Synthesis and Study of Supramolecular Structures

A Thesis

Submitted to
The Maharaja Sayajirao University of Baroda
for

the Degree of
Doctor of Philosophy
in

Organic Chemistry

By
Arpita S. Desai

Department of Chemistry
Faculty of Science
The M. S. University of Baroda.
Vadodara-390 002 India
February 2014

Certificate

This is to certify that the thesis entitled **"Synthesis and Study of Supramolecular Structures"** submitted by Ms. Arpita Satishchandra Desai, for the award of the degree of DOCTOR OF PHILOSOPHY in Chemistry to the M S University of Baroda, is her original research work and investigations carried out by her under my guidance and supervision at the Department of Chemistry, Faculty of Science. The subject matter of this thesis has not been previously submitted to any other university for the award of any other degree.

S/d-

(Prof. Shailesh R. Shah)
Guide

Professor,
Department of Chemistry
Faculty of Science,
The M. S. University of Baroda
Vadodara 390002

S/d-

(Dr. T. Rajamannar)
Co- Guide

Director,
Sunpharma Advance Research center,
Tandalja,
Vadodara-390012.

S/d-

(Prof. Neelima Kulkarni)

Head,
Department of Chemistry,
Faculty of Science,
The M. S. University of Baroda.

Statement

I hereby declare that the matter embodied in this thesis is the result of investigations carried out by me at the Department of Chemistry, Faculty of Science, the M.S.University of Baroda, Vadodara under the supervision of **Prof. Shailesh R. Shah** and **Dr. T. Rajamannar**. Keeping with the general practice of reporting scientific observations, due acknowledgements have been made where the work described is based on the findings of other investigators.

S/d-

Arpita S. Desai

Acknowledgments

It is my great pleasure to acknowledge my deep sense of gratitude to my research supervisors Dr. Shailesh R. Shah and Dr. T. Rajamannar for their valuable guidance.

I take an opportunity to thank Prof. Nilima Kulkarni, Head, Department of Chemistry, Prof. B. V. Kamath and Prof. Surekha Devi, former Heads of the Department of Chemistry for providing the laboratory and analytical facilities during my work.

I sincerely thank Prof. Nilima Kulkarni for her valuable guidance to carry out Host-Guest studies.

I am thankful to Zydus Research Centre (ZRC), Ahmedabad and Sunpharma Advance Research centre (SPARC), Vadodara for their analytical support. I also thank CSMCRI Bhavnagar for recording Circular Dichroism spectra and CHN analysis. I am grateful to Prof. H. Sakurai, Institute of Molecular Science, Okazaki, Japan for providing some of the 1H NMR, 13C NMR, and 2D NMR spectral analyses.

I especially thank Mr. Amol G. Dikundwar and Prof. T. N. Guru Row, Solid state and Structural Chemistry Unit, Indian Institute of Sciences, Banglore, Dr. E. Suresh, CSMCRI Bhavnagar and Dr. K. Ravikumar, IICT Hyderabad for carrying out single crystal X-ray analyses.

I am thankful to Mr. Shardul and Prof. Bhavna Trivedi for recording cyclic voltamogramms of silver(I) and copper(II) complexes. I also thank ‘SAIF ’IIT Bombay for providing ESR facility.

I thank Dr. D. P. Rajani, Microcare Laboratory, Surat for carrying out antibacterial and antifungal activities.

I am thankful to all teaching and non-teaching staff of the Department of Chemistry.

I sincerely thank Prof. Surekha Devi and my parents for their continuous inspiration and support to overcome all difficulties and developing a positive spirit to deal with all challenges.

Contents:

List of Abbreviations Used in This Thesis

COSY	Correlation spectroscopy
DABN	Diamino-binaphthalene
DACH	Diamino-cyclohexane
DADPE	Diamino-diphenyl-ethane
DCM	Dichloromethane
DEPT	Distortionless enhancement by polarization transfer
DMF	Dimethyl formamide
ESI	Electron spray ionization
ESR	Electron spin resonance
gl. HOAc	Glacial acetic acid
HMBC	Heteronuclear multiple bond correlation
HPLC	High performance liquid chromatography
HSQC	Heteronuclear single quantum coherence
IR	Infrared
MeOH	Methanol
NMR	Nuclear magnetic resonance
NOE	Nuclear Overhouser effect
Q-Tof	Quadrupole time of flight
TFA	Trifluoro acetic acid
TLC	Thin layer chromatography
TREN	Tris-2-aminoethylamine
TRPN	Tris-3-aminopropylamine
UPLC	Ultrahigh performance liquid chromatography
Uv-Vis	Ultraviolet-Visible
XRD	X-ray diffraction

Chapter 1

Introduction

1.1 Chemistry of Soft Interactions

The existence of life on the Earth makes this planet a very special one in the universe. Among many factors which help the life to grow on the Earth, the non-covalent interactions are responsible to make the biochemical processes go on in a specific way as required which makes a thing 'living'. With advances in science and technology we are still trying to understand the biological processes taking place in a cell, in a living system and thus in human body. It helps in making our life healthier. Understanding the biological processes help us to develop more specific and more potent medicine having minimum or no bad effects.

The smallest part of living organism is the cell. Number of reactions takes place in the cell simultaneously e.g. ion exchange, generation of energy, replication of DNA or RNA and many more with extreme accuracy and specificity. There is an auto reaction control and rate accelerations are observed. The base lies in the soft and reversible interactions, e.g. hydrogen bonding exists between two strands of DNA double helix which is a non-covalent interaction.[1] The 2013 Nobel Prize in medicine[2] is awarded for the work on machinery regulating vesicle traffic, a major transport system in our cell. The prize is shared by James E. Rothman, Randy W. Schekman and Thomas C. Sudhof. They have explained the precise control system for the transport and delivery of cellular cargo, which are mainly based on non-covalent interactions. Enzymes are made from proteins which self assemble for a specific task. Emil Fischer in 1894 gave lock and key model to explain enzyme action and provided the basis of molecular recognition.[3] In short non-covalent interactions are basis of biochemical processes.

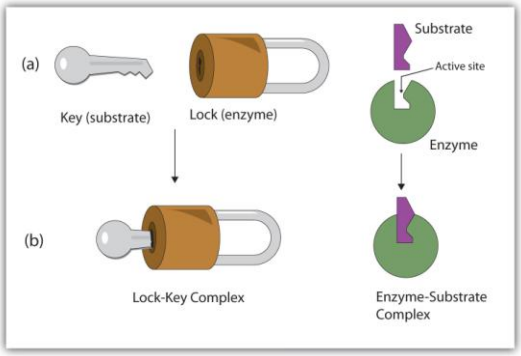

Comparison of enzyme specificity with lock and key

Fig. 1.1

Natural receptors are quite flexible and can adopt a necessary change in their structure as well as function depending on the environmental need. Because of these fascinating characteristics 21st century research has more focused on materials involving soft chemistry.

The research in this area started long before with the observation of Paul Ehrlich that 'molecules do not act if they do not bind'. The concept of receptor and substrate binding strengthened with lock and key model and resulted in enormous number of diverse molecules when Alfred Werner gave concept of coordination. In 1987 Jean Marie-Lehn, Donald J. Cram and Charles J. Pedersen got the Nobel Prize for their work in the area of soft interaction named as Supramolecular Chemistry: 'Chemistry beyond the molecule bearing on the organized entities of higher complexity that result from association of two or more chemical species held together by non-covalent interactions.'[4]

Supramolecular chemistry is also called the chemistry of molecular assemblies and of the intermolecular bond, chemistry of non-covalent bond and non-molecular chemistry.

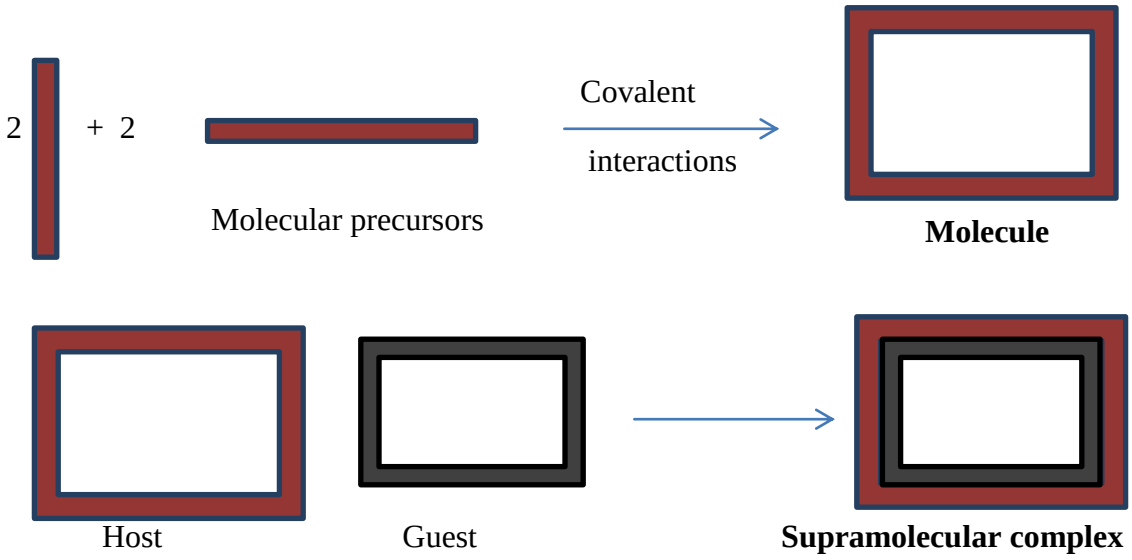

Concept of covalent and supramolecular bonding

Fig. 1.2

Supramolecular entities are thermodynamically less stable, kinetically more labile and dynamically more flexible than covalently bonded molecules.[5] The supramolecular chemistry deal with binding of a substrate to receptors where a receptor is generally bigger component which is capable of binding smaller molecules. The substrate is usually a smaller molecule whose binding is being sought.

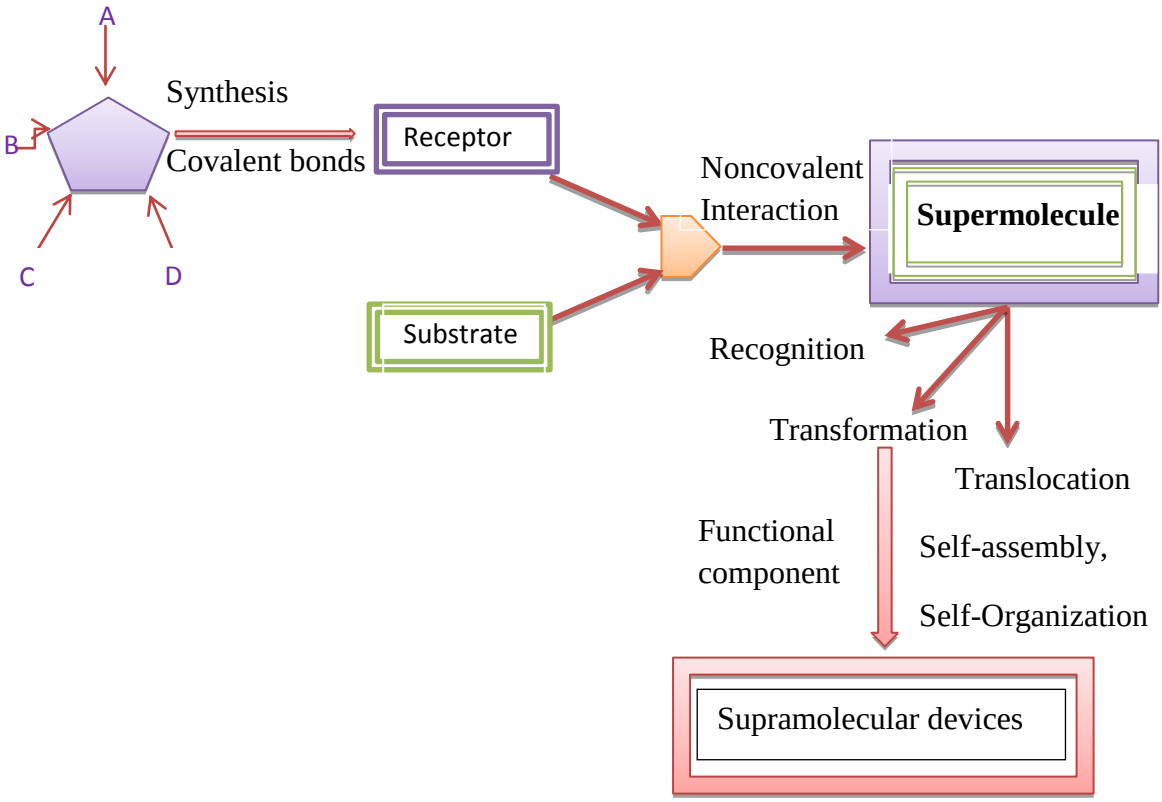

Components of Supramolecular Chemistry[4]
Fig. 1.3

Molecular recognition, transformation and translocation represent the basic functions of supramolecular species. Recognition is the preferential binding of a given substrate by the receptor molecule. Generally, recognition and subsequent binding of a substrate by a receptor are reflected in terms of a change in the physical properties of the receptor molecule. When receptor bears a reactive functionality, it makes chemical changes to the bound substrate and transforms it to the more stable or more suitable substrate and thus

acts as a supramolecular catalyst. Sherman's carceplexes and hemicarceplexes are appropriate examples of receptors having transformation capacities.[6] Benzyne was trapped in the cavity of a carceplex and reacted with the aromatic ring of the carceplex receptor. A lipophilic membrane soluble receptor may act as a carrier effecting the translocation of the bound substrate. Supramolecular chemistry comprises of all types of species held by non-covalent interaction including oligomolecular species like macrocycles or cage compounds as well as polymolecular species.

Supramolecular chemistry is divided into two broad classes.[4]

I Supermolecules: "Supermolecules are well defined discrete oligomolecular species that result from the intermolecular association of a few components based on the principles of molecular recognition**."**

II Supramolecular assemblies: "Supramolecular assemblies are polymolecular entities that result from the spontaneous association of a large undefined number of components into specific phase having more or less well-defined microscopic organization and macroscopic characteristics depending on its nature."

Supramolecular chemistry is also known as host-guest chemistry where receptor is called host molecule which possesses convergent binding sites like Lewis basic donor sites and guest is the molecule which possesses divergent i.e. counter interacting binding sites like Lewis acidic acceptor site. Commonly the host is a large molecule or aggregate such as macrocyclic compound possessing a central hole or cavity of a definite size. Commonly the guest may be cation, anion or neutral molecule such as a hormone, drug, pheromone or neurotransmitter. Pederson's crown ether complexation with metal ion is the first example of such man maid host-guest system. Sherman's carceplex and hemicarceplex formation is another well studied host-guest system, where guest itself act as template to organize the assembly of the host molecule and gets trapped at the end of the synthesis. Hemicarceplexes are more popular due to their application in stabilization of short lived reactive intermediates and to achieve direct reactions inside the cavity of the host molecule.[6]

1.2 Types of Supramolecular interactions[4]

The forces that drive the non-covalent binding between host and guest can be classified into a) ion-ion interaction, b) ion-dipole interaction, c) dipole-dipole interaction, d) hydrogen bonding, e) cation-π interactions, f) π-π stacking, g) Van der Waals forces, h) hydrophobic effects and i) combinations of these interactions.

➢ Ion-Ion interaction

Bond energy of ion ion interaction between host and guest molecules ranges from 100 kJ/mole to 350 kJ/mole. The common example of such reaction is NaCl. Where Na^+ ion is capable of organizing six Cl^- donor atoms around itself and Cl^- also attracts six Na^+ ions around itself. Another example of ion-ion interaction is between supramolecular tris-(diazabicyclooctane) host which carries 3+ charge and an anion such as $Fe(CN)_6^{3-}$.

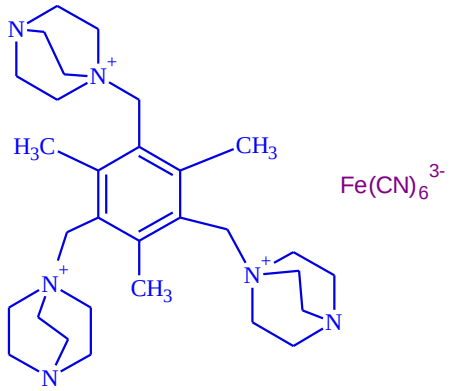

Ion-ion interaction between tris-(diazabicyclooctane) host and $Fe(CN)_6^{3-}$ guest

Fig. 1.4

➢ Ion-dipole interactions

Bond energy of ion-dipole interaction between host and guest molecules ranges from 50 kJ/mole to 200 kJ/mole. The well known example is the binding of K^+ with [18]-crown-6 (Fig. 1.5) or Zn^{2+} bound in octaaza-cryptand cavity[7] (Fig. 1.6).

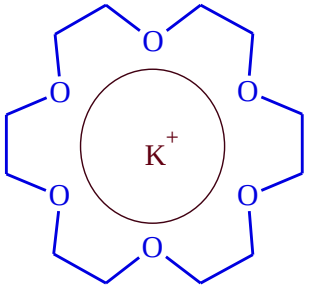

Ion-dipole interaction in $K^+ \subset$ [18]-Crown-6

Fig. 1.5

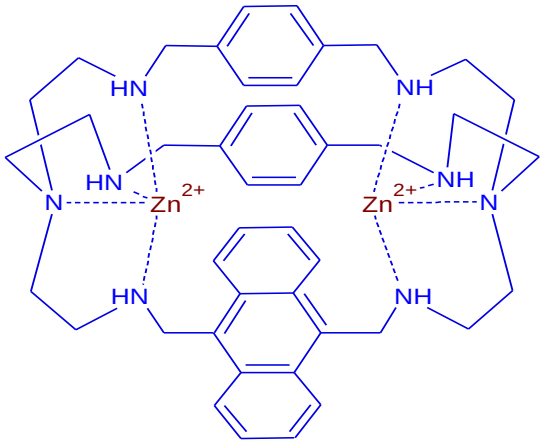

Ion-dipole interaction in $Zn^{2+} \subset$ Cryptand

Fig. 1.6

➢ Dipole-dipole interactions

Dipole-dipole interactions are relatively weak interactions having bond energies of 5-50 kJ/mole. This interaction exists between the molecules having permanent dipoles as carbonyl functionalities. (Fig. 1.7)

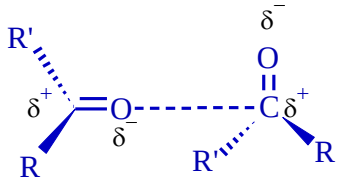

Dipole-dipole interaction between acetone molecules

Fig. 1.7

➢ Hydrogen bonding

- "The hydrogen bond is an attractive interaction between a hydrogen atom from a molecule or amolecular fragment X–H in which X is more electronegative than H, and an atom or a group of atoms in the same or a different molecule, in which there is evidence of bond formation."

It is a special type of dipole-dipole interaction in which a hydrogen atom attached to an electronegative atom is attracted to a neighbouring dipole on an adjacent molecule or functional group. 'It is known as master key interaction in supramolecular chemistry.'[4]

Hydrogen bonds are present in many supramolecular host-guest systems such as DNA double helix[2] (Fig. 1.8) or in enzyme action on different substrates in the body.

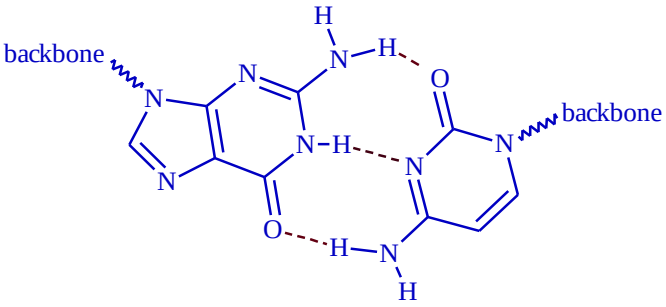

Hydrogen bonding between DNA double helix

Fig. 1.8

Many synthetic receptors undergo hydrogen bonding to make a stable supramolecular assemblies e.g. binding of barbiturate molecule with a macrocyclic host by six hydrogen bonds.[8]

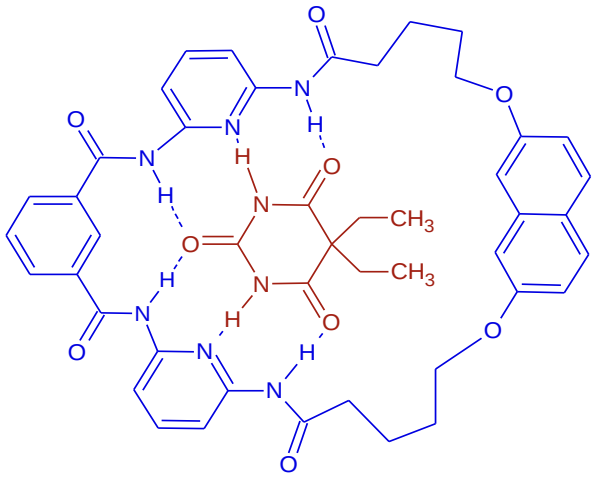

Barbiturate ⊂ Aza Corand

Fig. 1.9

When hydrogen atoms are attached to carbon rather than electronegative atoms and are attracted by neighboring dipole form **weaker hydrogen bonds.** This is possible with acidic hydrogens, where carbon containing hydrogen will be attached to electron withdrawing group. e.g. nitro methane encapsulated within the cavity of pyridine based crown ether. An example of such kind of weaker attraction is proposed when nitromethane gets encapsulated within the cavity of the pyridine based crown ethaer. (Fig. 1.10)

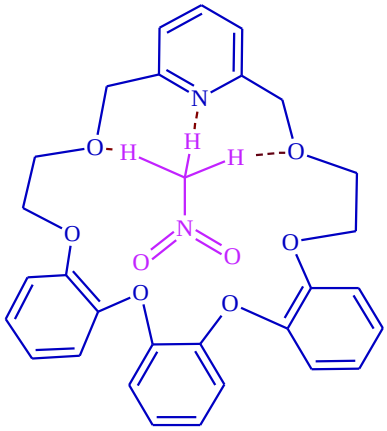

Nitromethane⊂ Pyridine linked Crown ether

Fig. 1.10

➢ Cation- π interactions

In cation- π interaction, bond energy varies from 5 to 80 kJ/mole. The well known example is of sandwich molecule ferrocene, were Fe^{2+} ion is attracted by two aromatic π electron clouds. Pt^{2+} also forms such compounds due to cation- π interactions. When alkali or alkaline earth metal ions gets encapsulated in the aromatic cavity of supramolecular hosts or form complexes with carbon-carbon double bonds, the interaction involved is much more noncovalent or weak and becomes important in the supramolecular chemistry.

➢ **π-π staking :** Bond energy of this interaction varies from 0 to 50 kJ/mole. When one aromatic ring is electron rich and other is electron poor, there exists a weak electrostatic interaction, known as π-π staking. It is of two general types: a) edge to face b) face to face (Fig. 1.11)

a. Edge to face π-π staking **b. Face to face π-π staking**

Fig. 1.11

➢ Hydrophobic effects

Hydrophobic effects are considered as exclusion from polar solvents such as water, alcohol etc. When few oil droplets are added to water they are repelled by water molecules. There is a strong attraction already present between the surrounding water molecules which squeeze out the oil droplets and agglomeration of such droplets takes place which is known as hydrophobic effect. In supramolecular chemistry the host such as cyclodextrins, cyclophanes etc are soluble in polar solvents but their interior is hydrophobic. When organic guest molecules are added to their aqueous solutions, water molecules from the cavity are thrown out and organic molecules are stabilized in hydrophobic cavity of such host molecules.(Fig. 1.12)

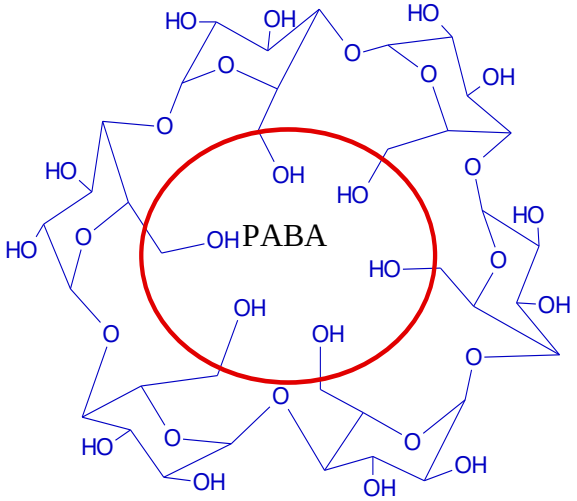

PABA= p-aminobenzoicacid⊂ α-cyclodextrin

Fig. 1.12

➢ **Van der Waals forces:**

The Van der Waals interactions are very weak having bond energy less than 5kJ/mole.

"Weak electrostatic attractions occur between dipoles and instantaneous dipoles created by polarization of the electron cloud of one atom/molecule by the nucleus of the adjacent atom/molecule are known as van der Waals forces." They are present in noble gases. p-*tert*-Butyl-calix[4]arene encapsulate toluene due to this interactions. (Fig. 1.13) Interaction mainly depends on distance between the two dipoles and attraction decreases with increase in the distance rapidly.

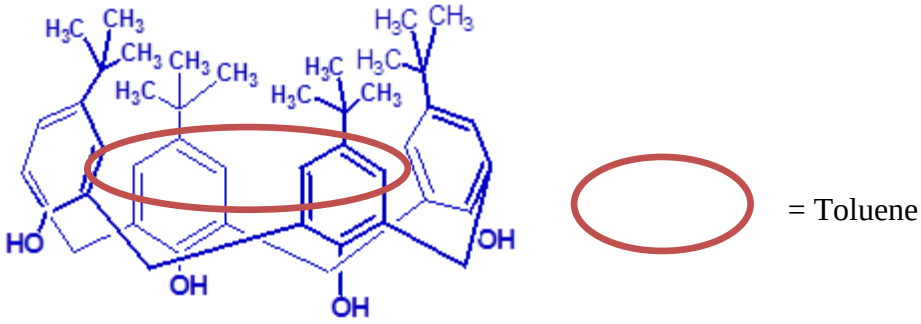

Toluene⊂ p-tert-Butylcalix[4]arene

Fig. 1.13

1.3 Classification of supramolecular interactions[4]:

The supramolecular interactions can be classified as summative or multiplicative interactions. In summative interaction the total stabilization energy is arithmetic sum of the individual stabilizations resulting from individual binding sites. While in case of multiplicative interactions the total stabilization energy of a supramolecular system is synergistically greater than the sum of individual stabilizations. Multiplicative interactions are found in most of the supramolecular species and comprise of chelate effect and macrocyclic effect.

➢ **Chelate effect:** Metal complexes of bidentate or polydentate ligands are more stable than corresponding monodentate ligands. e.g Ethylenediamine complexes. (Fig. 1.14)

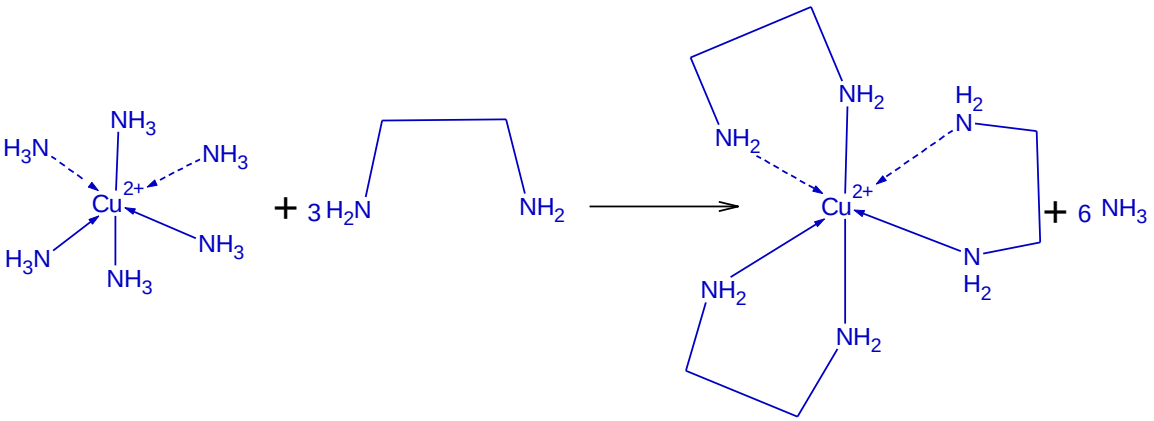

Monodentate ligand vs bidentate ligand
Fig. 1.14

When ethylenediamine is added to the copper hexamine complex this chelating bidentate ligand replaces six ammonia molecules to form a chelate complex of copper and ethylene diamine, thus increases the entropy of overall reaction as total entities on reactant side are four while on product side the total entities are seven. This makes Δ S positive and ΔG negative which ensures the feasibility of the reaction.

➢ Macrocyclic effect

Macrocyclic ligands are more stable than the corresponding acyclic analogous. This is due to presence of number of binding sites of the ligands at proper positions to chelate their guests. Such supramolecular entities are further stabilized by the macrocyclic effect. During the synthesis of macrocycle, the enthalpic penalty associated with bringing donor atom lone pairs in juxta positions with respect to one another in order to bind the guest molecule has been already paid in advance. The macrocyclic hosts such as corands are up to a factor of 10^4 times more stable than their acyclic analogous podands with similar binding sites. In case of acyclic molecules more number of host-solvent bonds are required to be broken to achieve a stable host-guest complex compared to the cyclic host, as cyclic nature of the host makes minimum interaction with the bulk solvent. This provides the enthalpic stabilization. Macrocyclic host losses less degree of freedom when gets complexed which is entropically favoured process.

1.4 Classification of Supramolecular Host-guest Compounds[4]

There are two types of supramolecular host-guest complexes. a) clathrates b) cavitates

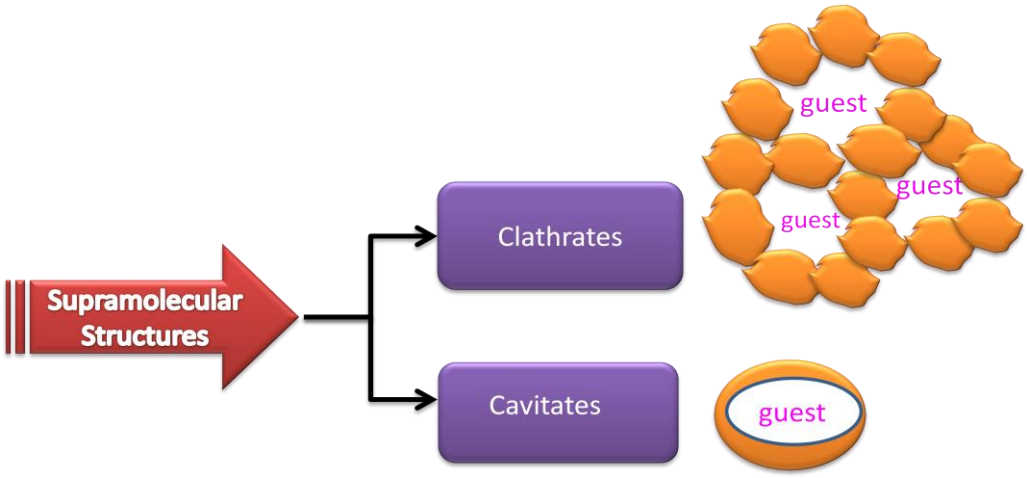

Representation of clathrates and cavitates

Fig. 1.15

Clathrates: "Clathrate is a kind of inclusion compound in which two or more components are associated without ordinary chemical union but through complete enclosure of one set of molecule in a suitable structure formed by another." Here host is known as clathrand which possess extramolecular cavity. These species are stable in crystalline or solid state only. Cyclotriveratrylene host (CTV) forms clathrates with acetone involving van der Waals interactions or gets stabilized due to crystal packing.

Cavitates: "Cavitate is a kind of inclusion compound in which one or more guest molecules are completely encapsulated within the cavity of host molecule." Here host is known as cavitand which possesses intramolecular cavities. These are stable in solid as well as solution state. Macrocyclic hosts possessing intramolecular cavity are capable of binding the guest molecule(s) by non-covalent interactions. When host is dissolved in a solvent, the solvent molecules get bound in the cavity of the host. If a suitable guest is added, the bonds between solvent and the host cavity gets broken and new bonds between host and guest molecules are formed. This happens only when the host has preferential selectivity to the added guest rather than a solvent molecule. Further this process should be entropically favoured.

Cavitates can be further classified on basis of the structures of host molecules. Fig. 1.16 represents various types of cavitates and the interaction presents between the host-guest molecules.

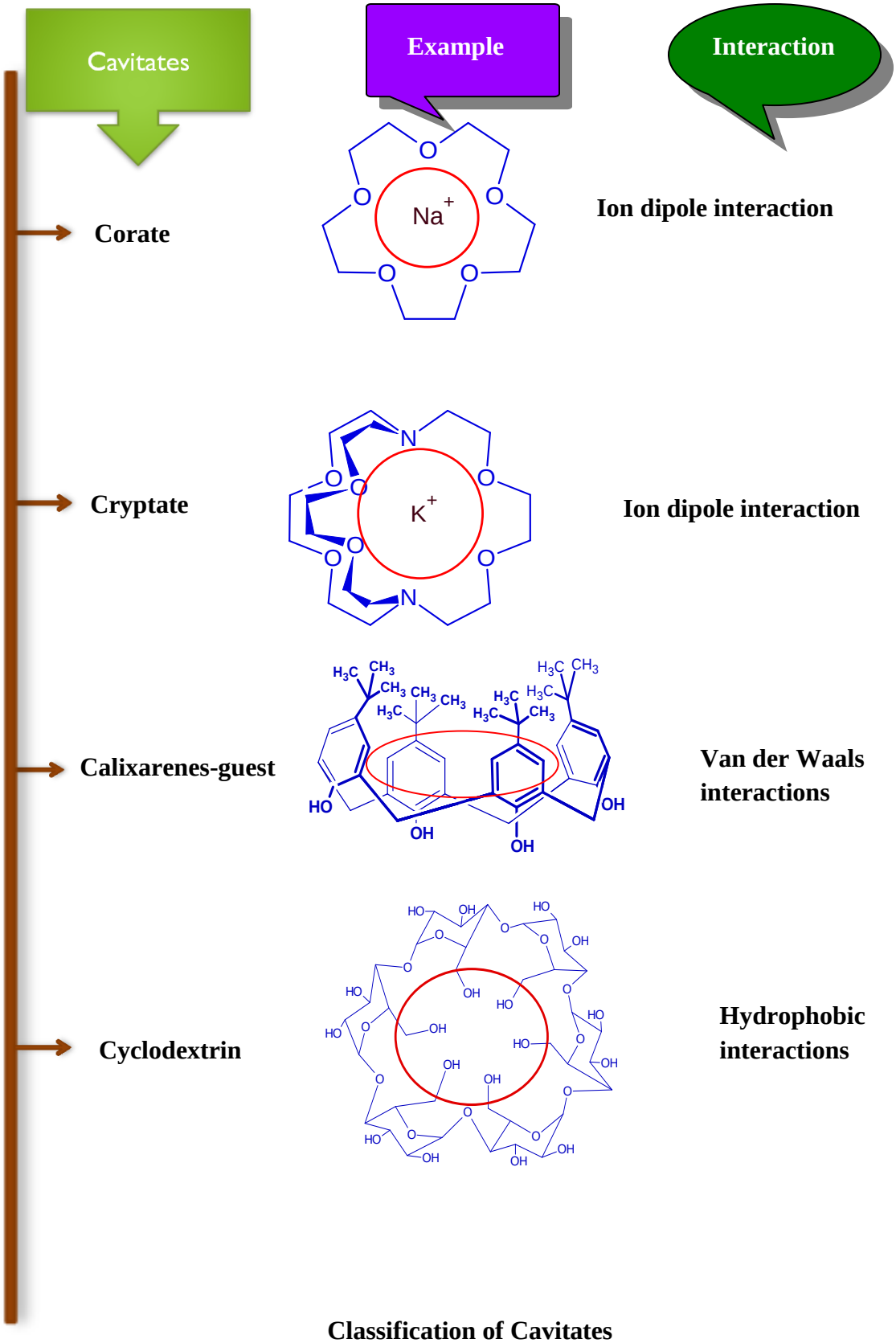

Classification of Cavitates

Fig. 1.16a

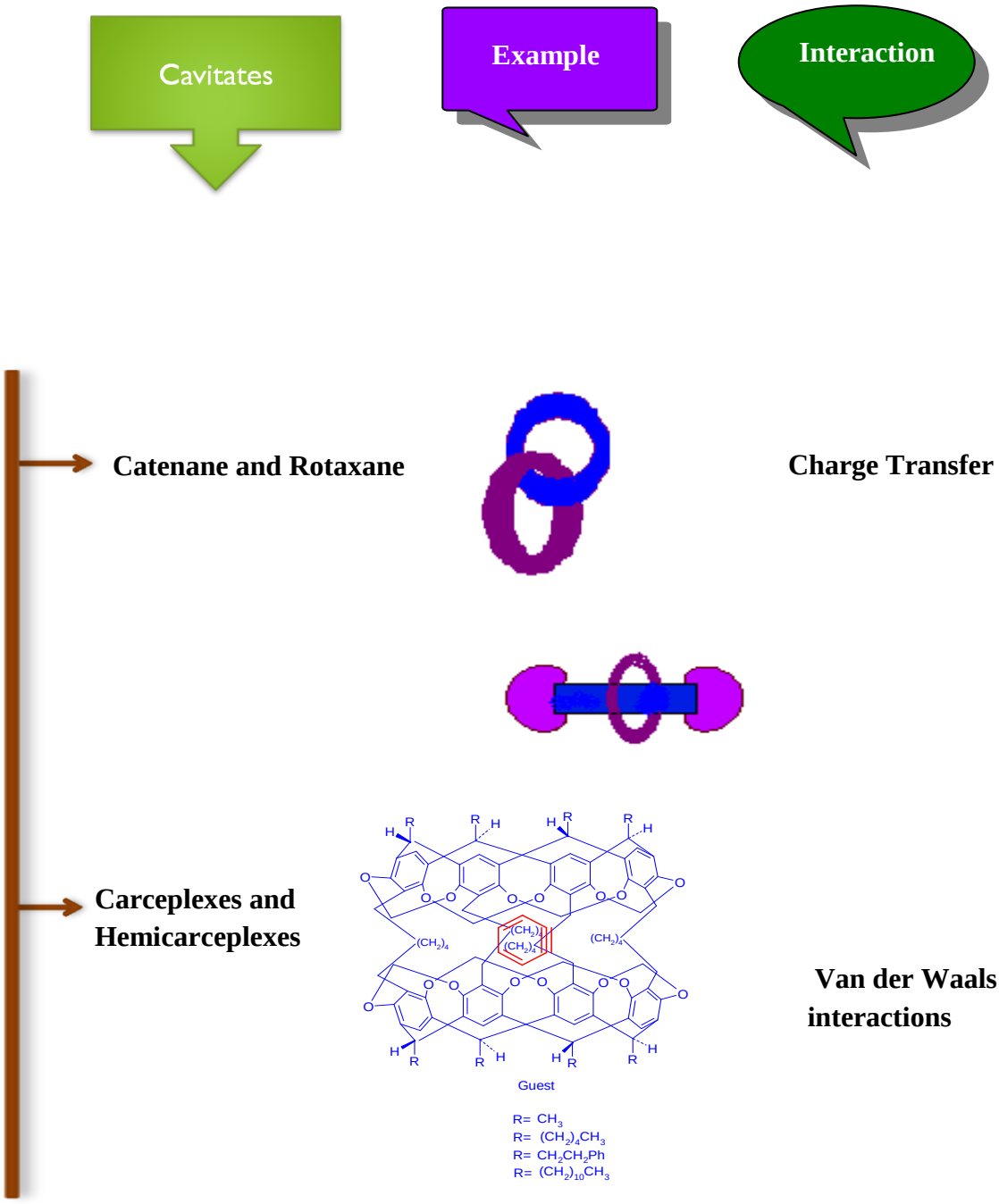

Classification of Cavitates

Fig. 1.16b

1.5 Molecular recognition[5]**:** Binding and selection of substrate(s) by a given receptor molecule is called molecular recognition. Mere binding is not recognition, but selective binding with a particular purpose is recognition. Recognition is due to geometrical and interactional complementarity between two or more associating entities.

Recognition depends on

- **Steric factors :** The best fit between receptor 'ρ' and substrate 'σ' is a steric complementarity i.e. presence of correct concave and convex domain at an appropriate positions on receptor and substrate

- **Interactional complementarity:** It means presence of complementary functionalities on 'ρ' and 'σ'. Generally receptors possess convergent binding sites which include presence of dipoles, hydrogen bond donor sites, negative or positive charges etc. which need to be matching to the binding functionalities on substrate molecules like positive or negative charges, dipoles, hydrogen bond acceptors in correct position on 'ρ' and 'σ'.
- **Large surface overlaps:** A maximum overlap is required between receptor and substrate to have multiple interaction sites.

In order to achieve efficient recognition, both high stability and selectivity are required. The natural receptors are flexible and can undergo conformational changes to bind a required substrate. These complexes are often less stable as the energy is utilized in making the conformational changes. Rigid receptors form more stable host-guest complexes but they lack in flexibility. Biological processes like exchange, regulation, transformations and transportations require built-in flexibility where a receptor needs to adapt and respond to the changes.

1.6 Chiral recognition

Biochemical systems involve enantiospecific receptor-substrate binding. Cram's group in 1976 reported a new class of macrocyclic chiral compound named chiral crown ether in enantiomerically pure form (R,R).[9] It does enantioselective recognition of chiral ammonium salts. It is useful in resolution of many drug molecules and thus has potential applications in pharmaceutical industry.

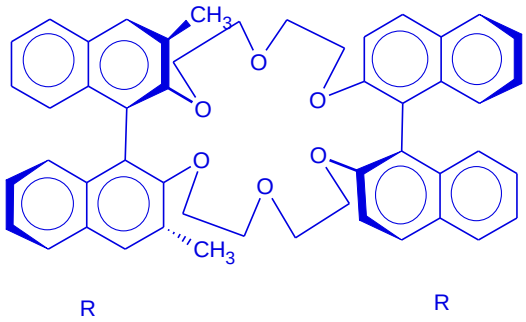

Chiral crown ether for enantiospecific binding of aminoacids

Fig. 1.17

The (R,R) chiral crown ether displays enantioselective binding with one of the enantiomers of chiral amino acids. Generally it is observed that this (R,R) host binds with D- amino acids and their esters much more strongly than the L-guest. The host-guest complexes can be extracted by chloroform from water. The D isomer selectively binds to the host having better fit and gets preferentially extracted.

Stoddart and co-workers in synthesized a number of chiral corands derived from mannitol and tartaric acid derivatives which were employed for resolution of various amino acids.[10]

Chiral recognition of amines and amino alcohols was possible by using azophenolic crown ethers (Fig. 1.18) where cis-1-phenylcyclohexane-1,2-diol was a chiral subunit which was responsible for chiral recognition while 2,4-dinitrophenyl-azophenol was introduced to generate a specific response in UV-Vis spectrum.[11,12]

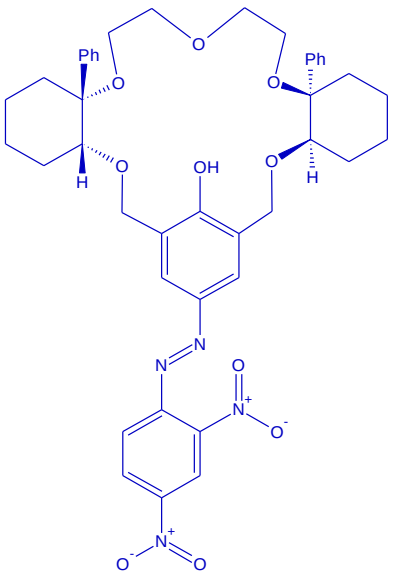

Chiral, light responsive azophenolic crown ether

Fig. 1.18

Resolution of racemic mixture of various aminoacids including methionine, phenylglycine, isolucine etc was done using [18]-crown-6-tetracarboxylicacid host. The chiral discrimination was studied with the help of their single crystal X-ray structures.[13]

➢ Chiral recognition with Podands and lariat ethers

Chiral recognition of amino acids with aromatic side chain (e.g. tryptophan and phenylalanine) can also be achieved with the help of chiral podands and lariat ethers.[14]

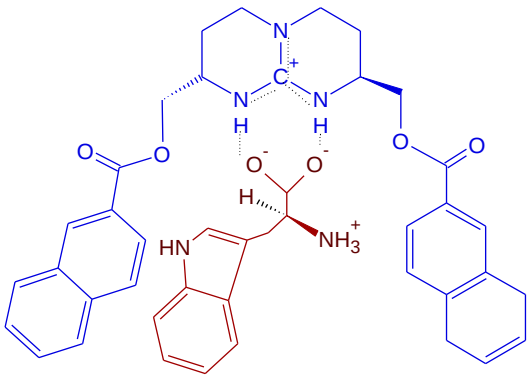

Recognition of L-tryptophan in (S,S) host

Fig. 1.19

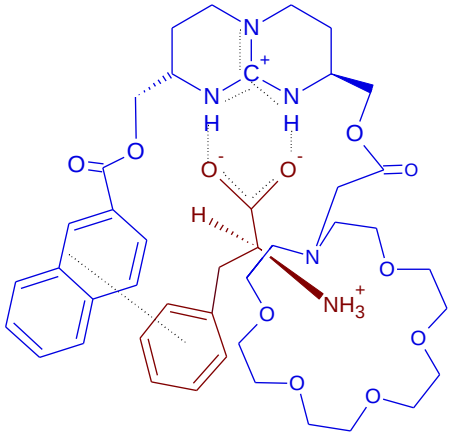

Recognition of L-phenylalanine in (S,S) host

Fig. 1.20

1.7 Methods of synthesis of supramolecular structures: [4]

1.7.1 Template assisted synthesis

Template: "The chemical specie which organizes an assembly of atoms, with respect to one or more geometric loci, in order to achieve a particular linking of the atoms is known as template"[6]

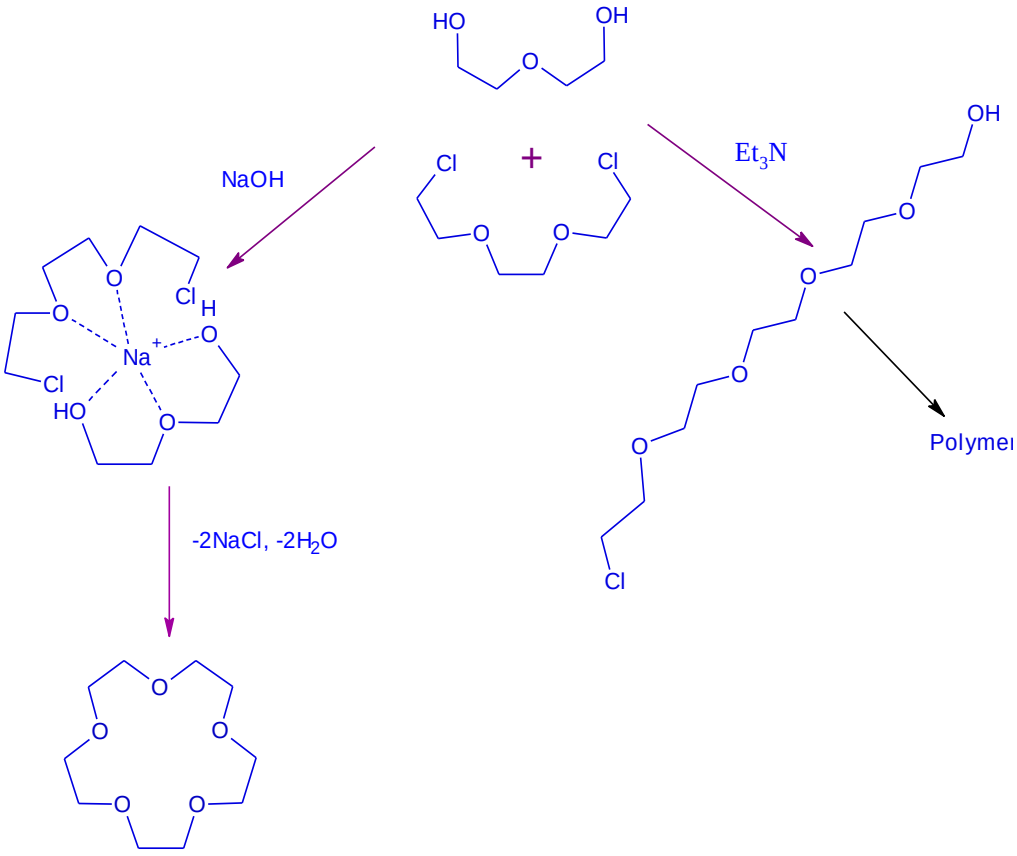

Template assisted synthesis of [15]crown-5
Fig. 1.21

Ether formation reaction between –OH and –Cl functional groups is a base catalyzed reaction. When triethylamine is used as a base in the reaction of dihalide with diol, an intermolecular reaction resulted in an oligomeric species, which may further react with diols and dihalides to form a polymer. When specific alkali metal carbonate is used, it orients the reactants diol and dihalide around itself in an appropriate geometry to achieve

macrocyclization. Here alkali metal ion like Na^+ is called template or more specifically a kinetic template and the specific macrocyclization in presence of cation or anion or a neutral molecule is known as template effect.

Template may be an organic molecule, a metal cation or an anion. Cs^+ is very effective as a template for the formation of cyclic products in good yields. The phenomenon is called 'caesium effect'. Although template assisted synthesis gives products in good yields, it is often observed that the template gets trapped into the cavity of the synthesized host. Open hosts like crown ethers are exceptions. It is also seen that some so-called template assisted synthesis proceeds similarly even in absence of a template e.g. synthesis of porphyrins and macrocycle formed by condensation between acetone and ethylenediamine.[15]

To obtain a template free host, high dilution technique is employed in absence of any specific ion or molecule to act as a template.

1.7.2 High Dilution Synthesis[4]

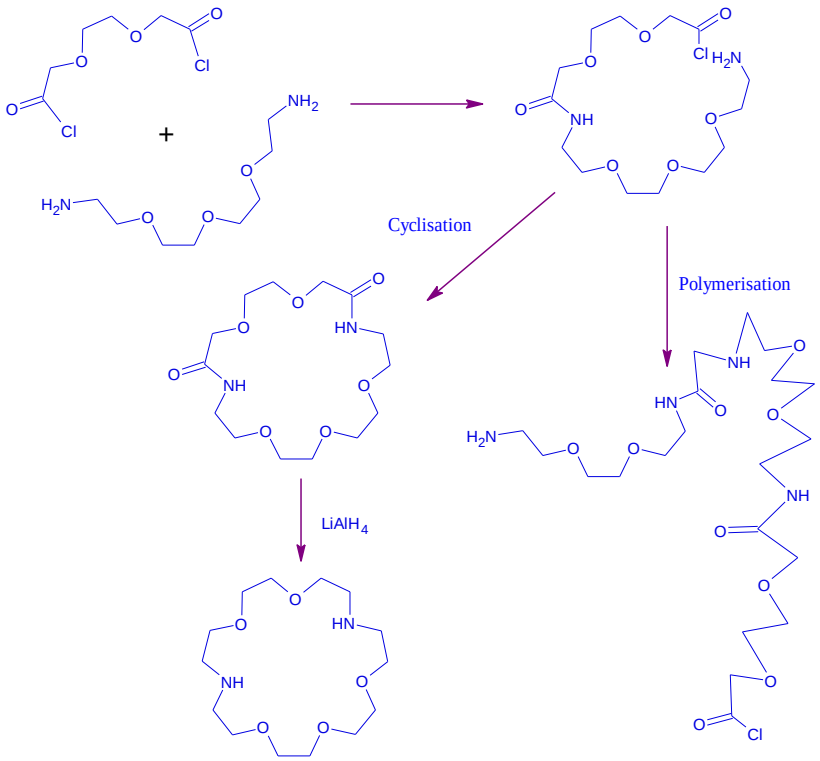

Template free high dilution synthesis of aza-crown ether

Fig. 1.22

When an appropriate template is not available for macrocyclic host formation or for metal free synthesis is to be done, reaction is carried out in excess of solvent, which is known as high dilution synthesis. Here the reactants are dissolved in an excess of solvent and simultaneously added drop wise at a very slow rate from addition funnels to a round bottom flask containing an excess of solvent. This ensures a very low concentration of reactants as well as intermediate products at a time and reduces chance of polymerization favouring intramolecular cyclization to yield the desired macrocycle.

If rate of cyclization of reactant A-B, $r_c=k_c[A\text{-}B]$ is compared with rate of polymerization $r_p=k_p[A\text{-}B]^2$

$r_c/r_p = k_c[A\text{-}B]/ k_p[A\text{-}B]^2$

$= k_c /kp[A\text{-}B]$

The lesser is the concentration of A-B, more is the rate of cyclization.

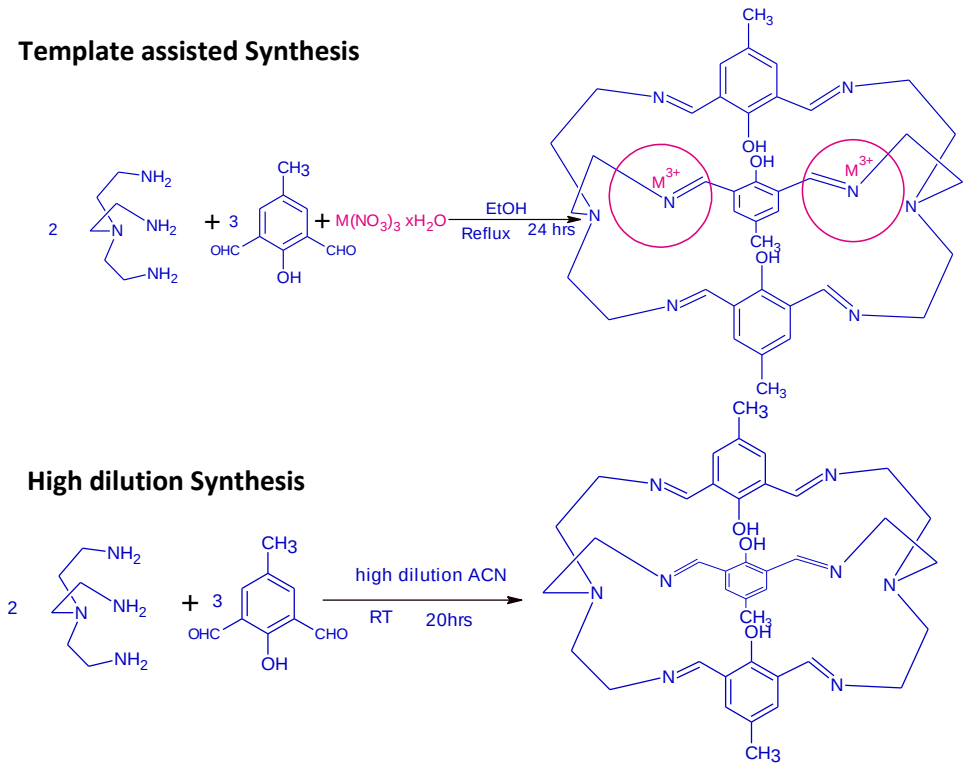

Cryptand formation under High dilution as well as template assisted synthesis[15,16]

Fig. 1.23

As depicted in Fig. 1.23 synthesis of TREN capped cryptand can be achieved using either lanthanide cations or under high dilution condition. In template assisted synthesis the yields are higher while in high dilution synthesis though the yields are lower, metal free cryptand is achieved.

1.8 Binding constant[17-20]

Binding constant is a specific numerical value assigned to the host guest entities reflects stability of the host guest system. Binding constant is also known as stability constant or protonation constant. Binding constant is quantification of supramolecular host-guest complexation. It is a result of mathematical operations on experimental observations. Normally the experimental observations are based on titration methods using different spectroscopic techniques. For titration most often the guest is gradually added to the solution of host molecule. Supramolecular interactions between the two components if results in a change in the spectroscopic behavior of the host, the binding between the two can be detected and the technique can be employed for determination of binding constant. Alternatively potentiometric titration can also be used for determination of binding constant especially when metal ions are involved.

- **Determination of binding constants.**

The most common approach to find out binding constant is the supramolecular titration method. Here one component (most often a guest) is gradually added to the solution of the other (Host) while monitoring a change in physical property such as chemical resonance in ^{1}H NMR, ^{13}C NMR or absorption band in UV that is sensitive to the supramolecular interactions of interest. The resulting information is further processed by chemical models and their mathematical equations to calculate association constant K_a also known as binding constant, Energetic and stoichiometry. Some of the most frequently used techniques for determining binding constant are outlined as follows.

1.8.1 Determination of Binding constant: pH measurement

Ligands are weak bronsted bases. In aqueous solutions the ligand can form metal-ligand complex or it can be protonated. There is a competition between metal ion and proton which can be monitored by PH-measurements or pH titration. This method was developed by Bjerrum.[21] Method is very precise and can be applied to various metal ions and ligands.

The most common procedure for binding constant determination is pH titration. A particular concentration of ligand solution is prepared to which stoichiometric amount of metal ion and acid is added under nitrogen atmosphere to prevent aerial oxidation or reaction with carbon dioxide. A standard base is added drop wise to a magnetically stirred solution and pH is measured.

1.8.2 Determination of Binding constant: NMR measurement

The most informative technique which is applicable to a wide range of organic ligands is protone NMR measurements at different host-guest concentration. Relative shifts in NMR monitored titration can give qualitative information such as changes in symmetry of the molecule, stoichiometry of guest to the host molecule and quantitative information such as binding constant for the guest molecule.

In case of host-guest complex having (1:1) stoichiometry, chemical shift (δ) of the signal of interest is assumed to be the weight average of the free host and the bound host complex. This is true for the equilibria that are fast on NMR time scale. For a slow exchange of complexed and uncomplexed host, the binding constant may be evaluated by simple integration of NMR signals.

Experiment is carried out in deuterated solvents where known quantity of host is taken and small aliquots of the guest are added and spectrum is monitored as a function of guest concentraion or host-guest ratio. Titration curve is monitored by computer programme such as EQNMR.

1.8.3 Determination of Binding constant: By UV-Visible measurement

Spectrophotometric method is convenient as compared to potentiometric method and less expensive as compared to NMR titration method. It can also be used for non-basic ligands such as halides. It is necessary to determine stoichiometry of the complex before calculation of binding constant.

Absorbance is measured at a wavelength where complex absorbs strongly but metal as well as ligand's absorbance is minimum or ideally they do not absorb at all.

In mole-ratio method a series of solutions is prepared where concentration of any one of the reactant is held constant and other's is varied.

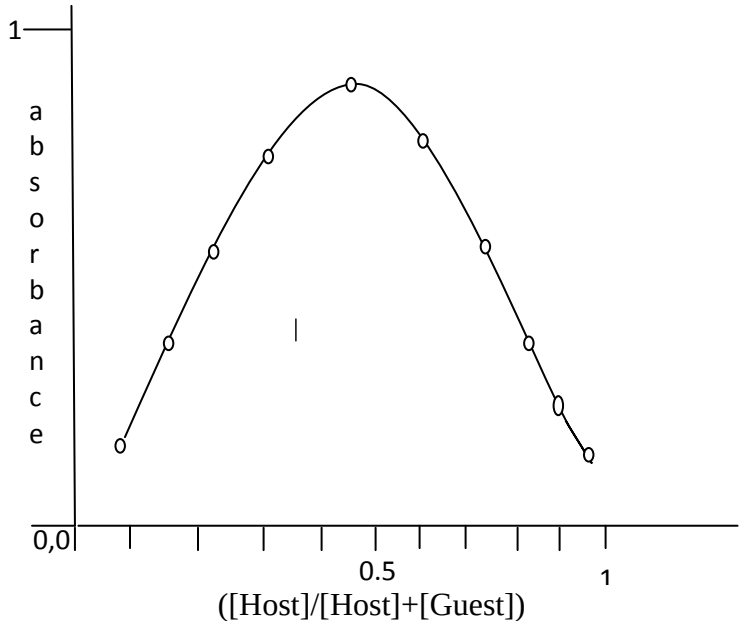

Job plot showing (1:1) Host : Guest ratio

Fig. 1.24

Absorbance is plotted against concentration of the component whose concentration is varied. If only one complex of high stability is formed, the graph consists of two linear intersecting parts. Intersection point refers to the stoichiometry of the complex.

Calculation of binding constant assuming 1:1 stoichiometry

$$K_a = [HG]/[H][G] \quad \text{Equation-1}$$

$$[G] = 1/2\left\{\frac{1}{G}_0 - H_0 - \frac{1}{K_a}\right\} - \sqrt{\left\{G_0 - H_0 - \frac{1}{K_a}\right\}2 + \frac{4G_0}{K_a}} \quad \text{Equation -2}$$

$$[HG] = 1/2\left\{\frac{1}{G}_0 + H_0 + \frac{1}{K_a}\right\} - \sqrt{\left\{G_0 + H_0 + \frac{1}{K_a}\right\}2 + 4[G_0][H_0]} \quad \text{Equation-3}$$

$$\Delta A_{obs} = \in_{HG}\{[HG]\} \quad \text{Equation-4}$$

From eq-3 and eq-4 binding constant 'K_a' can be calculated.

1.8.4 Determination of Binding constant: Fluorescence measurement

Fluorescence is one of the most popular, relatively cheap and most sensitive techniques. Due to its high sensitivity it can work with submicromolar or even nanomolar solutions.

Ideally fluorescence titrations are to be carried out with such a concentration where absorbance is less than 0.05 at a wavelength of excitation.

The best situation under which fluorescence experiments can be carried out is one where host and guest both are fluorescent inactive but complex is fluorescent active. But it may not be the case always still if either of the host or guest is fluorescent active and a complexation quenches the fluorescence, the binding constant can be measured. It can be static quenching or dynamic quenching.

Following equation is used for determination of binding constant.

$$\triangle F_{obs} = K_{\Delta HG}([HG])$$

1.9 Applications of supramolecular entities:

➢ Supramolecular hosts as Sensors:

"A sensor is a converter that measures a physical quantity and converts it into a signal which can be read by an observer or by an instrument." [22]

Supramolecular chemosensors are based on chemical changes which reflect the encapsulation of a particular guest into a well designed host molecule which acts as a sensor. Many techniques are employed to analyze the target entity including mass spectrometry and atomic absorption spectroscopy, however these methods are not popular as they are more time consuming or require sophisticated instrumentation. UV and fluorescence spectroscopy have been powerful tools due to their simplicity, high detection limit and application to bio imaging. These are fast, non-destructive, highly sensitive and suitable for high-throughput screening applications. Quantification is possible here with quite good efficiency.[23]

A number of supramolecular sensors have been developed to sense cations, anions as well as organic molecules such as carboxylic acids, esters etc. Metal cations especially transition metal ions are one of the widely used substrates because of their biological concern and presence in the environment.[24] Organic macrocyclic host molecules serve as efficient receptors for such metal ions and these ions could get bound in their cavity. If binding of these metal ions to the receptors result in a trivial colour change or affect the fluorescence properties by change in fluorescence intensities, can act as a colorimetric chemosensors or fluorescence chemosensors respectively.

1.9.1 Design principle for fluorescence chemosensors for detection of metal ions[25].

Depending on their mechanism of action they are classified in five different ways

1. Fluorescent ligands: They possess receptor unit capable of emitting fluorescence upon binding of the metal ion.

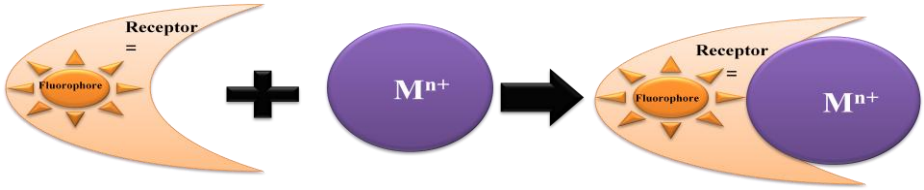

Fluorescent ligand as metal ion sensor

Fig. 1.25

Here an aromatic moiety which is a good fluorophore, is attached to the macrocyclic host or substituted with particular functional groups like amine, amide, imine, phenolic or carboxylic group. These functional groups help in binding the substrate which is generally a metal ion. Binding and selectivity depends strongly on number, type and geometrical arrangement of functional groups attached to the aromatic moiety. It is observed that paramagnetic ions are more strongly bound than the diamagnetic ions.

2. Intrinsic fluorescent probes: In case of intrinsic fluorescence probes, binding site and chromophore are in direct electronic conjugation.

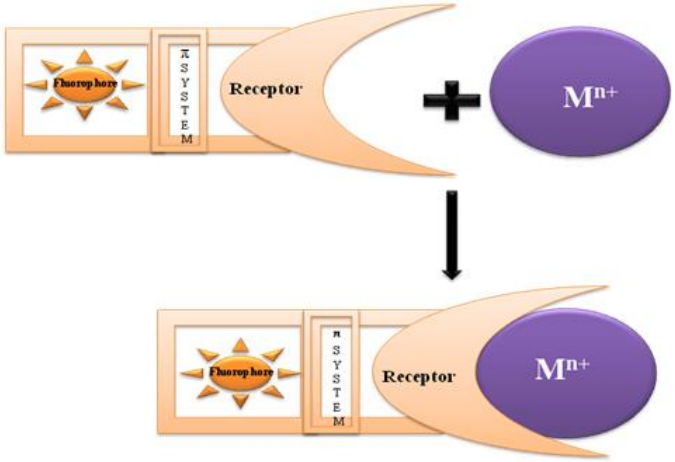

Intrinsic fluorescent probes as metal ion sensors

Fig. 1.26

This is achieved by connecting electron donating and electron accepting fragments by butadienyl, stilbenyl or phenyl groups. It can also be framed as donor-acceptor-donor type of system.

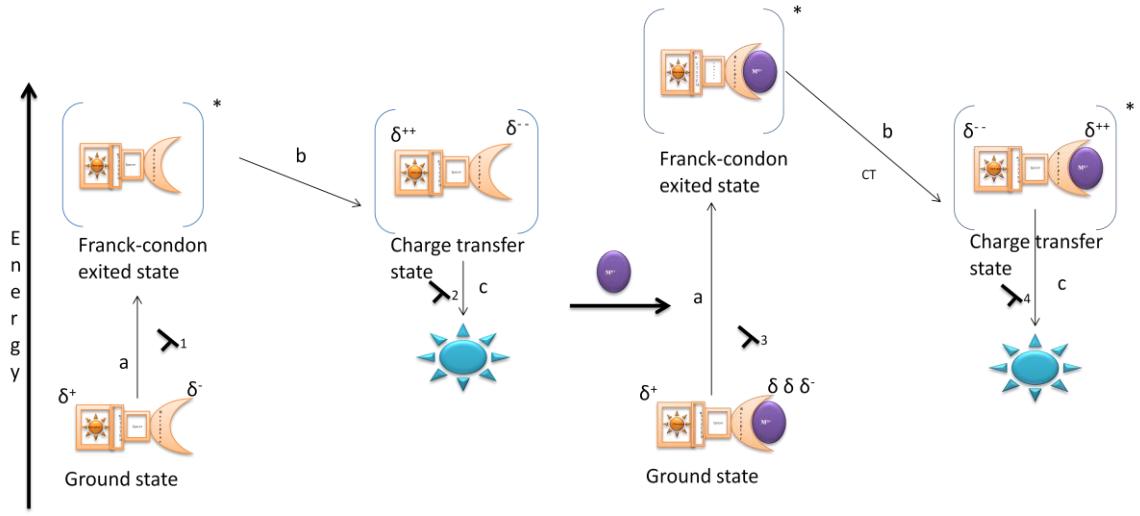

The mechanism of fluorescence sensing

Fig. 1.27

When donor-π-acceptor type of probe is excited at a particular wave length it goes to Frank-Condon excited state which undergoes charge transfer from donor to acceptor subunit of the probe. In charge transfer state as charge density separation increases, the dipole moment increases and emission takes place at higher wavelength. Now when metal binding takes place, the receptor uses its electrons in binding with the metal ion and hence its delta negativity and electron donating capacity decreases. This leads to a blue shift in absorption spectrum of the complex as compared to that of the unbound probe. When such complex is to be excited to Frank Condon state, higher energy is required.

After excitation, charge transfer process still proceeds which make the donor like a radical cation. As this donor site is bound to a metal ion an electrostatic repulsion takes place which weakens the coordinative bond, resulting in a very little blue shift observed in emission spectrum as compared to the unbound probe.

When there is a large energy gap between Frank Condon excited state and charge transfer state, the rapid and quantitative population of the weakly emissive charge transfer state is achieved. Here energy level position of charge transfer state is still lower than the other available non-emissive states, and thus the conversion from Frank Condon excited state to charge transfer state still dominates. This is reflected in the emission spectrum where very little shift is observed. As a result, all complexes of such donor acceptor probes are highly fluorescent than the free probes.

If the donor-acceptor probe is designed in such a way that different energy states are very close to one another, than complexation promotes fluorescence quenching due to reduction in charge transfer characteristic of probe after complexation. Here energy level of charge transfer state is raised, which results in conversion from Frank Condon excited state to other lower energy non radiative states. This results in fluorescence quenching. Examples of such probes are shown in Fig. 1.28:[26,27]

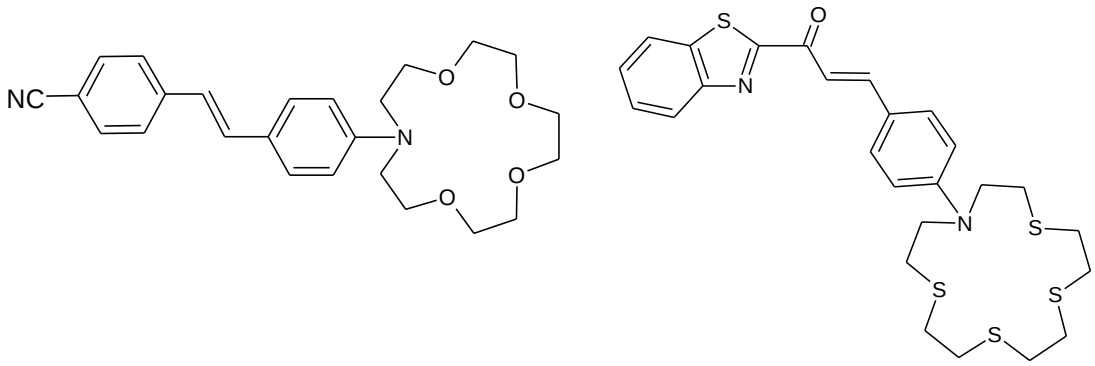

Azacorwn based intrinsic fluorescent probes

Fig. 1.28

3. Composite fluorophore-spacer-receptor systems:

Here ligand and fulorophore are electronically decoupled by a spacer.

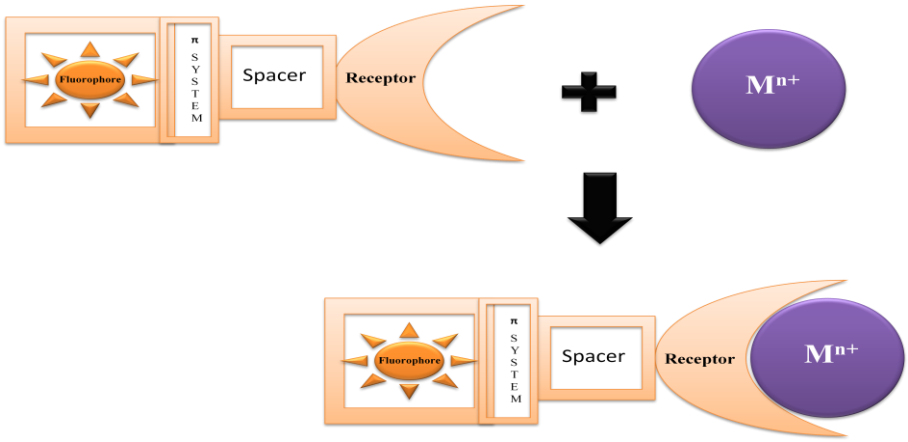

Composite fluorophore-spacer-receptor system as metal ion sensor
Fig. 1.29

In most of the fluorophore-spacer-receptor systems highest occupied molecular orbital (HOMO) of receptor has energy in-between that of HOMO and LUMO of excited fluorophore. When excitation of electron from HOMO of such a probe takes place to its LUMO, simultaneous electron transfer takes place from free receptor to HOMO of the excited fluorophore. This results in fluorescence quenching. When complexation is achieved, loan pair of the receptor is bound with the cation, which prevents photo induced electron transfer to HOMO of the excited fluorophore. This allows electron from LUMO of the excited fluorophore to come to its HOMO followed by fluorescence enhancement (Fig. 1.30). Such probes are generally used as switch-ON type fluorescence sensors.

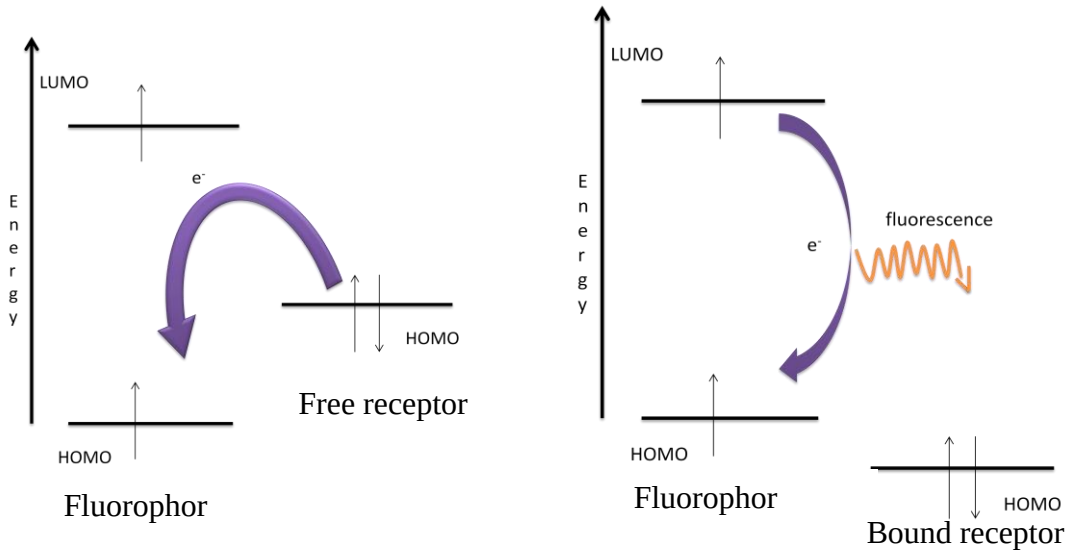

Photoinduced electron transfer

Inhibition of photoinduced electron transfer (PET) after complexation

Fig. 1.30

Examples of fluorophor-spacer-receptor systems are shown in Fig. 1.31.[28,29]

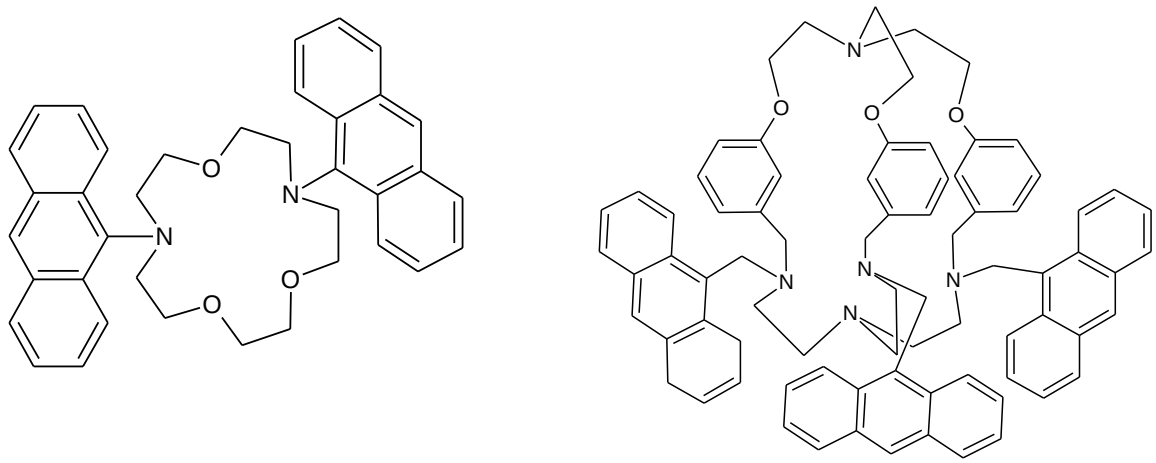

Fluorophore-spacer-receptor type of ligands

Fig. 1.31

4. Exciplex or excimer forming probes:

Here binding and signalling units can form an intramolecular exciplex or excimer and encapsulation of the metal ions causes strong conformational changes which result in increasing or decreasing ratio of excimer-to-monomer emission. (Fig. 1.32)

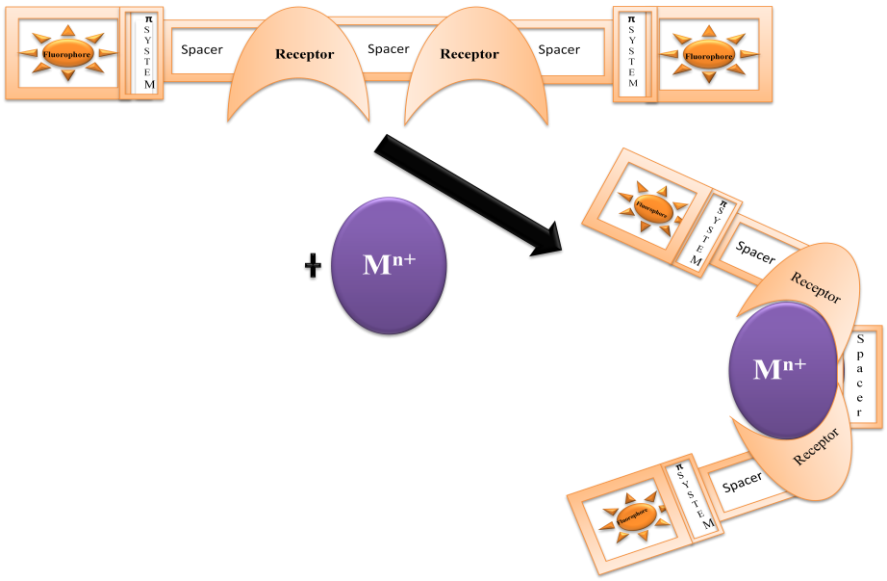

Design of excimer forming probes

Fig. 1.32

Exciplex or excimer forming probes are designed in such a way that their geometrical arrangement gets changed on cation binding which results in fluorescence enhancement or quenching.

When one or two fluorophores are attached to cyclic or acyclic receptor via short alkyl spacers, they prevent PET in excited state after complexation as well as adopt particular geometrical conformation which results in excited state photo physical processes like intramolecular excimer or exciplex formation. Due to this phenomenon a new red shifted band in emission spectrum is observed due to charge transfer interactions in polar solvents. These are capable of switch-on the fluorescence after complexation.

Reverse is possible when geometry of the probe is such that in unbound state they form excimer or exciplex, but cation binding changes the geometry and prevents excimer or exciplex emission.

Examples of exciplex or excimer forming probes[30,31] are shown in **Figure 1.33**.

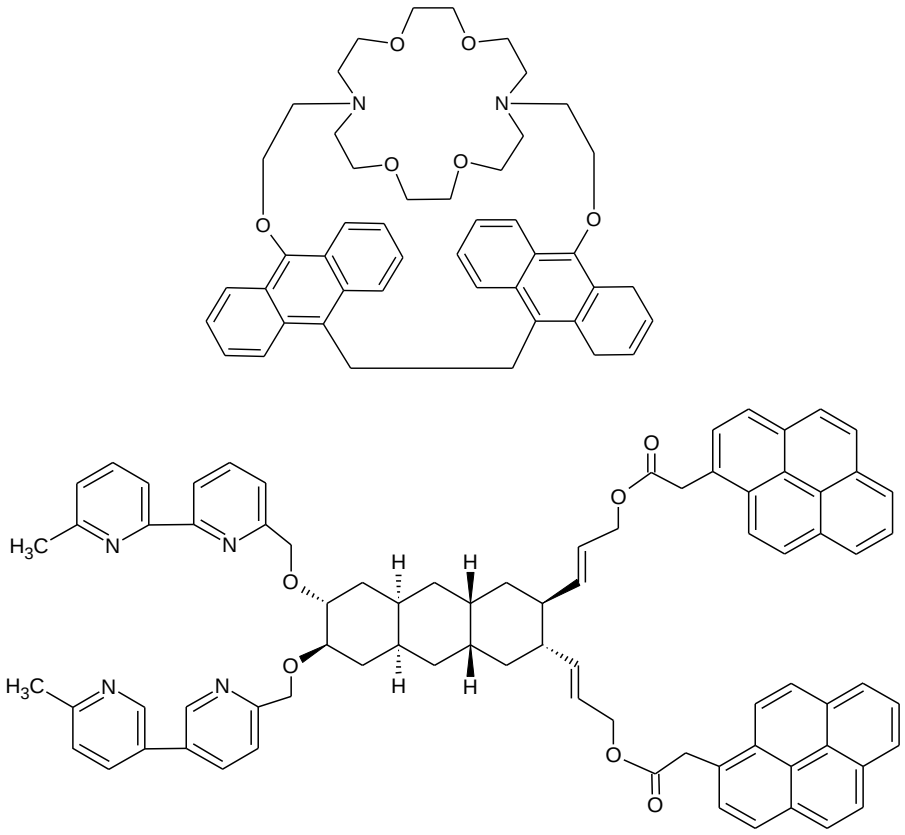

Fluorescent receptors with anthracenyl and pyrene fluorophore
Fig. 1.33

5. Chemodosimeter:

Weakly fluorescent probe reacts with redox active metal ions which greatly enhances its fluorescent activity. (Fig. 1.34)

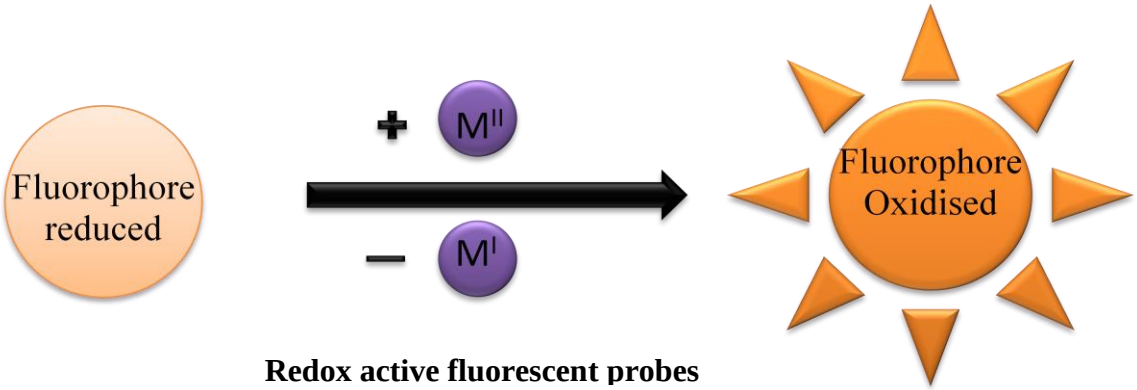

Redox active fluorescent probes

Fig. 1.34

Here a receptor which itself is non-fluorescent reacts with a metal ion to yield a fluorescent product and acts as switch-ON type fluorescent chemosensor. Selectivity amongst different metal ion depends on specificity of a reaction employed. The extent of fluorescence enhancement depends on reaction yield. Supramolecular hosts not only detect ions but are also used as molecular sensors.

1.9.2 Molecular Sensors

Explosives like trinitrotoluene (TNT) do need to be detected at ppm or ppb levels due to security reasons as well as due to environmental concerns. The macrocyclic host (Fig. 1.35) is found to bind 2,4-DNT and TNT molecules in its cavity. The films of different thickness were made by surface casting method based on the micrometric nanofibres of the macrocycle. These films show intense fluorescence which is immediately quenched on exposure to saturated TNT or 2,4-DNT vapours. The fluorescence can be slowly recovered on arial exposure or it can be immediately recovered on exposure to hydrazine vapours.[32]

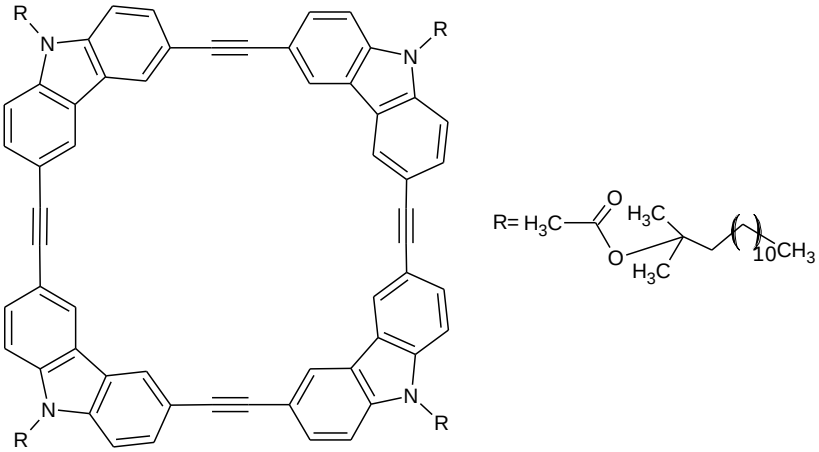

Fluorescencce sensor for 2,6-DNT and TNT
Fig. 1.35

Another fluorescence sensor for TNB and TNT is pyrene derivative of amidocalix[4]arene-[15]crown-5. (Fig. 1.36) It gives two emission bands at 375 nm and 450 nm when excited at 343nm. TNB and TNT quench the fluorescence significantly while moderate quenching is observed with 2,6-DNT or 1,3-DNB with detection limit of 1ppb. It can also colorimetrically detect TNT and TNB. $CHCl_3$ solution of host gives intense bands at 320-360nm interval due to pyrene functionality. The host solution in chloroform appears colourless but turns yellow on addition of TNT and turns reddish orange on addition of TNB.[33]

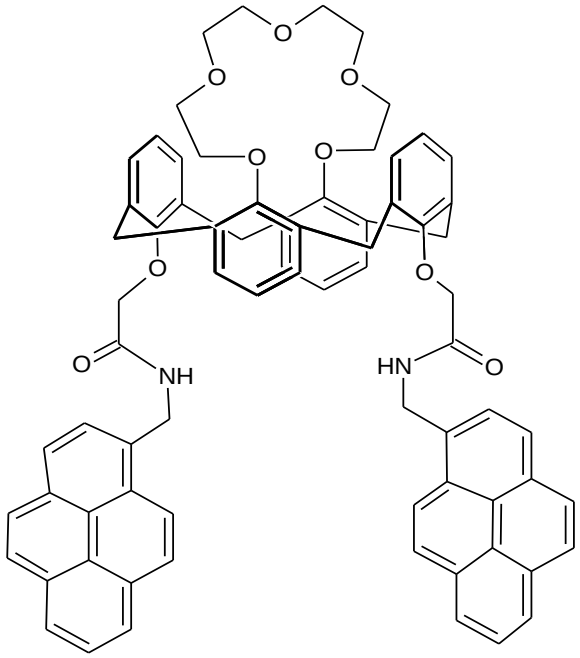

Pyrene based hybrid fluorescent probe for TNB and TNT sensing
Fig. 1.36

1.9.3 Stabilization of reactive intermediates:

Supramolecular structures are also known for stabilization of reactive intermediates. The molecules like benzyne, cyclobutadiene etc. are extremely reactive and thus do not survive under normal reaction conditions. They can be formed and trapped within the interiors of macrocyclic cages where they are not affected by bulk reactants (Figure 1.37). This provides an opportunity for their complete characterization.[34]

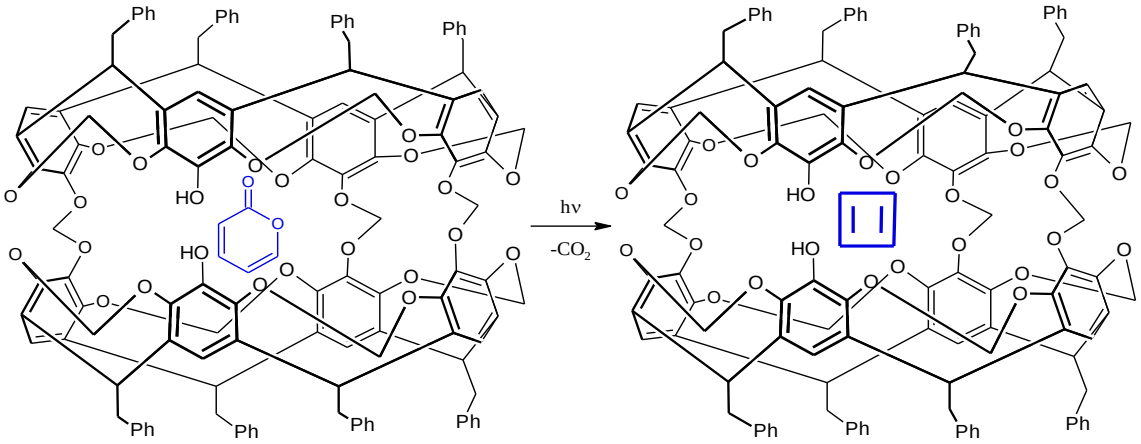

Stabilization of cyclobutadiene in carceplex cavity

Fig. 1.37

1.9.4 Nano reaction chamber:

Benzocyclobutenedione was encapsulated within the hemicarcerand by heating empty hemicarcerand in molten benzocyclobutenedione. Subsequent photolysis of the encapsulated guest converted it to benzocyclopropenone which on irradiation at 77K was converted it to benzyne.[35] (Fig. 1.38) The hemicarcerand not only stabilizes benzyne in the cavity but also undergoes Diels-Alder reaction with it at ambient temperature. This reveals that the macrocyclic cavity not only acts as a container but also transforms the encapsulated guest.[36]

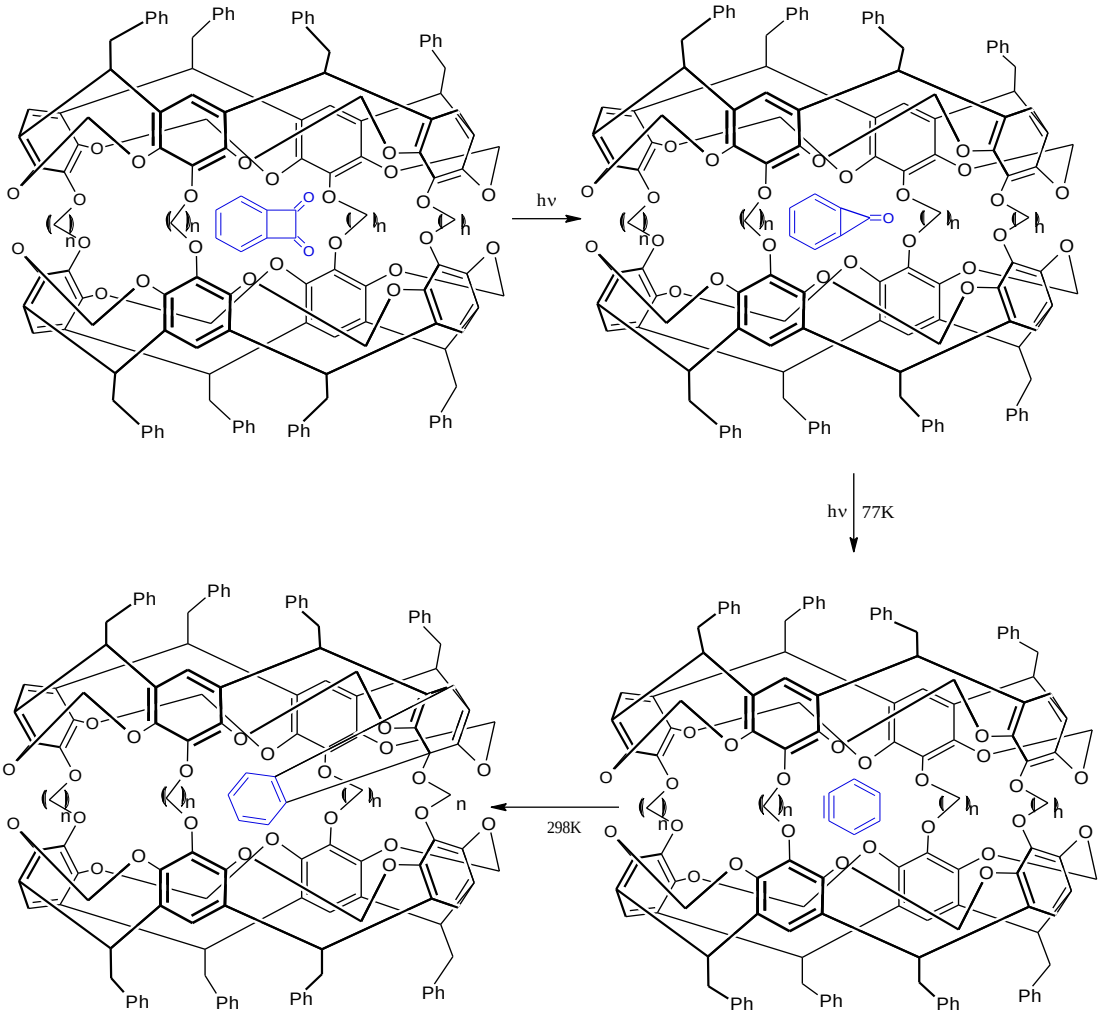

Generation of benzyne within the isolated interior of hemicarceplex

Fig. 1.38

The other most versatile hosts known for supporting the reactions to undergo in its cavity without influence of the solution environment are cyclodextrins (CDs). Imidazole derivatized β-CD encapsulated and efficiently hydrolysed the phosphodiester 120 times faster as compared to the hydrolysis of the phosphodiester in the NaOH solution without β-CD. The reaction inside the cavity of β-CD also resulted in 99% selectivity for one of the two possible products (Fig. 1.39).[37-38]

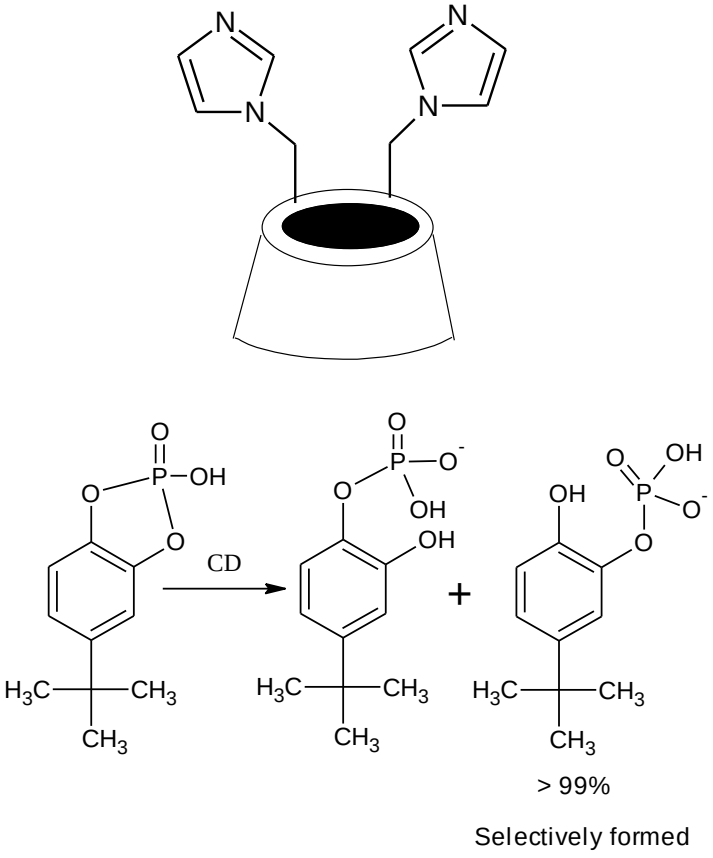

Highly selective hydrolysis of phosphodiester within the cavity of β-CD

Fig. 1.39

Similar to the covalently bonded macrocyclic hosts, the host which are stabilized by non-covalent interactions like hydrogen bonding also provide an isolated interior to the encapsulated guests for their reactions. The hydrogen bonded resorcarene capsule encapsulated phenyl acetylene and phenyl azide molecules which underwent 1,3-dipolar cycloaddition reaction with efficient rate enhancement.[39-40]

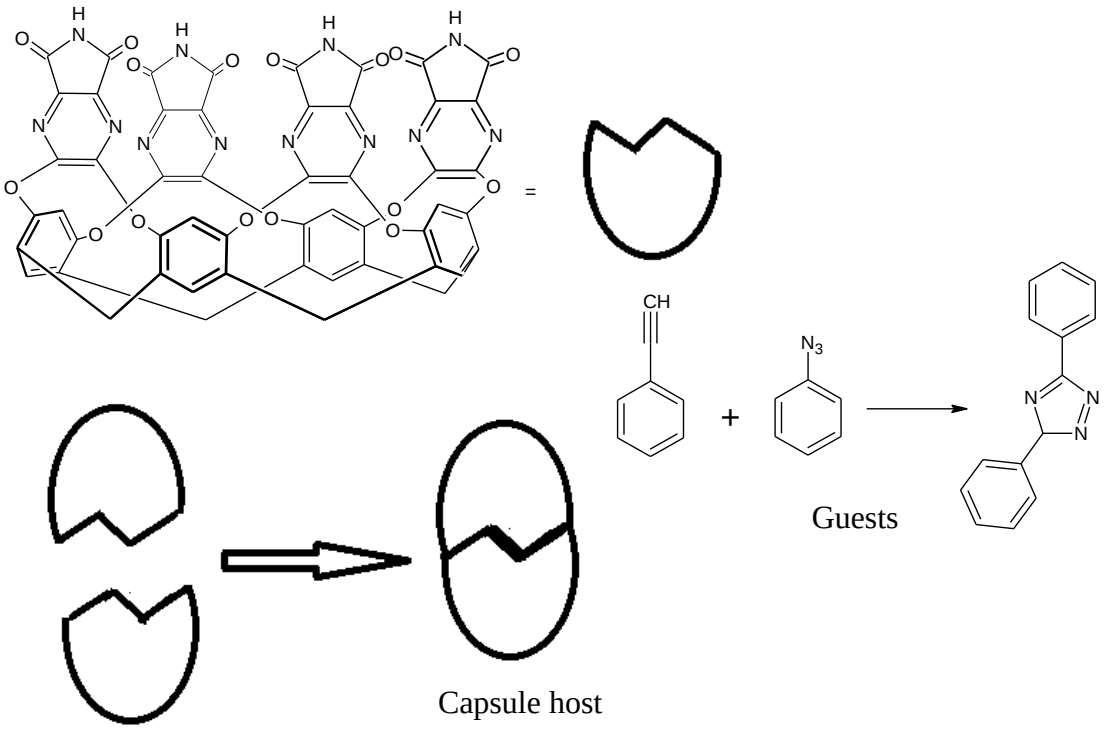

1,3-dipolar cycloaddition reaction within the resorcarene capsule

Fig. 1.40

1.9 References:

1. Fcrsht, A. R. *Trends Biochem. Sci.,* **1987***,* 12, 3.

2. See the Nobel Prize in Physiology or Medicine 2013, at *http://www.nobelprize.org*

3. The image has been taken from the website *Creativecommons.org.*

4. Steed, J. W.; Atwood, J. L. *Supramolecular Chemistry*., John Wiley & Sons, Ltd. **2002**.

5. Lehn, J. M. *Supramolecular Chemistry concepts and perspectives, VCH* **1995.**

6. Jasat, A.; Sherman, J.; *Chem. Rev.,* **1999**, 99(4), 931.

7. Amendola, V.; Fabbrizzi, L.; Mangano, C.; Pallavicini, P.; Poggi, A.; Taglietti, A. *Coord. Chem. Rev.,* **2001**, 219, 821.

8. Chang, S. K.; Van Engen, D.; Fan, E.; Hamilton, A. D.; *J. Am. Chem. Soc.*, **1991**, 113, 7640.

9. Peacock, S. C.; Cram, D. J. *J.Chem.Soc. Chem, Comm.,* **1976**, 282**.**

10. Curtis, W. D.;Laidler, D. A.;Stoddart, J. F.; Jones, G. H *J. Chem. Soc. Perkin Trans. 1.*,**1977**, 1756.

11. Naemura, K.; Ueno,K.; Takeuchi, S.; Hirose,K.; Tobe, Y.; Kaneda, T.; Sakata, Y. *J. Chem. Soc. Perkin Trans. 1*,**1996**, 383.

12. Naemura, K.; Ueno,K.; Takeuchi, S.; Hirose,K.; Tobe, Y.; Kaneda, T.; Sakata, Y. *J. Chem. Soc. Perkin Trans. 1*,**1995**, 213.

13. Nagata, H.; Nishi, H.; Kamigauchi, M.; Ishida, T. *Org . Biomol. Chem* ., **2004** , *2* , 3470.

14. Kalsi, P. S.; Kalsi, J. P. *Bioorganic, Bioinorganic and Supramolecular Chemistry,* New Age International Publishers **2007**.

15. Curtis, N.F. *Coord. Chem. Rev.*, **1968**, 3, 3.

16. Avecilla, F.; Bastida, R.; Blas, A.; Fenton, D.; Macias, A.; Rodriguez, A.; Blas, T.; Granda, S.; Suarez, R. *J. Chem. Soc., Dalton Trans*., **1997**, 409.

17. Hargrove, A.; Zhong, Z.; Sessle, J.; Anslyn, E. *New J. Chem.*, **2010**, 34, 348.

18. Thordarson, P. *Chem. Soc. Rev.*, **2011**, 40, 1305.

19. Schalley, C. A. *Analytical Methods in Supramolecular Chemistry*, Wiley-VCH, Weinheim, **2005**.

20. Billo, J. E. *Excel for Chemists: A Comprehensive Guide* John Wiley & Sons **2001**.

21. Bjerrum, J. *Metal-ammine formation in aqueous solution*. P. Haase & Son, Copenhagen, **1941.**

22. For more information see *http:// en.wikipedia.org.*

23. Jeong, Y.; Yoon, J. *Inorg. Chim. Acta*, **2012**, 381, 2.

24. Bazzicalupi, C. *Inorg. Chim. Acta*, **2012**, 381, 162.

25. Rurack, K. *Spectrochimica Acta Part A*, **2001**, 57, 2161.

26. Letard, J. F.; Lapouyade, R.; Rettig, W.; *Pure Appl.Chem*., **1993,** 65, 1705.

27. Rurack, K.; Bricks, J. L.; Reck, G.; Radeglia, R.; Resch-Genger, U. *J. Phys. Chem. A*, **2000**, 104, 3087.

28. Al Shihadeh, Y.; Benito, A.; Lloris, J. M.; Martinez-Manez, R.; Pardo, T.; Soto, J.; Marcos, M. D. *J. Chem. Soc. Dalton Trans*., **2000**, 1199.

29. Ghosh, P.; Bharadwaj, P. K.; Mandal, S.; Ghosh, S. *J. Am. Chem. Soc.*, **1996**, 118, 1553.

30. Desvergne, J. P.; Lauret, J.; Bouas-Laurent, H.; Marsau, P.; Lahrahar, N.; Andrianatoandro, H.; Cotrait, M. *Recl. Trav. Chim. Pays-Bas*, **1995**, 114, 504.

31. Krauss, R.; Weinig, H. G.; Seydack, M.; Bendig, J.; Koert, U. *Angew. Chem. Int. Ed*., **2000**, 39, 1835.

32. Naddo, T.; Che, Y.; Zhang, W.; Balakrishnan, K.; Yang, X.; Yen, M.; Zhao, J.; Moore, J. S.; Zang, L. *J. Am. Chem. Soc.*, **2007**, 129, 6978.

33. Lee, Y. N.; Liu, H.; Lee, J. Y.; Kim, S. H.; Kim, S. K.; Sessler J. L.; Kim, Y.; Kim, J. S. *Chem. Eur. J*., **2010**, 16, 5895.

34. Cram, D. J.; Tanner, M. E.; Thomas, R., *Angew Chem. Int. Ed*., **1991**, 30, 1024.

35. Warmuth, R. *J. Chem. Soc., Chem. Commun*., **1998**, 59.

36. Warmuth, R. *Angew Chem. Int. Ed*., **1997**, 1347.

37. Breslow, R.; Schmuck, C. *J. Am. Chem. Soc.,* **1996**, 118, 6601.

38. Breslow, R.; Anslyn, E. *J. Am. Chem. Soc.*, **1989**, 111, 8931.

39. Heinz, T.; Rudkevich, D. M.; Rebek, J. Jr. *Nature*, **1998**, 394, 764.

40. Chen, J.; Rebek, J. Jr., *Org. Lett*., **2002**, 4, 327.

Chapter 2

Synthesis of Methylene-bis-aldehydes as Linkers for Construction of Macrocyclic Structures

2.1 Introduction

The compounds containing formyl group are very useful in organic synthesis because of their reactivity and diverse products they form. The compounds containing two of this functionality embedded in a molecule can be used as a monomer in polymerization or as a linker in a condusive environment for construction of supermolecules such as cage compounds. Single ring containing two aldehydes e.g. phthalaldehyde, isophthalaldehyde, terephthalaldehyde, pyridine-2,6-dicarbaldehyde, pyrrole-2,5-dicarbaldehyde, furan-2,5-dicarbaldehyde, thiophene-2,5-dicarbaldehyde have been employed as linkers in syntheses of supermolecules.[1-5]

Rather than employing the compounds containing two formyl groups on same aromatic or hetero-aromatic ring, we looked for the use of methylene linked mono aldehydes as bifunctional linkers for the synthesis of supramolecular structures in context with earlier work reported from our laboratory employing methylene-bis-salicylaldehyde as a linker.[6] The synthesis of 5,5'-methylene-bis-salicylaldehyde from salicylaldehyde and formaldehyde is an example of useful reaction for converting a monoformyl compound to diformyl substrate with an additional ortho functionality present. Methylene-bis-salicylaldehyde has been used for the synthesis of binucleating ligands for the preparation of metal complexes.[7]

These methylene-bis-aldehydes have also been employed as monomers for the synthesis of low cost resins[8]. On reaction with aromatic amines and thioacid they result in antimicrobial and nematicidal agents[8-14] Methylene-bis-salicylaldehydes themselves exhibit tyrosinase inhibitory activity in which the conversion of L-tyorsine to L-DOPA and subsequently to melanine is inhibited.[15]

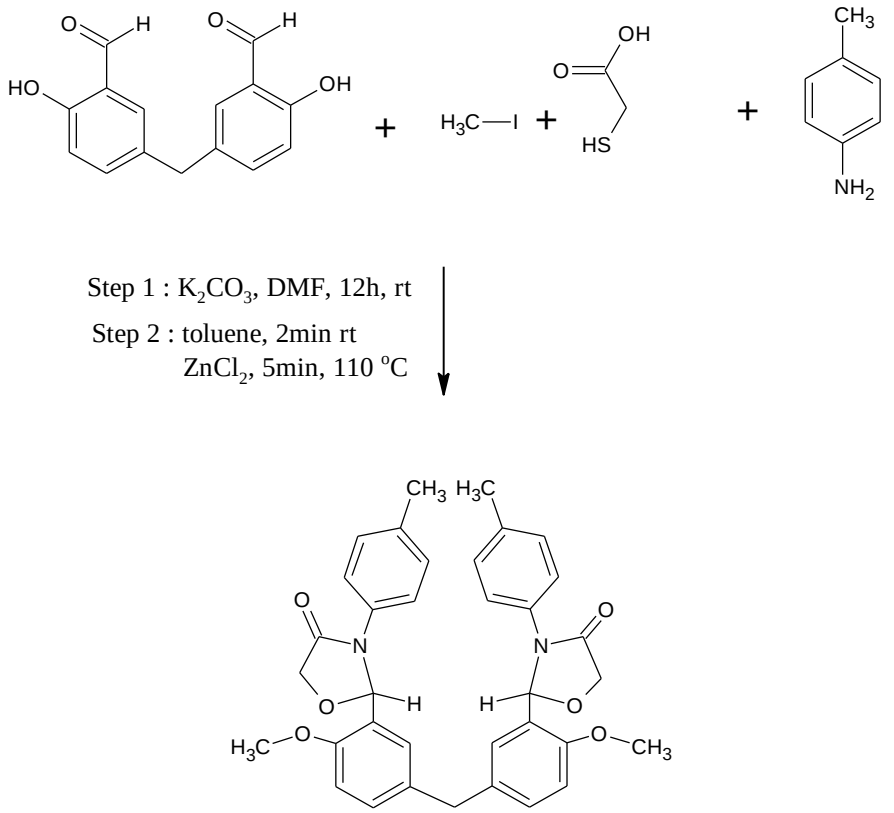

Scheme 2.1 : Synthesis nematicidal compounds from methylene-bis-salicylaldehyde

Formyl group in aromatic ring can be introduced by various well known methods including some famous name reactions.

➢ The Reimer Tiemann reaction.[16-18]

The Reimer Tiemann reaction is used in the synthesis of 2-hydroxyaldehydes for example, when phenol is subjected to Reimer-Tiemann reaction, it gives salicylaldehyde and 4-hydroxybenzaldehyde in 37% and 9% respectively.

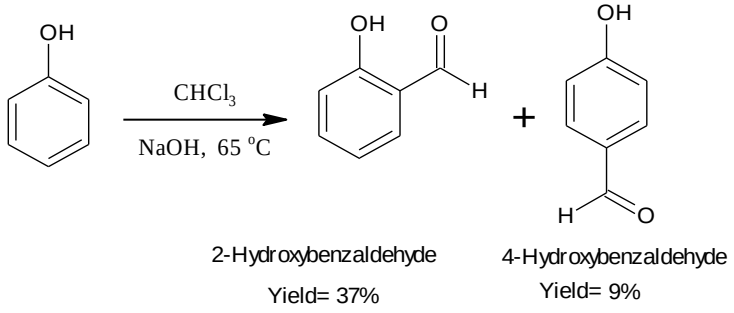

Scheme 2.2: Synthesis of hydroxybenzaldehydes

➢ The Vilsmeier Haack reaction.

The Vilsmeier Haack reaction is extensively used for synthesis of aromatic aldehydes of activated or conjugated system.[19,20] The Vilsmeier reagent has also been extensively employed for the synthesis of a variety of heterocyclic compounds often with a formyl group.[21-23]

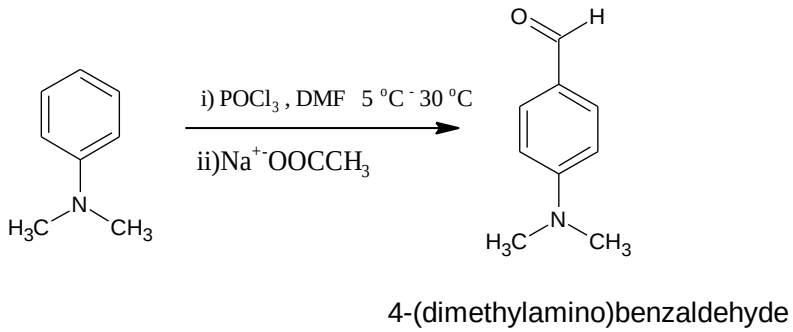

Scheme 2.3 : Synthesis of 4-N,N-dimethylaminobenzaldehyde

Formylation using $SnCl_4$ and paraformaldehyde:

2-Hydroxybenzaldehydes can also be prepared by the use of $SnCl_4$ as an acid catalyst and tributylamine in nonpolar solvent like toluene by using para-formaldehyde as a formylating agent in good yields[24-27]

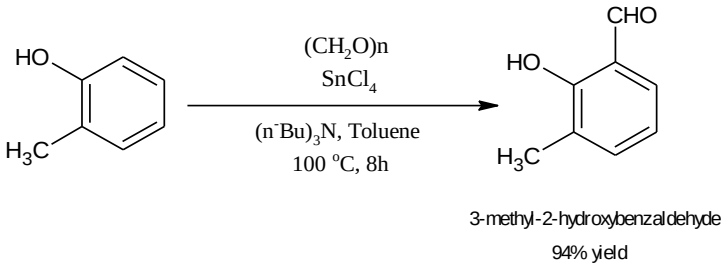

Scheme 2.4 : Synthesis of 3-methyl-2-hydroxybenzaldehyde.

➢ The Skattebol reaction

A highly regeoselective ortho formylation of substituted phenols has been reported by Skettebol and co-workers by using $MgCl_2$ beads, instead of $SnCl_4$ in high yields.[28-30] The limiting factor here is high cost of $MgCl_2$ beads.

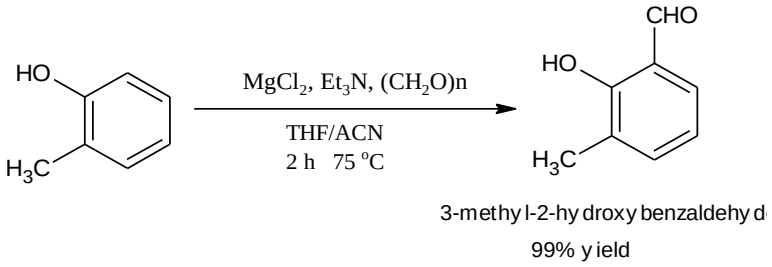

Scheme 2.5 : Synthesis of 3-methyl-2-hydroxybenzaldehyde

Synthesis of this bis-salicylaldehyde involves the use of 1,3,5-trioxane as a source of formaldehyde in presence of catalytic amount of conc. H_2SO_4 in gl. CH_3COOH as a solvent.[31] (Scheme: 2.6) We also looked for some more methylene-bis-aromatic aldehydes which can be used similarly as linkers for the synthesis of new supramolecular compounds.

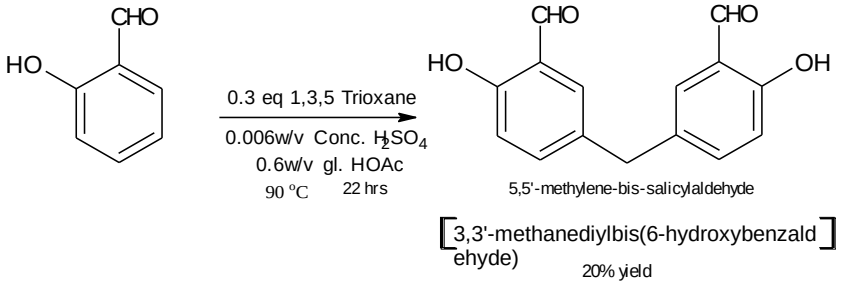

Scheme 2.6: Synthesis of 5,5'-methylene-bis-salicylaldehdye

Di-formylation of 4,4'-methylene-bis-2-substituted phenols converts them into 5,5'-methylene-bis-3-substituted aldehydes using the duff reaction.[32]

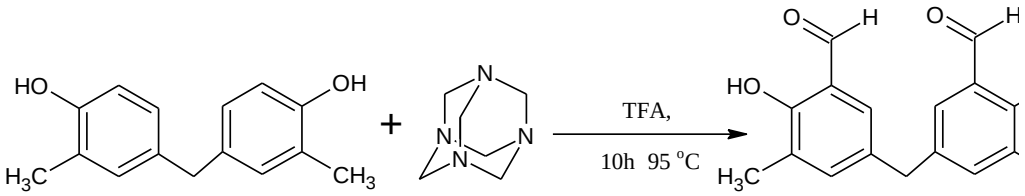

Scheme 2.7: Diformylation of bis phenols.

2.2 Aim and Objectives

In view of usefulness of di-aldehydes in the synthesis of various macrocyclic compounds, as stated earlier, we planned to synthesize methylene-bis-aromatic aldehydes for their application as linkers for the synthesis of some new supramolecular compounds. We visualised that the flexibility or spacer introduced in this bifunctional aldehydes may be advantageous in the formation of supramolecular structure compare to the di-aldehydes with rigid aromatic ring contining the two reactive functionalities. The major differences between the two are the increased distance between the two formyl groups in methylene-bis-aldehydes compared to the dialdehydes and an angle formed between the two reactive functionalities.

The present chapter encompasses the experiments dealing with the synthesis of some aromatic aldehydes and their application in the synthesis of methylene-bis-aldehydes.

The results of these experiments have been included and discussed in this chapter.

2.3 Results and Discussion

We have synthesized or attempted to synthesize a number of methylene-bis-aldehydes starting from various aromatic and hetero-aromatic aldehydes. 5,5'-Methylene-bis-salicylaldehyde has been synthesized and widely employed for various purposes[1,8-14,33-38] The method employed for the synthesis of methylene-bis-aldehydes was based on the synthesis of bis-salicylaldehyde reported by Marvel and Torkoy in 1957.[31]

Thus we started with the synthesis of the known methylene-bis-salicylaldehyde following the same procedure. The reaction of salicylaldehyde with trioxane in presence of sulphuric acid results in formation of 5,5'-methylene-bis-salicylaldehyde as a major product. (Scheme: 2.8) Due to the presence of the hydroxyl group in salicylaldehyde, the para position to the hydroxyl group is most reactive but at the same time the ortho position is also activated.

We carefully studied the reaction of salicylaldehyde which was reported to give 5,5'-methylene-bis-salicylaldehyde. In this reaction the ratio of H_2SO_4 to gl.CH_3COOH plays an important role. It is also important to adhere to required equivalence of trioxane for getting consistent yields. The reaction temperature was also found to play an important role. At temperature lesser than 90 ^oC the reaction preceded slowly and conversion was incomplete while with the increased temperature, above 100 ^oC resulted in multiple product formation as oligomerization was facilitated at higher temperatures. An increased amount of sulphuric acid also resulted in more polar impurities.

After finding out the best reaction conditions for bridging salicylaldehyde through a methylene carbon the reported product 5,5'-methylene-bis-salicylaldehyde could be obtained on crystallising the crude from acetone. On careful investigation of the filterate obtained from this crystallization, the presence of the other minor compounds was detected as number of spots on TLC. Column chromatography of the residue from the filterate resulted in isolation of two more compounds which have not been reported earlier.

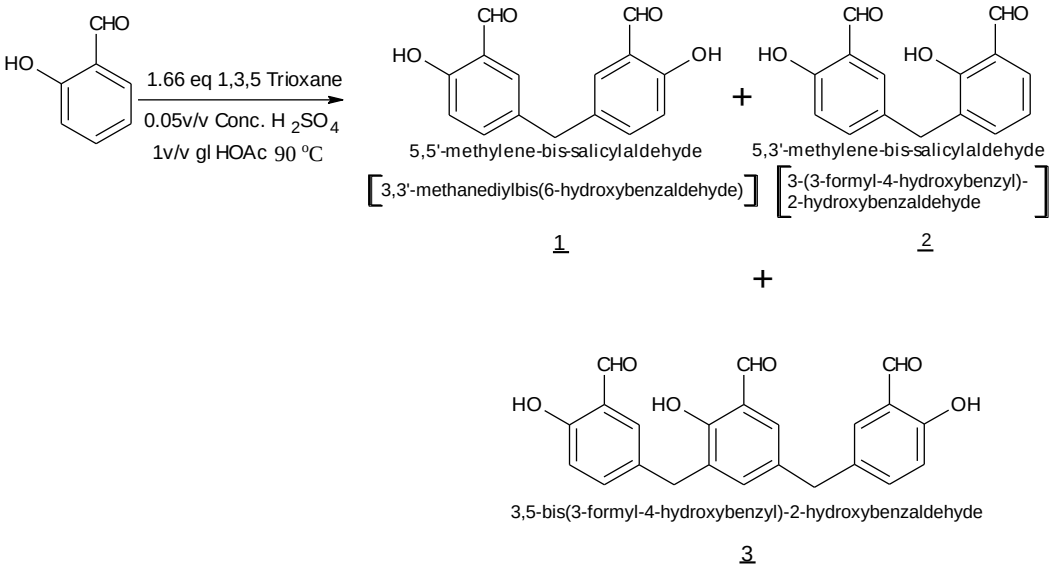

Scheme 2.8: S**ynthesis of 5,5'-methylene-bis-salicyalaldehyde and its derivatives**

One of the minor compounds could be assigned as unsymmetrical structure formed by coupling of two salicylaldehyde molecules at para position to phenolic group and the other via the ortho position of the phenolic group resulting in 5,3'-methylene-bis-salicylaldehyde. The proposed structure was confirmed by presence of two distinct aldehyde signals at 9.92δ and 9.86δ and two different signals corresponding to phenolic groups at 11.36δ and 10.91δ in proton NMR spectroscopy.

Reaching to the structure of the other product just from its NMR, Mass and IR analysis was found to be difficult. Its structure could be realized form the result of single crystal X-ray analysis as the compound was crystalline. It turned out to be interesting combination of the earlier two structure giving rise to coupling of three salicylaldehyde molecules via two methylene bridges with the central ring substituted at both the para and ortho positions available with respect to the phenolic group. Single crystal X-ray analysis was carried out at solid state and the structural chemistry unit IISC Banglore by A. G. Dikundwar from Prof. T. N. Guru Row's research group.

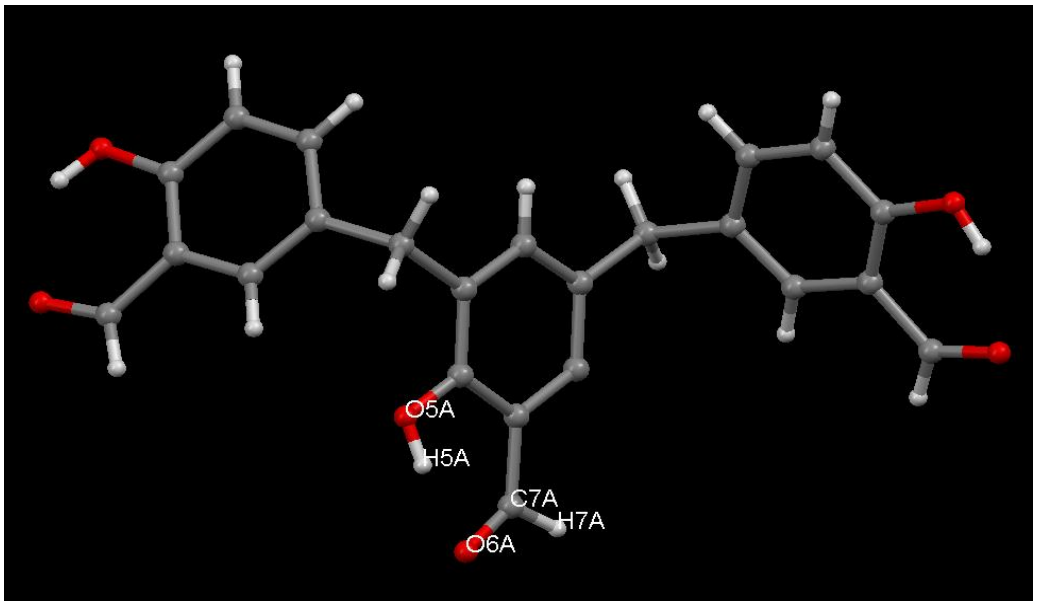

ORTEP diagram of trialdehyde 3

Fig. 2.01

We also carried out coupling of the other oxygen containing aromatic aldehydes such as 4-hydroxy-3-methoxy-benzaldehyde (vanilline) and 2-hydroxy-3-methoxy-benzaldehyde (o-vanilline) to get the corresponding 5,5'-methylene-bis-benzaldehyde derivatives in low yields. [15,40-42] (Scheme: 2.9) While the attempts to couple 3,4-dimethoxy-benzaldehyde (veratraldehyde) were not successful, giving a black solution on addition of sulphuric acid.

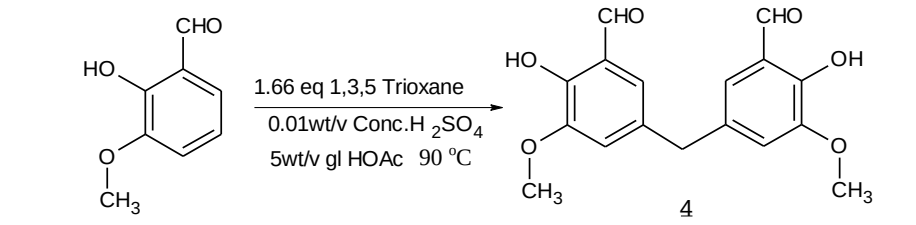

4

3,3'-methanediylbis(6-hydroxy-5-methoxybenzaldehyde)

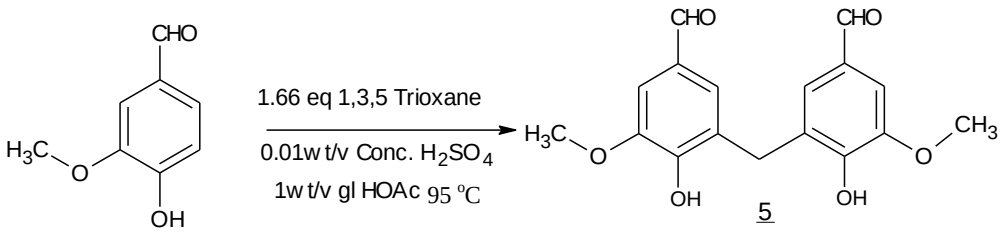

5

3,3'-methanediylbis(4-hydroxy-5-methoxybenzaldehyde)

Scheme 2.9: Synthesis of 5,5'-methylene-bis-o-vanilline and 5,5'-methylene-bis-vanilline

For the synthesis of the other substituted methylene-bis-salicylaldehydes we first targeted at the preparation of alkyl substituted salicylaldehydes. 2-Methylphenol and 2-*tert*-butylphenol were formylated by using para-formaldehyde and catalytic amount of $SnCl_4$ in the presence of a base by using toluene as solvent giving good yields.[24-27] Both the alkylated salicylaldehyde were subjected to the same reaction conditions which were employed for the preparation of 5,5'-methylene-bis-salicylaldehyde. The desired products were isolated and characterized. (Scheme: 2.10)

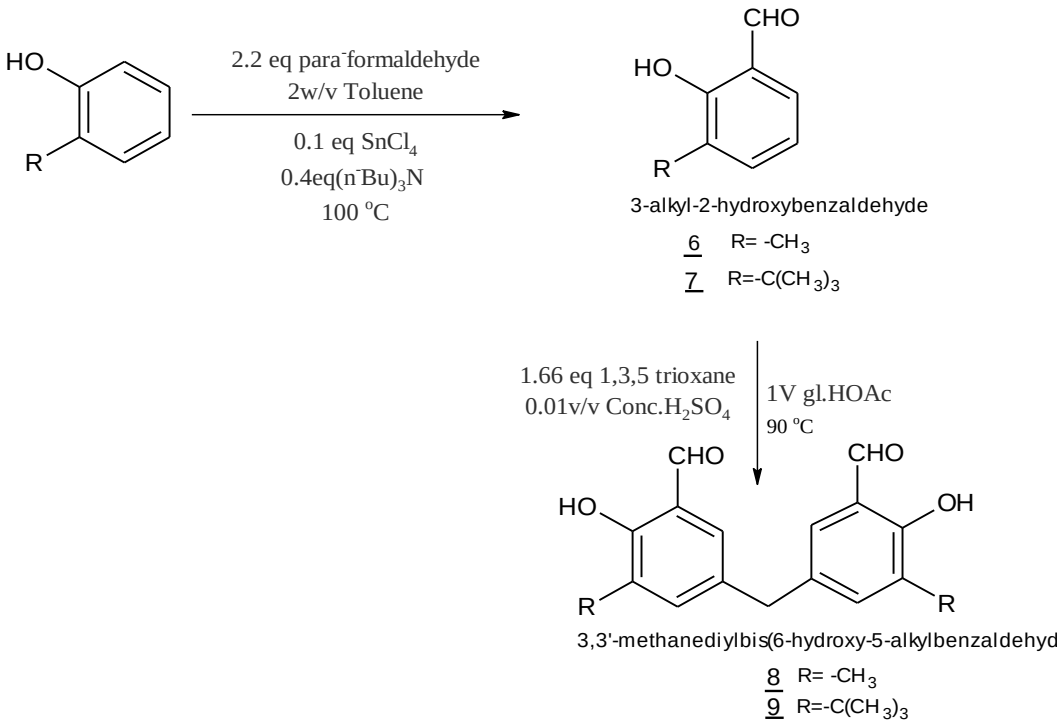

Scheme 2.10: Synthesis of 5,5'-methylene-bis-(3-alkyl-salicylaldehyde)[8,43-47]

2,4-Dihydroxybenzaldehyde is also a good example of activated benzaldehyde derivative which can be subjected to the methylene coupling reaction. The aldehyde was prepared by subjecting resorcinol to the Vilsmeier reaction.[15,23,48] The resulting resorcylaldehyde when subjected to the coupling reaction using trioxane, it was found that reaction proceeds even at lower temperatures compared to the earlier experience. Due to higher reactivity of this aldehyde the reaction gave multiple products at room temperature. Careful and repeated column chromatography resulted in isolation of three major

isomeric products which were characterized by subjecting them to spectral and elemental analyses. They were found to be 5,5'-methylene-bis-2,4-dihydroxybenzaldehyde, 3,3'-methylene-bis-2,4-dihydroxybenzaldehyde and 5,3'-methylene-bis-2,4-dihydroxybenzaldehyde, an unsymmetrical methylene-bis-resorcylaldehyde. (Scheme: 2.11)

In mass spectra the molecular ion peak is observed at m/z = 288 for all of them. (Spectra 3.20, 3.22, 3.25) In proton NMR the unsymmetrical isomer could be differentiated because of two distinct signals for the formyl groups at δ 9.73 and 9.81. (Spectrum 3.24) The symmetrical isomer could be differentiated based on proton NMR analysis. 5,5'-isomer shows two singlets for aromatic protons while 3,3'-isomer shows two doublets with J = 8.4 Hz. (Spectrum 3.19, 3.21) Elemental analysis of these isomers is in accordance with the expected values.

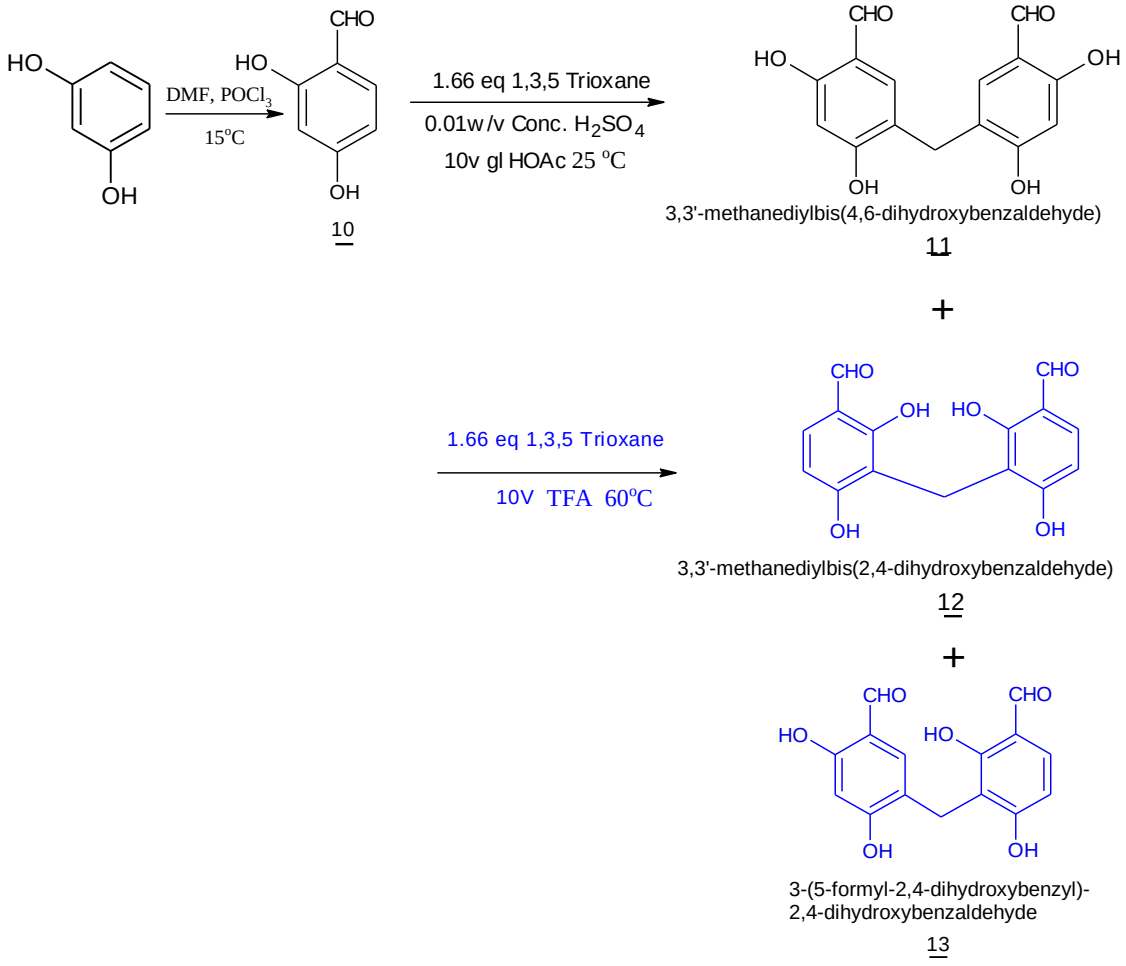

Scheme 2.11: Synthesis of methylene-bis-resorcylaldehydes[15]

It was observed that change in reaction conditions affect relative ratio of these three isomers. The effect of temperature on this reaction was studied in detail. HPLC technique was used to monitor the reactions. The reactions were carried out at 10 ^{o}C, 30 ^{o}C, 60 ^{o}C, 90 ^{o}C and 120 ^{o}C (reflux temperature).

At lower temperature reaction doesn't proceed due to lack of solubility of the β-resorcylaldehyde. The reaction at 30 ^{o}C was found to be most conducive for the synthesis of 5,5'-isomer. The higher temperature reactions gave more of the polar products which could not be isolated and characterized. The effect of the available concentration of trioxane in the reaction mixture was also studied at different temperatures. For this slow addition of trioxane was carried out. It did not help in increasing the yield of the desired 5,5'-isomer.

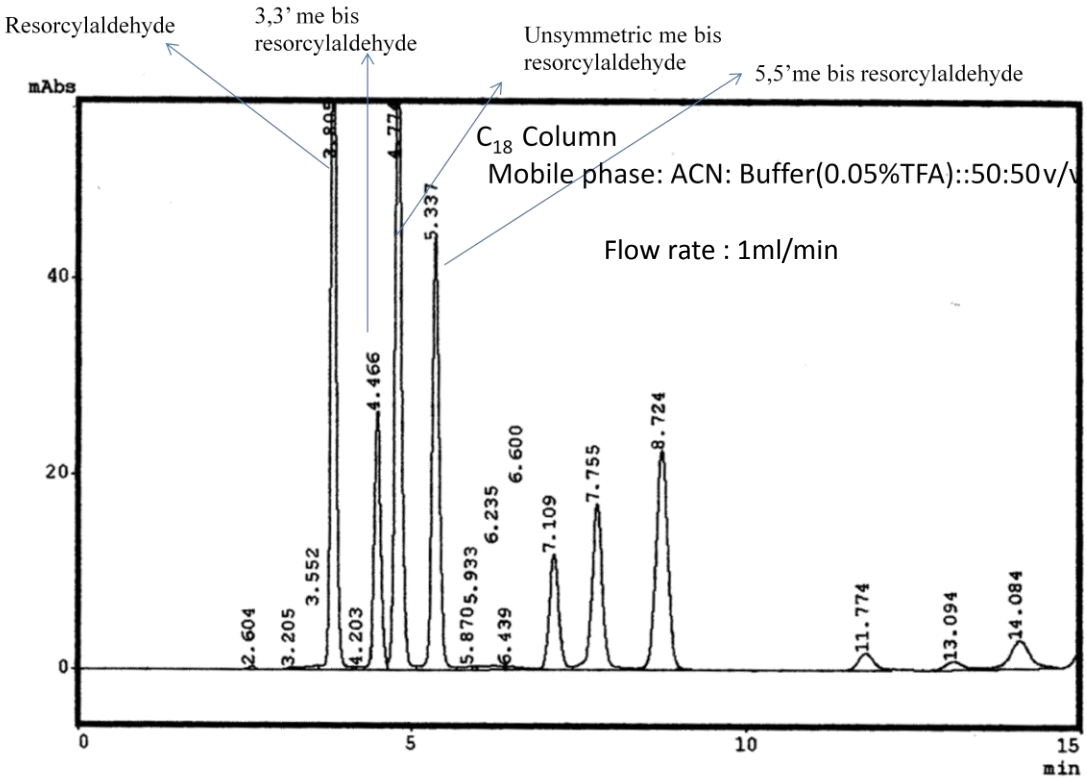

HPLC chromatogram of crude containing mixture of isomeric aldehydes and starting material

Fig: 2.02

2,4-Dihydroxy benzaldehyde being solid, requires a higher quantity of acetic acid to make it soluble because of which the ratio of reactants and catalyst with respect to solvent could not be retained as reported for salicylaldehyde reaction. This led us to an idea of consideration of alternate acid catalyst and solvent. Trifluoroaceticacid (TFA) being a strong organic acid was initially employed only as a catalyst replacing sulphuric acid. While investigating further modifications, the reaction was found to be better when TFA was used as solvent as well as a catalyst, so the reaction was further studied in detail in this medium. The reaction was carried out at lower temperature of 0-5 ^{o}C, at R.T. and at 60 ^{o}C. Resorcylaldehyde having higher solubility in TFA, the reaction at lower temperature was possible but was not satisfactory. The ratio of isomeric products was found to be different at R.T. and at 60 ^{o}C. The higher temperature reaction significantly reduced the generation of 5,5'-isomer. In TFA the 3,3'-isomer was produced in greater amounts compared to that in acetic acid and the 5,5'-isomer was being formed in minor quantities at 60 ^{o}C. It was convenient to separate 3,3'-isomer being the major product from this reaction. Purification of the unsymmetrical isomer on column chromatography could not be achieved. The enriched fractions containing this isomer were subjected to preparative reverse phase HPLC to obtain the unsymmetrical product in pure form.

o-Anisaldehyde, the methyl ether of salicylaldehyde when subjected to the coupling reaction smoothly resulted in 5,5'-methylene-bis-(o-anisaldehyde) giving better yield compared to that of 5,5'-methylene-bis-salicylaldehyde. The product was isolated in similar way by crystallising from acetone. Later on, it was found that crystal packing of this bis-aldehyde has been studied, where the 5,5'-methylene-bis-anisaldehyde were prepared by formylating 4,4'-methylene-bis-anisole using $TiCl_4$ and dichloromethyl methyl ether.[9,10,12,49] (Scheme:2.12)

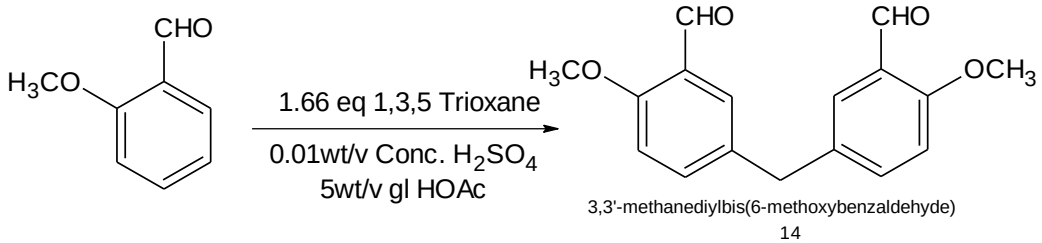

Scheme: 2.12 Synthesis of 5,5'-methylene-bis-o-anisaldehyde

After exploring compounds with phenolic and alkoxy group activated benzaldehydes, we considered an amino group activated benzaldehyde, 4-(N-dimethylamino-benzaldehyde) which also should undergo similar coupling reaction as per our expectation. This kind of coupling on amino-benzaldehydes has not been reported in literature earlier. Thus 4-(N-dimethylaminobenzaldehyde) was subjected to the coupling reaction with 1,3,5-trioxane

in gl. acetic acid in the presence of conc. sulphuric acid which successfully resulted in 3,3'-methylene-bis-(4-dimethylamino-benzaldehyde) as expected though in low yield of 10%. The reaction was found not to go to completion and some of the starting material was recovered (Scheme: 2.13). The newly synthesized compound was characterized with the help of IR, NMR, MASS spectral analysis and elemental analysis. In NMR, the formyl proton is observed at 9.8 δ while the methyl protons give singlet at δ 2.8. Methylene protons are observed at 4.1δ. The aromatic protons are observed at δ 7.71, 7.49, 7.13 with expected splitting and coupling pattern. (Spectrum 3.31)

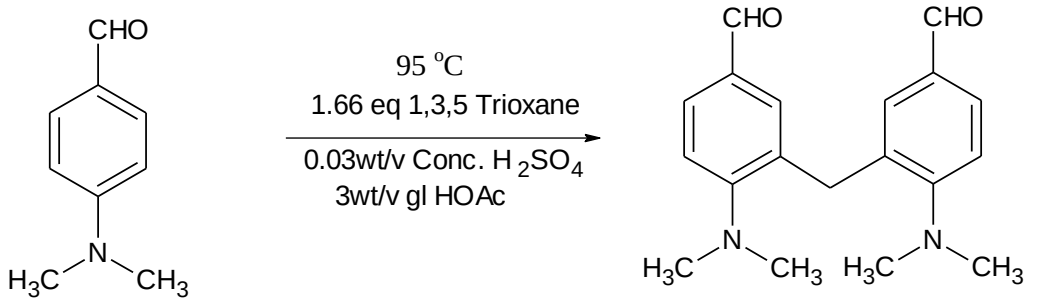

Scheme 2.13: Synthesis of 3,3'-Methylene-bis-(4-N,Ndimethylaminobenzaldehyde)

The bis-aldehyde gave golden yellow crystals form ethanol. The crystals were subjected to single crystal X-ray diffraction analysis at IISc Bangalore with the help of Mr. Amol Dikundwar from Prof. Guru Row's research group. For the Analysis Bruker Kappa Apex2 CCD area detector and Mo-Kα X-ray radiation source were used. The structure refinement was carried out using SHELXL97. The compound was crystallized with the space group R-3. The orientation of formyl groups of same molecule can attain two different arrangements. Both the arrangements were found to be present in the ORTEP diagram of the given molecule Fig. 2.03.

As such there was no conventional hydrogen bonding found between two or more molecules of the given compound but a soft interaction between hydrogen of N-CH_3 group and aldehyde oxygen of the adjacent molecule was observed. 3,3'-Methylene-bis(4-N-dimethylaminobenzaldehyde) molecules were stacked due to π-π interactions between the aromatic rings. Top view of the crystal packing from space fill model shows the propeller shaped packing of the molecules with hexagonal voids have been generated. (Fig. 2.07) The angle formed between the planes of the two aromatic rings connected via methylene bridge is 64.34˙ . The angle formed at the methylene bridge carbon connecting the two aromatic rings (C(6)-C(7)-C(8) angle) is found to be 117.38˙(Fig. 2.03).

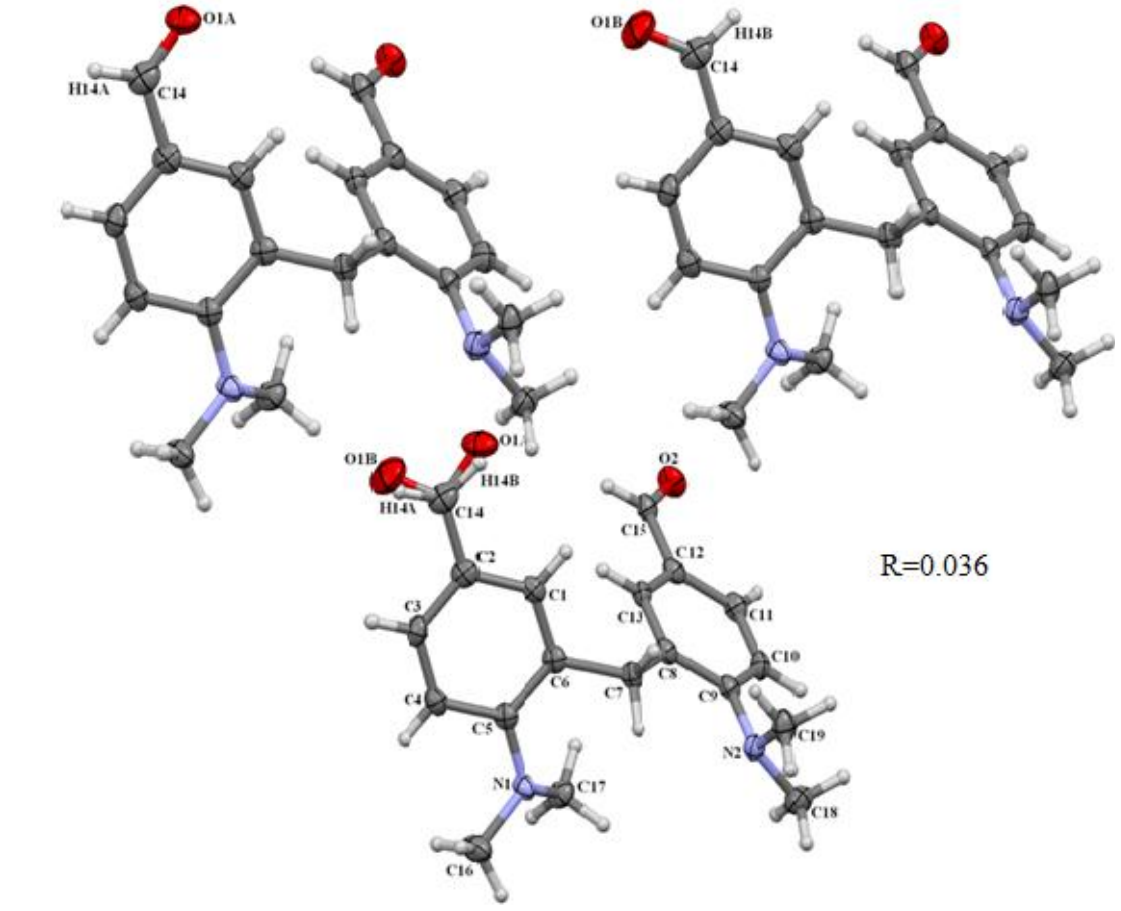

Ortep diagram of 3,3'Methylene-bis-(4-N,N dimethylamino-benzaldehyde)

Fig.2.03

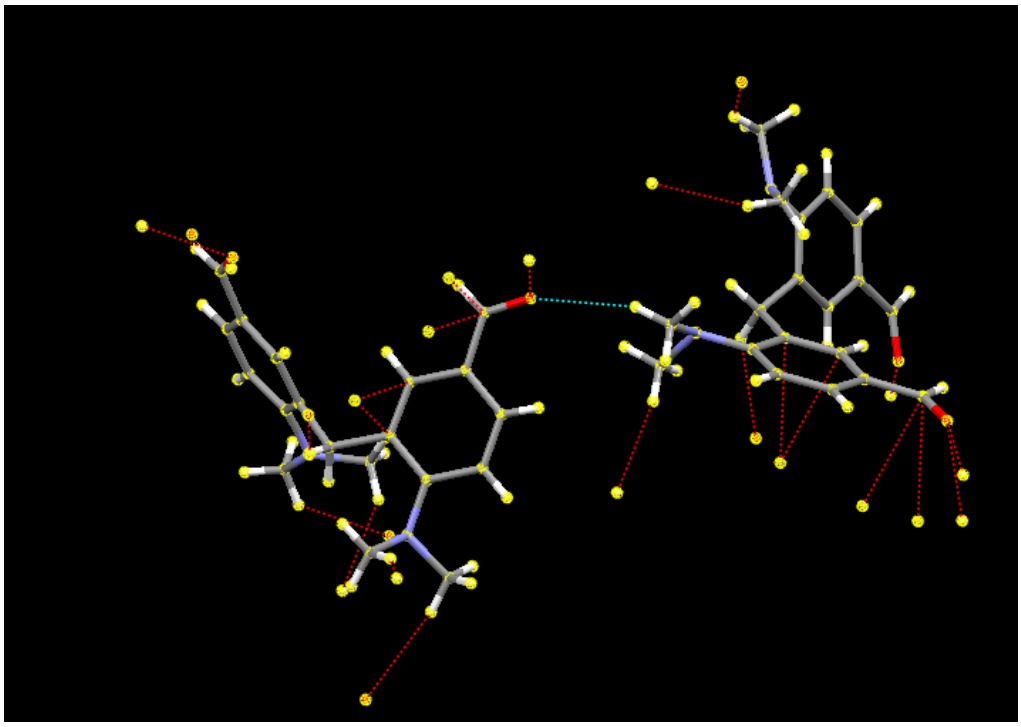

Single crystal X-ray image showing O----H-CH_2N soft Hydrogen bonding of 3,3'-Methylene-bis-(4-N,N dimethylamino-benzaldehyde)

Fig. 2.04

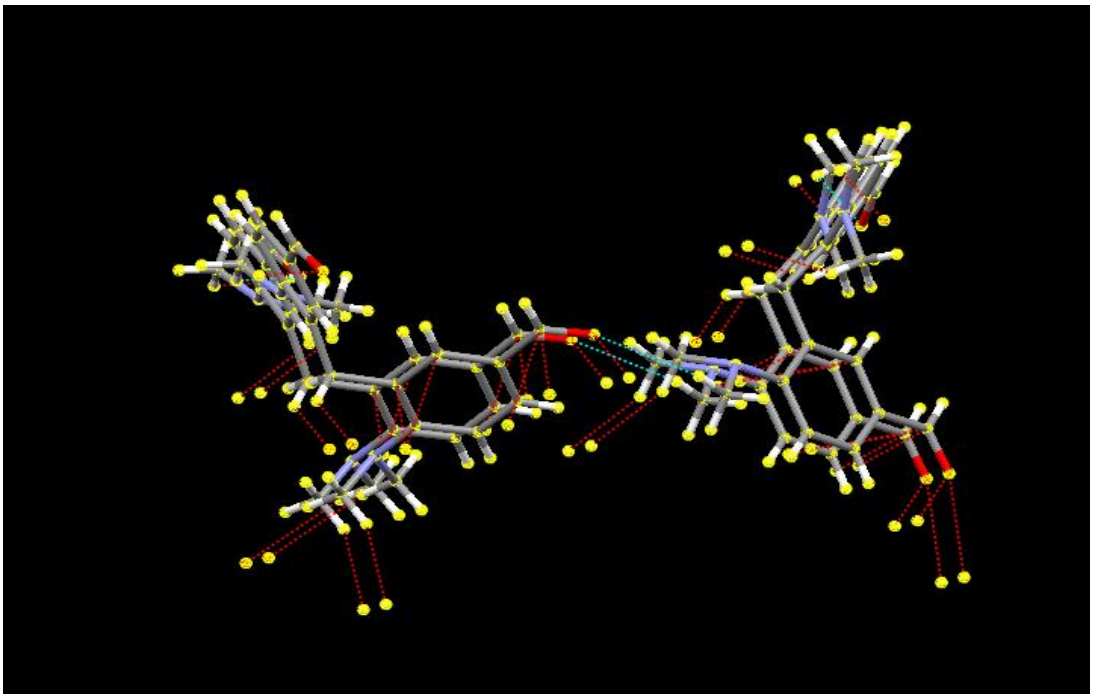

Single crystal X-ray image of 3,3'-Methylene-bis-(4-N,N-dimethylaminobenz-aldehyde) showing π-π stacking.

Fig. 2.05

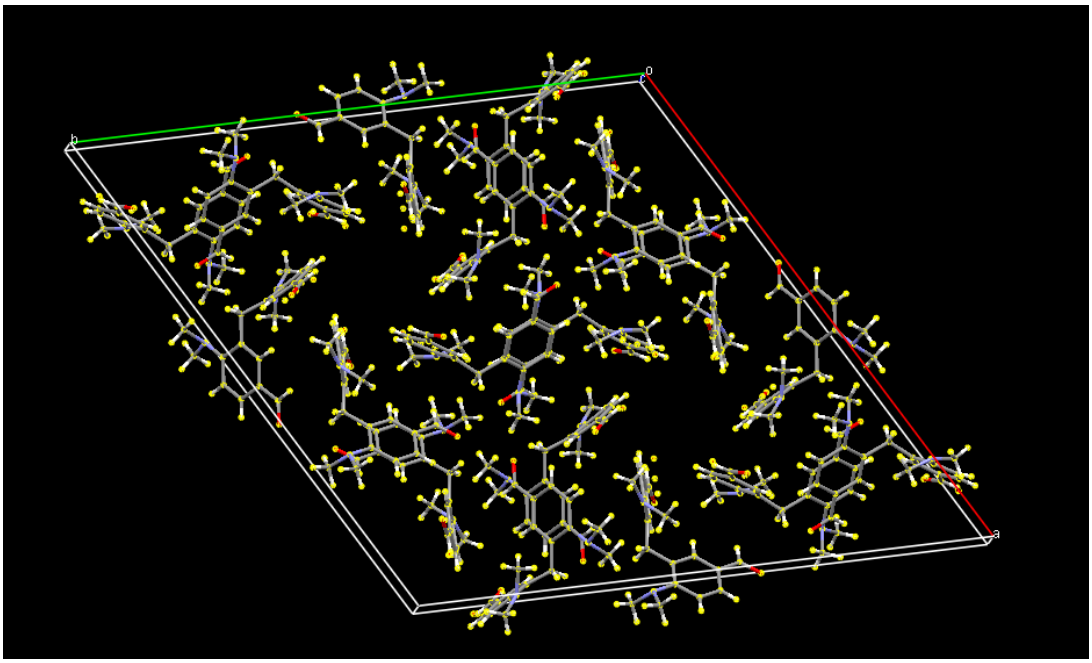

Single crystal X-ray image of 3,3'-Methylene-bis-(4-N,N dimethylamino-benzaldehyde) showing crystal packing pattern.

Fig.2.06

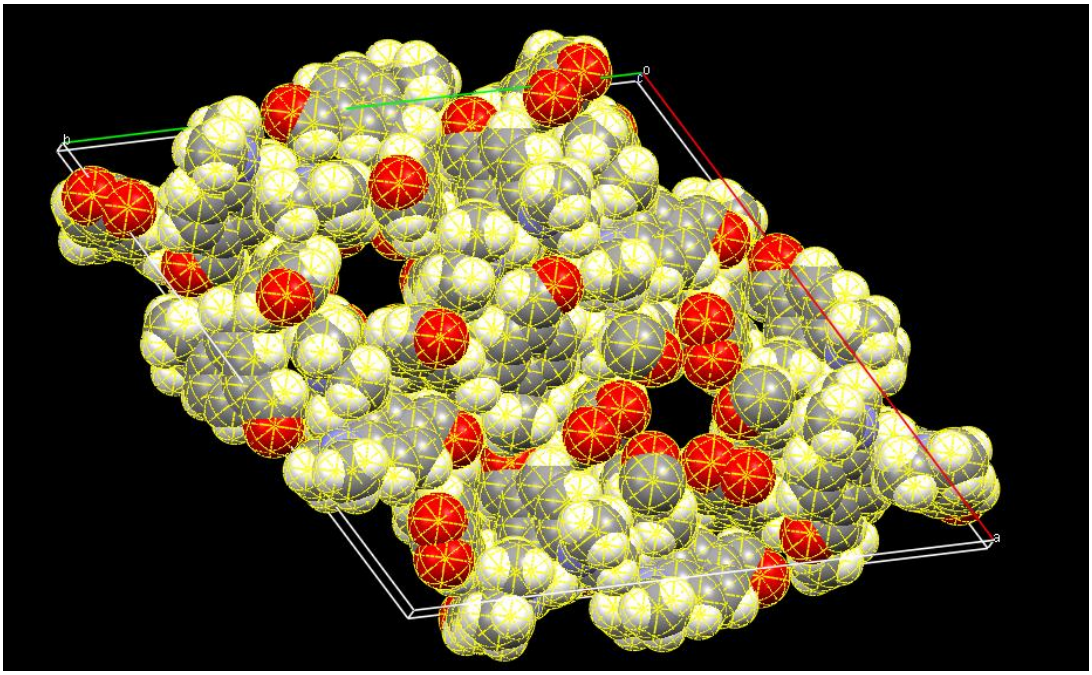

Single crystal X-ray image of 3,3'-Methylene-bis-(4-N,N dimethylamino-benzaldehyde) showing crystal packing pattern in space-fill pattern.

Fig.2.07

Crystal parameters of 3,3'-methylene-bis-(4-N-dimethylaminobenzaldehyde) are listed in the Table No. 1

Table No. 1 Crystal data and structure refinement

1.	Formula	$C_{19}H_{22}N_2O_2$
2.	Formula Weight	310.39
3.	Cell Volume (Å)	7740.9(11)
4.	T(K)	295
5.	Crystal system	Trigonal
6.	Space group	R-3
7.	Z	18
8.	a Å	29.5739(18)
9.	b Å	29.5739(18)
10.	c Å	10.2198(12)
11.	α (°)	90
12.	β (°)	90
13.	γ (°)	120
14.	goodness of fit	1.018
15.	Calculated density($mg/m^{3)}$	1.200
16.	Absorption coefficient (mm^{-1})	0.078
17.	F(000)	2987.5
18.	θ ranges for data collection	2.15-24.99
19.	Index ranges	$-35 \leq h \leq 35$ $-35 \leq k \leq 35$ $-12 \leq l \leq 12$
20.	Reflection collected	3024
21.	R indices	R1=0.0363(2793), wR2=0.0998(3024)

In order to acquire some more linkers in the form of methylene-bis-aromatic-aldehydes we used 5,5'-methylene-bis-salicylaldehyde as a starting material and derivatized the same. Bromination of the bis-aldehyde was carried out in gl. acetic acid at 20 °C with two equivalents of bromine in acetic acid giving 3,3'-dibromo-5,5'-methylene-bis-salicylaldehyde in good yield[50]. Similarly the methylene-bis-salicylaldehyde was subjected to nitration by using conc. nitric acid in acetic acid giving the analogous dinitro-bis-aldehyde.[50] (Scheme: 2.14) For both of this reactions a large amount of gl. acetic acid was required to dissolve the starting materials. The use of nitrating mixture or the reaction at greater temperature resulted in formation of picric acid.

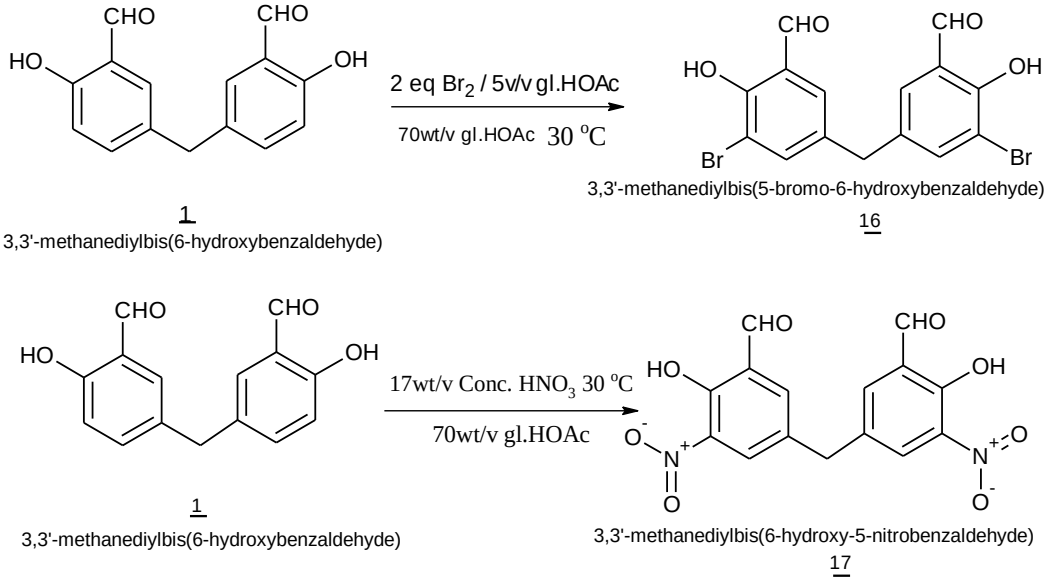

Scheme 2.14: Synthesis of 5,5'-methylene-bis-(3-bromosalicylaldehyde) and 5,5'-methylene-bis-(3-nitrosalicylaldehyde)

Following the synthesis of a number of methylene-bis-aldehydes as linkers we decided to synthesize methylene-bis-acetophenone which may also be used as a linker for the synthesis of macrocyclic structures. Thus 2-hydroxy-acetophenone was subjected to the coupling reaction using 1,3,5-trioxane under the conditions which were employed for coupling of benzaldehyde derivatives.[39] (Scheme: 2.15) Resulting methylene-bis-acetophenone was characterized by using spectral analysis.

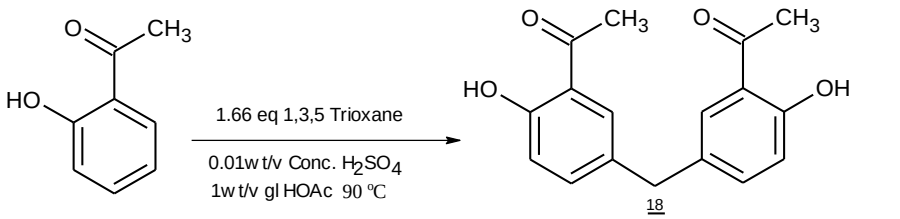

Scheme 2.15: Synthesis of 2,2'-dihydroxy-5,5'-methylene-bis-acetophenone

With the success in coupling of the acetophenone derivative it was planned to extend the same coupling reaction is extended for coupling of hetero-aromatic aldehydes and in particular five member heterocyclic aldehydes. This should result in linkers with hetero atoms included in them. Furfural, pyrrole-2-carbaldehyde and thiophene-2-carbaldehyde were subjected to the same coupling reaction using paraformaldehyde and sulphuric acid (Scheme: 2.16). The hetero-aromatic rings were found to be too sensitive to the acid catalysed coupling reactions and were resulting in dark reaction mixture without indication of any product on TLC. We also subjected these aldehydes to mild acid catalysed reactions for which Lewis acids such as $AlCl_3$ and Amberlyst-15 were employed. The coupling was also attempted by replacing paraformaldehyde by dimethoxymethane (methylal). All these attempts didn't meet with success. The coupling reactions were also attempted on the other aromatic aldehydes such as benzaldehyde, p-hydroxy-benzaldehyde, veratraldehyde and 2-hydroxy-1-naphthaldehyde but were unsuccessful. (Scheme: 2.17)

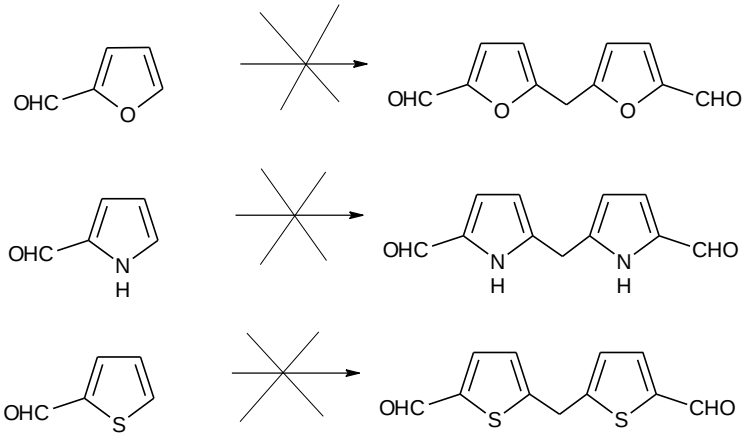

Scheme 2.16: Attempted synthesis of heterocyclic linkers.

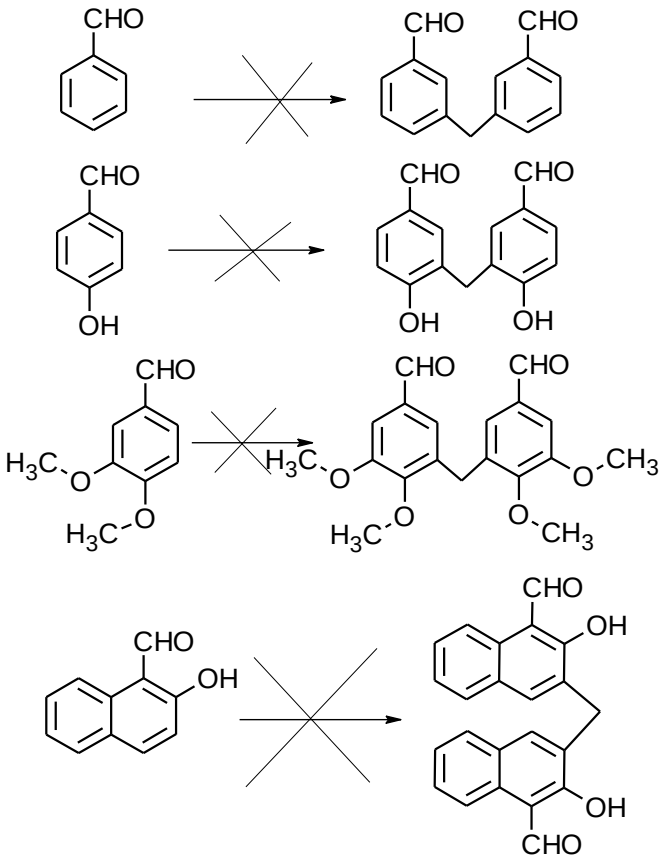

Scheme 2.17: Attempted synthesis of some other Methylene-bis-derivatives as linkers.

2.4 Conclusion

Several bifunctional linking agents useful in the synthesis of supramolecular structures have been synthesized by employing acid catalyzed coupling of aromatic aldehydes using the help of formaldehyde in acetic acid. Modification in synthetic methodology has also been studied. During the synthesis of bifunctional linking agents, several new compounds were isolated and characterized. Thus this chapter is comprised of a practical synthetic methodology leading to a library of several useful bifunctional linking agents for construction of supramolecular assemblies.

2.5 Experimental

General Remarks

All the chemicals and reagents were purchased from Sigma-Aldrich, Merck, or Spectrochem. All solvents were distilled before use. Column chromatography was carried out using silicagel (60-120 mesh). Thin layer chromatography was performed on pre-coated silicagel $60F_{254}$ (Merck) aluminium sheets.

Infrared spectra were recorded on Perkin-Elmer FT-IR 16PC spectrophotometer as KBr pellets. ^{1}H NMR and ^{13}C NMR were recorded on Bruker 200 or 400 MHz NMR spectrophotometer in $CDCl_3$, DMSO or D_2O. Elemental analyses were carried out at different places (ZRC, SPARC and CSMCRI). ESI mass were recorded on Shimadzu LC-MS 2010-A and EI and CI mass were recorded on Thermo Fisher DSQ II mass spectrometer. HPLC was carried out using Shimadzu LC-10AT and UFLC using Shimadzu LC-20AD. Melting points were measured in open capillaries and are uncorrected.

2.5.1 Synthesis of 2,4-dihydroxybenzaldehyde[23,48] **10**

.

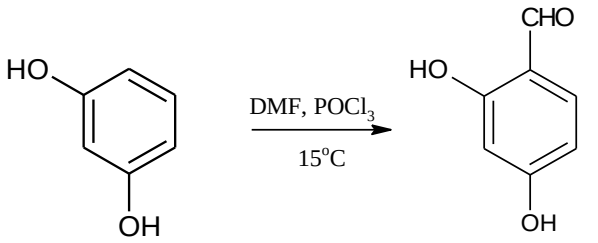

M.P.= 135
10

In a 500 ml beaker, resorcinol (50g, 0.45 mol) was dissolved in dimethyl formamide (36 ml, 0.44 mole). The solution mixture was cooled to 10 ^{o}C in ice bath. $POCl_3$ (60g, 0.39 mole) was added drop wise over 45 minutes with stirring. Reaction mixture became sticky near the completion of addition of $POCl_3$ and needed to stir manually. An exotherm was observed after 30 minutes of stirring which was followed by precipitation of white solid. The reaction mixture was poured in to a cold solution of sodium acetate (50%) in water with stirring. A yellowish solution was filtered and kept in refrigerator for crystallization. White needle shaped crystals were obtained. Crystals were filtered and washed with cold water. It was necessary to cool solution of sodium acetate as decomposition of white solid was exothermic. At higher temperature (~ 80 ^{o}C) yellowish undersirable product precipitated out.

Yield: 25g (40%)

M.P. = 135 °C (135-137 °C)

IR (KBr disc, cm^{-1}): 3129 (phenol,υ(O-H)), 1891, 1633 (aldehyde, υ(OC-H), 1582, 1498 (aromatic ring, υ(C=C)), 1444(phenol, δ(O-H)), 1395(aldehyde, δ(OC-H)) 1329 (phenol, δ(O-H)), 1231 (phenol, υ(C-O)), 1166 (out of plane, δ(C-H)), 1130 (phenol, υ(C-O)), 974, 856, 823 (aromatic, out of plane, δ(C-O)), 746, 695, 635, 460, 427 (aromatic ring, δ(C=C)).

2.5.2 Synthesis of 3-alkyl-2-hydroxybenzaldehydes[24-27] 6,7

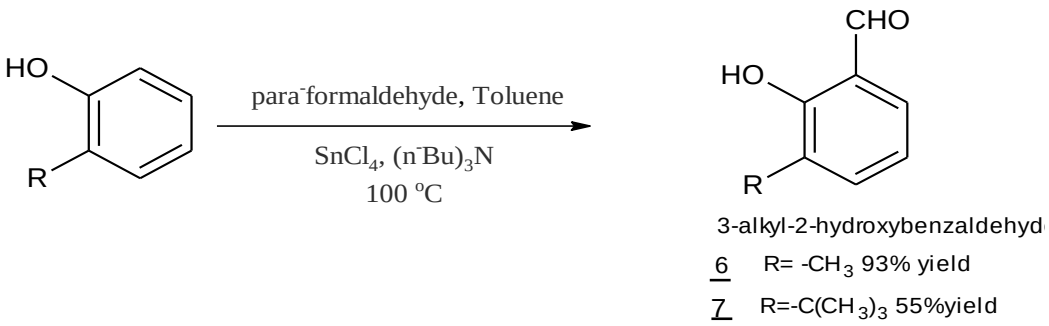

General procedure:

2-Alkyl phenol (0.23 mol), tri n-butylamine (0.09 mol) and 2v/v toluene was placed in a 250 ml three necked round bottom flask equipped with a condenser and an addition funnel under N_2 atmosphere. To a stirred mixture $SnCl_4$ (0.02 mol) was added dropwise over 30 minutes at room temperature (30 ^oC) with stirring. After this time paraformaldehyde (0.5 mol) was added in single portion. The reaction mixture was heated to reflux for 8hrs (TLC). The reaction mixture was poured in to aqueous HCl (5%, 600ml) solution and was extracted with diethyl ether (3x100ml). Combined organic layers were washed with water, brine and were dried over Na_2SO_4. Diethyl ether was removed using rotary evaporator. Brownish oil was subjected to column chromatography using Pet-ether : dichloromethane (gradient) was done using pet-ether:MDC mixtures. Pure product was separated as yellowish oil which solidified later.

3-Methyl-2-hydroxybenzaldehyde[24,26] **6**

2-Methylphenol (24 ml, 0.23 mol), paraformaldehyde (15 g, 0.5 mol), $SnCl_4$ (2.7 ml, 0.02 mol) and tri-n-butylamine (22.1 ml, 0.09 mol) were reacted in toluene (50 ml) to give compound **6** as yellow oil which partially solidifies on standing.

Yield: 29.0g (93%)

M.P.= 204 °C (730 mm of Hg) (Reported)

^{1}H NMR (400 MHz, $CDCl_3$): δ 11.27 (s, 1H), 9.78 (s, 1H), 7.31(d, *J* = 7.6 Hz, 2H), 6.86 (t, *J* = 7.6 Hz ,1H), 2.22(s, 1H)

^{13}C NMR (400 MHz, $CDCl_3$): δ 196.7, 159.8, 137.7, 131.3, 126.6, 119.9, 119.3, 14.9

3-*tert*-Butyl-2-hydroxybenzaldehyde[27] **7**

2-*tert*-Butylphenol (25.6ml, 0.17mole), paraformaldehyde (11g, 0.37mole), $SnCl_4$ (2.0ml, 0.02mol) and tri-n-butylamine (15.9ml, 0.07mole) were reacted in toluene 50ml to give the **7** as yellowish oil.

Yield: 16.0g (55%)

B.P.= 78-79 °C (1mm of Hg) (Reported)

^{1}H NMR (400 MHz, $CDCl_3$): δ 11.30 (s, 1H), 7.53 (dd, *J* = 1.6 Hz ,*J* = 7.6 Hz, 1H), 7.44 (dd ,*J* = 1.6 Hz, *J* = 7.6 Hz, 1H), 6.86 (t, *J* = 7.6 Hz, 1H), 1.48 (s, 1H)

^{13}C NMR (400 MHz, $CDCl_3$): δ 204.2, 161.0, 138.6, 132.9, 131.6, 120.1, 117.8, 35.1, 29.4

2.5.3 5,5'-Methylene-bis(3-substituted-salicylaldehyde)

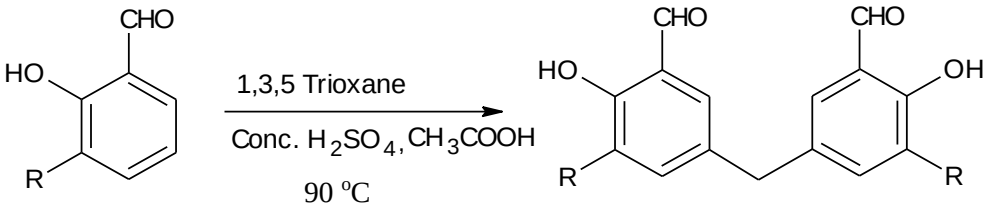

General Procedure[31]:

3-Substituted-salicylaldehyde (0.39 mol), 1,3,5-trioxane (0.06 mol) and gl. CH_3COOH (1v/v) were placed in a 250 ml round bottom flask equipped with a condenser and N_2 balloon. Reaction mixture was warmed to 90 ^oC. A solution of conc. H_2SO_4 (0.01v/v) in gl. CH_3COOH (0.05v/v) was added drop wise using a syringe to the magnetically stirred reaction mixture maintained at 90^oC under N_2 atmosphere. The stirring was continued at 90 ^oC for 5hrs. (TLC). The Reaction mixture was poured in to ice-water (1L). Yellowish semi solid was obtained after decantation of water which was washed with pet.ether (3x 100ml) and recrystallized from acetone to give off white product.

2.5.4 Preparation of 5,5'-Methylene-bis-salicylaldehyde[31] 1

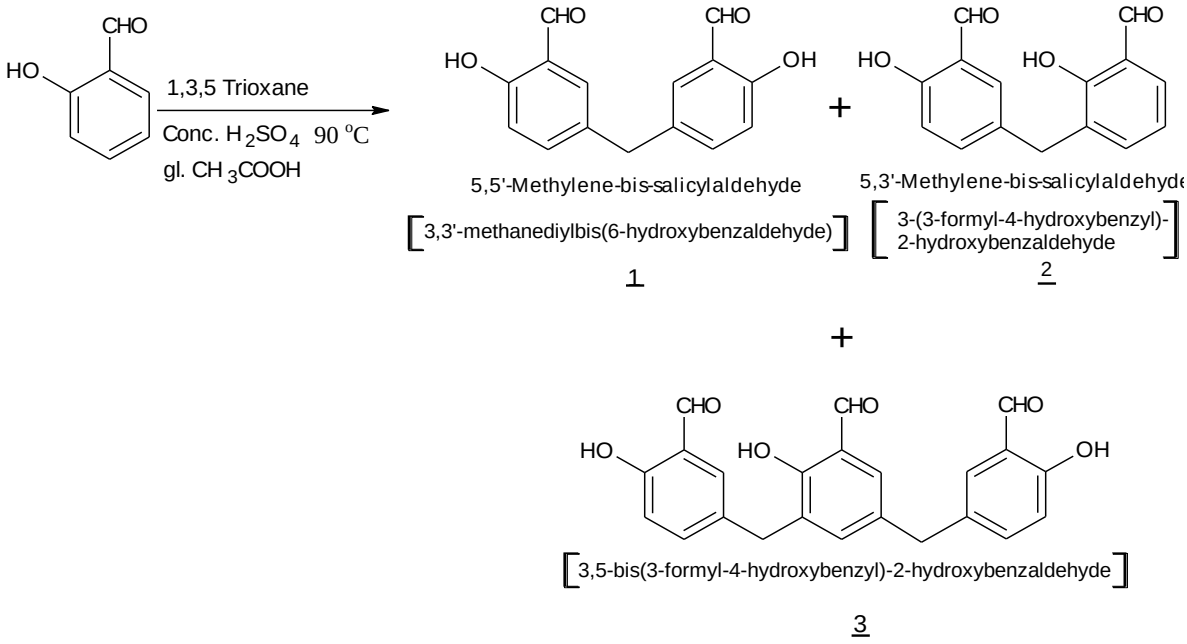

Salicylaldehyde (41ml, 0.39 mol), 1,3,5-trioxane (5.9g, 0.06 mol) and conc. H_2SO_4 (0.4ml, 0.01v/v) in 41ml gl. HOAc (1v/v) were reacted as per the general procedure (2.5.3) to yield title compound **1** as off white solid.

Yield= 12 g (25%) M.P.= 149 °C.

The residue obtained from concentrating mother liquor after crystallization from acetone was subjected to column chromatography using pet-ether ethyl acetate solvent system in gradient manner. Compound **2** and **3** were obtained successively as white crystals.

Compound **2 :** 0.1g (0.2%yield)
Compound **3 :** 2.5g (5%yield), M.P.= 141 °C.

5,5'-Methylene-bis-salicylaldehyde 1

^{1}H NMR (400 MHz, $CDCl_3$): δ 10.95 (s, 1H), 9.86 (s, 1H), 7.34-7.38 (m, 2H), 6.65 (d, 1H), 3.98 (s, 1H)

^{13}C NMR (400 MHz, $CDCl_3$): δ 196.4, 160.2, 137.6, 133.2, 131.9, 120.4, 117.9, 39.4

IR (KBr disc, cm^{-1}): 3424 (phenol,υ(O-H)), 2915, 2858, 2744 (Fermiresonance,υCHO), 2364, 1656(aldehyde, υ(C-H), 1590, 1483 (aromatic ring, υ(C=C)), 1440 (phenol, δ(O-H)), 1376 (aldehyde, δ(C-H)) 1332 (phenol, δ(O-H)), 1277 (phenol, υ(C-O)), 1199(out of plane, δ(C-H)), 956, 896, 844, 811 (aromatic, out of plane, δ(C-O)), 768, 718, 617, 553, 423 (aromatic ring, δ(C=C)).

CHN: 70.39 %C, 4.69 %H (Theoretical cal value: 70.31 %C, 4.72 %H)

Mass: 256m/z

5,3'-Methylene-bis-salicylaldehyde 2

^{1}H NMR (400 MHz, $CDCl_3$): δ 11.36 (d, *J* = 6.8 Hz, 1H), 10.91 (d, *J* = 12 Hz,1H), 9.92(d, *J* = 6 Hz, 1H), 9.86 (d, *J* = 6 Hz, 1H), 7.33-7.48 (m, 4H), 6.91-7.00(m, 2H), 3.99 (s, 1H)

^{13}C NMR (400 MHz, $CDCl_3$): δ 196.8, 196.6, 160.1, 159.5, 137.8, 137.3, 133.5, 132.3, 131.5, 129.4, 120.5, 120.4, 119.8, 117.7, 33.9

IR (KBr disc, cm^{-1}): 3420 (phenol,υ(O-H)), 1652(aldehyde, υ(C-H), 1568, 1482 (aromatic ring, υ(C=C)), 1436 (phenol, δ(O-H)), 1373 (aldehyde, δ(C-H)) 1319 (phenol, δ(O-H)), 1274 (phenol, υ(C-O)), 1148(out of plane, δ(C-H)), 995, 904, 841, 811 (aromatic, out of plane, δ(C-O)), 737, 673, 656, 458 (aromatic ring, δ(C=C)).

3,5-bis(3-formyl-4-hydroxybenzyl)-2-hydroxybenzaldehyde 3

^{1}H NMR (400 MHz, $CDCl_3$): δ 11.27(s, 1H), 10.91 (d, 1H), 9.84 (s, 1H), 7.39(t, *J* = 9.6 Hz, 2H), 7.33(t, *J* = 9.6 Hz, 2H), 7.20 (dd, *J* = 9.6 Hz, 2H), 6.90-6.96 (m, 2H), 3.94 (d, 2H)

^{13}C NMR (400 MHz, $CDCl_3$): δ 196.6, 196.5, 196.4, 160.3, 160.1, 158.2, 137.9, 137.7, 137.6, 133.4,133.3, 131.9, 131.8, 131.7, 131.4, 129.9, 120.5, 120.4, 120.3, 118.0, 117.7, 39.4, 33.9

IR (KBr disc, cm^{-1}): 3059 (phenol,υ(O-H)), 2923, 2834, 2364, 1683(aldehyde, υ(C-H), 1591, 1554 (aromatic ring, υ(C=C)), 1436 (phenol, δ(O-H)), 1324 (phenol, δ(O-H)), 1275 (phenol, υ(C-O)), 1193(out of plane, δ(C-H)), 916, 896, 833, 800 (aromatic, out of plane, δ(C-O)), 768, 736, 675, 544, 420 (aromatic ring, δ(C=C)).

CHN: 70.67%C, 4.60%H (Theoretical cal value: 70.76 %C, 4.65 %H)

2.5.5 5,5'-Methylene-bis-(3-methoxy-salicylaldehdye)[15,40,41] **4**

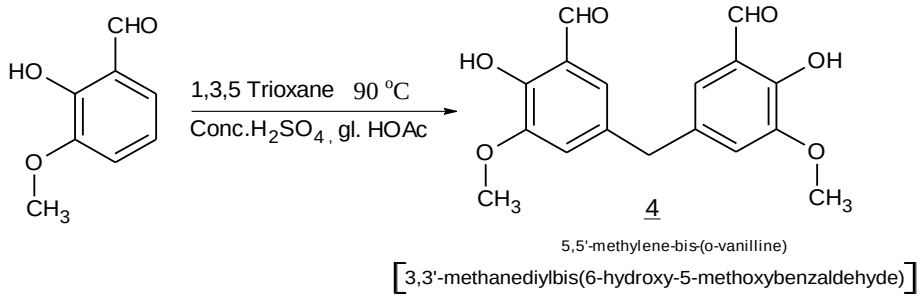

o-Vanilline (20g, 0.23mol), 1,3,5-trioxane (2g, 0.02mol) and H_2SO_4 (0.2ml, 0.01v/wt) were reacted in 100 ml gl. HOAc (5v/wt) using similar procedure as that of 5,5'methylene-bis-(3-substituted-salicylaldehyde) (2.5.3) to yield the title compound **4** as light brown powder.

Yield= 4g (20%)

M.P. = 151 °C.

^{1}H NMR (400 MHz, $CDCl_3$): δ 9.82 (s, 1H), 6.76 (d, 1H), 6.59 (d, 1H), 5.23 (s, 1H), 3.47(s, 3H), 3.39 (s, 1H)

2.5.6 5,5'-Methylene-bis-(4-hydroxy-3-methoxy-benzaldehyde)[42] 5

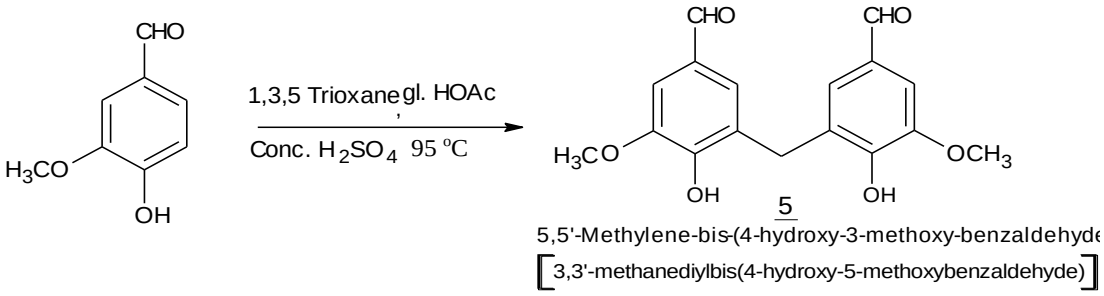

The compound **5** was synthesized using similar procedure as that of 5,5'methylene-bis-(3-substituted-salicylaldehyde) (2.5.3) Vanilline (7.6g, 0.05 mol), 1,3,5-trioxane (0.75g, 0.01 mol) and H_2SO_4 (0.07ml, 0.01wt/v) in 8ml gl. HOAc (1wt/v) were reacted at 95 ^oC to yield the title compound **5**

Yield: 1.2 g (15%)

M.P.= 276 ^oC .

^{1}H NMR (400 MHz, $CDCl_3$): δ 9.71 (s, 1H), 9.00 (s, 1H), 7.67 (s, 2H), 3.95 (s, 1H), 3.06 (s, 3H)

IR (KBr disc, cm^{-1}) : 3203 (phenol, υ(O-H)), 2966 (methyl, υ(C-H)), 2934 (CH_2, asymmetric υ(C-H)), 2832, 2725 (aldehyde, fermiresonance, υ(CHO)), 2367, 2345, 1666 (aldehyde, υ(CHO)), 1591, 1498 (aromatic ring, υ(C=C)), 1469 ($\delta_s(CH_2)$), 1427 (phenol, δ(O-H)), 1368 (aldehyde, δ(CHO)), 1321 (phenol, δ(O-H)), 1276 ($\delta(CH_2)$),, 1261 (ether, υ_{as}(C-O)), 1145, 1091(ether, υ_s(C-O)), 998, 958, 930, 875, 850, 813, 782, 694, 616, 588 (out of plane, δ(C-H))

2.5.7 5,5'-Methylene-bis-(3-methyl-salicylaldehyde)[43-45] **8**

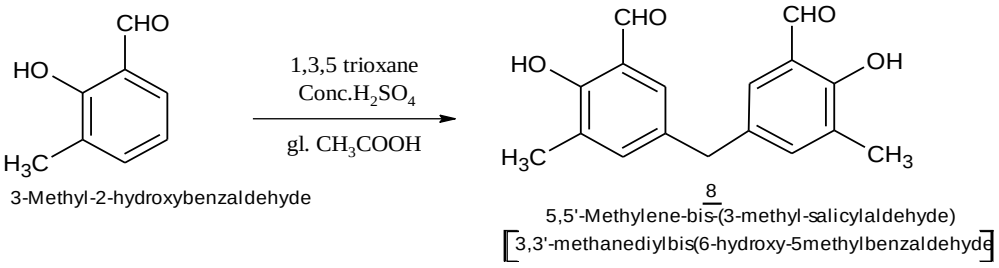

3-Methyl-2-hydroxybenzaldehyde

8

5,5'-Methylene-bis-(3-methyl-salicylaldehyde)

[3,3'-methanediylbis(6-hydroxy-5methylbenzaldehyde]

Compound **8** was synthesized using the general procedure described earlier (2.5.3). 3-Methylsalicylaldehyde (10g, 0.07mol), 1,3,5-trioxane (1.1g, 0.01mol) and H_2SO_4 (0.1ml, 0.01wt/v) in 10 ml gl. HOAc (1wt/v) were reacted to yield the title compound **8** as yellow crystals.

Yield= 8.26 g (79.12%)

M.P.= 150 ^{o}C.

^{1}H NMR (400 MHz, $CDCl_3$): δ 11.19 (s, 1H), 9.83 (s, 1H), 7.23 (s, 1H), 7.19 (d, 1H), 3.90 (s, 1H), 2.25 (s, 3H)

^{13}C NMR (400 MHz, $CDCl_3$): δ 196, 2 .14.7, 158.6, 138.6, 131.7, 130.8, 127.2, 119.8, 39.6

2.5.8 5,5'-Methylene-bis-(3-*tert*-butyl-salicylaldehyde)[36,43-47] **9**

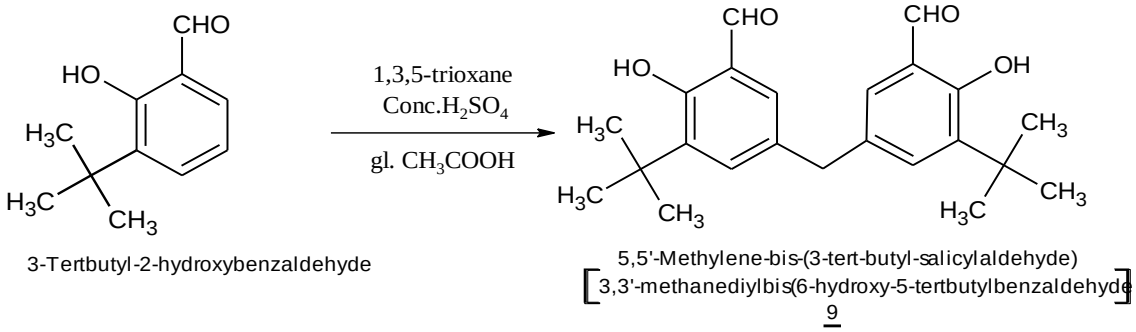

Compound **9** was synthesized using similar procedure as that of 5,5'-methylene-bis-(3-substituted-salicylaldehyde) (2.5.3). 3-*tert*-Butyl-salicylaldehyde (10g, 0.06mol), 1,3,5-trioxane (0.84g, 0.01mol) and H_2SO_4 (0.1ml, 0.01wt/v) in 10 ml gl. HOAc (1wt/v) were reacted to yield title compound **9** as light yellow crystals.

Yield= 3.24 g (31%)

M.P.= 105 ^{o}C.

^{1}H NMR (400 MHz, $CDCl_3$): δ 11.74 (s, 1H), 9.84 (s, 1H), 7.40 (d, *J* = 2 Hz, 1H), 7.17 (d, *J* = 2 Hz, 1H), 3.97 (s, 1H), 1.43 (s, 9H)

^{13}C NMR (400 MHz, $CDCl_3$): δ 197.1, 159.8, 138.6, 135.0, 131.3, 131.2, 120.5, 40.1, 34.9, 29.2

2.5.9 Synthesis of 5,5'-methylene-bis-resorcylaldehyde[15] 11

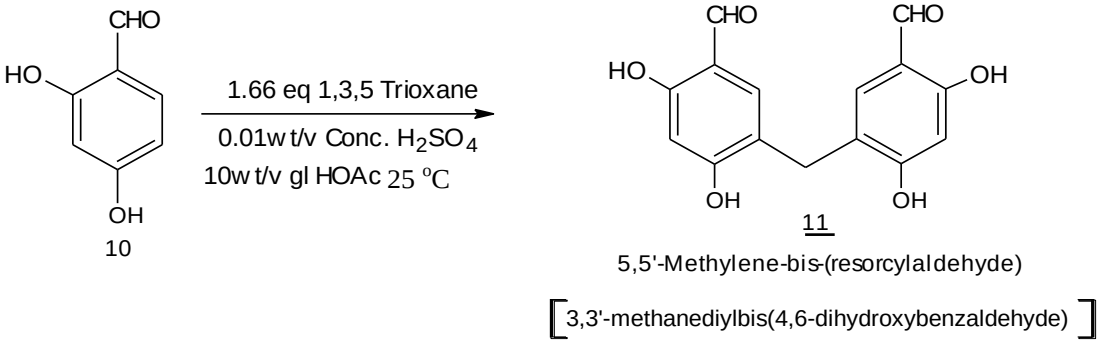

Compound **11** was synthesized using similar procedure as that of 5,5'-methylene-bis-(3-substituted-salicylaldehyde)(2.5.3). Resorcylaldehyde (14 g, 0.10mol), 1,3,5-trioxane (1.5 g, 0.02 mol) and H_2SO_4 (0.14 ml, 0.01wt/v) in 84 ml gl. acetic acid (6 wt/v) were reacted at 25 ^oC to yield title compound **11**

Yield= 4g (30%) (HPLC)

M.P.= 260 ^oC (d)

^1H NMR (400 MHz, $CDCl_3$+DMSO): δ 11.28 (s, 1H), 10.35 (s, 1H), 9.60 (s, 1H), 7.20 (s, 1H), 6.44 (s, 1H), 3.79 (s, 1H)

IR (KBr disc, cm^{-1}): 3175 (phenol,υ(O-H)), 2848, 1636 (aldehyde, υ(C-H), 1515 (aromatic ring, υ(C=C)), 1424 (phenol, δ(O-H)), 1386 (aldehyde, δ(C-H)) 1354 (phenol, δ(O-H)), 1247 (phenol, υ(C-O)), 1130 (out of plane, δ(C-H)), 935, 888, 864, 805 (aromatic, out of plane, δ(C-O)),751, 687, 625, 560, (aromatic ring, δ(C=C)).

Mass: 289.13 (M+H)

Elemental Analysis: Calculated for $\mathbf{C_{15}H_{12}O_6}$: C= 62.50%, H= 4.20%

Found: C= 62.07%, H= 4.37%

2.5.10 3,3'methylene-bis-resorcylaldehyde 12 and Unsymmetrical methylene-bis-resorcylaldehyde 13

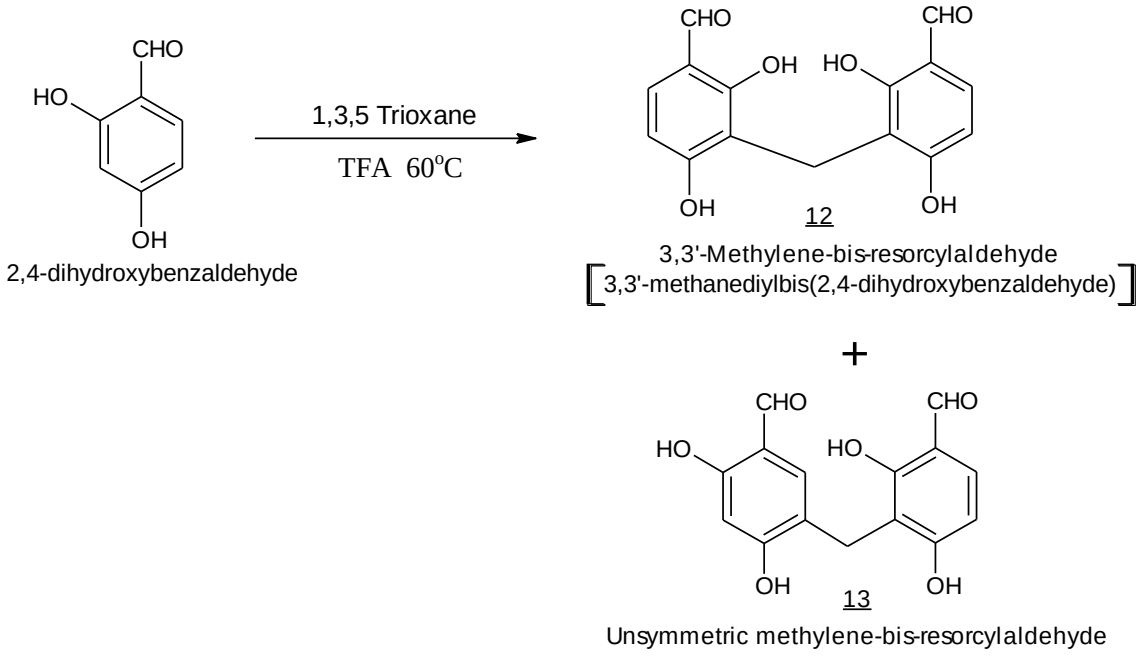

Resorcylaldehyde (1g, 0.007mol), 1,3,5-trioxane (0.11 g, 0.001 mol) and TFA (10 ml, 1wt/v) were placed in a 50ml round bottom flask equipped with a condenser, N_2 balloon and warmed to 60 ^oC. The stirring was continued at 60 ^oC for 3hrs (TLC). Reaction mixture was poured in 1L ice-water. The solid obtained was filtered and washed with distilled water (10x20ml) to yield pinkish solid giving a mixture of compound **12** (23%, by HPLC), **13** (40%, by HPLC) and some more polar impurities. The crude mixture was subjected to column chromatography using petether-ethylacetate. (gradient). Pure compound **12** was obtained as white crystalline solid and compound **13** was obtained with some contamination of **12**. The compound **13** was then purified using preparative HPLC.

Yield : 0.9 g (Crude mixture (12+13))

Yield of Compaund 12: 23% (HPLC),

M.P.= 205 °C (d)

Yield of Compaund 13: 40% (HPLC),

M.P.= 215 °C

3,3'-Methanediylbis(2,4-dihydroxybenzaldehyde) 12

^{1}H NMR (400 MHz, DMSO-d_6): δ 11.67 (s, 2H), 10.64 (s, 2H), 9.72 (s, 2H), 7.45 (d, *J* = 8.4 Hz, 2H), 6.51 (d, *J* = 8.4 Hz, 2H), 3.87 (s, 2H)

^{13}C NMR (400 MHz, $CDCl_3$): δ 194.8, 163.4, 159.9, 134.1, 114.4, 112.3, 111.3, 15.1

Mass: 289.02(M+H)

Elemental Analysis: Calculated for **$C_{15}H_{12}O_6$**: C= 62.50%, H= 4.20%

Found: C= 62.44%, H= 4.17%

IR (KBr disc, cm^{-1}): 3348 (phenol,υ(O-H)), 2922, 2852, 1689 (aldehyde, υ(OC-H), 1617 (aromatic ring, υ(C=C)), 1429 (phenol, δ(O-H)), 1391 (aldehyde, δ(OC-H)) 1301 (phenol, δ(O-H)), 1220 (phenol, υ(C-O)), 1080 (out of plane, δ(C-H)), 832, (aromatic, out of plane, δ(C-O)),756, 640, 536, (aromatic ring, δ(C=C)).

3-(5-formyl-2,4-dihydroxybenzyl)-2,4-dihydroxybenzaldehyde 13

^{1}H NMR (400 MHz, DMSO-d_6): δ 11.59 (s, 1H), 10.76 (s, 2H), 10.62 (s, 1H), 9.81 (s, 1H), 9.74 (s, 1H), 7.54 (d, *J* = 8.8 Hz, 1H), 6.83 (s, 1H), 6.61 (d, *J* = 8.8 Hz, 1H), 6.40 (d, 1H) 3.67 (s, 2H)

^{13}C NMR (400 MHz, $CDCl_3$): δ 195.7, 190.3, 164.3, 163.5, 162.1, 161.9, 134.6, 128.9, 119.5, 115.2, 114.6, 112.5, 108.8

Mass: 287.9 M^+

IR (KBr disc, cm^{-1}): 3256 (phenol,υ(O-H)), 2928, 2837, 2754 (fermiresonance,υCHO), 1612 (aldehyde, υ(OC-H), 1501 (aromatic ring, υ(C=C)), 1439 (phenol, δ(O-H)), 1385 (aldehyde, δ(OC-H)) 1331 (phenol, δ(O-H)), 1252 (phenol, υ(C-O)), 1113 (out of plane, δ(C-H)), 982, 872,841, 802 (aromatic, out of plane, δ(C-O)),784, 700, 636, 540, (aromatic ring, δ(C=C)).

2.5.11 5,5'-Methylene-bis-anisaldehyde[9,12] 14

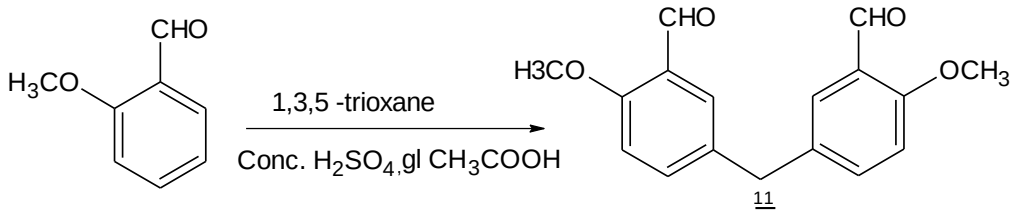

11

5,5'-Methylene-bis-(anisaldehyde)
3,3'-methanediylbis(6-methoxybenzaldehyde)

The compound **14** was synthesized using similar procedure as that of 5,5'-methylene-bis-salicylaldehyde (2.5.3). Anisaldehyde (10 g, 0.05mol), 1,3,5-trioxane (0.69 g, 0.01 mol) and H_2SO_4 (0.1 ml,0.01wt/v) in 50ml gl. HOAc (5wt/v) were reacted at 90^oC to yield the compound **14**

Yield : 3 g (30%)

M.P.= 135 ^oC .

^{1}H NMR (400 MHz, $CDCl_3$): δ 10.40 (s, 1H), 7.60 (d, *J* = 2.4 Hz, 1H), 7.32 (dd, *J* = 2.4 Hz, *J* = 8.4 Hz, 1H), 6.89 (d, *J* = 8.4 Hz, 1H), 3.87 (s, 1H)

^{13}C NMR (400 MHz, $CDCl_3$): δ 189.8, 160.5, 136.3, 133.1, 128.3, 124.6, 112.0, 55.7, 39.6

IR (KBr disc, cm^{-1}) : 3031(aromatic,υ(C-H)), 2964 (methyl, υ(C-H)), 2915 (CH_2, asymmetric υ(C-H)), 2876, 2773 (aldehyde, fermiresonance, υ(CHO)), 2334, 2359, 1676 (aldehyde, υ(CHO)), 1606, 1494 (aromatic ring, υ(C=C)), 1445 (CH_2, δ_s), 1401, 1257, 1215, 1192 (ether, υ_{as}(C-O)), 1112, 1027 (ether, υ_s(C-O)), 976, 965, 907, 888, 837, 824, 814, 792, 749, 648, 552, 473 (out of plane, δ(C-H))

2.5.12 3,3'-Methylene-bis-(4-N,Ndimethylaminobenzldehyde) **15**

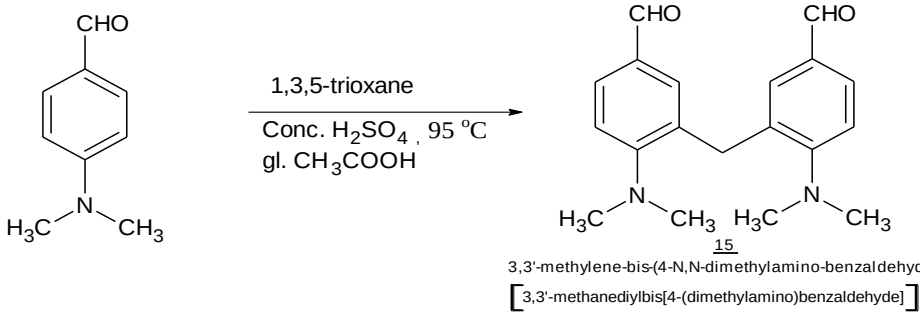

Compound **15** was synthesized using similar procedure as described for 5,5'-methylene-bis-(3-substituted-salicylaldehyde) (2.5.3).

4-N,N-dimethylaminobenzaldehyde (20 g, 0.13mol), 1,3,5-trioxane (2 g, 0.02mol) and H_2SO_4 (0.6 ml,0.03wt/v) in 60 ml gl. Acetic acid (3wt/v) were reacted at 95 ^oC to yield compound **15** . Here 50% of the starting material was recovered from water work up.

Yield: 2g (20% on recovery base)

M.P.= 104 ^oC

^1H NMR (400 MHz, $CDCl_3$) δ 9.79 (s, 1H), 7.71 (dd, J_1 = 1.9Hz, J_2 = 8.3 Hz, 1H), 7.50 (d, J = 1.7 Hz, 1H), 7.13 (d, J = 8.3 Hz, 1H), 4.15 (s, 1H), 2.80 (s, 6H)

Mass: 311.18 (M+H)

Elemental Analysis: Calculated for $C_{19}H_{22}O_2N_2$: C= 73.52%, H= 7.14%, N= 9.03%

Found: C= 72.47%, H= 7.07%, N= 9.67 %

IR (KBr disc, cm^{-1}) : 2954 (methylene, υ_{as}(C-H)), 2840 (methylene, υ_s(C-H)), 2798, 2723 (aldehyde, fermiresonance, υ(CHO)), 2365, 2345, 1681 (aldehyde, υ(CHO)), 1595, 1499 (aromatic ring, υ(C=C)), 1469 ($\delta_s(CH_2)$), 1378 (aldehyde, δ(CHO)), 1340 (aromatic, υ(C-N)), 1317 (δ(CH_2)),, 1243 (aromatic, υ(C-N)), 1221, 1188, 1170, 1084, 1052 (aliphatic, υ(C-N)), 980, 952, 931, 876, 826, 799, 754, 645, 616, 582, 475 (out of plane, δ(C-H))

2.5.13 Synthesis of 5,5'methylene-bis(3-bromo-salicylaldehyde)[50] 16

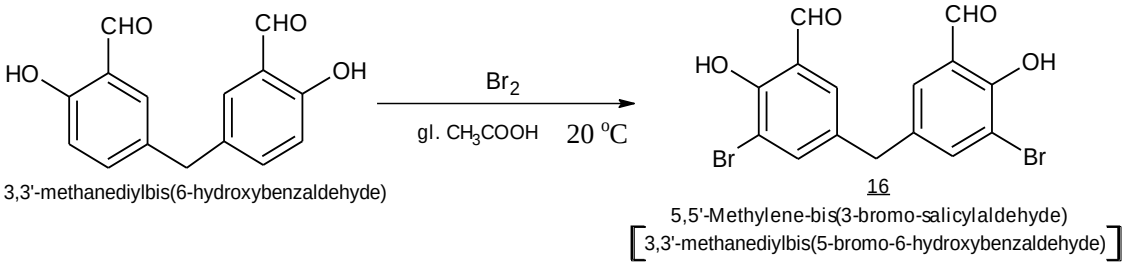

3,3'-methanediylbis(6-hydroxybenzaldehyde)

16

5,5'-Methylene-bis(3-bromo-salicylaldehyde)

[3,3'-methanediylbis(5-bromo-6-hydroxybenzaldehyde)]

5,5'-Methylene-bis-salicylaldehyde **1** (5 g, 0.02 mol) and gl. acetic acid (350 ml ,70 wt/v) were placed in a 500ml round bottom flask equipped with addition funnel. Reaction mixture was cooled to 20 ^{o}C. Bromine (2.1ml, 6.2 g, 0.03mole) in 10ml gl. acetic acid was added dropwise at 20 ^{o}C over 30 min. Allowed to come at R.T. (TLC). Reaction mixture was poured into 1L ice-water. Off white solid was filtered and washed with distilled water (4x100ml) to remove trapped acid. The crude product was recrystallized from absolute alcohol to yield pure compound **16**

Yield : 4g (54%)

M.P.=188 ^{o}C.

^{1}H NMR (400 MHz, DMSO-d_6): δ 11.11 (s, 1H), 10.03 (s, 1H), 7.86 (d, *J* = 2 Hz, 1H), 6.46 (d, *J* = 2 Hz, 1H), 3.94 (s, 1H)

^{13}C NMR (400 MHz, DMSO-d_6): δ 195.2, 155.6, 139.9, 134.4, 131.7, 123.3, 111.7, 38.0

2.5.14 Synthesis of 5,5'methylene-bis(3-nitro-salicylaldehyde)[50] 17

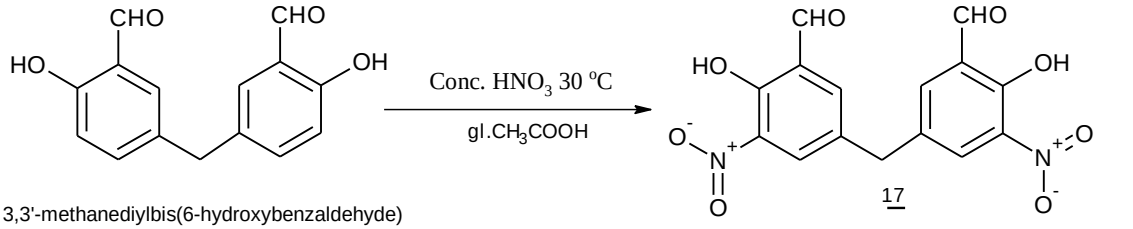

3,3'-methanediylbis(6-hydroxybenzaldehyde)

1

17

5,5'-Methylene-bis(3-nitro-salicylaldehyde)

[3,3'-methanediylbis(6-hydroxy-5-nitrobenzaldehyde)]

5,5'-Methylene-bis-salicylaldehyde 1 (5g, 0.02 mol, 1eq) and gl. HOAc (350 ml ,50wt/v) were placed in a 500 ml round bottom flask equipped with addition funnel carrying $CaCl_2$ guard tube. Reaction mixture was cooled to 20 ^oC and solution of conc.HNO_3 (119 ml, 17 wt/v) in 140 ml gl. acetic acid was added dropwise at 20 ^oC over 30 min. Reaction mixture was allowed to warm to R.T. (TLC). Reaction mixture was poured in 1L ice-water. Yellow solid obtained. The solid was filtered and washed with distilled water (4x 100 ml) to remove trapped acid. The crude product was recrystallized from MDC:EtOAc :: 50:50 to yield compound **17**

Yield: 5 g (54%)

M.P.=218 ^oC.

^{1}H NMR (400 MHz, $CDCl_3$): δ 11.31 (s, 1H), 10.44 (s, 1H), 8.18 (d, *J* = 2.4 Hz, 1H), 7.94 (d, *J* = 2.4 Hz, 1H), 4.09 (s, 1H)

^{13}C NMR (400 MHz, DMSO-d_6): δ 191.0, 153.6, 138.3, 136.0, 132.2, 131.7, 126.3, 37.6

2.5.15 Synthesis of 5,5'-methylene-bis-acetophenone[33] 18

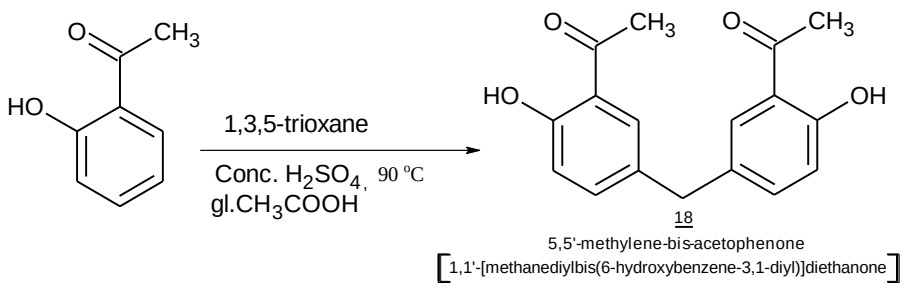

18

5,5'-methylene-bis-acetophenone

[1,1'-[methanediylbis(6-hydroxybenzene-3,1-diyl)]diethanone]

The title compound **18** was synthesized using general procedure as described for synthesis of 5,5'-methylene-bis-(3-substituted-salicylaldehyde) derivatives.(2.5.3)

2-Hydroxyacetophenone (44 ml, 50g, 0.37 mole), 1,3,5-trioxane (5.5g, 0.06 mol) and H_2SO_4 (0.5ml, 0.01wt/v) in 50ml gl. acetic acid (1wt/v) were reacted at 95 ^oC to yield compound **18**

Yield : 10g (20%)

M.P.= 139^oC.

^{1}H NMR (400 MHz, $CDCl_3$) δ 12.20 (s, 1H), 7.53 (d, *J* = 2 Hz, 1H), 7.30 (dd, *J* = 2 Hz, *J* = 8.4 Hz, 1H), 6.95 (d, *J* = 8.4 Hz, 1H), 3.93 (s, 1H), 2.62 (s, 3H)

^{13}C NMR (400 MHz, $CDCl_3$) δ 204.4, 161.0, 137.1, 131.0, 130.4, 119.5, 118.8, 39.9, 26.7

2.6 Analytical Data:

Spectrum 2.1

IR

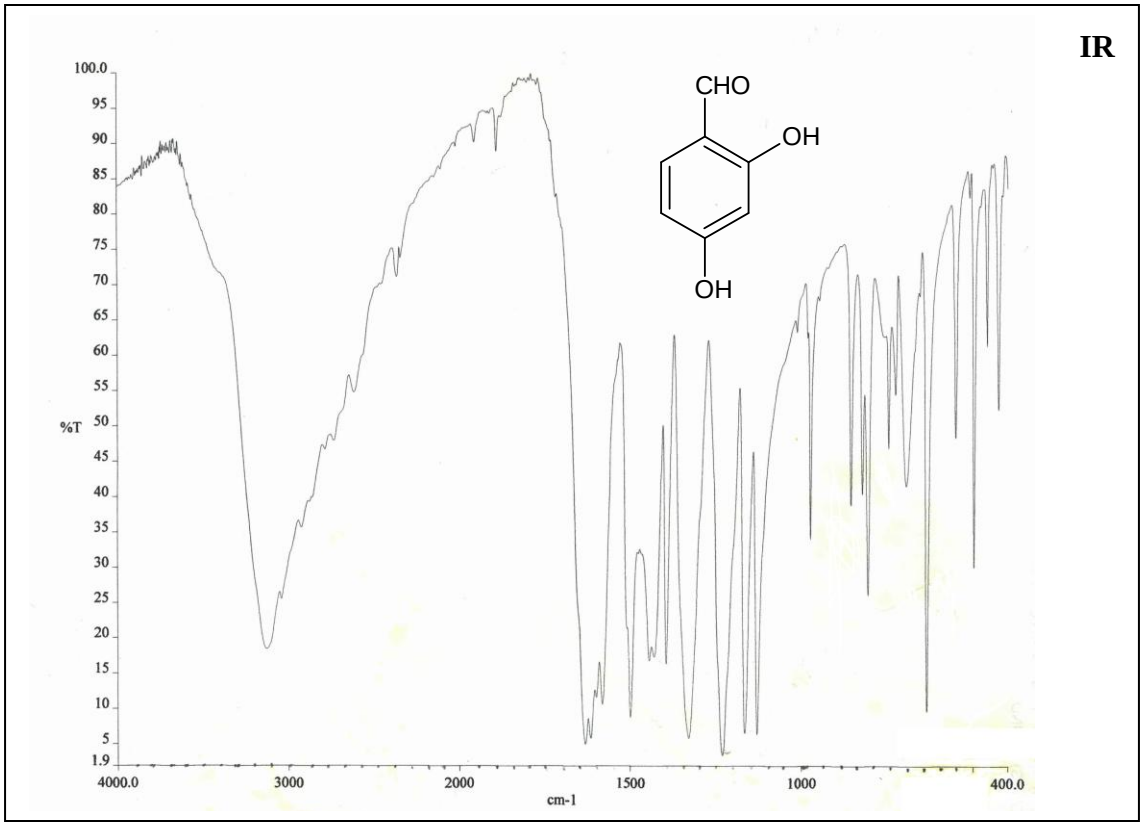

Spectrum 2.2

^{1}H NMR

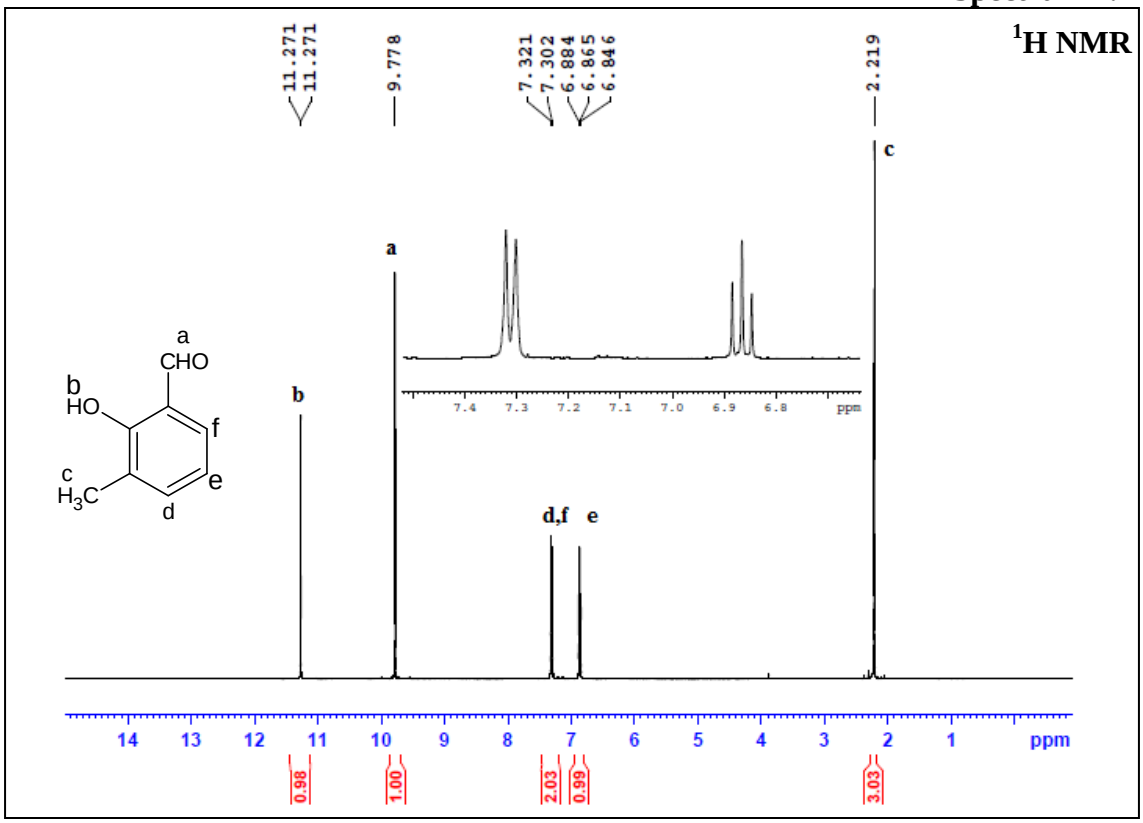

Spectrum 2.3

^{13}C NMR

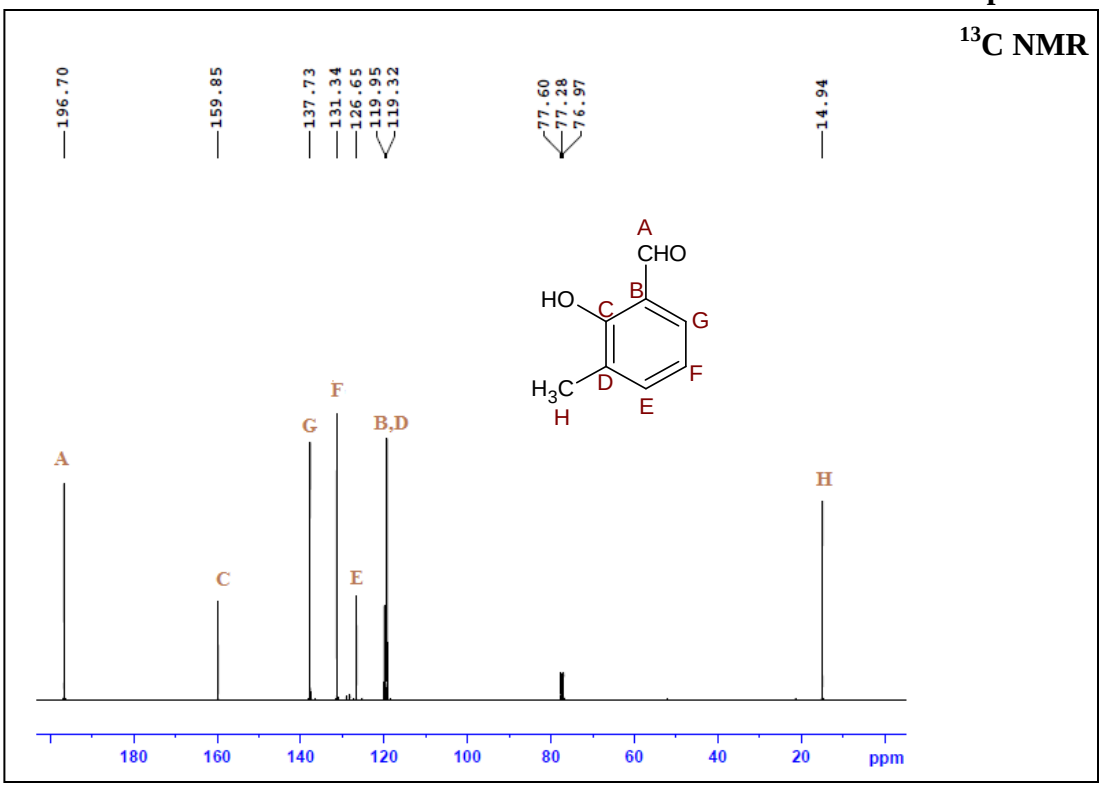

Spectrum 2.4

^{1}H NMR

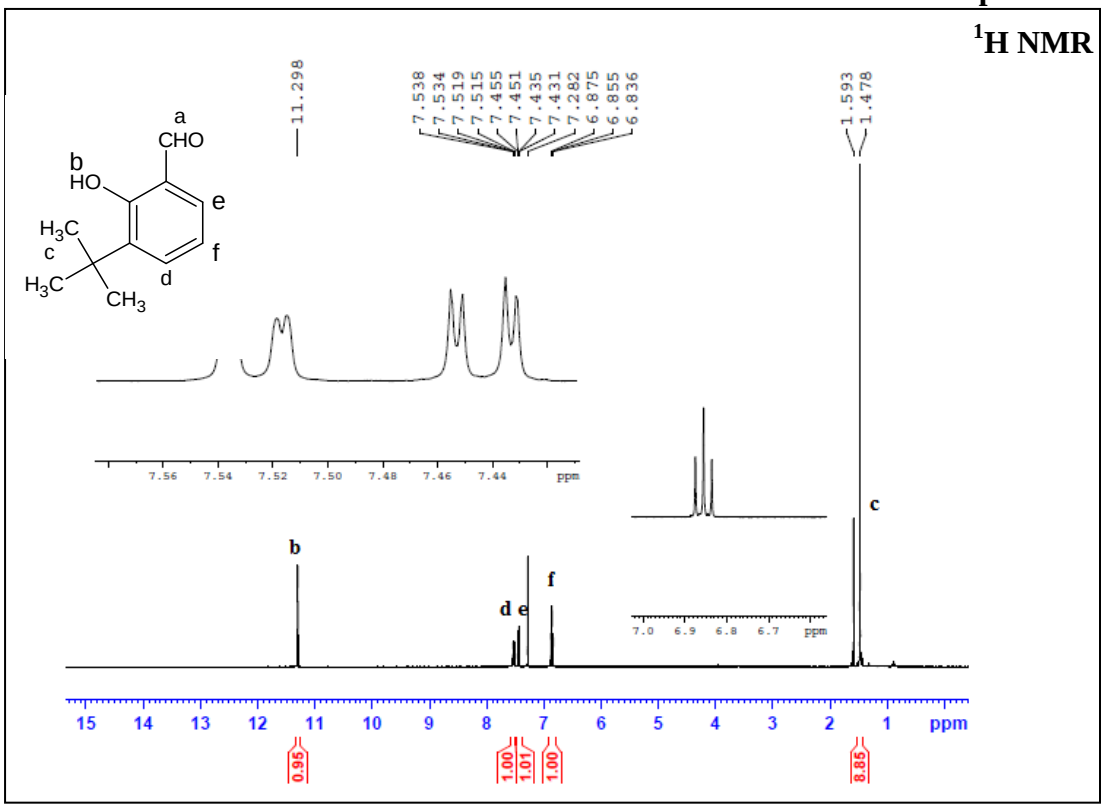

Spectrum 2.5

^{13}C NMR

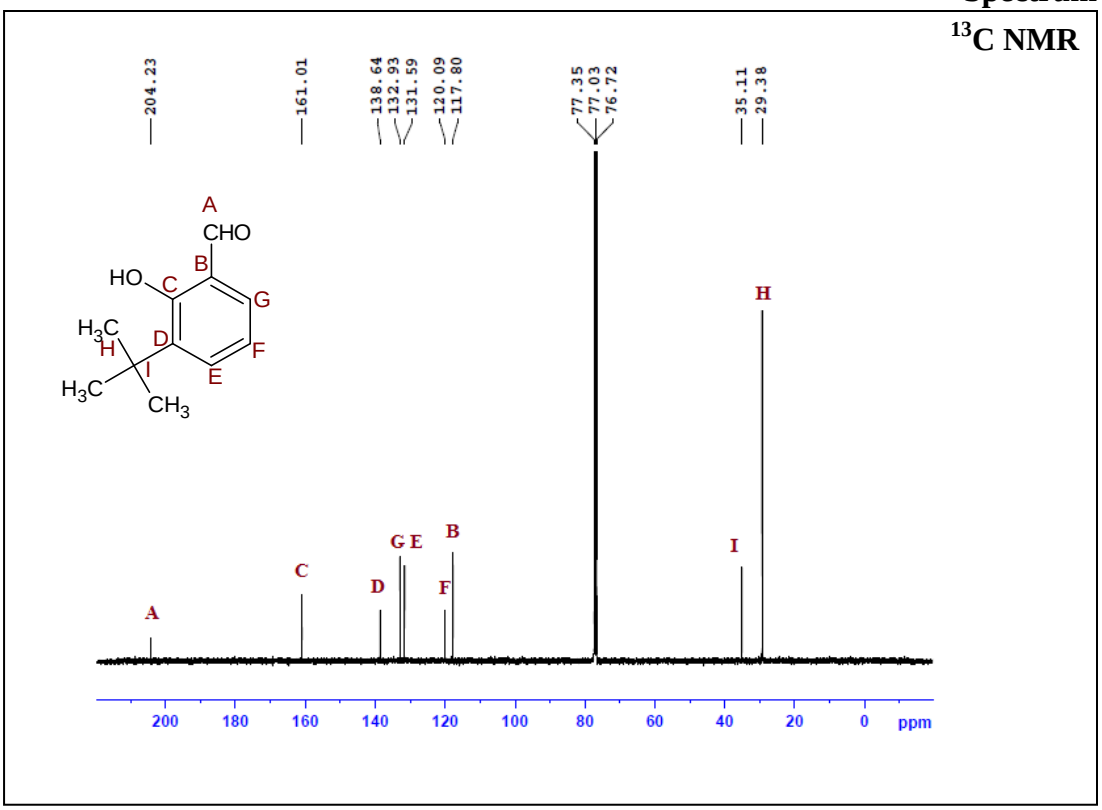

Spectrum 2.6

IR

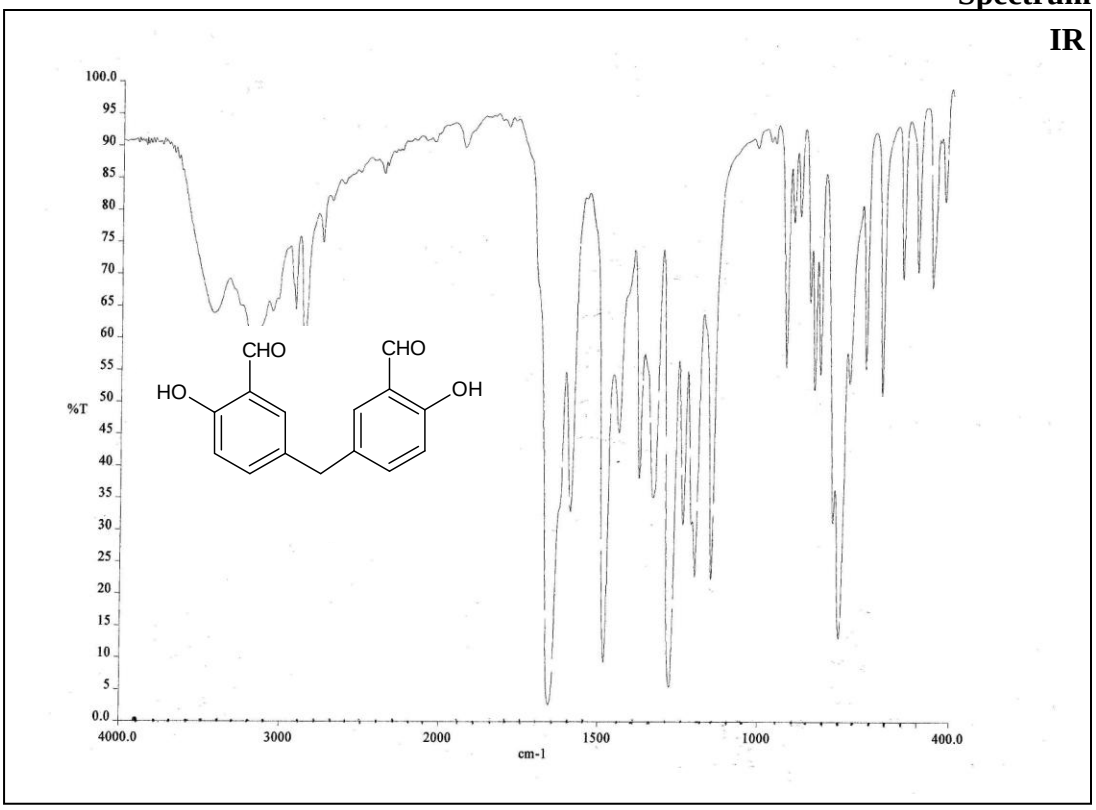

Spectrum 2.7

^{1}H NMR

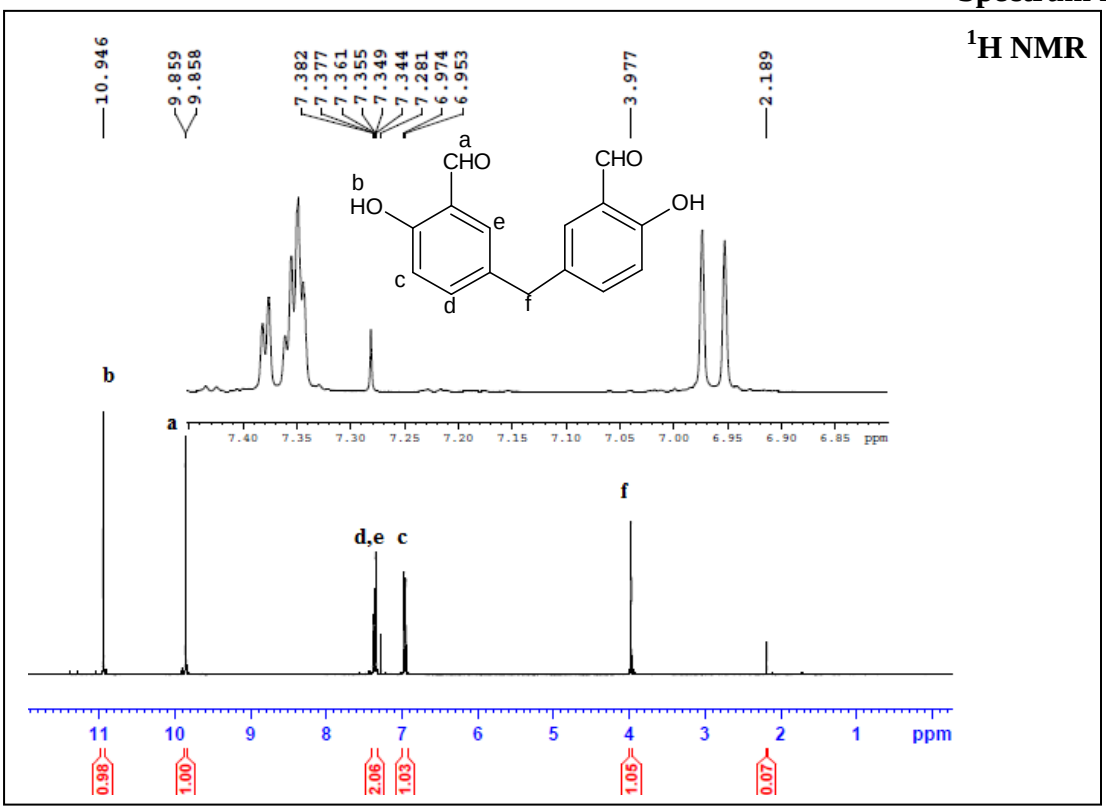

Spectrum 2.8

^{13}C NMR

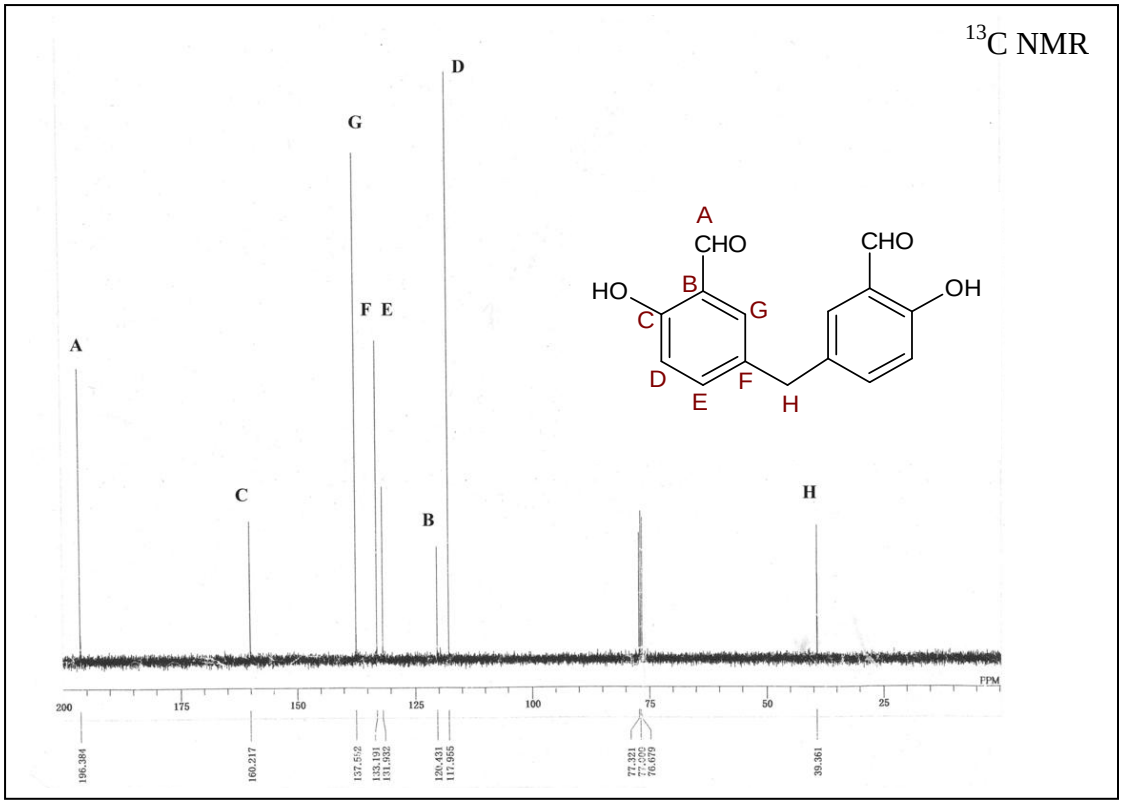

Spectrum 2.9

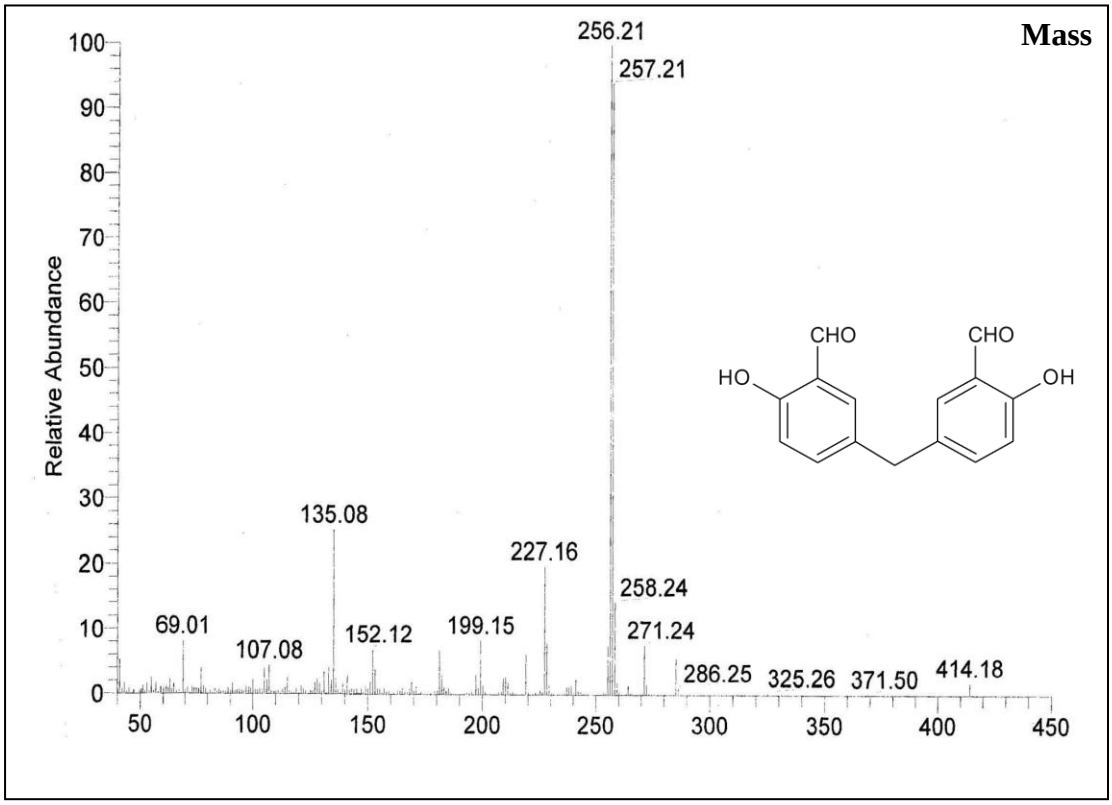

Spectrum 2.10-a

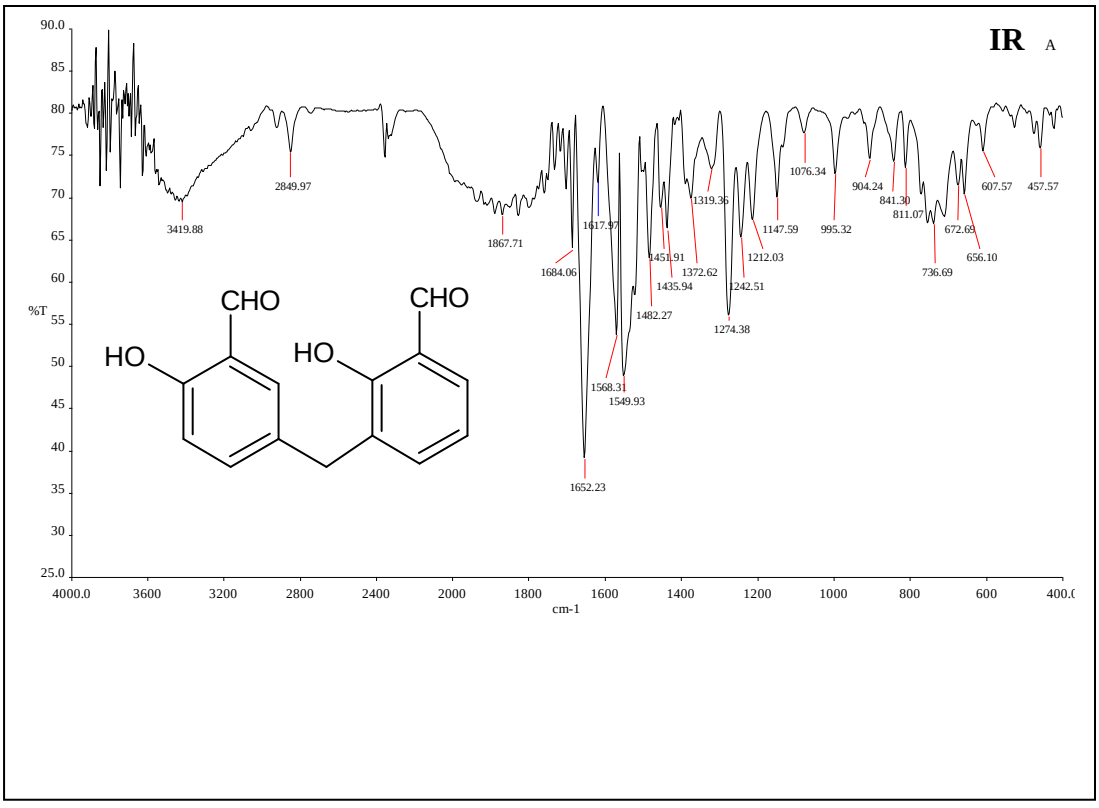

Spectrum 2.10

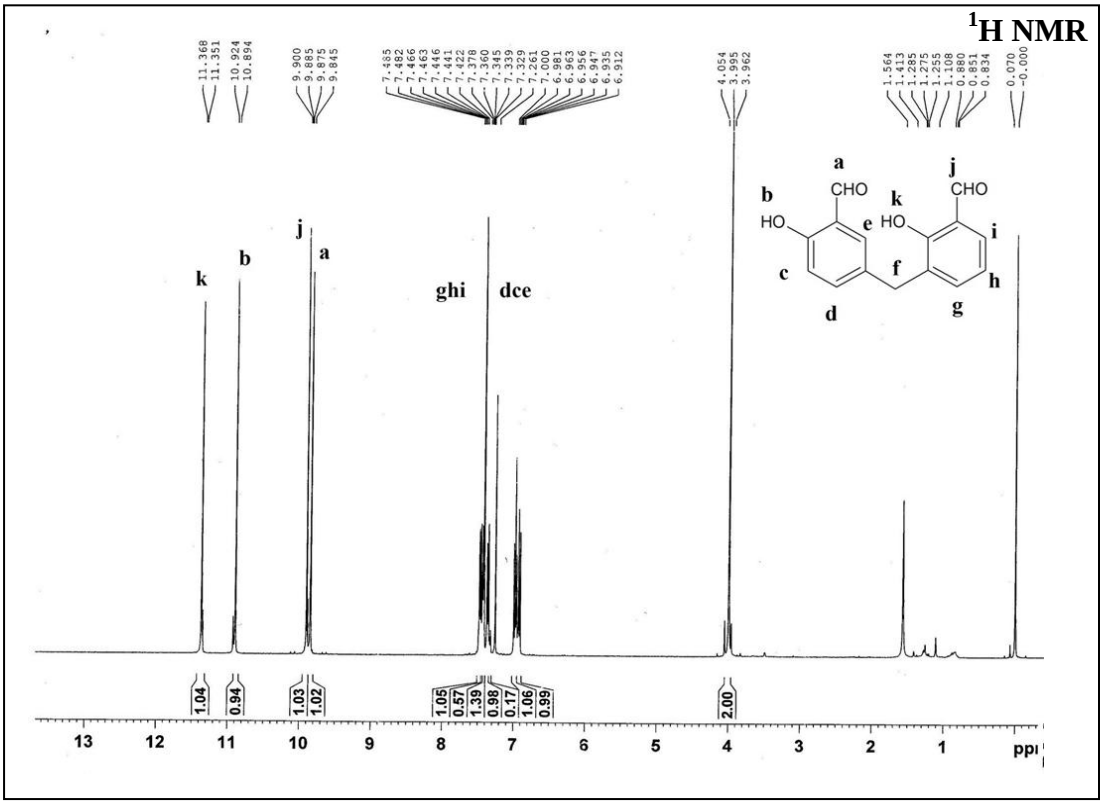

Spectrum 2.10-b

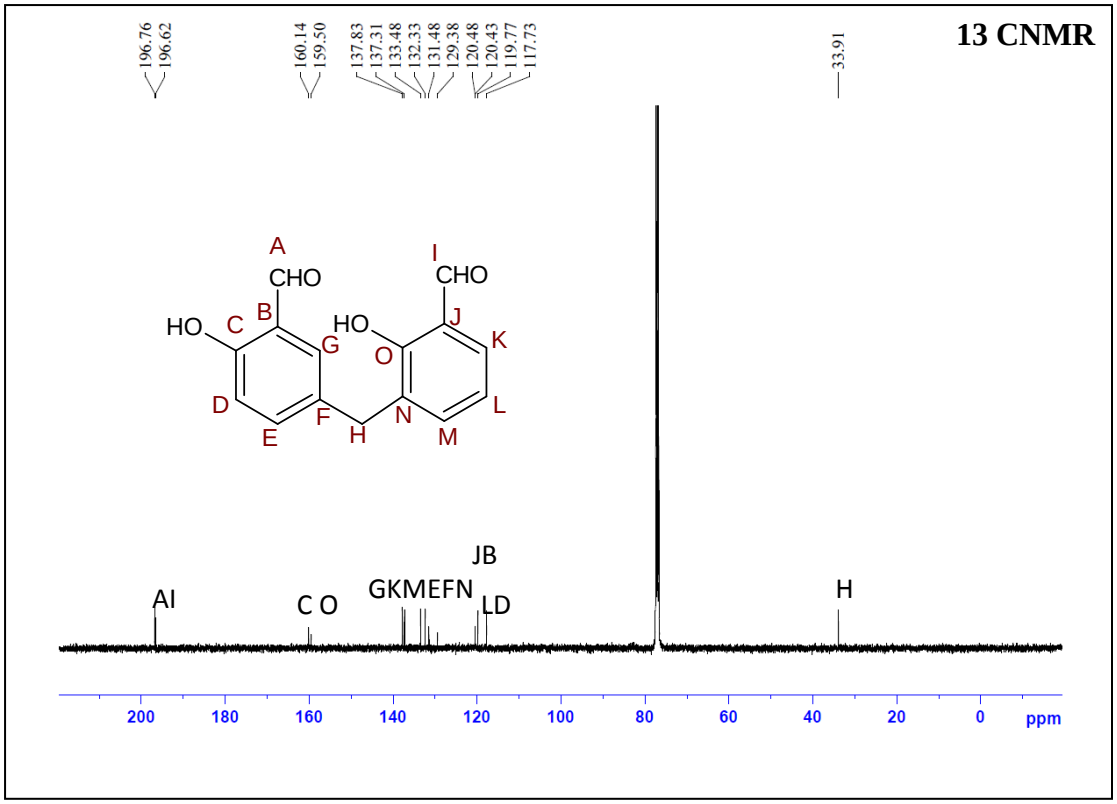

Spectrum 2.10-c

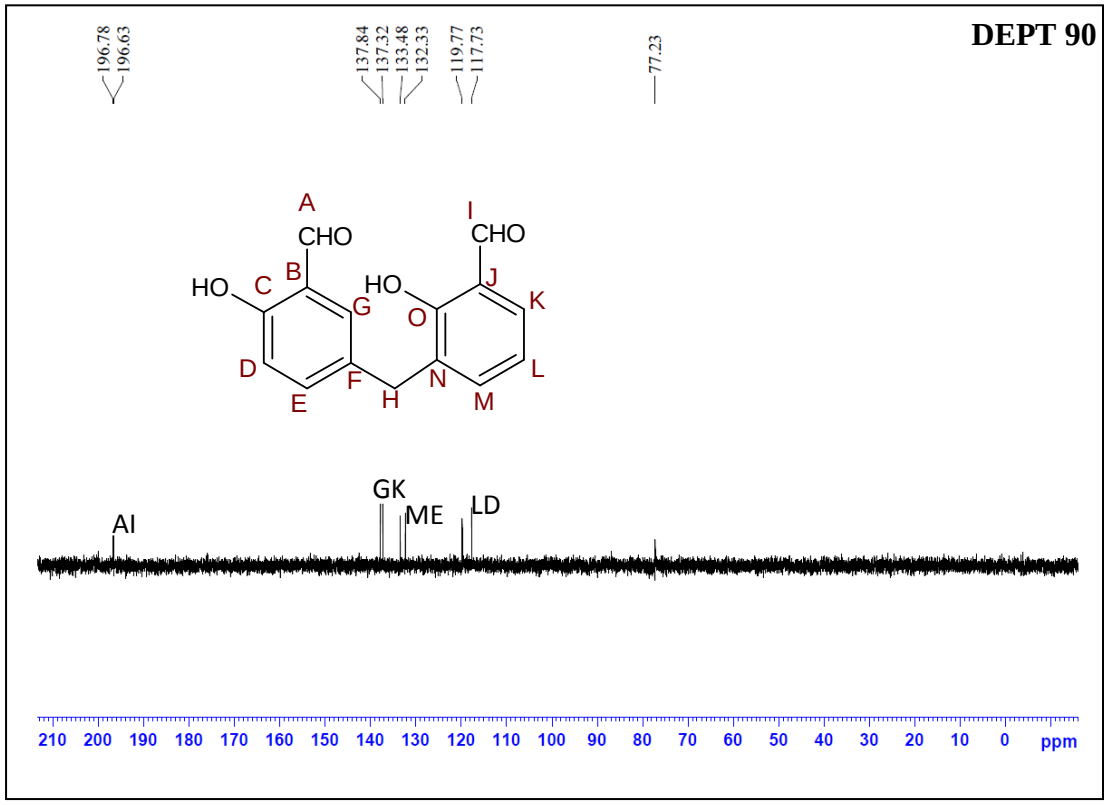

Spectrum 2.10-d

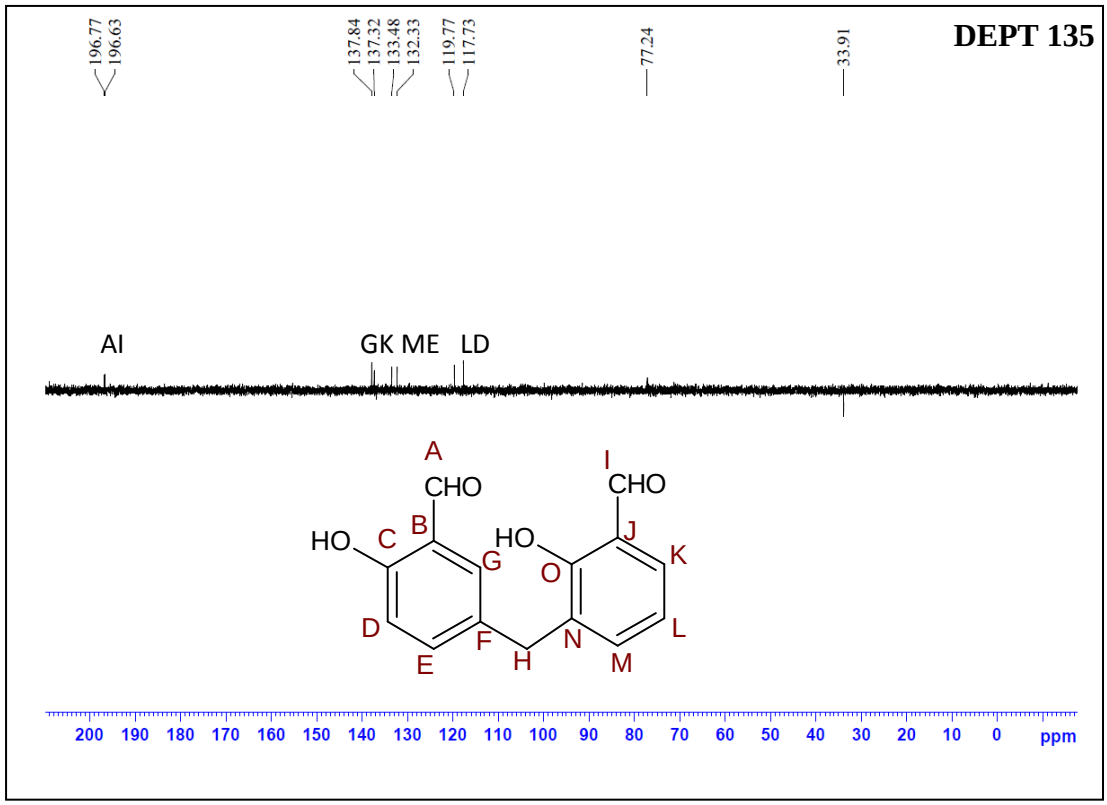

Spectrum 2.11-a

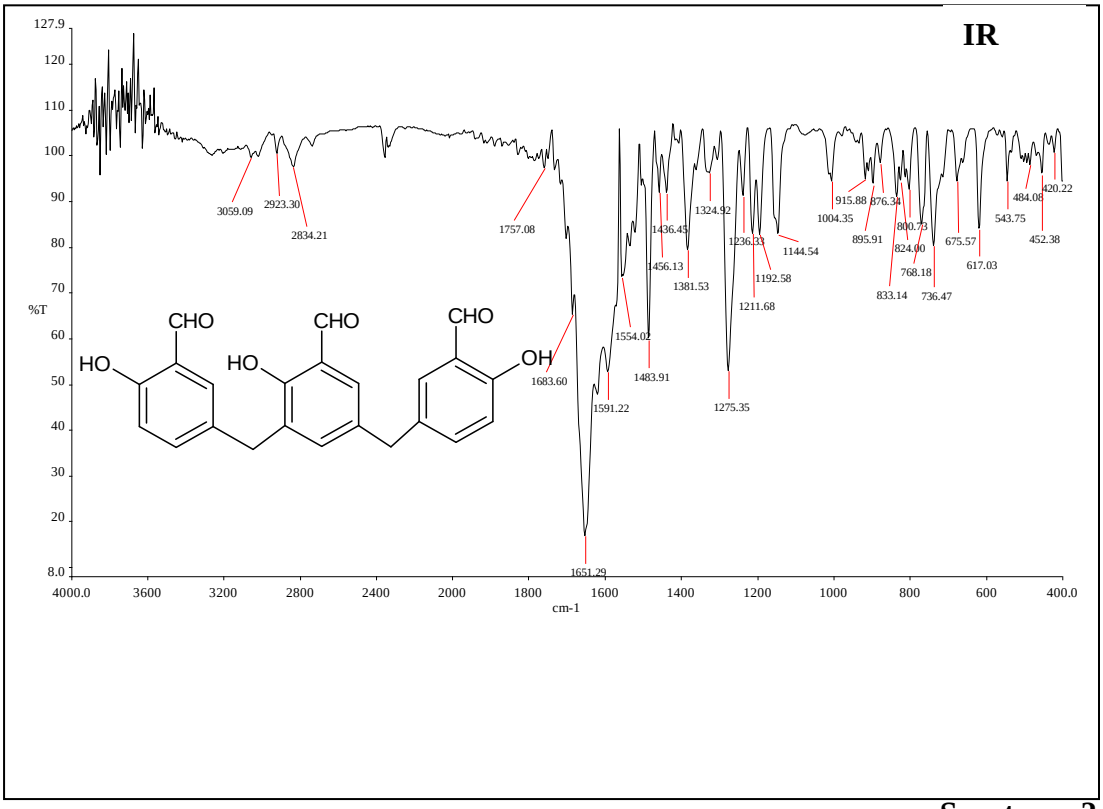

Spectrum 2.11

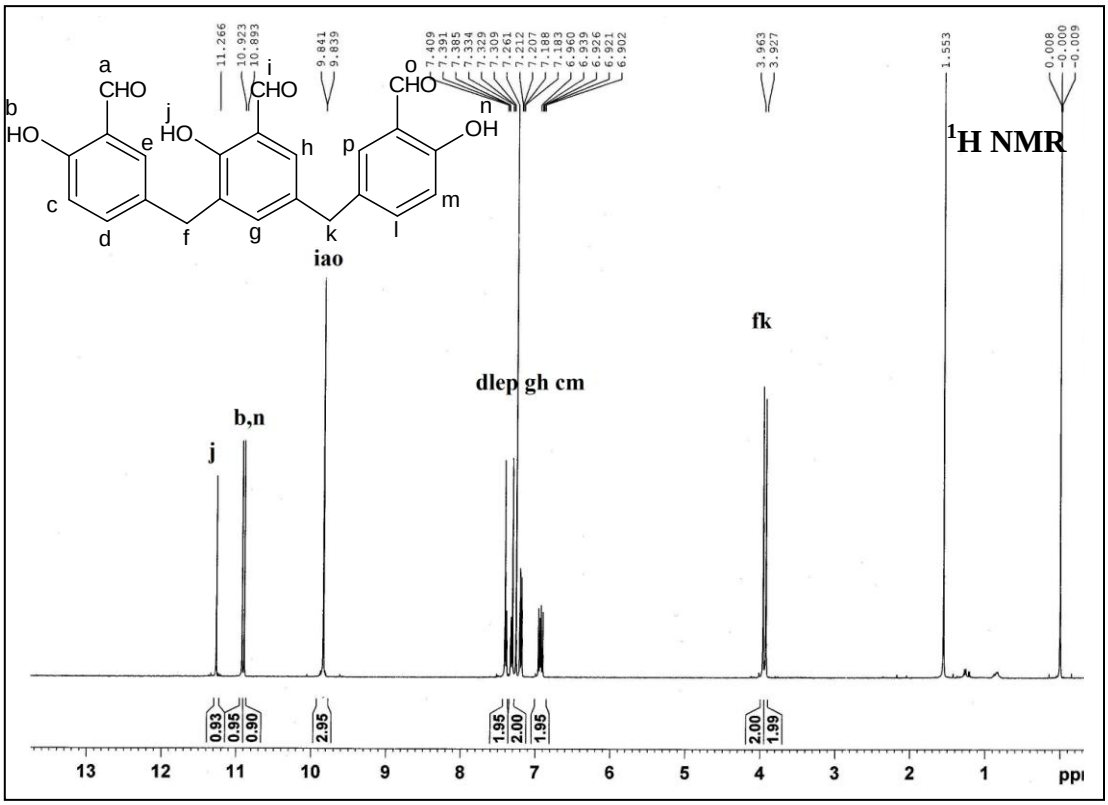

Spectrum 2.11-a

13 CNMR

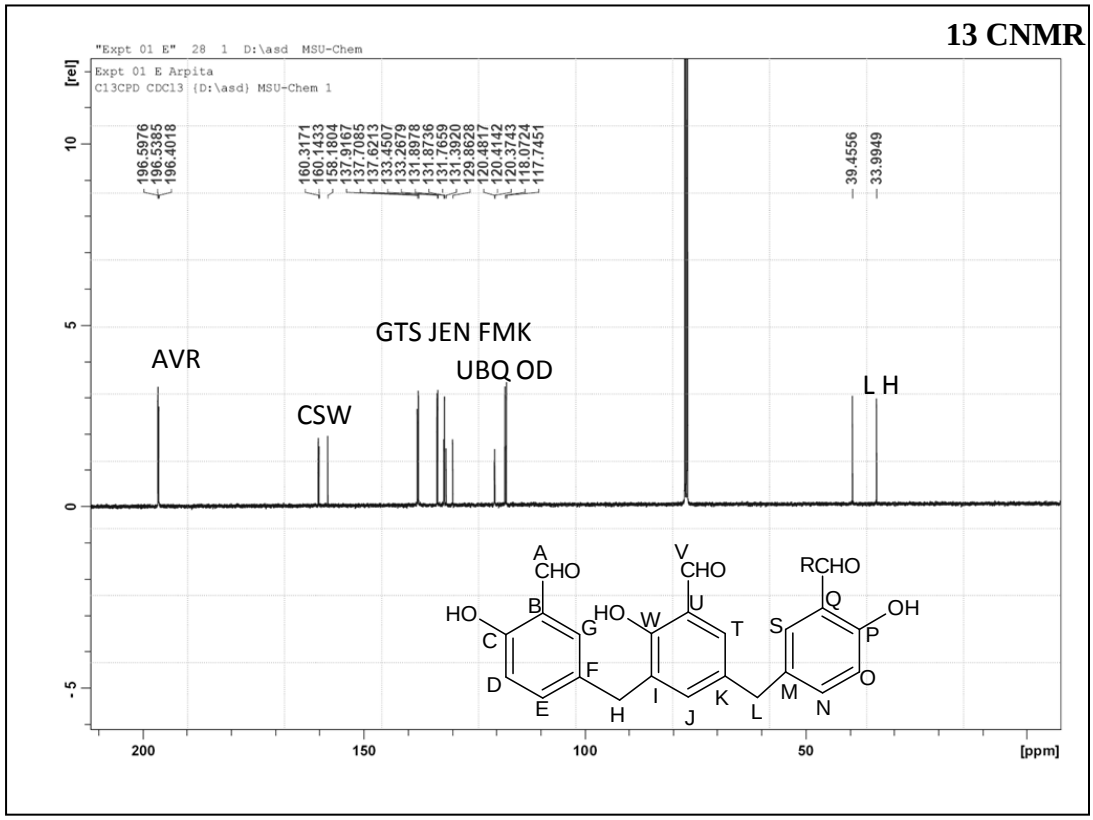

Spectrum 2.11-b

DEPT 90

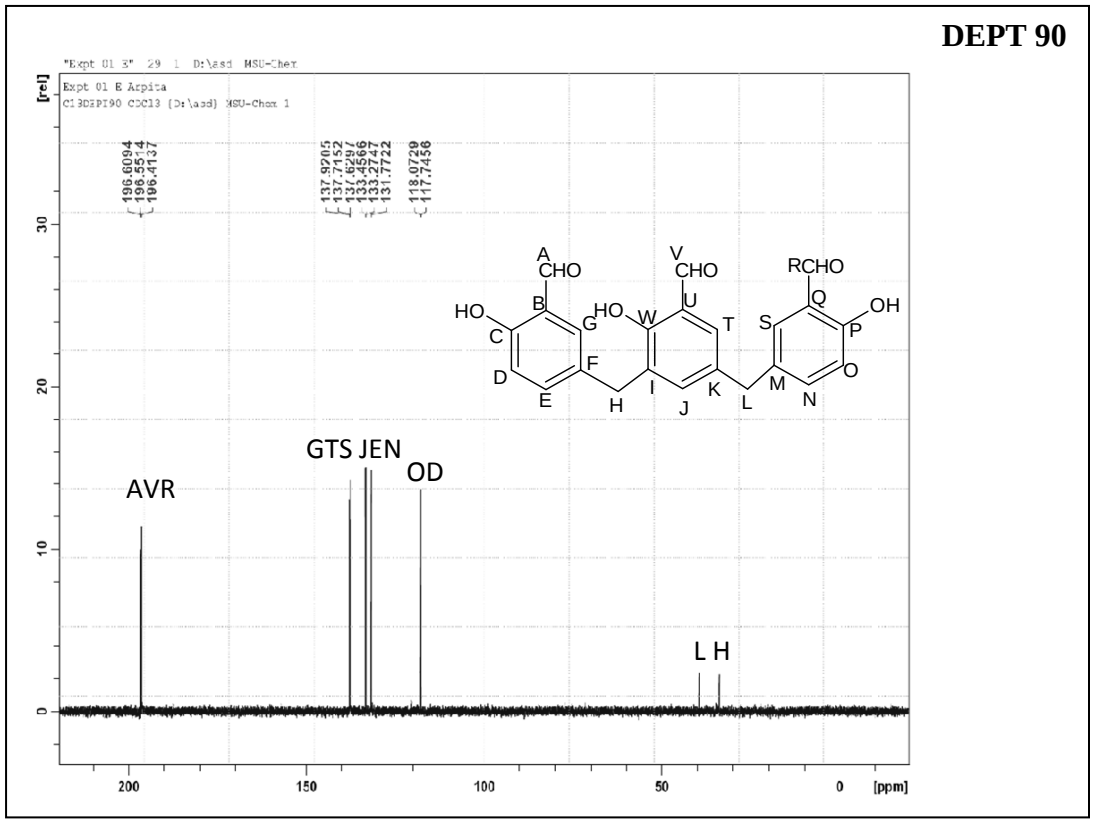

Spectrum 2.11-c

DEPT 135

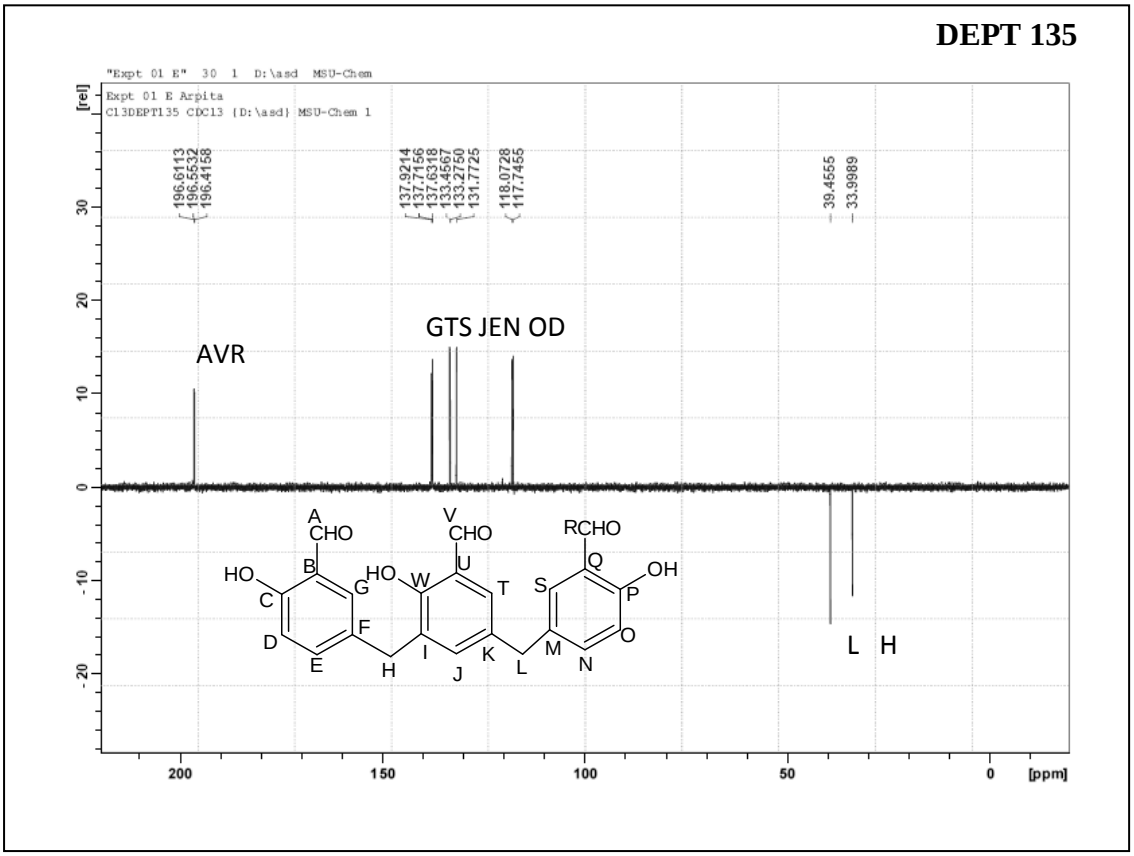

Spectrum 2.11-d

MASS

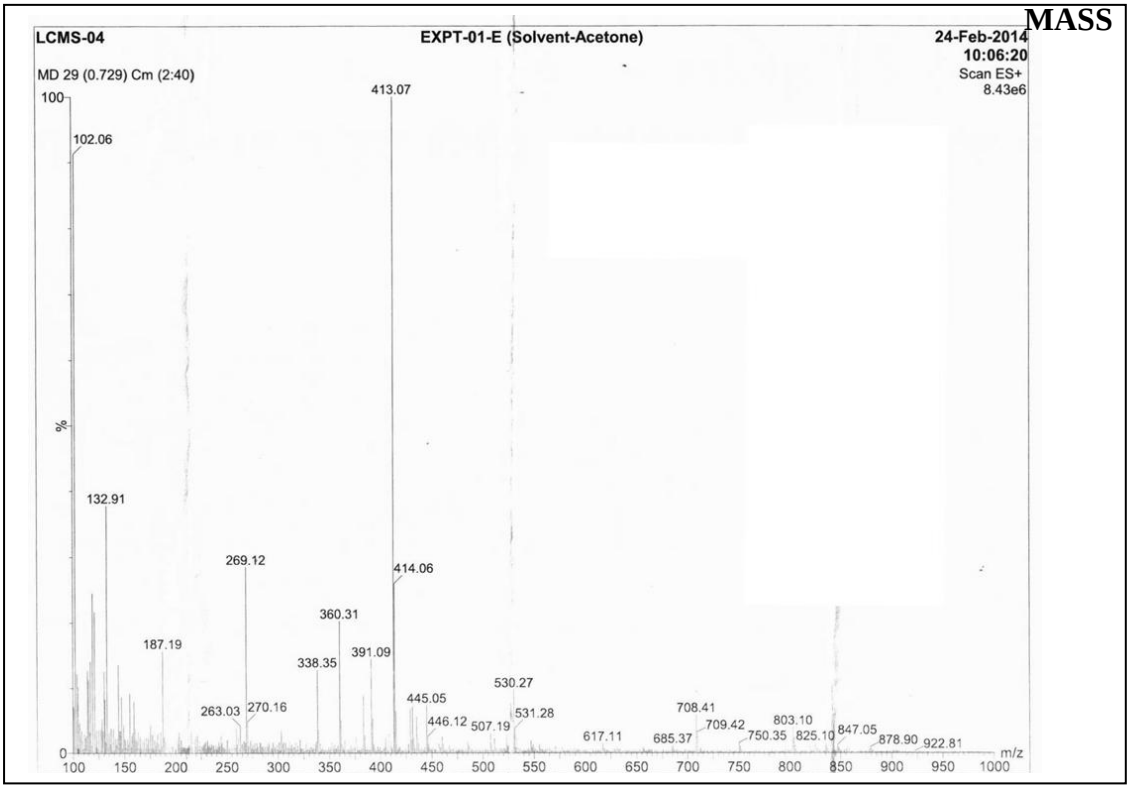

Spectrum 2.12

^{1}H NMR

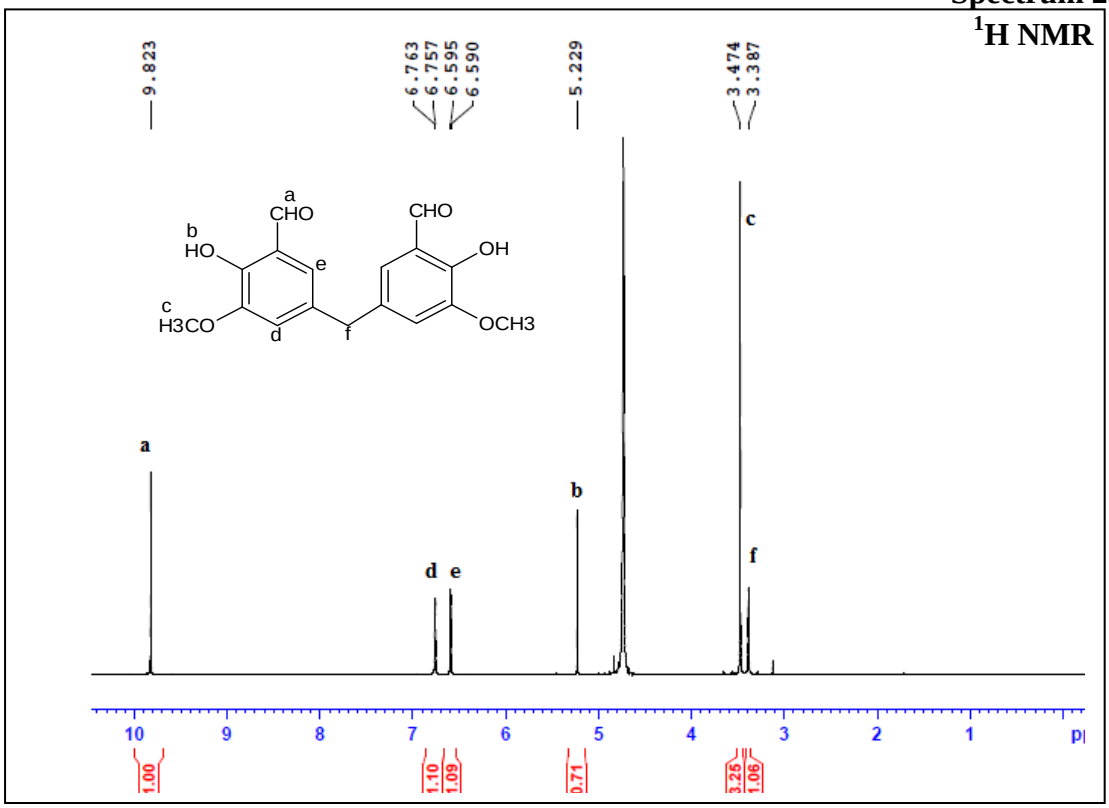

Spectrum 2.13

IR

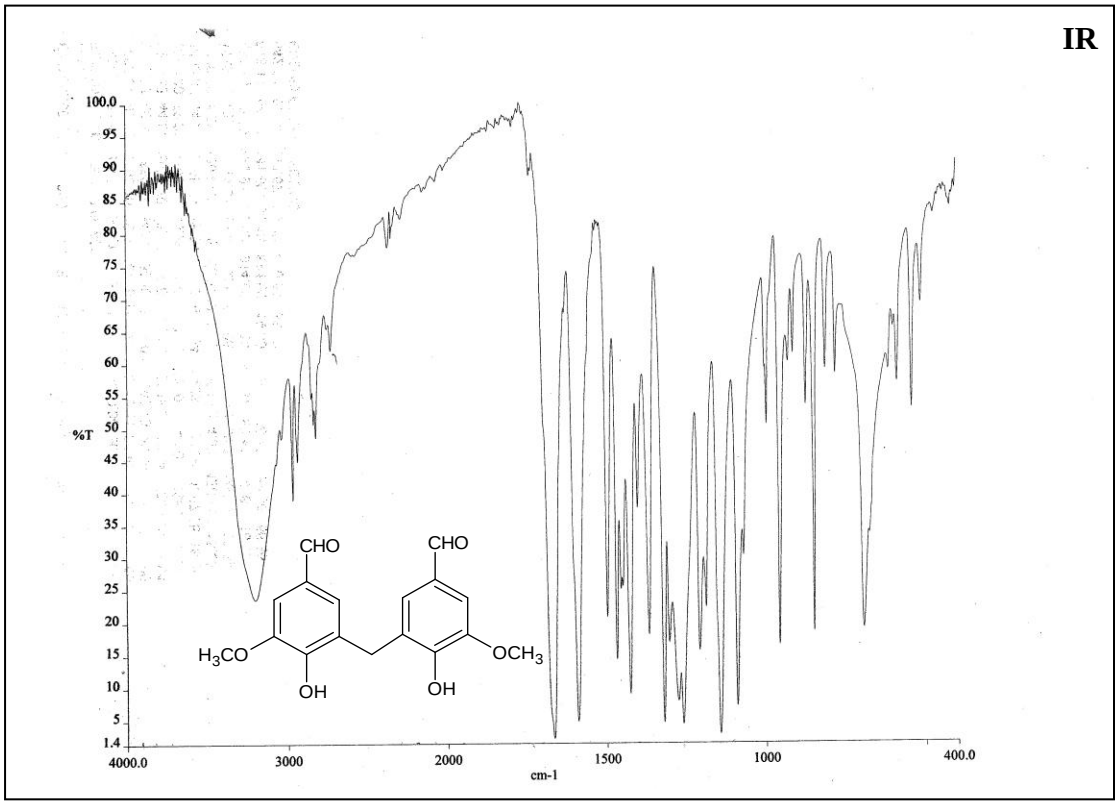

Spectrum 2.14

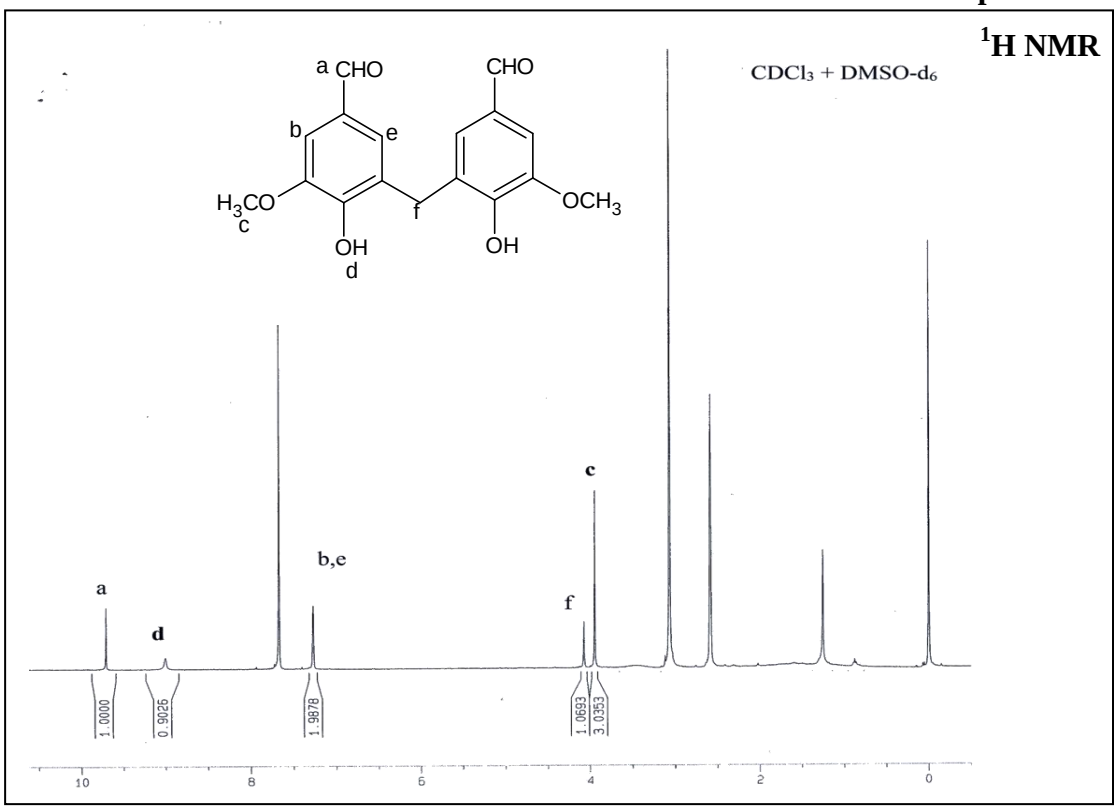

Spectrum 2.15

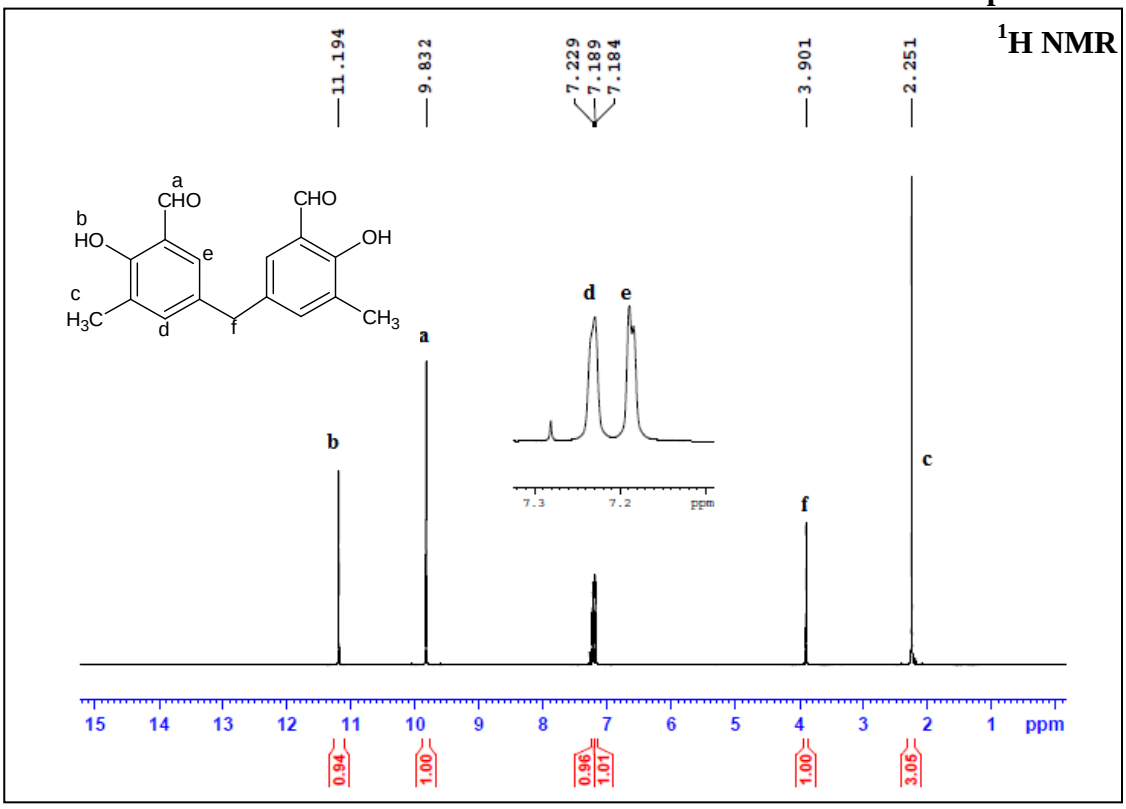

Spectrum 2.16

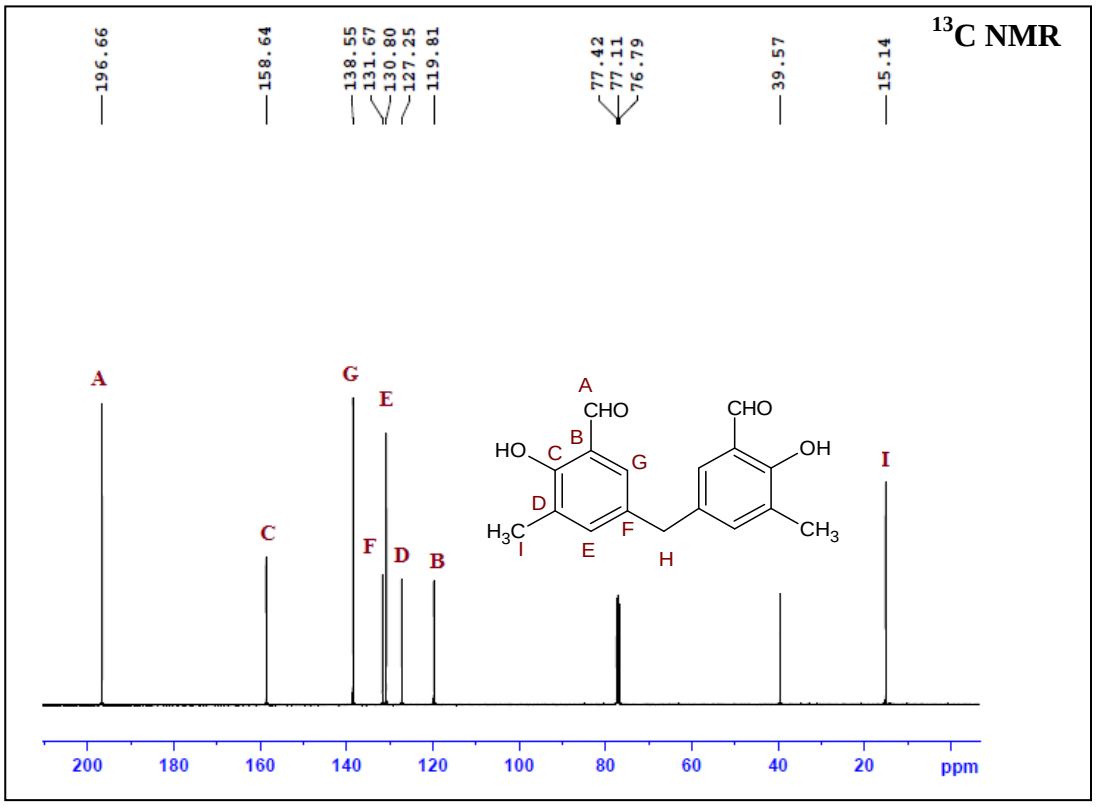

Spectrum 2.17

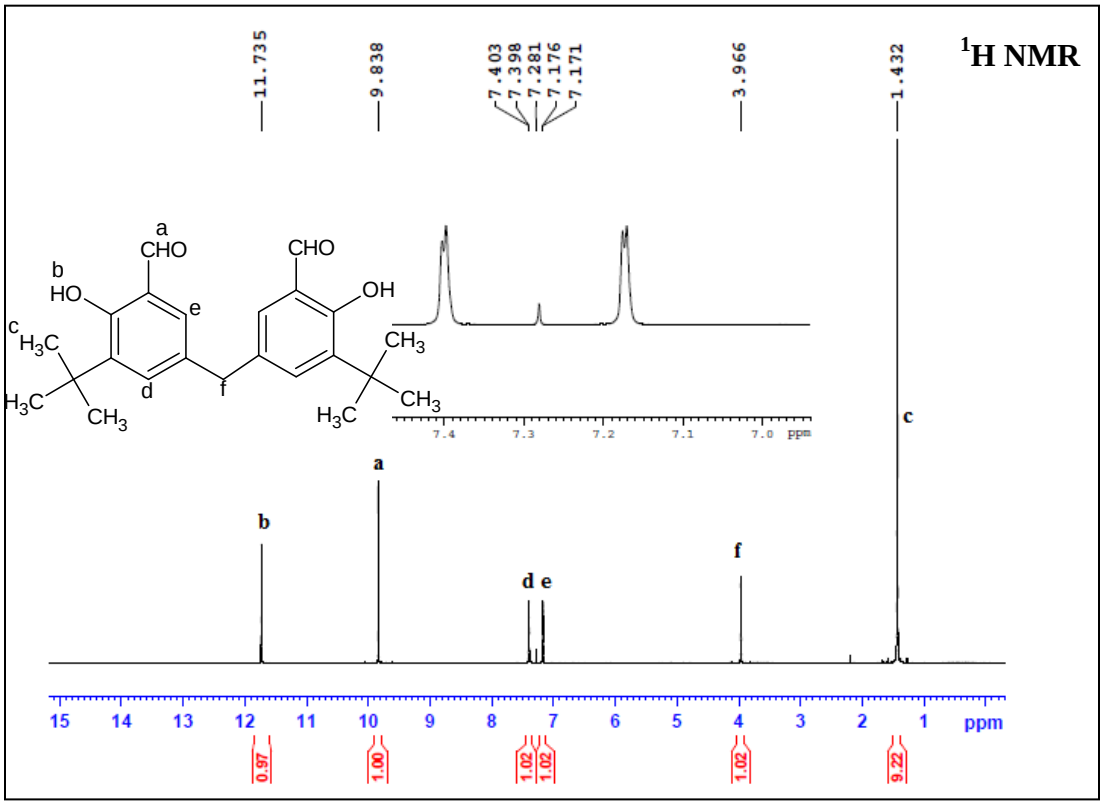

Spectrum 2.18

^{13}C NMR

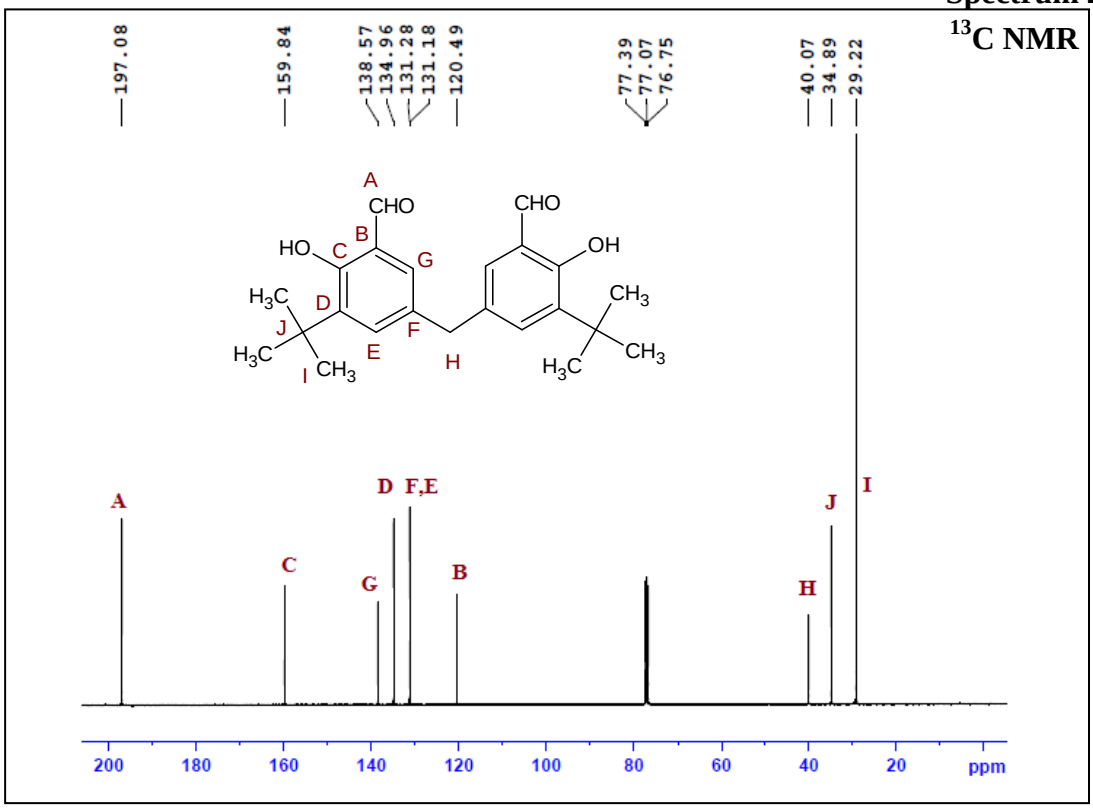

Spectrum 2.19-a

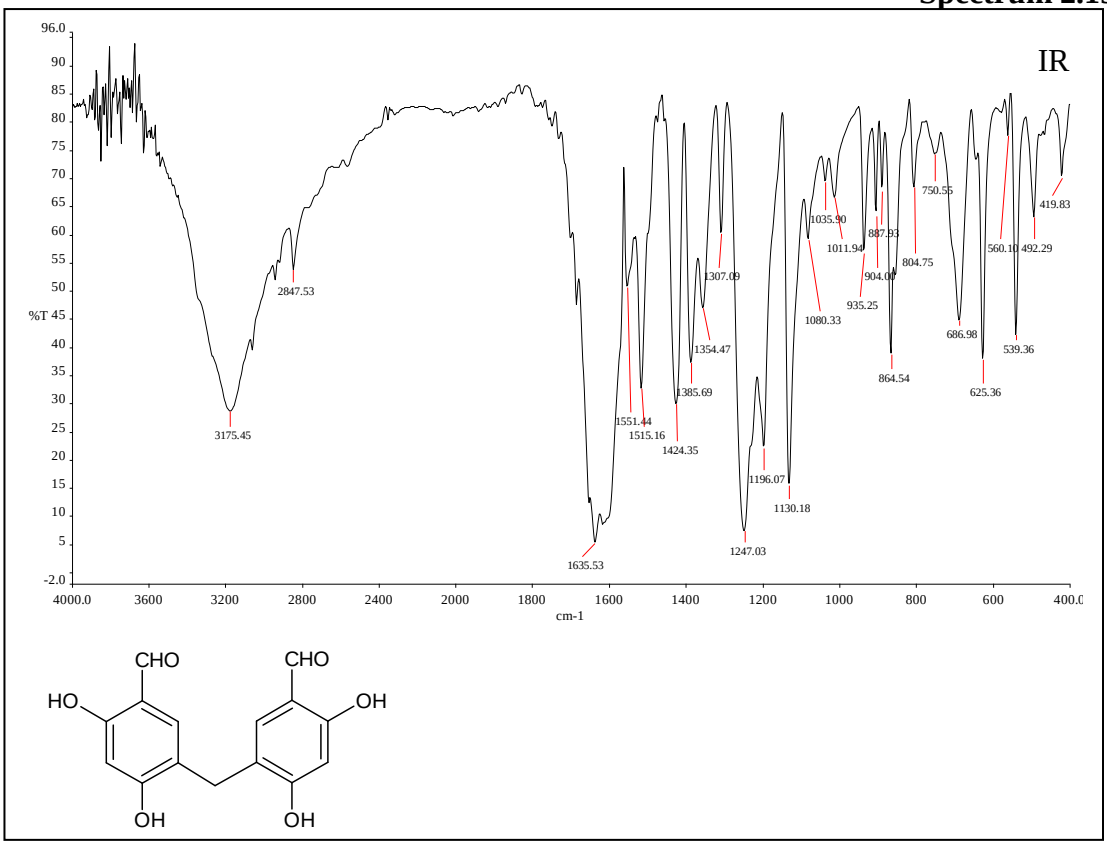

Spectrum 2.19-b

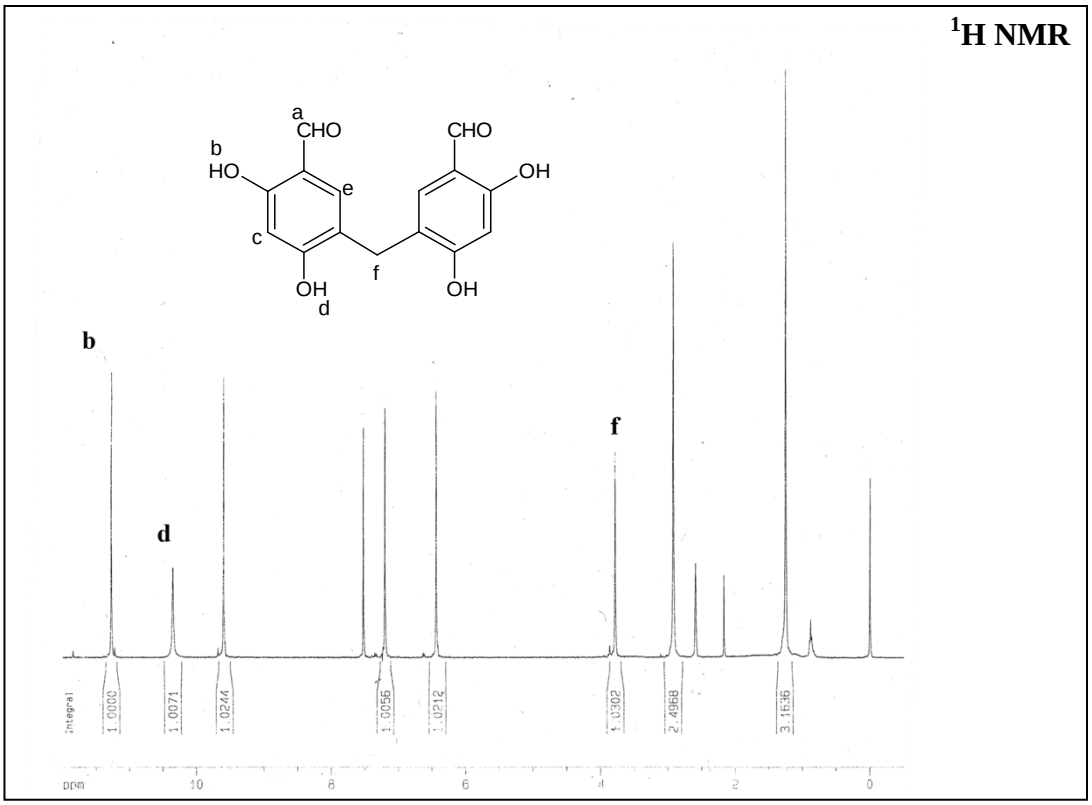

Spectrum 2.20

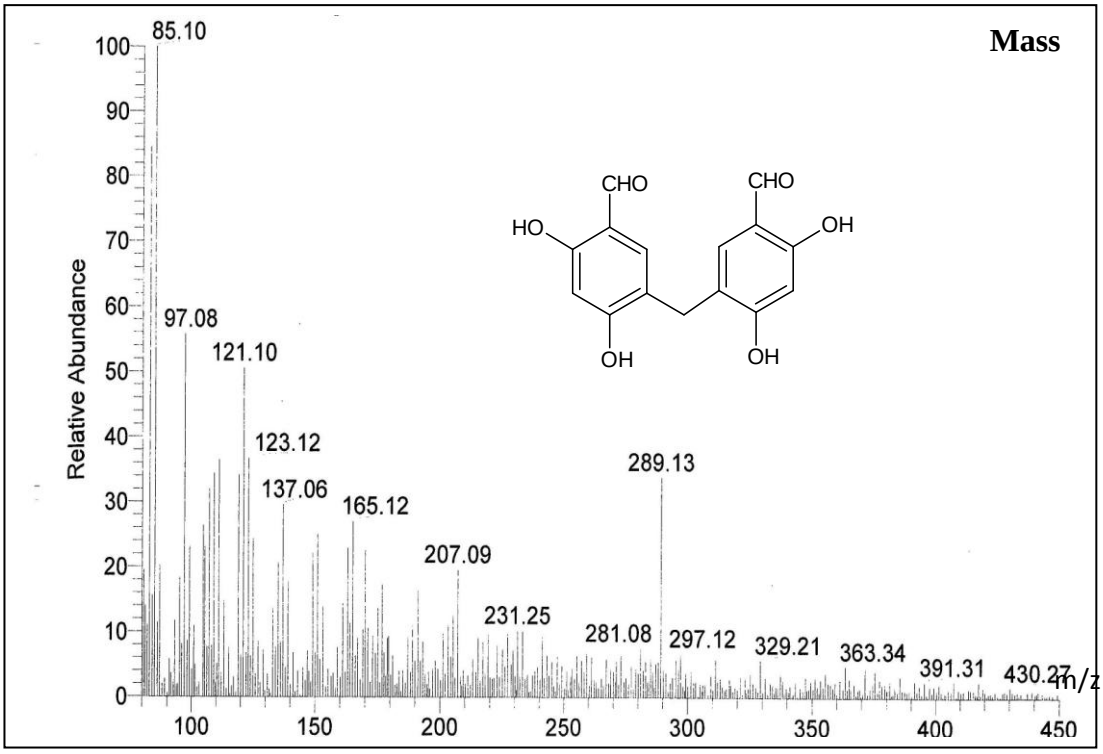

Spectrum 2.21

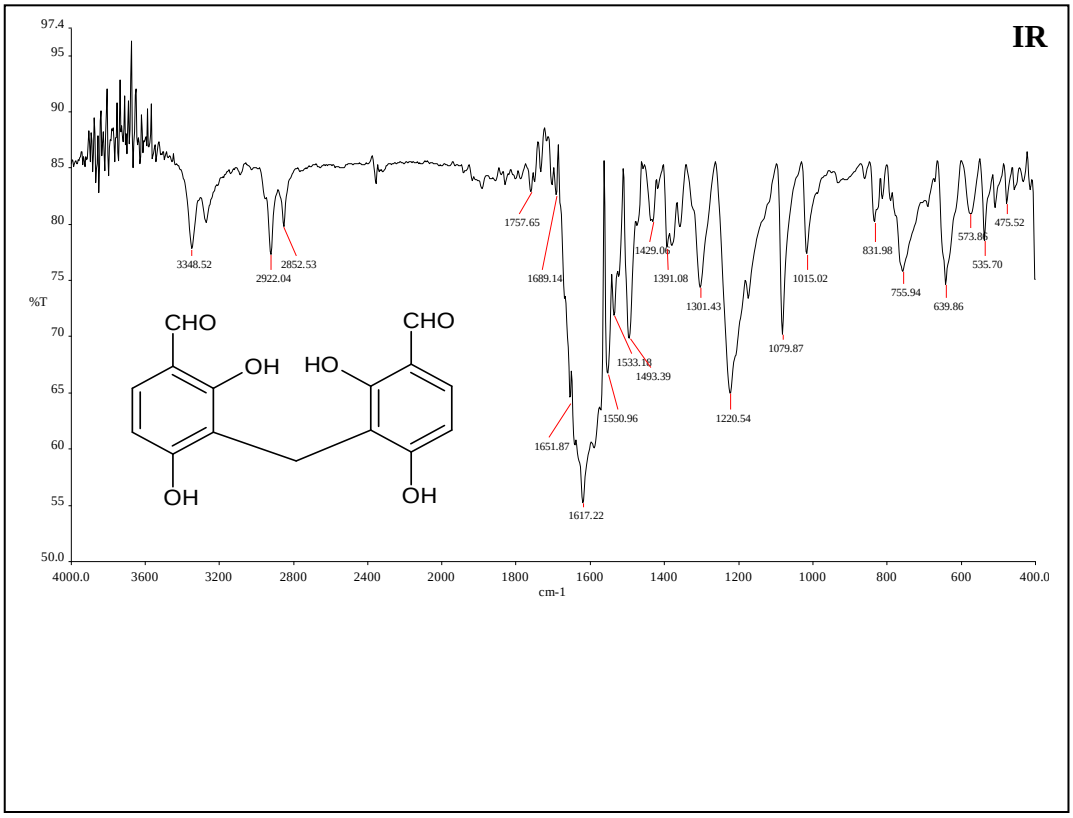

Spectrum 2.21-b

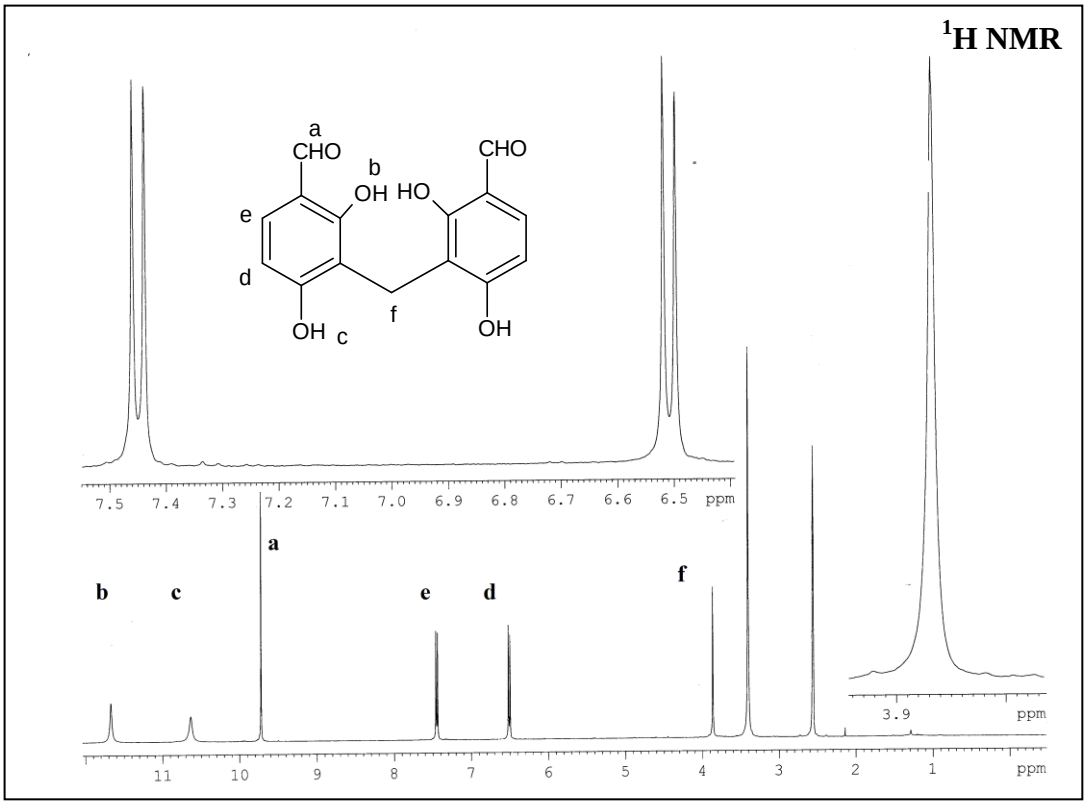

Spectrum 2.21-c

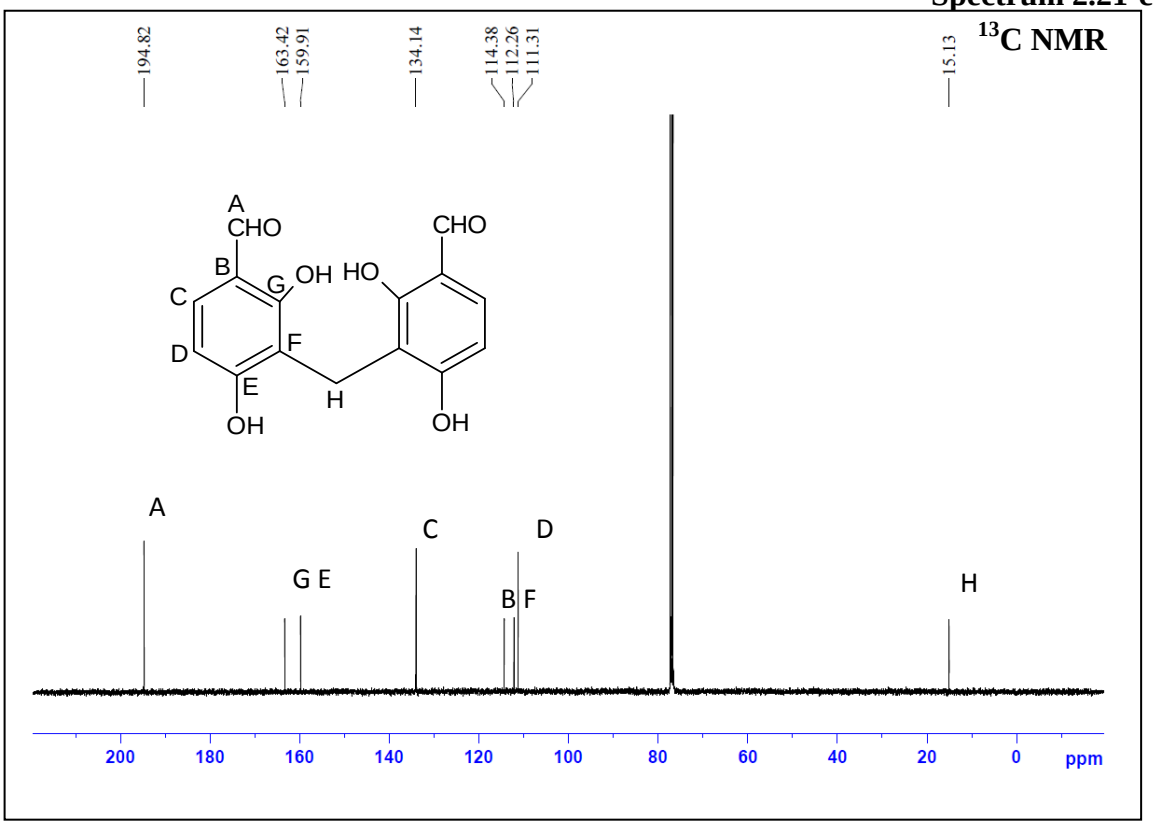

Spectrum 2.21-d

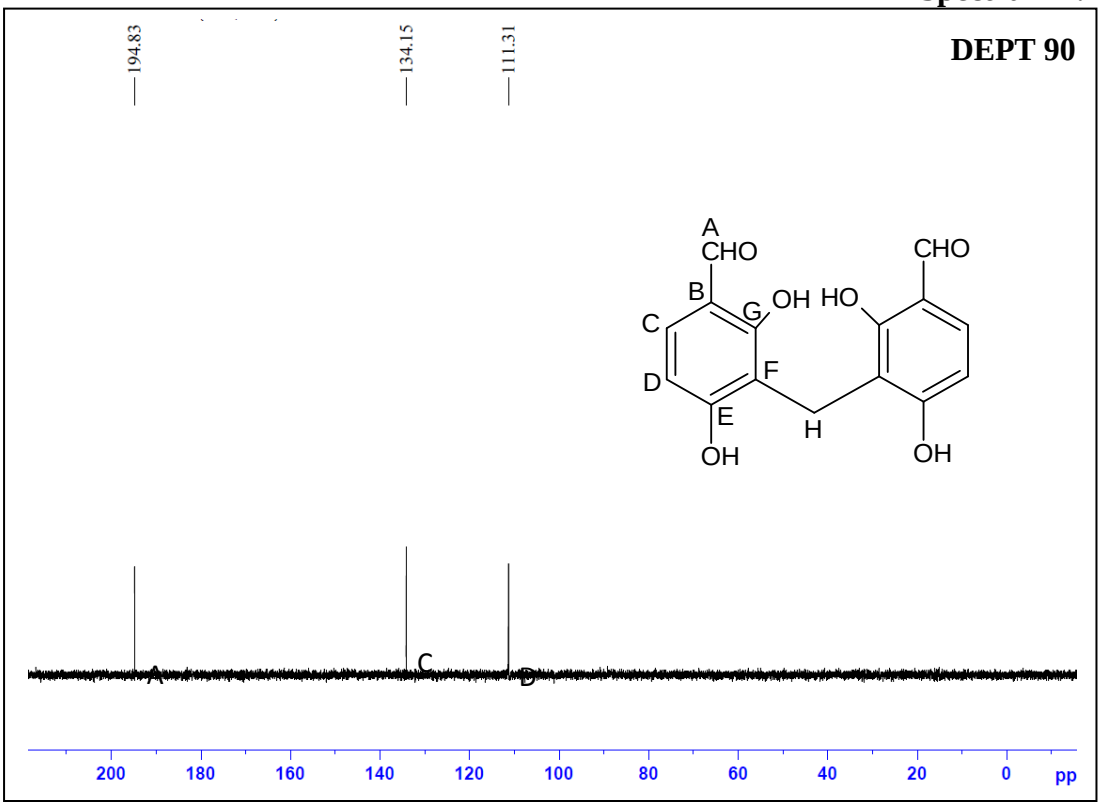

Spectrum 2.21-e

DEPT 135

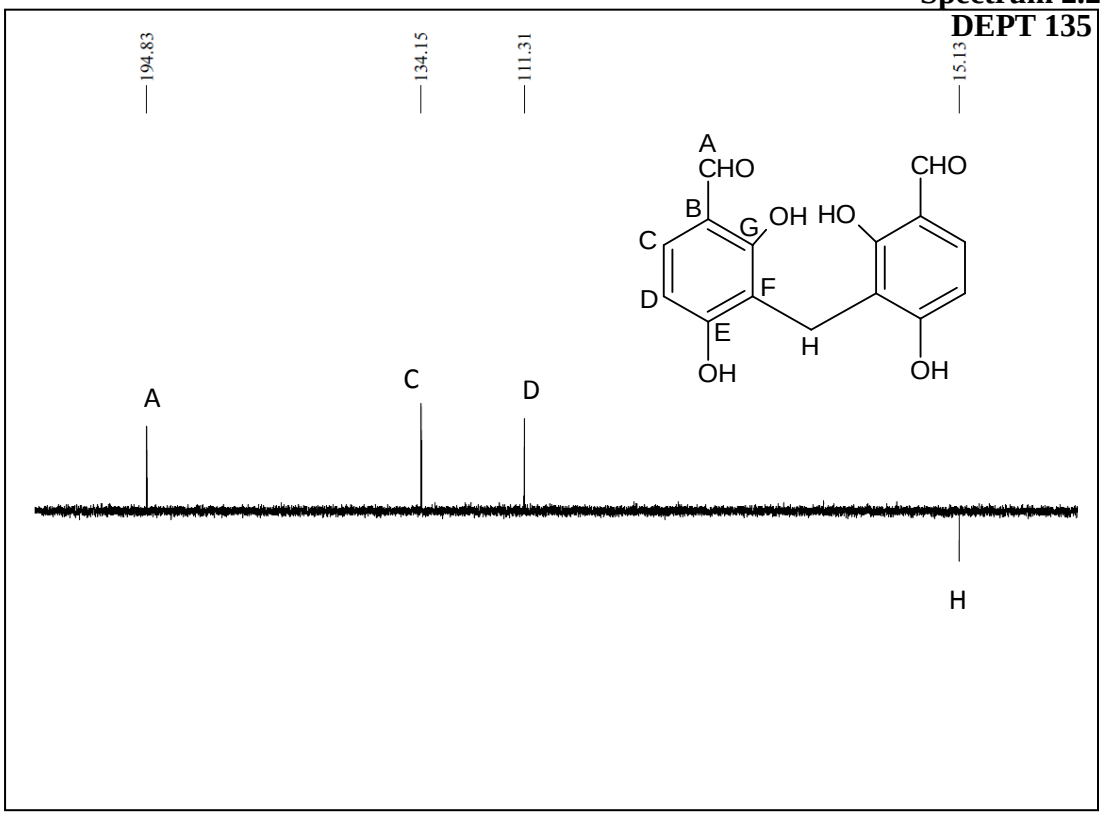

Spectrum 2.22

Mass

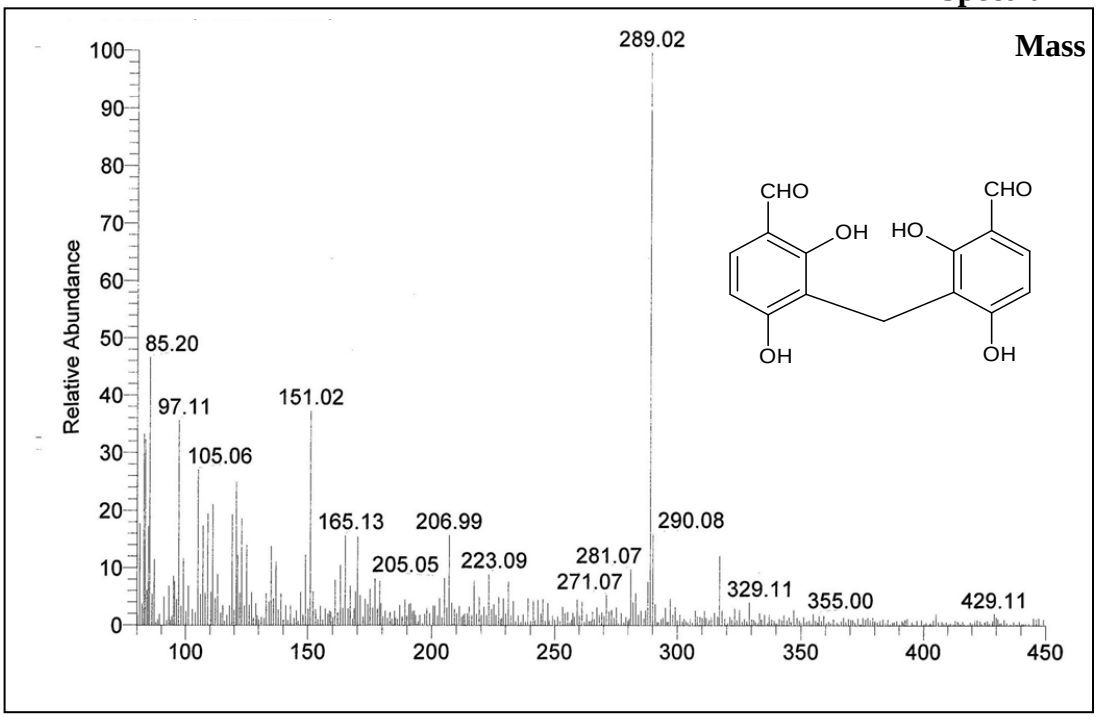

Spectrum 2.23

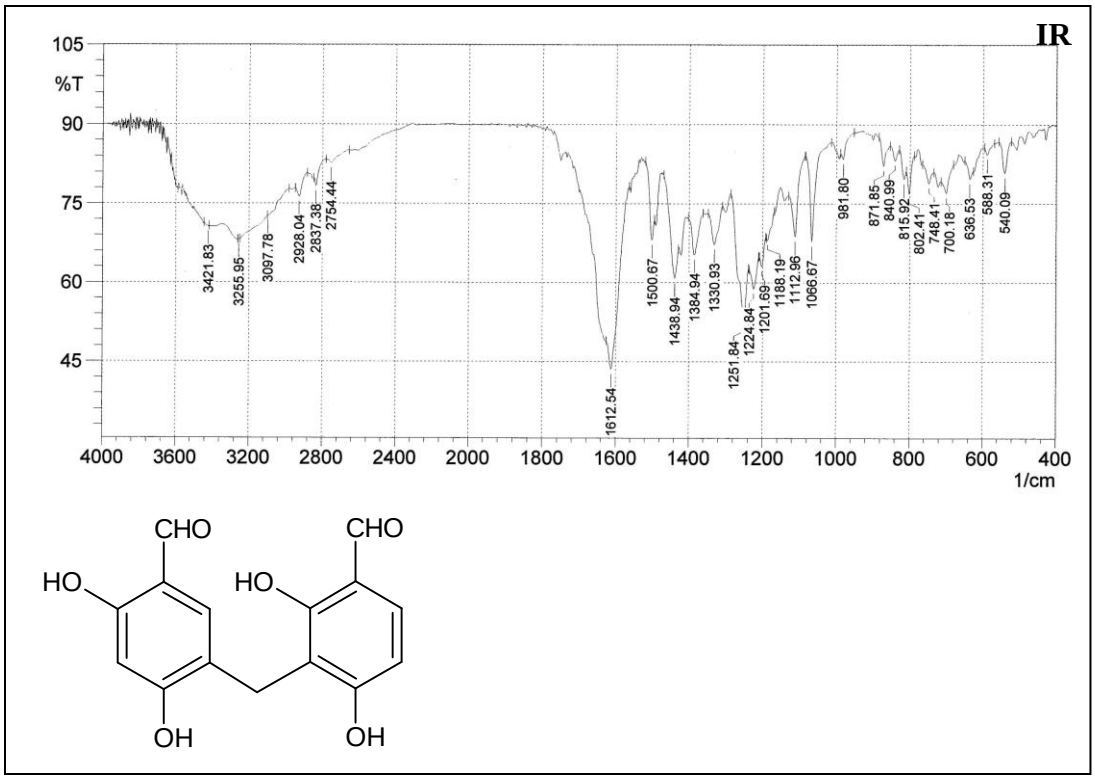

Spectrum 2.24

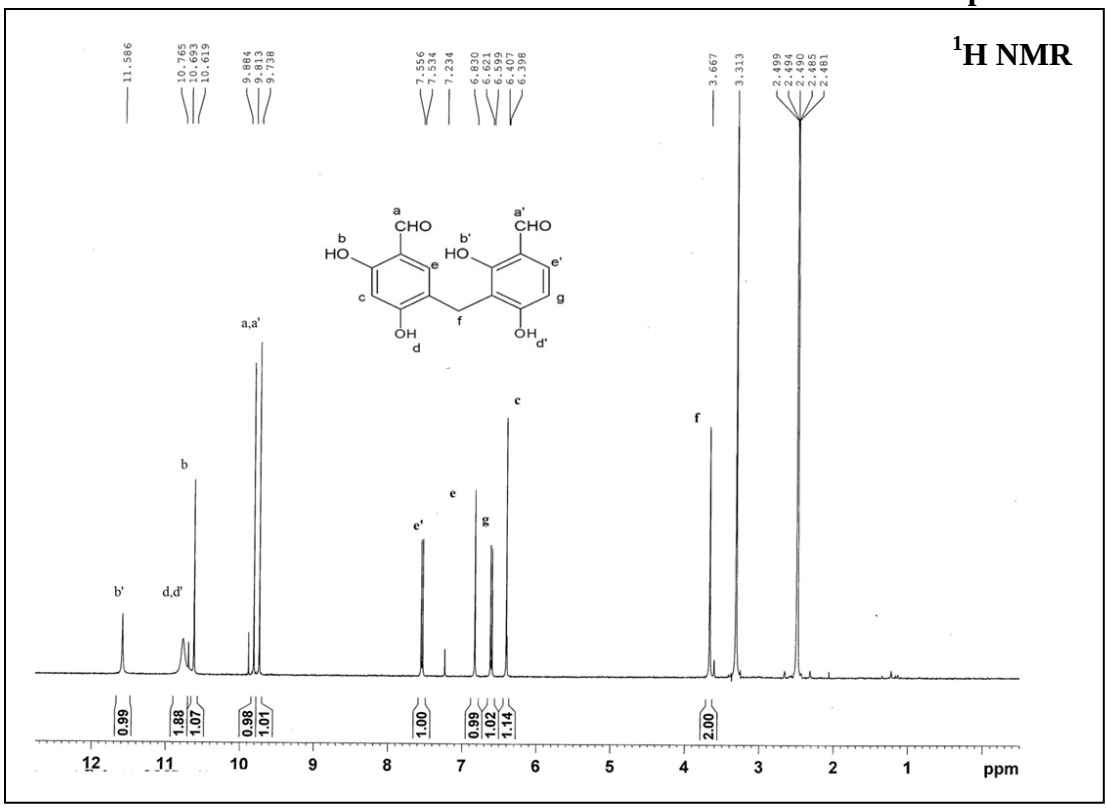

Spectrum 2.24-a

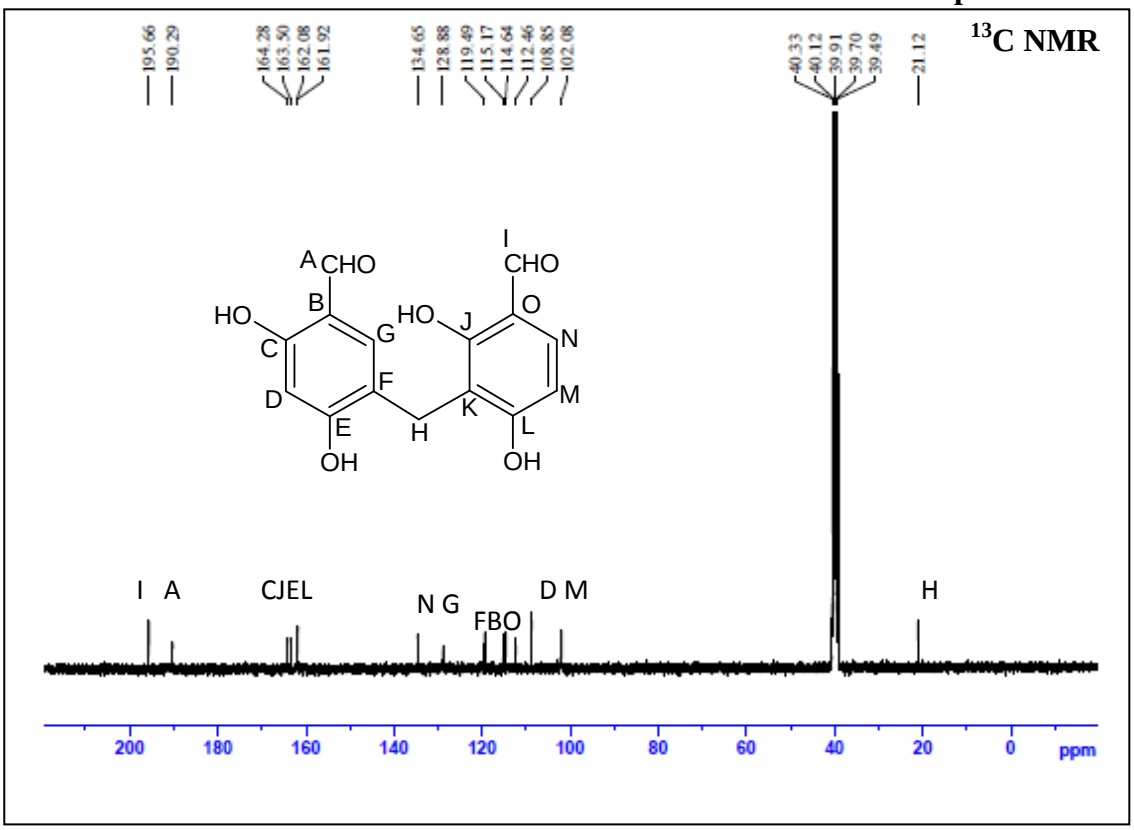

Spectrum 2.24-b

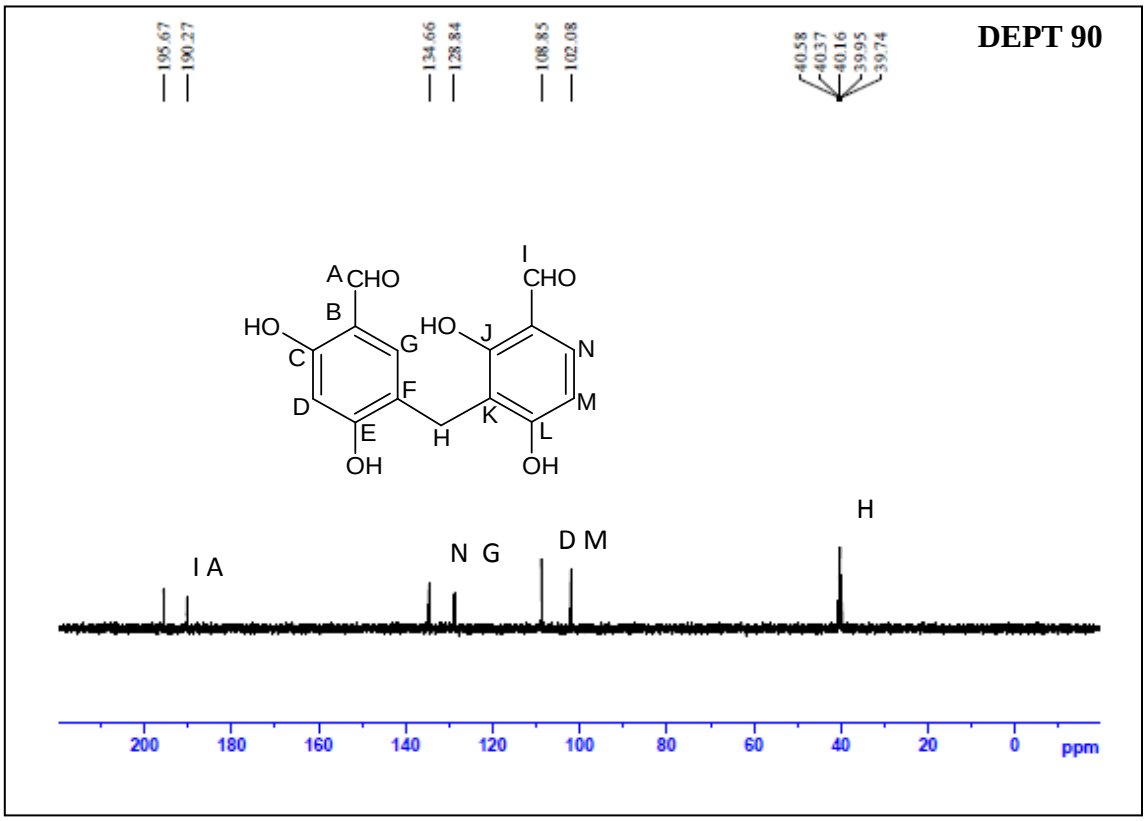

Spectrum 2.24-c

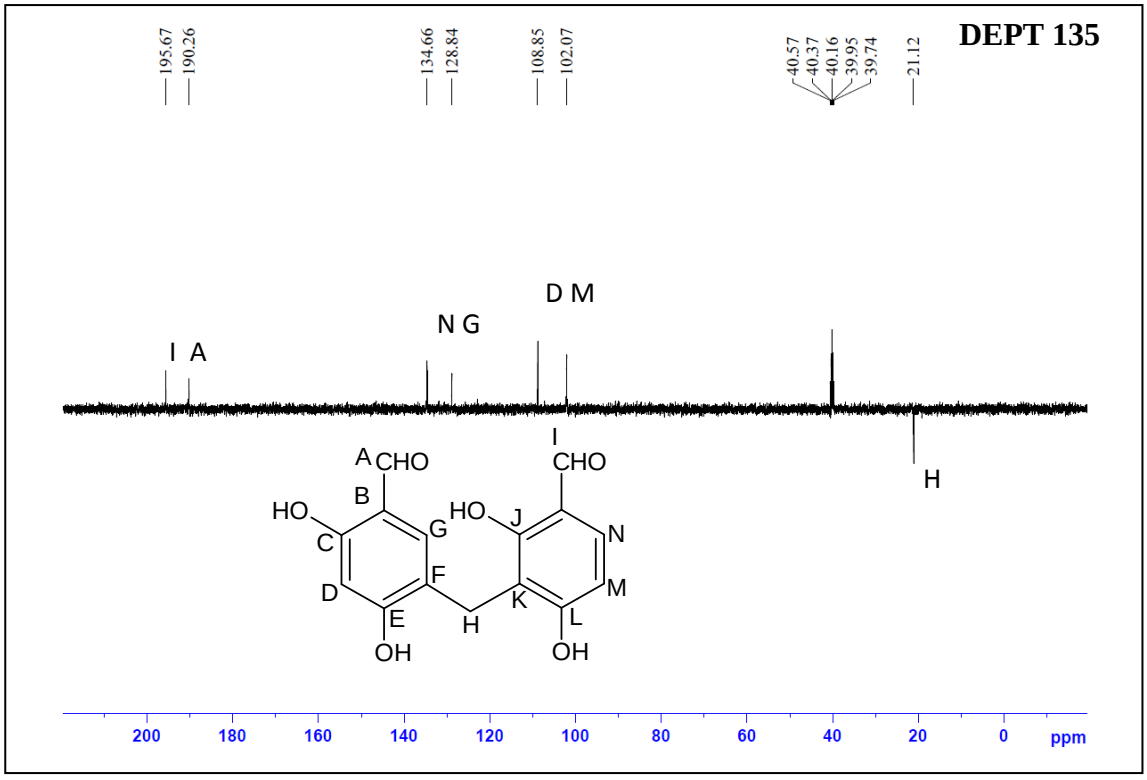

Spectrum 2.25

Mass

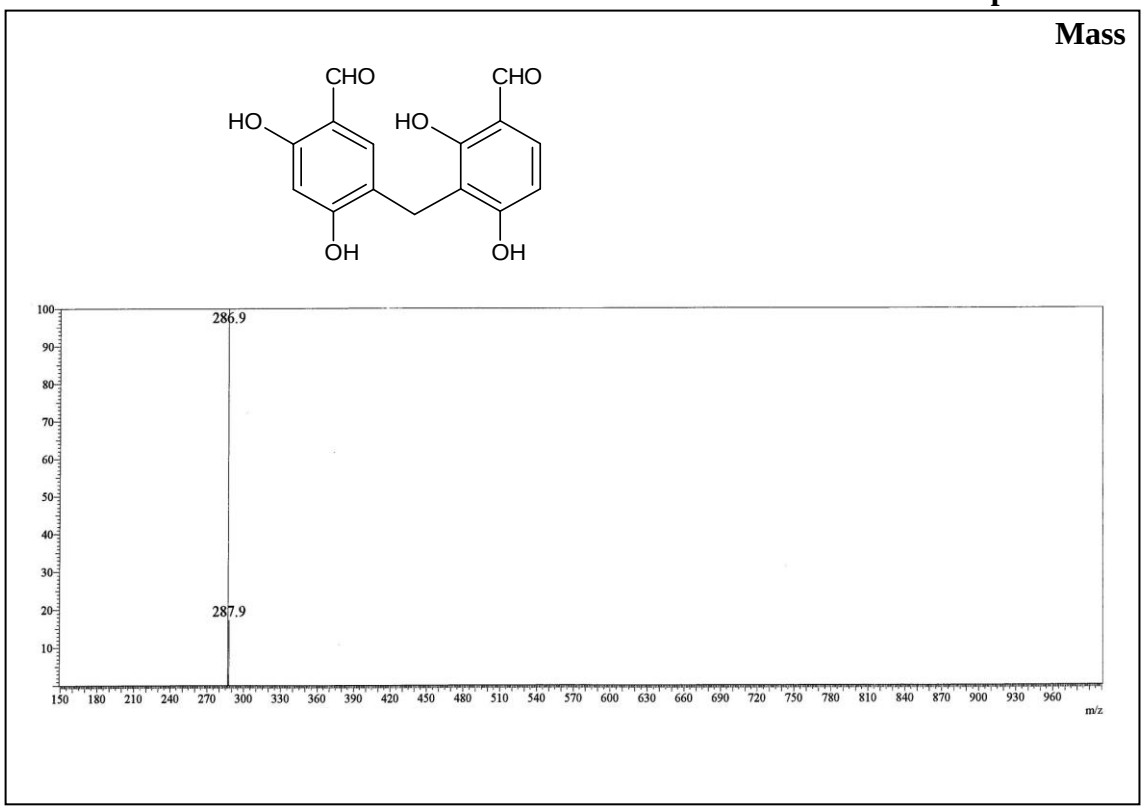

Chromatogram 2.26

HPLC

COLUMN : YMC J'SPHERE C18(150 X4.6mm)4u
M.PHASE: 0.05%TFA BUFFER : ACN (GRADIENT)
F.RATE : 1.0 ML/MIN @ 220 nm

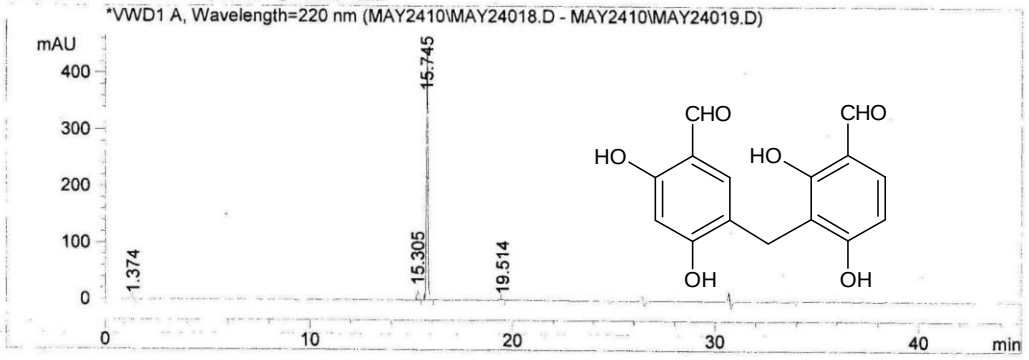

Peak #	RetTime [min]	Type	Width [min]	Area mAU *s	Height [mAU]	Area %
1	1.374	BBA	0.0673	6.79830e-1	1.59180e-1	0.0281
2	15.305	BBA	0.0810	89.93205	17.29946	3.7160
3	15.745	BBA	0.0802	2324.67847	442.93002	96.0548
4	19.514	BBA	0.0777	4.86765	9.90393e-1	0.2011
Totals :				2420.15800	461.37906	

Spectrum 2.27

IR

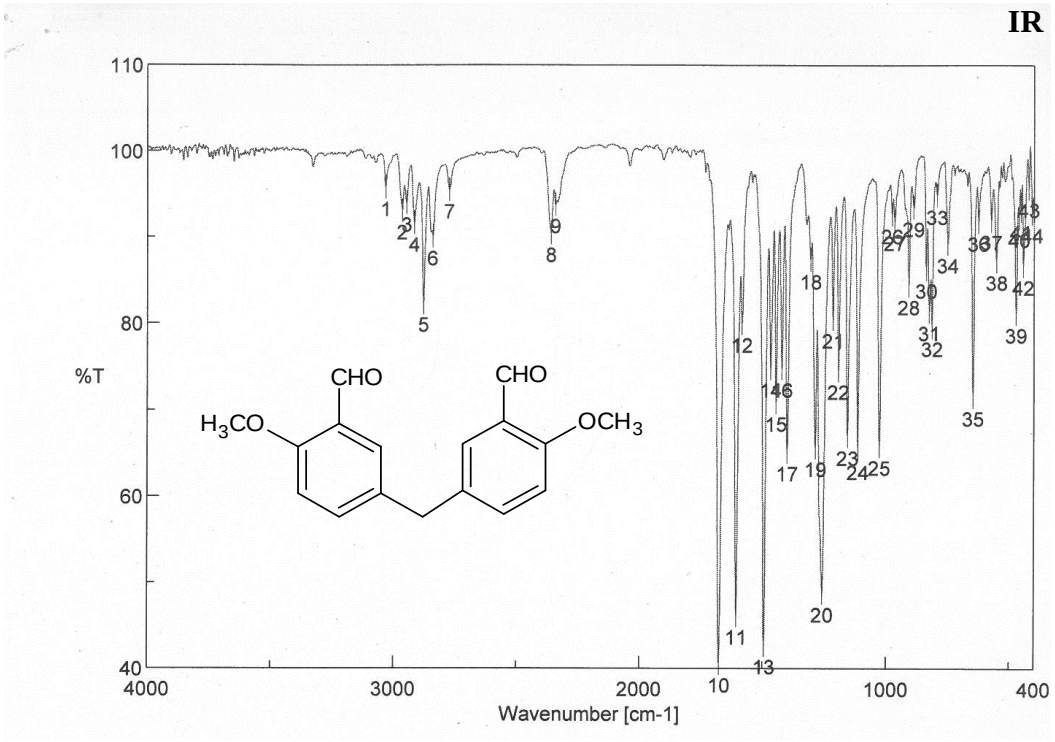

Spectrum 2.28

^{1}H NMR

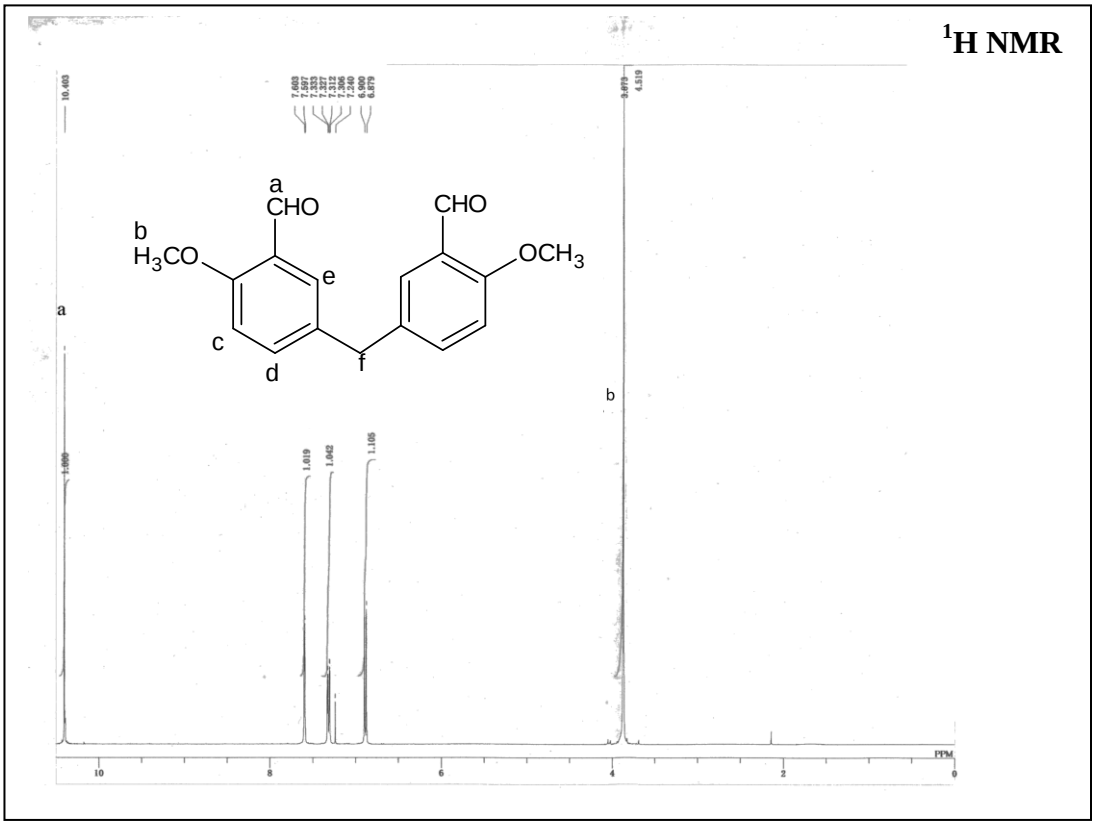

Spectrum 2.29

^{13}C NMR

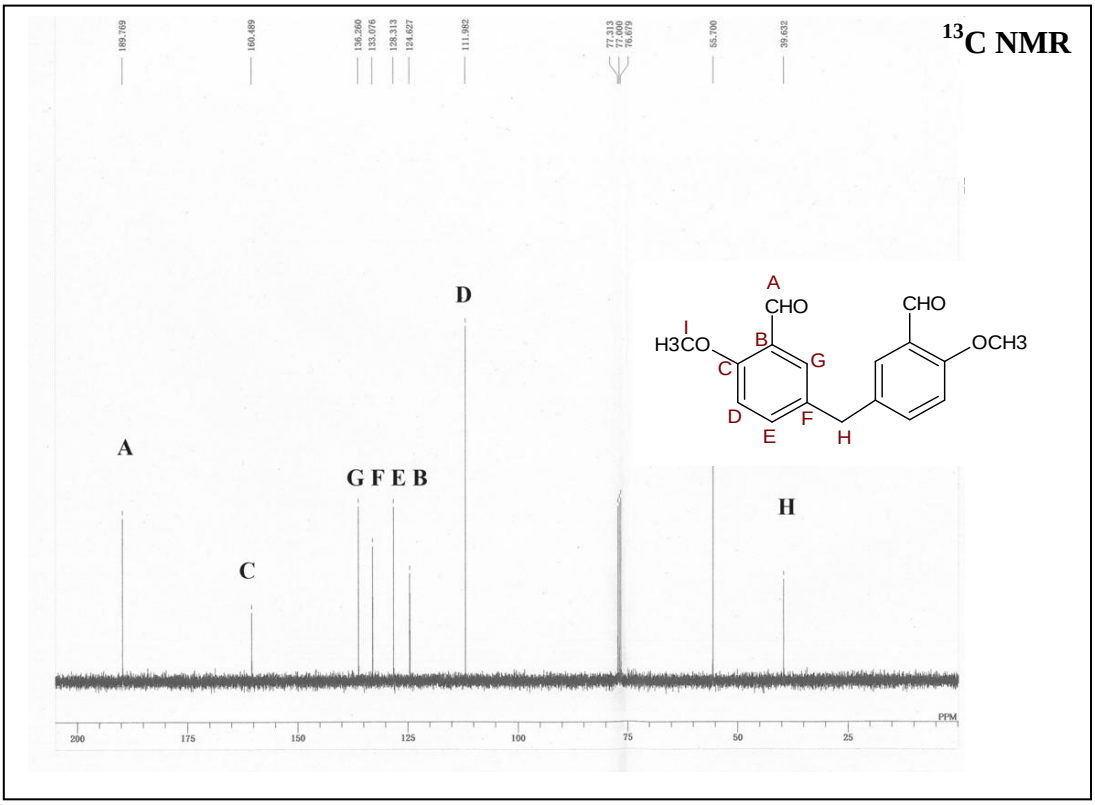

Spectrum 2.30

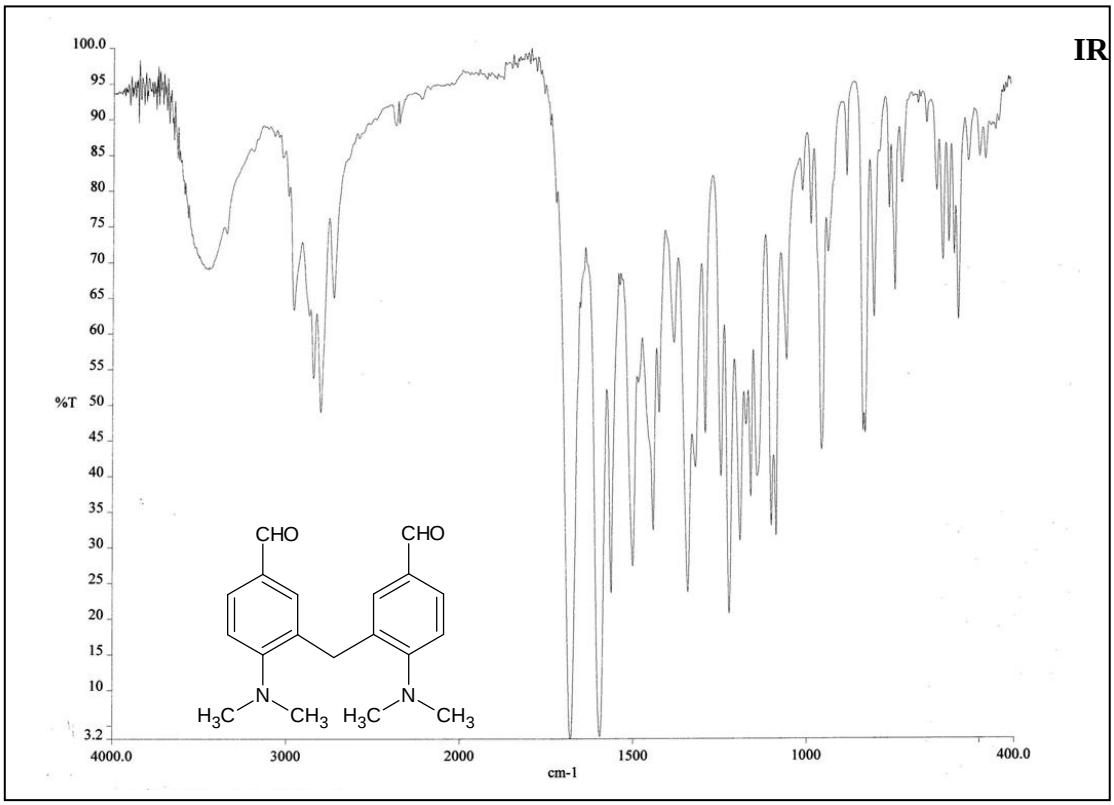

Spectrum 2.31

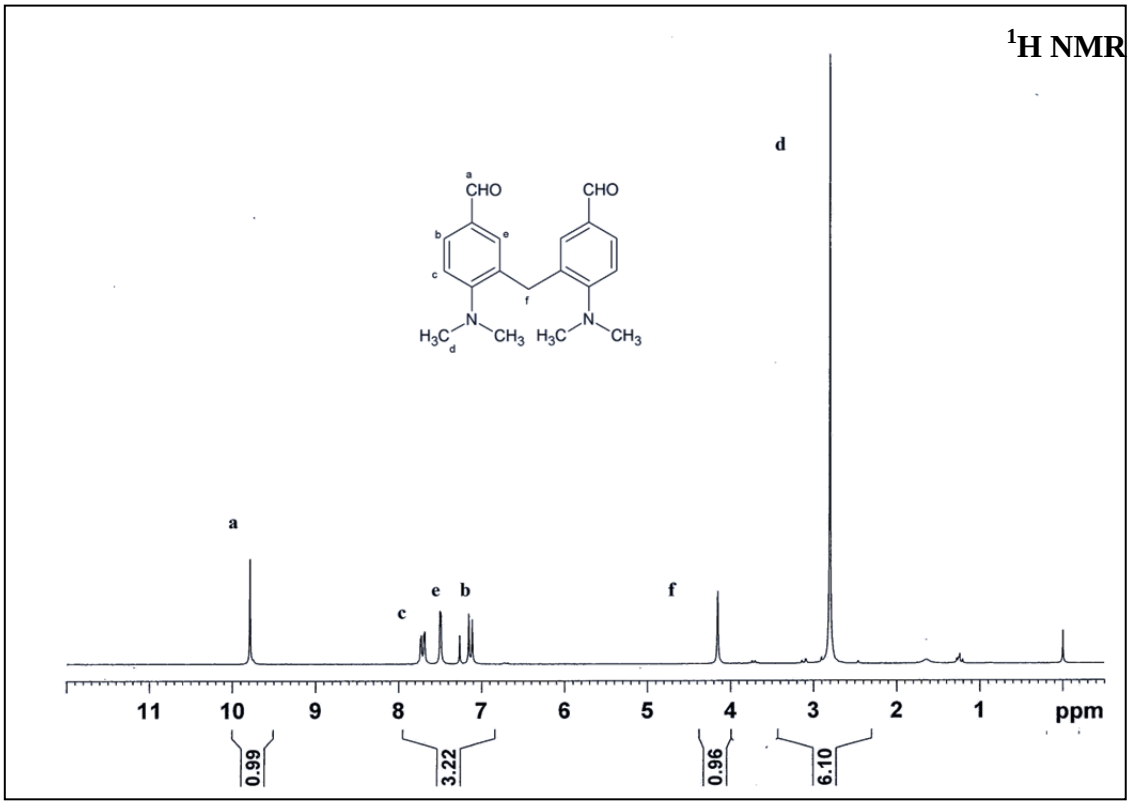

Spectrum 2.32

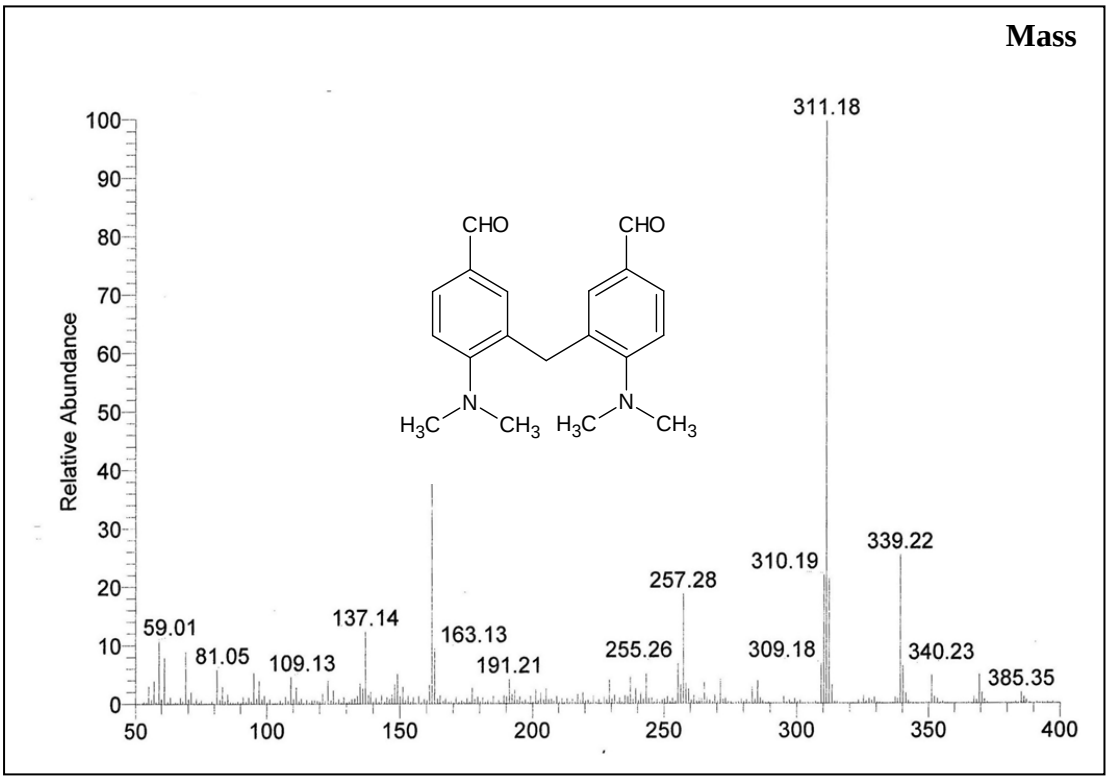

Spectrum 2.33

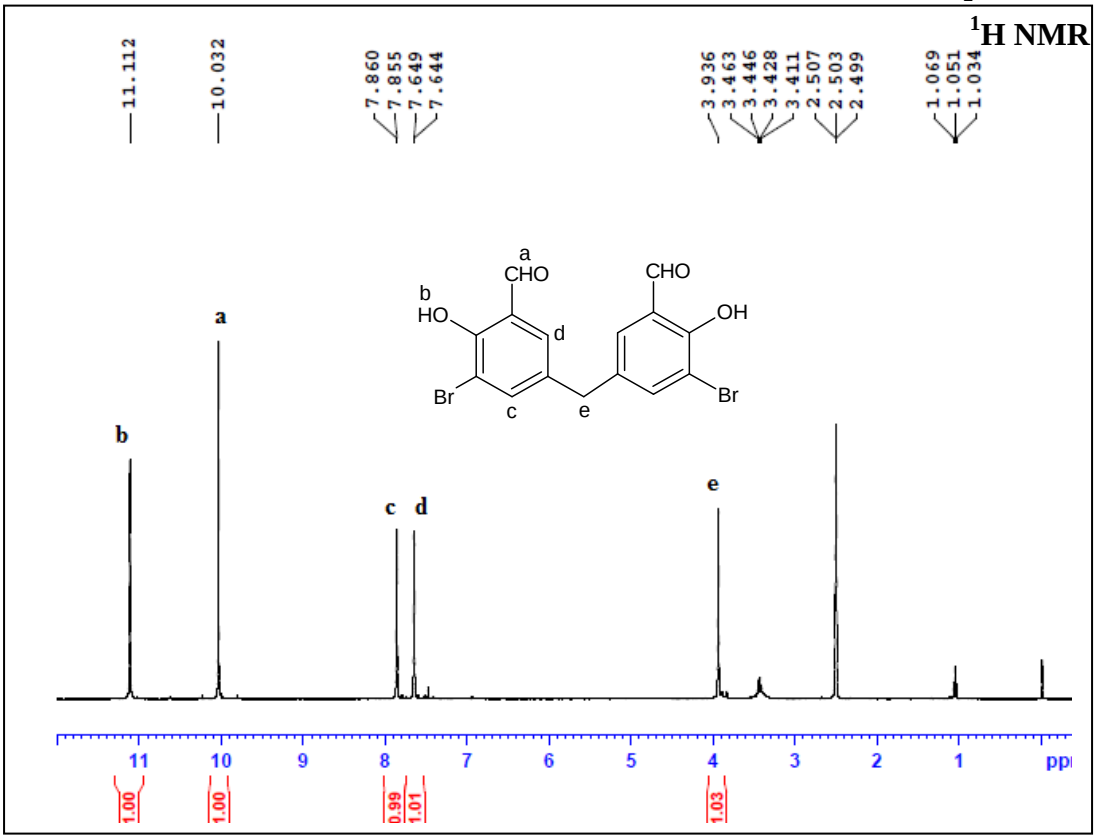

Spectrum 2.34

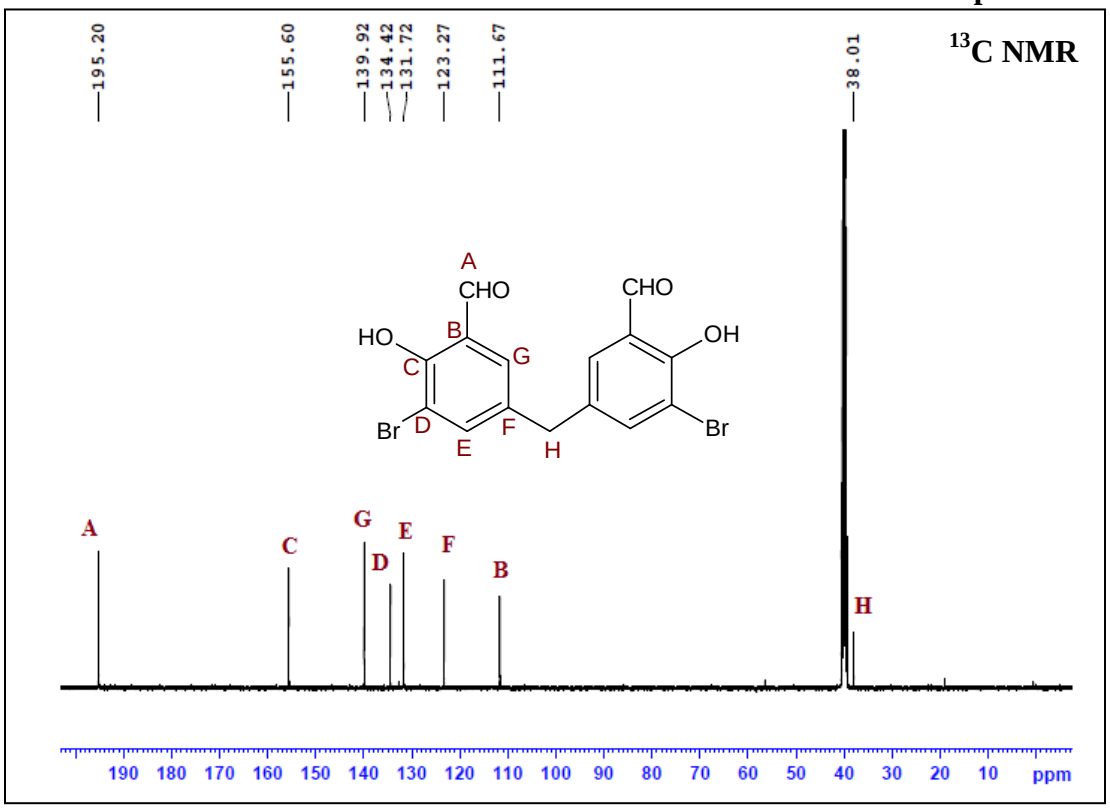

Spectrum 2.35

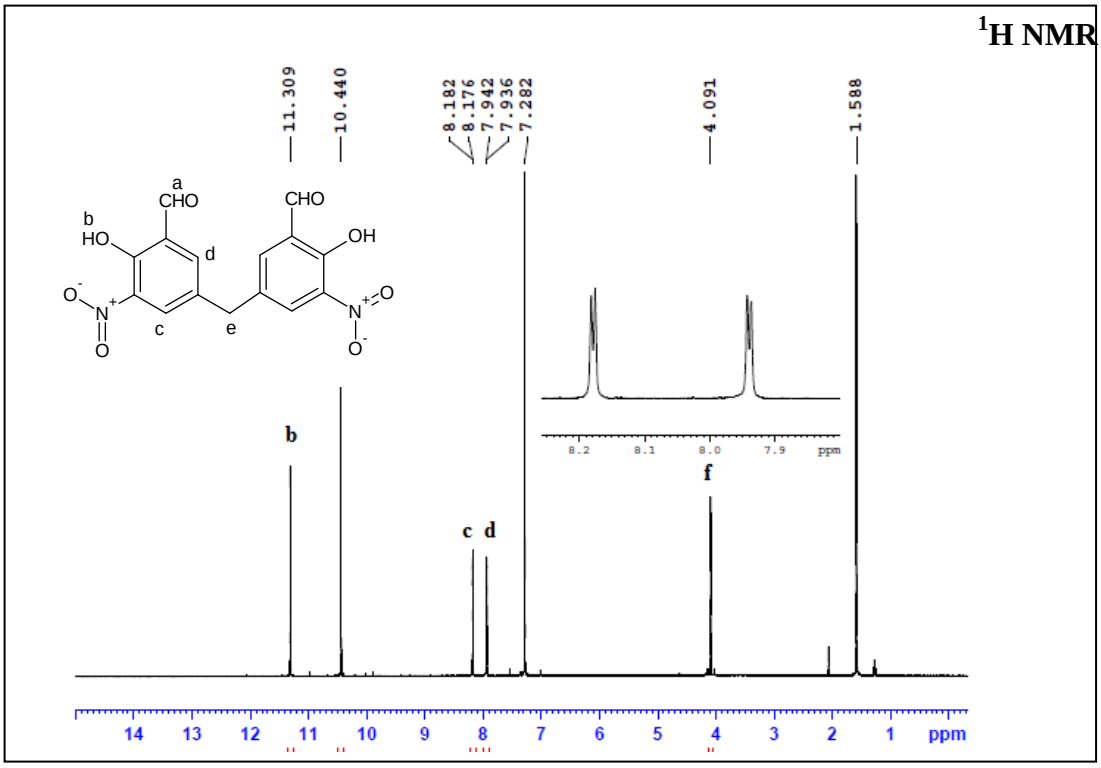

Spectrum 2.36

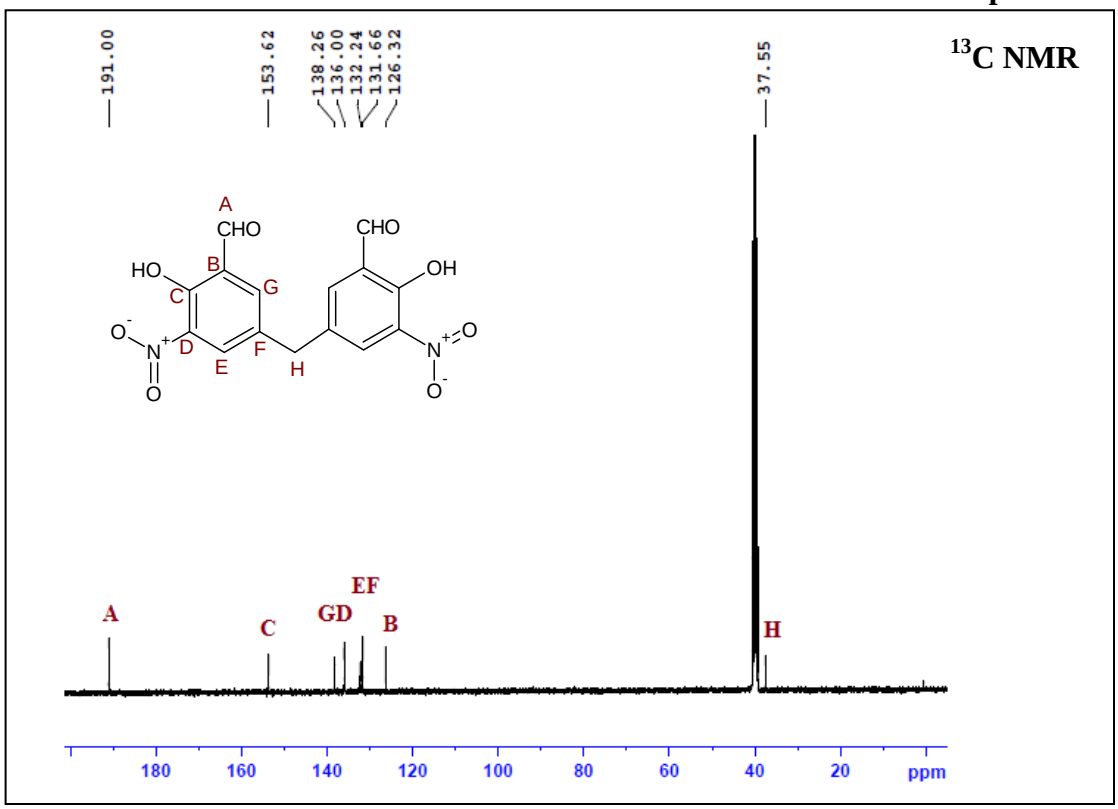

Spectrum 2.37

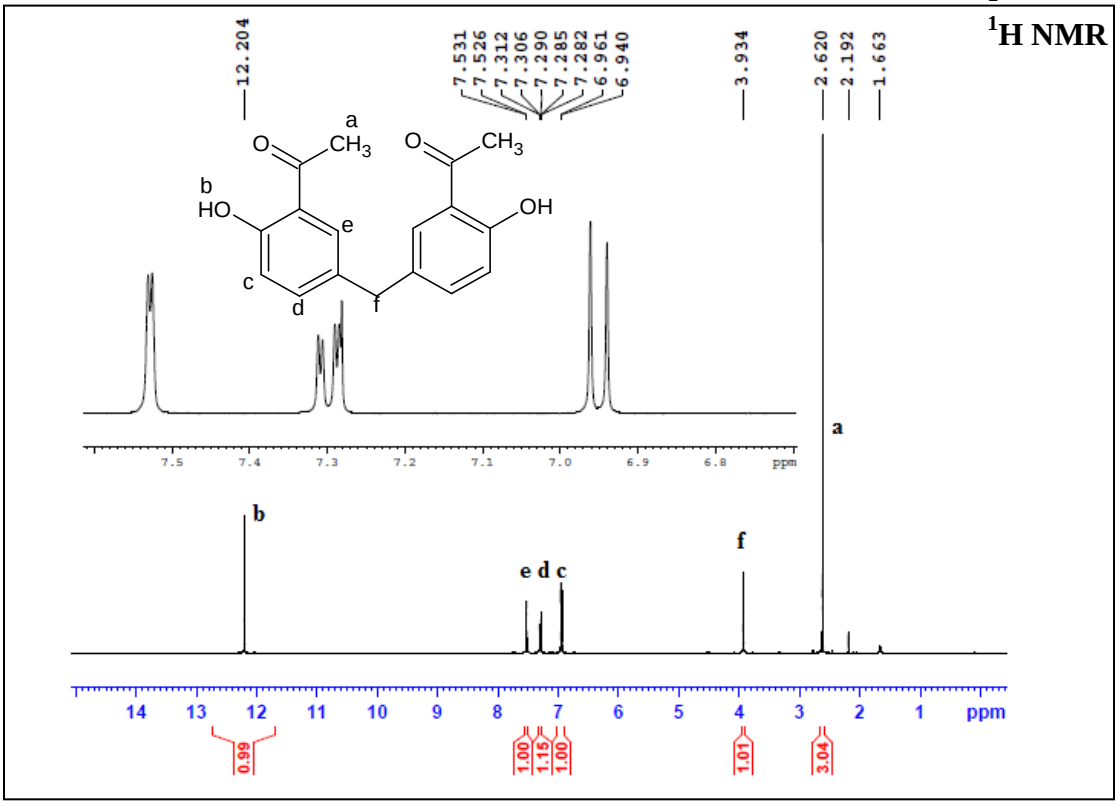

Spectrum 2.38

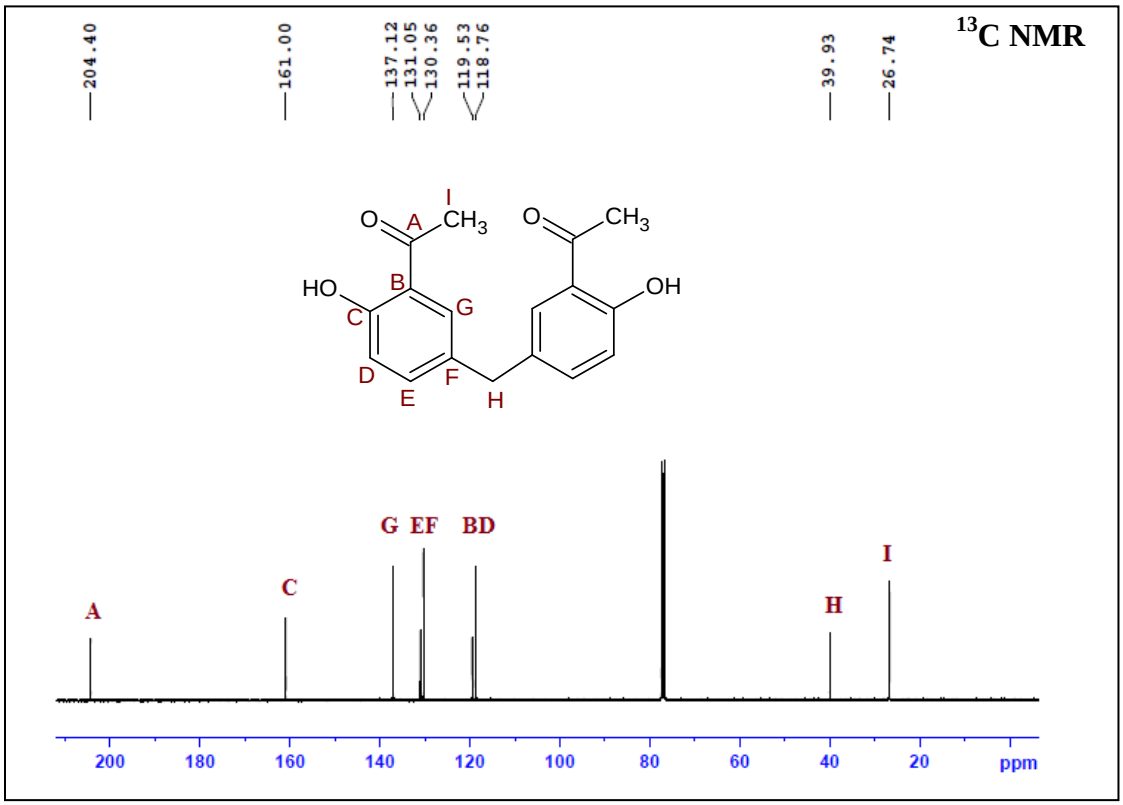

2. 7 References

1. Moder, M.; Wichmann K.; Gloeb, K.; Vogtle, F. *Int. J. Mass Spectrom.,* **2001**, 210/211, 327.

2. Fenton, D. E.; Najera, B. A. *J. Coord. Chem.,* **2011**, 54, 239.

3. Menif, R.; Reibenspies, J.; Martell, A. E. *Inorg. Chem.,* **1991**, *30*, 3446

4. Basallote, M. G.; Durán, J.; Fernández-Trujillo, M. J.; Máñez, M. A. *J. Chem. Soc*., *Dalton Trans*., **1999**, 3817.

5. Lennartsona, A.; McKeeb, V.; Nelsona, J.; Arthurs, M., McKenziea, C. *J. Supramolecular Chem*., **2012**, 24(8), 604.

6. Vyas, T. A., *PhD Thesis,* The M. S. University of Baroda **2004**.

7. Sureshan, C. A.; Bhattacharya, P. K. *Polyhedron*, **1997**, 16(3), 489.

8. Reddy C. S.; Srinivas, A.; Sunitha, M.; Nagaraj A. *J. Heterocycl. Chem.,* **2010,** 47, 1303.

9. Srinivas, A.; Nagaraj, A.; Reddy, C. S. *Eur. J. Med. Chem.,* **2010**, 45(6), 2353.

10. Reddy, C. S.; Srinivas, A.; Nagaraj, A. *Chem. Pharm. Bull*. **2009**, 57(7), 685.

11. Srinivas, A.; Nagaraj, A. Reddy C. S. *J. Heterocycl. Chem.* **2009**, 46(3), 497.

12. Cochran; Melville; *Synth. Commun.* **1990**, 20, 609.

13. Lindoy, L. F.; Meehan, G.V.; Svenstrup, N. *Synthesis*, **1998**, 1029.

14. Srinivas, A.; Nagaraj, A.; Reddy, C. S. *J. Heterocycl. Chem.,* **2008** 45(4), 1121.

15. Giovanna, D; Behedetta, F. M.; Antonella, F.; *Benedetta, E. Bioorg. Med. Chem. Lett.,* **2010**, 20(20), 6138.

16. Wynberg, H.; Meijer, E. W., *Org. React*., **1982**, 28, 1.

17. Thoer, A.; Denis, G.; Delmas, M.; Gaset, A., *Synth. Commun*. **1988**, 18, 2095.
18. Winberg, H., *Chem.. Rev.* **1960**, 60(2), 169.

19. Jones, G.; Stanforth, S. P.; *Org. React.*, Pacquette, L. A., Ed. Wiley: New York, **1997**, 49, 1.

20. Jones, G.; Stanforth, S. P. *Org. React.*, Overman, L. E., Ed. Wiley: New York, **2000**, 56, 355.

21. Meth-Cohn, O; Tarnowski, B. *Adv. Heterocycl. chem*., Katritzky, A. R. Ed. Academic press: New York **1982**, 31, 207.

22. Shah, S. R.; Navathe, S. S.; Dikundwar, A. G.; Guru Roa, T. N.; Vasella, A. T. *Eur.J. Org. Chem.,* **2013**, 264.

23. García-Beltrán,O.; Mena, N.; Pérez, E. G.; Cassels, B. K.; Nuñez, M. T.; Francisca, W.; Zavala, D.; Aliaga, M. E.; Pavez, P. *Tetrahedron Lett.* **2011**, 52, 6606.

24. Aspinall, H. C.; Beckingham, O.; Farrar, M. D.; Greeves, N.; Thomas, C. D. *Tetrahedron Lett.* **2011**, 52(40), 5120.

25. Payne, P.; Tyman, J. H.P.; Mehet, S. K.; Ninagawa, A. *J. Chem. Res.,* **2006**, 6, 402.

26. Casiraghi, G.; Casnati, G.; Puglia, G.; Sartori, G.; Terenghi, G. *J. Chem. Soc., Perkin Trans. 1*, **1980**, 1862.

27. Wong, Y.; Mak,C.; Kwan,H. S.; Lee, H. K. *Inorg. Chim. Acta*. **2010**, 363(6), 1246.

28. Hansen, T.V.; Skettebol, L., *Organic Synthesis*, **2009**, Coll Vol XI, 267.

29. Hofslokken, N. U.; Skattebol, L. *Acta Chem. Scand.*, **1999**, 53(4), 258.

30. Jin, Z.; Yang, R.; Du, Y.; Tiwari, B.; Ganguly, R.; Chi, Y. R. *Org. Lett.,* **2012**, 14(12), 3226.

31. Marvel, C. S.; Torkoy, N. *J. Am. Chem. Soc.*, **1957**, 79, 6000.

32. Tan R., Yin, D.; Yu, W.; Ding, Y.; Zhao, H.; Yin, D., *Catal Lett.* **2009**, 129(3-4), 471.

33. Maurya, M. R.; Kumar, A.; *J. Mol. Catal. A-Chem.*, **2006**, 250(1-2) 190.

34. Nashed, A. W.; Elbokl, T. A.; Khalil, T. E.; Haase W.; Iskander M. F. *J. Coord. Chem.*, **2005** 58(2), 153.

35. Maurya, M. R.; Khan, A. A.; Azam, A.; Ranjan, S.; Mondal, N.; Kumar, A.; Avecilla, F.; Pessoa, J. C. *J. Chem. Soc., Dalton Trans.*, **2010, 39**, 1345.

36. Shrimurugan, S.; Viswanathan, B.; Varadarajan, T. K.; Varghese, B. *Tetrahedron Lett.*, **2005**, 46, 3151.

37. Maurya, M. R.; Haldar, C. Khan, A., A.; Azam, A.; Salahuddin, A.; Kumar A.; Pessoa J. C. *Eur. J. Inorg. Chem.,* **2012,** 15, 2560.

38. Kuo, K. *J. Chem. Soc., Dalton Trans.*, **2008, 29**, 3889.

39. Guieu, S.; Rocha J.; Silva, A. M. S. *Tetrahedron*, **2013**, 69, 9329.

40. Guili, J.; Xiaoyan, L.; Ruixia, C.; Min, L. *Acta Crystallogr., Sect. E: Struct. Rep. Online*, **2005**, E61(12), o4298-o4299.

41. Mustaga, O.; Cigdem, A.; Orhan, B. *Acta Crystallogr., Sect. E: Struct. Rep. Online*, **2006**, E62(1), o239-o240.

42. Agus, S.; Nourmamode, A.; Gardrat, C., Fritsch, A.; Castellan, A. *J. Mol. Struct.*, **2003**, 649(1) 177.

43. Kureshy, R. I.; Khan, N. H. Sayed H. R. A.; Patel, S. T.; Jasra, R. V. *Tetrahedron Asymmetry.*, **2001**, 12(3), 433.

44. Loredana, P.; Tudorache, M.; Neatu, S.; Grecu, M. N.; Kemnitz, E.; Filip, P.; Parvulescu,V. I.; Coman, S. M. *J. Phys. Chem. C*, **2011,** 115(4). 1112.

45. Yang, S.; Ning, T.; *J. Mol. Catal. A: Chem.*, **2006** 255(1) 171.

46. Longhai, C.; Feixiang, C.; Lei, J; Aijiang, Z.; Jincai, W.; Ning, T. *Chirality*, **2011** 23(1), 69.

47. Janssen, K. B. M.; Dehaen, I. L. W.; Parton, R. F.; Vunkelecom I. F. J.; Jacobs, P. A. *Tetrahedron Asymmetry*., **1997**, 8(20), 3481.

48. Johnson , T. B.; Lane, F. W. *J. Am. Chem. Soc.*, **1921**, 43 (2), 348.

49. Narasimha, M. J.; Natarajan, R.; Venugopalan, P. *J. Mol. Struct.*, **2005,** 741(1) 107.

50. Patel, P.; Bhattacharya, P. K.; *Can. J. Chem.*, **1993**, 71, 1253.

Chapter 3

Synthesis and Study of

Chiral Calix Salen Corands

3.1 Introduction

One of the most challenging tasks in supramolecular chemistry is the design of supramolecular host molecules having selectivity in binding with guest molecules or ions. Generally host-guest assembly formed by binding of guest molecules with acyclic host entity is stabilised by chelate effect while in the case of cyclic host, macrocyclic effect also operates which provides extra stabilisation to such host-guest systems. Thus the cyclic host molecules have greater binding ability and selectivity over their acyclic analogous. The monocyclic host molecules are termed as corands. The most common corands are crown ethers with different size and shape. Their chemistry began with the synthesis of dibenzo[18]-crown-6 which was a minor side product during ether formation reaction of chatechol and di-(chloroethyl)ether by Pederson.[1a] He was awarded Nobel prize along with Lehn and Cram in 1987 for his contribution in supramolecular chemistry in form of crown ethers. In general, synthesis of corands, macromonocyclic host molecules, can be achieved by reacting two bifunctional compounds as in the case of synthesis of crown ethers.[1]

Similar to crown ethers, calixarenes were also isolated as side products during the synthesis of Bakelite from phenol and formaldehyde by Alois Zinke. Calixarenes are isomeric monocyclic metacyclophanes formed during the polymerisation process. They are named as calixarenes because of their bowl shaped conformation which was in resemblance with Greek vase called calix-crater.[1]

Salens are Schiff bases formed by condensation of amines with salicylaldehyde or its derivatives. Their unique coordination capacity and high solubility in various organic solvents have made them the ligands of choice especially for cation recognition. Calix-salens are corands having salen linkage and calixarene like structure.[2] Macrocyclic salen host molecules are synthesized from 2,6-diformyl phenols and α,ω-di-amines e.g. 2,6-diformylphenol derivatives when reacted with different diamines in the presence of metal ions, give various metal corates.[3,4] Metal corates were observed to undergo intramolecular electron transfer in the case of mixed valence copper complexes (Fig. 3.1).[5]

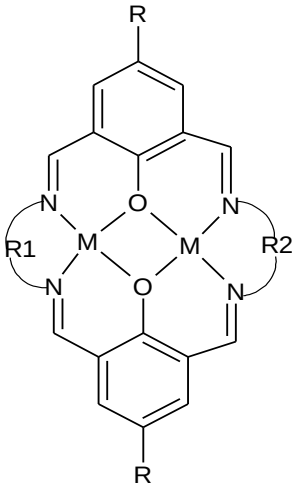

$R = -CH_3, -C(CH_3)_3$

$R_1=R_2$= propylene

$R_1=R_2$= 2,2’ dimethylpropylene

$R_1=R_2$=butylenes

$R_1=R_2$=biphenylene

R_1= propylene, R_2= 2,2’ dimethylpropylene

R_1= propylene, R_2= biphenylene

Dinuclear metal complex from Schiff base corand

Fig 3.1

Di-iron complexes of these ligands were prepared and their electrochemistry, X-ray structure and magnetochemistry were studied.[6] Similarly 2,6-diformyl-4-methyl phenol on reaction with α,ω-di-amine separated by polyether chain formed larger corands which were converted to the corresponding zinc conplexes (**Fig. 3.2**).[7]

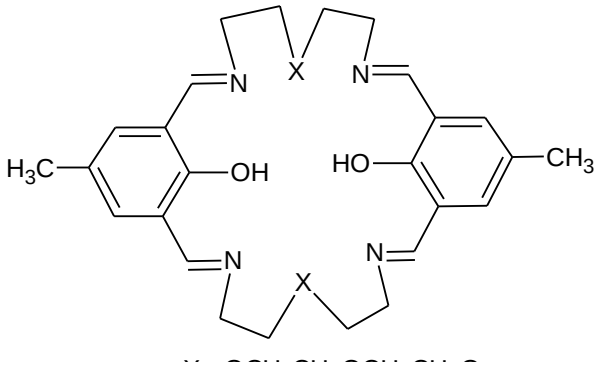

Imine-Crown ether hybrid corand

Fig 3.2

Heteronuclear macrocyclic complexes containing both Ni^{2+} and Pd^{2+} ions were synthesized and characterized by X-ray crystal structure.[8] When these aldehydes were reacted with substituted o-phenylene-di-amines in the presence of catalytic amount of acid gave macrocyclic compaunds having π-conjugated system (**Fig. 3.3**).[9]

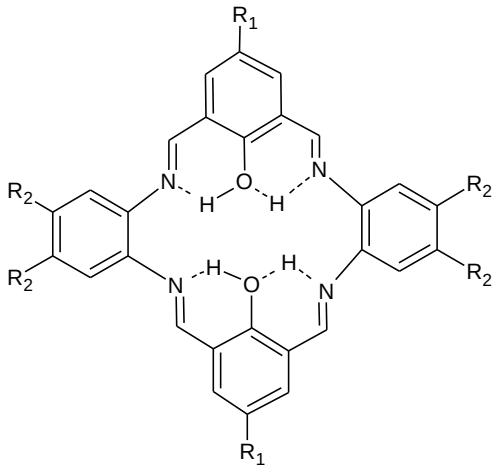

Conjugated aromatic imino corand

Fig. 3.3

The dialdehydes were reacted with diamines connected by pyridazine thio-ether spacer in the presence of $Cu(ClO_4)_2$ forming dinuclear complexes of the corresponding cryptand[10] (Fig. 3.4).

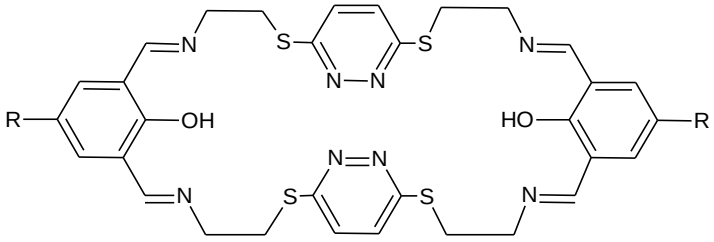

R= -CH_3, -$C(CH_3)_3$

Heteroatom-heterocycle linked imino corand

Fig. 3.4

4-Alkyl-2,6-diformylphenol on reaction with chiral vicinal diamines or chiral binaphthyldiamine gave chiral salen ligands. Co^{2+} and Mn^{2+} complexes of chiral salen ligands were evaluated in asymmetric oxidation of olefins and reduction of ketones giving high enantioselectivity (Fig. 3.5).[2,11]

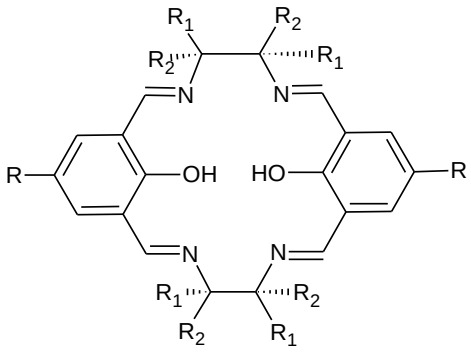

Chiral salen corands

Fig. 3.5

The macrocyclization between more number of these bifunctional reactants results in formation of larger cryptands. Thus the larger cryptands from the reaction between 4-substituted-2,6-diformylphenols and various diamines in [4+4] manner along with their metal complexes have been studied by various groups[12-15] e.g. as shown in Fig. 3.6.

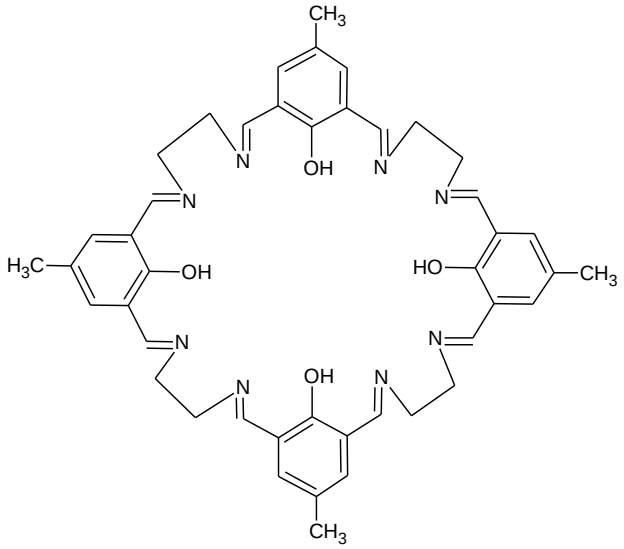

Larger corand with imino-phenolic cavity from [4+4] condensation

Fig. 3.6

Larger macrocyclic cryptands can also be synthesized by applying two formyl groups situated on interconnected two different aromatic rings. Lehn and co-workers used 4,4'-methylene-bis-benzaldehyde for the condensation with different diamines giving polyazamacrocycles.(Fig. 3.7) Condensation of optically active diamino-succinicacid with the dialdehyde resulted in the chiral macrocycle (**Fig. 3.8**).[16]

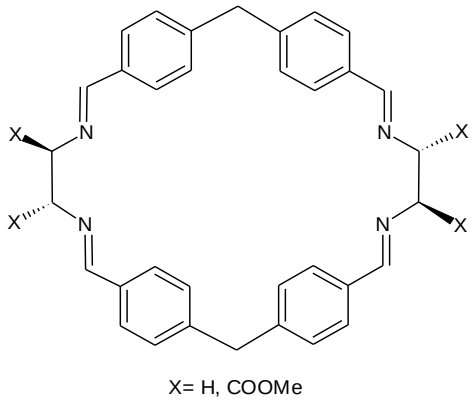

Chiral corand from methylene-bis-aldehyde

Fig 3.7

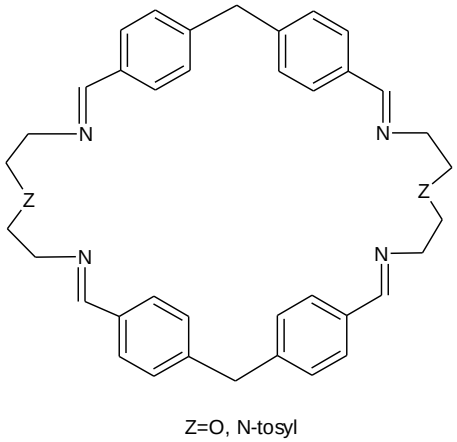

Larger corand from methylene-bis-aldehyde

Fig 3.8

When chiral 3,3'-diformyl-bis-binaphthol was reacted with chiral 1,2-diphenylethylenediamine or with chiral cyclohexane-1,2-diamine, resulted in the [2+2] macrocyclic salen compounds which on borohydride reduction gave the corresponding chiral amines. These corands were found to behave as enantioselective fluorescence sensors for recognition of chiral carboxylic acids (**Fig. 3.9, 3.10**).[17,18]

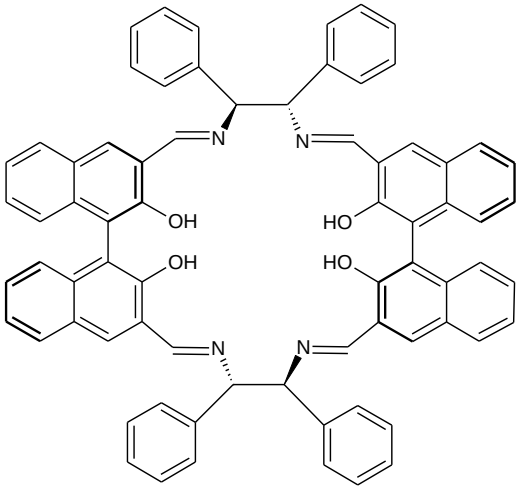

Chiral phenolic corand from diphenylethylenediamine

Fig. 3.9

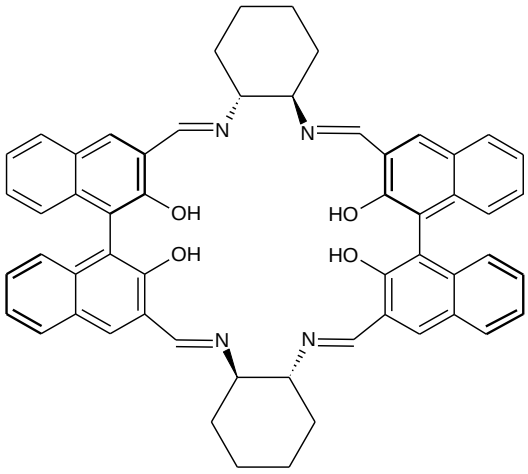

Chiral phenolic corand from cyclohexane 1,2-diamine

Fig. 3.10

The cyclocondensation of (1R,2R)-cyclohexane diamine (DACH) with various 5,5'-methylene-bis-salicylaldehydes resulted in macrocyclic chiral calix-salen corands under different reaction conditions.[19-23] Barium templated synthesis of the chiral macrocycles was employed for the synthesis of ligands which form manganese complexes which were found to catalyze enantioselective epoxidation of styrene[19] **(Fig. 3.11**).

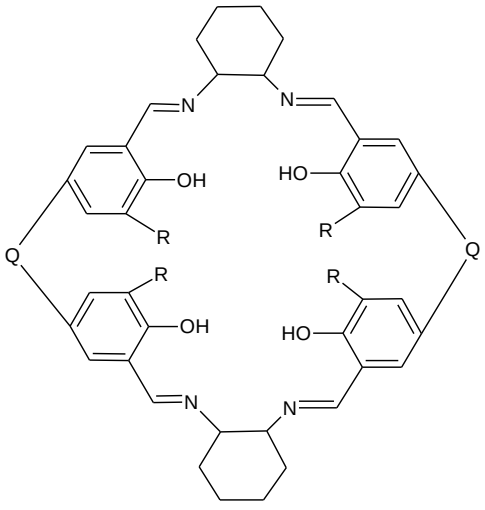

Calix-salen corands from cyclohexane diamine

Fig. 3.11

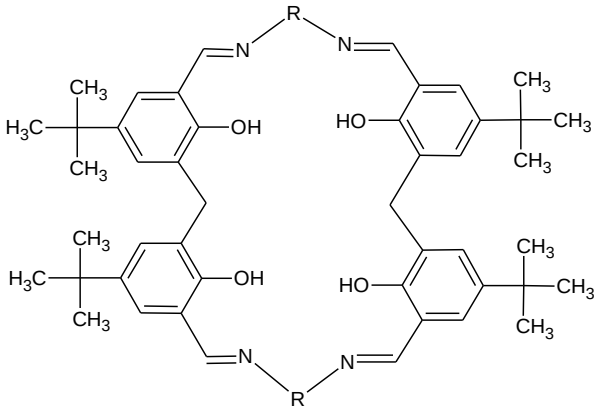

Calix-salen corands from various aromatic and aliphatic diamines

Fig. 3.12

They also afforded solvent controlled mono and binuclear Ni^{2+} complexes.[20] The salen corands from 3,3'-methylene-bis-salicylaldehyde having *tert*-butyl substitutents were prepared in the presence of boric acid in good yields[21,22](**Fig. 3.12**).

Microwave assisted cyclocondensation of chiral diamines including DACH gave [2+2] macrocycles with methylene or sulphone linked bis-aldehydes while [3+3] macrocycles were formed as major products when aromatic dialdehydes were used[23,24](Fig. 3.13).

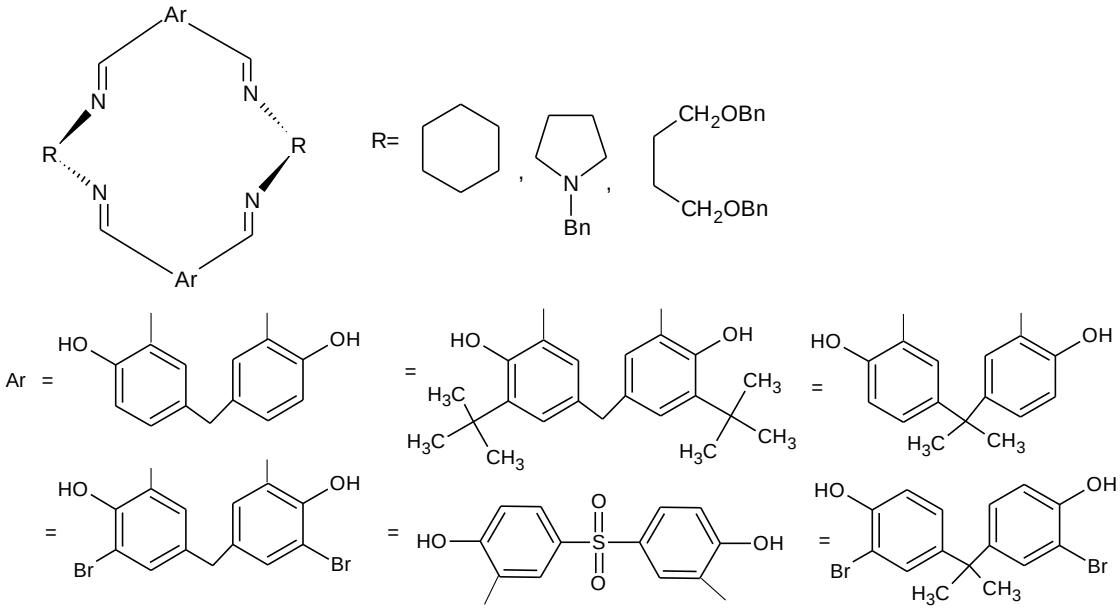

Calix-salen corands from [2+2] cyclocondensation

Fig. 3.13

Trans (1R,2R)-DACH on reaction with 4-methyl-2,6-diformylphenol gave [3+3] salen macrocycle whose dinuclear transition and lanthanide metal complexes were formed and characterised.[25-27] The chiral [3+3] salen macrocycles derived from 4-substituted-2,6-diformyl phenols exhibited enantioselective fluorescence recognition of mandelic acid derivatives.[28] The heximine reduced chiral amine macrocycle was found to be useful as

NMR chiral shift reagent for carboxylic acids.[29] The analogous but novel chiral imine macrocycles exhibited thermally reversible photochromism on photo irradiation.[30]

The preference for [3+3] cyclocondensation of trans DACH with rigid aromatic dialdehydes having benzene, biphenyl, terphenyl, quaterphenyl, anthryl, styrene, divinylbenzene, stilbene or heterocyclic spacers was explained by Gawronski and coworkers who studied their chiroptical properties.[31-33] They also isolated and characterized [2+2], [3+3] and [4+4] macrocycles derived from DACH and 2,6-diformylpyridine.[34] When terephthalaldehyde was employed for [3+3] cyclocondensation the resulting molecular triangles exhibited stereoselective solid state stacking into microporous chiral columns.[35] Reduction of this trianglimine resulted in trianglamine which was studied for asymmetric catalysis.[36] The macrocycles were also found to recognize tricarboxylic acids due to shape complimentarity.[37,38] Kuhnert *et. al.* have studied the scope and limitations in the synthesis of trianglimines.[39] They synthesized and studied a number of trianglimine macrocycles using various aromatic and heteroaromatic dialdehydes (**Fig. 3.14, 3.15**).[39-45]

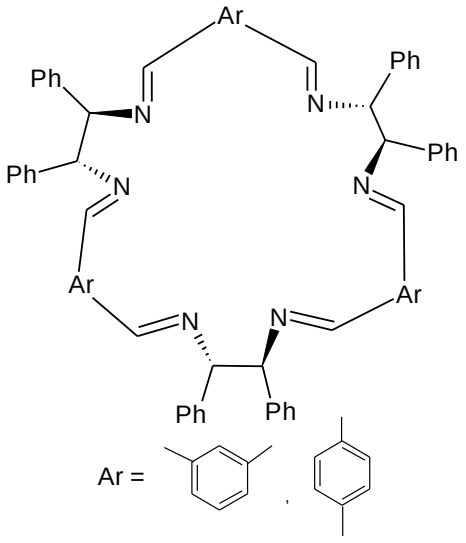

Chiral corands from [3+3] cyclocondensation

Fig. 3.14

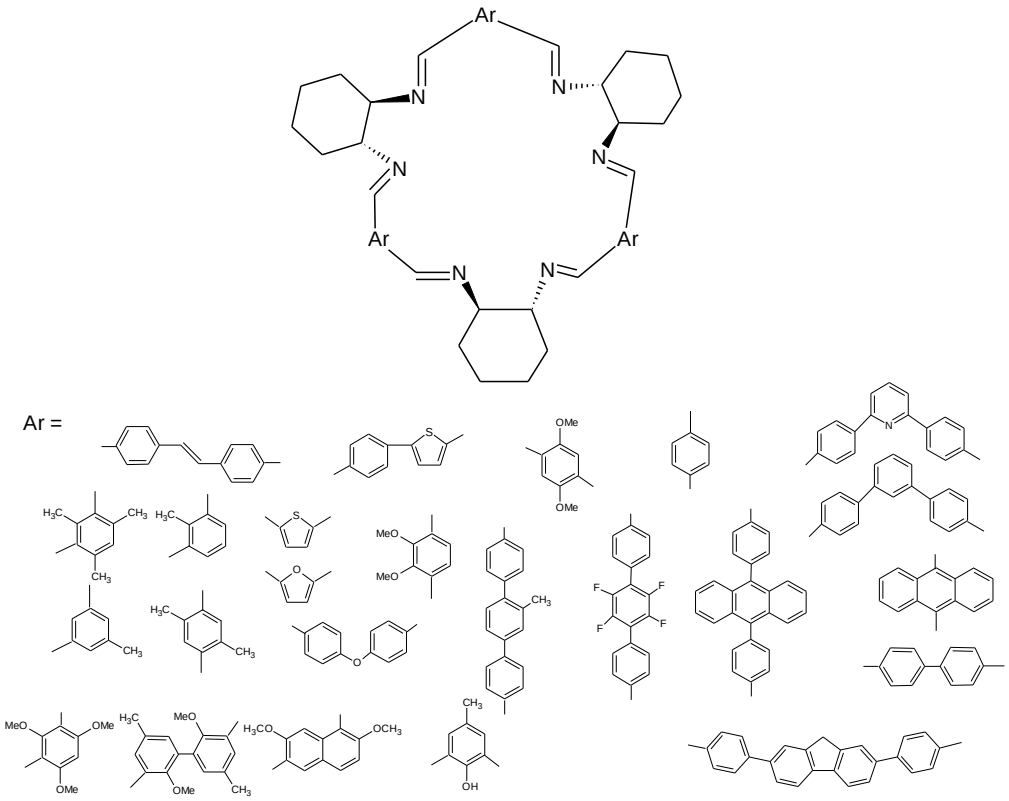

Variety of corands from [3+3] cyclocondensation

Fig. 3.15

3.2 Aim and objectives:

The chiral salen macrocycles have attracted attention of organic chemists mainly due to their well organized chiral interiors and their ability towards enantioselective recognition of chiral organic molecules. Various chiral amino acids and other carboxylic acids have been recognised using such macrocycles.[28-30] They also provide chiral environment for enantioselective syntheses. Most of these corands have been prepared from aromatic dialdehydes.[40-44] Due to versatility in structures and in applications we undertook the synthesis and study of chiral calix-salen macrocycles by using distantly located diformyl linkers in the form of 5,5'-methylne-bis-salicylaldehydes and chiral diamines. During course of our study we synthesized several new corands. We carried out recognition studies of 1st series transition metal ions with the newly synthesized macrocycles.

3.3 Results and Discussion

With an aim to synthesize some chiral calix-salen type corands using methylene-bis-aldehydes and methylene-bis-acetophenones we looked for chiral diamines with different structural features. The chiral diamines selected were (1R,2R)-diaminocyclohexane (DACH) which is a reactive cyclic aliphatic diamine, (1R,2R)-(+)-1,2-diamino-1,2-diphenylethane (DADPE) which is substituted ethylenediamine with benzylic 1,2-diamino functionality having lower reactivity as compare to DACH and R-(+)-1,1'-binaphthalenyl-2,2'-diamine (BNDA) as an aromatic diamine with chirality induced due to atropisomerism.

The high dilution methodology was successfully adopted for macrocyclic salen formation free from any metal ion contrary to template assisted synthesis. Large volume of solvent allows low concentration of reactants at a given time leading to macrocyclization reducing the probability of polymerisation.

Prior art reported the use of ethanol or methanol[19,20,22] as a reaction medium which when used by us found to give more of insoluble material due to polymerization. Dichloromethane was found to be a better solvent for the desired macrocyclization.

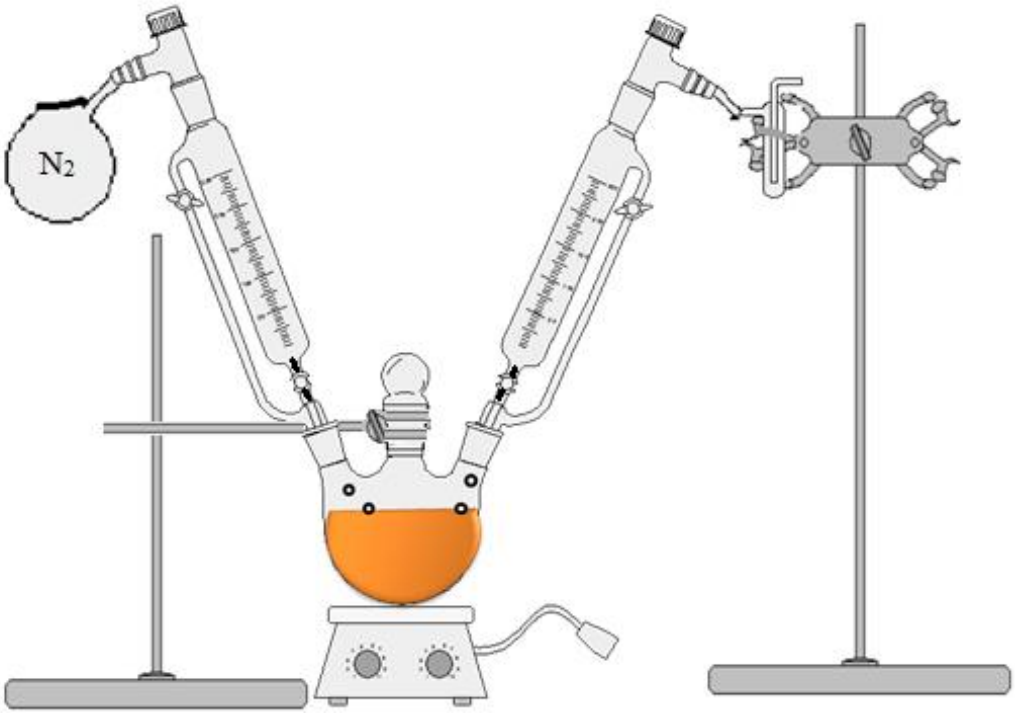

Schematic diagram of high dilution macrocyclization reaction
Fig. 3.16

3.3.1 Application of (1R,2R)-Diaminocyclohexane (DACH) in Synthesis of Calix-Salen Corands

The reaction of (1R,2R)-diaminocyclohexane (DACH) and 5,5'-methylene-bis-salicyclaldehyde under high dilution condition in dichloromethane showed several spots on TLC indicating possibility of different size calix-salen formation. The major product out of these was found to be calix-salen from [2+2] cyclocondensation of the reactants obtained in 20% yield after column chromatography.

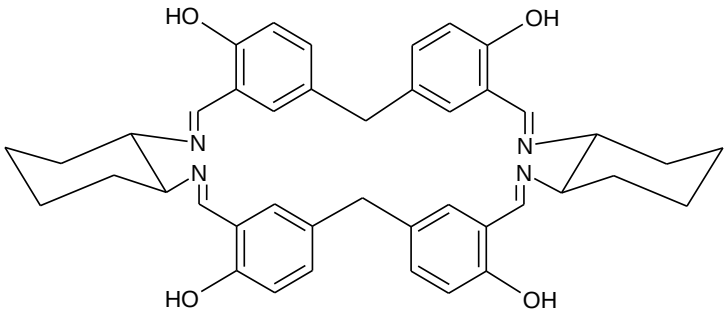

Corand C 247

Fig. 3.17

The structure was assigned based on detailed spectral analysis. IR spectrum of the corand shows νO-H at 3521 cm^{-1}, strong νC-H due to cyclohexane at 2927 and 2855 cm^{-}. The band at 1634cm^{-} is due to νC=N and at 1489 cm^{-1} is due to the δCH_2 while the band at 1273 cm^{-1} is due to νAr-O (Spectrum 3.1).

In proton NMR phenolic proton is observed at 13.09 δ and CH proton of the imine linkage is observed as a sharp singlet at 7.99 δ. The aromatic protons are observed between 7.2 δ to 6.6 δ. The most downfield of these is observed as a doublet of doublet having both ortho and meta coupling with coupling constants 8.4 Hz and 2.0 Hz respectively. The other two protons have either ortho or meta coupling only. The methylene bridge protons are observed as a singlet at 3.57 δ. The most downfield proton of the cyclohexane protons is for CH attached to nitrogen at 3.16 δ which appears as a multiplet. The other aliphatic methylene protons of cyclohexane ring are found between 1.8 δ to 1.3 δ (Spectrum-3.2).

^{13}CNMR shows 7 downfield signals between 165 δ to 115 δ, most downfield of these is for imine carbon. Four carbons are observed in aliphatic region, three from cyclohexane ring having nitrogen attached carbon peak at 72.9 δ. Methylene bridge carbon connecting aromatic rings is observed at 40.9 δ (Spectrum 3.3).

The DEPT experiment supports the assignments (Spectrum 3.4, 3.5). COSY spectrum of the corand shows correlation between protons on cyclohexane ring which are undergoing mutual coupling. The axial protons on the carbon connected to the nitrogen shows cross

peaks with the protons of the neighbouring methylene group's axial and equatorial protons which can be identified separately. Similarly correlation is observed in between the aromatic protons which are ortho and meta coupled (Spectrum 3.6).

NOESY spectrum shows through space interaction between CH proton of imine linkage with the proton on the carbon of cyclohexane ring attached to nitrogen and with the aromatic proton at its ortho position. Methylene protons on the carbon connecting the aromatic rings show correlation with both the aromatic protons situated on its ortho position. Interestingly the axial proton of the chiral carbon of cyclohexane ring shows through space NOE with the axial proton on third position because of 1,3-diaxial relation (**Fig. 3.18**; Spectrum 3.7).

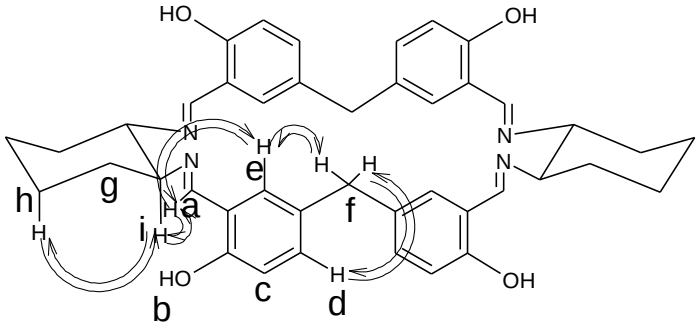

^{1}H-^{1}H Correlation as observed in NOESY

Fig. 3.18

With the help of HSQC location of all the protons on respective carbons were assigned precisely (Spectrum 3.8). The same was supported by HMBC spectrum of the corand ((Spectrum 3.9). Variable temperature proton NMR experiments were carried out from room temperature to -33°C and recording NMR at about 10°C intervals. A gradual intensity change was observed in the proton signals of the cyclohexane ring finally resulting in broad signals (spectrum 3.10).

The Q-TOF mass spectrum of the corand shows mass peak at 669.4 m/z corresponding to (M+H) as the base peak (spectrum 3.11). In HPLC analysis the corand shows 98.93%

purity. The microanalysis values of C, H, N were in accordance with the calculated values. Optical specific rotation of corand at 0.3% concentration in DCM shows [α]= -383.00. CD spectrum shows double Cotton effect at 220nm and 380nm in ethylacetate (Fig. 3.19).

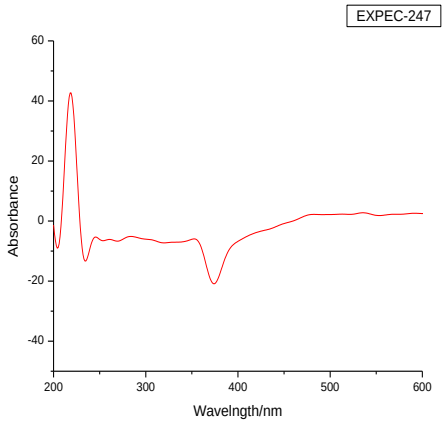

CD spectrum of C-247

Fig. 3.19

The compound was crystallized from acetone giving solvent supported crystals which were found suitable for single crystal X-ray analysis but were fragile. The single crystal X-ray analysis was carried out at IICT Hyderabad by Ravikumar and co-workers. Orthorhombic crystals confirm composition of the corand as [2+2] cyclocondensation of the reactans, DACH and 5,5'-methylene-bis-salicylaldehyde with two acetone molecules present in the cavity. The crystal structure shows the 1,3-dialternate arrangement of the aromatic rings in the calix-salen corand. The crystal packing shows the presence of two hollow channels.

Table No. 3.1 Crystal data and structure refinement

1.	Formula	$C_{42}H_{44}N_4O_4$, $2(C_3H_6O)$
2.	Formula Weight	784.97
3.	Cell Volume (Å)	4573.45
4.	T(K)	294
5.	Crystal system	Orthorhombic
6.	Space group	P 21 21 21
7.	Z	4
8.	a Å	11.2169(7)
9.	b Å	13.4138 (9)
10.	c Å	30.3962(19)
11.	α(°)	90.00
12.	β(°)	90.00
13.	γ(°)	90.00
14.	goodness of fit	1.023
15.	Calculated density diffrn ($mg/m^{3)}$	1.140
16.	Absorption coefficient (mm^{-1})	0.075
17.	F(000)	1680
18.	θ ranges for data collection	2.46-23.39
19.	Index ranges	$-13 \leq h \leq 13$ $-15 \leq k \leq 15$ $-26 \leq l \leq 26$
20.	Reflection collected	8321
21.	R indices	4.94

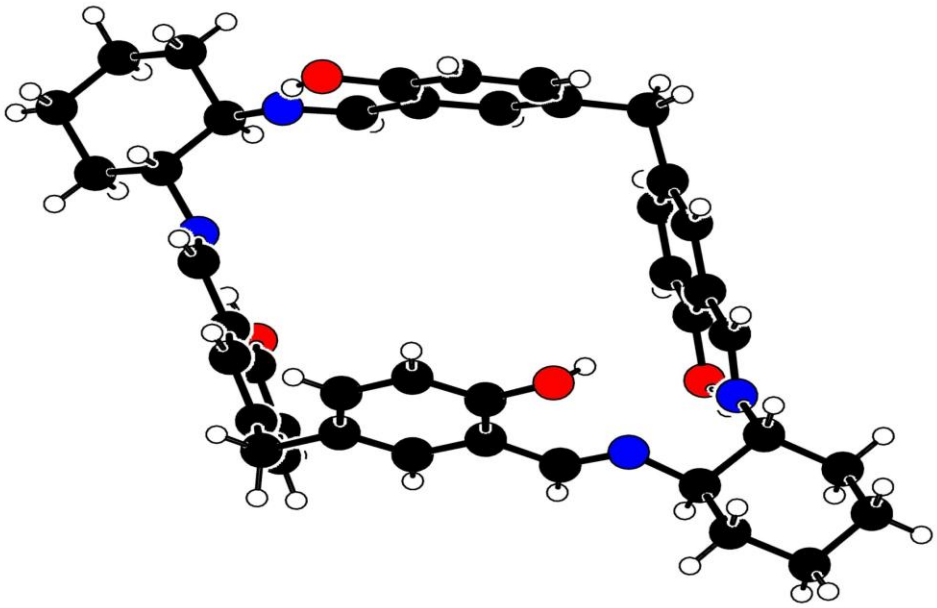

ORTEP diagram of Calix salen C-247 showing 1,3-dialternate conformation

Fig. 3.20

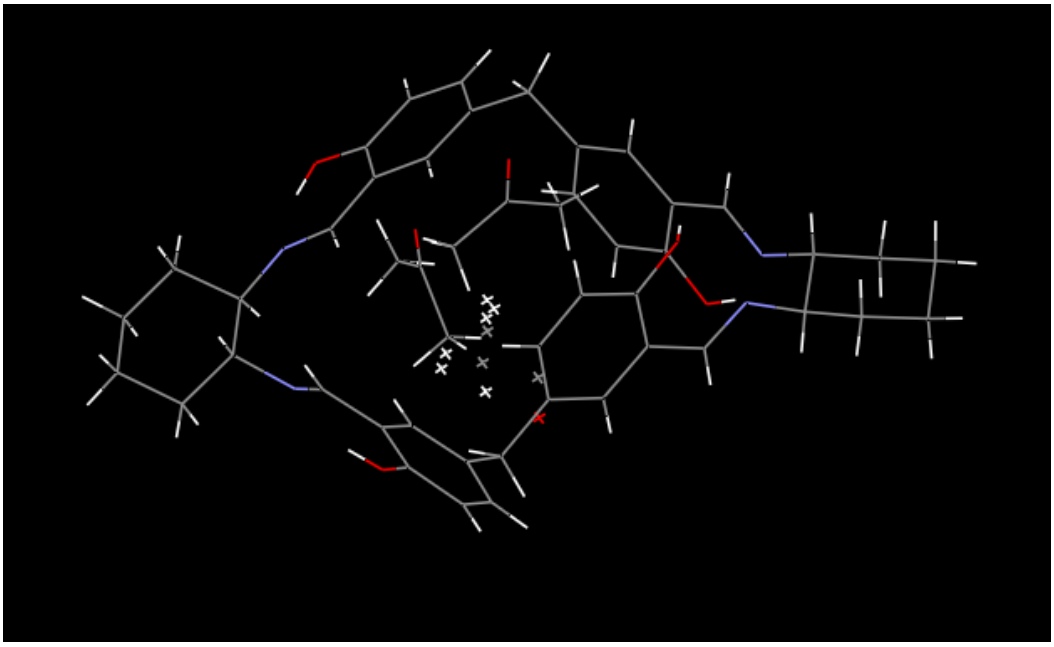

Wireframe image of Calix salen C-247 with acetone molecules in its cavity.

Fig. 3.21

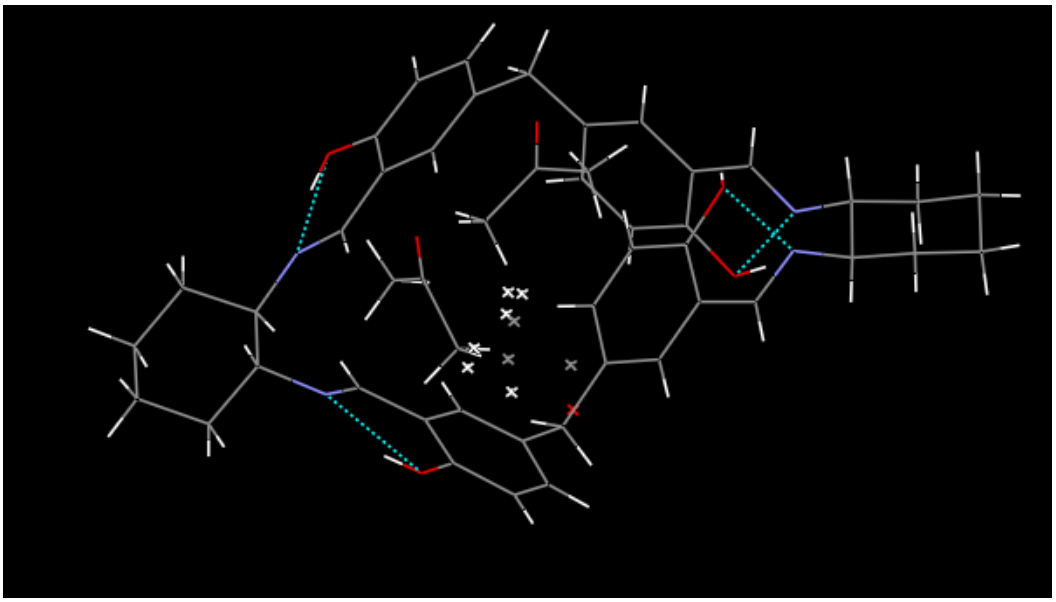

Wire frame image of C-247 showing hydorgen bonding between imine N---HOphenol

Fig. 3.22

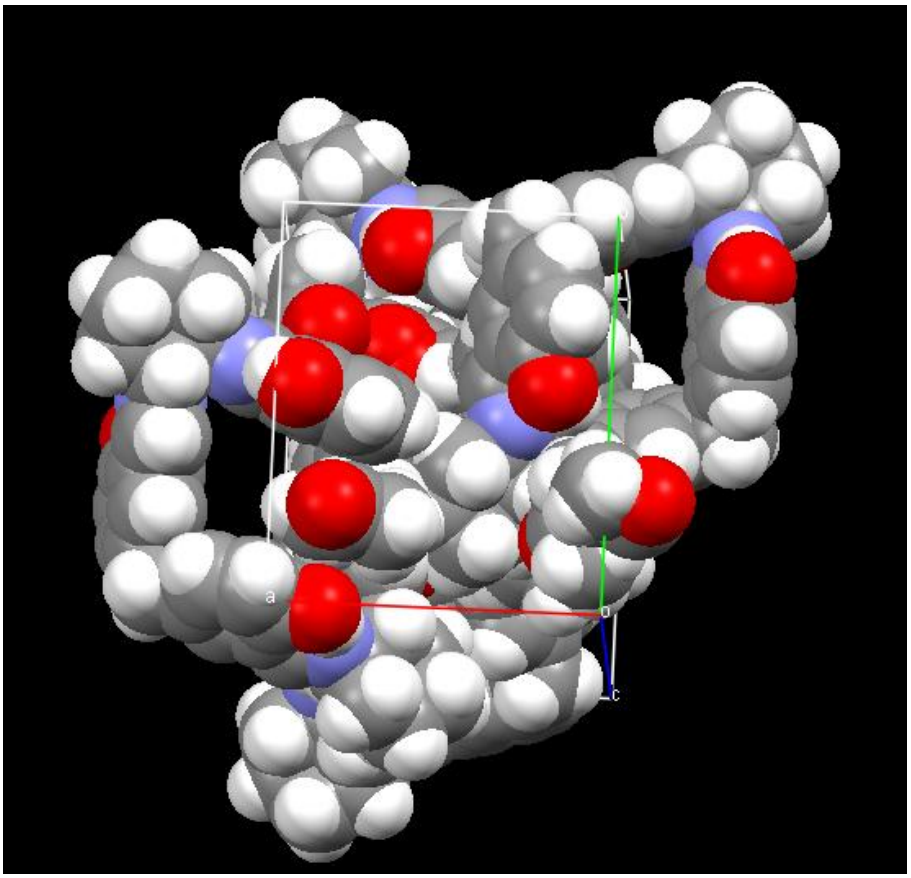

Space filling image showing voids in crystal packing of calix-salen corand C-247

Fig. 3.23

The Ba^{2+} template directed synthesis of the same corand (Fig. 3.17) was reported by Li *et. al.*[19,20] in MeOH-THF mixture as solvent in 1999. They also reported the single crystal X-ray showing monoclinic crystals with space group $P2_1/c$ different from orthorhombic crystals obtained by us. This shows that we have obtained another polymorph of the corand as compared to that reported by Li *et. al.*[19,20] Latter on, another paper reported microwave assisted reaction of methylene-bis-aldehyde and (1R,2R)-DACH monotartrate in water- ethanol mixture in presence of K_2CO_3. It was proposed that the reaction resulted in [1+1], [2+2] and [3+3] cyclocondensed products on the basis of mass analysis of the reaction mixture. None of the proposed products were isolated and characterised.[23]

Thus our methodology differs from the earlier reports in the sense that reaction was carried out in single solvent (DCM) under high dilution condition without addition of any metal salt. As a result, we obtained another polymorph of the cryptand with an isolated yield of 27% after column chromatography.

- **Solution studies of corand with transition metal ions**

Host-guest study between calix-salen corand (C 247) and 1st transition series metal ions was carried out at $2.5x10^{-4}$M concentration of host corand in DCM and $2.5x10^{-3}$ M concentration of guest ions in DMSO. Concentration of guest molecules was taken 10 times to the host molecule to ensure complete complexation. Corand shows unique absorption bands for Fe^{3+}, Cu^{2+}, Fe^{2+} and Ni^{2+} in the visible region (Fig. 3.24).

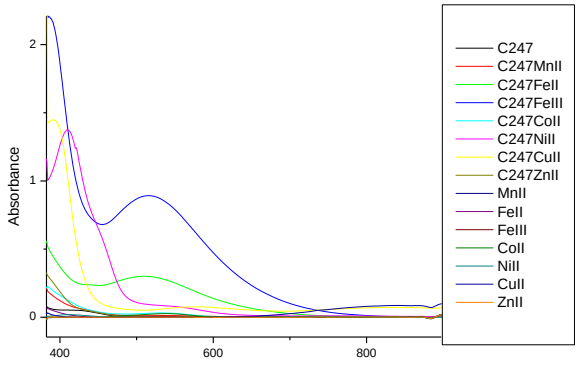

Electronic spectra of calix-salen corand C-247 in presence of 1st transition series metal ions.

Fig. 3.24

Selectivity study was carried out by adding solution of host macrocycle ($0.8x10^{-3}$M) to the solution mixture of two metal ions ($8x10^{-3}$M each) at a time. Study reveals that the macrocycle selectively recognizes Cu^{2+} among all the metal ions with very small interference of Fe^{3+} (green coloured complex was immediately formed due to Cu^{2+} complexation). In absence of Cu^{2+} the corand shows marked preference for Fe^{3+} among the other metal ions and produces intense red coloured complex (Fig. 3.25, 3.26).

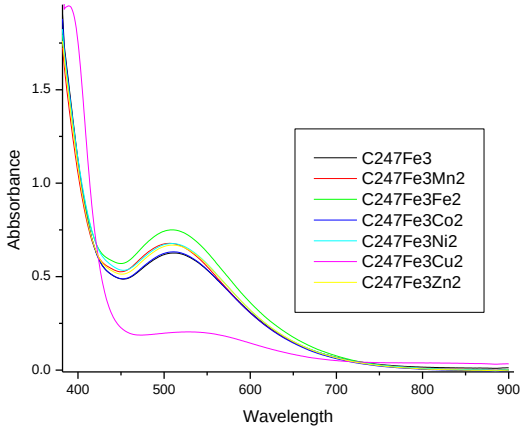

Fe^{3+} selectivity study observed with uv-vis spectra.

Fig. 3.25

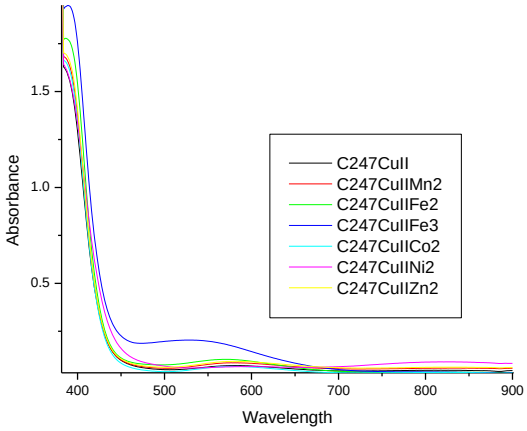

Cu^{2+} selectivity study observed with uv-vis spectra.

Fig. 3.26

Determination of stoichiometry by Job's method

To determine the number of metal ions binding with the host molecule having multiple binding sites, titration of the host molecule with $Fe(ClO_4)_3$ in DMSO was carried out to find nature of curve in Job's plot. The result shows that there is 1:1 binding between metal ion and the corand. This means that only one metal ion has been included in the cavity formed by the corand (Fig. 3.27).

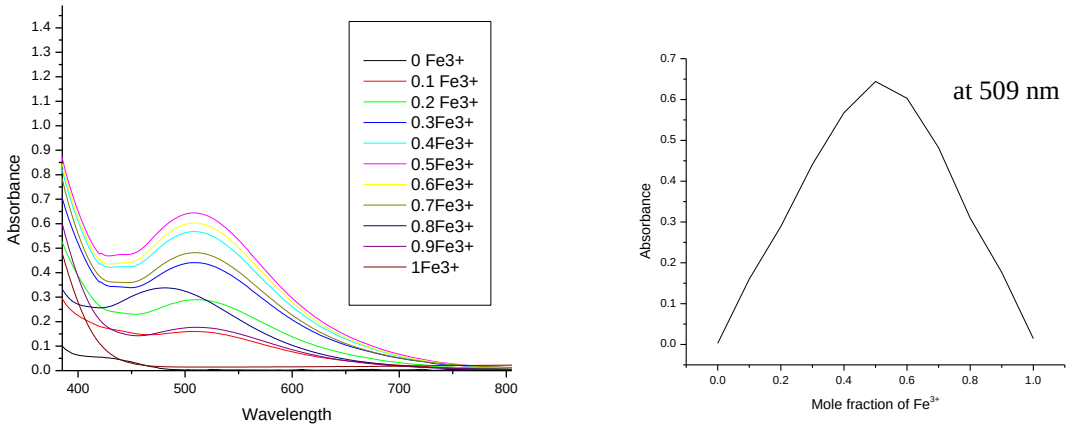

Stoichiometry determination by Job's method

Fig. 3.27

Photoluminescence study was also carried out with the calix-salen corand C-247 (2.5x 10^{-4} M in DCM) and 1st transition series metal ions (2.5x 10^{-3} M in DMSO).The result shows that salicylaldehyde derived calix-salen corand is a weak fluorophore. Binding of Zn^{2+} with calix-salen corand showed remarkable enhancement in fluorescence intensity while other metal ions did not show any enhancement on their binding. When fluorescence study was carried out with Zn^{2+} in the presence of other transition metal ions, it was observed that there is a decrease in fluorescence due to their interference and maximum quenching was observed in the presence of Cu^{2+}. This is in accordance with our observation that there is preference for Cu^{2+} binding from UV-Vis spectroscopy study (Fig. 3.28).

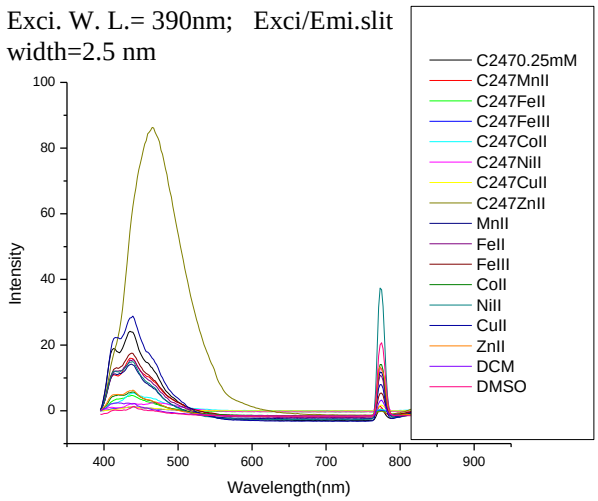

Photoluminescence results of calix-salen corand C 247 in presence of 1st transition series metal ions.

Fig. 3.28

In order to prepare more densely functionalised corand the reaction of 5,5'-methylene-bis-vanilline with (1R,2R)-DACH was carried out in dichloromethane under high dilution conditions, but did not result in any desired product, as was observed on TLC even after 24 hrs. However when its isomeric bis-aldehyde, 5,5'-methylene-bis-(2-hydroxy-3-methoxybenzaldehyde) was reacted with (1R,2R)-DACH under high dilution condition using dichloromethane as a solvent the reaction proceeded smoothly with a clear major spot on TLC along with some other minor products. The major product was isolated in 57% yield after purification of reaction mixture by column chromatography using DCM-MeOH elluent system.

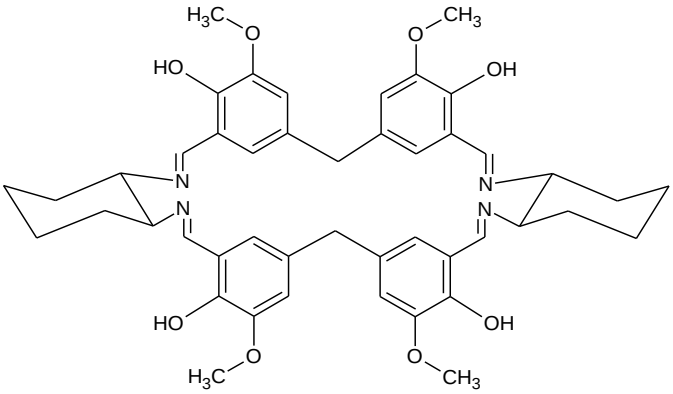

Corand C 139

Fig. 3.29

In IR spectrum a strong and slightly broader band for C-O stretching is observed at 1266 cm^{-1} in addition to the other characteristic IR bands (Spectrum 3.13). In proton NMR the methoxy protons were observed at 3.93 δ in addition to the other proton signals as were observed for the unsubstituted salen corand (Spectrum3.14). The methoxy group carbon was observed at 56.2 δ in ^{13}CNMR (Spectrum 3.15). Nature of carbon atoms in the corand was confirmed by DEPT studies. 2DNMR study of the corand was carried out with the help of COSY, NOESY, HSQC and HMBC techniques which gave clear connectivity between the carbons and protons.

NOESY correlation shows through space interaction of methylene bridge protons with that of the neighbouring ortho protons on aromatic ring as well as due to 1,3-diaxial related protons on cyclohexane ring as was observed in earlier case in addition to NOE of CH proton of the imine linkage with a cyclohexane proton and with an aromatic proton. An additional NOESY cross peak is observed between protons on methoxy group with the aromatic proton at the ortho position to the methoxy group (**Spectrum 3.19, Fig. 3.30**).

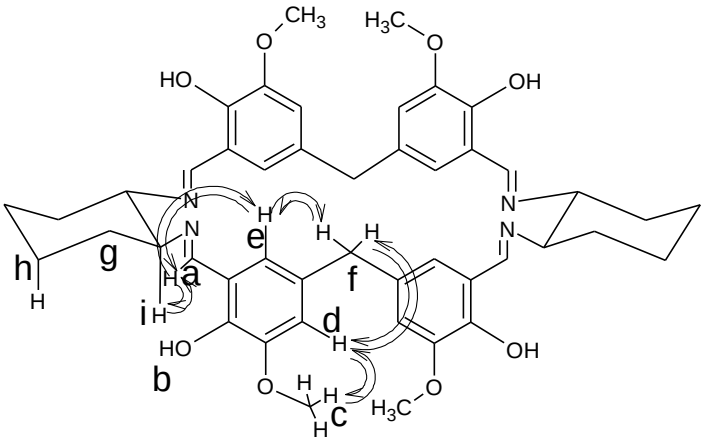

^{1}H-^{1}H Correlation as observed in NOESY

Fig. 3.30

In Q-TOF mass spectrum [M+H] peak is observed at 789.4 m/z and a base peak for [M+Na] at 811.4 m/z which is in accordance with the proposed [2+2] cyclocondensed corand structure (Fig. 3.29). A mass peak at 1600.8 is also observed in the mass spectrum

indicative of existence of [4+4] corand which can be ultimately proved with the help of single crystal X-ray analysis (Spectrum 3.22). The attempts to grow single crystals of the corand are in progress. HPLC purity of the corand was found to be 98.1%. Specific optical rotation at 0.3% concentration was found to be [α] = -215.14 in DCM. CD spectrum of the corand is shown in Fig. 3.31.

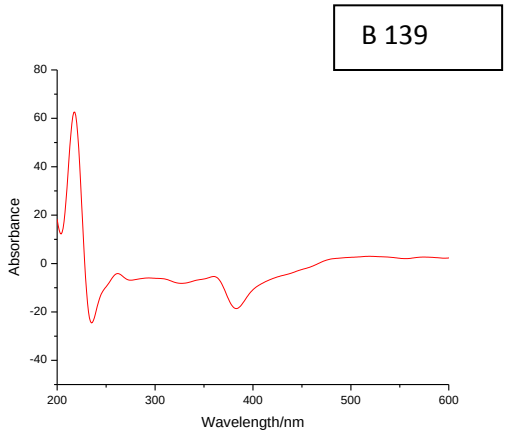

CD Spectrum of C-139

Fig. 3.31

Solution studies

Host-guest complexation studies with the newly synthesized calix-salen corand dissolved in DCM was carried out by adding 10 times more concentrated solution of various transition metal ions to it in DMSO. There was significant response for Cu^{2+}, Fe^{3+}, Fe^{2+} and Ni^{2+} (**Fig. 3.32**). Selectivity study was carried out by mixing solution of two metal ions at a time with host (corand) solution. It was found that there is the preference for Cu^{2+} ions compared to the other transition metal ions except for Fe^{3+} and Fe^{2+} which show some interference (**Fig. 3.33**).

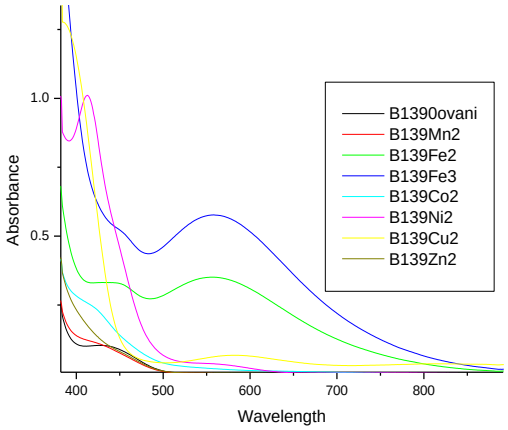

Uv-vis spectra of calix-salen corand (B139) in presence of 1st transition series metal ions.

Fig. 3.32

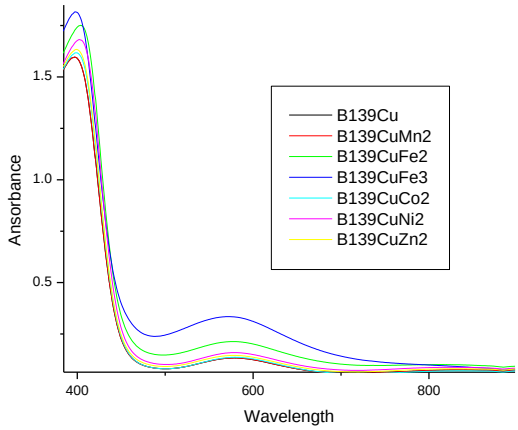

Cu^{2+} selectivity observed with Uv-vis spectra.

Fig. 3.33

The host-guest stoichiometry was determined using Job's method. It was found that corand binds the metal ion in (1:1) stoichiometry (**Fig. 3.34, 3.35**).

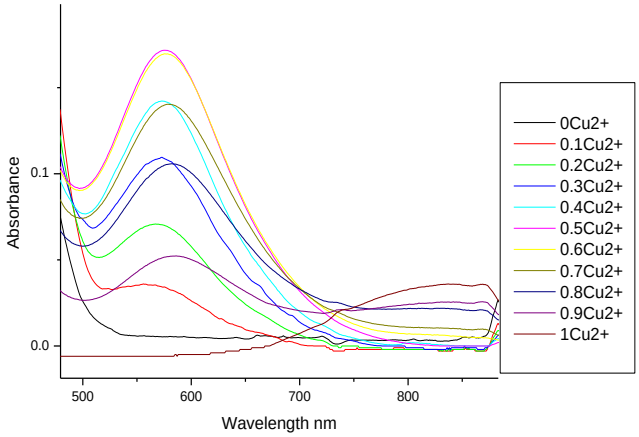

Uv-Visible spectrum of corand B 139- Cu^{2+} titration

Fig. 3.34

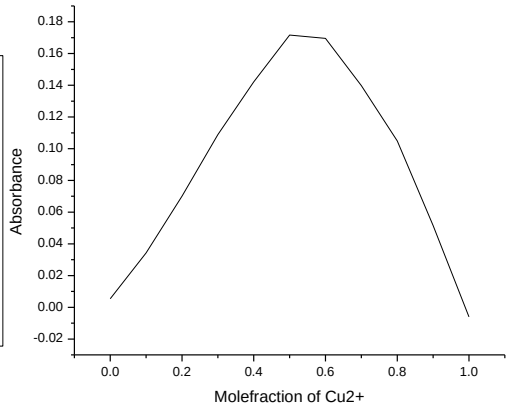

Job's plot of corand B 139 and Cu^{2+}

Fig. 3.35

Photoluminescence study between calix-salen corand B 139 in presence of 1st transition series metal ions showed greater fluorescence response for binding of Mn^{2+} within the

macrocycle. The phtoluminiscence study was also carried out with the macrocycle and mixture of metal ions (**Fig. 3.36**). Cu^{2+} quenched the fluorescence observed, due to its preferential binding with the macrocycle even in presence of Mn^{2+} ions.

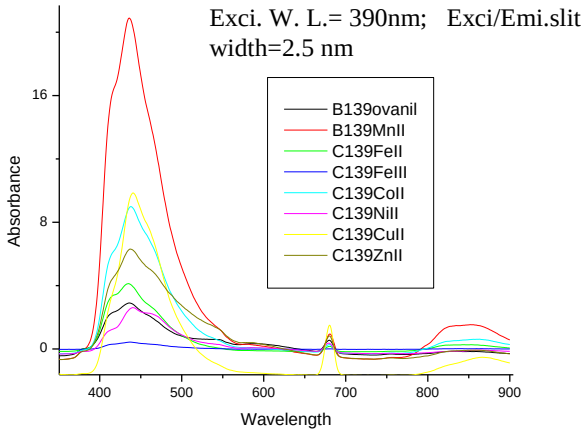

Photoluminescence spectra of calix-salen corand (B-139) and 1st T.M. ions

Fig. 3.36

We also prepared 5,5'-methylene-bis-(3-alkyl-2-hydroxybenzaldehyde) for their application as linkers for constructionof supramolecular structures. When 5,5'-methylene-bis-(3-methyl-2-hydroxybenzaldehyde) was subjected to macrocyclocondensation with (1R,2R)-DACH it resulted in a mixture of products having major product with at least two overlapping spots on TLC. The attempts to purify the mixture from column chromatography were unsuccessful. Further analysis of the products was not carried out at this stage and pursued in future.

The macrocyclisation of 5,5'-methylene-bis-(3-*tert*-butyl-salicylaldehyde) with (1R,2R)-DACH gave a major product along with some other minor products as was observed on TLC. The major product on column chromatrography could be isolated in pure form in about 18% yield. The structure of the macrocyclic corand was established based on its spectral characteristics (**Fig. 3.37**). In proton NMR as well as in ^{13}CNMR strong peaks were observed corresponding to *tert*-butyl groups present (Spectra 3.25, 3.26).

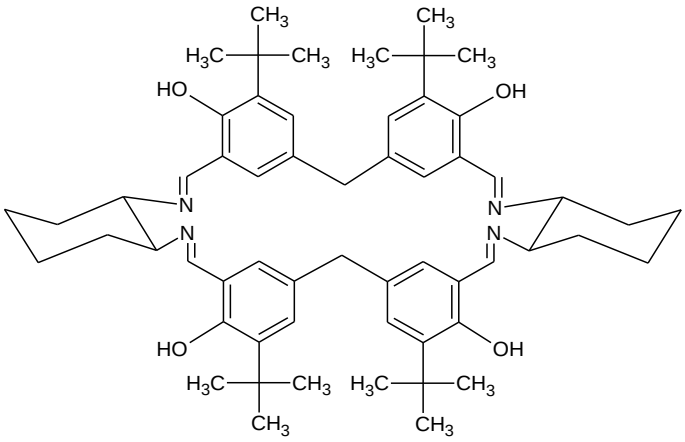

Corand C 240

Fig. 3.37

Carbon and proton assignments were done on basis of its 1D and 2D NMR characteristics in form of ^{1}H NMR, ^{13}CNMR, DEPT, COSY, HSQC, HMBC and NOESY NMR studies. (Spectra 3.25 to 3.32) In NOESY spectrum, NOE interaction between the *tert*-butyl protons was observed with the proton on its ortho position as a cross peak (Spectrum 3.30).

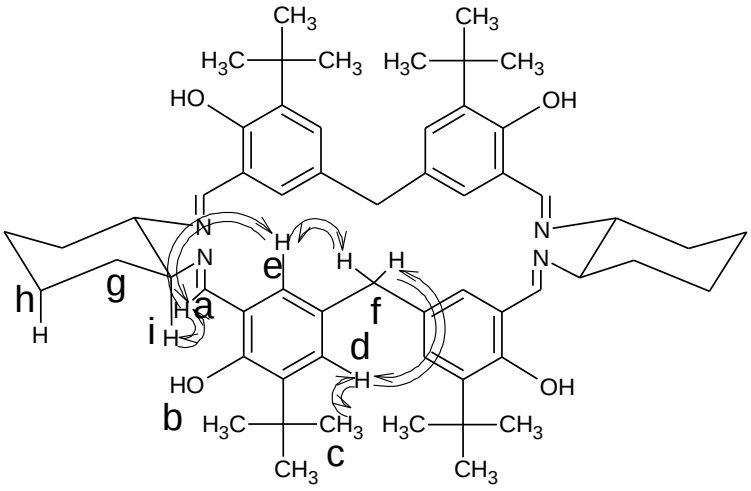

^{1}H-^{1}H Correlation as observed in NOESY

Fig. 3.39

Q-TOF mass spectrum of the corand B-139 is having mass value 893.4 m/z corresponding to the molecular ion peak supports the proposed corand structure from [2+2] cyclocondensation of the reactants. Its HPLC profile shows 99.9% purity of the corand. The specific optical rotation of the corand at 0.3% concentration in DCM was measured to be [α]= -308.1. Its CD spectrum is shown in Fig 3.38.

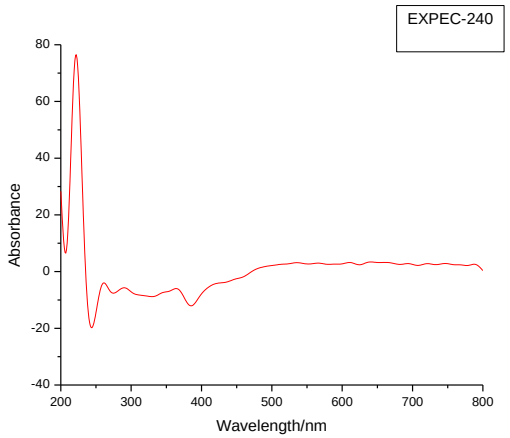

CD spectrum of C-240

Fig. 3.38

- **Solution studies**

Host-guest complexation studies of the *tert*-butyl corand with 1st transition series metal ions show higher absorption in the presence of Ni^{2+}, Fe^{2+}, Fe^{3+}. Selectivity study didn't show any preference for a particular metal ion. The fluorescence was not observed in photoluminescence study (**Fig. 3.40**).

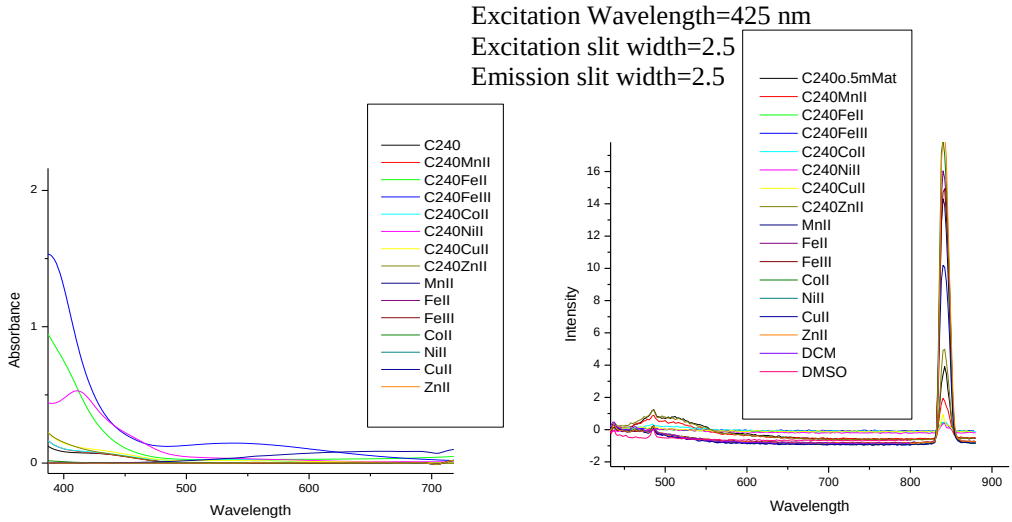

Uv-vis and fluorescence spectra of *tert*-butyl calix-salen corand (C240) in presence of 1st transition series metal ions.

Fig. 3.40

The Ba^{2+} template synthesis of *tert*-butyl calix-salen corand was reported by Li. *et. al*. who also studied its Manganese and Nickel complexes.[19,20]

In the next phase we looked at the linkers having electron withdrawing substituents present. Thus the reaction with 5,5'-methylene-bis-(3-bromosalicylaldehyde) and (1R,2R)-DACH was carried out under high dilution condition which resulted in the formation of calix-salen macrocycle due to [2+2] cyclocondensation of the reactants. The major product was isolated in about 30% yield after column chromatographic purification of the mixture of products obtained.

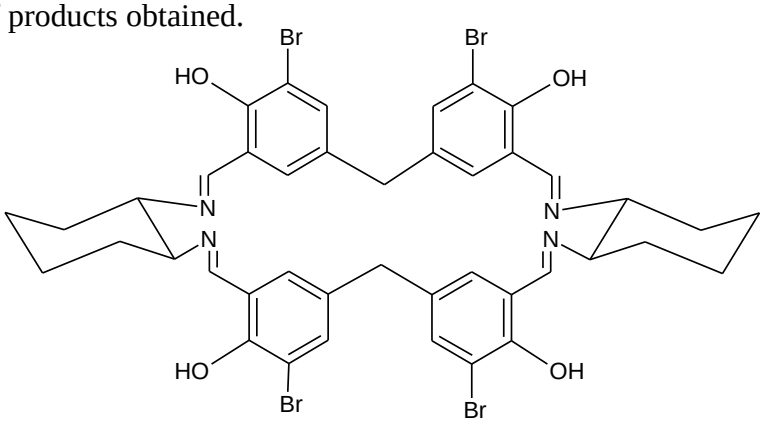

Corand C 242

Fig. 3.41

The structure of the corand was confirmed by various spectral analyses. In proton NMR one of the two aromatic protons is showing resolved meta coupling (Spectrum 3.36). ^{13}CNMR, DEPT, COSY, HSQC, HMBC and NOESY NMR studies were carried out showing characteristics observed as in earlier cases (Spectra 3.35 to 3.44). Its mass spectrum showed a base peak at 985.23 m/z corresponding to [M+H] mass value (Spectrum 3.44). HPLC shows only single peak corresponding to 100% purity. Specific rotation was found to be [α]= -175.59 at 0.3% concentration in DCM. Its CD spectrum was also measured as shown in Fig. 3.42.

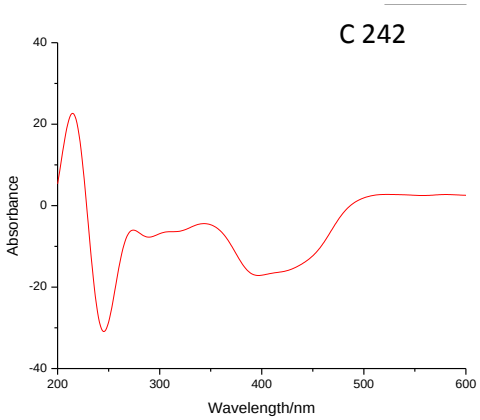

CD spectrum of corand C 242

Fig. 3.42

Microwave assisted cyclocondensation of the methylene-bis-aldehyde with (1R,2R)-DACH tartrate in presence of K_2CO_3 in MeOH-THF mixture was reported to yield the bromo corand without any spectral data.[23]

Solution studies.

Binding and selectivity studies of the corand was carried out using 1st transition series metal ions which indicated preference for Ni^{2+}, Fe^{2+}, Fe^{3+} ions but no specificity was observed for them when ion mixtures were used for the same study (Fig. 3.43). The bromo corand itself shows fluorescence when excited at 430nm with emission at 540nm.

In the presence of Zn^{2+}, Mn^{2+}, Co^{2+} and Cu^{2+} fluorescence is retained while the other metal ions quench the fluorescence of the corand (**Fig. 3.44**).

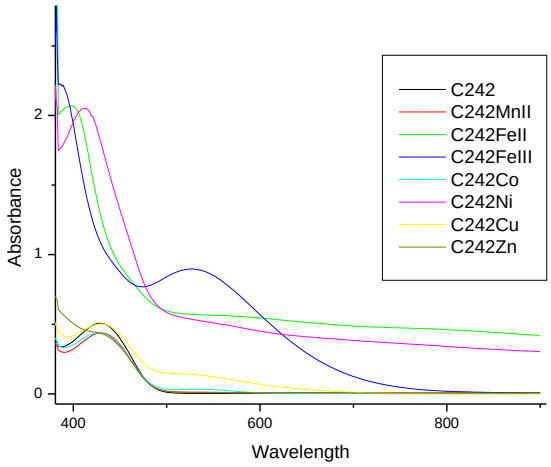

Uv-vis spectra of *tert*-butyl calix-salen corand (C242) in presence of 1st T. M. ions.

Fig.3.43

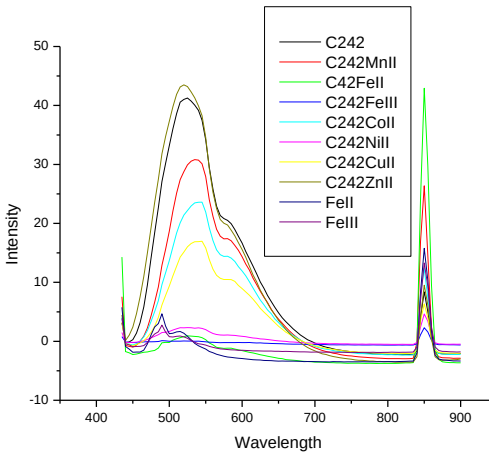

Fluorescence spectra of *tert*-butyl calix-salen corand (C242) in presence of 1st T. M. ions.

Fig.3.44

The cyclocondensation of 5,5'-methylene-bis(3-nitrosalicylaldehdye) with (1R,2R)-DACH was a smooth reaction giving a clear spot on TLC of a major product which was isolated by column chromatography in about 40% yield. The product had a poor solubility in the other organic solvents compared to the other corands and was soluble in DMSO. The corand was assigned the structure as [2+2] cyclocondensed product based on its analytical data (Fig. 3.45).

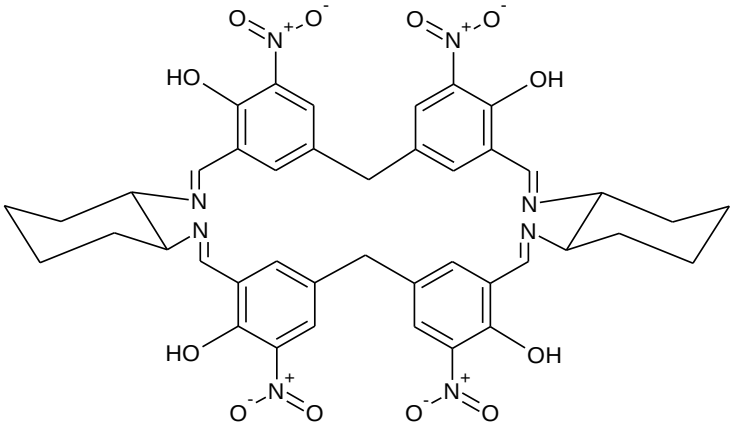

Corand C 188

Fig. 3.45

IR spectrum of the product shows strong bands corresponding to νC=N and $\nu_{as}NO_2$ at 1639 cm^{-1} and 1530 cm^{-1} while medium intensity band at 1351cm^{-1} for ν_sNO_2 (Spectrum 3.46). In proton NMR -OH proton was observed at 15.9 δ, the CH proton of imine linkage at 8.52 and aromatic protons at 8.0 δ and 7.4 δ with meta coupling of 2Hz. The methylene bridge protons and the proton attached to carbon of cyclohexane ring which is attached to nitrogen are found close to each other at 3.77 δ and 3.72 δ as a singlet and a multiplet respectively. Each remaining proton on cyclohexane ring is seen separately located at axial and equatorial positions (Spectrum3.47). In ^{13}C NMR eleven signals are observed between 167 δ to 23 δ due to symmetry present in corand (Spectrum 3.48). Secondary, tertiary and quaternary carbons were differentiated with the help of DEPT experiments (Spectra 3.49, 3.50). COSY spectrum shows the cross peaks due to coupling of N attached CH with the protons on neighbouring carbon on cyclohexane ring (Spectrum 3.51). HSQC, HMBC and NOESY 2D NMR spectra helped in establishing carbon-hydrogen correlation and through space correlation between various protons (Spectra 3.3.51-3.54, **Fig. 3.46**).

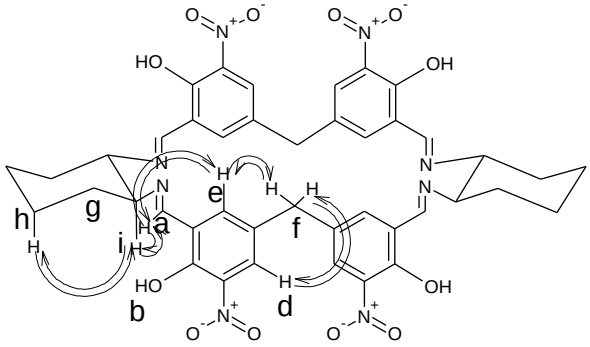

Correlation of protons from NOESY
Fig. 3.46

ESI mass spectrum of the nitro substituted corand shows base peak at 849.56 m/z corresponding to [M+H] supporting [2+2] corand structure (Spectrum 3.55). HPLC showed 99.95% purity of the product. (Chromatogram 3.56) Specific optical rotation of the nitro substituted calyx-salen corand was found to be [α]= -812.95 at 0.3% w/v concentration in DMSO at 26 °C. The CD spectrum was recorded in DMSO at concentration of 3mg/5ml as shown in Fig. 3.47.

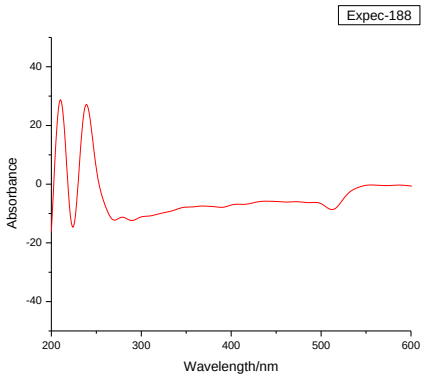

CD spectrum of Corand C188

Fig. 3.47

All the transition metal ions show characteristic bands due to their binding with the corand (C188). Cu^{2+}, Ni^{2+} and Fe^{3+} show specific absorption bands at different λ_{max} as compare to host corand (**Fig. 3.48**). Selectivity study was carried out for Fe^{3+}, Cu^{2+} and Ni^{2+} in presence of other metal ions. In presence of Fe^{3+} all other ions lost their identity except Cu^{2+} and Ni^{2+} while Ni^{2+} did not show any effect on the absorption bands of the other metal complexes (**Fig. 3.49, 3.50**). Selectivity study for Cu^{2+} revealed that corand recognizes Cu^{2+} even in presence of other metal ions (**Fig. 3.51**).

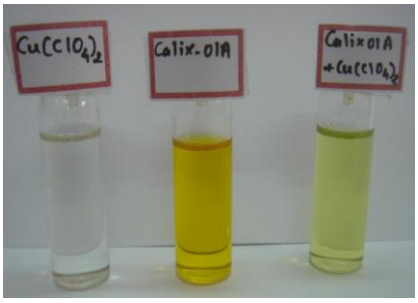

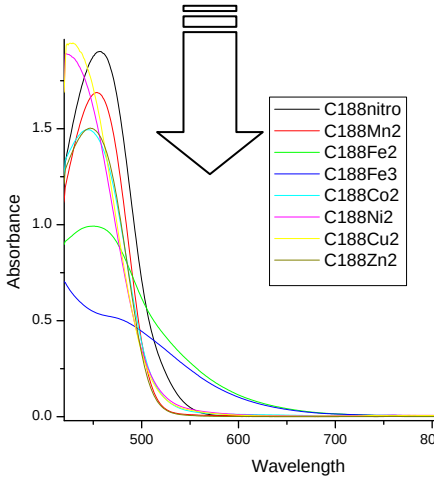

Uv-vis spectra of *tert*-butyl calix-salen corand (C240) in presence of 1st transition series metal ions.

Fig. 3.48

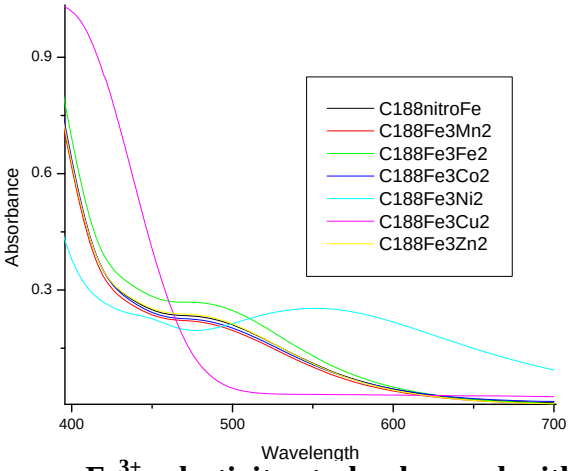

Fe^{3+} selectivity study observed with Uv-vis spectra.

Fig. 3.49

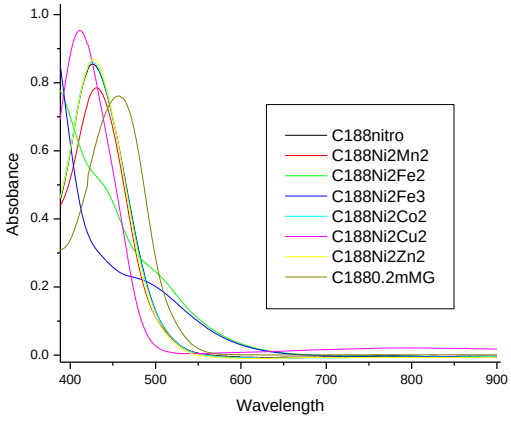

Ni^{2+} selectivity study observed with Uv-vis spectra.

Fig. 3.50

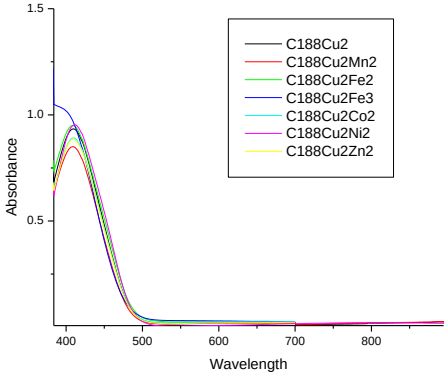

Cu^{2+} selectivity study observed with Uv-vis spectra.

Fig. 3.51

Synthesis of calix-salen corand (C-188) was attempted by another group under microwave conditions which resulted in some insoluble material which was not characterized[23].

3.3.2 Chiral calix salen corand from (1R,2R)-diamino-diphenylethane (DADPE)

The other chiral (1R,2R)-diamine selected for synthesis and study of some new corands was (1R,2R)-diamino-diphenylethane (DADPE). (1R,2R)-DADPE was subjected to cyclocondensation with various methylene-bis-aromaticaldehyes under high dilution condition in dichloromethane as a solvent. Most of the bis-aldehydes did not react with (1R, 2R)-DADPE, the only bis-aldehyde which successfully gave [2+2] cyclocondensed calix-salen macrocycle was 5,5'-methylene-bis(3-nitrosalicylaldehyde) apparently due to its higher reactivity. The observation shows that (1R, 2R)-DADPE is having lower reactivity compared to that of (1R, 2R)-DACH. The major product from the reaction of 5,5'-methylene-bis(3-nitrosalicylaldehyde) and (1R, 2R)-DADPE was isolated using column chromatography in 30% yield (Fig. 3.52).

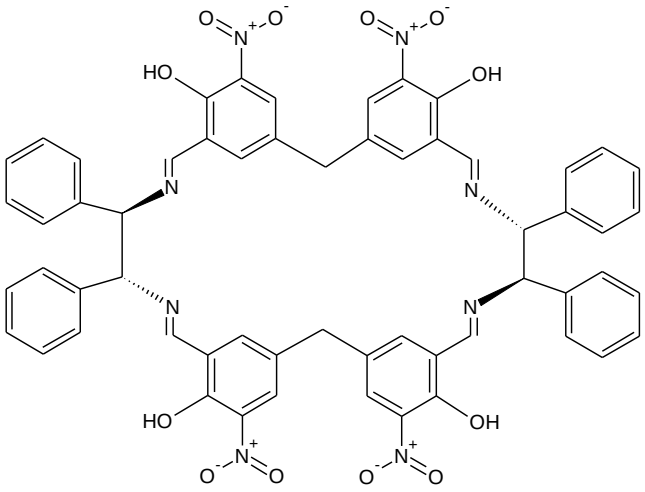

Corand C 221
Fig. 3.52

The chiral corand was assigned the structure based on its spectral analysis. In IR it showed characteristic bands for OH, C=N and NO_2 streching frequencies at 3465, 1636 and 1530, 1351cm^{-1} respectively (Spectrum 3.57). In proton NMR phenolic OH proton is observed at 15.4 δ, CH of imine linkage at 8.76 δ as a singlet, aromatic protons of the aldehyde linker were observed at 8.1 δ and 7.6 δ having meta coupling of 2 Hz. The other monosubstituted phenyl ring protons are observed as a three set signals between 7.3 -7.1 δ. The proton on chiral carbon is observed as a singlet at 5.43 δ while methylene protons are observed at 3.8 δ as a singlet with no other signal at high field (Spectrum 3.58). In ^{13}C NMR the aromatic carbons are bunched between 138 δ and 129 δ. The benzylic chiral carbon is observed at 75.2 δ while the methylene bridge carbon is seen at 38.1δ (Spectrum 3.59). DEPT study separated out the proton attached carbons (Spectra 3.60, 3.61). From COSY spectrum no additional information could be obtained (Spectrum 3.62). Q-TOF mass analysis was helpful in establishing the composition of the new corand as [2+2] cyclocondensation reaction product with the mass value at 1045.15 m/z. (Spectrum 3.63). Specific optical rotation of the chiral corand C 221 was observed to be [α]= +10.604 at 0.1% w/v concentration in DMSO at 26 ^{o}C. Multiple cotton effect was observed CD spectrum of the corand C-221which was recorded in DMSO at concentration of 1mg/5ml. (**Fig. 3.53**)

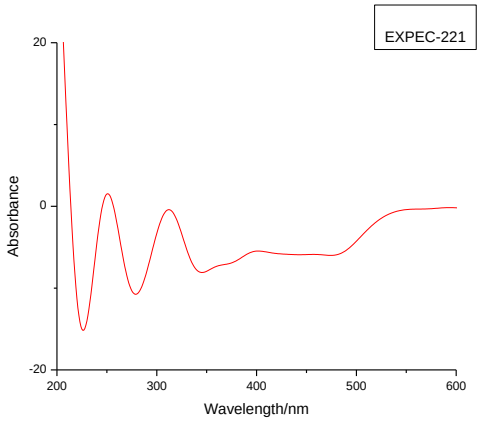

CD spectrum of Corand C-221
Fig. 3.53

Solution Studies

Electronic spectra of the corand (C-221) were recorded to explore their binding as well as selectivity towards 1st transition series metal ions. Host concentration was $5x10^{-4}$ M in DMSO and metal ion concentration was $5x10^{-3}$M in DMSO. Study reveals that it binds with all the metal ions giving different absorption bands (Fig. 3.54).

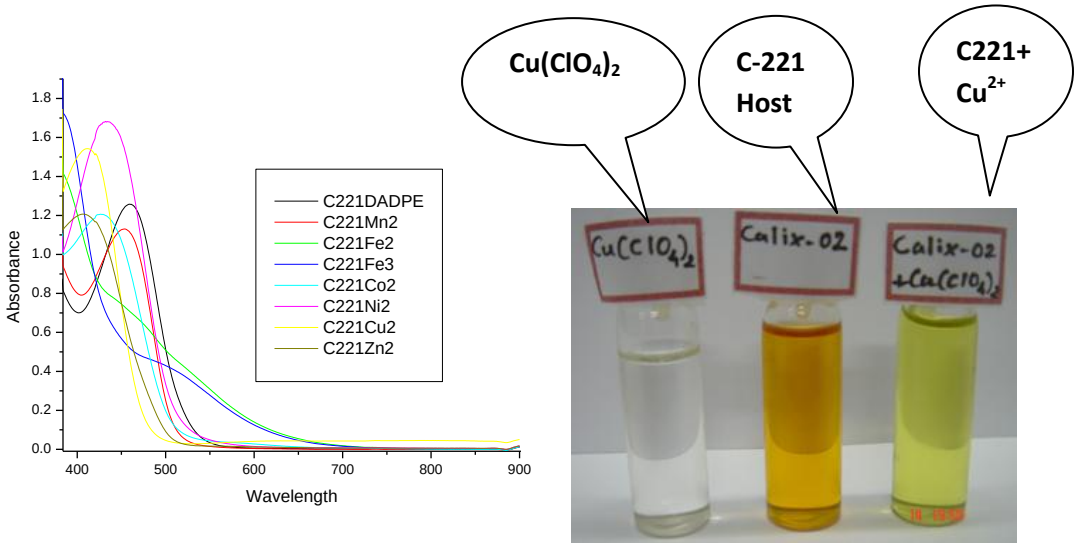

Uv-vis spectra of nitro substituted calix-salen corand (C 221) in presence of 1st transition series metal ions.

Fig. 3.54

It showed unique response towards Fe^{3+} and Ni^{2+}, so selectivity study was carried out with Fe^{3+} and Ni^{2+} in the presence of the other metal ions. There wasn't any selectivity observed for Ni^{2+} (Fig. 3.55). Corand shows unique abosorption band similar to that of binding of Fe^{3+}even when added to the mixture of Fe^{3+} and other transition metal ions except Cu^{2+} (Fig. 3.56).

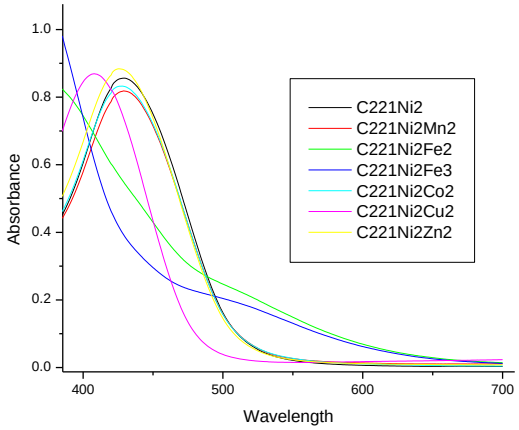

Ni^{2+} selectivity study observed though uv-vis spectra

Fig. 3.55

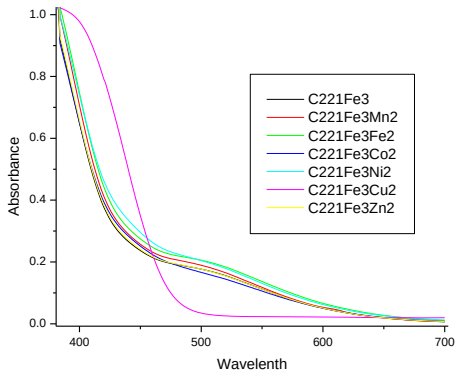

Fe^{3+} selectivity study observed though uv-vis spectra

Fig. 3.56

Cu^{2+} shows marked deviation in the characteristic pattern of absorption band of Fe^{3+}. The corand showed characteristic band of Cu^{2+} complexation even when added to the mixture of other metal ions with Cu^{2+}. This reveals that chiral caix-salen corand (C 221) is also a promising candidate of colorimetric Cu^{2+} ion sensor amonst 1st transition series metal ions (**Fig. 3.57**).

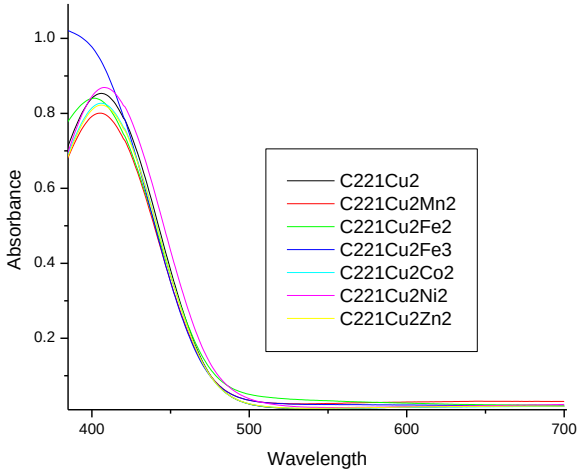

Cu^{2+} selectivity study observed through uv-vis spectra

Fig. 3.57

3.3.3 Chiral Calix-Salen Corand from R-(+)-2,2'-Diamino-binaphthalene

The other novel chiral diamine R-(+)-2,2'-diamino-binaphthalene (DABN) was selected for the synthesis of new calix-salen corands. This diamine was different from the earlier two in the sense that it is not a vicinal diamine and has no stereogenic centre in its structure but has a chiral axis. The chirality is due to restricted rotation along C-C bond connecting two naphthyl rings. The cyclocondensation of this diamine with various methylene-bis-aldehydes when carried out under high dilution condition in DCM did not show any progress even after long reaction times and starting materials were recovered unreacted. Once again 5,5'-methylene-bis(3-nitro-salicylaldehdye) was found to be undergoing reaction with R-(+)-DABN with a gradual colour change from colourless to yellow of the reaction mixture showing major spot on TLC. The product was isolated in poor yield of 11% after column chromatography separation on silica-gel.

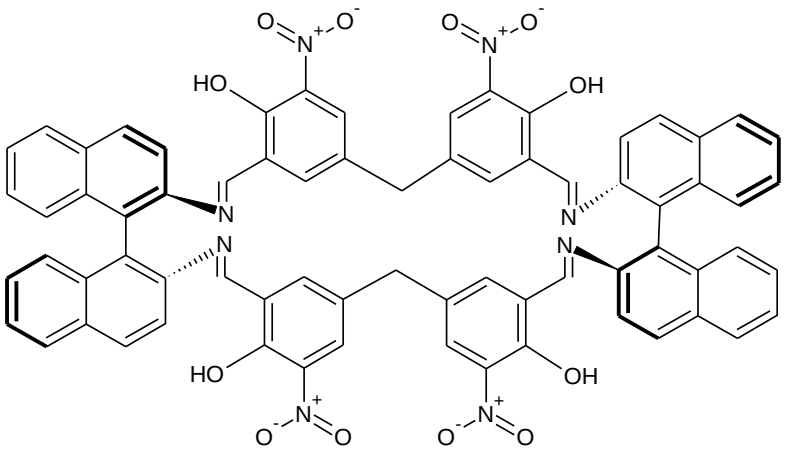

Corand C 238

Fig. 3.58

Symmetry of the corand was reflected in its ^{1}H NMR and ^{13}C NMR. In ^{1}H NMR phenolic OH proton is observed at 14.02 δ, the CH proton of imine linkage is observed downfield at 9.14 δ, the aromatic protons from the linker dialdehyde were observed at 7.90 and 7.59 δ with meta coupling of 2 Hz. The six protons of naphthalene ring are distinctively seen in the aromatic region with appropriate splitting of the signals between 8.30 to 7.0 δ. The

methylene bridge protons are observed at 3.83 δ as a singlet (Spectrum 3.66). In ^{13}CNMR, methylene carbon being only SP^3 hybridized carbon is observed at 37.9 δ while the carbon of the imine linkage is observed most downfield at 162.4 δ next to the OH attached aromatic carbon which is observed at 154.5 δ. All the other aromatic carbons are giving signals between 140-116 δ (Spectrum 3.67). Assignment of each carbon and each proton was done by in depth study of DEPT, COSY, HSQC, HMBC and NOESY. Identification of each proton peak was possible on the basis of its COSY spectrum (Spectrum 3.70). All protons of naphthalene rings show cross peaks due to coupling with their neighbouring protons on the ortho positions. The two aromatic protons of methylene-bis-aldehyde linker show cross peaks due to their mutual coupling (Spectrum 3.70). With the help of HSQC, location of all the protons on respective carbons was assigned precisely. (Spectrum 3.72) The same was supported by HMBC spectrum of the corand (Spectrum 3.73). The NOESY spectrum shows through space coupling between CH proton of imine functionality with aromatic proton of methylene-bis-aldehyde at its ortho positon as well as with proton at 3rd position of the naphthalene ring (**Fig. 3.59**, Spectrum 3.71).

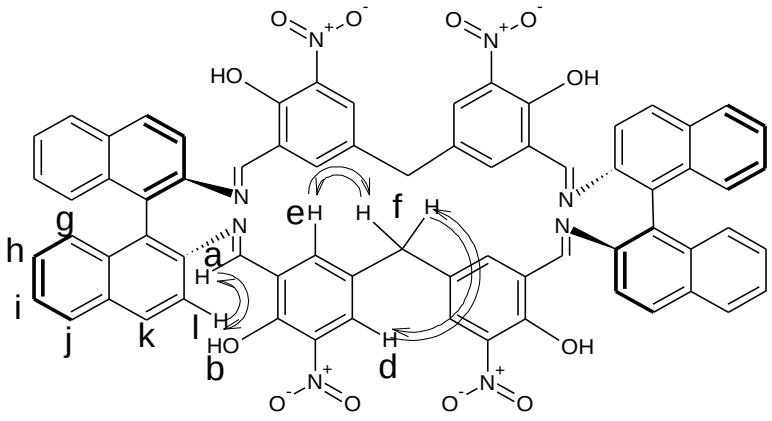

1H-1H Correlation as observed in NOESY
Fig. 3.59

IR spectrum of the corand shows both bonded and non-bonded OH stretching frequency at 3487 and 3640 cm^{-1} respectively. -C=N stretching frequency is observed at 1628 while asymmetric stretching frequency for NO_2 group is observed at 1527 cm^{-1} and symmetric

stretching frequency for the same is observed at 1343 cm^{-1}. Some broad bands are observed in the spectrum seems to be due to higher concentration of the corand in KBr. (Spectrum 3.65). The corand was found to be 99.89% pure by HPLC. Specific rotation was found to be [α] = -617.416 at 26 ^{o}C in DMSO with concentration of 0.3%w/v. CD spectrum was recorded in DMSO at concentration of 3.25mg/5ml (Fig. 3.60).

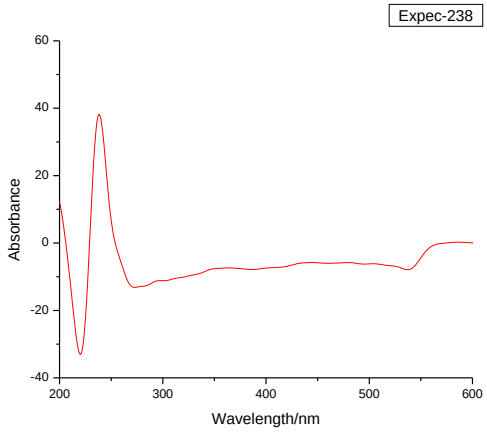

CD-spectrum of corand C-238
Fig. 3.60

Solution studies

With the help of electronic spectroscoapy it was observed that the corand binds with the 1st transition series metal ions in DMSO as a solvent with shift in absorption value in their presence. The Cu^{2+} and Ni^{2+} showed different absorption bands with the higher intensities. Selectivity study of corand among the 1st transition metal ions in the presence of Cu^{2+} and Ni^{2+} was carried out (**Fig. 3.61**).

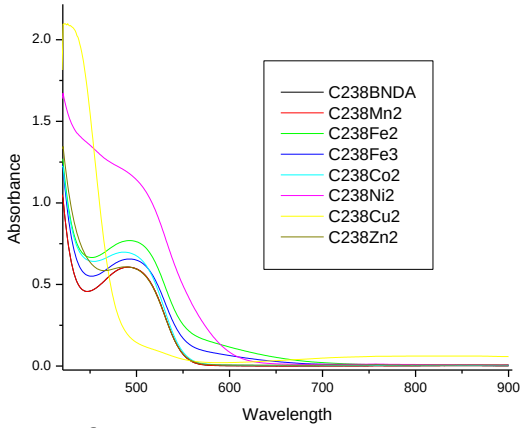

Uv-vis spectra of nitro substituted calix-salen corand (C 238) in presence of 1st transition series metal ions.
Fig. 3.61

The corand did not show any selectivity for Ni^{2+} (**Fig. 3.62**) while it had preference for Cu^{2+} even in the presence of the other transition metal ions except Ni^{2+} which shows some interference as reflected in the absorption spectra. (**Fig. 3.63**).

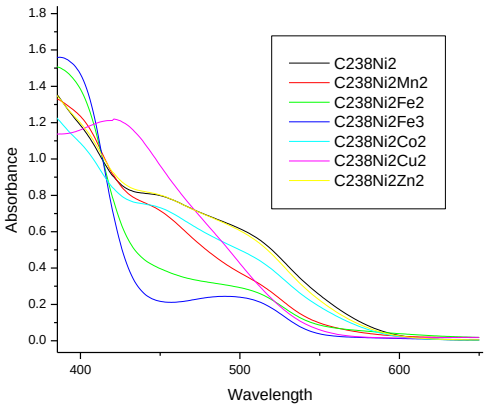

Ni^{2+} selectivity study observed though uv-vis spectra

Fig. 3.62

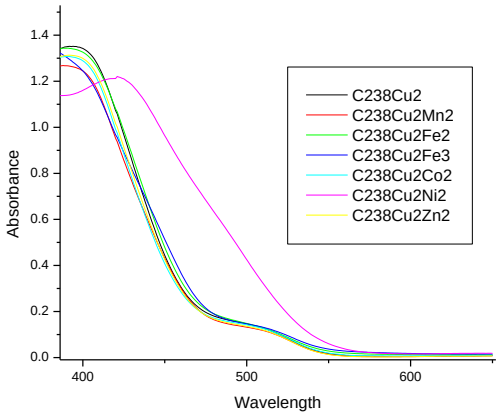

Cu^{2+} selectivity study observed though uv-vis spectra

Fig. 3.63

As soon as a solution of $Ni(ClO_4)_2$ was mixed with the calix-salen corand (C238), an intense reddish orange colour was observed which gradually faded to yellow on storing in an atmospheric condition at room temperature for more than one hour. The kinetics of this process was studied with the help of UV-Vis spectroscoapy. The change in its absorption pattern was monitored with UV-Vis spectrum of the complex at every 10 min interval. The absorption band at 380 nm decreased in its intensity with time while the band at 450 nm increased in its intensity, the decrease in intensity with time was also observed for the band at 520 nm value. These changes in absorption pattern with time result in change in the colour of the host-guest complex (**Fig. 3.64**).

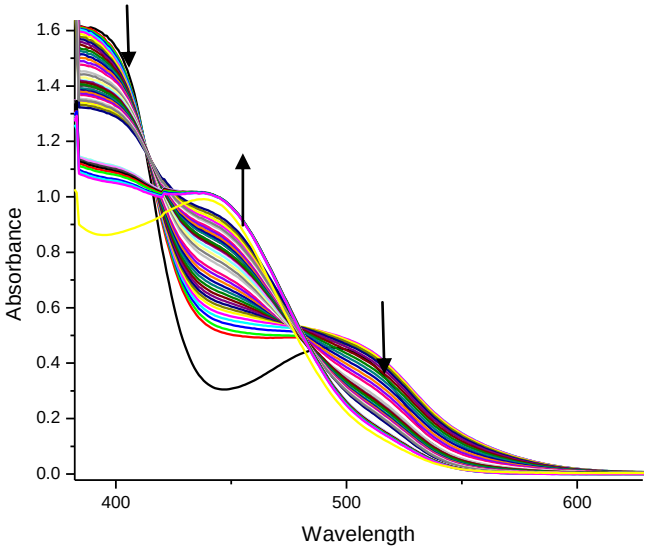

Kinetic study of Ni^{2+} complexation with calix-salen corand C-238 using uv-visible spectroscopy.

Fig. 3.64

Photoluminescence study of the corand shows fluorescence when excited at 425 nm with emission at 590 nm due to the presence of binaphthyl moieties with extended conjugated system present in the corand. The fluorescence study of the corand was carried out in the presence of 1st transition series metal ions which showed that the original fluorescence is decreased in their presence except for Mn^{2+} in whose presence intensity of fluorescence is increased while Cu^{2+} totally quenched the fluorescence (**Fig. 3.65**).

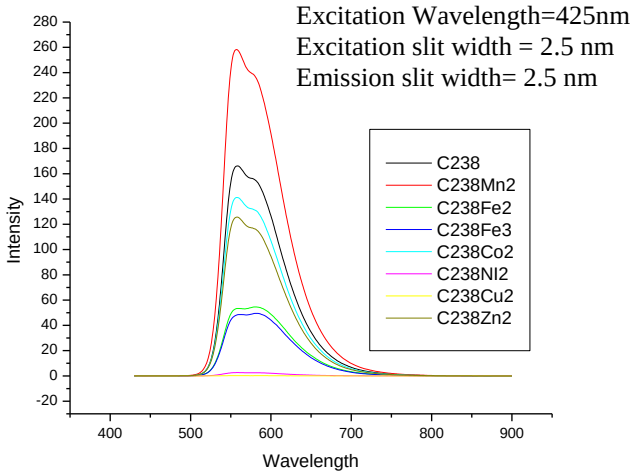

Photoluminescence spectra of the nitro substituted calix-salen corand (C 238) in presence of 1st transition series metal ions.

Fig. 3.65

Following this observation selectivity in binding was also studied with the help of fluorescence spectroscoapy. The results were in accordance with the results from the UV-Vis studies. Mixture of different transition metal ions and Cu^{2+} when added to corand solution the result was no-fluorescence. This shows that corand has a greater preference for Cu^{2+} compared to the other transition metal ions studied. The results show that the calix-salen corand C-238 can be used as fluorescence sensor for Cu^{2+} even in the presence of the other 1st transition metal ions (**Fig. 3.66**).

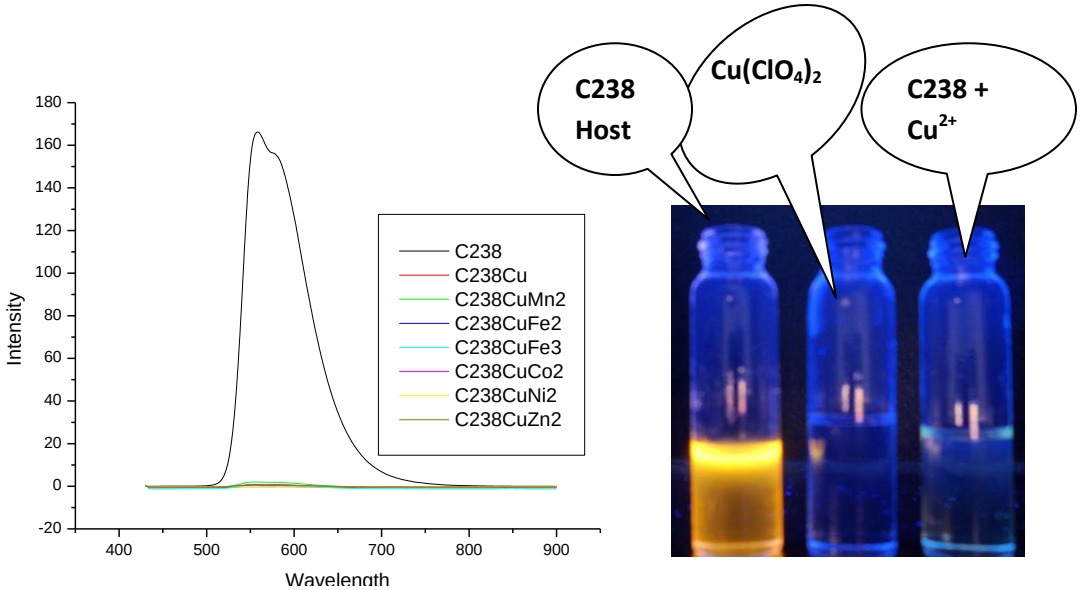

Cu^{2+} selectivity study through photoluminescence spectra

Fig. 3.66

Kinetics of the gradual change with time of the Ni(II) complex of the corand was also studied with the help of fluorescence spectroscopy. The fluorescence spectra of the complex showed gradual decrease in fluorescence with time when recorded at an interval of 10 minutes each (**Fig. 3.67**) The results of the kinetic studies both from UV-Vis and fluorescence spectroscoapy indicates that the type of binding or the location of binding of Ni^{2+} ion changes with time specially in the case of the present corand.

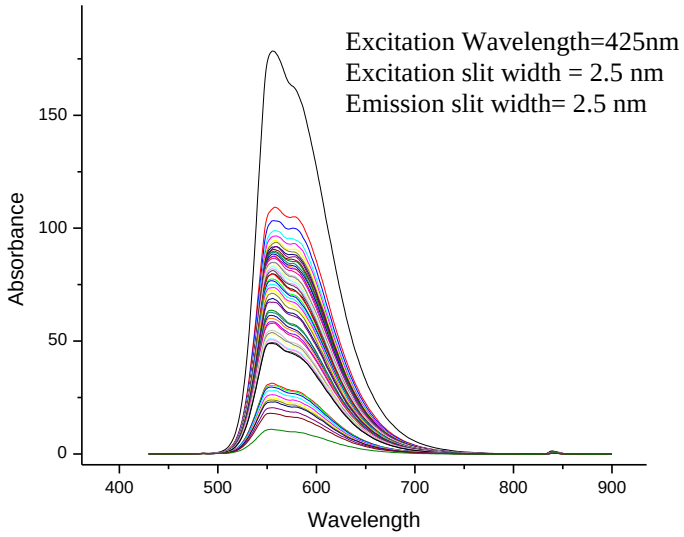

Kinetics of Ni^{2+} complexation with calix-salen corand C-238 using photoluminiscence spectroscopy.

Fig. 3.67

3.4 Conclusion

Several chiral calix-salen corands have been prepared by [2+2] macrocyclization of 5,5'-methylene-bis-salicylalhedydes and chiral diamines namely (1R,2R)-diaminocyclohexane, (1R,2R)-diamino-diphenylethane and R(+)-2,2'-diamino-binaphthalene. All the corands have been well characterized by various spectral methods and all the data have been included here.

Single crystal X-ray analysis of one of the chiral corands shows a different morphology of the crystals than the measured earlier. Specific optical rotation and CD-spectra of all the chiral corands have been recorded and reported here.

The macrocyclic corands have been studied for host-guest complexation with 1st transition series metal ions exhibiting a very good response using UV-Vis. spectroscopy. Selectivity study shows that the corands from 5,5'-methylene-bis(3-nitrosalicylaldehyde) and (1R,2R)-DACH as well as (1R,2R)-DADPE preferentially binds Cu^{2+} in the presence of the other metal ions and thus can act as Cu^{2+} colorimetric chemosensors.

Photoluminescence study of host guest complexes have been carried out. Fluorescence enhancement is observed in case of some of the corands in the presence of metal ions. The corand from R(+)-DABN itself is found to be fluorescent in nature. Cu^{2+} quenches its fluorescence completely even in the presence of other metal ions. Thus the calix salen corand from R(+)-DABN and 5,5'-methylene-bis-(3-nitrosalicylaldehyde) is found to be an effective switch-off type fluorescence chemosensor.

3.5 Experimental

General Remarks

All the chemicals and reagents were purchased from Sigma-Aldrich, Merck, or Spectrochem. All solvents were distilled before use. Column chromatography was carried out using silica-gel (60-120 mesh). Thin layer chromatography was performed on pre-coated silicagel $60F_{254}$ (Merck) aluminium sheets.

Infrared spectra were recorded on Perkin-Elmer FT-IR 16PC spectrophotometer as KBr pellets. ^{1}H NMR and ^{13}C NMR were recorded on Bruker 200 or 400 MHz NMR spectrophotometer in $CDCl_3$, DMSO or D_2O. Elemental analyses were carried out at different places (ZRC, SPARC and CSMCRI). ESI mass were recorded on Shimadzu LC-MS 2010-A and Waters micromass Quattro micro T. M. API. EI and CI mass were recorded on Thermofisher DSQ II mass spectrometer. UV spectra were recorded on Perkin-Elmer Lambda 35 Uv-Vis spectrometer. HPLC was carried out using Shimadzu LC-10AT and UFLC using Shimadzu LC-20AD. Photoluminiscence was measured on Jasco FP6300 Spectrofluorometer. Melting points were measured in open capillaries and are uncorrected. Optical rotation was measured on Rudolph Autopol IV.

Calix-Salen Corand from (1R, 2R)-Diaminocyclohexane.

General procedure for the synthesis:

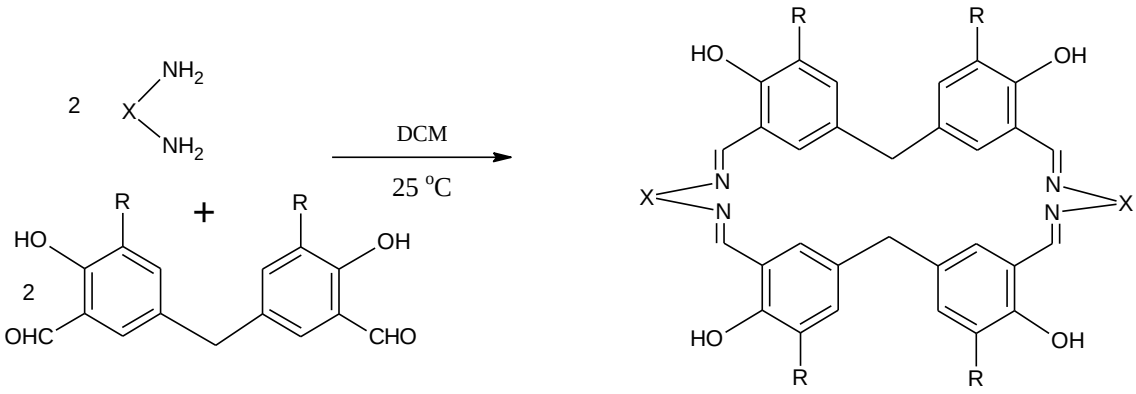

Dichloromethane (2000ml) was placed in a 5L 3 necked Round bottom flask equipped with two addition funnels. Solution of 5,5'-methylene-bis-aldehydes (0.004mol) in dichloromethane (1000ml) and diamine (0.005mol) in dichloromethane (1000ml) were added drop wise from addition funnels over 12 hrs to the magnetically stirred dichloromethane under N_2 atmosphere. Bright yellow colour was slowly developed. Solvent was removed on rotary evaporator till 50 ml solution left. The concentrate was got adsorbed on silicagel for column chromatography. TLC showed very small amount of starting material, nonpolar product spot and many polar impurities. Starting material was eluted in MDC and pure yellow product was separated using MDC:methanol solvent system (gradient).

Calix-salen corand[19,20,23] from (1R, 2R)-diaminocyclohexane and 5,5'-methylene-bis-salicylaldehyde. (C-247)

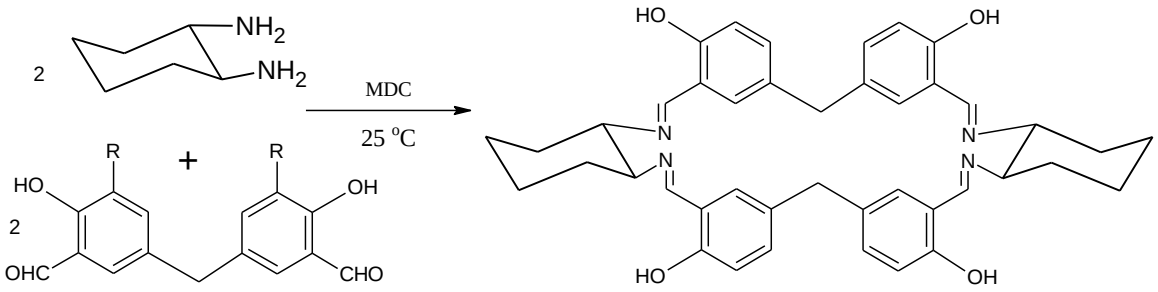

5,5'-Methylene-bis-salicylaldehyde (1 g, 0.004 mol) and (1R, 2R) Diaminocyclohexane (0.53 g, 0.005 mol) reacted in 4000ml MDC to yield the compound (C-247)

Yield: 0.352 g (27%), M.P.= 148 °C.

^{1}H NMR (400 MHz, $CDCl_3$): δ 13.09 (s, 1H), 7.99 (s, 1H), 7.10 (dd, J_1 = 2.0 Hz, J_2 = 8.4 Hz, 1H), 6.85 (d, J = 2.0 Hz, 1H), 6.68 (d, J = 8.4 Hz, 1H), 3.58 (s, 1H), 3.17-3.10 (m, 1H), 1.765(d, J = 8.4 Hz, 2H), 1.60 (q, 1H), 1.37(t, 1H).

^{13}C NMR (400 MHz, $CDCl_3$): δ 164.2, 159.3, 132.0, 131.9, 131.0, 119.0, 116.7, 72.9, 40.9, 33.3, 24.2

Mass: 669.4 (M+H)

HPLC Purity: 98.9%

Specific rotation: -383.000 (C=0.3% wt/v in DCM at 26 °C)

Elemental Analysis:

Calculated for **$C_{42}H_{44}O_4N_4$** : C= 75.42%, H= 6.63%, 8.38%N
Found: C= 74.98%, H= 7.01%, 7.79%N

IR (KBr disc, cm^{-1}) : 3521(phenol, υ(O-H)), 2927 (methylene, $υ_{as}$(C-H)), 2855 methylene, $υ_s$(C-H)), 1634(imine, υ(C=N)), 1586, 1447 (aromatic ring, υ(C=C)), , 1489 ($δ_s(CH_2)$), 1378, 1273 (ν(Ar-O)), 1221 (aromatic, υ(C-N)), 1161, 1041 (aliphatic, υ(C-N)), 982, 939, 931.05, 821, 783, 675, 633, 571, 424 (out of plane, δ(C-H))

Calix-salen corand from (1R,2R)-diaminocyclohexane and 5,5'-methylene-bis-(3-methoxy-salicylaldehyde). (B-139)

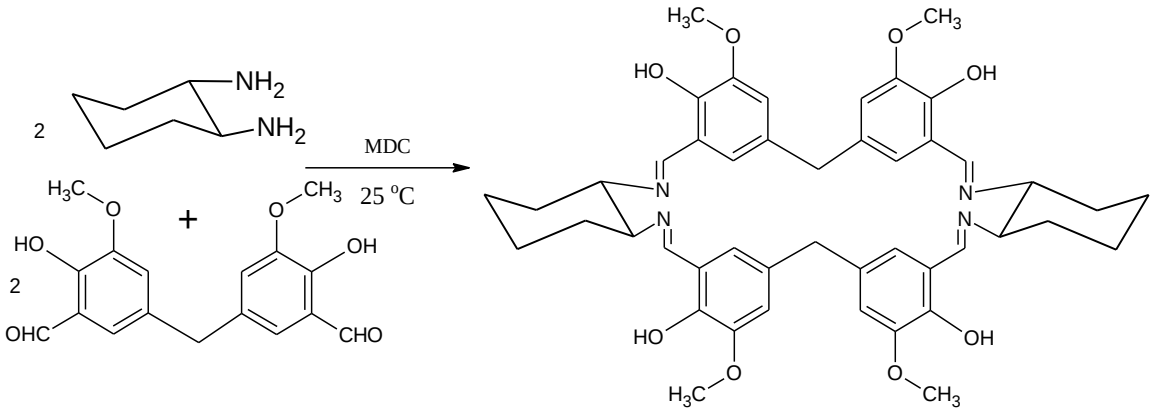

5,5'-Methylene-bis-(3-methoxy-salicylaldehyde) (1g, 0.003mol) and (1R, 2R)-diaminocyclohexane (0.43g, 0.004mol) when reacted in 4000ml MDC yield the corand **(B-139)**.

Yield: 0.710 g (57%)

M.P.= 193 °C.

^{1}H NMR (400 MHz, $CDCl_3$): δ 13.82 (s, 1H), 8.08 (s, 1H), 6.83 (s, 1H), 6.61 (s, 1H), 3.93 (s, 3H), 3.67 (s, 1H), 3.22 (d, 1H), 1.88 (d, 2H), 1.44 (t, 1H).

^{13}C NMR (400 MHz, $CDCl_3$): δ 164.3, 149.8, 148.0, 131.2, 122.2, 118.5, 114.5, 72.6, 56.2, 41.9, 33.2, 24.0

Mass: 789.4 (M+H)

HPLC Purity: 98.12%

Specific rotation: -215.142 (C=0.3% wt/v in DCM at 26 °C)

IR (KBr disc, cm^{-1}) : 2924 (methylene, υ_{as}(C-H)), 2854 methylene, υ_s(C-H)), 1628 (imine, υ(C=N)), 1471 (aromatic ring, υ(C=C)), 1440($\delta_s(CH_2)$), 1380, 1266 (aromatic, υ(C-N)), 1161(ether, υ_sC-O), 1094 (aliphatic, υ(C-N)), 1035 (ether, υ_{as}C-O), 974, 940, 861, 797, 749,709, 578, 477 (out of plane, δ(C-H))

Calix-salen corand[19,20] **from (1R, 2R)-diaminocyclohexane and 5,5'-methylene-bis-(3-*tert*-butylsalicylaldehyde). (C-240)**

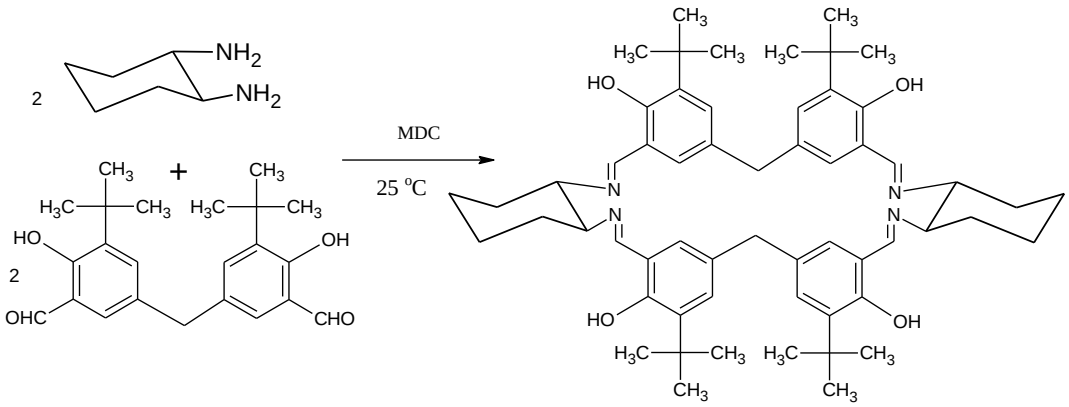

5,5'-Methylene-bis(3-tertbutylsalicylaldehyde) (1g, 0.003mol) and (1R,2R) Diaminocyclohexane (0.31g, 0.003mol) were reacted in 4000ml MDC to yield the corand (C-240).

Yield: 0.222 g (18%), **M.P**.= 260 °C (decomposed).

^{1}H NMR (400 MHz, $CDCl_3$): δ 13.81 (s, 1H), 8.09 (s, 1H), 7.16 (d, *J* = 2 Hz, 1H), 6.75 (d, *J* = 2.4 Hz, 1H), 3.65 (s, 1H), 3.27-3.24 (m, 1H), 1.88 (t, 2H), 1.72 (q, 1H), 1.61 (s, 1H), 1.38 (d, 1H).

^{13}C NMR (400 MHz, $CDCl_3$): δ 165.1, 158.6, 136.8, 130.8, 129.4, 129.2, 118.8, 72.3, 41.5, 34.6, 33.5, 29.4, 24.3

Mass: 894.46 (M^+)

Specific rotation: -308.10 (C=0.3% wt/v in DCM at 26 °C)

HPLC purity: 99.97%

IR(KBr disc, cm^{-1}) : 3414 (phenol, υ(O-H)), 2950 (methylene, υ_{as}(C-H)), 1628 (imine, υ(C=N)), 1597 (aromatic ring, υ(C=C)), 1440 ($\delta_s(CH_2)$), 1389, 1360, 1267 (aromatic, υ(C-N)), 1206,1161 (aliphatic, υ(C-N)),1091, 982, 943, 862, 800, 773, 707, 674, 493 (out of plane, δ(C-H))

Calix-salen corand[23] from (1R,2R)-diaminocyclohexane and 5,5'methylene-bis-(3-bromosalicylaldehyde). (C-242)

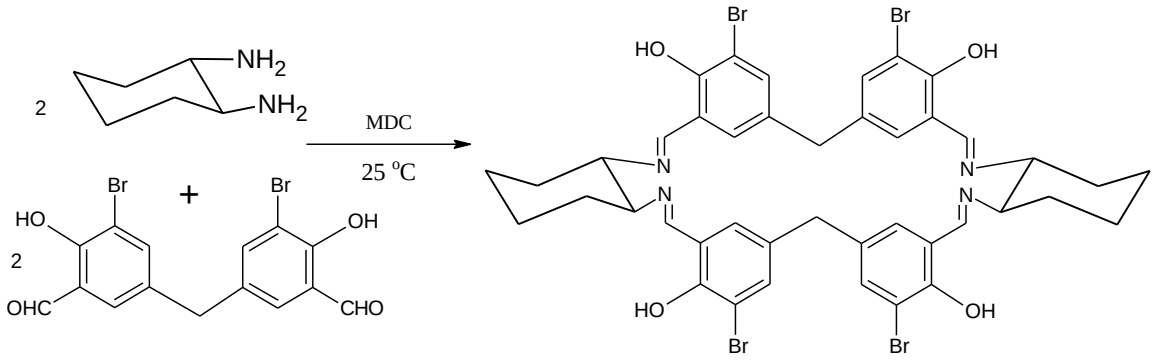

5,5'-Methylene-bis(3-bromosalicylaldehyde) (0.7g, 0.002mol) and (1R,2R) diaminocyclohexane (0.19g, 0.002mol) when reacted in 2100ml MDC, yield the corand **(C-242)**.

Yield: 0.249 g (30%)

M.P.= 260 °C (decomposed).

^{1}H NMR (400 MHz, $CDCl_3$): δ 14.38 (s, 1H), 8.09 (s, 1H), 7.48 (d, 1H), 6.96 (s, 1H), 3.64 (s, 1H), 3.28 (d, 1H), 1.88 (d, 2H), 1.69 (s, 1H), 1.44 (t, 1H).

^{13}C NMR (400 MHz, $CDCl_3$): δ 163.7, 156.8, 135.1, 132.1, 130.3, 119.5, 110.8, 72.3, 40.2, 33.19, 24.0

Mass: 985.23 (M+1), 987.18(M+3), 988.17(M+4), 989.12(M+5), 990.10(M+6)

HPLC Purity: 99.9%

Specific rotation: -175.598 (C=0.3% wt/v in DCM at 26 °C)

IR (KBr disc, cm^{-1}) : 2924 (methylene, υ_{as}(C-H)), 2854 (methylene, υ_{s}(C-H)), 1627 (imine, υ(C=N)), 1570, 1456 (aromatic ring, υ(C=C)), 1376, 1345, 1277 (aromatic, υ(C-N)), 1235, 1149 (aliphatic, υ(C-N)), 973, 941, 847,804, 743, 696, 669, (out of plane, δ(C-H)) 579, 499 (aromatic, υ(C-Br))

Calix-salen corand from (1R,2R)-diaminocyclohexane and 5,5'-methylene-bis-(3-nitro-salicylaldehyde). (C-188)

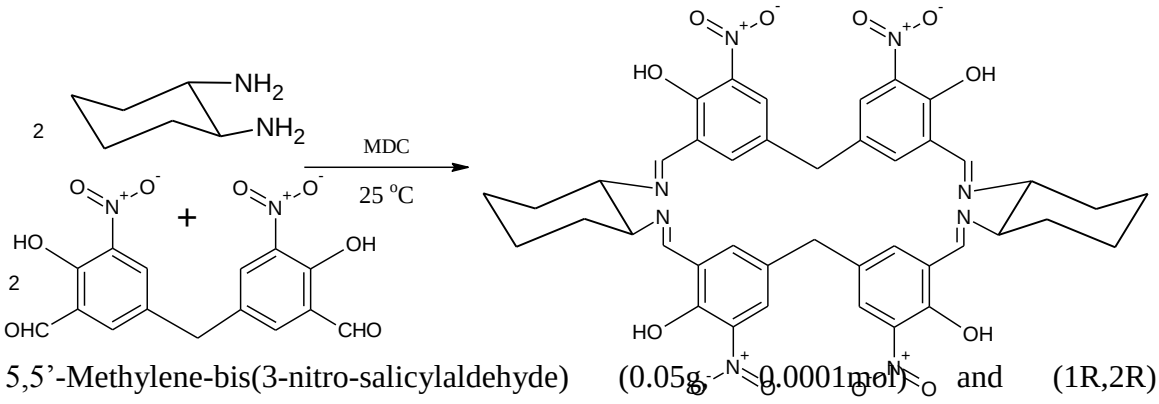

5,5'-Methylene-bis(3-nitro-salicylaldehyde) (0.05g, 0.0001mol) and (1R,2R) diaminocyclohexane (0.016g, 0.0001mol) reacted in 100ml MDC to yield the corand (C-188).

Yield: 0.25 g (41%), **M.P**.= 257 °C (decomposed).

^{1}H NMR (400 MHz, DMSO-d_6) δ 15.09 (s, 1H), 8.53 (s, 1H), 8.06 (d, *J* = 2 Hz, 1H), 7.46 (d, *J* = 2, 1H), 3.77(s, 1H), 3.73-3.70 (m, 1H), 1.92 (d, *J* = 10.8, 1H),1.75 (d, *J* = 6.8, 1H), 1.64-1.56 (m, 1H), 1.38 (d, *J* = 9.6, 1H).

^{13}C NMR (400 MHz, DMSO-d_6): δ 166.5, 160.5, 139.3, 139.0, 130.8, 127.5, 120.3, 67.4, 37.9, 32.82, 23.9

Mass: 849.56 (M+H)

Specific rotation: -812.950 (C=0.3% wt/v in DMSO at 26 °C)

HPLC Purity: 99.95%

IR (KBr disc, cm^{-1}) : 3456 (phenol, υ(O-H)), 2990 (methylene, υ_{as}(C-H)), 2858 (methylene, υ_s(C-H)), 1639 (imine, υ(C=N)), 1530 (nitro, $\upsilon_{as}(NO_2)$), 1351 (nitro, $\upsilon_s(NO_2$)), 1239 (aromatic, υ(C-N)), 1150,1086 (aliphatic, υ(C-N)), 992, 926, 698, 566, 504 (out of plane, δ(C-H))

Calix-salen corand from (1R,2R)-diaminodiphenylethane and 5,5'-methylene-bis-(3-nitrosalicylaldehyde) (C-221).

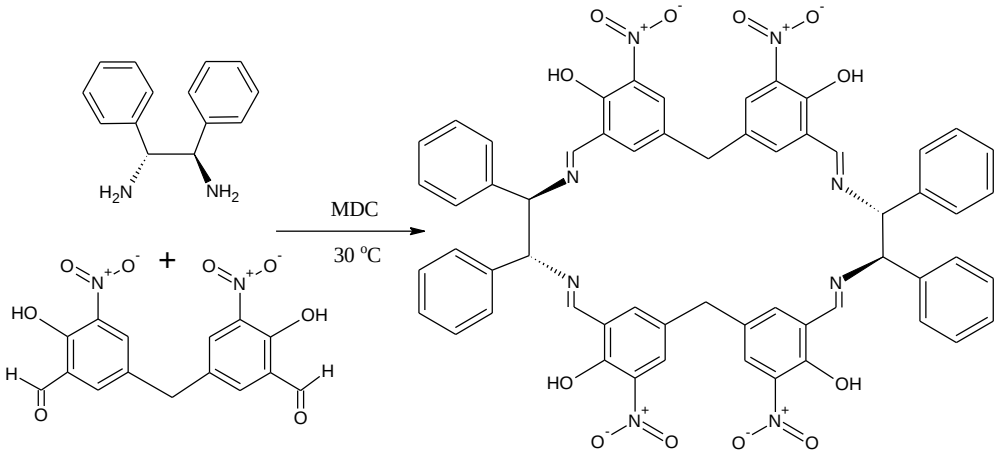

5,5'-Methylene-bis(3nitrosalicylaldehyde) (1 g, 0.003 mol) and (1R,2R) diamino-diphenylmethane (0.61g, 0.003mol) reacted in 4000ml MDC to yield the corand **(C-221)**.

Yield: 0.437 g (29%), **M.P.=** 195 ^{o}C.

^{1}H NMR (400 MHz, DMSO-d_6): δ 15.42 (s, 1H), 8.76 (s, 1H), 8.12 (d, *J* = 2,1H), 7.60 (d, *J* = 2, 1H), 7.32 (d, *J* = 7.2, 2H), 7.24 (t, *J* = 7.6, 2H), 7.21-7.13 (m, 1H), 5.43 (s, 1H), 3.83 (s, 1H)

^{13}C NMR (400 MHz, DMSO-d_6): δ 166.8, 157.1, 139.0, 138.4, 138.3, 130.1, 129.4, 129.1, 128.3, 120.9, 75.3, 38.1

Mass: 1045.15 (M^{+}) HPLC Purity: 99.57%

Specific rotation: +10.60 (C=0.1% wt/v in DMSO at 26 ^{o}C)

IR (KBr disc, cm^{-1}) : 3465 (phenol, υ(O-H)), 3031 (methylene, $υ_{as}$(C-H)), 2874 (methylene, $υ_{s}$(C-H)), 1636 (imine, υ(C=N)), 1590, 1530 (nitro, $υ_{as}$(N--O)), 1351 (nitro, $υ_{s}$(N--O)), 1252 (aromatic, υ(C-N)), 1150,1050 (aliphatic, υ(C-N)), 997, 919, 818, 767, 699, 557, 510 (out of plane, δ(C-H))

Calix-salen corand from R-(+)-2,2'-diamino-binaphthalene and 5,5'-methylene-bis-(3-nitrosalicylaldehyde) (C-238).

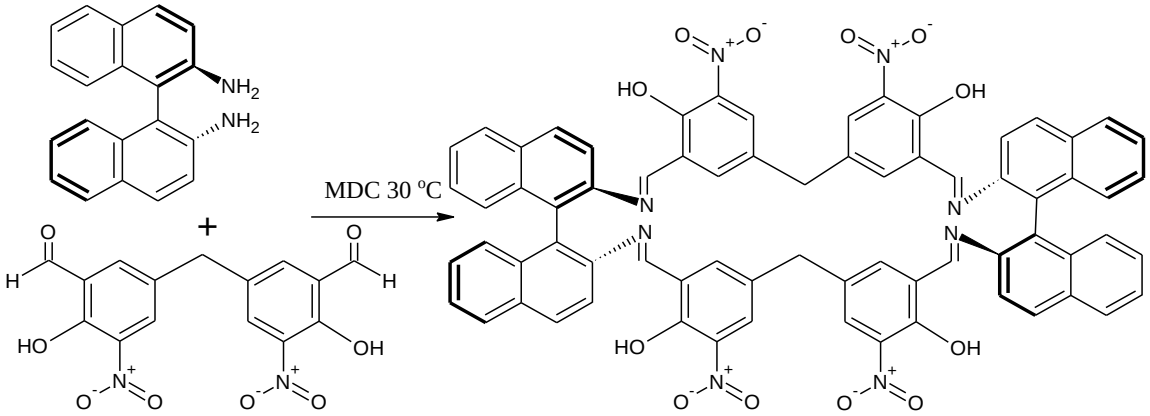

5,5'-Methylene-bis(3-nitro-salicylaldehyde) (1g, 0.003mol) and R-(+)-2,2'-diamino-binaphthalene (0.82g, 0.003mol) reacted in 4000ml MDC to yield the corand (C-238).

Yield: 0.188 g (11%)

M.P. = 259 ^{o}C (decomposed).

^{1}H NMR (400 MHz, DMSO-d_6): δ 14.02 (s, 1H), 9.15 (s, 1H), 8.28 (d, *J* = 8.8, 1H), 8.12 (d, *J* = 8.4, 1H), 8.03 (d, *J* = 9.2, 1H), 7.98 (d, *J* = 2, 1H), 7.60 (d, *J* = 2, 1H), 7.54 (t, *J* = 8, 1H), 7.35-7.31 (m, 1H), 7.03 (d, *J* = 8.4, 1H), 3.84 (s, 1H)

^{13}C NMR (400 MHz, DMSO-d_6): δ 162.4, 154.5, 141.5, 138.8, 137.4, 133.2, 132.6, 130.8, 129.0, 128.0, 127.2, 126.3, 121.6, 117.0, 38.0

Mass (ESI): 1189.19

HPLC Purity: 99.89%

Specific rotation: -617.42 (C=0.3% in DMSO, wt/v at 26 ^{o}C)

IR (KBr disc, cm^{-1}) : 3467 (phenol, υ(O-H)), 3052, 2917 (methylene, υ_{as}(C-H)), 2843 methylene, υ_{s}(C-H)), 1756, 1628 (imine, υ(C=N)), 1578, 1527 (nitro, υ_{as}(N--O)), 1462, 1343 (nitro, υ_{s}(N--O)), 1256 (aromatic, υ(C-N)), 1144 (aliphatic, υ(C-N)), 964, 865, 811, 748, 665, 525, 469,430 (out of plane, δ(C-H))

Host-Guest studies using UV-Visible spectroscoapy:

Host-guest study of following host corands were carried out.

1. C-247 (from (1R, 2R)-DACH and 5,5'-methylene-bis-salicylaldehyde)
2. B-139 (from (1R, 2R)-DACH and 5,5'-methylene-bis-(3-methoxy-salicylaldehyde)
3. C-188 (from (1R, 2R)-DACH and 5,5'-methylene-bis-(3-nitro-salicylaldehyde)
4. C-240 (from (1R, 2R)-DACH and 5,5'-methylene-bis-(3-*tert*-butyl-salicylaldehyde)
5. C-242 (from (1R, 2R)-DACH and 5,5'-methylene-bis-(3-bromo-salicylaldehyde)
6. C-221 (from (1R, 2R)-DADPE and 5,5'-methylene-bis-(3-nitro-salicylaldehyde)
7. C-238 (from R-(+)-DABN and 5,5'-methylene-bis-(3-nitro-salicylaldehyde)

with the following 1st transition series metal ions

a. Mn^{2+} b. Fe^{2+} c. Fe^{3+} d. Co^{2+} e. Ni^{2+} f. Cu^{2+} g. Zn^{2+}

at the concentration of $2.5x10^{-4}$M of host corand in DCM and $2.5x10^{-3}$ M concentration of guest ions in DMSO. Both the solutions of the host and the guest molecules were mixed in equal amount (2ml+2ml) to give total 4ml of test solution.

Selectivity study in case of C-247 and B-139 corands was carried out by preparing 0.8mM of host solution in DCM and 8.0 mM of metal ion solution in DMSO. Total seven sets of test solutions were prepared by mixing 1ml solution of host corand to the solution mixture of 1 ml Cu^{2+}solution with 2 ml DMSO and subsequently mixing 1ml solution of host corand with solution mixture of 1ml of Cu^{2+}, 1 ml other transition metal ion and 1ml DMSO. Selectivity study between mixture of Fe^{3+} and other transition metal ions was carried out by preparing similar test solutions. UV-Vis spectra of all these test solutions were recorded at 26 °C and graph were plotted.

Selectivity studies in case of C-188, C-221 and C-238 corands were carried out by preparing 0.2 mM of host solution in DMSO and 2 mM of metal ion solution in DMSO. Total seven sets of test solutions were prepared by mixing 1ml solution of host corand to the solution mixture of 1ml Cu^{2+}solution with 2ml DMSO and subsequently mixing 1ml solution of host corand with solution mixture of 1ml of Cu^{2+} solution, 1ml other transition metal ion solution and 1ml DMSO. Selectivity study between mixture of Fe^{3+} and Ni^{2+} with other transition metal ions was carried out by preparing similar test solutions. UV-Vis spectra of all these test solutions were recorded at 26°C and graphs were plotted.

Solution studies for host-guest stoichiometry determination:

Job's method was used for determination of Host:Guest stoichiometry. Stock solution of 0.5 mM salicylaldehyde derived corand was prepared in DCM while 0.5 mM $Fe(ClO_4)_3$ solution was prepared in DMSO. Both the solutions were mixed in amounts shown in the following table and ectronic spectrum of each set was recorded at 26 °C. Same procedure using same concentrations was followed for o-vanilline derived corand for determination of its binding stoichiometry with Cu^{2+}.

0.5mMCorand	5ml	4.5ml	4ml	3.5ml	3ml	2.5ml	2ml	1.5ml	1ml	0.5ml	0ml
0.5mM Metal perchlorate	0ml	0.5ml	1ml	1.5ml	2ml	2.5ml	3ml	3.5ml	4ml	4.5ml	5ml

Photoluminescence study

Photoluminescence studies were carried out using $2.5x10^{-4}$ M stock solutions of calix-salen corand (C-247 salicylaldehyde derived corand, B-139 o-vanilline derived corand, C-240 tert-butyl-salicylaldehyde derived corand or C-242 bromo-salicylaldehyde derived corand) in DCM and $2.5x10^{-3}$M 1^{st} transition series metal ions in DMSO. Spectroscoapy grade DCM and DMSO were used for the study. The host-guest complexes were excited

at 390 nm, 340 nm, 425 nm and 430 nm with 2.5 mm excitation and emission slit width using Jasco FP6300. Photoluminescence spectra for solvents were also recorded with no response in the 390 to 900nm range.

Photoluminescence study was also carried out by mixing 1ml $1x10^{-3}$ M solution of calix-salen corand (C-238) synthesized from R-(+)-2,2'-diamino-binaphthalene and 5,5'-methylene-bis(3-nitrosalicylaldehyde) and 2ml $5x10^{-3}$M solution of 1st transition series metal ions in DMSO. The host-guest complexes were excited at 425 nm with 2.5 mm excitation and emission slit widths using Jasco FP6300. Selectivity studies were carried out by addition of 1ml, $1x10^{-3}$ M solution of host corand (C-238) to the solution mixture of 1ml, $1x10^{-2}$ M Cu^{2+}, 1ml $1x10^{-2}$ M other metal ion.

Kinetic study

Kinetic studies were carried out by mixing an equal volume of $1x10^{-3}$M solution of host corand (C-238) with $1x10^{-2}$ M solution of $Ni(ClO_4)_2$. Changes in its UV spectral band as well as fluorescence intensity was observed at an interval of 10 minute each for 8 hrs and than recorded after gap of 16 hrs for further 5 hrs at an interval of 10 minute each and then last reading was taken after 24 hours.

3.6Analytical data

Spectrum 3.1

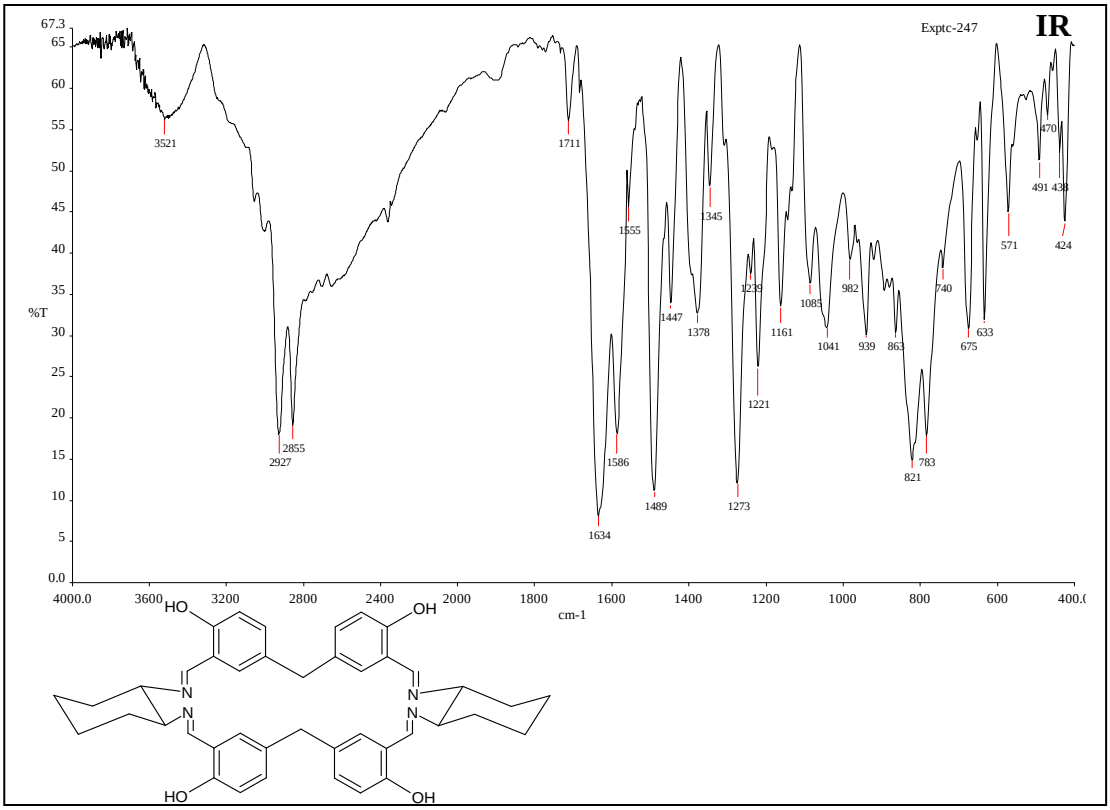

Spectrum 3.2

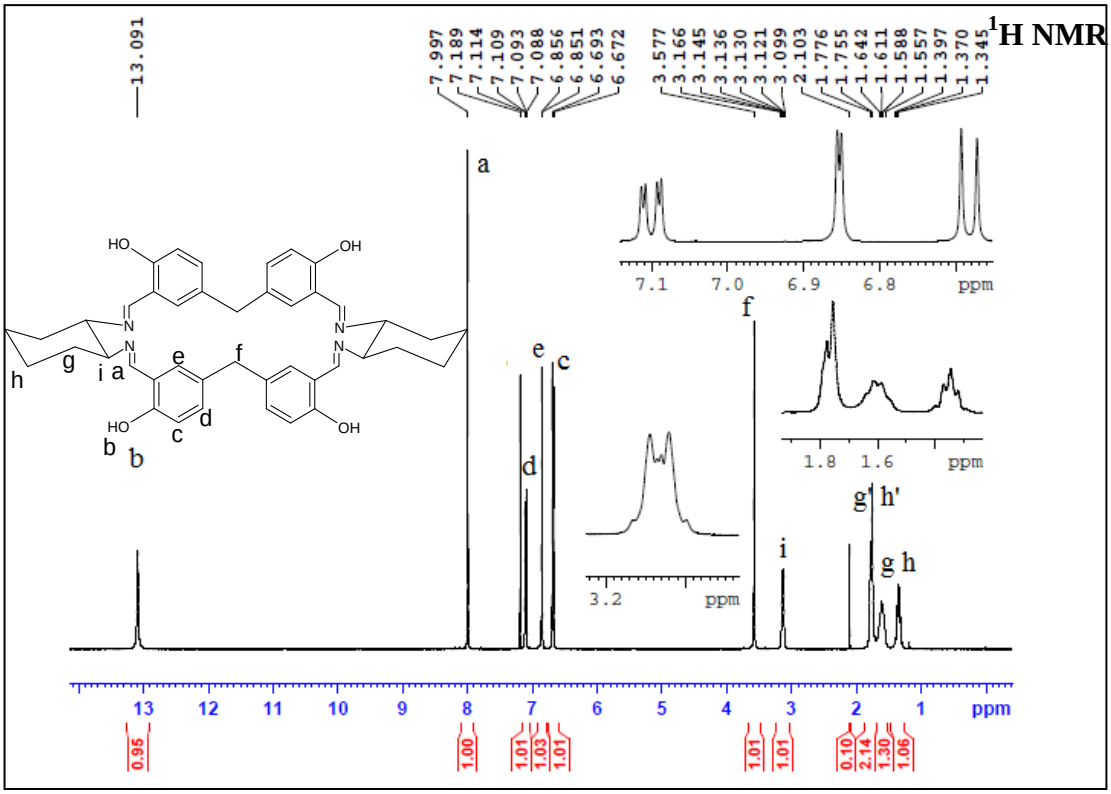

Spectrum 3.3

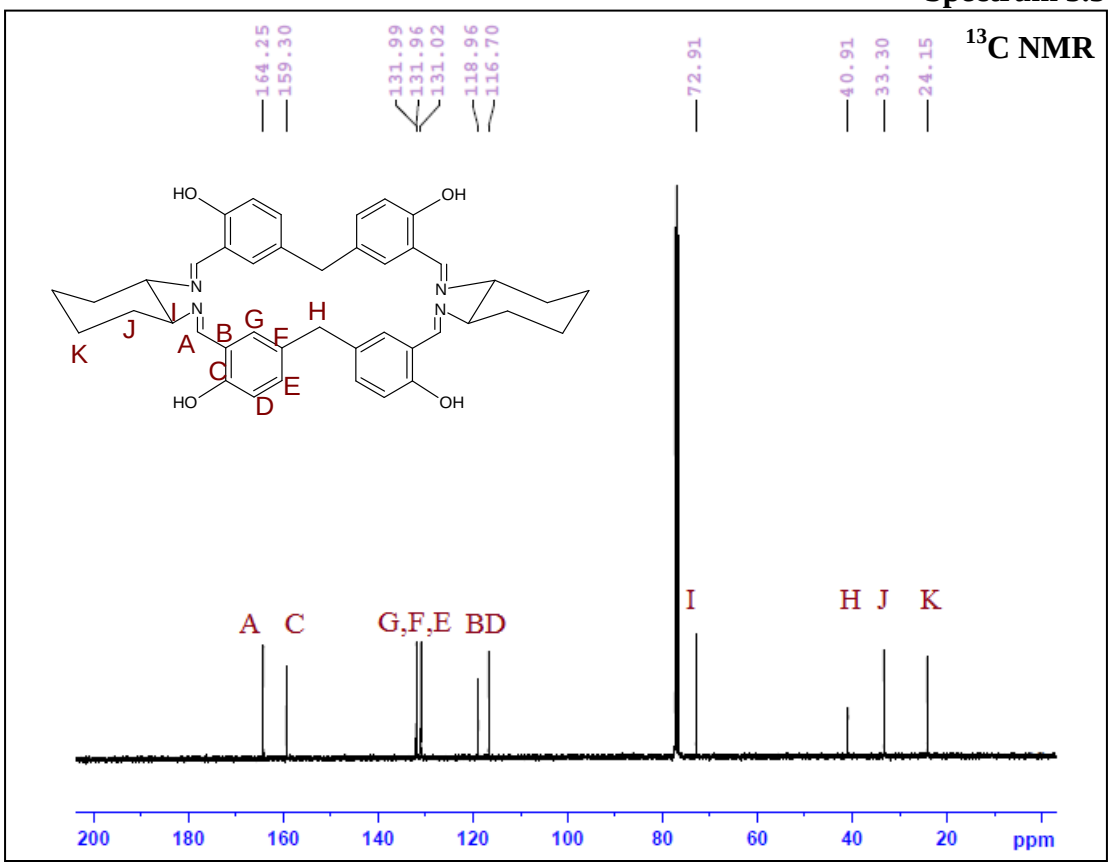

Spectrum 3.4

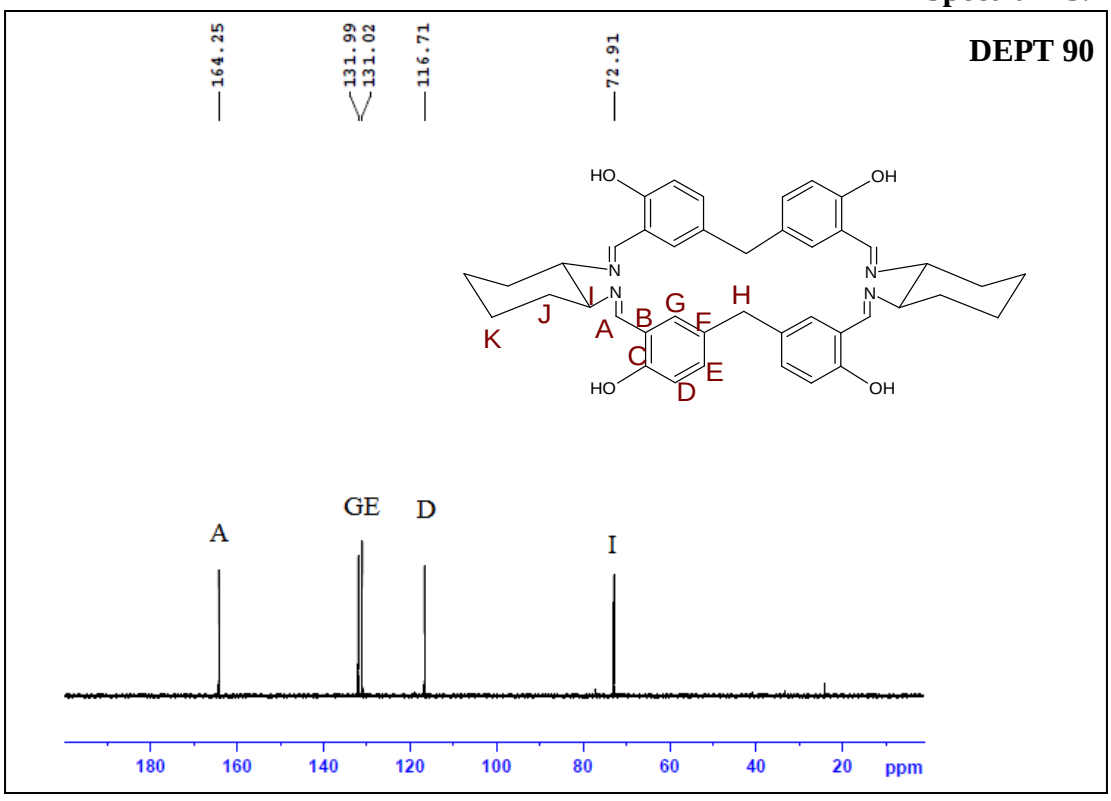

Spectrum 3.5

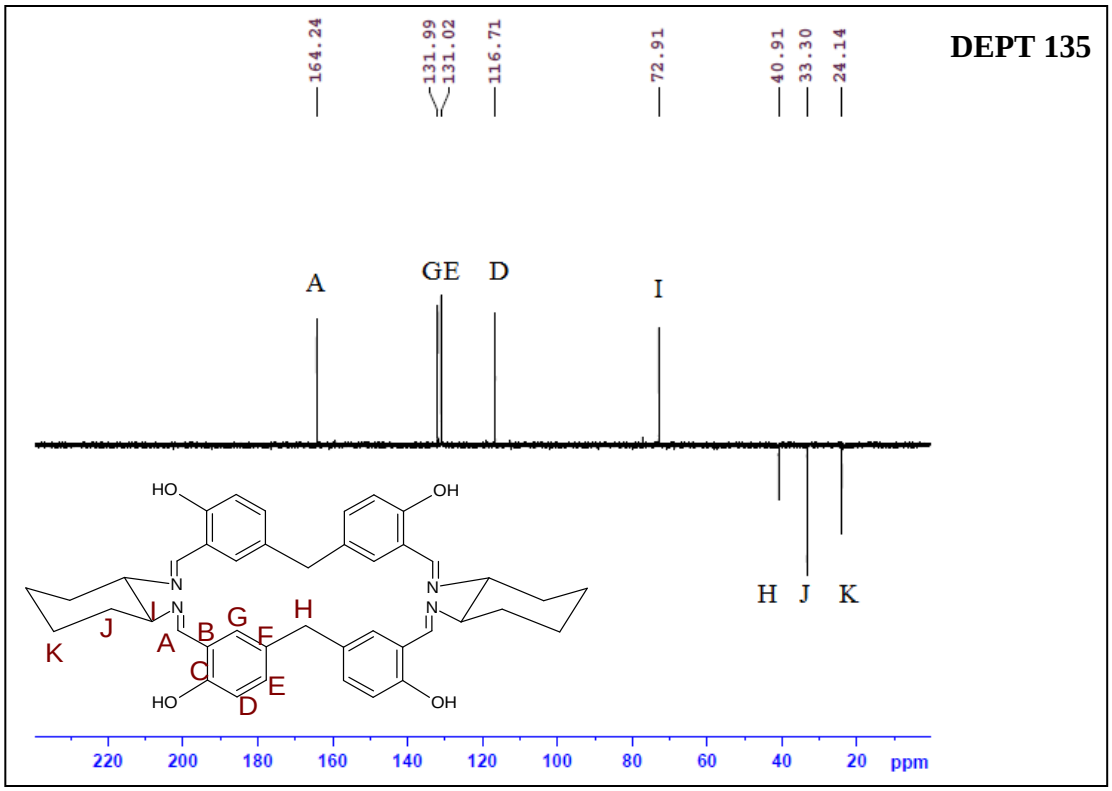

Spectrum 3.6

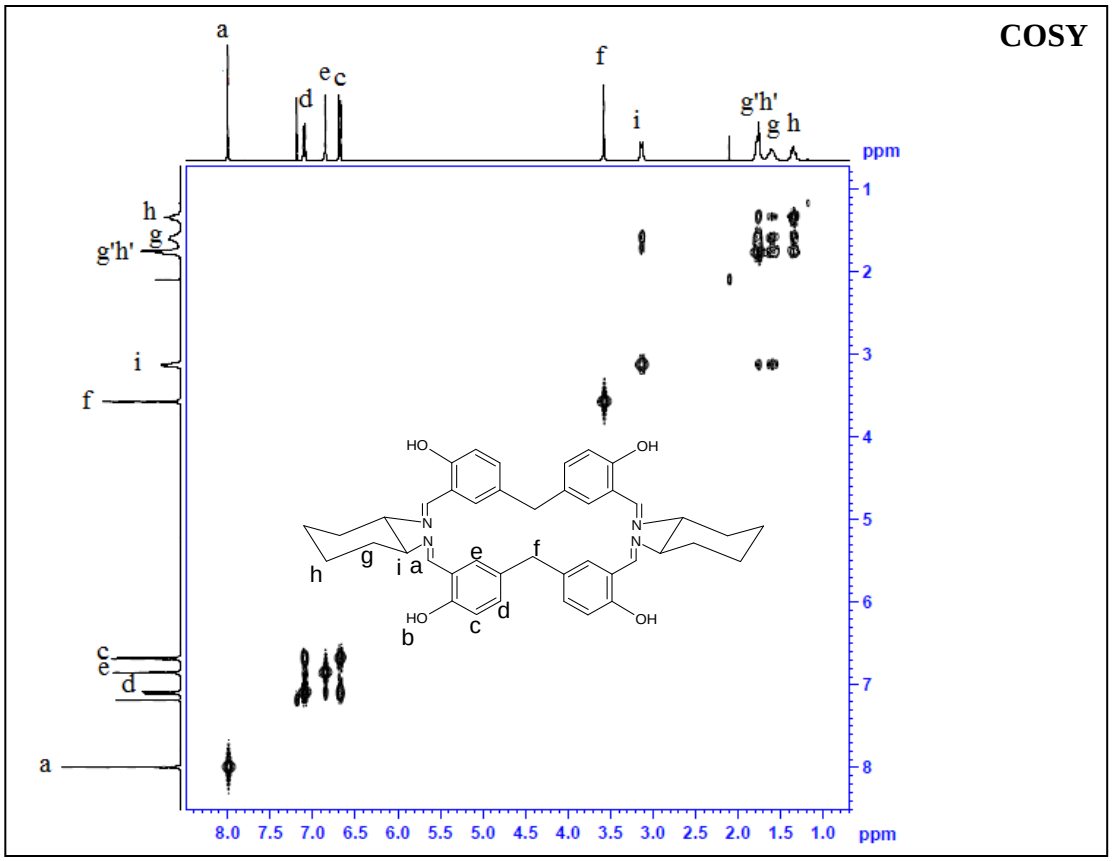

Spectrum 3.7

NOESY

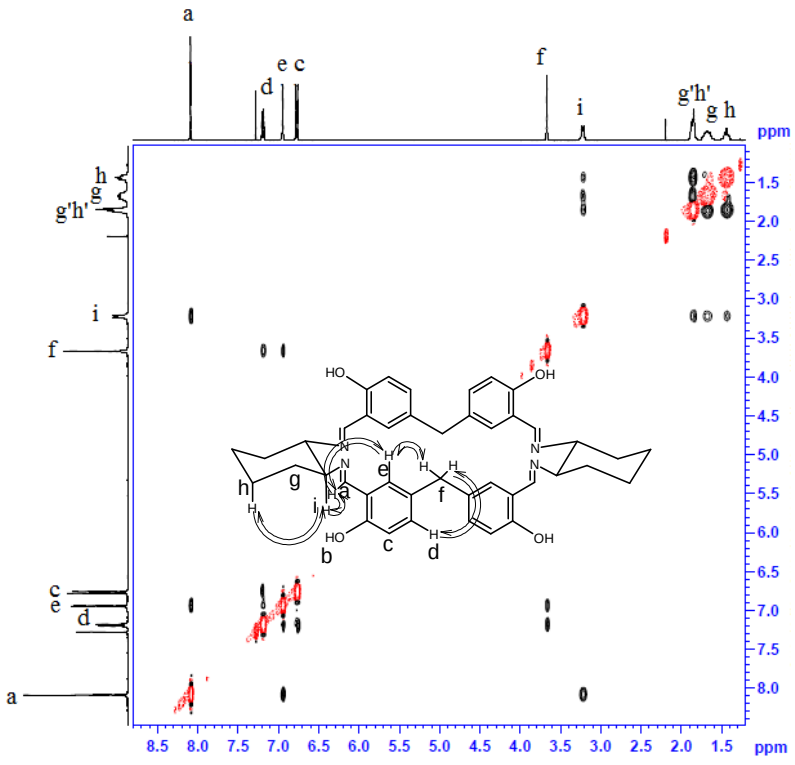

Spectrum 3.8

HSQC

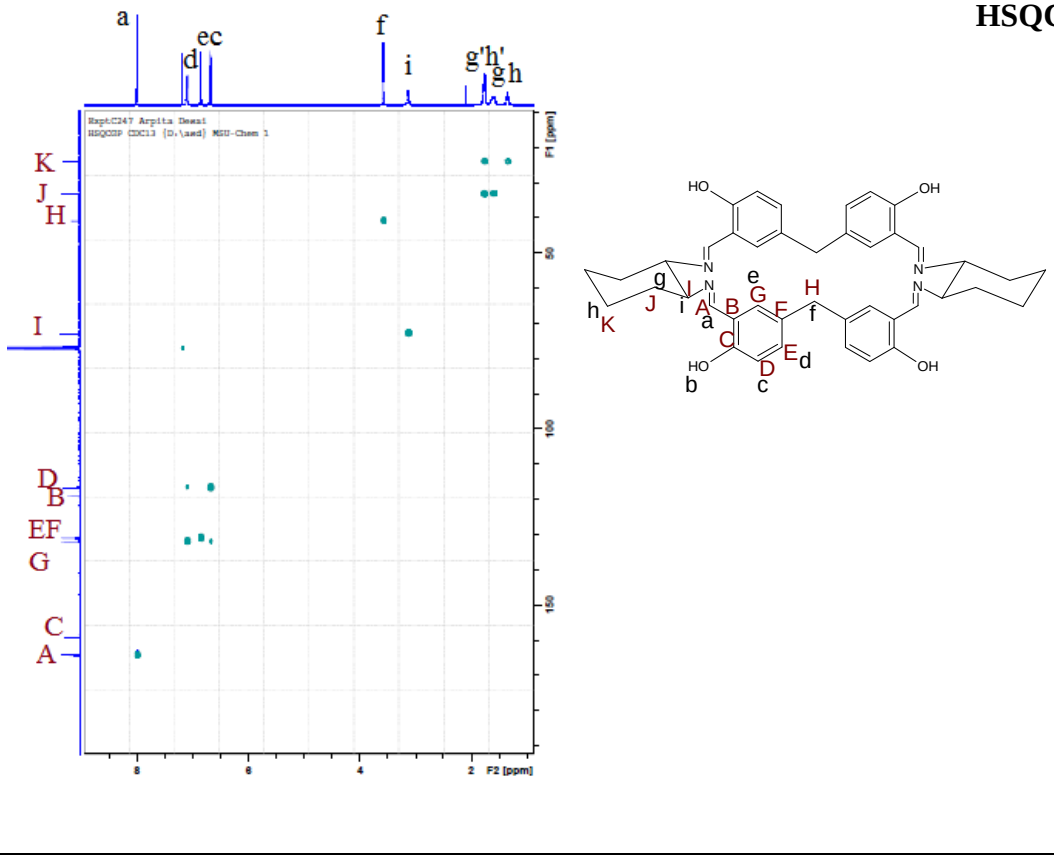

Spectrum 3.9

HMBC

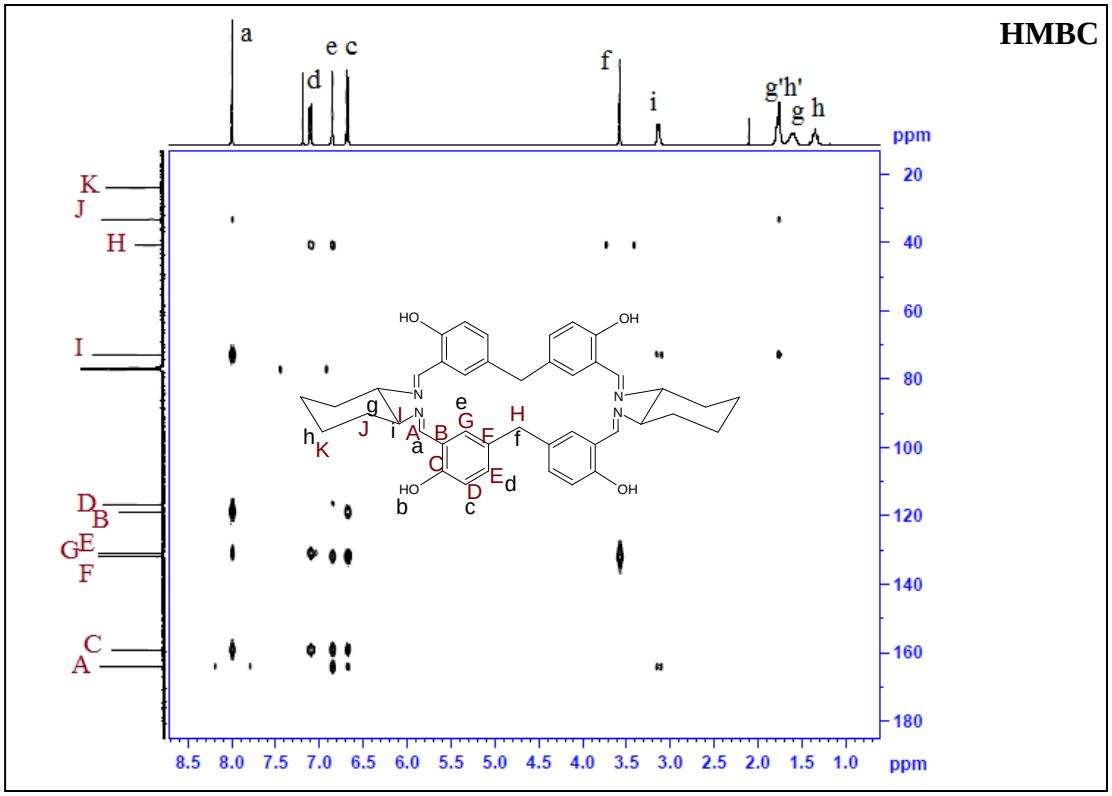

Spectrum 3.10

Variable temperature NMR

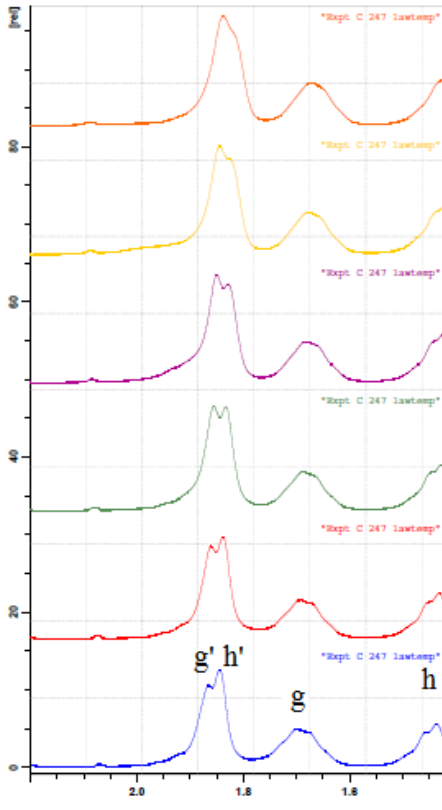

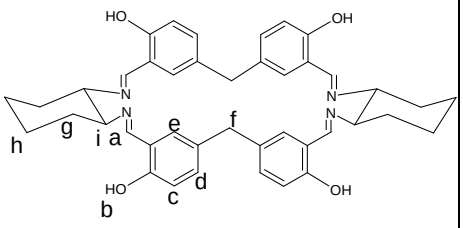

Spectrum 3.11

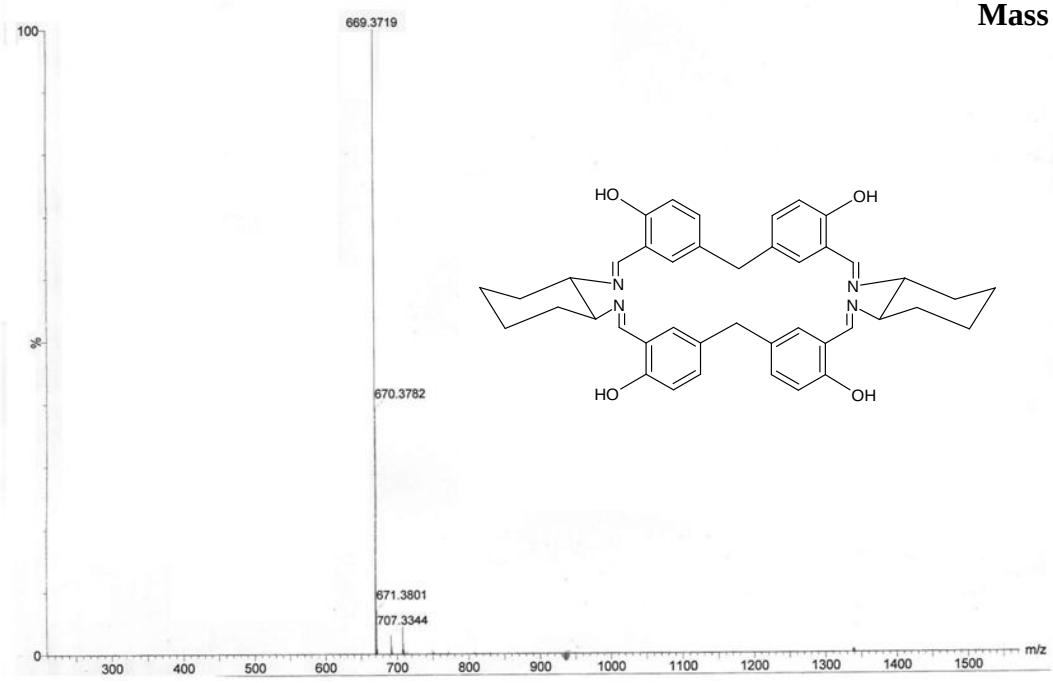

Chromatogram 3.12

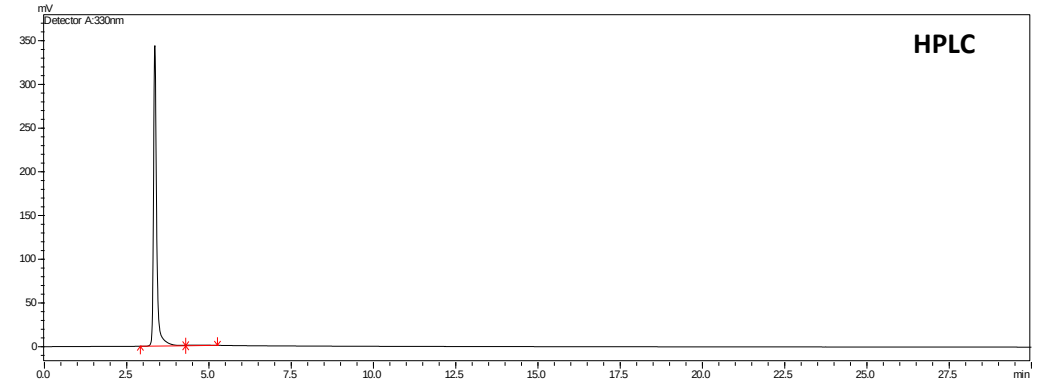

Silica column

Mobile phase: MDC:MeOH:: 98:2(v/v)

Peak	Name	Ret. Time	Area%
1	EXPT C-247(calix-salen corand from DACH and 5,5'methylene –bis-salicylaldehyde)	3.351	98.9330
2	RT4.572	4.572	1.0670

Spectrum 3.13

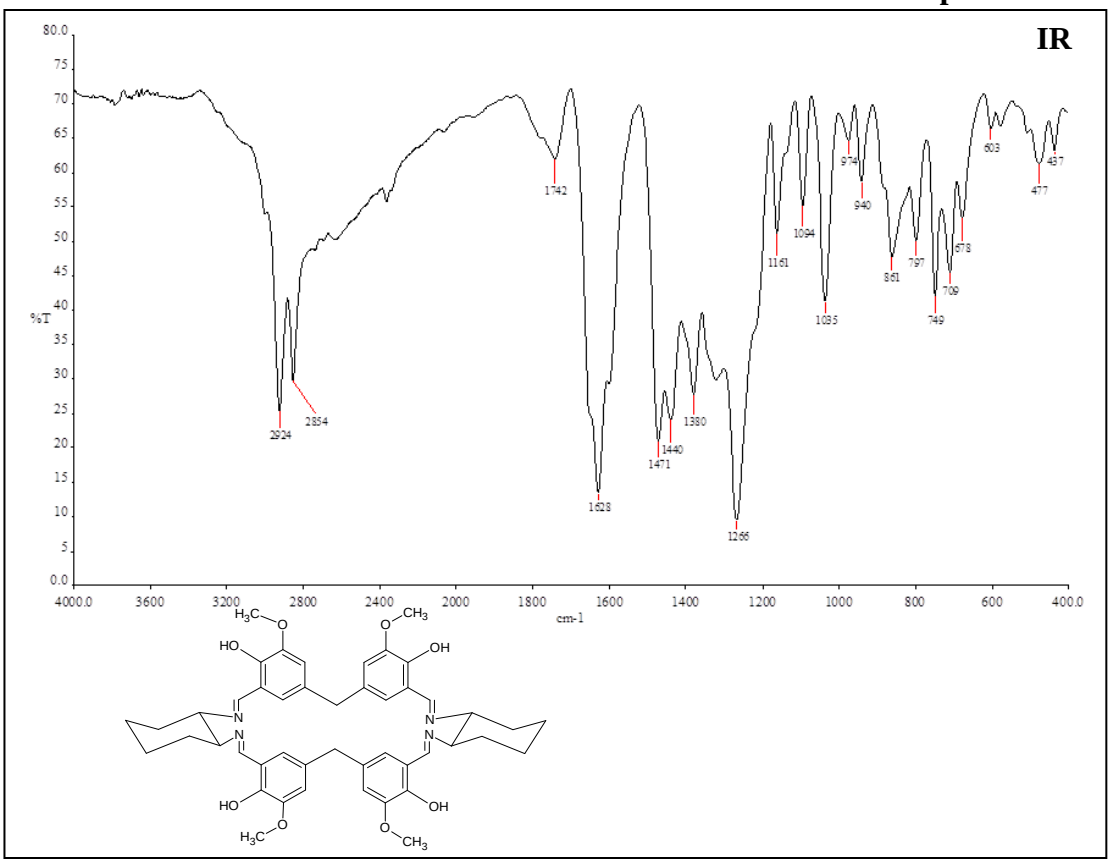

Spectrum 3.14

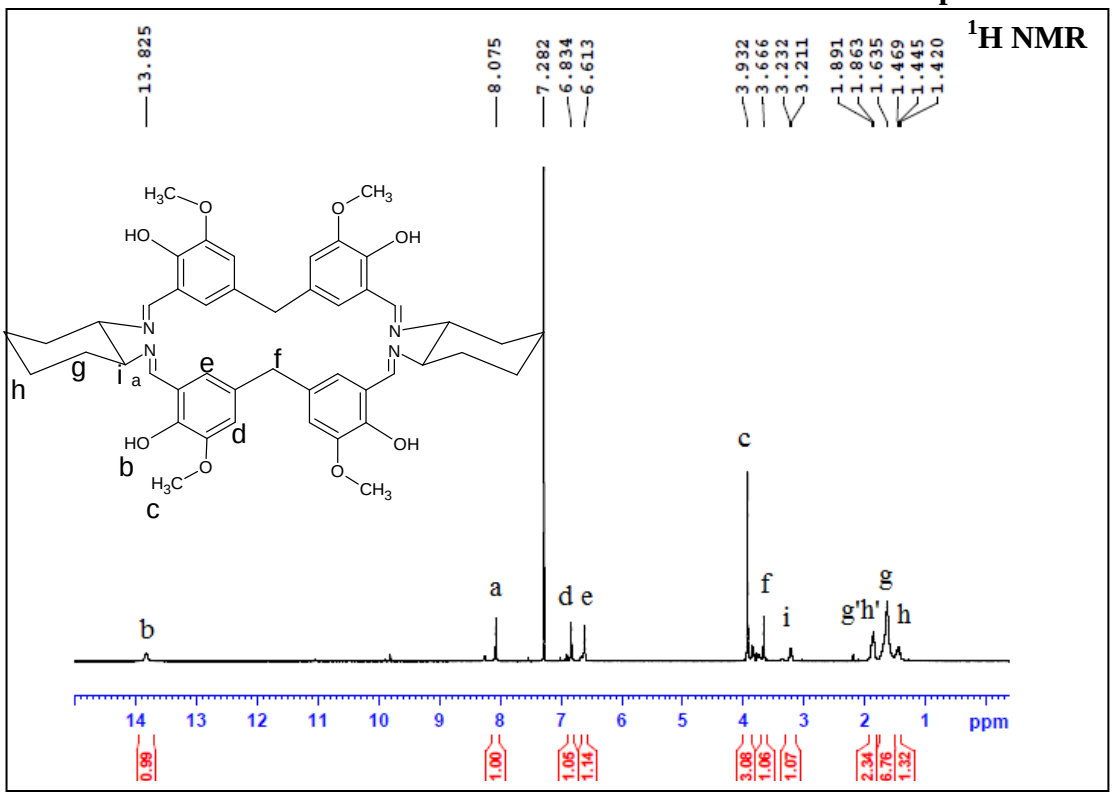

Spectrum 3.15

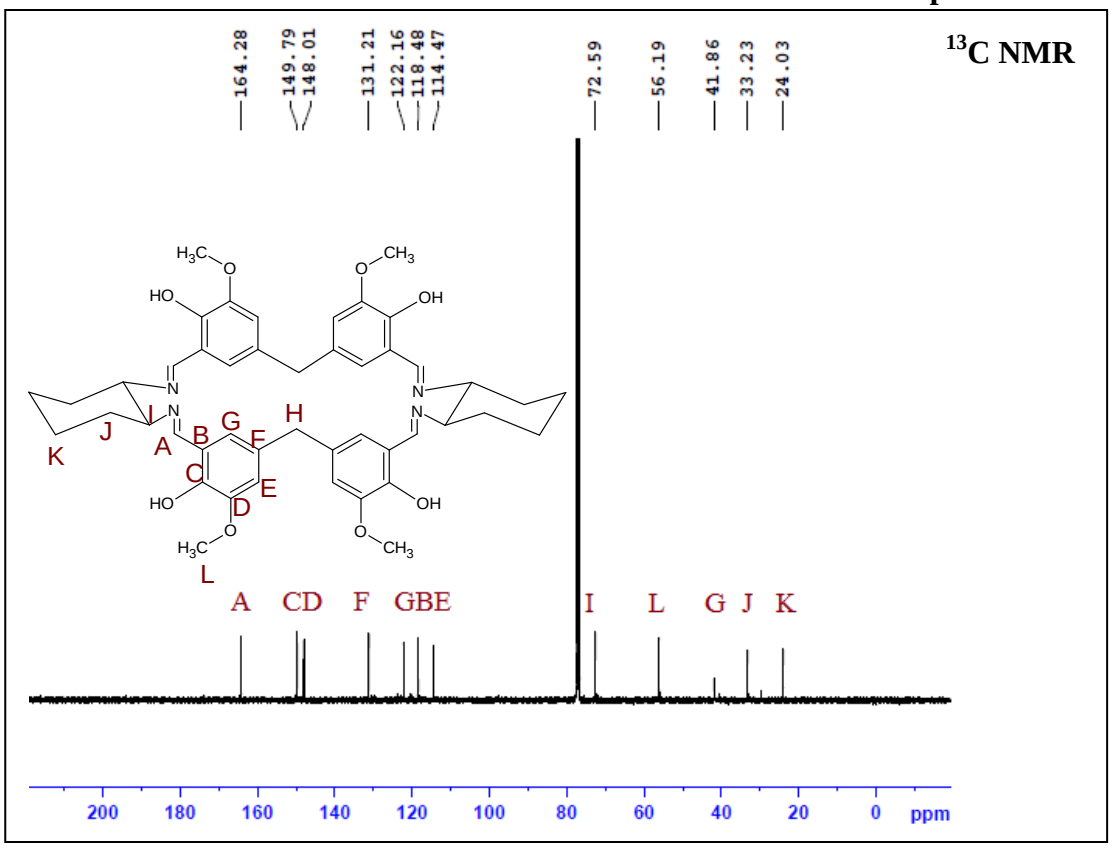

Spectrum 3.16

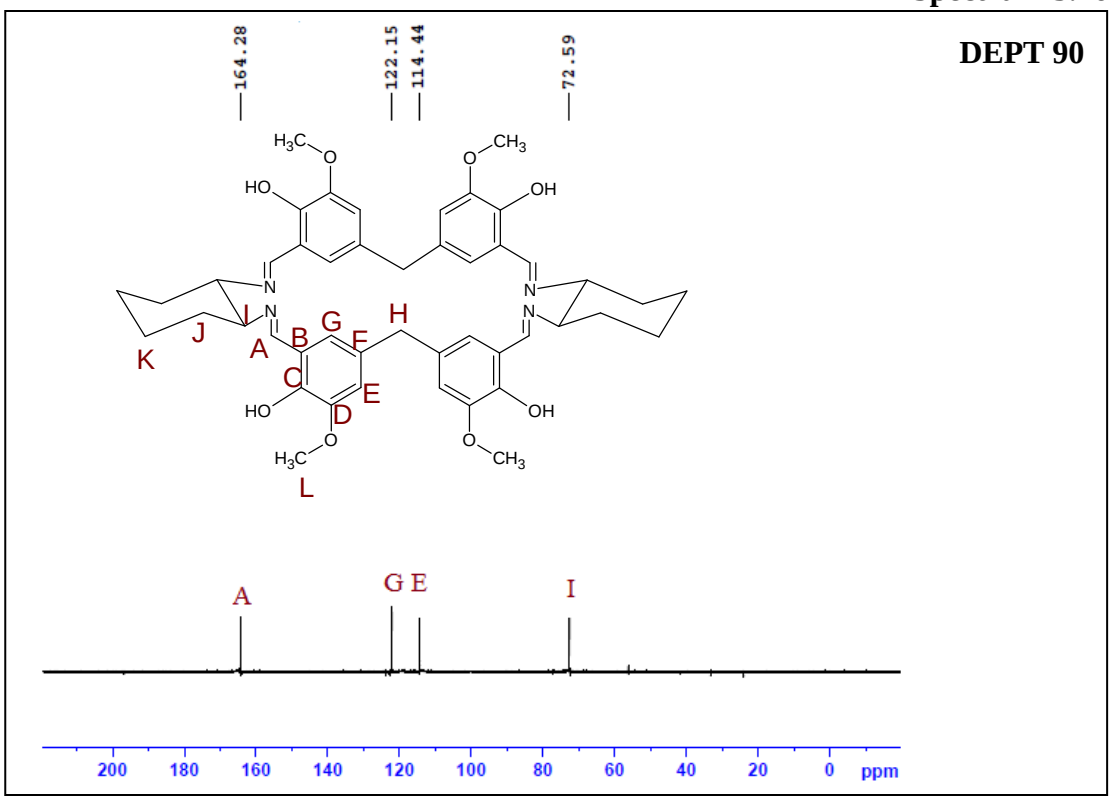

Spectrum 3.17

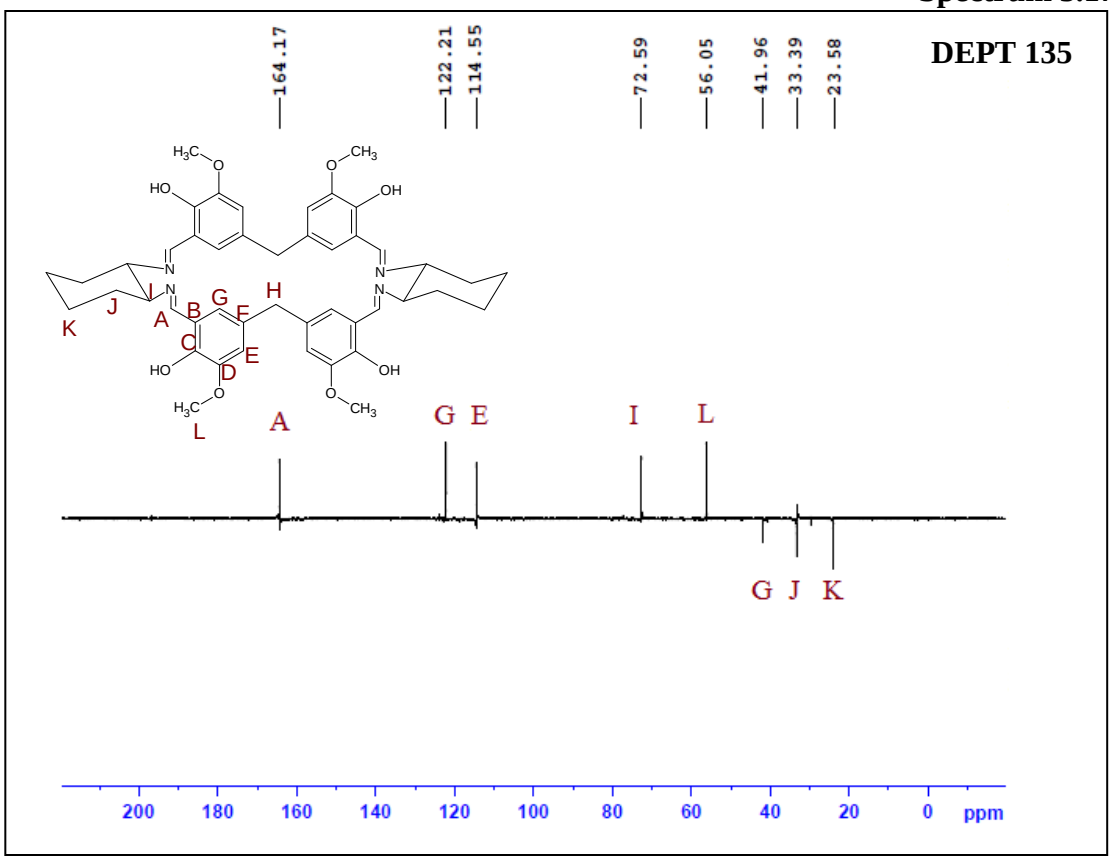

Spectrum 3.18

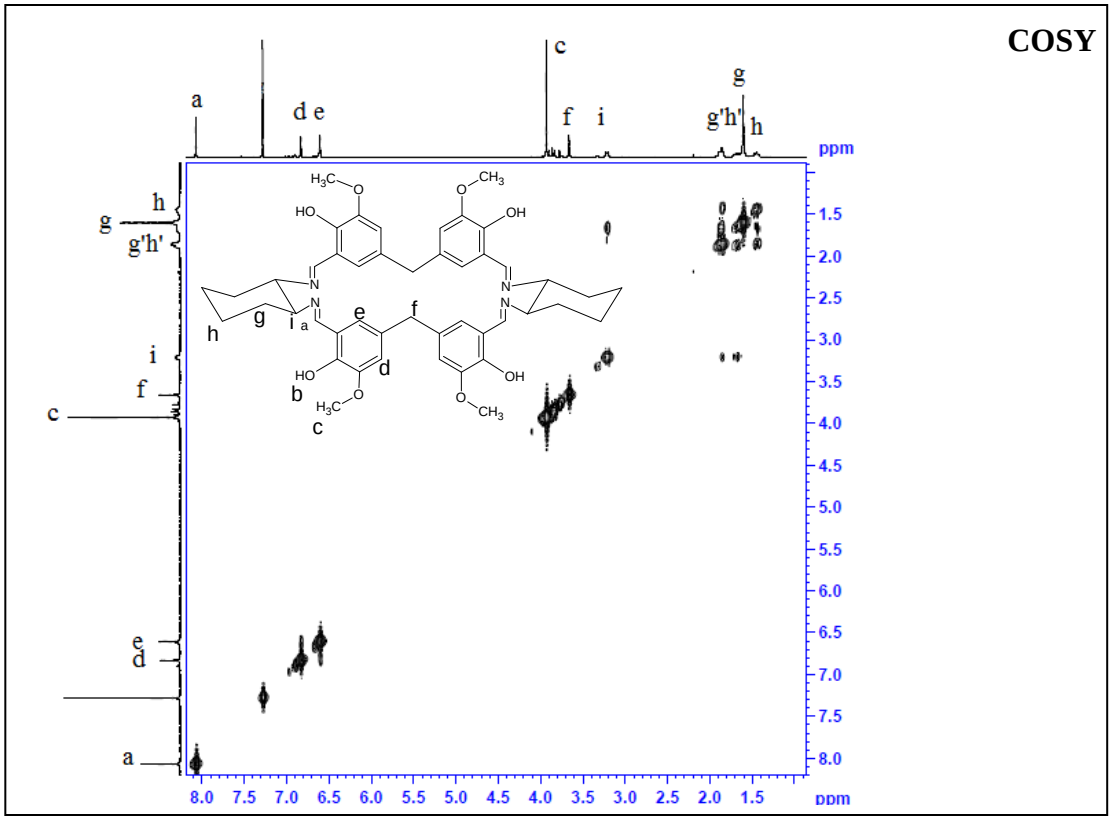

Spectrum 3.19

NOESY

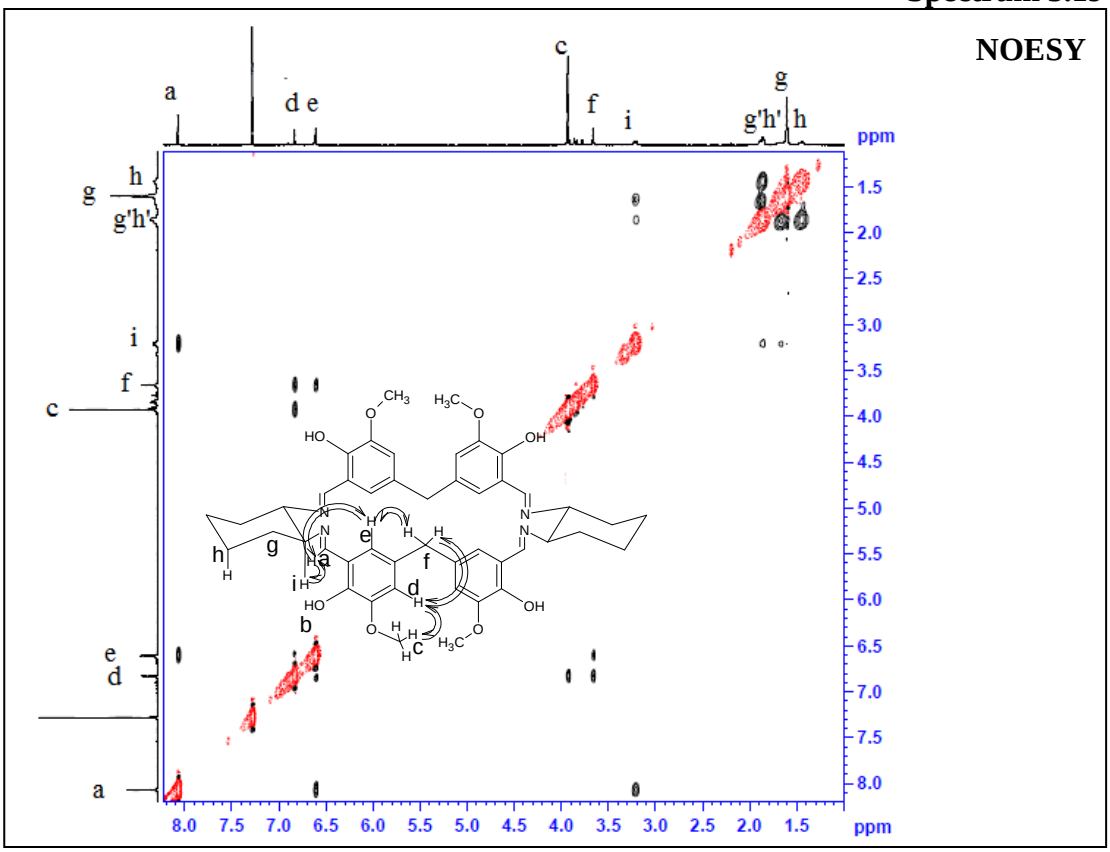

Spectrum 3.20

HSQC

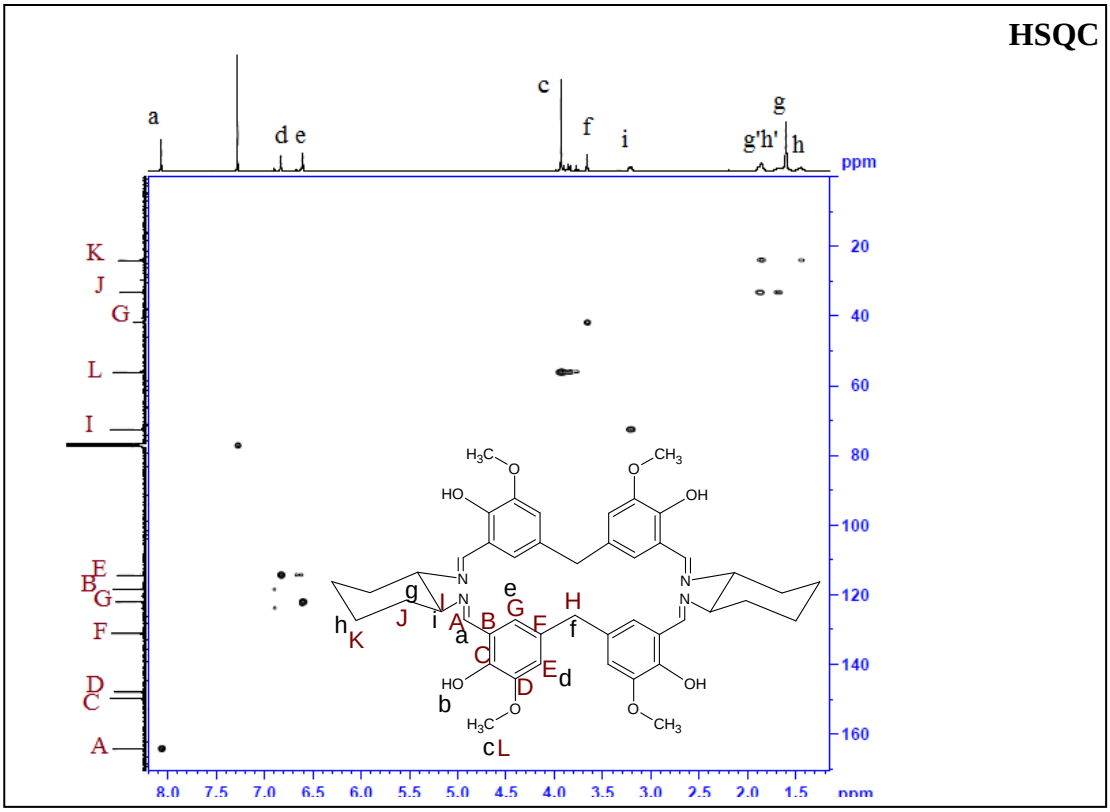

Spectrum 3.21

HMBC

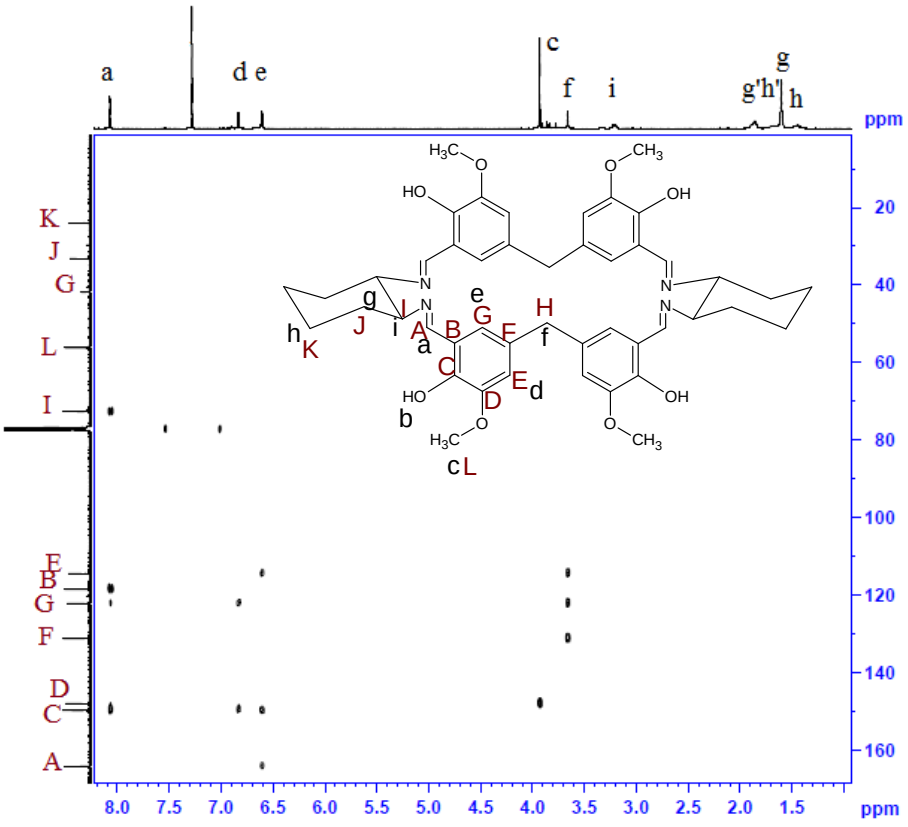

Spectrum 3.22

MASS

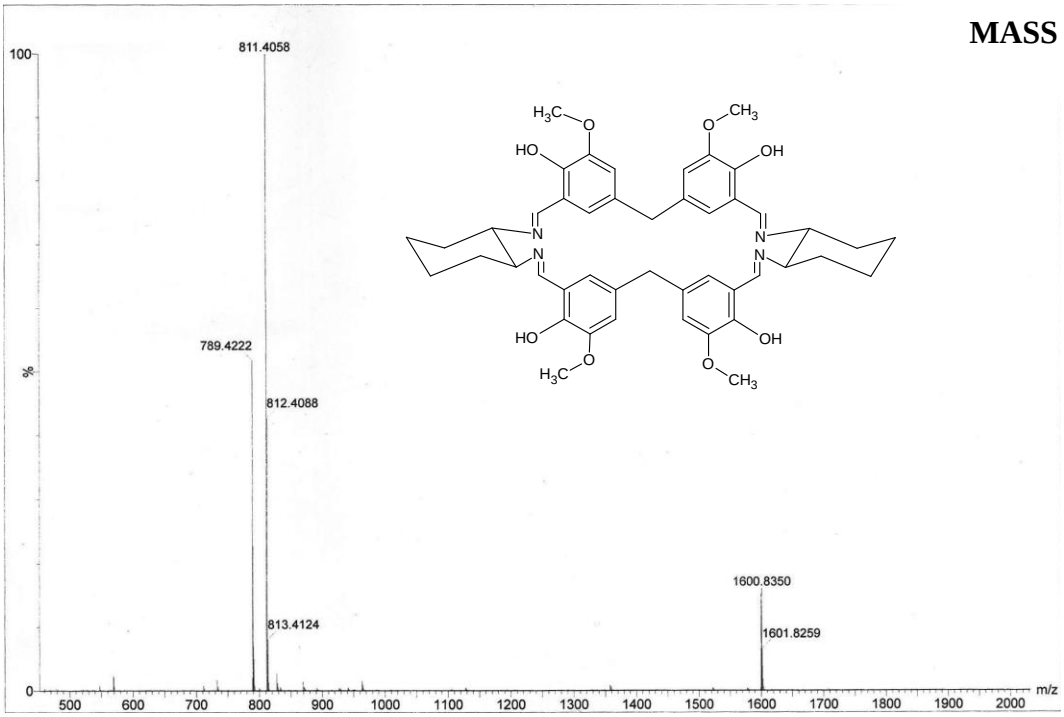

Chromatogram 3.23

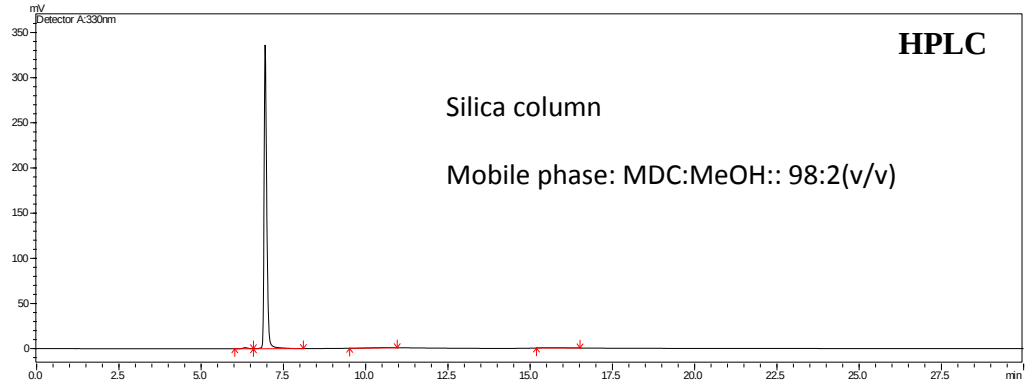

Peak	Name	Ret. Time	Area%
1	Imp-a	6.331	0.6241
2	Calix-salen corand from dach and 5,5'methylene-bis-o-vanilline	6.941	98.1207
3	Imp-b	10.652	0.5383
4	Imp-c	15.672	0.7169

Spectrum 3.24

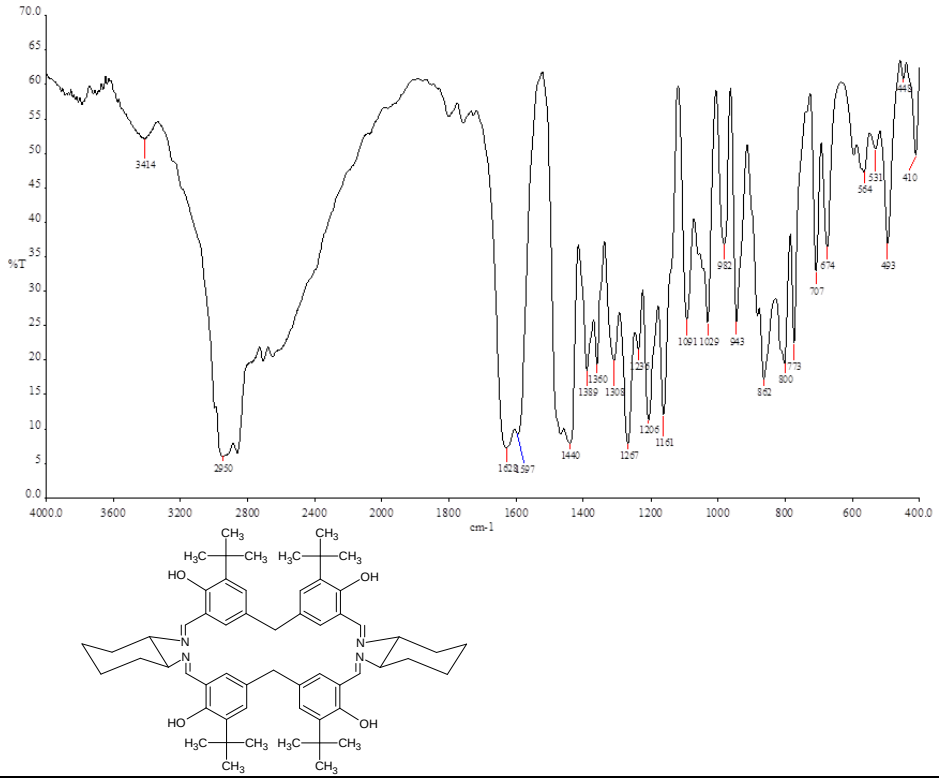

Spectrum 3.25

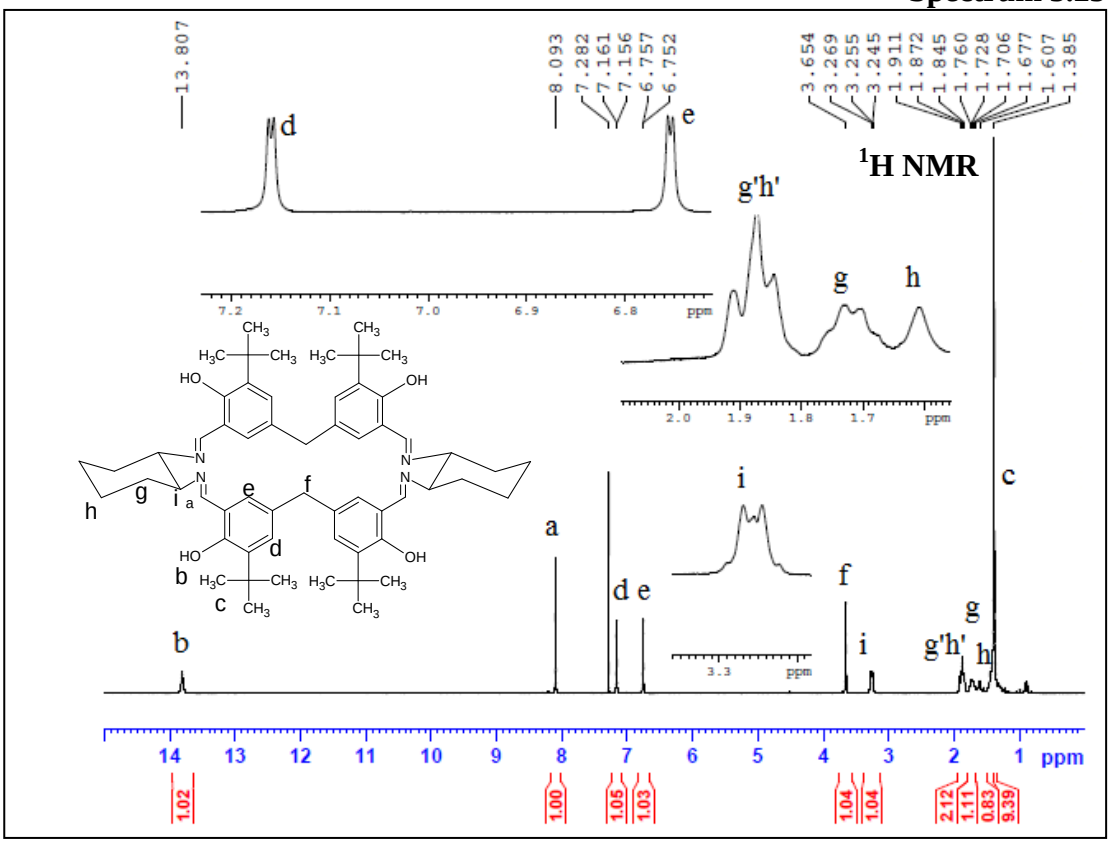

Spectrum 3.26

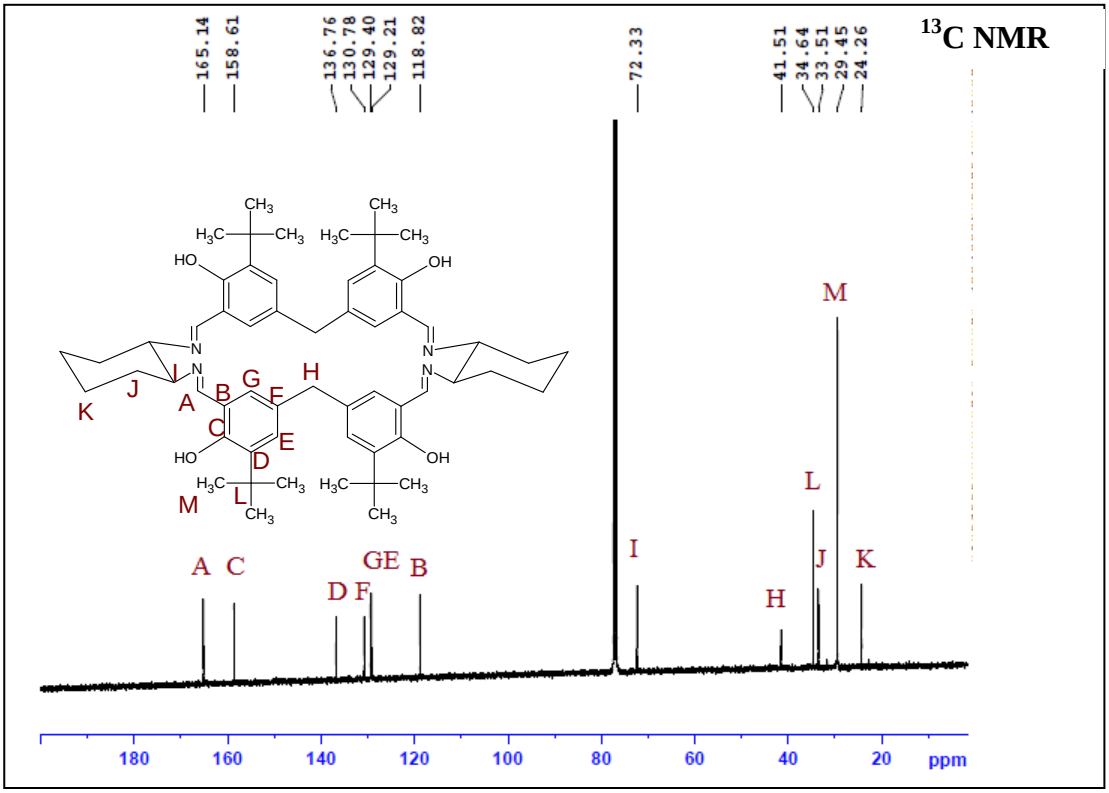

Spectrum 3.27

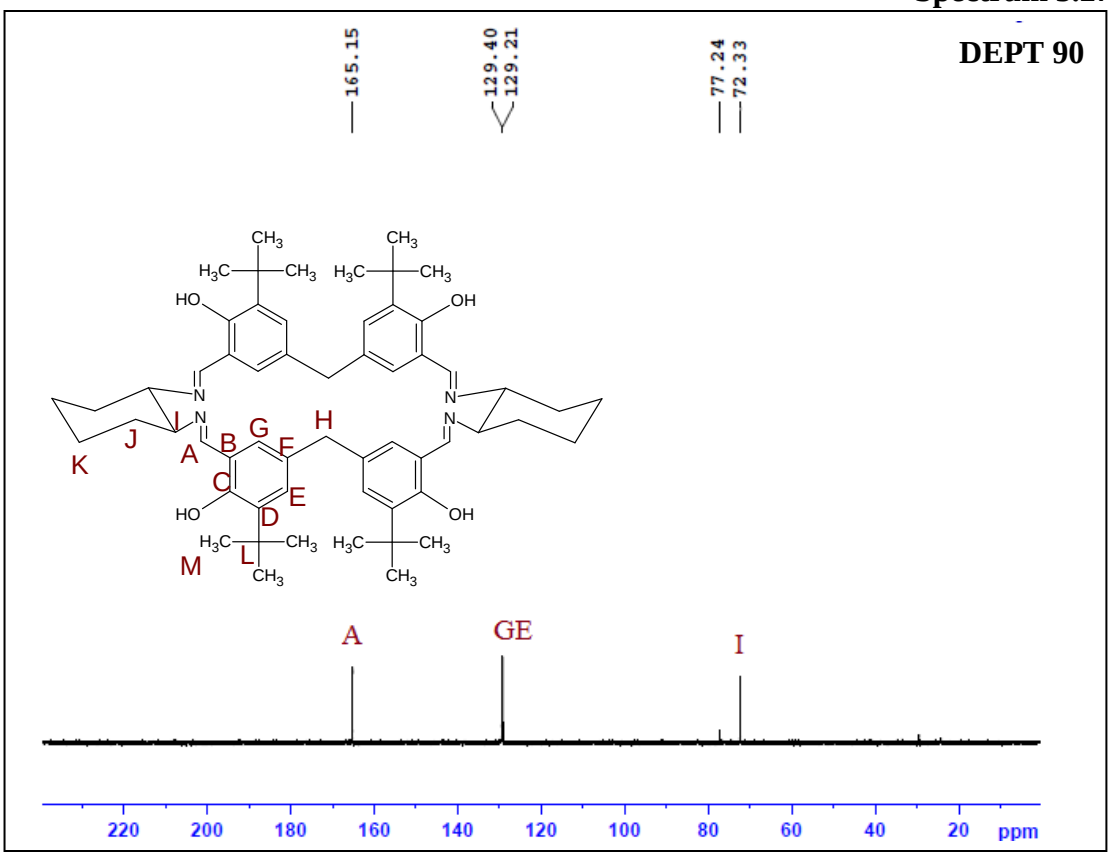

Spectrum 3.28

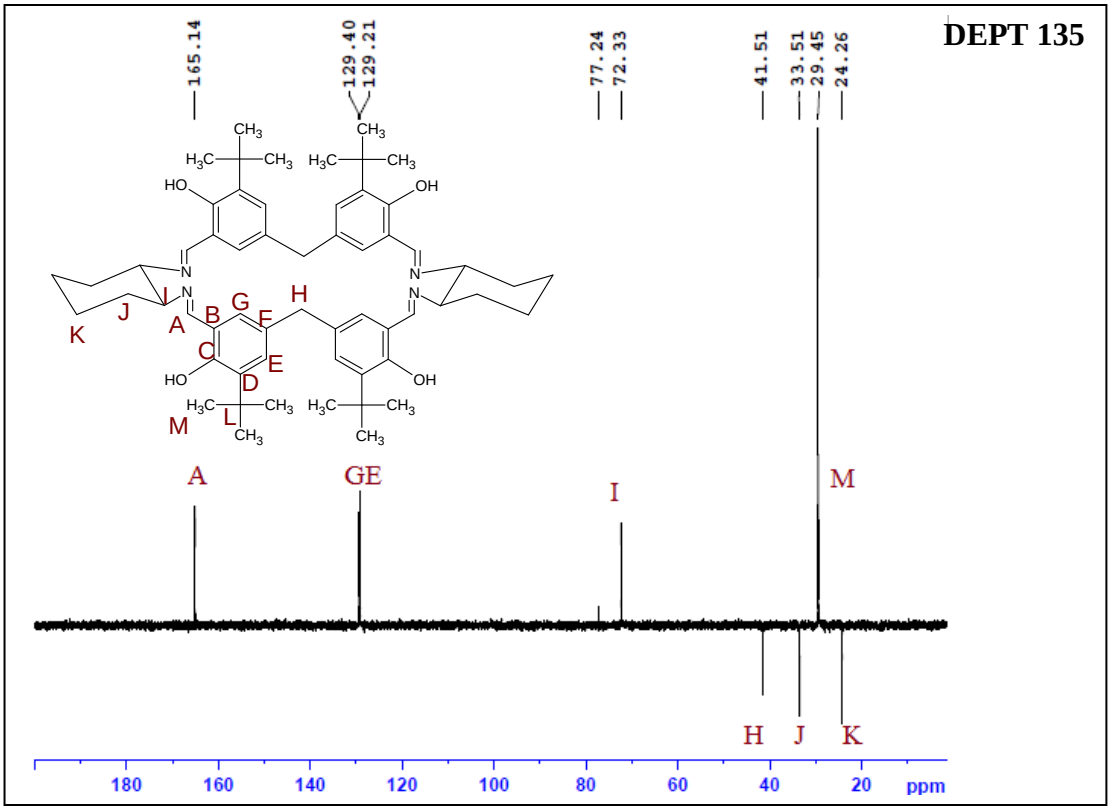

Spectrum 3.29

COSY

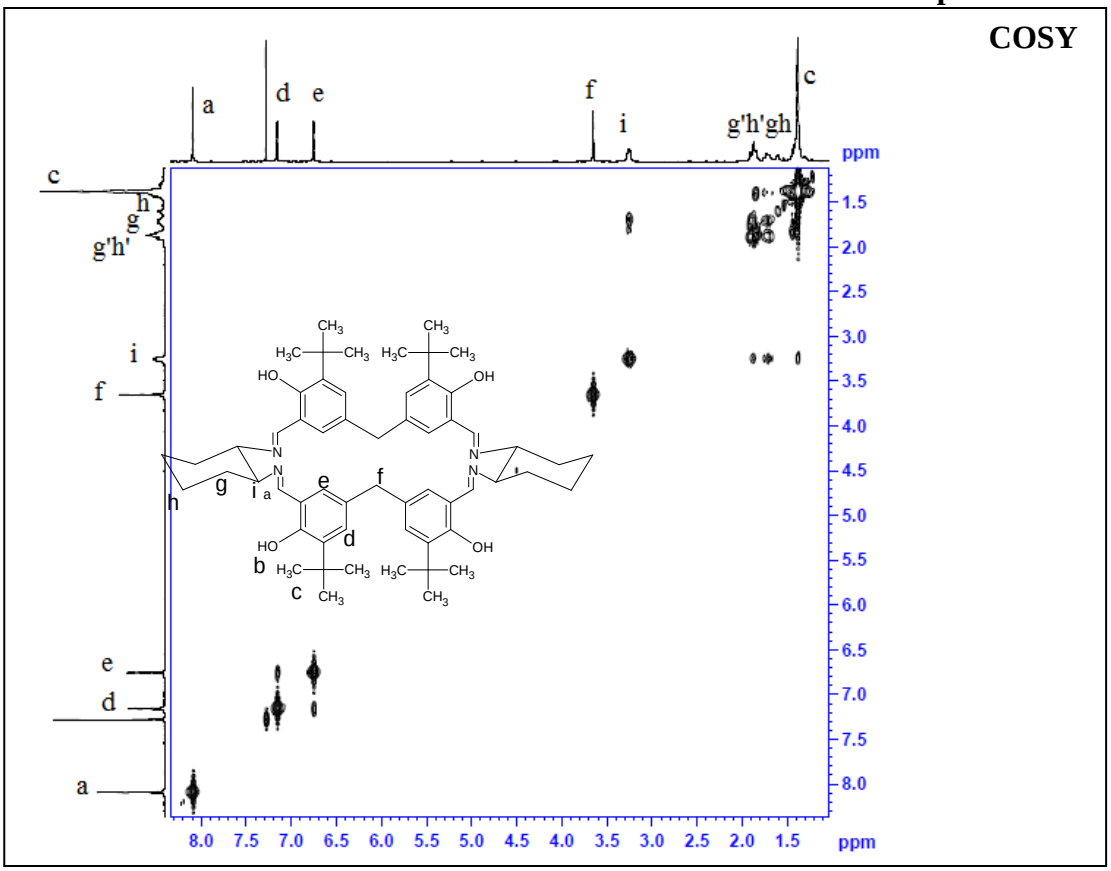

Spectrum 3.30

NOESY

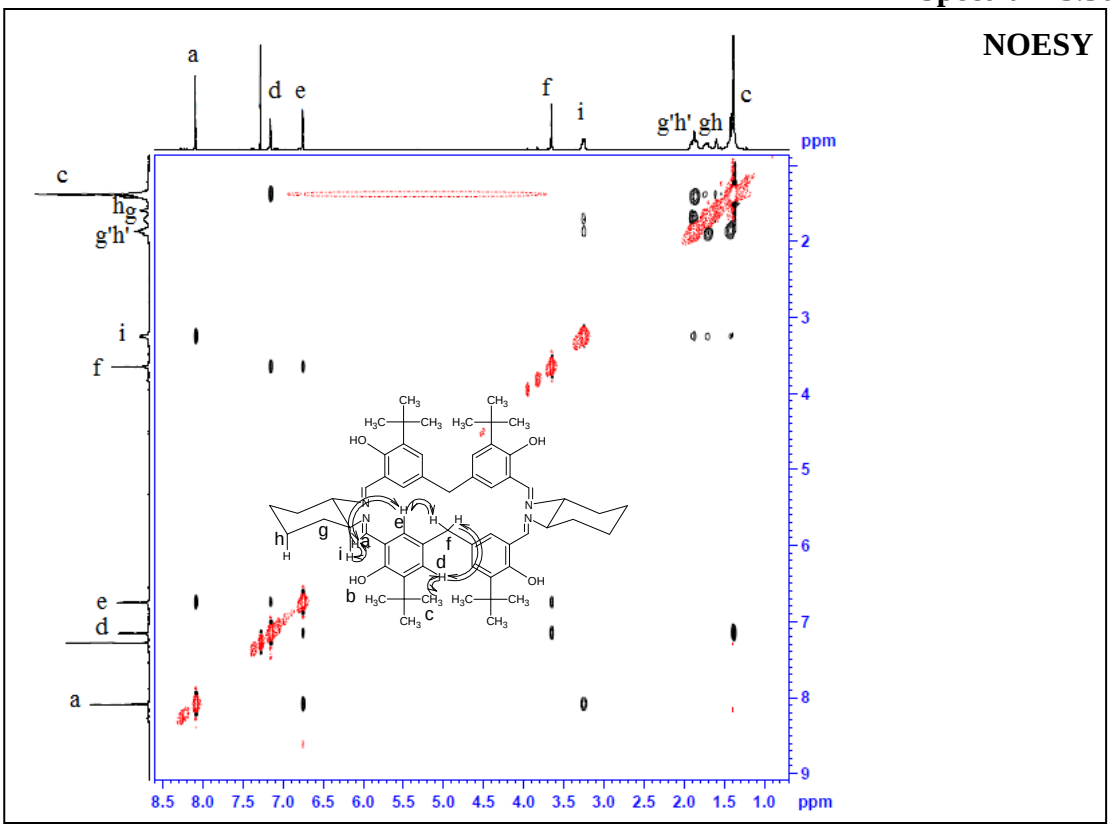

Spectrum 3.31

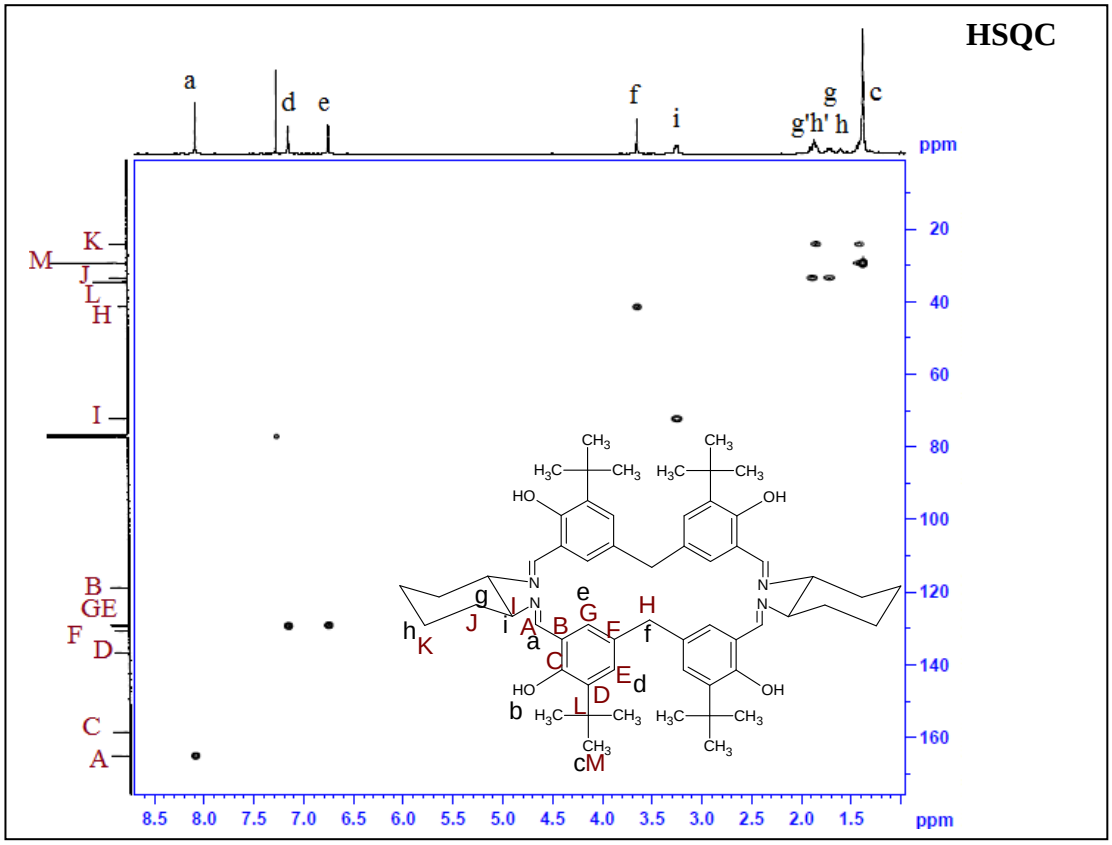

Spectrum 3.32

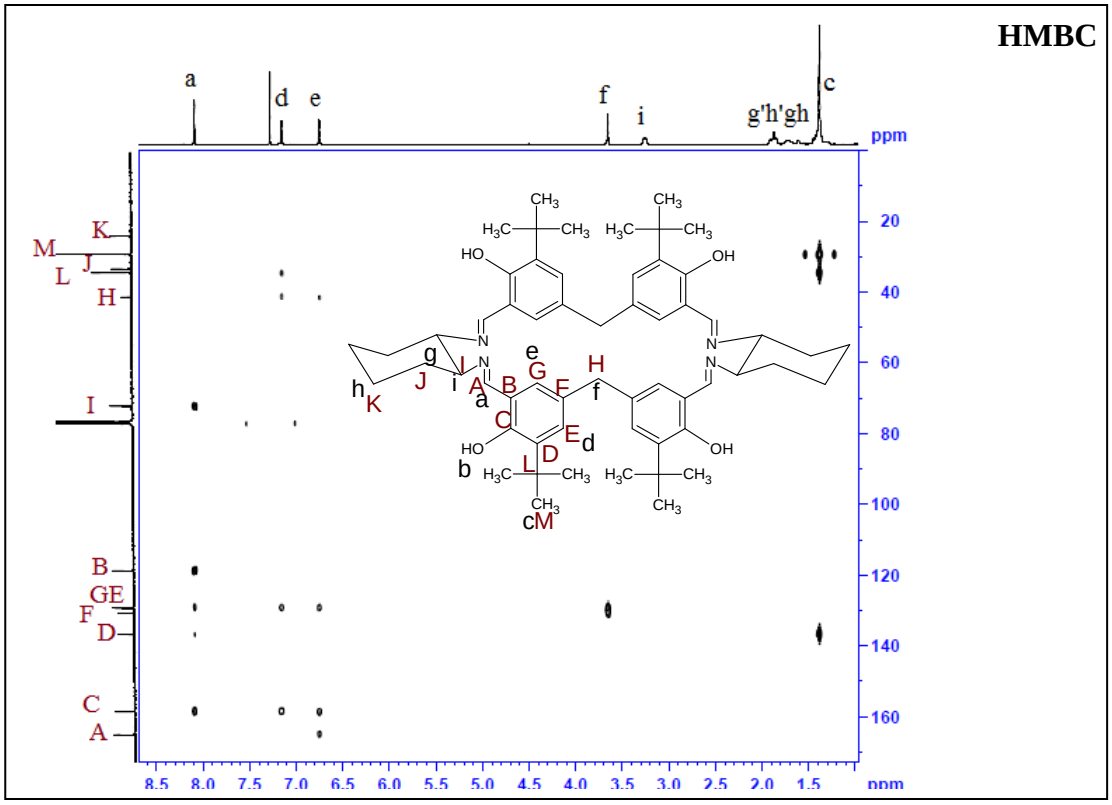

Spectrum 3.33

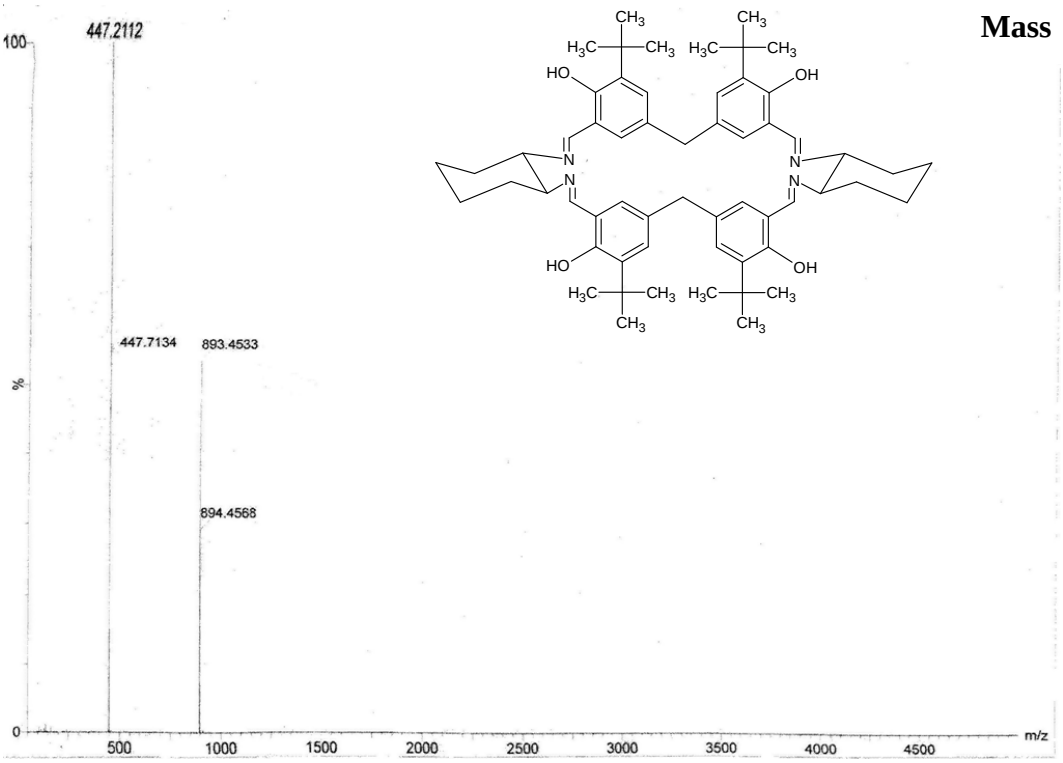

Chromatogram 3.34

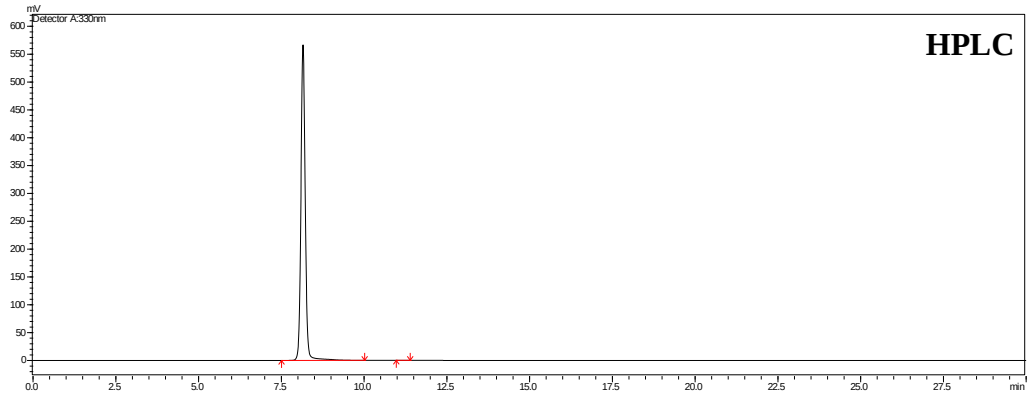

Silica column

Mobile phase: MDC

Peak	Name	Ret. Time	Area%
1	Calix-salen corand from dach and 5,5'methylene-bis(3-tertbutylsalicylaldehyde)	8.150	99.9790
2		11.122	0.0210

Spectrum 3.35

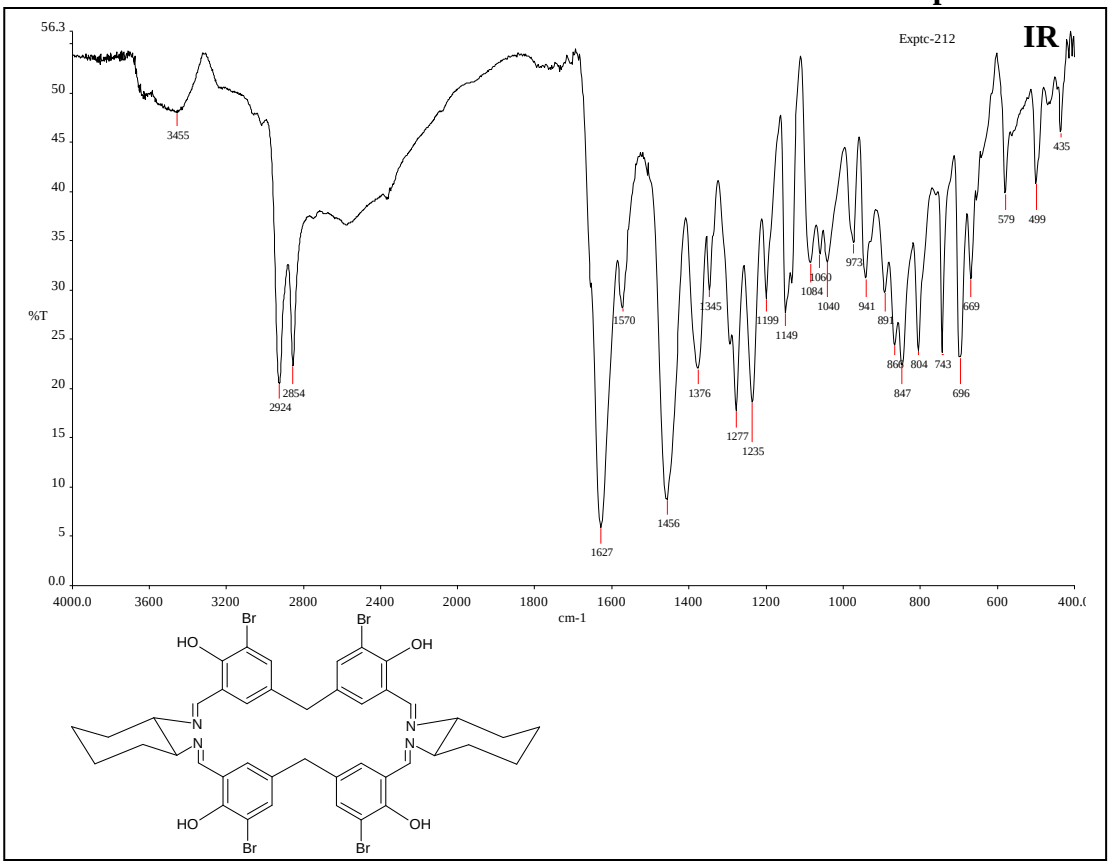

Spectrum 3.36

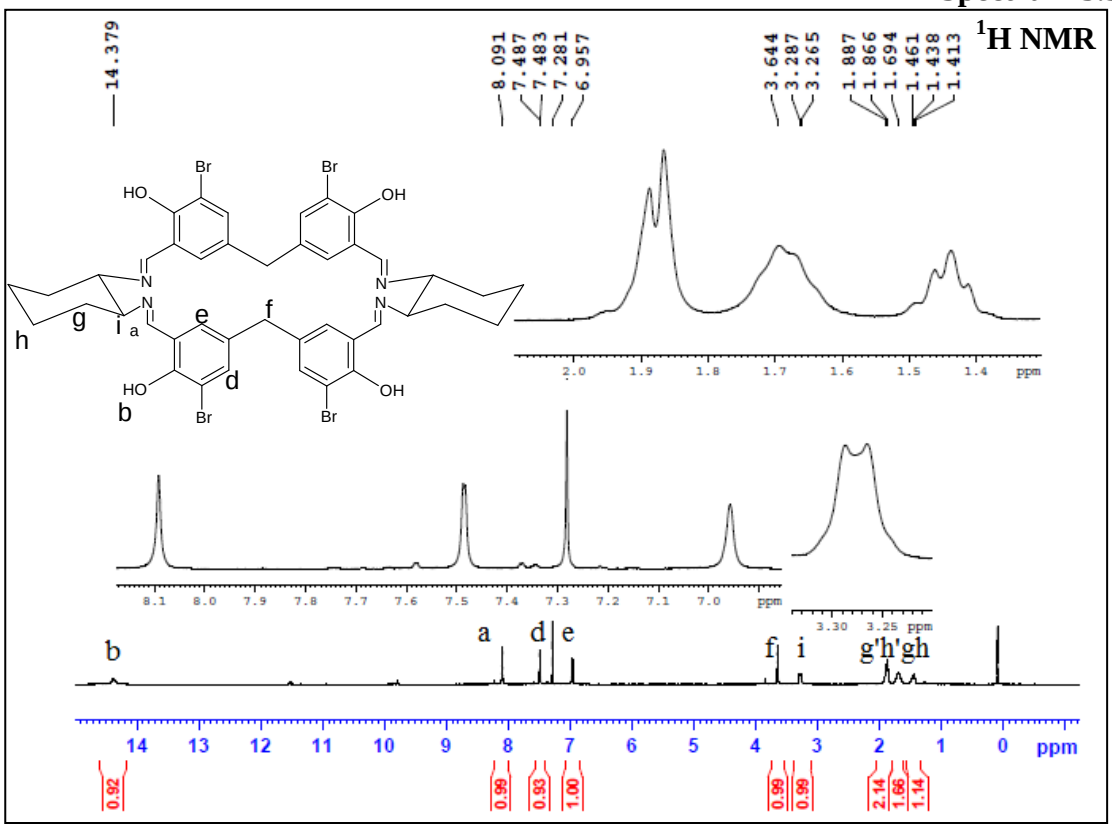

Spectrum 3.37

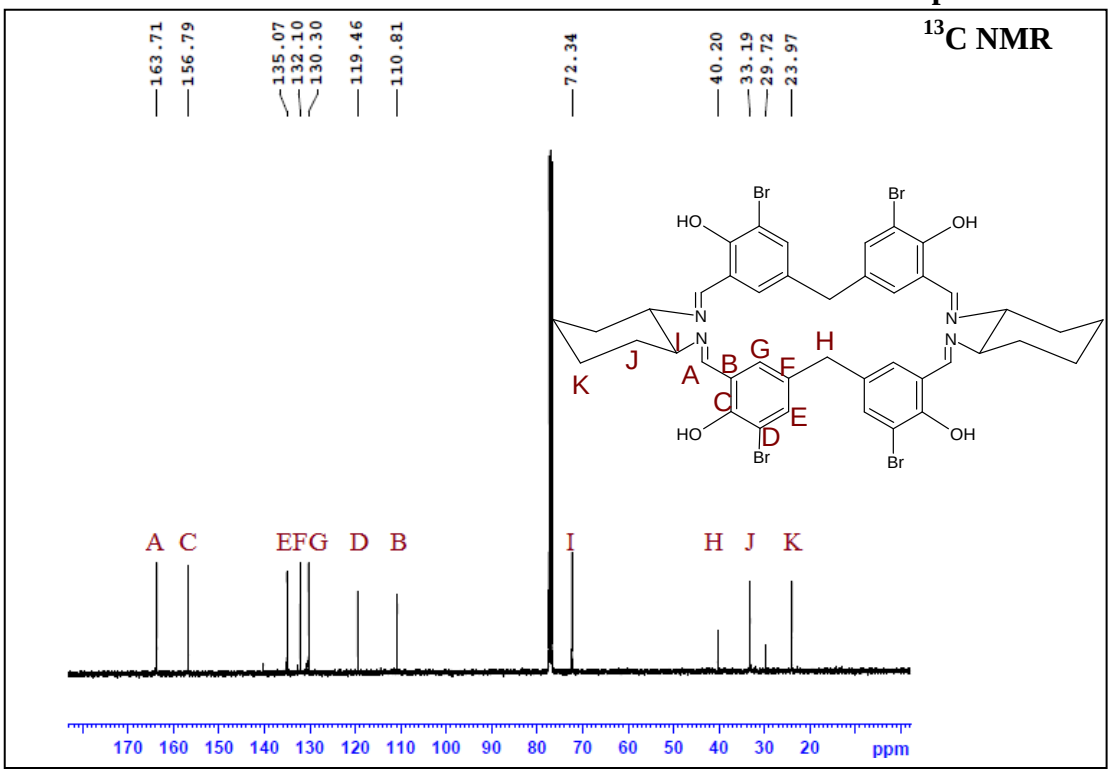

Spectrum 3.38

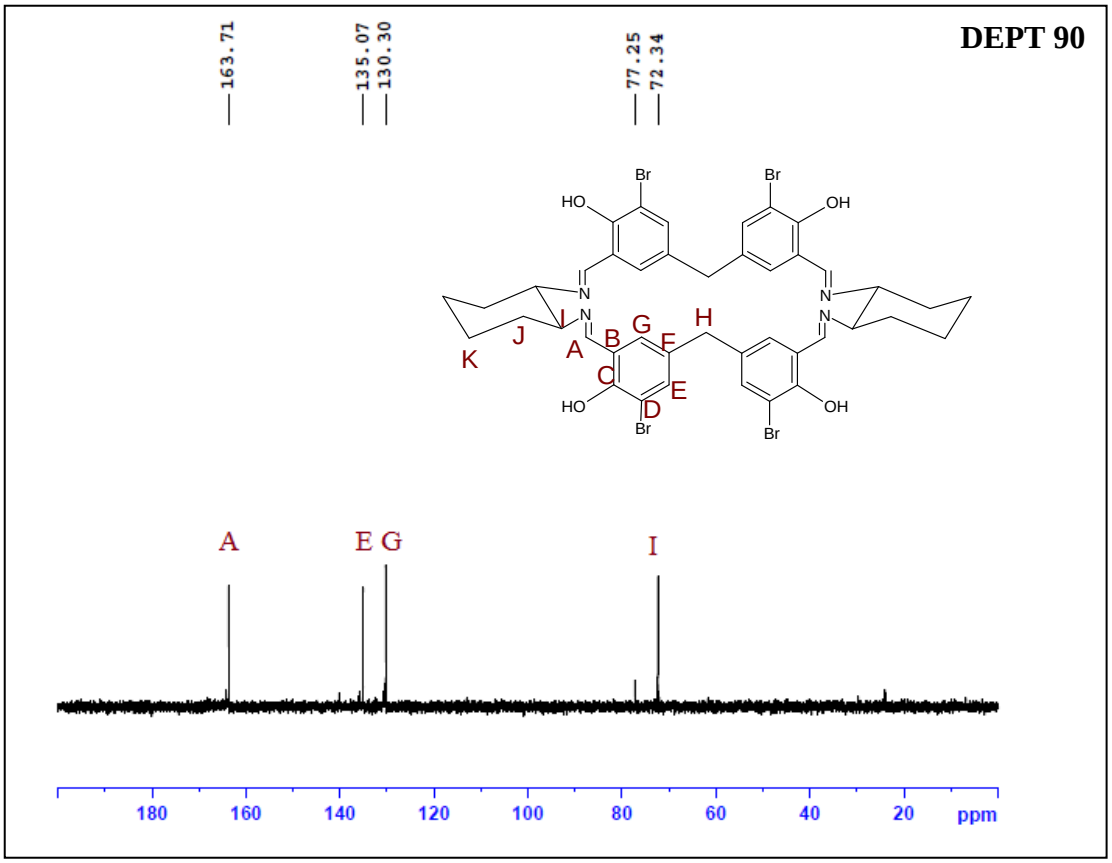

Spectrum 3.39

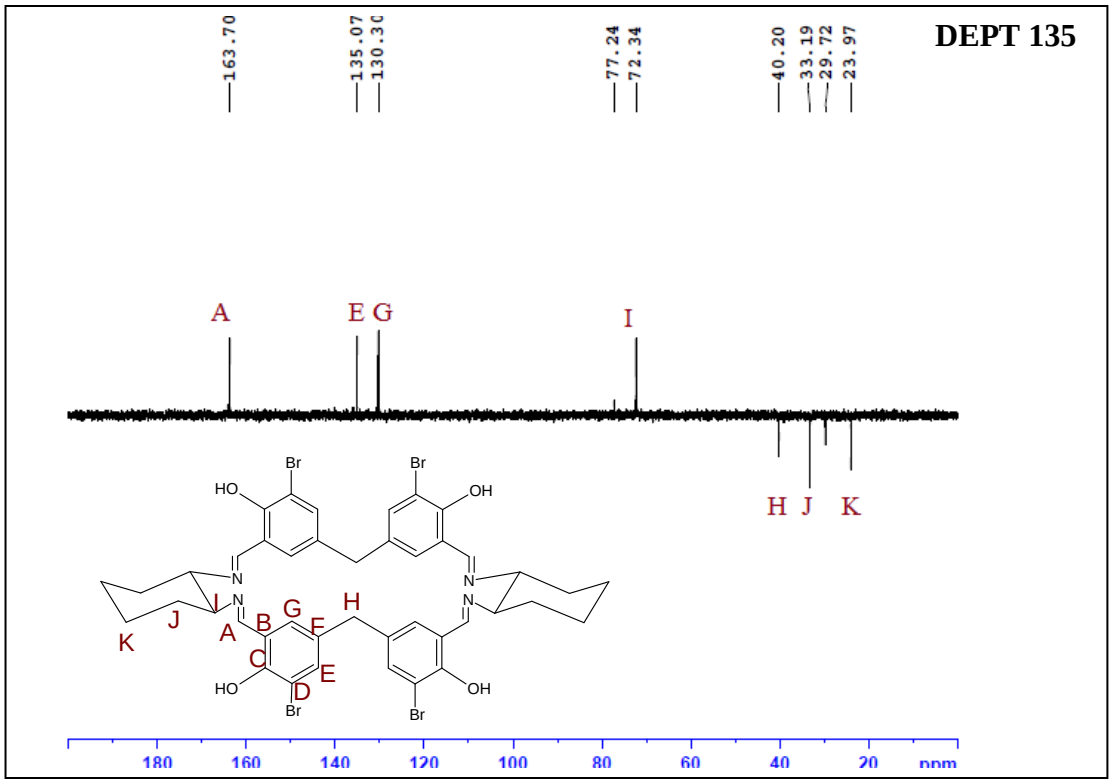

Spectrum 3.40

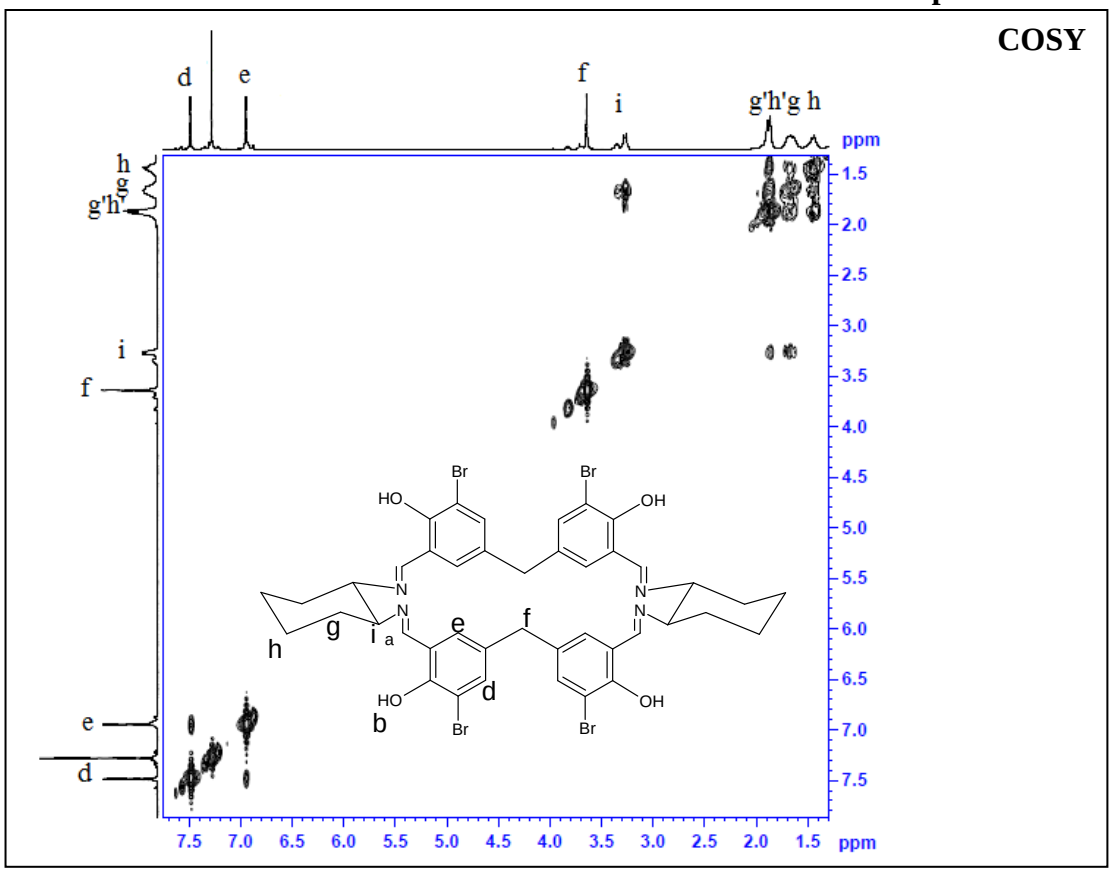

Spectrum 3.41

NOESY

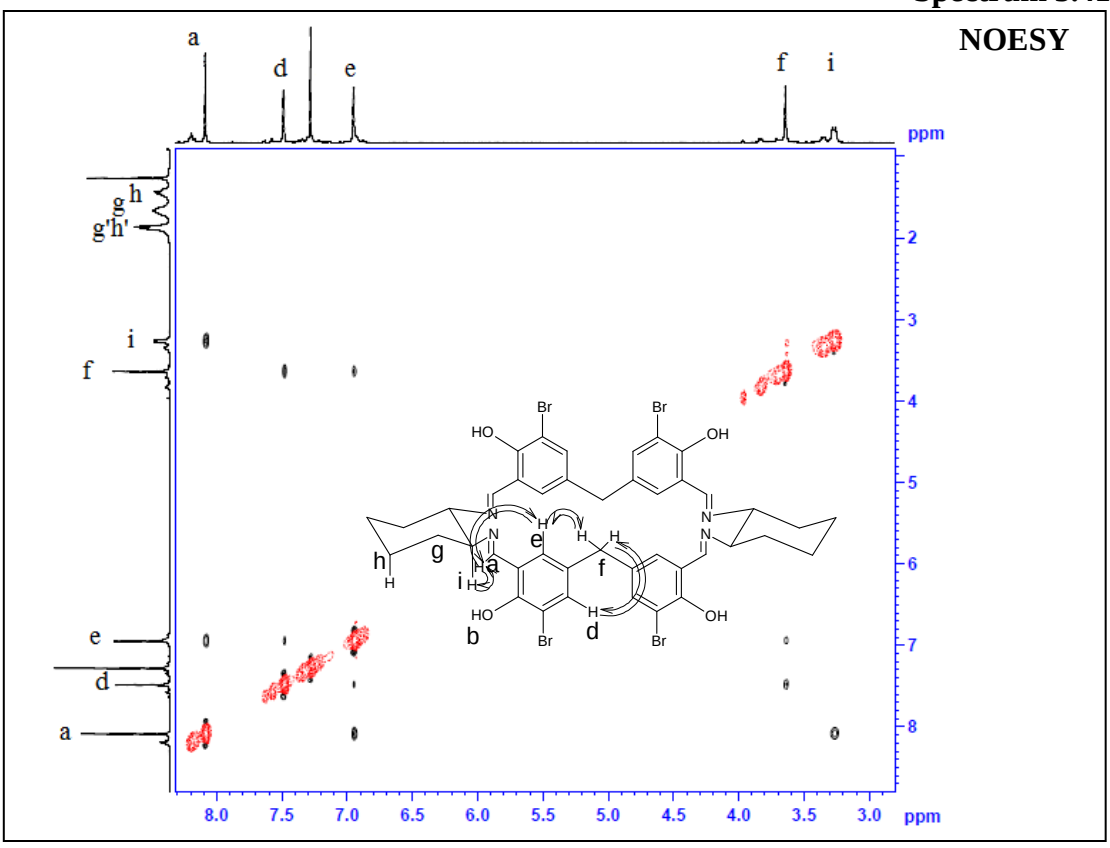

Spectrum 3.42

HSQC

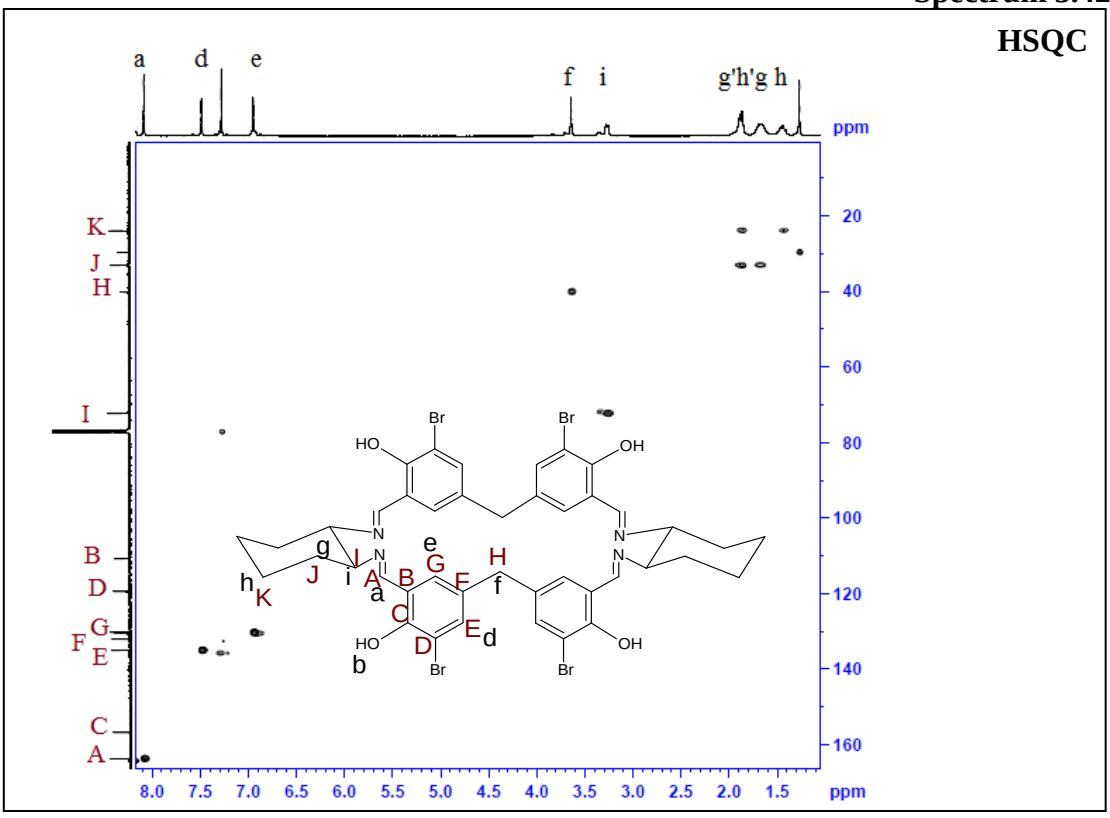

Spectrum 3.43

HMBC

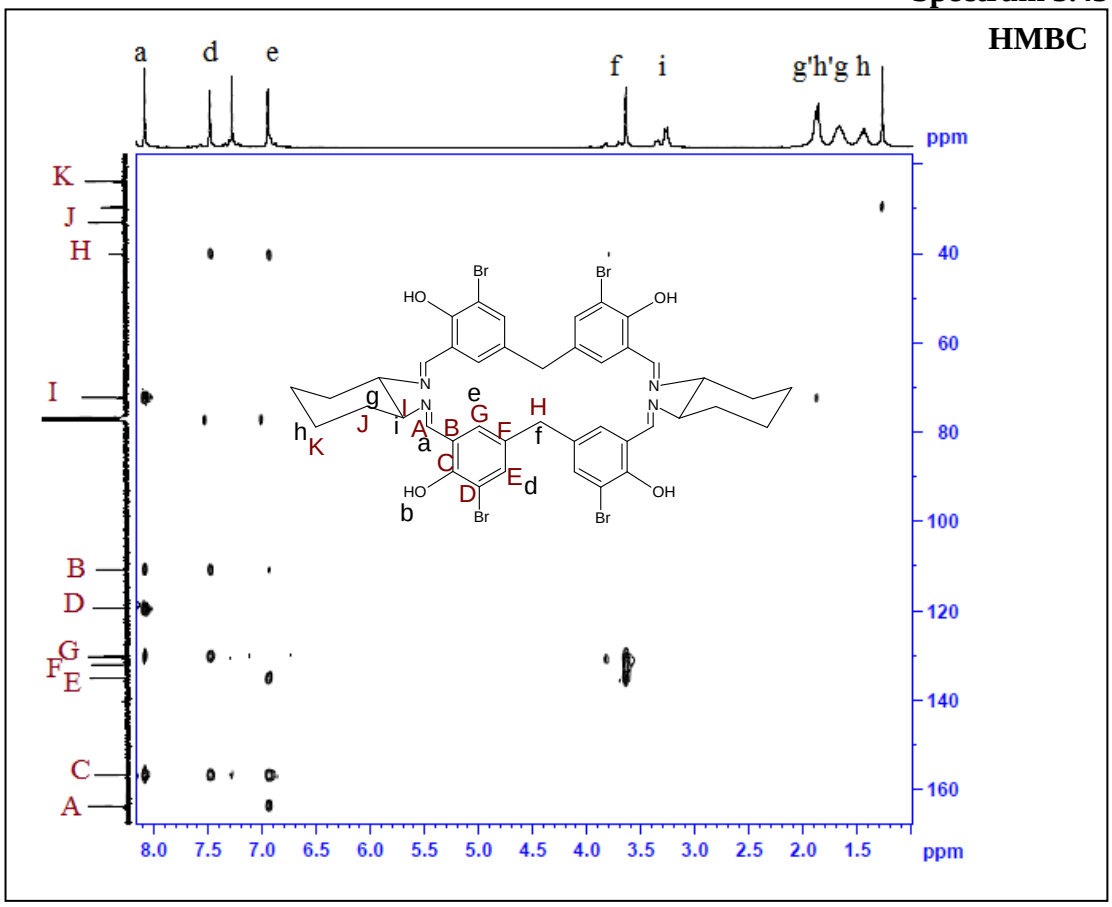

Spectrum 3.44

MASS

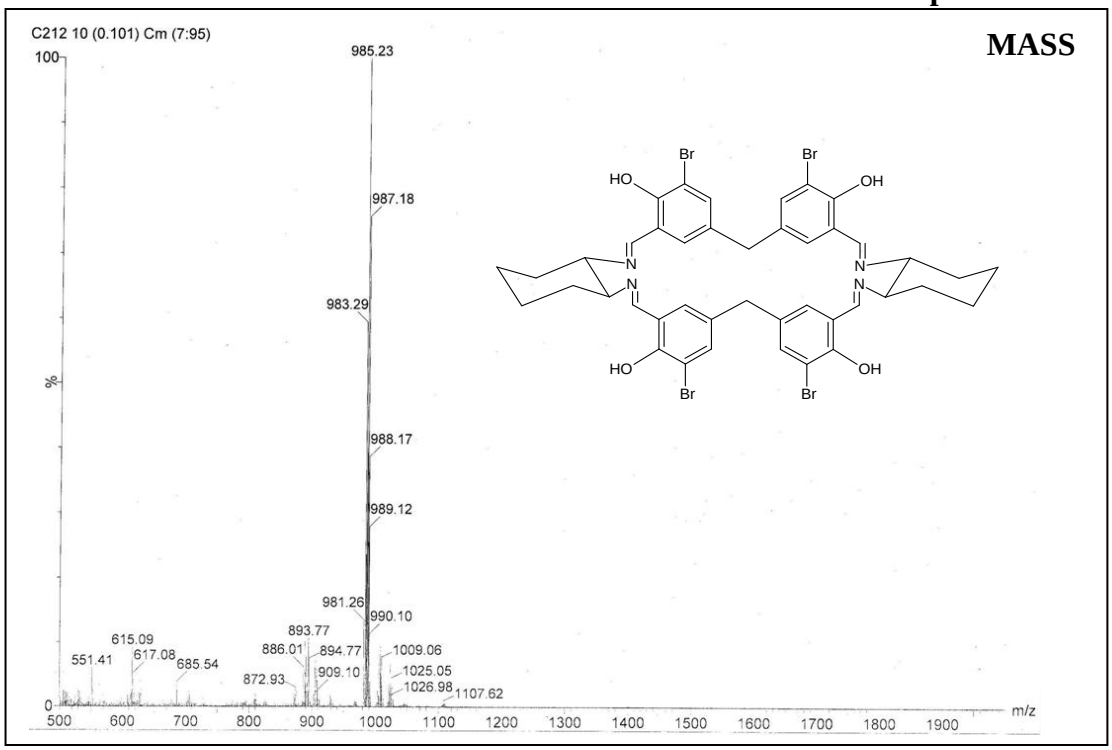

Chromatogram 3.45

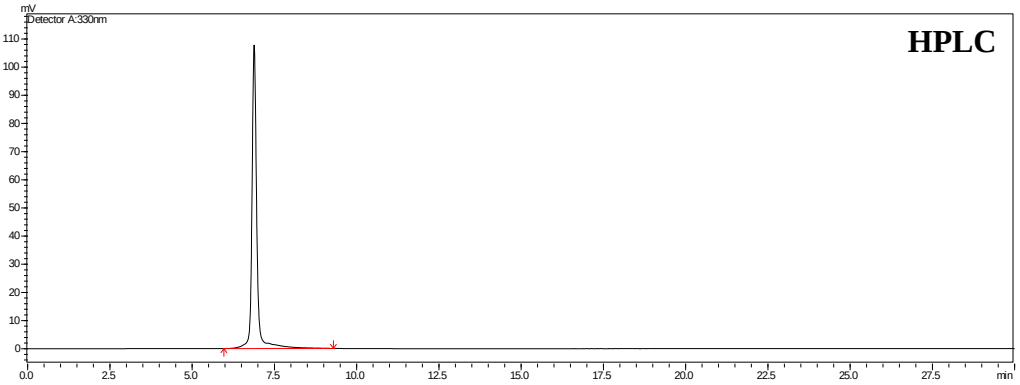

Silica column

Mobile phase: MDC:MeOH:: 98:2(v/v)

Peak	Name	Ret. Time	Area%
1	calix-salen corand from dach and 5,5'methylene bis(3-bromosalicylaldehyde)	6.881	100.0000

Spectrum 3.46

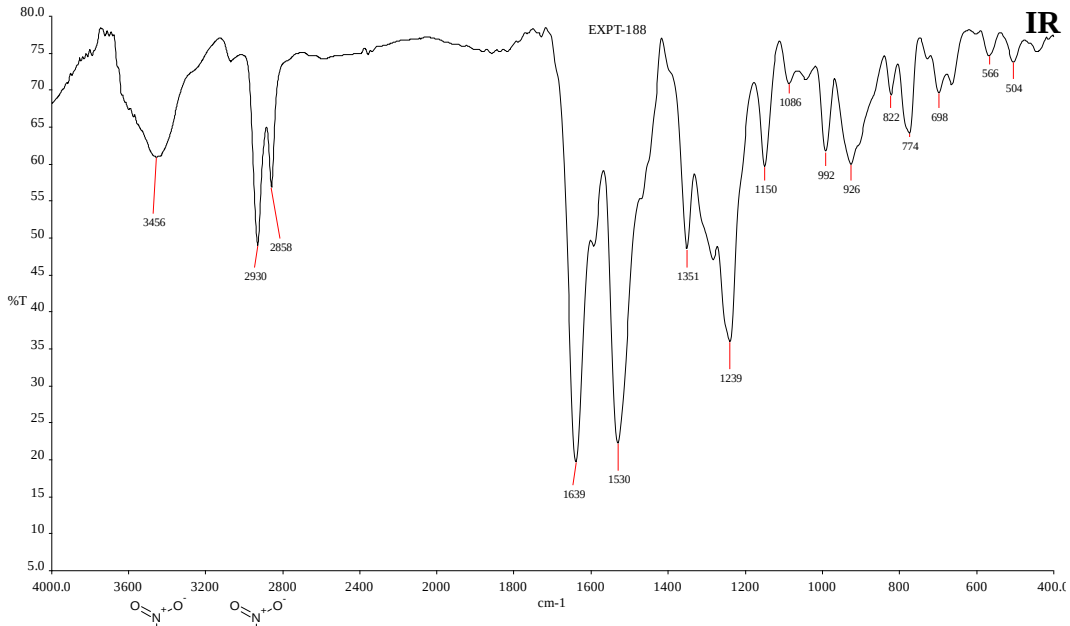

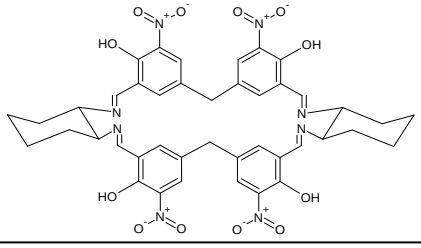

Spectrum 3.47

^{1}H NMR

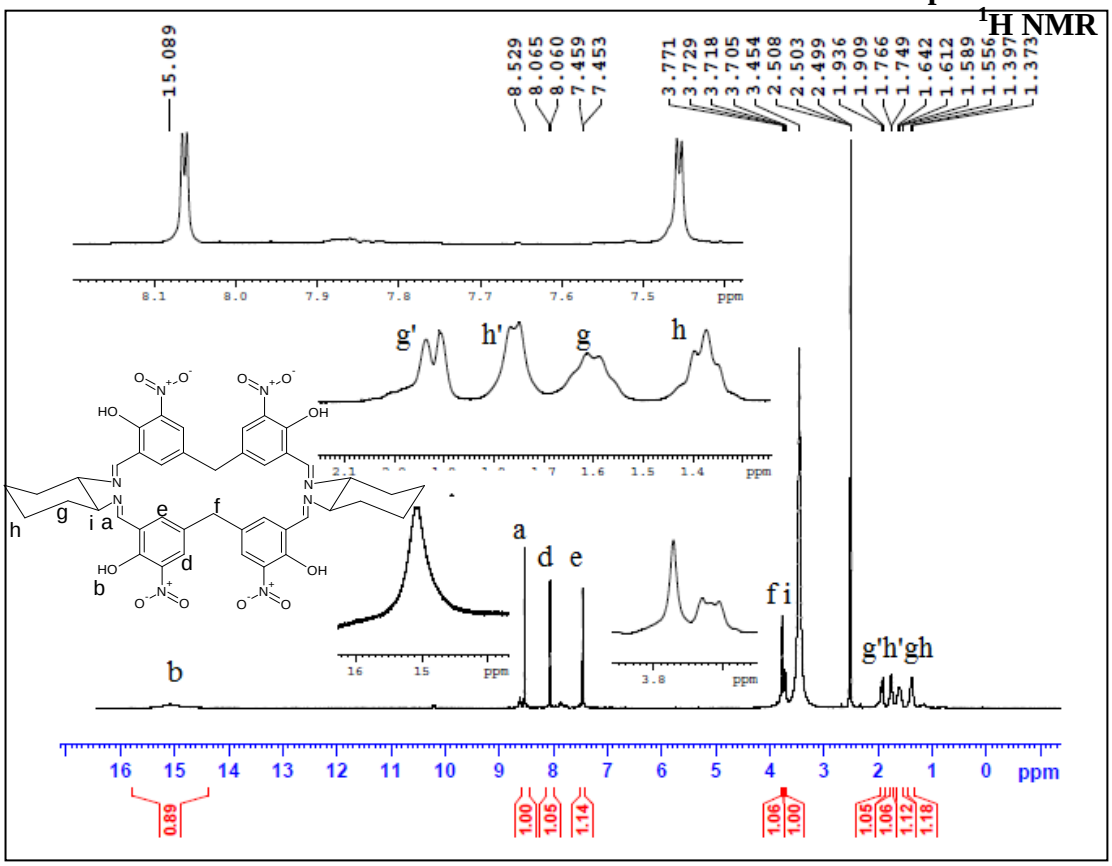

Spectrum 3.48

^{13}C NMR

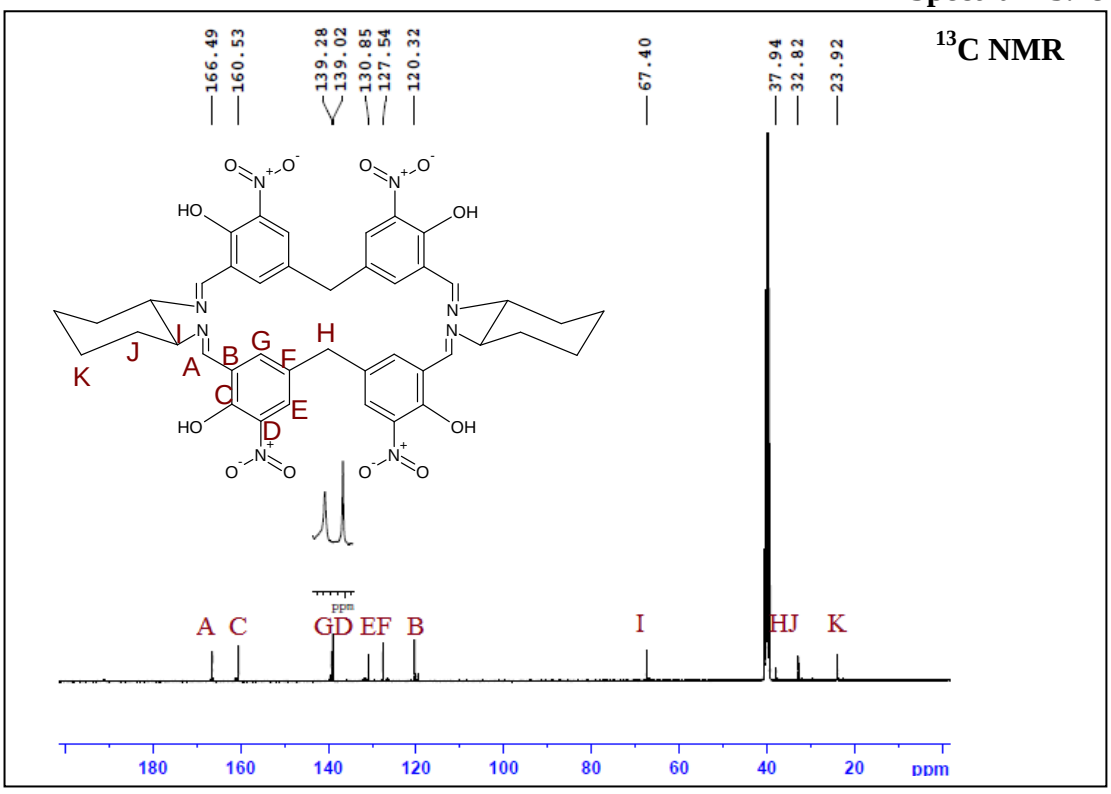

Spectrum 3.49

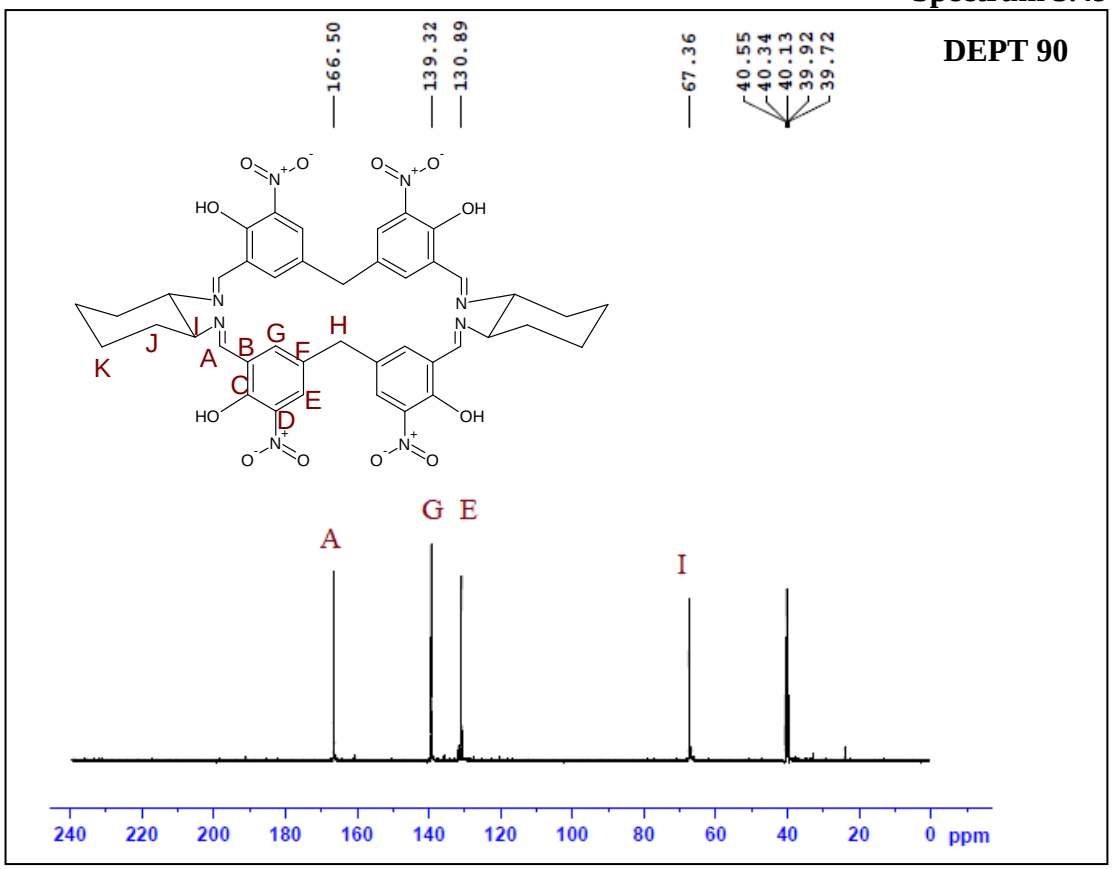

Spectrum 3.50

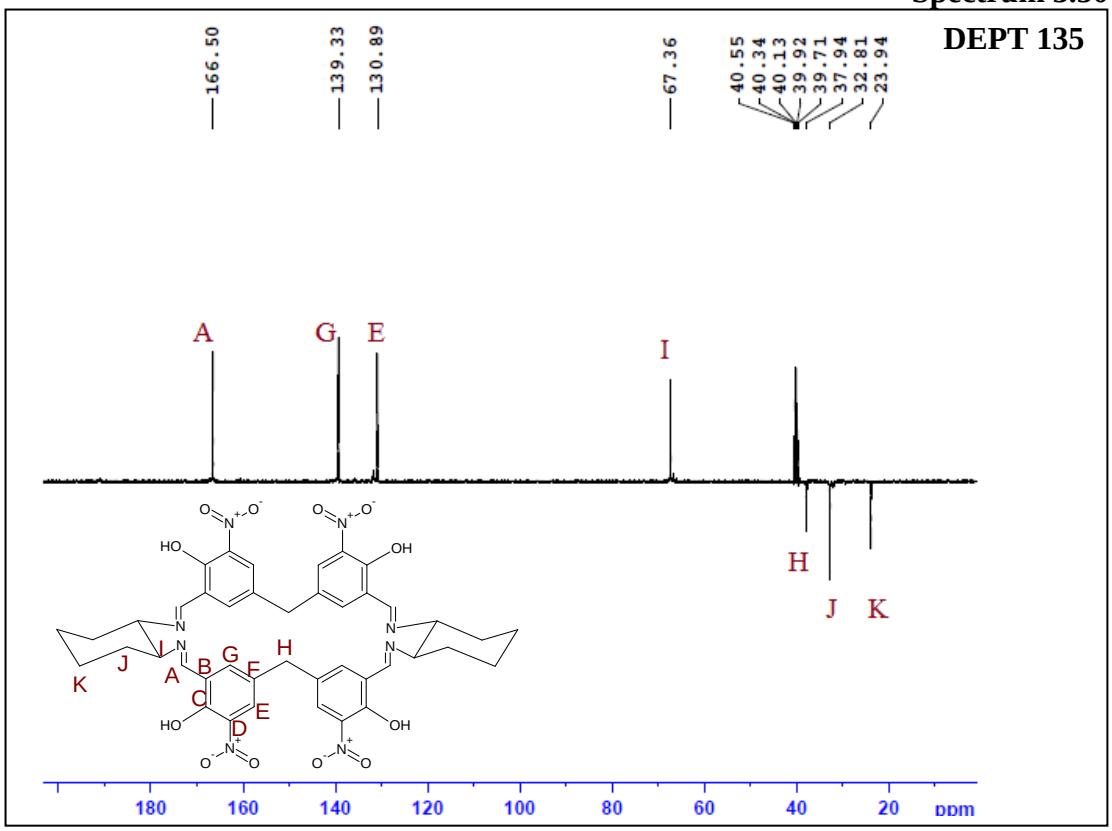

Spectrum 3.51

COSY

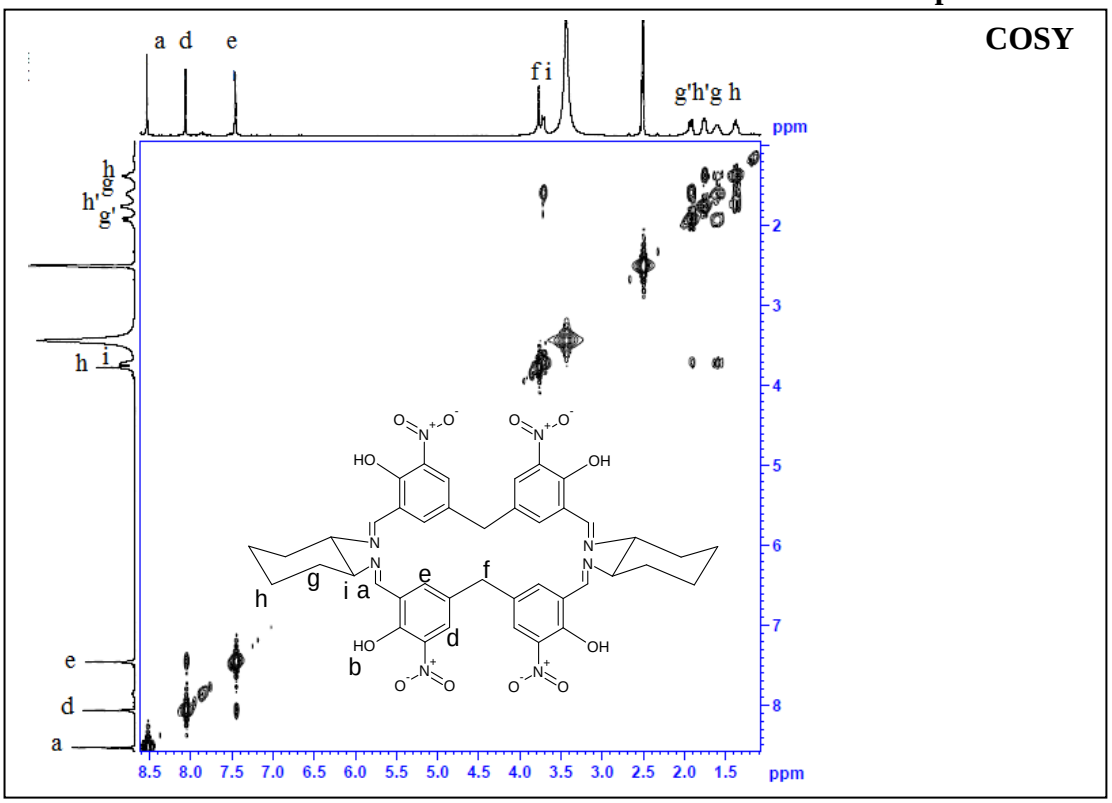

Spectrum 3.52

NOESY

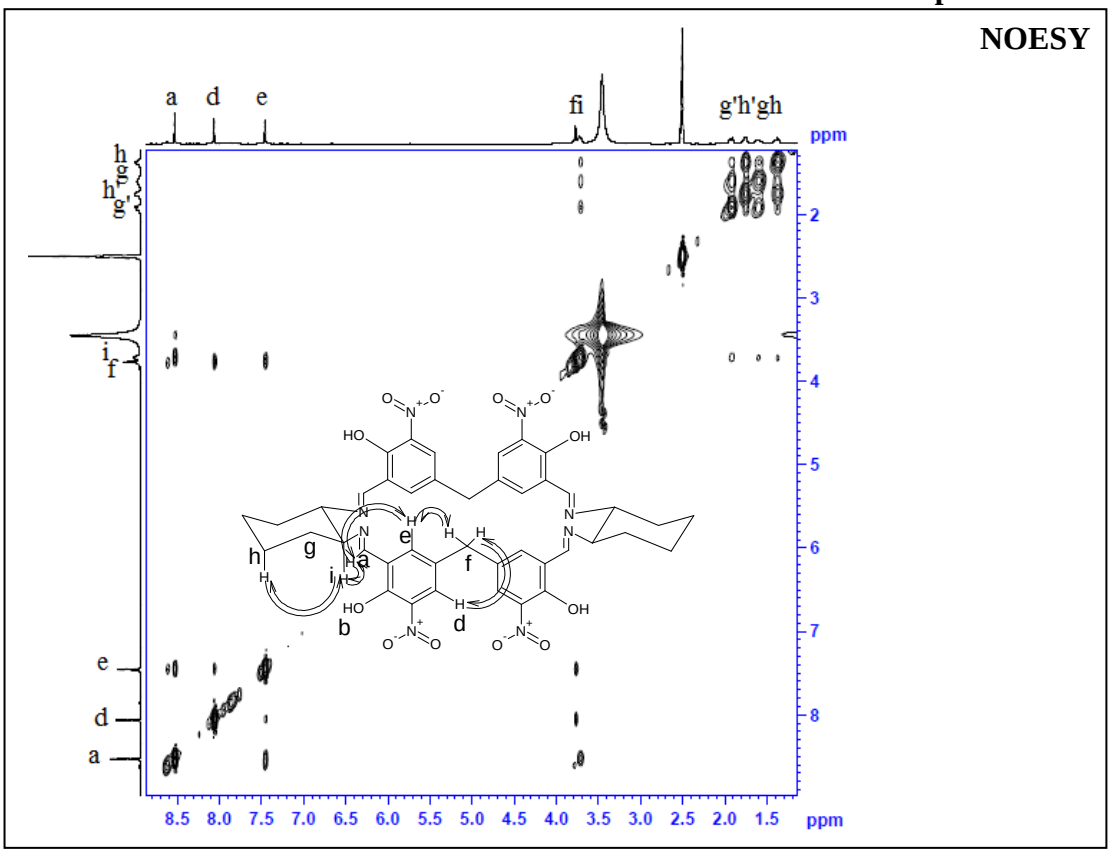

Spectrum 3.53

HSQC

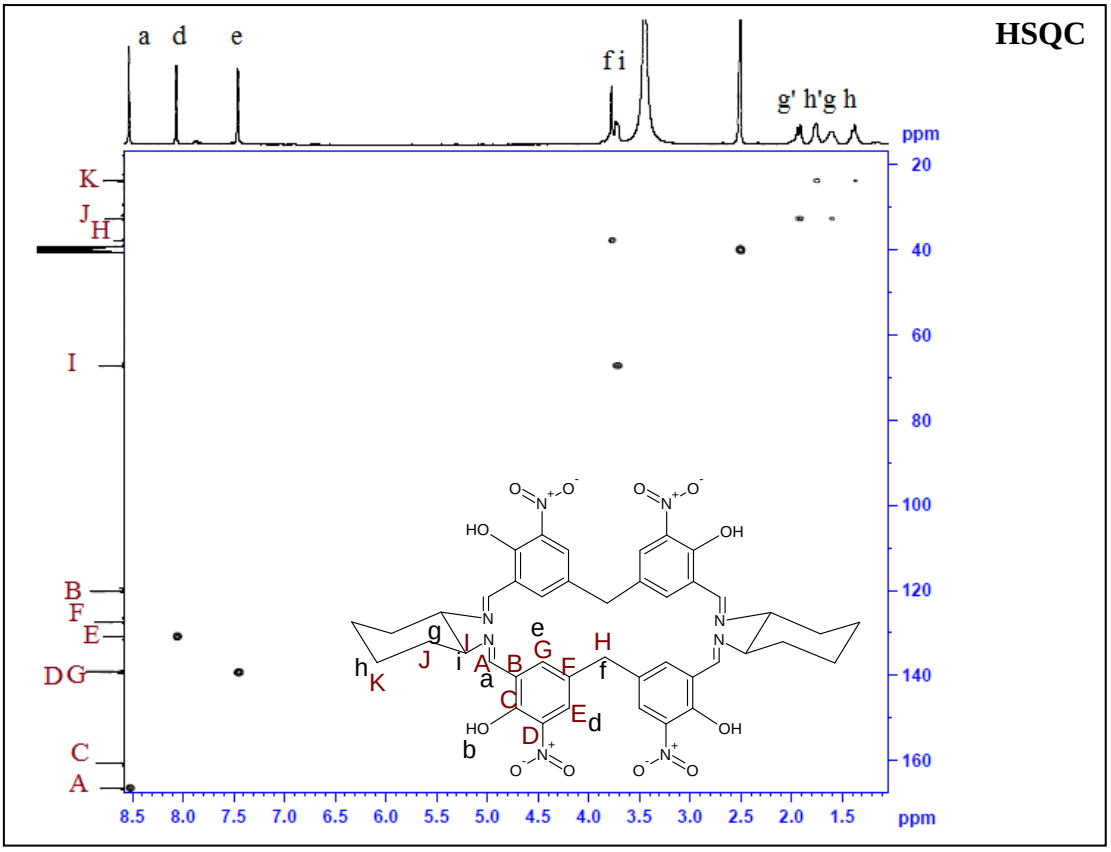

Spectrum 3.54

HMBC

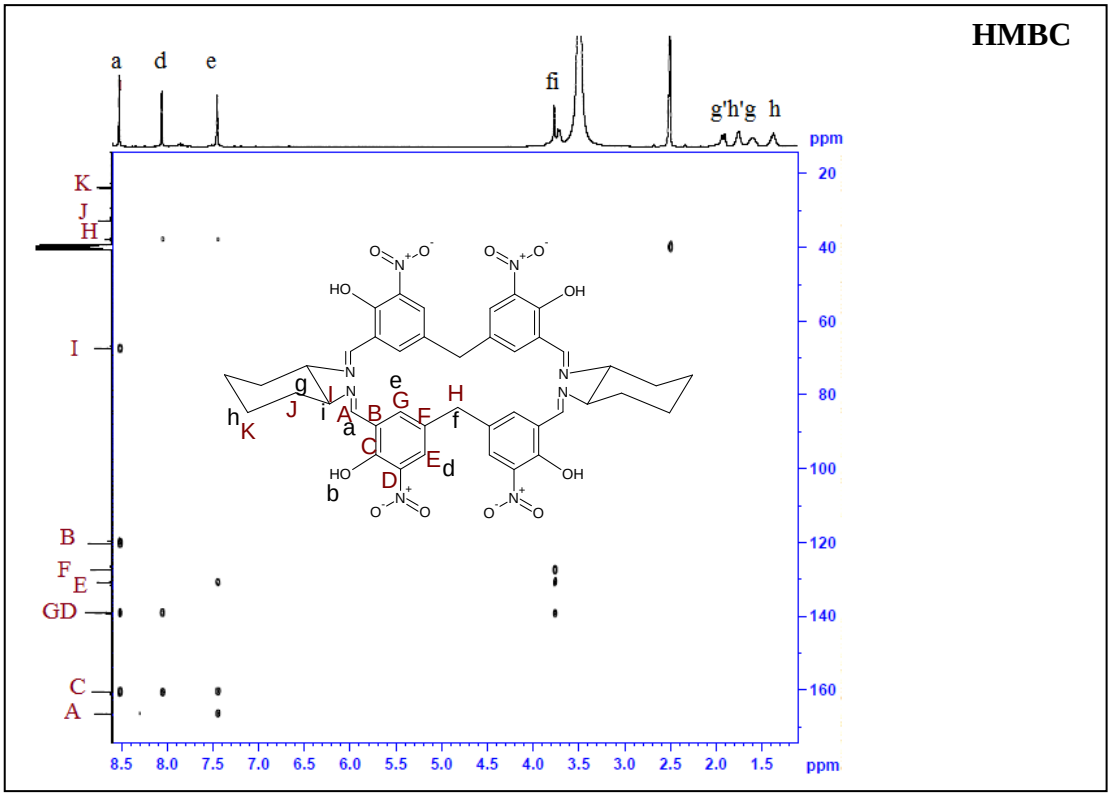

Spectrum 3.55

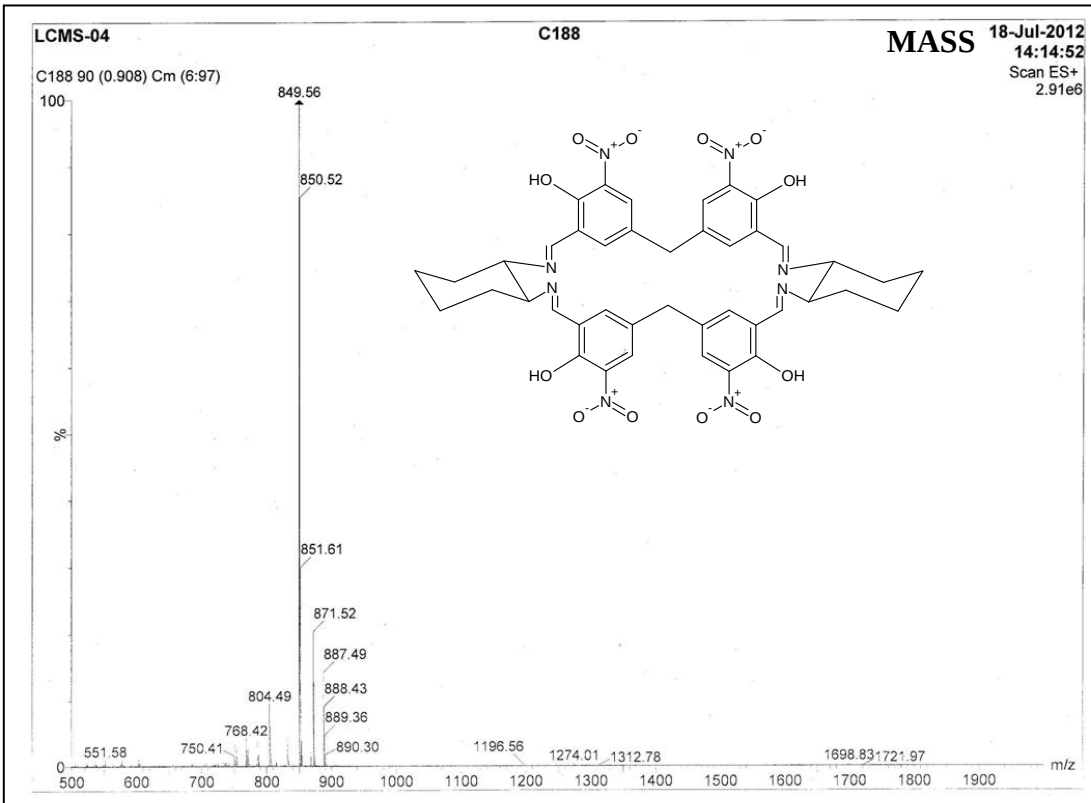

Chromatogram 3.56

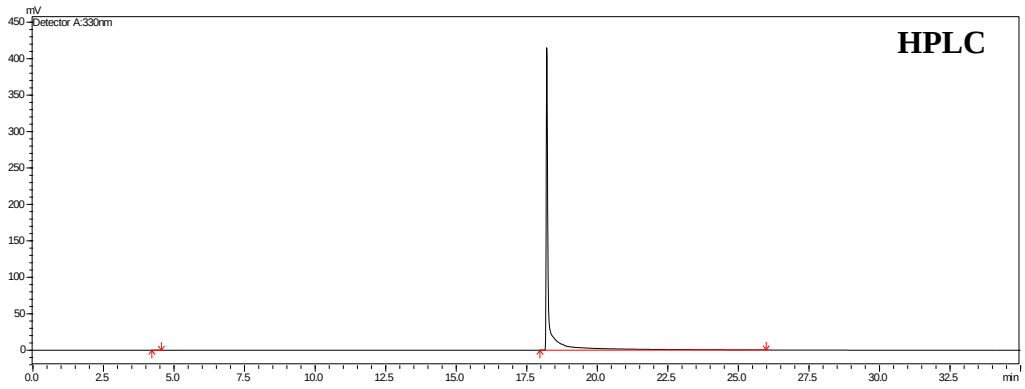

Silica column

Mobile phase: MDC:MeOH:: 95:5(v/v)

Peak	Name	Ret. Time	Area%
1	imp	4.372	0.0417
2	Calix-salen corand from dach and 5,5'methylene-bis-(3-nitrosalicylaldehyde)	18.207	99.9583

Spectrum 3.57

IR

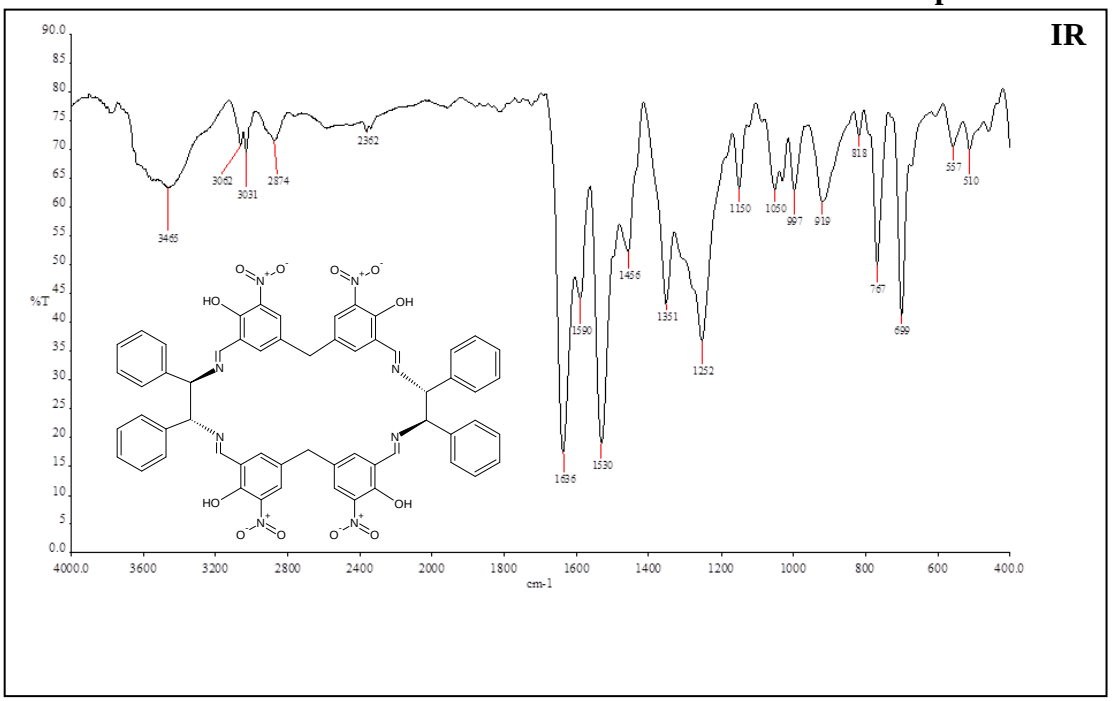

Spectrum 3.58

^{1}H NMR

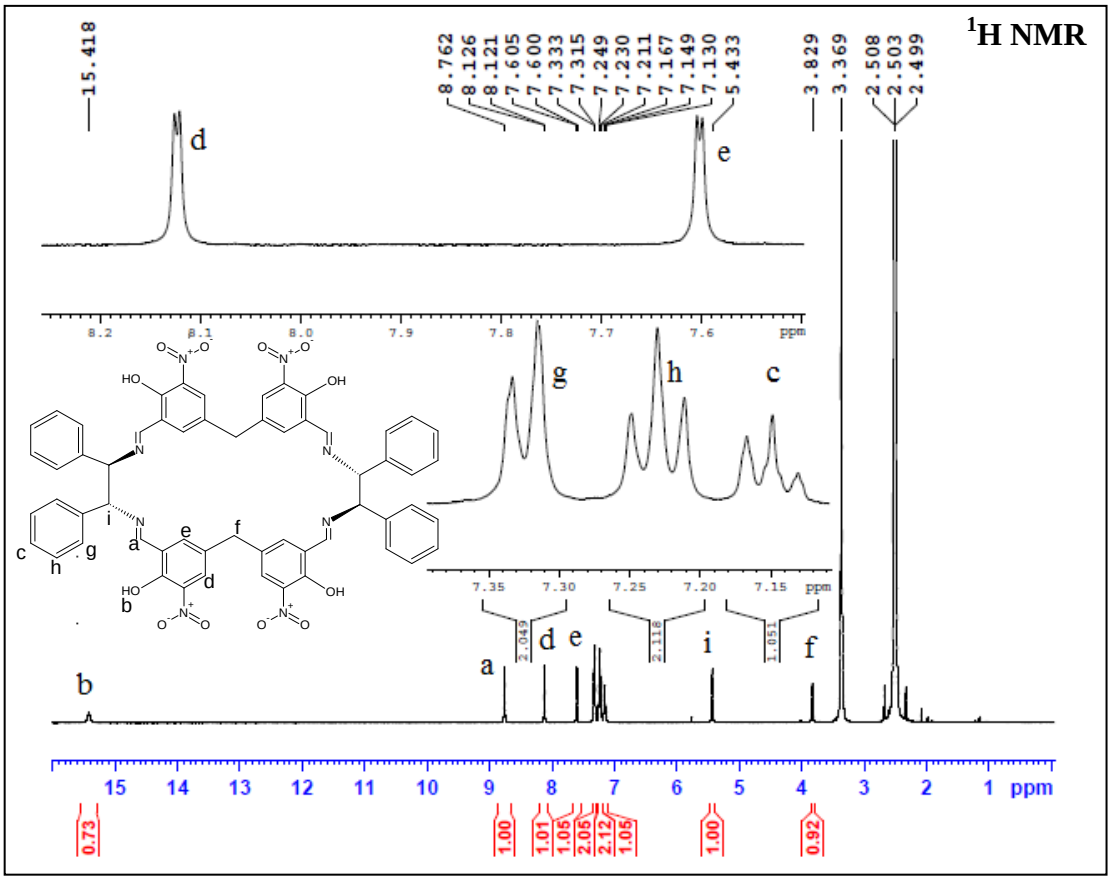

Spectrum 3.59

^{13}C NMR

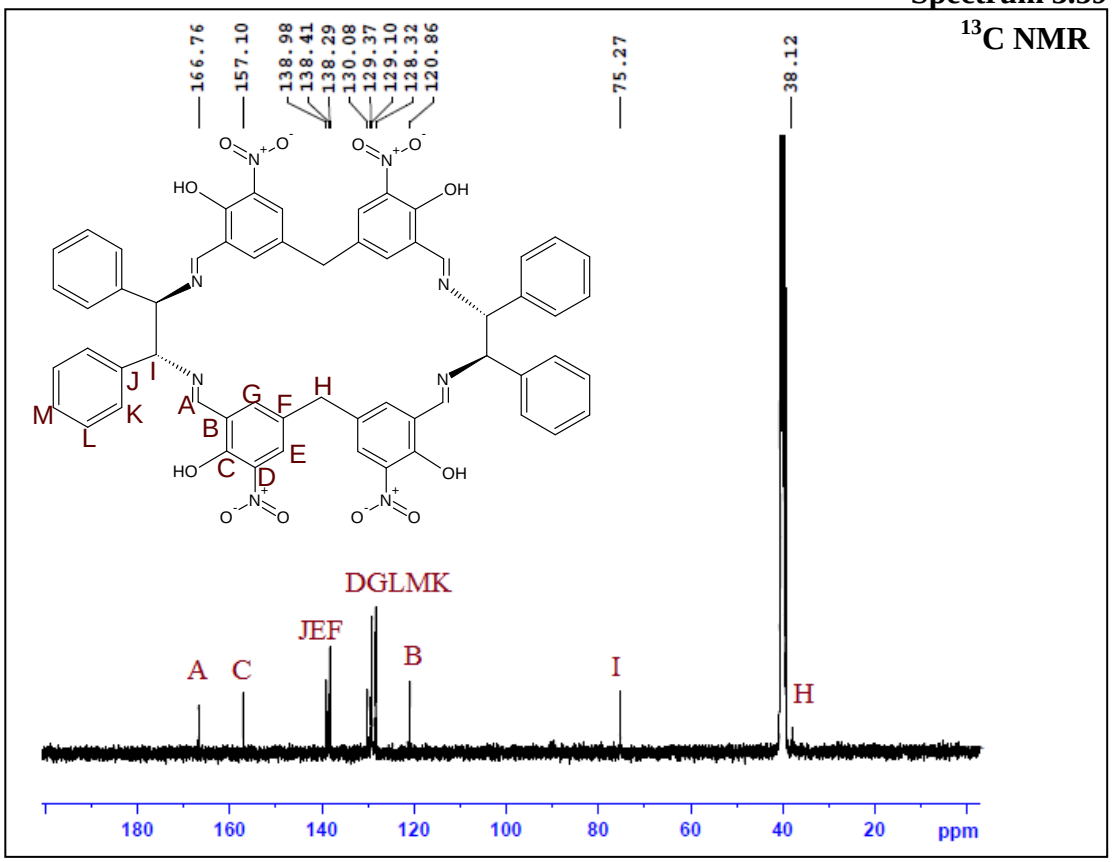

Spectrum 3.60

DEPT 90

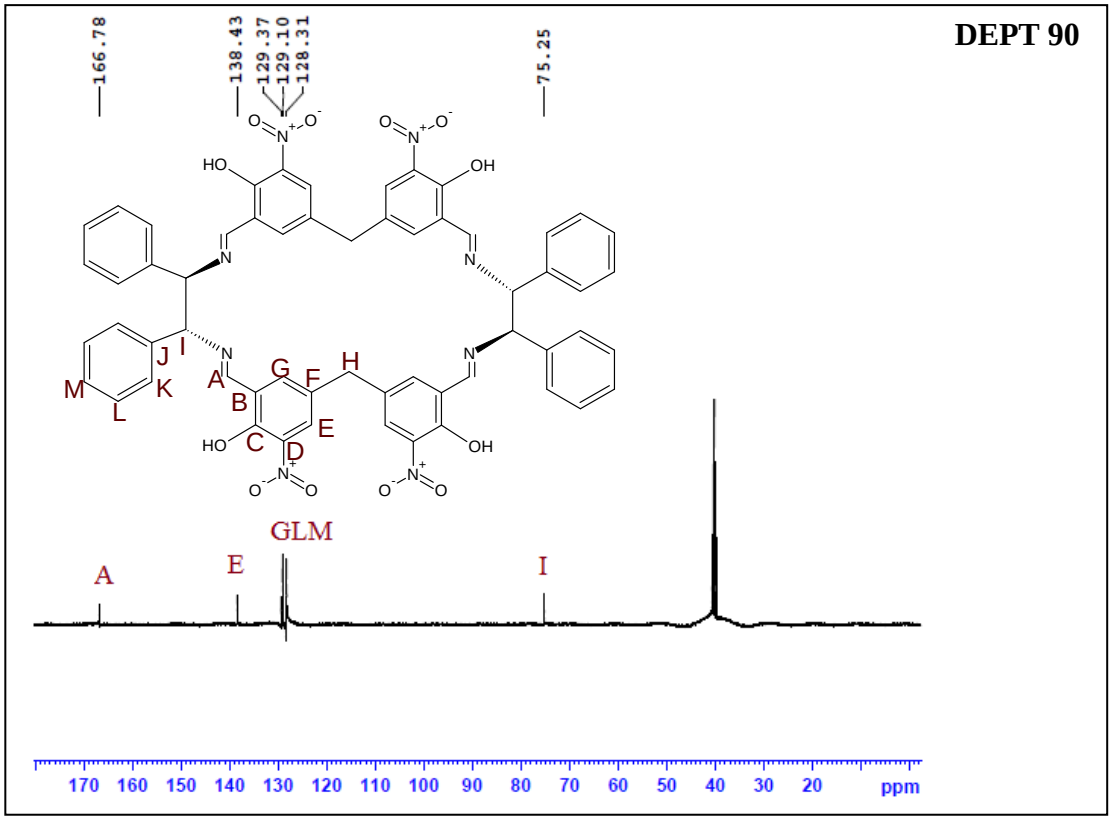

Spectrum 3.61

DEPT 135

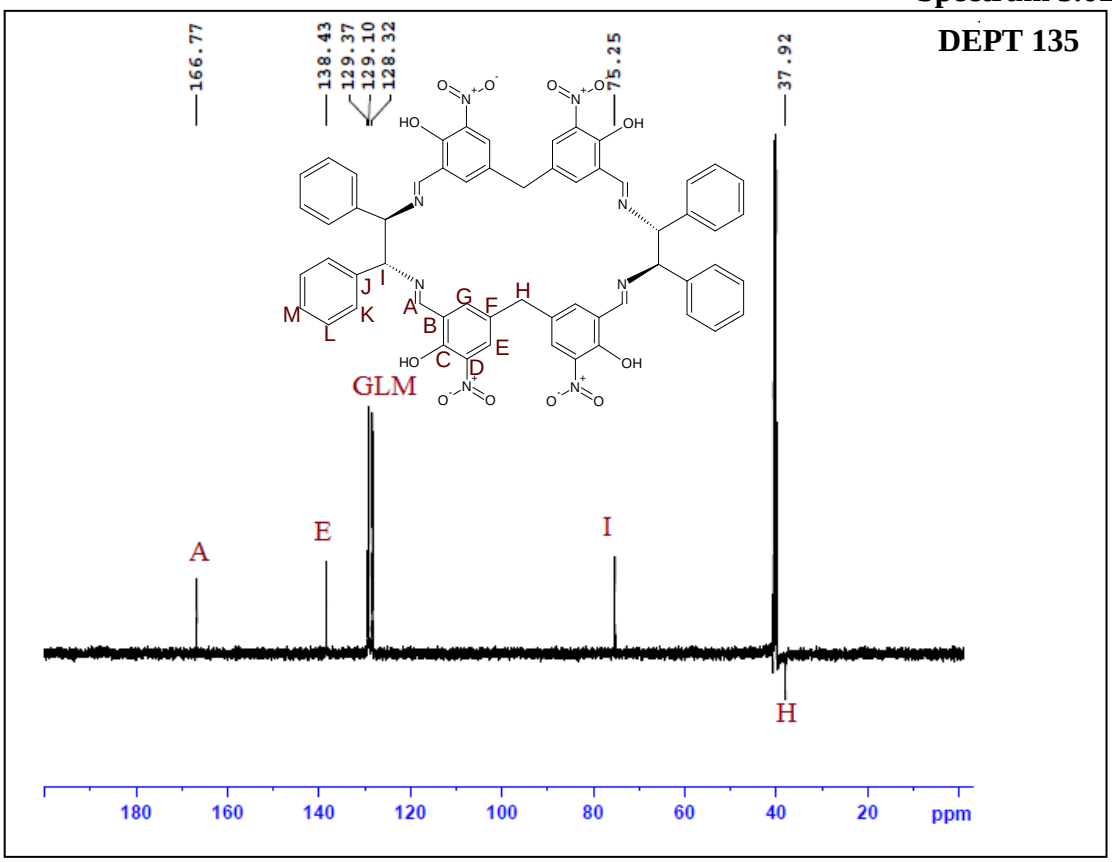

Spectrum 3.62

Cosy 90

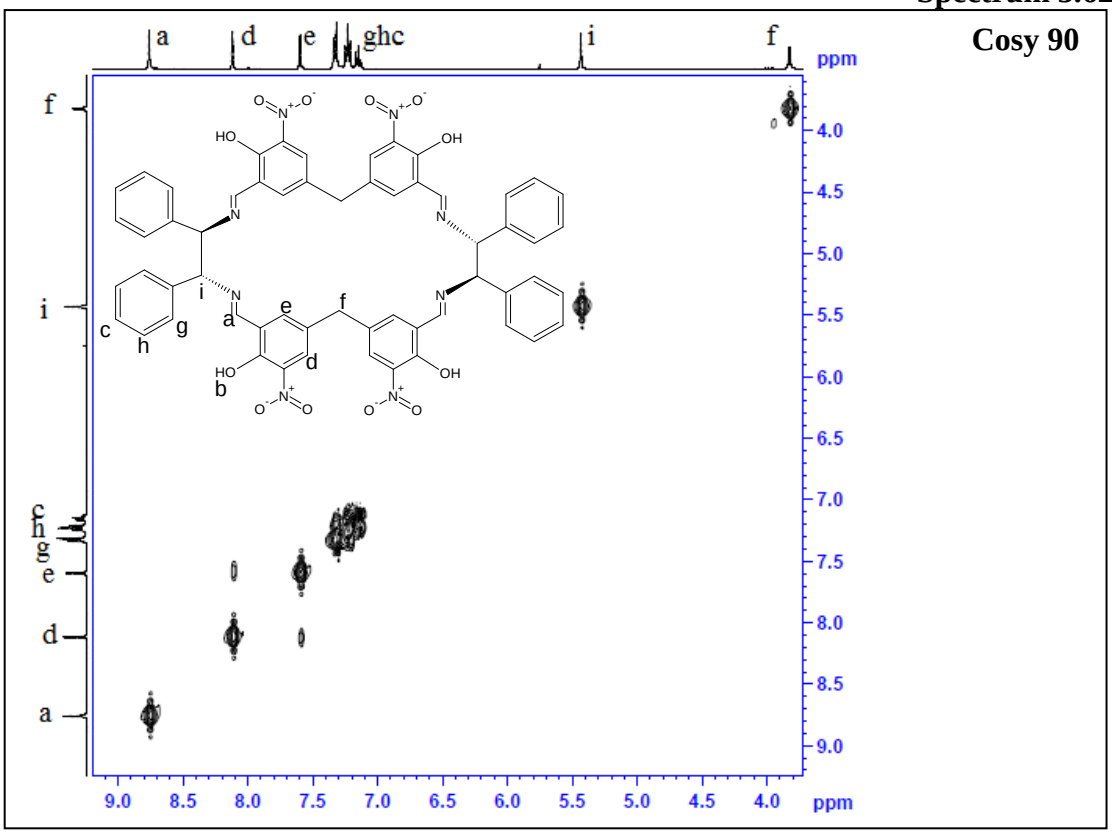

Spectrum 3.63

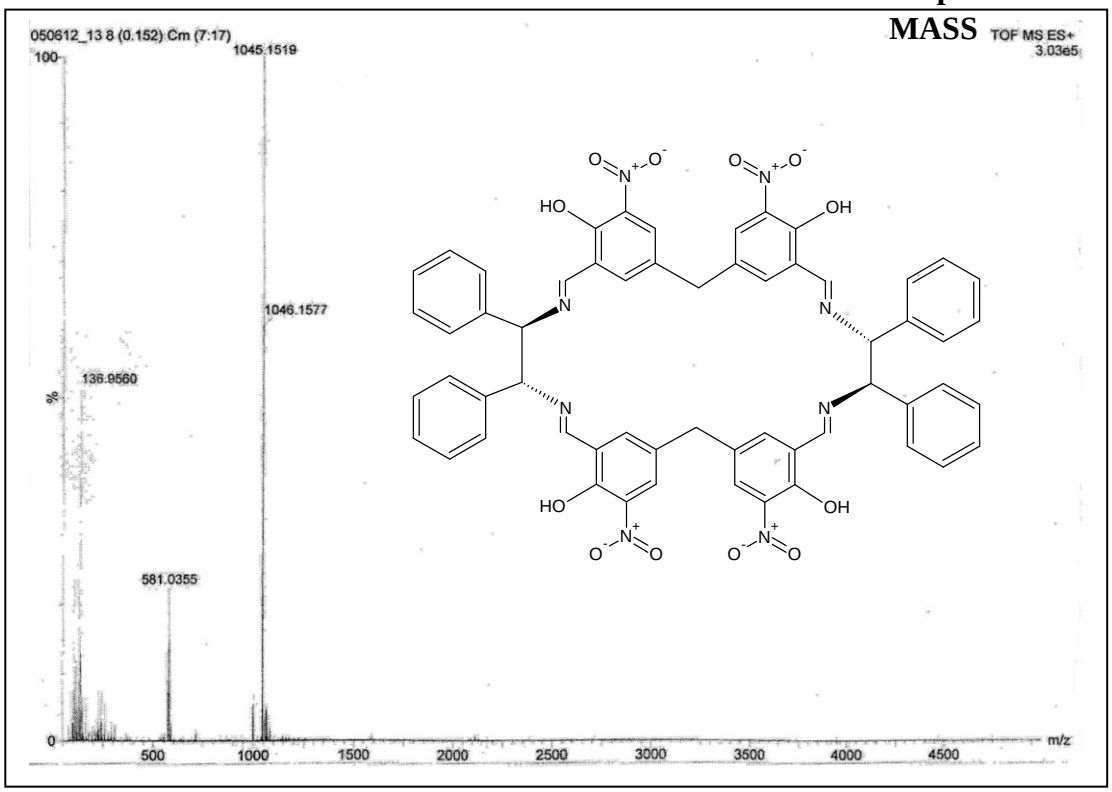

Chromatogram 3.64

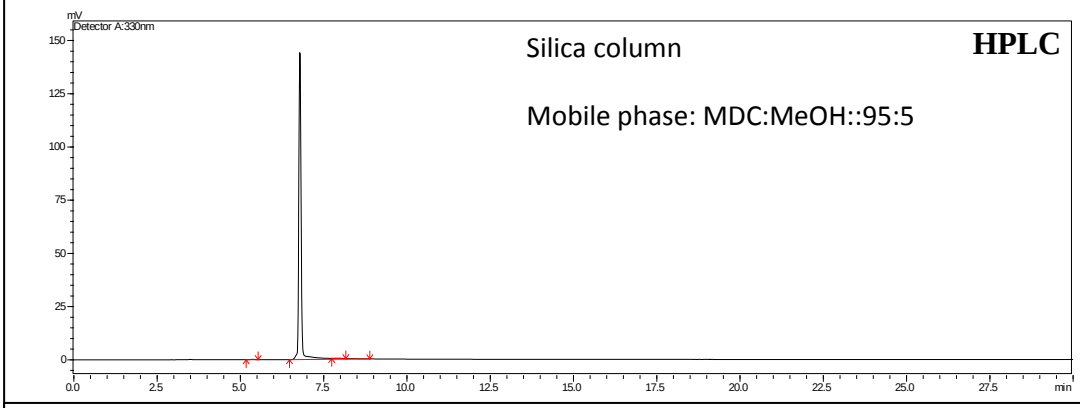

Peak	Name	Ret. Time	Area%
1	imp-a	5.362	0.1901
2	Calix-salen corand from dadpe and 5,5'methylene-bis-(3-nitrosalicylaldehyde)	6.783	99.5715
3	imp-b	7.952	0.2384

Spectrum 3.65

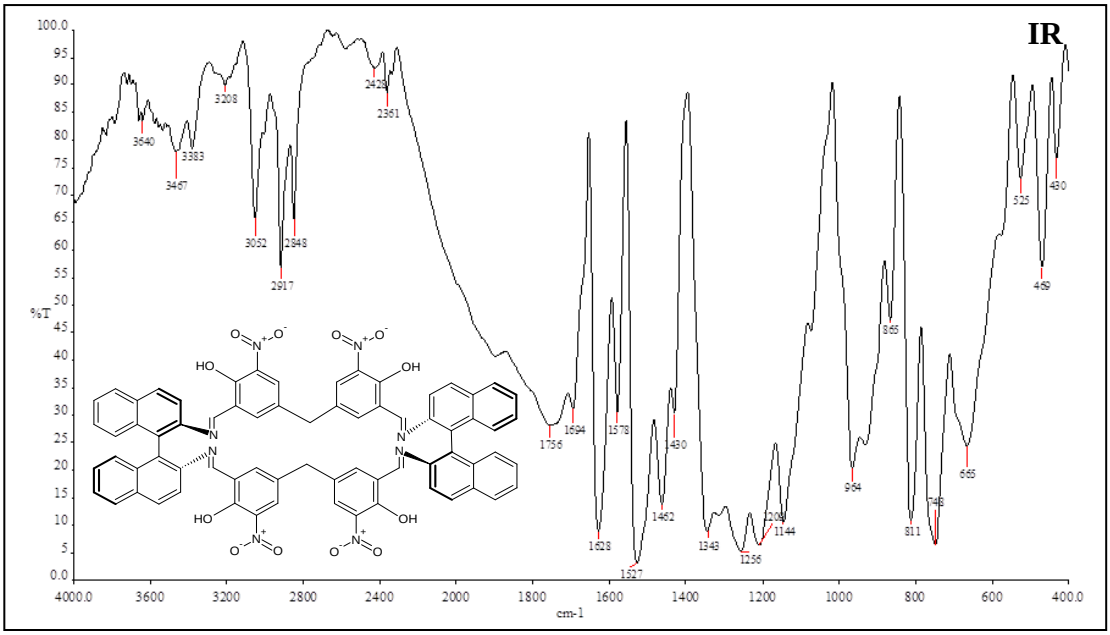

Spectrum 3.66

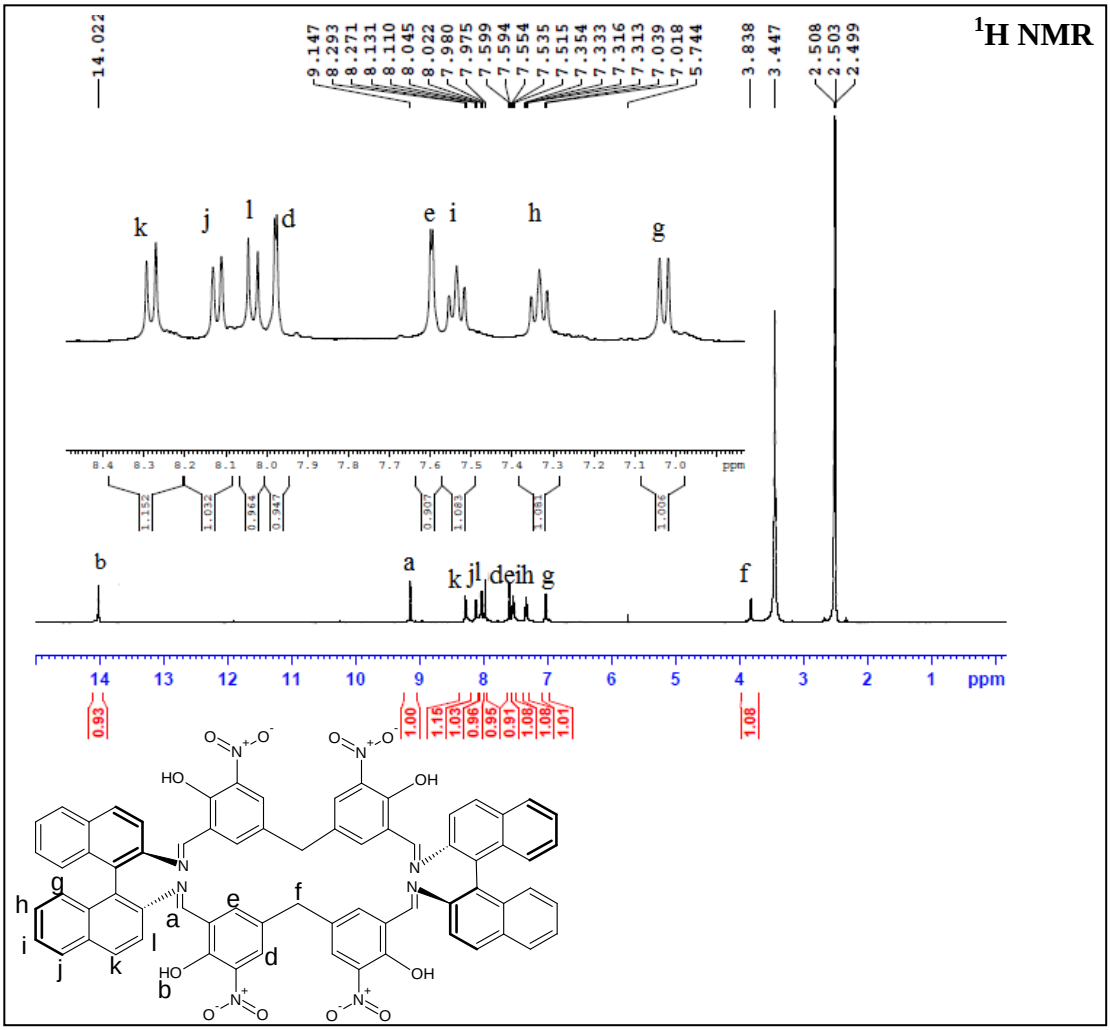

Spectrum 3.67

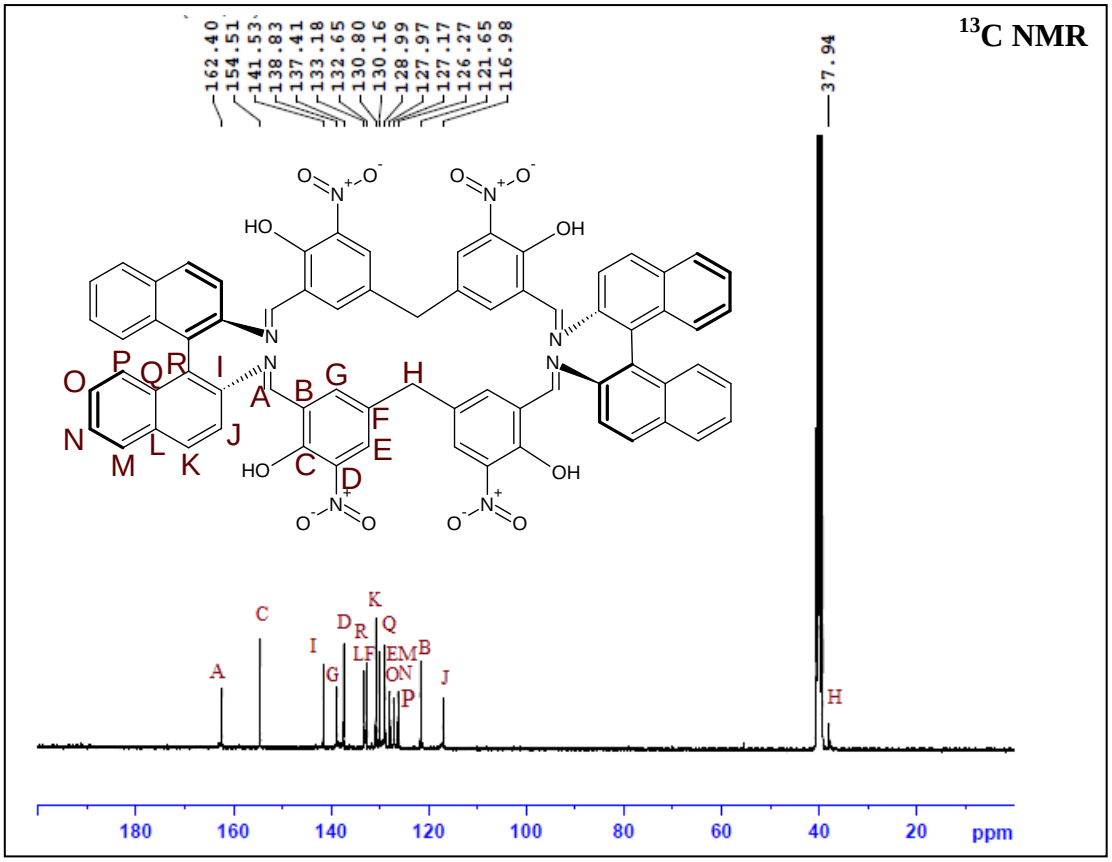

Spectrum 3.68

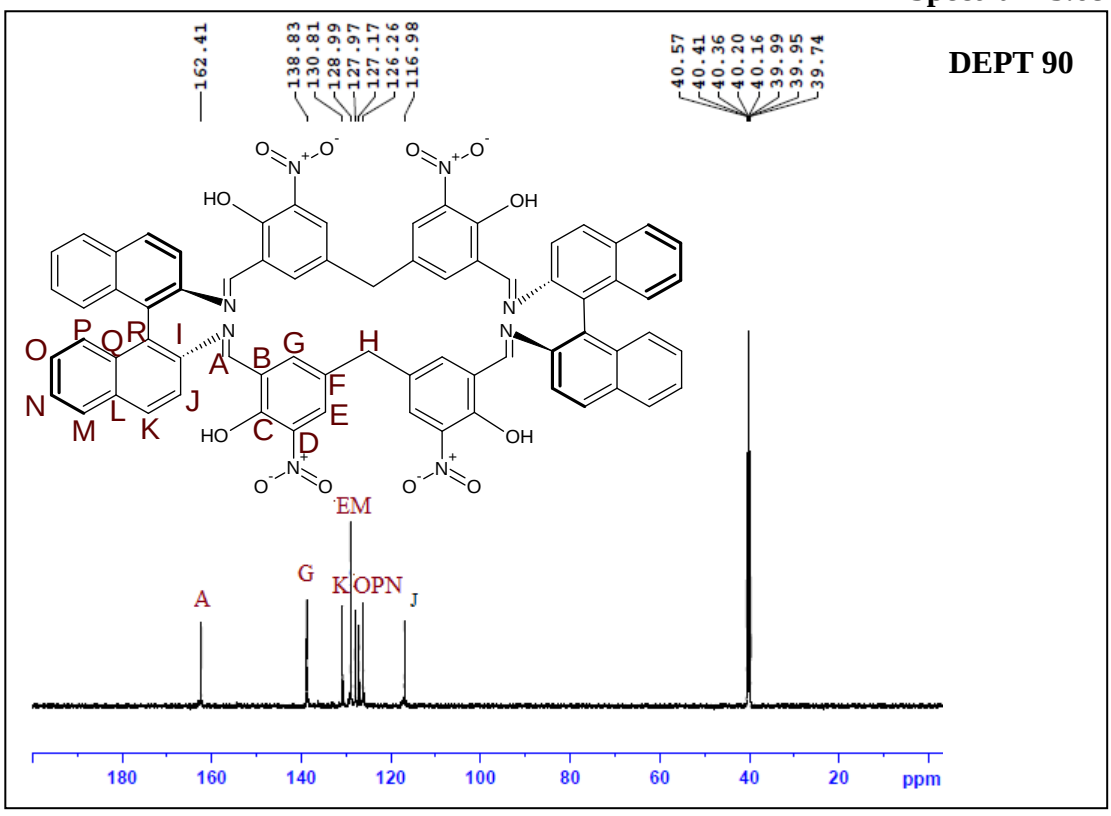

Spectrum 3.69

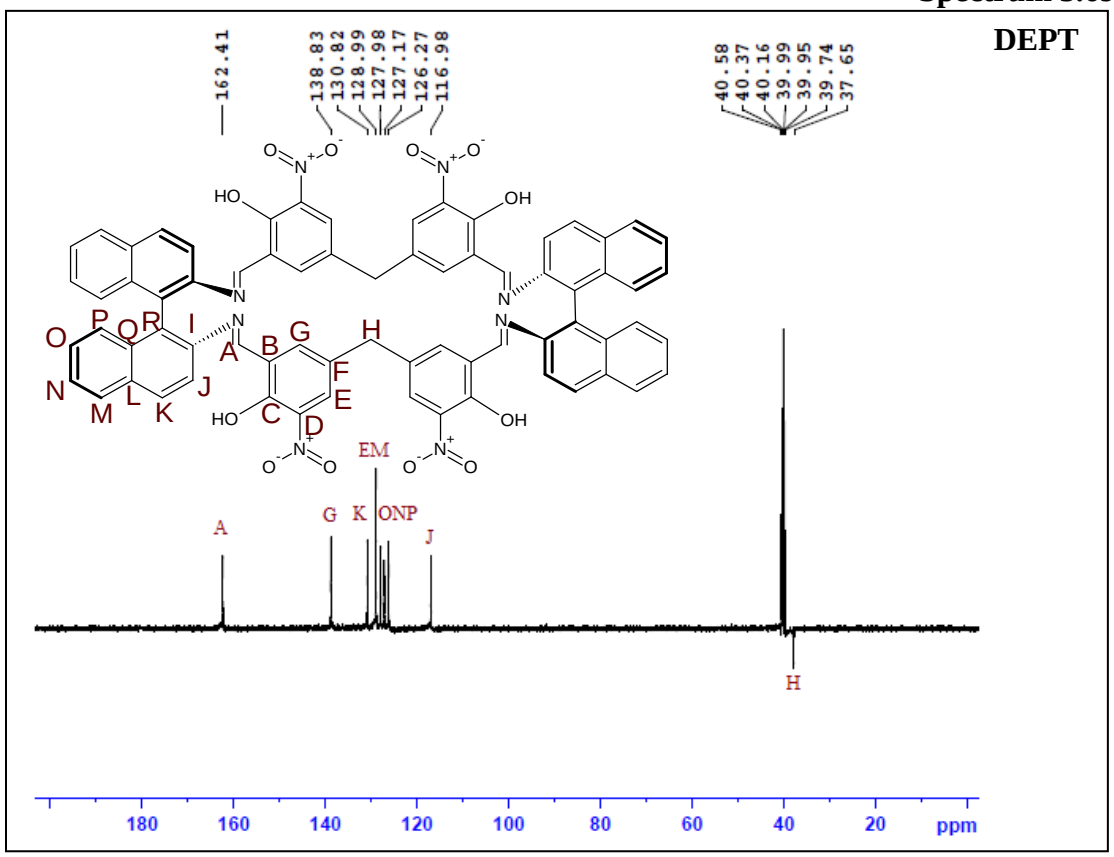

Spectrum 3.70

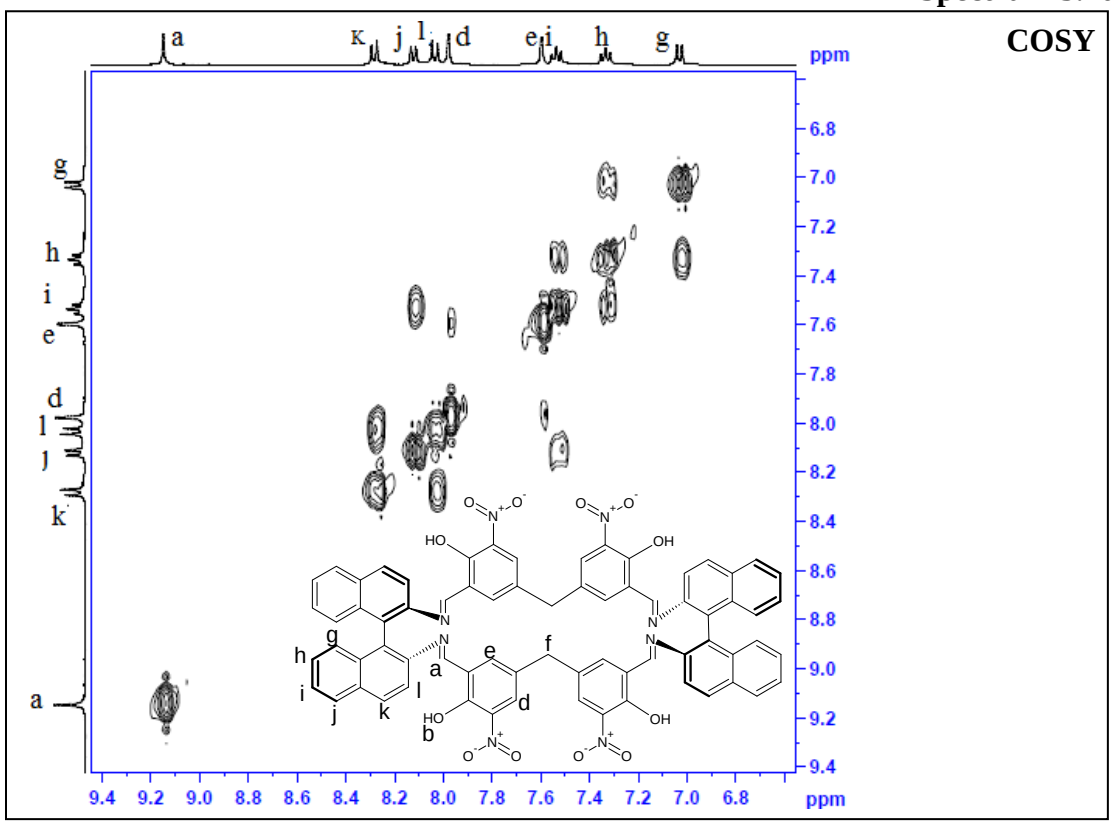

Spectrum 3.71

NOESY

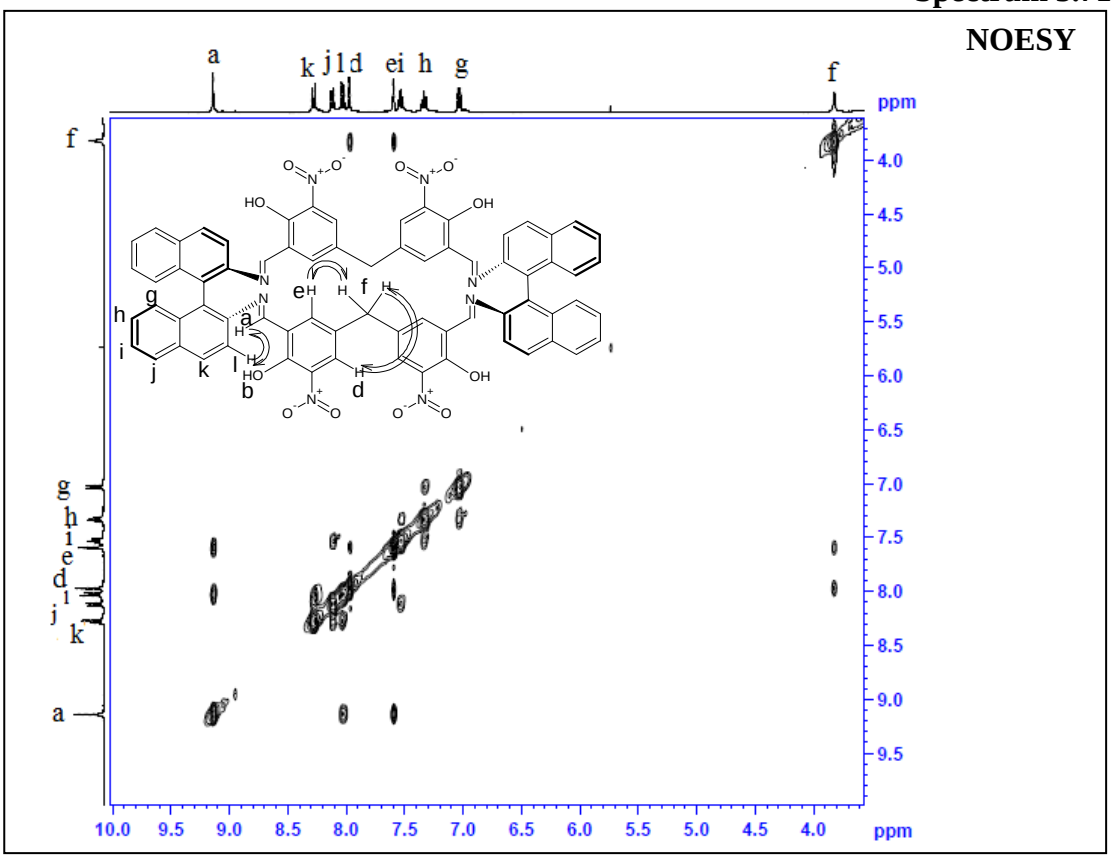

Spectrum 3.72

HSQC

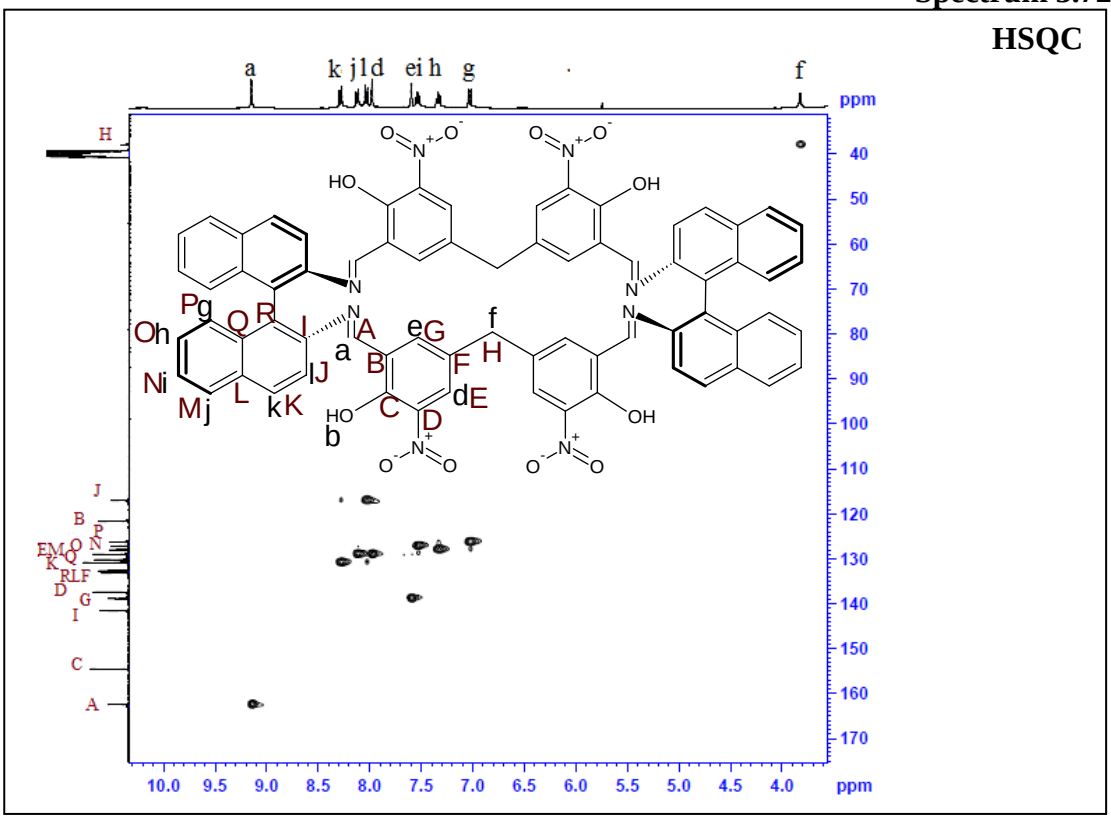

Spectrum 3.73

HMBC

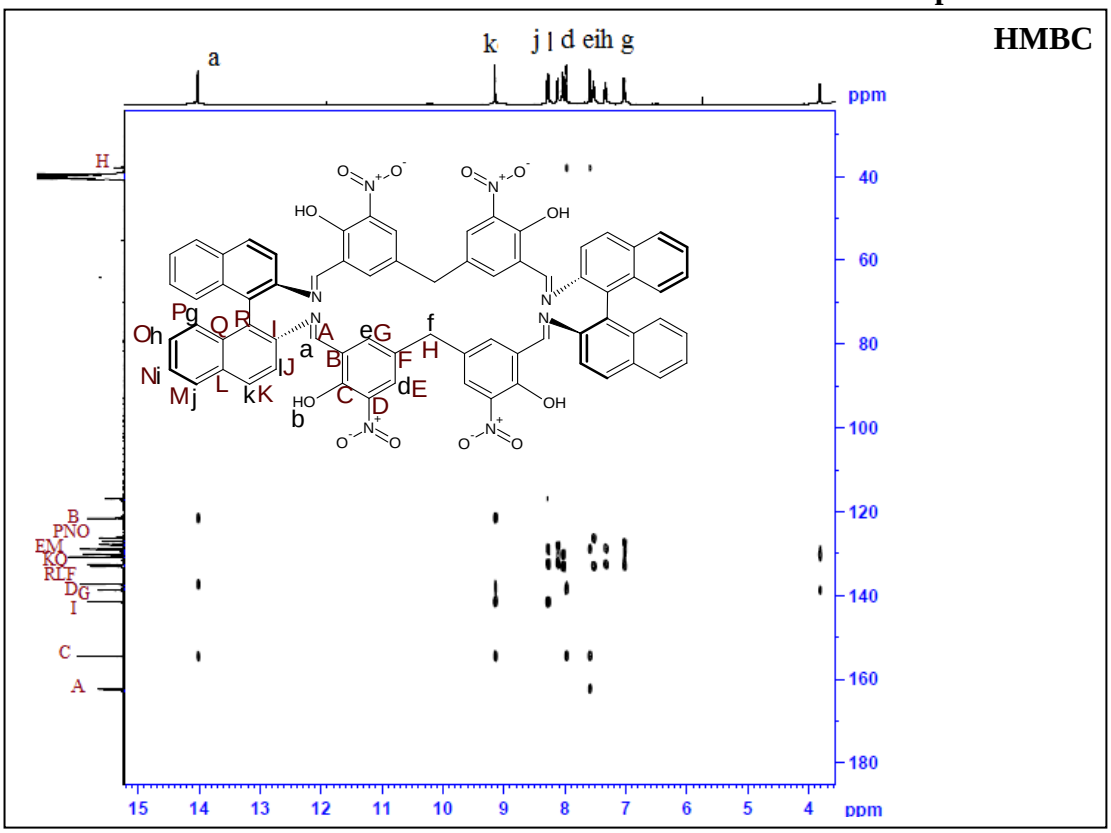

Spectrum 3.74

MASS

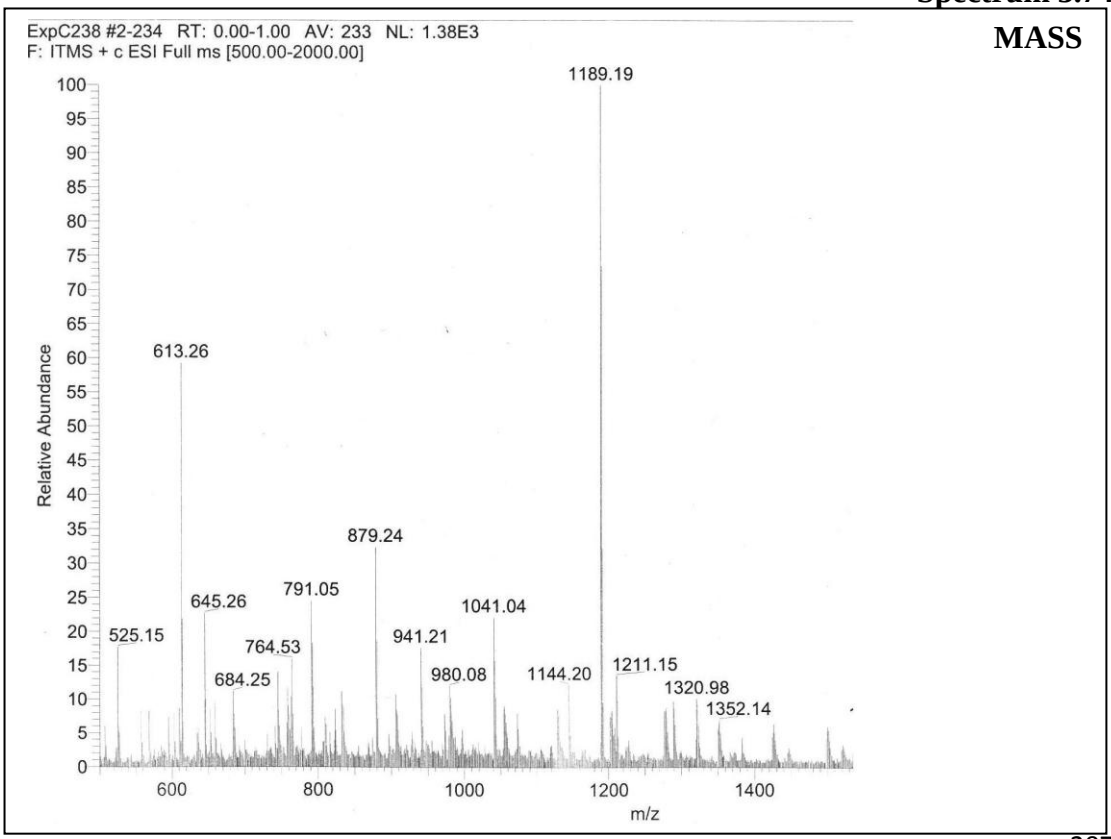

Chromatogram 3.75

HPLC

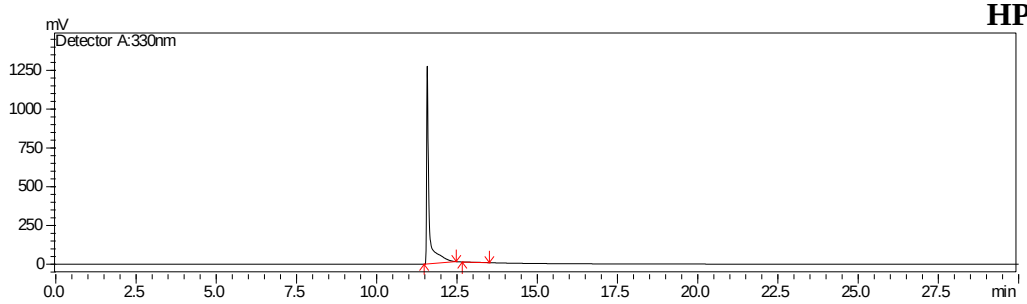

Silica column

Mobile phase: MDC

Peak	Name	Ret. Time	Area%
1	Calix-salen corand from Binaphthalenyldiamine and 5,5'methylene-bis-(3-nitrosalicylaldehyde)	11.570	99.8916
2	Impurity	12.675	0.1084

3.7 References:

1. Steed, J. W.; Atwood, J. L. *Supramolecular Chemistry*, John Wiley & Sons, **2002**.

1. a) Pederson, C. J. *J. Am. Chem. Soc.*, **1967**, 89(26), 7017.

2. Gao, J.; Reibenspies, J. H.; Zingaro, R. A.; Woolley, F. R.; Martell, A. E.; Clearfield, A. *Inorg. Chem.*, **2005**, 44, 232.

3. Long R. C.; Hendrickson D. N. *J. Am. Chem. Soc.*, **1983**, 105,1513.

4. Zanello P. *Coord. Chem. Rev*., **1987,** 77, 165.

5. Gagne R. R.; Spiro C. L.; Smith T. J.; Hamann C. A.; Thies W. R.; Shiemke A. K. *J. Am. Chem. Soc.*, **1981**, 103, 4073.

6. Vogtle, F.; Hoss, R. *J. Chem. Soc., Chem. Commun.*, **1992**, 1584.

7. Asato, E.; Furutachi, H.; Kawahashi, T.; Mikuriya, M. *J. Chem. Soc. Dalton Trans.*, **1995**, 3897.

8. Starynowicz, P.; Lisoowski, J. *Chem. Commun*., **1999**, 769.

9. Tian, Y.; Tong, J.; Frenzen, G.; Sun, J. Y. *J. Org. Chem*., **1999**, 64, 1442.

10. Tandon, S. S.; Thompson, L. K.; Bridson, J. M. *Inorg. Chem*., 1993, 32, 32.

11. Kim, G. J.; Park, D. W.; Tak, Y. S. *Catalysis Lett*., **2000**, 65, 127.

12. Mohanta, S.; Nanda, K. K.; Werner, R.; Haase, W.; Mukherjee, A. K.; Dutta, S. K.; Nag, K. *Inorg. Chem.*, **1997**, 36, 4656.

13. Nakamura, Y.; Yonemura, M.; Arimura, K.; Usuki, N.; Ohba, M.; Okawa, H. *Inorg. Chem*., **2001**, 40, 3739.

14. Sun, Y.; Zeng, Q.; Gou, S.; Huang, W.; Duan, C.; Yao, J *J. Inclusion Phenom. Macrocyclic Chem.*, **2002**, 42, 131.

15. Hewitt, I. J.; Tang, J. K.; Madhu, N. T.; Pilawa, B.; Anson, C. E.; Brooker, S.; Powell, A. K. *J. Chem. Soc., Dalton Trans*, **2005**, 429.

16. Jazwinski J.; Lehn, J. M.; Meric R.; Vigneron J. P.; Cesario, M.; Guilhem, J.; Pascard C. *Tetrahedron Lett.*,**1987**, 28(30), 3489.

17. Lin, J.; Zhang, H. C.; Pu, L. *Org. Lett.*, **2002**, 4(19), 3297.

18. Li, Z.; Lin, J.; Sobat, M.; Hyacinth, M.; Pu, L. *J. Org. Chem*., **2007,** 72, 4905.

19. Li, Z.; Jablonski, C.; *Chem*. *Commun.*,1999, 1531.

20. Li, Z.; Jablonski, C.; *Inorg. Chem*., **2000**, 39, 2456.

21. Shimakoshi, H.; Takemoto, H.; Aritome, I.; Hisaeda, Y. *Tetrahedron Lett*., **2002**, 43, 4809.

22. Shimakoshi, H.; Kai, T.; Aritome, I.; Hisaeda, Y. *Tetrahedron Lett*., **2002**, 43, 8261.

23. Shrimurugan, S.; Viswanathan, B.; Varadarajan, T. K.; Varghese, B. *Tetrahedron Lett.*, **2005**, 46, 3151.

24. Shrimurugan, S.; Viswanathan, B.; Varadarajan, T. K.; Varghese, B. *Org. Biomol. Chem.*, **2006**, 4, 3044.

25. Korupoju, S. R.; Mangayarkarasi, N.; Ameerunisha, S.; Valente, E. J.; Zacharias, P. S. *J. Chem. Soc. Dalton Trans*., **2000**, 2845.

26. Kwit, M.; Gawronski, J. *Tetrahedorn Asymmetry*,**2003**, 14, 1303.

27. Paluch, M.; Lisowski, J.; Lis, T. *J. Chem. Soc.,Dalton Trans*., **2006**, 381.

28. Tanaka, K.; Tasuchitani, T.; Fukuda, N.; Masumoto, A.; Arakawa, R. *Trahedron Asymmetry*. **2012**, 23, 205.

29. Tanaka, K.; Fukuda, N.; *Trahedron Asymmetry*, **2009**, 20, 111.

30. Tanaka, K.; Shimoura, R.; Caira, M. R. *Tetrahedron Lett.*, **2010**, 51, 449.

31. Gawronski, J.; Kolbon, H.; Kwit, M.; Katrusiak A. *J. Org. Chem.*, **2000**, 65, 5768.

32. Kwit, M.; Skowronek, P.; Kolbon, H.; Gawronski, J. *Chirality*, **2005**, 17, S93.

33. Gawronski, j.; Gawronska, K.; Grajewski, J.; Kwit, M.; Plutecka, A.; Rychlewska, U. *Chem. Eur. J.* **2006**, 12, 1807.

34. Gregolinski, J.; Lisowski, J.; Lis, T. *Org. Biomol. Chem.*, **2005**, 3, 3161

35. Chadim, M.; Budesinsky, M.; Hodacova, J.; Zavada, J.; Junk, P. C. *Tetrahedron Assymetry*, **2001**, 12, 127.

36. Gao, J.; Martell A. E. *Org. Biomol. Chem.*, **2003**, 1, 2795.

37. Hodacova, J.; Chadim, M.; Zavada, J.; Aguilar, J.; Espana, E. G.; Luis, S. V.; Miravet, J. F. *J. Org. Chem*., **2005**, 70, 2042.

38. Ma, C.; Lo, A.; Abdolmaleki, A.; MacLachlan, M. J. *Org. Lett*., 2004, 6(21), 3841.

39. Kuhnert, N.; Rossignolo, G. M.; Periago, A. L. *Org. Biomol. Chem.*, **2003,** 1, 1157.

40. Kuhnert, N.; Periago, A. M. L. *Tetrahedron Lett.*, **2002,** 43, 3329.

41. Kuhnert, N.; Strabnig, C.; Periago, A. L. *Tetrahedron Asymm.*, **2002,** 13, 123.

42. Kuhnert, N.; Periago, A. L.; Rossignolo, G. M. *Org. Biomol. Chem.*, **2005,** 3, 524.

43. Kuhnert, N.; Patel, C.; Jami, F. *Tetrahedron Lett*., **2005,** 46, 7575.

44. Kuhnert, N.; Burzlaff, N.; Patel, C.; Periago, A. L. *Org. Biomol. Chem.*, **2005,** 3, 1911.

45. Gao, J.; Martell A. E. *Org. Biomol. Chem.*, **2003**, 1, 2801.

Chapter 4

High Dilution Synthesis of The Cryptands from Tris-(-2-aminoethyl)amine and Their Study

4.1 Introduction

The macrocyclic supramolecular structures having more than one macrocycle included in them are termed cryptands. 'Cryptand' is derived from the Greek word *kruptos* meaning hidden.[1] Cryptands have multiple binding sites through which they can include metal cations with the help of supramolecular interactions. This inclusion is like hiding of cations in the pocket(s) formed by such macrocycles. Cryptands bound with such cations are known as cryptates.[2] Binding of these supramolecular hosts with guest cations or molecules is stronger compared to binding by analogous corands or podands and is more specific. Nowadays some simple cryptands are even commercially available. The synthesis of cryptands is much more challenging than the synthesis of podands or corands because their synthesis one step synthesis requires formation of more number of cycles at a time through multiple covalent bond formation in competition with the formation of linear macromolecules. Thus their syntheses are low yielding in general. Azacryptands are cryptands containing nitrogen binding sites as part of macrocycle. A promising starting material for synthesis of azacryptand is tris(2-aminoethylamine) which is abbreviated as TREN. It was first employed in cryptand synthesis by Lehn and co-workers to get octaazacryptand.[3]

TREN being a trifunctional flexible molecule on reaction with bifunctional linkers has probability of giving a cryptand structure under appropriate reaction conditions. Cryptand formation requires two of the TREN molecules acting as a capping agent in a three dimensional structure by reacting with three molecules of bifunctional linkers. Majority of the linkers employed are aromatic dialdehydes. 1,3- and 1,4-dialdehydes have been employed for the synthesis of azacryptands. Some of the dialdehydes which have been employed for this purpose are pyridine-2,6-dicarbaldehyde[3-9], pyridazine-3,6-dicarbaldehyde[10-13], pyrazole-3,5-dicarbaldehyde[14], triazole-2,5-dicarbaldehyde[15], acridine-2,7-dicarbaldehyde[16], furan-2,5-dicarbaldehyde[17,18], pyrrole-2,5-di-carbaldehyde,[18] isophthalaldehyde[19-23,], terephthalaldehyde [24-32]. The reaction of TREN with dialdehydes in 2+3 reaction results in imino functionalities present in the crypand which can be reduced to secondary amines.

The cryptands with amide linkage can be obtained from the reaction of TREN with carboxylic acids or their derivatives such as acylhalides.

Pyridine containing octa-azacryptands were synthesized and found to be distinguishing Cu(I) and Cu(II)[3] (**Fig. 4.1**). They have been also studied in detail for their formation and stability of various metal complexes with metal cations such as Ag^{+}, Co^{2+}, Ni^{2+}, Zn^{2+}, Hg^{2+} using ESI mass spectrometry.[4] Pyridine and salicylaldehyde derived dialdehyde resulted in expanded cryptand which was synthesized under metal free conditions[5] (**Fig. 4.2**).

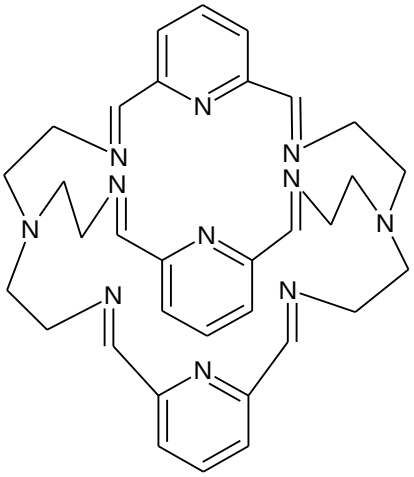

Imino cryptand with pyridine linkers

Fig. 4.1

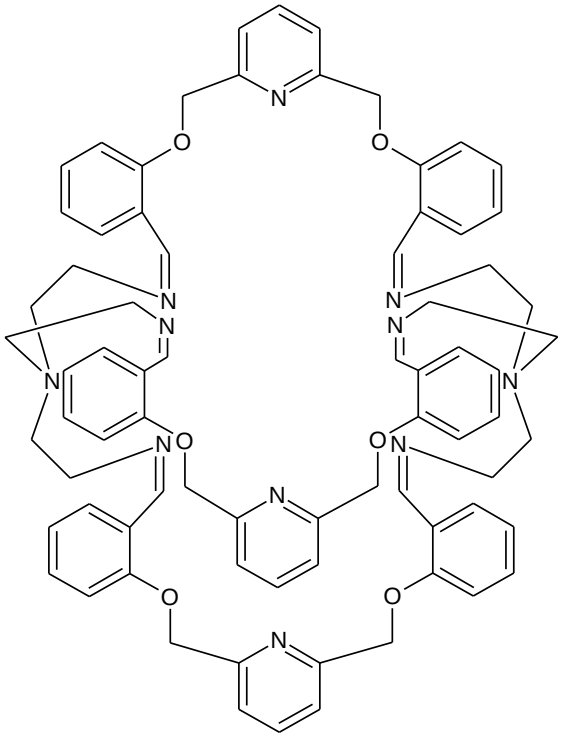

Larger cryptand with a hybrid linker
Fig. 4.2

Pyridine derived polyamide cryptands were synthesized by [2+3] condensation of TREN and 2,6-pyridinedicarbonyl dichloride in dichloromethane. It recognized anions like F^{-}, Cl^{-}, $H_2PO_4^{1-}$ and CH_3COO^{-} with marked preference for fluoride ions[6-8] (**Fig. 4.3**). Unsymmetrical octamidocryptand was prepared by introducing a spacer between two pyridine-2,6-diester and reacting in stepwise manner with the prepared spacer. The resulting unsymmetrical cryptand hosted both anions and metal ions.[6] Pyridazine

containing cryptand was found to give heterobinuclear cryptates with Cu^{+}, Cu^{2+} and Co^{2+} ions[10-13] (**Fig. 4.4**).

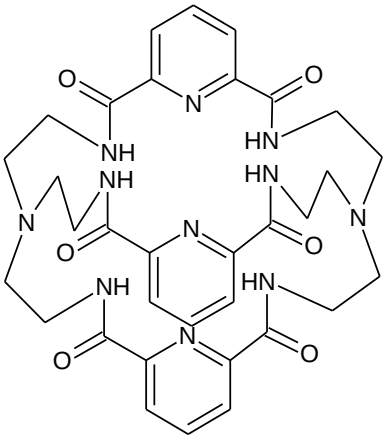

Hexaamido cryptand from2,6-pyridinedicarbonyl dichloride

Fig. 4.3

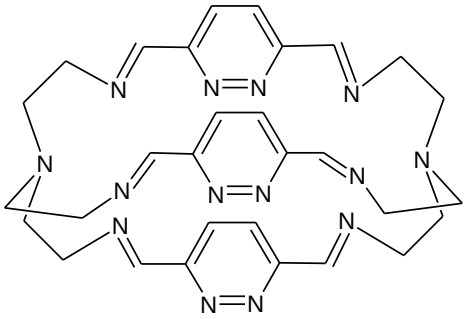

Hexa-imino cryptands with pyridazine linkers

Fig. 4.4

The trispyrazole derived cryptand and its disilver complex were obtained by [2+3] condensation of TREN and 3,5-pyrazoledicarbaldehyde in absence as well as in presence of silver(I) ions respectively. The reduced cryptand was found to form di and tetra nuclear Cu^{2+} and Zn^{2+} complexes[14] (**Fig.4.5**). Similarly 1,2,4-triazole-3,5-dicarbaldehyde derived cryptands were found to give dinuclear Ag^{+}, trinuclear Cu^{+}, trinuclear Ni^{2+} and Cu^{2+} complexes[15] (**Fig.4.6**).

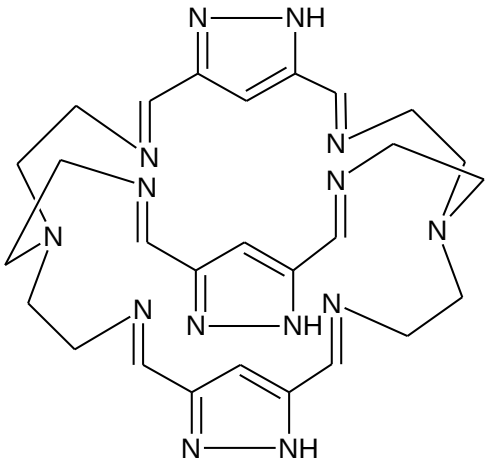

Imino cryptand from pyrazole dicarbaldehyde

Fig. 4.5

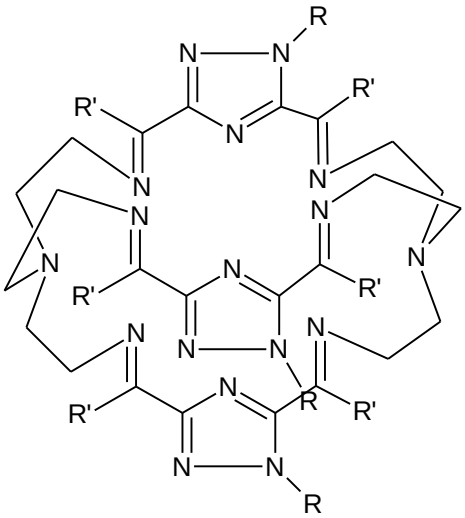

TREN derived imino cryptand from triazole dicarbonyl linkers

Fig. 4.6

A water soluble macrobicyclic cryptand was obtained from reaction of TREN with acridine-2,7-dicarbaldehyde followed by reduction and protonation with hydrochloric acid. The cryptand was used for the detection of organic anions through complexation enhanced fluorescence[16] (**Fig. 4.7**).

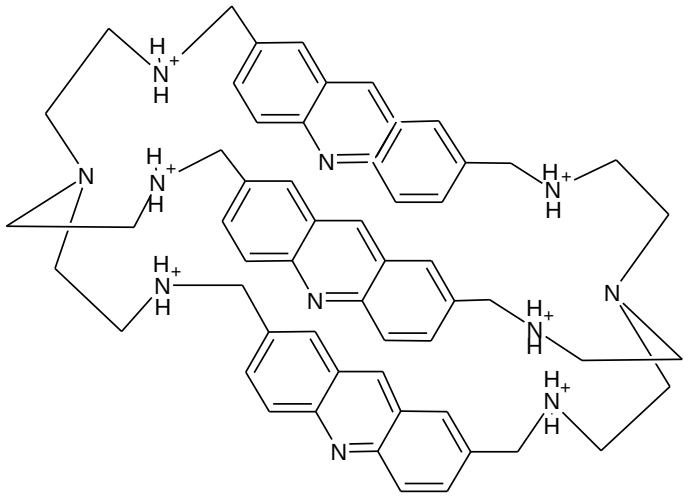

Acridine dicarbaldehyde derived octa-aza cryptand

Fig. 4.7

The reaction of TREN with isophthalaldehyde or terephthalaldehyde resulted in isomeric cryptands. Isophthalaldehyde derived cryptands and their cryptates with Cu^{2+} and Co^{2+} were studied for their binding constant determination and their ability to bind with hydroxide and carbonate ions.[19,20] These cryptands when incorporated in sol-gel material were found to undergo reversible binuclear Cu^{2+} complex formation and same were studied for various properties including optical sensing capability of azide anion[21,22] (**Fig. 4.8**). The cryptand with amide linkage was prepared by reacting TREN with isophthaloyl dichloride or isophthaloyldiester which was found to recognize fluoride ions[23] (**Fig. 4.09**). Its cofacial dicobalt complex was used to recognize cyanide ion.[24]

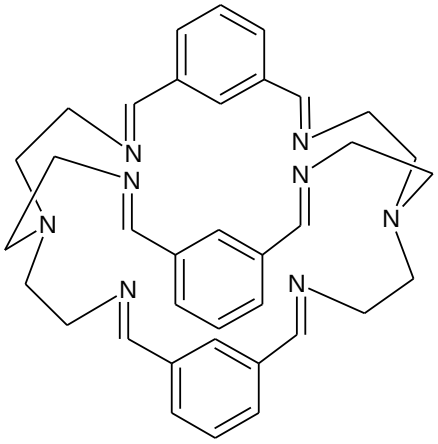

Imino cryptand using isothalaldehyde linker

Fig. 4.8

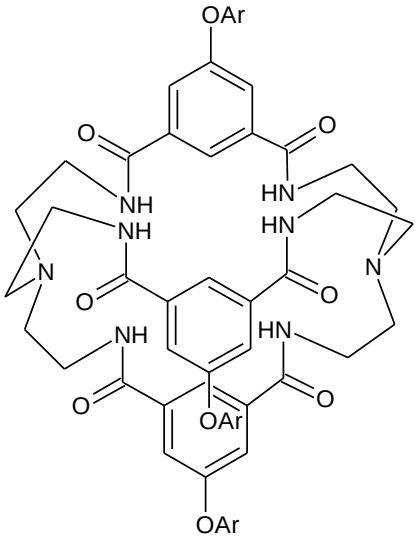

Amido cryptand from corresponding isophthaloyl chloride

Fig. 4.9

The octaazacryptands from TREN and terephthalaldehyde were prepared either in presence or absence of template[25-32] (**Fig. 4.10**).

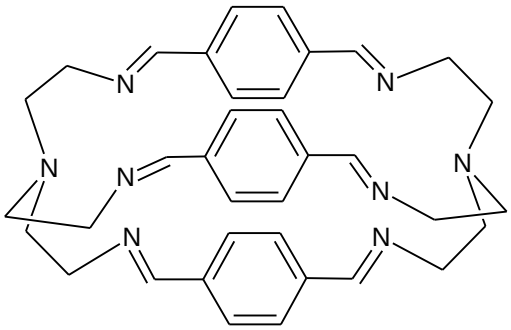

Terephthalaldehyde derived hexa-imino cryptand

Fig. 4.10

These cryptands have been studied in detail for their complexation and other properties. Their copper cryptates were found to recognize azide ion with linear geometry.[25] The corresponding zinc cryptate with one of the phenyl ring replaced with anthracenyl group acting as a fluorophore showed azide sensing ability due to quenching of fluorescence in its presence[26] (**Fig.4.11**).

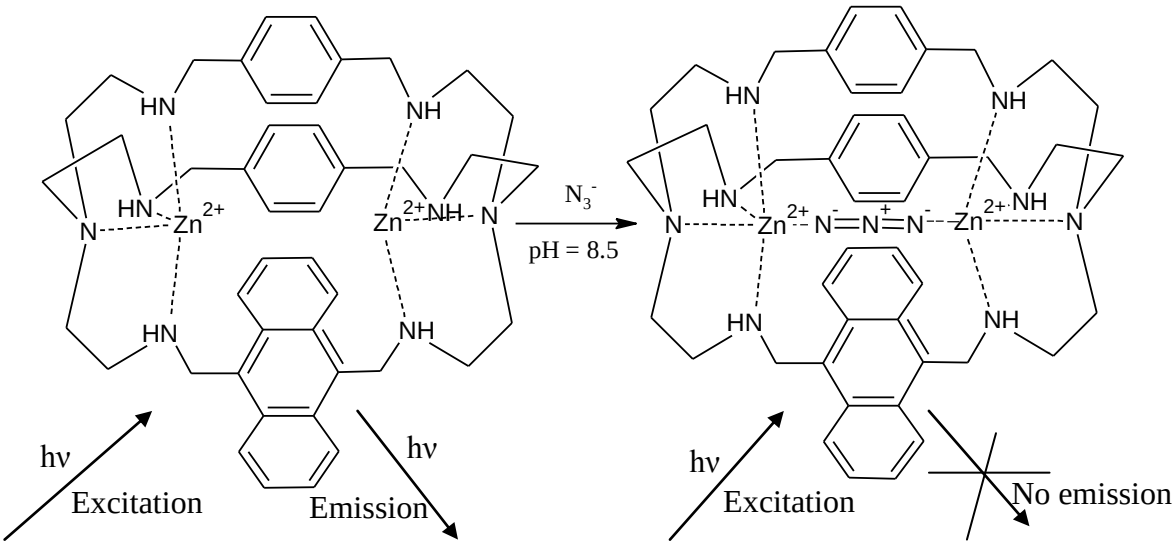

Azide recognition by zinc cryptate
Fig. 4.11

Crystal structure of the saturated azacryptate revealed a strong affinity towards water molecules[27] and were found to incorporate water clusters depending on anion in the cryptates[28] (**Fig. 4.12**). The cryptand was also found to form infinite 2D-layered water due to its cluster formation with cryptand.[29] Vesicular microcapsules were formed when secondary nitrogen of the saturated cryptand was acylated with long chain acid chlorides. It was found that they encapsulate hydrophilic dye molecules.[32]

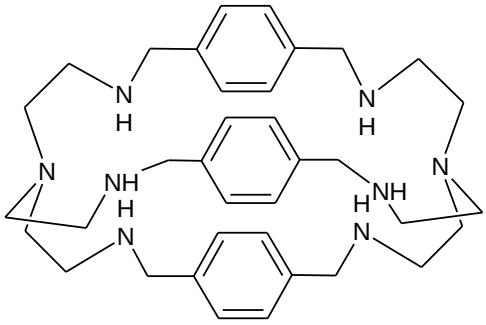

Octaamino cryptand
Fig. 4.12

When 2,6-diformylphenol was used as a linker for the cryptand formation with TREN, it resulted in the cryptands with three phenolic groups which can be easily converted to phenolate ions (**Fig. 4.13**). They formed dinuclear lanthanide (Ln(III)) complexes.[33,34] They were also studies by electron spray mass spectrometry. [35] Photophysical property study of their lanthanide complexes suggested them to be good candidates for designing of nanometric light converting devices due to their ability to convert absorbed visible light into emitted NIR radiation.[36] Their heterodinuclear cryptates were synthesized by using Ln(III)-Cu(II) mixed salts.[37] $Cd^{2+}$and Ag^{+} ions could act as templates to form [2+3] thiocryptates which have higher hydrolytic sensitivity than the phenolate analogue.[38]

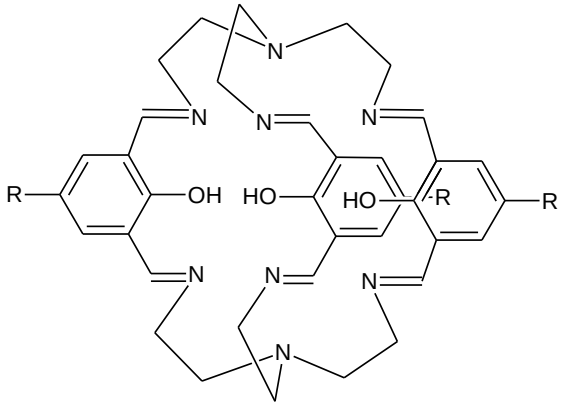

Imino cryptand with phenolic functionality

Fig. 4.13

Laterally nonsymmetric or heterodiatopic cryptands were prepared by two step synthesis. In the first step phenolic aldehyde was reacted with tris(2-chloroethylamine) or equivalent trihalide giving tripodal trialdehydes with ether linkage which were then reacted with TREN in the presence of sodiumborohydride resulting in the heterodiatopic cryptands with tetraaza binding site at one end and triether at the other[39,40] **(Fig. 4.14, 4.15)**.

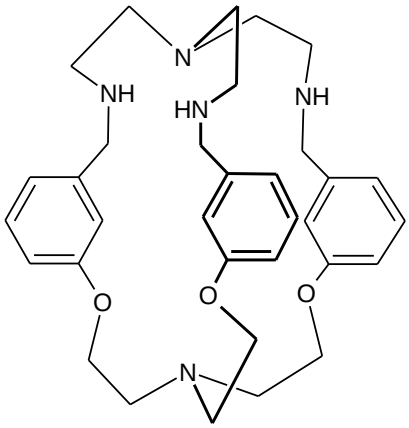

Cryptand with heterogeneous binding pockets

Fig. 4.14

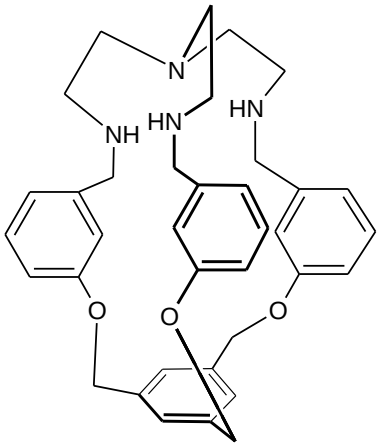

Tetra amino unsymmetrical cryptand with different pockets

Fig. 4.15

Such cryptands were prepared with the aim of binding a metal cation at only one receptor site, leaving the other site available. The other binding site could accept the other guest anion depending on the first guest accommodated. This made the metal cryptate an efficient anion sensor. Transition metal ions enter the cavity with weaker counter anions. On addition of coordination anions such as Cl^-, N_3^-, SCN^-, the metal ion comes out the cavity and binds the cryptand outside. Thus a metal ion can be translocated depending on nature of the counter anions.[41]

When a strong π-acceptor group such as 2,4-dinitrobenzene was attached to one of the secondary amines, the binding could be monitored by photoluminescence study. The free cryptand did not show any fluorescence due to photoinduced intramolecular electron transfer (PET) process but when metal ions like Cd(II) are bound to the cryptand, the PET is disturbed which results in fluorescence of metal cryptate. When stronger anions are added the fluorescence is quenched due to restoration of intramolecular PET because of translocation of metal ion outside the cavity.[42] The thioether analogous of the cryptand with anthracene fluorophores substituting the nitrogens were shown to undergo translocation of copper ion inside the cavity reversibly which was detected by fluorescence on-off process[43] (**Fig. 4.16**).

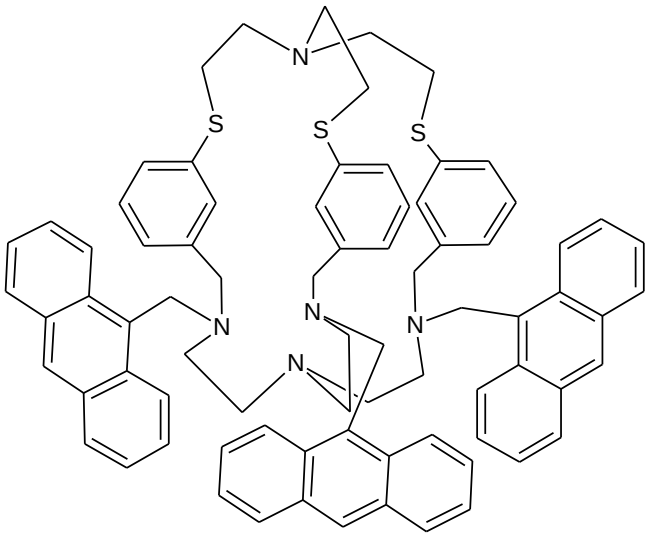

Unsymmetrical thia-aza cryptand with anthracene fluorophore

Fig. 4.16

The cobalt(II) cryptate of the heterodiatopic cryptand with ether linkage exhibited efficient catalytic oxidation ability for conversion of olefins to epoxides and benzylic compounds to corresponding carbonyl compounds.[44] Such kind of heterodiatopic and homodiatopic polyoxa-azacryptands were obtained in high yields by reaction of tripodal trialdehyde with TREN or ethylenediamine.[45] Various tripodal trialdehydes were reacted with TREN resulting in the creation of dynamic combinatorial libraries of cryptands.[46]

3,3'-Bis-salicylaldehydes separated by three carbon bridges were employed for the synthesis of dinuclear lanthanide cryptates by their reaction with TREN in the presence of lanthanide ions as template[47] (**Fig. 4.17**). A flexible dialdehyde with ethylene-dioxy bridges connecting two benzaldehyde moieties at para positions has also been employed with TREN for the synthesis of the corresponding cryptand[48] (**Fig. 4.18**).

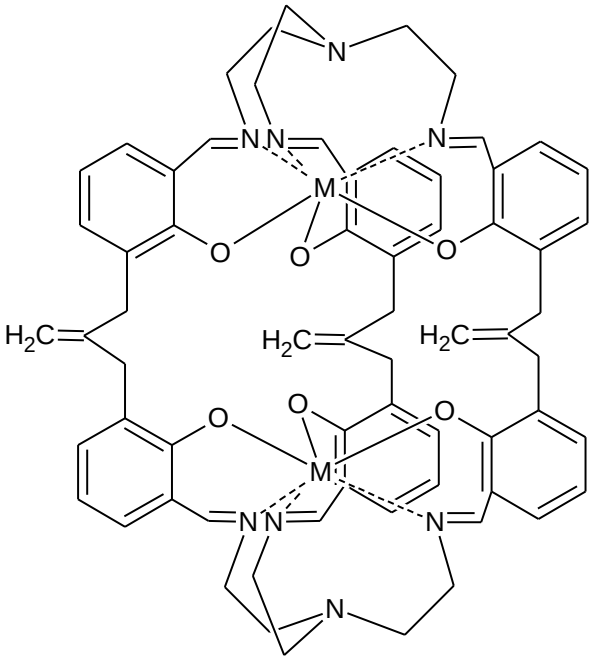

M=Lanthanide ion

Lanthanide cryptate

Fig. 4.17

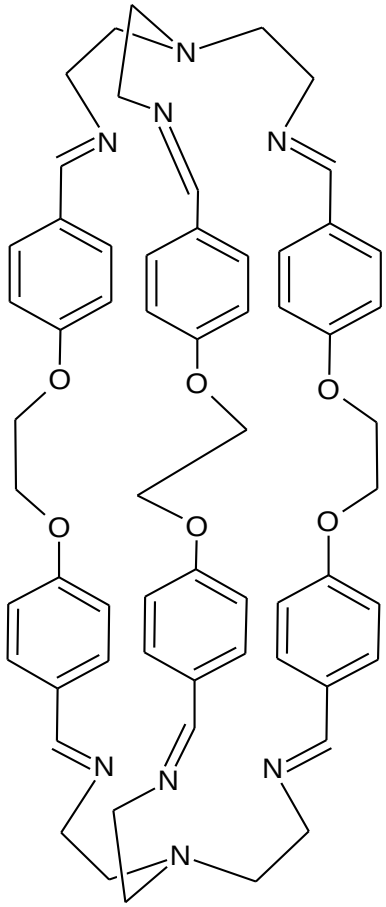

Larger imino cryptand from ether bridged dialdehyde linkers

Fig. 4.18

4.2 Aim and Objectives

After studying the supramolecular structures of corands by using chiral diamines we targeted the synthesis of cryptands by reacting the bis-aldehydes as linkers with the tripodal triamine namely tris(2-aminoethylamine) TREN, as its reactions with dialdehydes are well documented for the synthesis of variety of cryptands. The first bis-aldehyde employed for the synthesis of cryptand using TREN was 4,4'-methylene-bis-benzaldehyde by Lehn *et. al*. [3](Fig. 4.19)

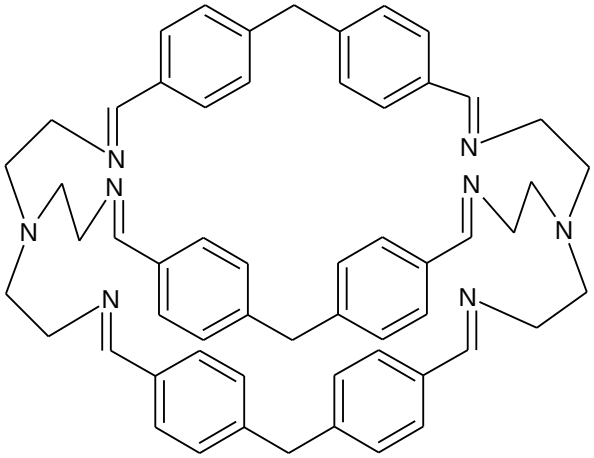

TREN-bisaldehyde derived hexa-imino Cryptand
Fig. 4.19

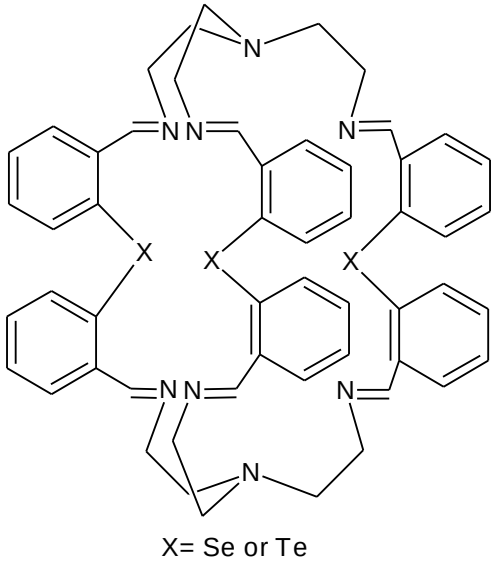

Metallo bridged hexa-imino cryptand from TREN
Fig. 4.20

Metal bridged bis aldehydes such as 2,2'-selenium-bis-benzaldehyde and 2,2'-tellurium-bis-benzaldehyde have also been employed with TREN for cryptand synthesis[49] (Fig. 4.20). The octaazacryptands which can be obtained by the use of TREN are versatile hosts for a variety of guests including cations, anions and neutral molecules[5-13] as expected, they have higher binding constants compared to the corands. Their Gd(III) cryptates can be used as NMR contrast agents.

A work on synthesis of cryptands by using TREN and methylene-bis-aldehyde was also initiated in our laboratory.[50] In continuation of the work with the aim of the synthesis of

some novel cryptands we decided to employ different methylene-bis-aldehydes synthesized by us, as linkers and TREN as a tripodal capping partner.

4.3 Results and Discussion

With the expectation of the formation of cryptands by application of methylene-bis-aldehydes and ketones prepared by us (Chapter-2) by [2+3] cyclo condensation with the trifunctional TREN, we carried out the reaction under high dilution conditions. Various modifications in this reaction conditions were also studied when the reactions under high dilution conditions were unsuccessful.

Thus 5,5'-methylene-bis-(3-*tert*-butylsalicylaldehyde) was subjected to macrocyclization by its reaction with TREN under high dilution condition in dichloromethane. The progress of the reaction was slow as could be visualised by colour change of reaction mixture and by TLC monitoring. After the completion of reaction and evaporation of solvent the residue was subjected to column chromatography. The starting material and less polar products were removed by elution with 80:20 mixture of pet-ether:MDC. The major product was collected by eluting the column with dichloromethane : methanol in 99:1 ratio in 21% yield. The product was confirmed to be [2+3] cryptand with the help of its mass spectrum and was characterized by various spectral techniques while its purity was established with the help of HPLC (**Fig. 4.21**).

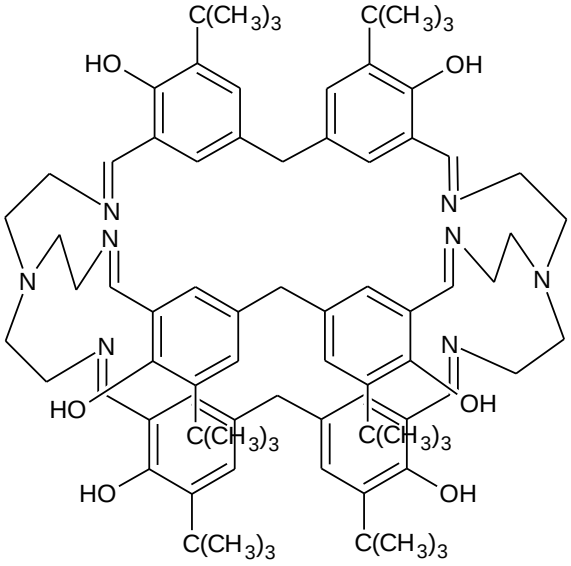

TREN & methylene-bis(*tert*-butyl salicylaldehyde) derived hexa-imino cryptand <u>1</u>

Fig. 4.21

In its proton NMR a phenolic protons show a broad singlet at 14.45 δ, CH protons of imine linkage are observed at 7.80 δ and two meta coupled aromatic protons are observed as doublets at 7.14 δ and 6.23 δ. Protons at the methylene bridge are observed as a singlet at 3.58 δ and the protons on the ethylene bridge from TREN are observed at 3.50 δ and 2.88 δ with a poor resolution. An intense singlet is observed for protons of *tert*-butyl group at 1.34 δ. All these signals have expected integration values. From proton NMR the inclusion of a minute quantity of starting bis-aldehyde was also detected. Repeated crystallization or column chromatography did not help in its removal (Spectrum 4.2). ^{13}C NMR shows twelve signals as expected ranging between 167 δ to 29 δ proving symmetrical structure of the cryptand (Spectrum 4.3).

The 2D NMR studies include a COSY establishing a clear correlation between various aliphatic and aromatic protons. The ethylene bridge correlation is observed as cross peaks at 3.5 δ and 3.88 δ (Spectrum 4.6). The cross peaks are observed in NOESY spectrum due to through space interactions between CH proton of imine linkage with aromatic proton at carbon '6' as well as between *tert*-butyl group protons and aromatic proton at carbon '4' (Fig. 4.22, Spectrum 4.7).

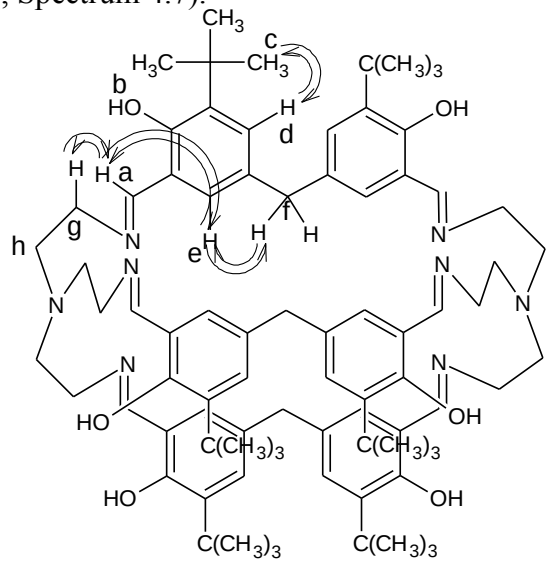

^{1}H-^{1}H correlation in cryptand <u>1</u> as observed in NOESY

Fig. 4.22

HSQC spectrum of the cryptand helps in clear assignment of each carbon signal due to its correlation with corresponding protons (Spectrum 4.8). HMBC of the cryptand was

helpful in confirming the assignments of various carbon and proton nuclei by interpreting the cross peaks observed. The up field signal for the aromatic proton between methylene bridge and imine linkage is observed at higher field as it is pointing inside the cavity experiencing the anisotropic shielding effect (Spectrum 4.9). In IR spectrum ν(OH) is observed as weak bend at 3421 cm^{-1} compared to strong broad bend due to various νCH. νC=N is observed at 1635 cm^{-1}. $\delta_{as}(CH_3)$ and $\delta_s(CH_2)$ are observed at 1439cm^{-1} while $\delta_s(CH_3)$ is observed at 1360 cm^{-1}. (Spectrum 4.1) Q-TOF mass analysis of the cryptand shows mass peak at 1289.9 m/z corresponding to its molecular ion which supports the proposed structure corresponding to [2+3] cycloimination (Spectrum 4.10).

One of the other bis-aldehydes which resulted in a successful synthesis of the cryptand was 5,5'-methylene-bis-(3-bromosalicylaldehyde) which was prepared by bromination of 5,5'-methylene-bis-salicylaldehyde in acetic acid. The reaction of bromo-bis-salicylaldehyde with TREN carried out under high dilution condition, gave a low isolated yield, compared to the earlier case, of 12% after column chromatography on silica gel (Fig. 4.23).

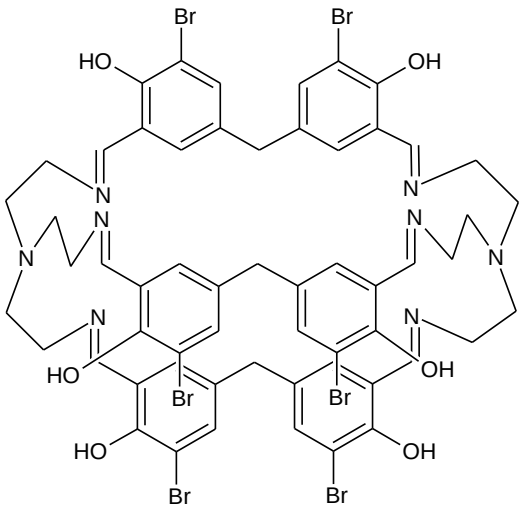

TREN & methylene-bis(bromo-salicylaldehyde) derived hexa-imino cryptand 3

Fig. 4.23

In proton NMR phenolic OH protons are observed at 15.49 δ, CH protons of the imine linkage at 8.16 δ, aromatic protons doublet at 7.91 δ and 5.50 δ, methylene singlet at 3.54 δ and protons of ethylene bridge are observed at 3.76 δ, 3.31 δ and 2.87 δ (Spectrum 4.13).

In IR ν(OH) is observed at 3450 cm^{-1}, νC=N at 1632 cm^{-1} and $\delta_s(CH_2)$ at 1459. νAr-Br is observed at 1038 cm^{-1}. (Spectrum 4.12) Its Q-TOF mass spectrum gave mass peak at 1448.99 corresponding to M+23 (Spectrum 4.14).

Simillarly when 5,5'-methylene-bis-(3-methyl-salicylaldehyde) was reacted with TREN under high dilution conditions with slow addition of reactants in dichloromethane showed multiple spots which included a small amount of starting material and more polar impurity along with distinct spot of product on TLC. The residue obtained after removal of solvent gave 20% of the product after column chromatography on silicagel with DCM:MeOH mixture. The yellow solid product isolated on removal of solvent was found to be insoluble in most of the organic solvents. (Fig. 3.24) The unusual solubility and medicinal properties of compounds containing methyl group compared to the other substituents is well documented[51]

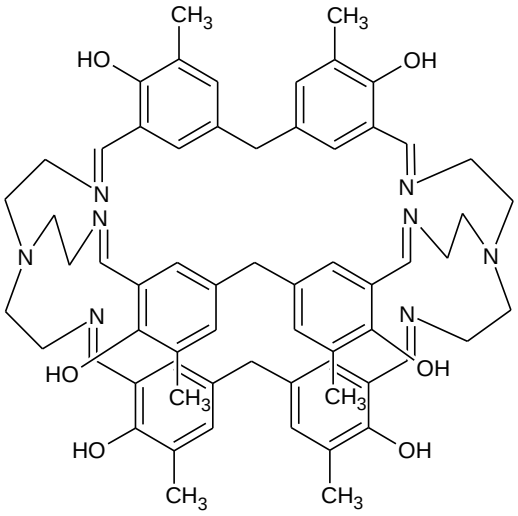

TREN & methylene-bis(methyl-salicylaldehyde) derived hexa-imino cryptand 3
Fig. 3.24

Due to insoluble nature its characterization was a challenge except IR spectroscopy, for studying its NMR the sample was dissolved in CD_3COOD. Some unusual chemical shifts were observed in this solvent. The phenolic –OH is not observed due to its exchange with CD_3COOD which showed signal for residual proton for –COOH at 10.97 δ. CH protons of imine linkage shifted much downfield to 9.85 δ. The aromatic protons are in close proximity at 7.35 δ and 7.32 δ. The methylene bridge protons are seen as a singlet at

3.93 δ. The ethylene bridge connecting nitrogens give four distinct signals for all four protons between 3.7 to 2.9 δ. The methyl protons give singlet at 2.22 δ. Proton NMR (Spectrum 4.17) after adding D_2O resulted in shift due to –COOH group which was exchanged and residual water was seen at 6.84 δ (Spectrum 4.18).

In ^{13}C NMR imine 'C' showed unsually downfield shift in CD_3COOD at 197.6 δ. The other ten carbons are observed between 158 to 14 δ value (Spectrum 4.19). In IR, stretching frequency of OH is observed at 3448 cm^{-1}, stretching frequency of imine linkage is observed at 1633 cm^{-1}, asymmetric bending of methyl group is observed at 1474 cm^{-1}, C-O stretching frequency is observed as a sharp bend at 1268 cm^{-1} (Spectrum 4.12). In Q-TOF mass, the compound being [2+3] cryptand, mass peak corresponding to M^+ is observed at 1037.6 m/z which is also a base peak. (Spectrum 4.20) Normal phase HPLC shows 99.77% purity of the cryptand (Chromatogram 4.21).

The closely related methylene-bis-aldehdyes employed for synthesis of cryptand which did not result in the formation of the desired macromolecules were

1. 5,5'-methylene-bis-(3-nitro-salicylaldehyde)

2. 5,5'-methylene-bis-(2-methoxy-benzaldehyde)

3. 5,5'-methylene-bis-(2,4-dihydroxy-benzaldehyde)

4. 5,5'-methylene-bis-(4-hydroxy-3-methoxy-benzaldehyde)

5. 3,3'-methylene-bis-(4-N-dimethylamino-benzaldehyde)

The macrocyclisation with TREN was also attempted without success by using 5,5'-methylene-bis-(2-hydroxy-acetophenone) as a linker. The failure of this reaction is attributed to a low reactivity of ketone functionality. Failure in macrocyclisation in case of nitrosalicylaldehyde is due to higher reactivity of the formyl group which led the reaction towards polymerization rather than macrocylization. The failure of other bis-aldehydes can't be satisfactorily explained.

4.4 Conclusion

Synthesis of octazacryptands by [2+3] cyclocondensation of TREN and 5,5'-methylene-bis-aromatic aldehydes containing methyl, *tert*-butyl or bromo substitution along with a hydroxyl group at ortho position of aldehyde group involving the formation of six imine linkages has been achieved by using high dilution synthetic methodology. The structures of these macrobicyclic cryptands have been proposed on the basis of detailed NMR, studies and mass spectral characteristics. Attempts for the synthesis of cryptands by several other linking agents prepared by us did not result in any characterizable or desired product. Their reasons and remedies can be studied in future. The presence of ortho-hydroxy group seems to be a necessity due to its hydrogen bonding capability with formyl group. Increased activity of the formyl group due to the presence of nitro group has also proved to be a disadvantage. Attempts to obtain crystals for single crystal X-ray study are in progress.

4.5 Experimental

General Remarks

All the chemicals and reagents were purchased from Sigma-Aldrich, Merck, and Spectrochem. All solvents were distilled before use. Column chromatography was carried out using silica-gel (60-120 mesh). Thin layer chromatography was performed on pre-coated silicagel $60F_{254}$ (Merck) aluminium sheets.

Infrared spectra were recorded on Perkin-Elmer FT-IR 16PC spectrophotometer as KBr pellets. ^{1}H NMR and ^{13}C NMR were recorded on Bruker 200 or 400 MHz NMR spectrophotometer in $CDCl_3$, DMSO or D_2O. ESI mass were recorded on Shimadzu LC-MS 2010-A and Waters Micromass Quattro micro T. M. API.. HPLC was carried out using Shimadzu LC-10AT and UFLC using Shimadzu LC-20AD. Melting points were measured in open capillaries and are uncorrected.

Synthesis of TREN (tris(3-aminoethyl)amine) derived cryptands

General synthesis.

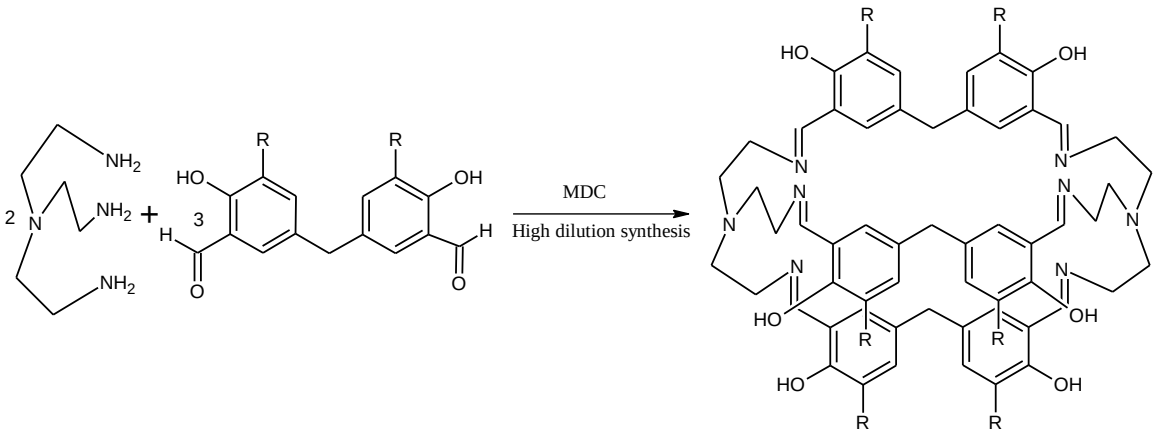

Dichloromethane 2000ml was placed in 5L three necked round bottom flask equipped with two addition funnels and nitrogen balloon. Nitrogen gas was purged for 30 minutes. Solution of 5,5' methylene-bis-aldehydes (0.003mol, 1eq) in 1000ml dichloromethane and TREN (tris(3-aminoethyl)amine)(0.002mol, 0.66eq) in 1000ml dichloromethane was added drop wise from addition funnels over 12 hrs to the magnetically stirred dichloromethane under N_2 atmosphere. Yellow colour was developed. Stirring was continued for further twelve hours. Solvent was removed on rotary evaporator till 50 ml solution left, which was got adsorbed on silica-gel for column chromatography. TLC showed very small amount of starting material, nonpolar product spot and many polar impurities. Starting material was eluted in MDC and single spot yellow product was separated using MDC : Methanol system (gradient).

Cryptand from TREN and 5,5'-methylene-bis-(3-*tert*-butyl-salicylaldehyde) <u>1</u>.

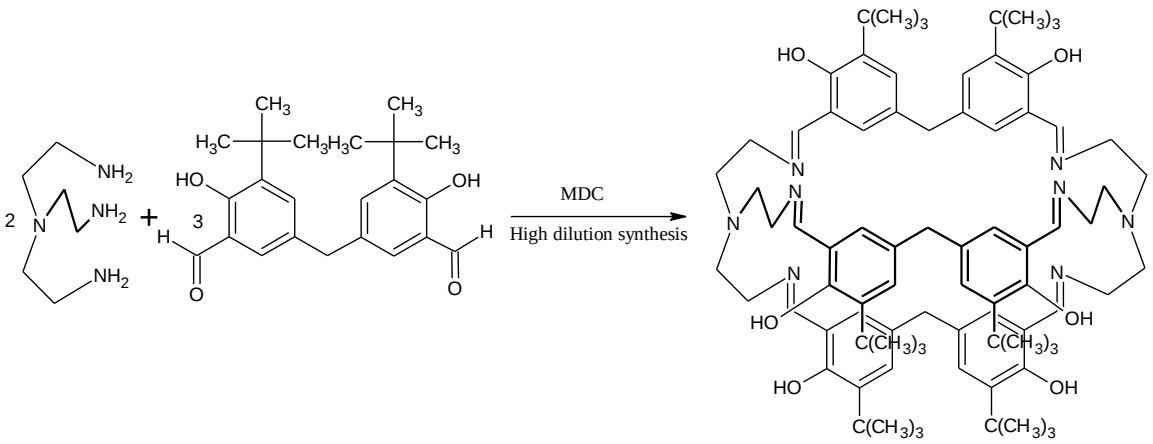

<u>1</u>

5,5'-Methylene-bis-(3-*tert*-butyl-salicylaldehyde) (1g, 0.003mol) and TREN (tris(3-aminoethyl)amine) (0.26g, 0.002mol) reacted in 4000ml MDC to yield the compound **<u>1</u>**.

Yield: 0.371g (21%)

M.P.= 245 ^{o}C (decomposed).

^{1}H NMR: ($CDCl_3$) δ 14.44 (s, 1H), 7.80 (s, 1H), 7.15 (d, *J* = 1.6 Hz, 1H), 6.23 (d, *J* = 1.6 Hz, 1H), 3.58 (s, 1H), 3.51 (d, *J* = 4 Hz, 2H), 2.87 (d, *J* = 4 Hz, 2H), 1.34 (s,1H).

^{13}C NMR: ($CDCl_3$) δ 166.8, 159.0, 137.2, 130.3, 129.7, 128.5, 118.4, 57.6, 57.2, 39.4, 34.9, 29.3

Mass: 1289.9 (M^+)

HPLC Purity: 99.47%

IR (KBr disc, cm^{-1}) : 3421 (phenol, υ(O-H)), 2955 (methylene, υ_{as}(C-H)), 1635 (imine, υ(C=N)), 1596 (aromatic ring, υ(C=C)), 1439 ($\delta_s(CH_2)$), 1360, 1266, 1210 (aromatic, υ(C-N)), 1158, 1026 (aliphatic, υ(C-N)), 929, 885, 852, 800, 772, 692, 670, 588, 572 (out of plane, δ(C-H))

Cryptand from TREN and 5,5'-methylene-bis-(3-bromo-salicylaldehyde) 2

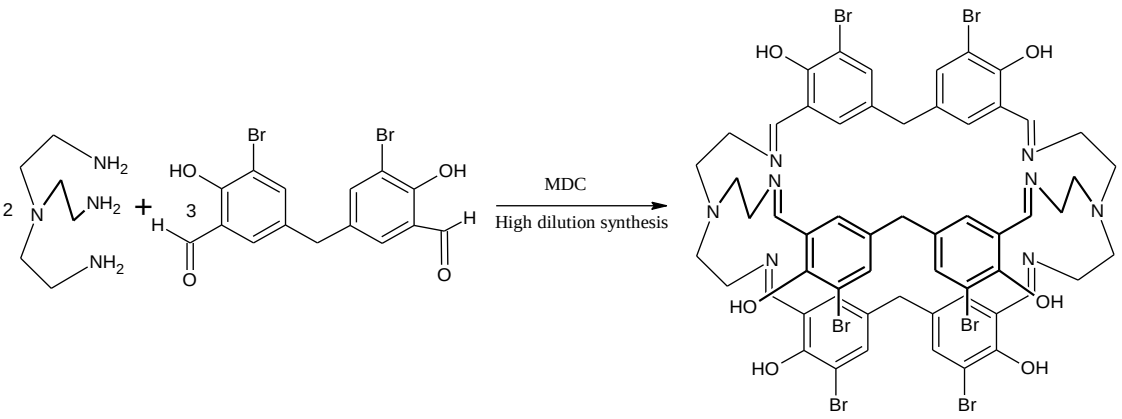

2

5,5'-Methylene-bis-(3-bromo-salicylaldehyde) (1g, 0.002mol) and TREN (tris(3-aminoethyl)amine) (0.26g, 0.002mol) were reacted in 4000ml MDC to yield the compound **2**.

Yield: 135mg (12%)

M.P. = 230^{o}C (decomposed).

^{1}H NMR: ($CDCl_3$) δ 15.49 (s, 1H), 7.92 (d, *J* = 1.6 Hz, 1H), 7.49 (s, 1H), 5.51 (d, *J* = 2.0 Hz, 1H), 3.76 (d, *J* = 8.4 Hz, 1H), 3.54 (s, 1H), 3.31 (d, *J* = 8.4 Hz, 1H), 2.87 (s, 2H).

Mass: 1448.9 (M+23)

HPLC Purity: 93.74%

IR (KBr disc, cm^{-1}) : 3400 (phenol, υ(O-H)), 2899 (methylene, υ_{as}(C-H)), 2842 (methylene, υ_{s}(C-H)), 1632 (imine, υ(C=N)), 1576 (aromatic ring, υ(C=C)), 1459 ($\delta_{s}(CH_2)$), 1368, 1278, 1235 (aromatic, υ(C-N)), 1139, 1038 (aliphatic, υ(C-N)), 977, 888, 843, 806, 743, 668 (out of plane, δ(C-H)).

Cryptand from TREN and 5,5'-methylene-bis-(3-methyl-salicylaldehyde) <u>3</u>

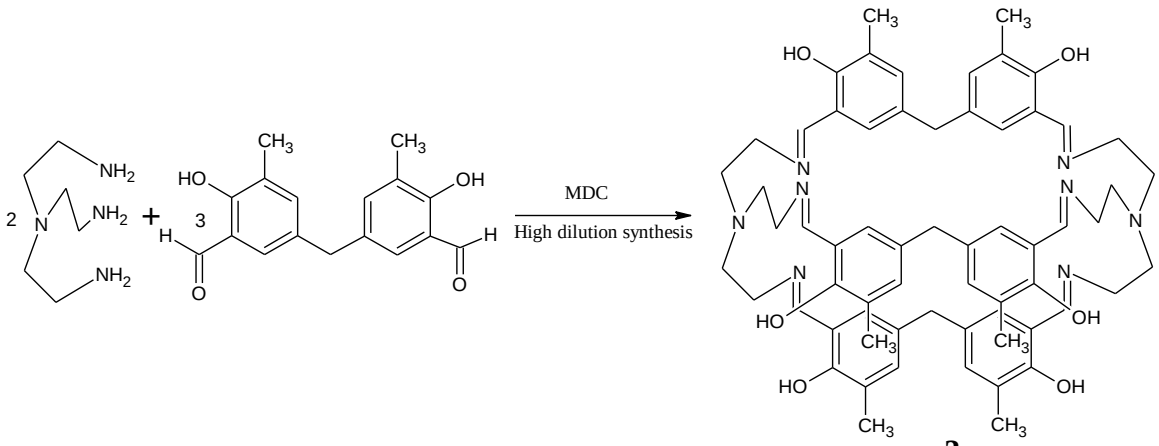

<u>3</u>

5,5'-Methylene-bis-(3-methyl-salicylaldehyde) (1g, 0.004mol) and TREN (tris(3-aminoethyl)amine) (0.34g, 0.002mol) were reacted in 4000ml MDC to yield the compound **<u>3</u>**.

Yield: 0.230 g (19% yield)

M.P.= 232 ^{o}C (decomposed).

^{1}H NMR: (CD_3COOD) δ 9.85 (s, 1H), 7.33 (s, 1H), 7.35 (s, 1H), 3.93 (s, 1H), 3.69 (t, *J* = 5.6 Hz, 1H), 3.54 (t, *J* = 5.6 Hz, 1H), 3.30 (d, *J* = 5.6 Hz, 1H), 2.90 (t, *J* = 5.2 Hz, 1H), 2.22 (s, 3H).

^{13}C NMR: ($CDCl_3$) δ 197.6, 158.1, 138.4, 132.2, 131.1, 126.8, 119.8, 53.6, 39.0, 34.6, 14.0

Mass: 1037.6 (M^+)

HPLC Purity: 99.77%

IR (KBr disc, cm^{-1}) : 3448 (phenol, υ(O-H)), 2915 (methylene, υ_{as}(C-H)), 2843 (methylene, υ_s(C-H)), 1633(imine, υ(C=N)), 1438 ($\delta_s(CH_2)$), 1383, 1268 (aromatic, υ(C-N)), 1164, 1075,1029 (aliphatic, υ(C-N)), 927, 867, 791,752, 701, 673 (out of plane, δ(C-H)).

4.6 Spectra

Spectrum 4.1

IR

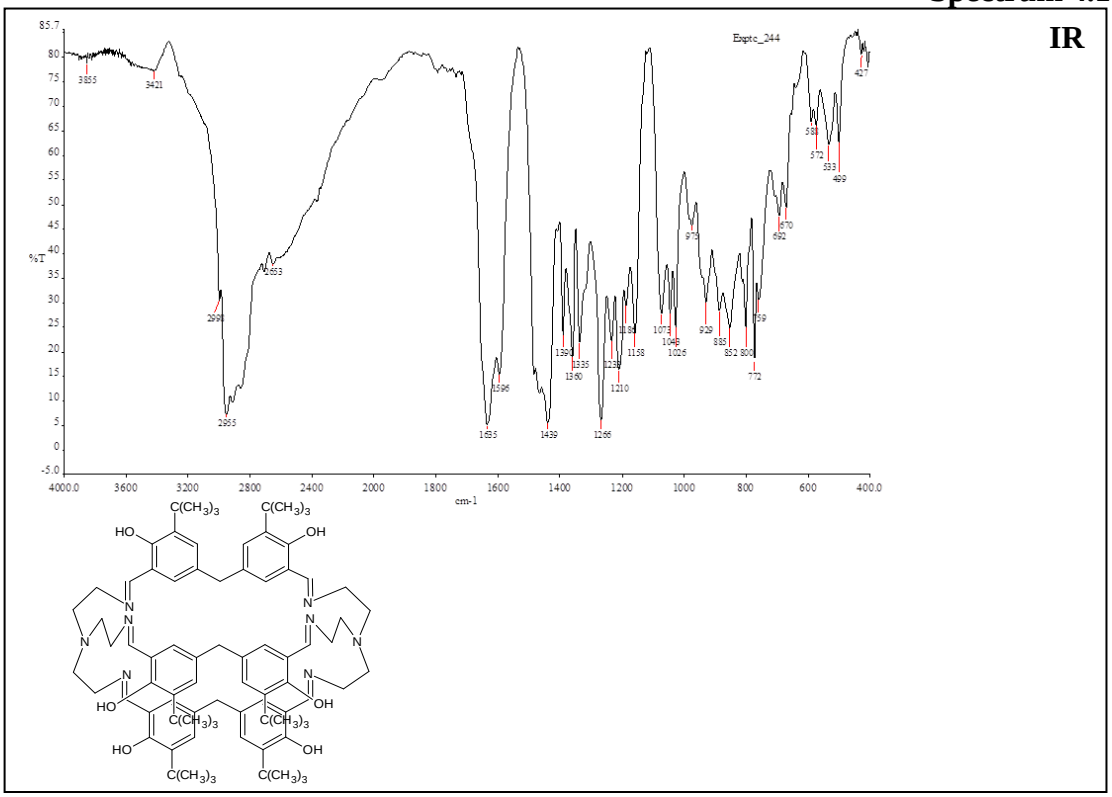

Spectrum 4.2

^{1}H NMR

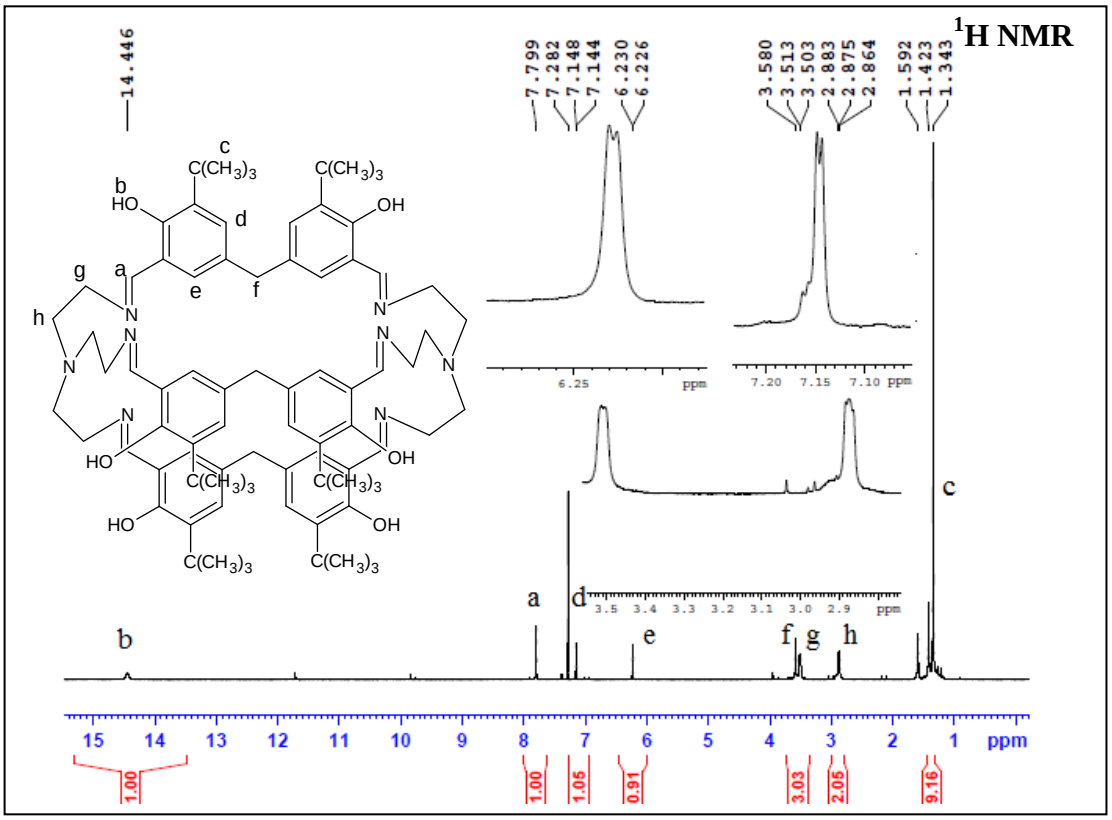

Spectrum 4.3

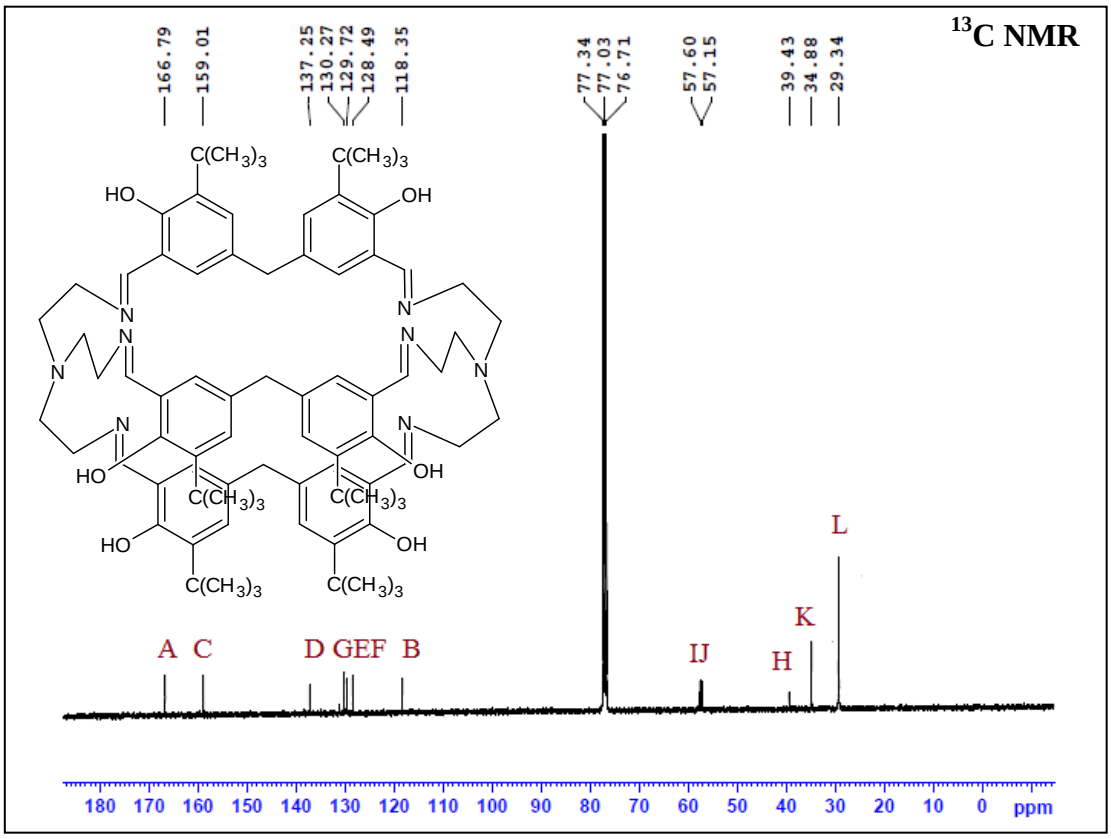

Spectrum 4.4

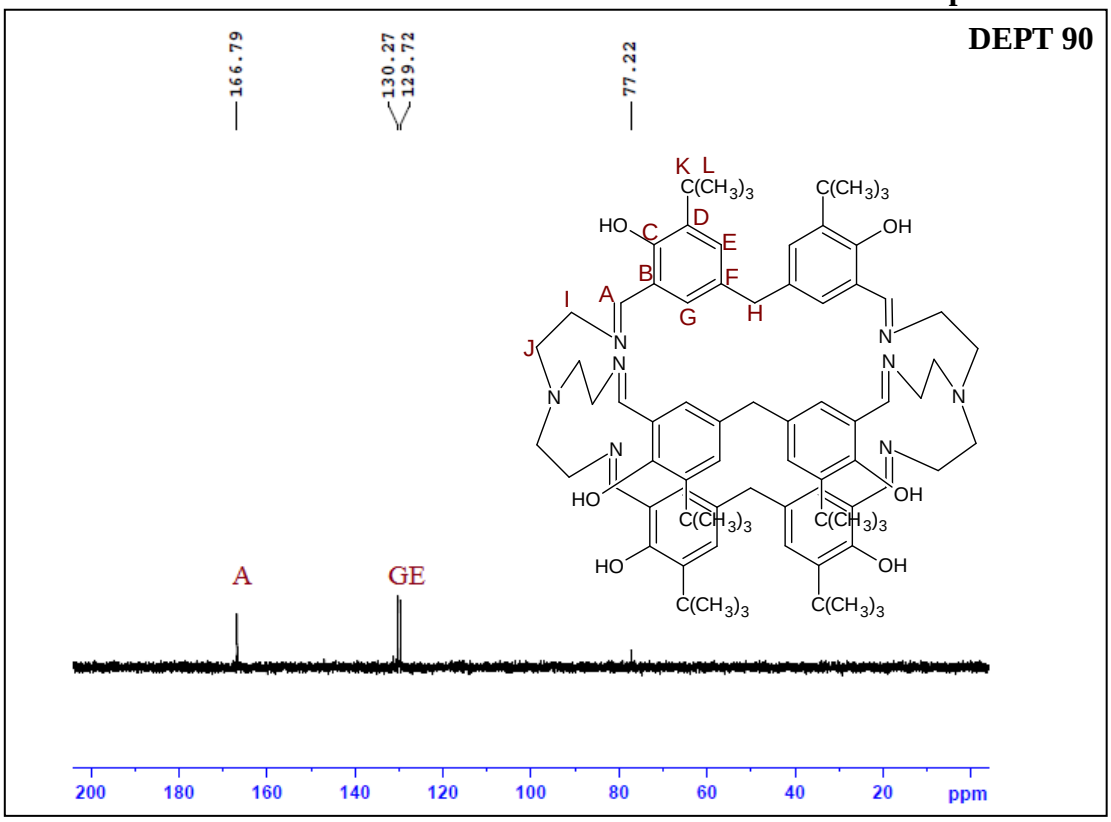

Spectrum 4.5

DEPT 135

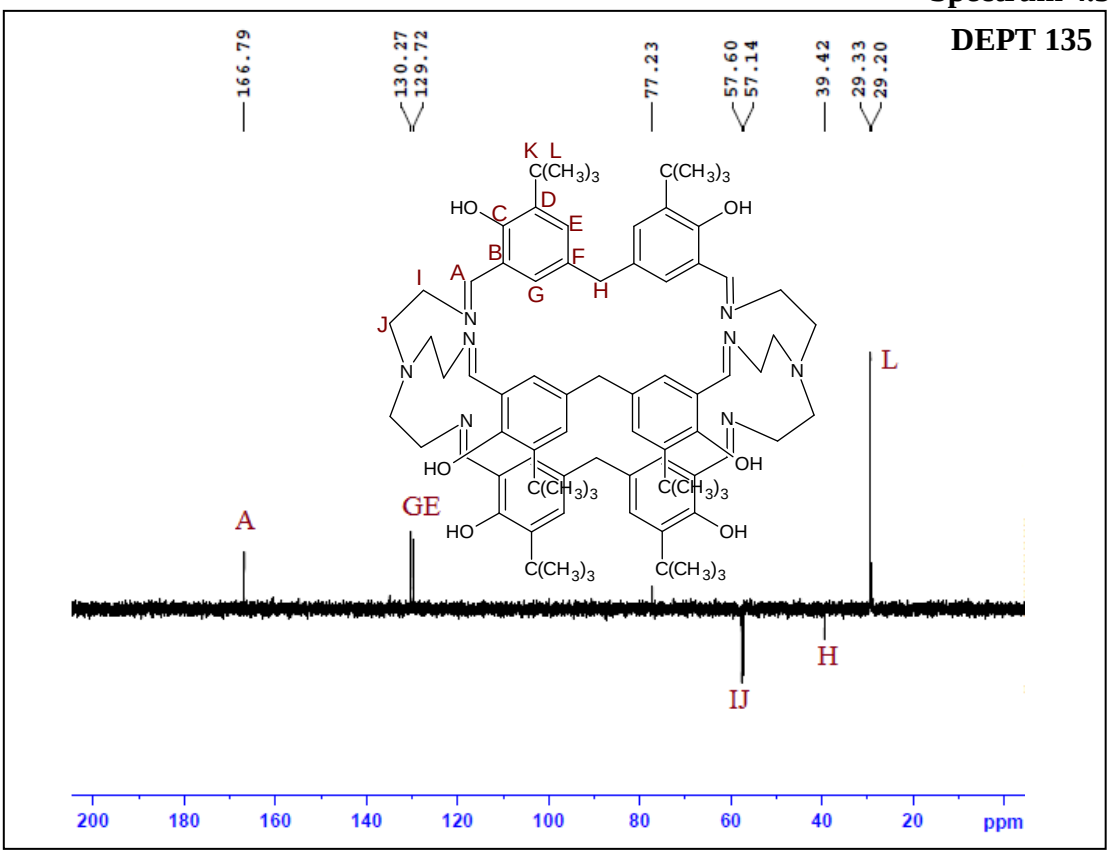

Spectrum 4.6

COSY

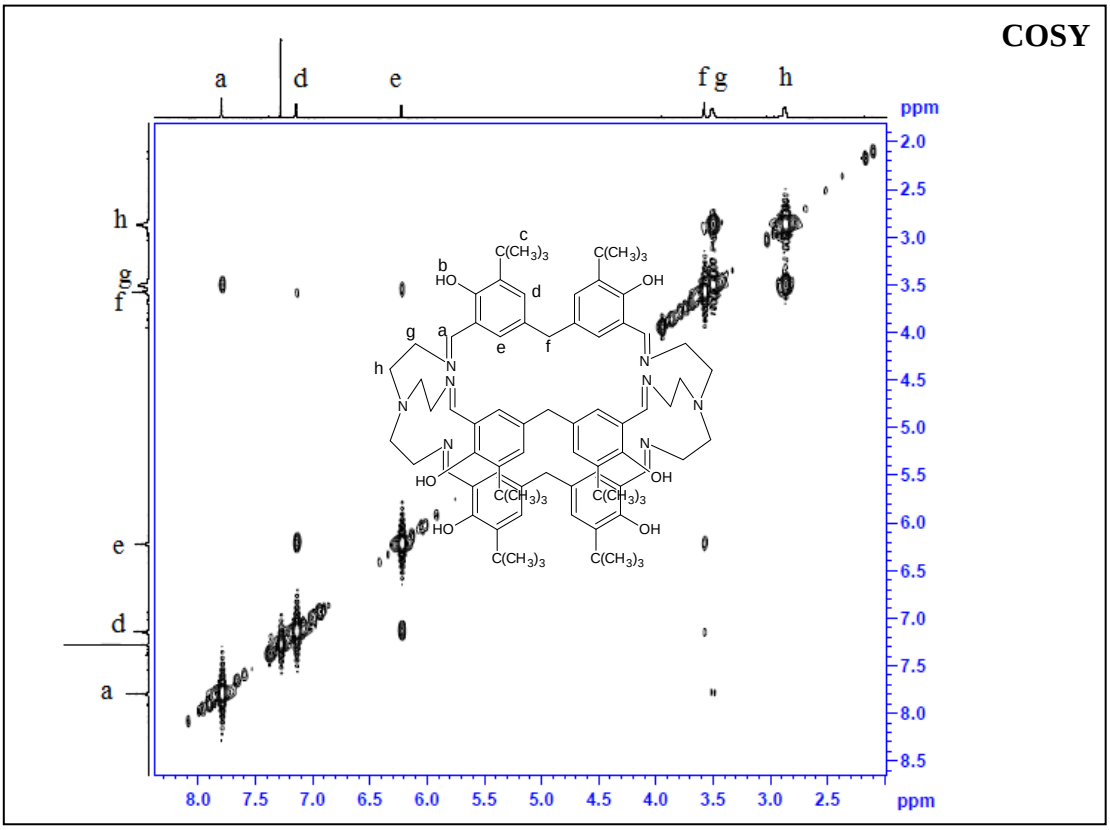

Spectrum 4.7

NOESY

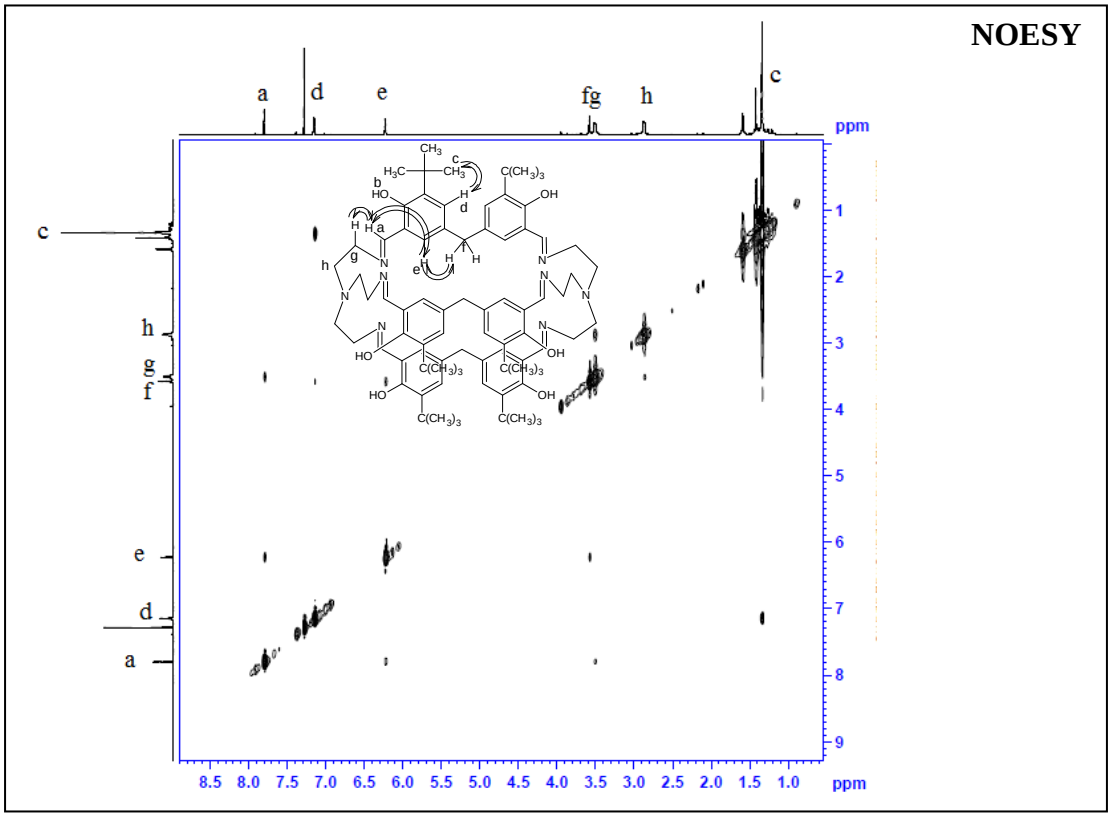

Spectrum 4.8

HSQC

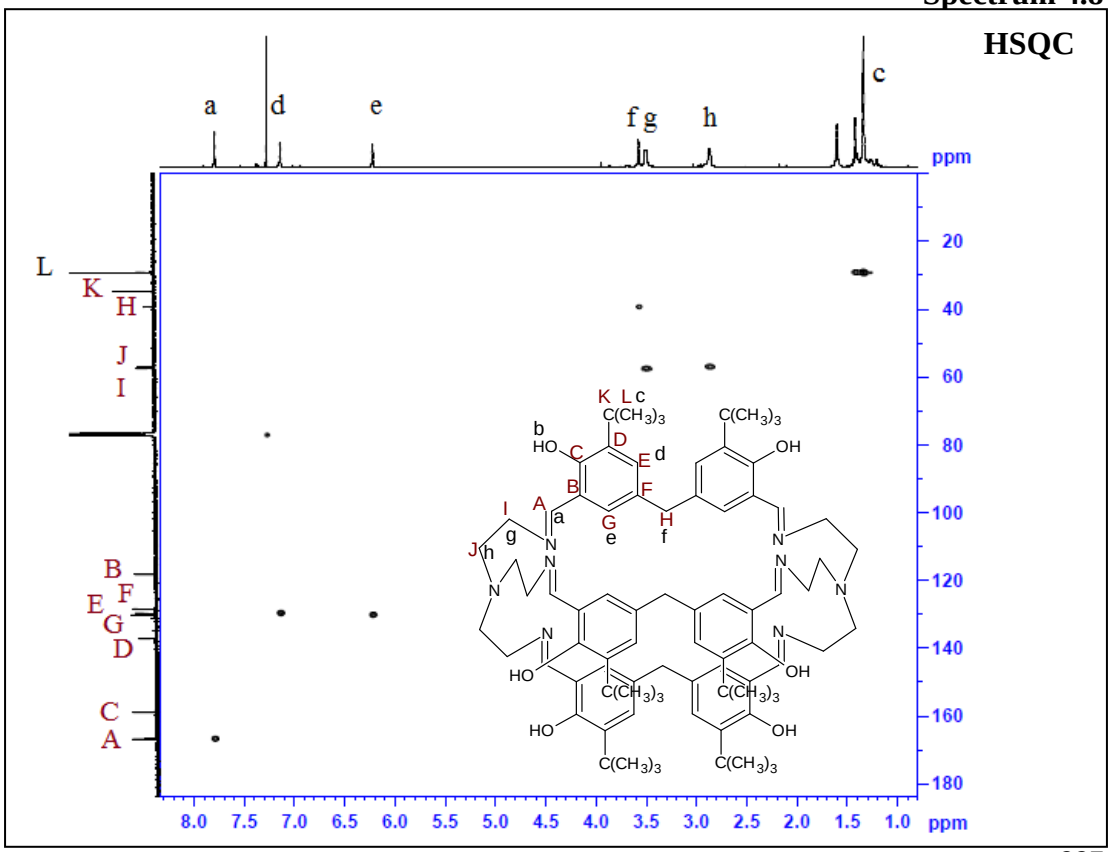

Spectrum 4.9

HMBC

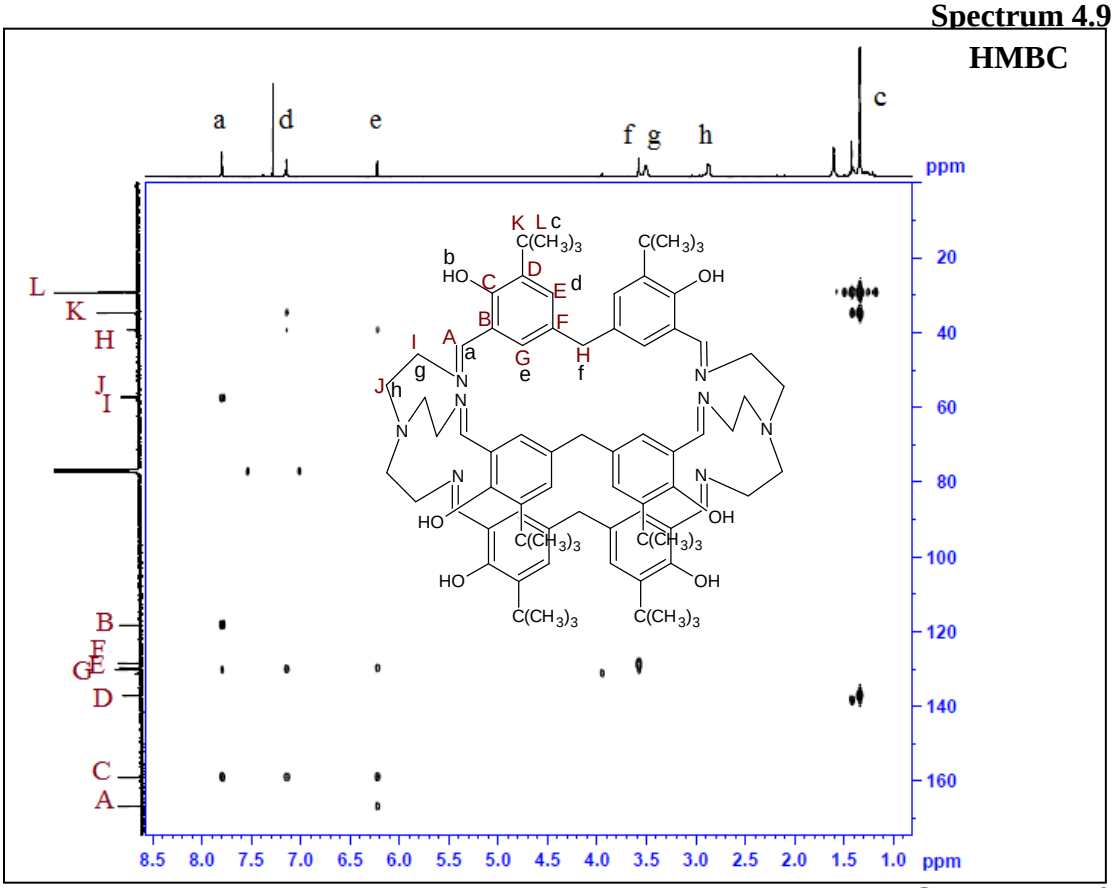

Spectrum 4.10

Mass

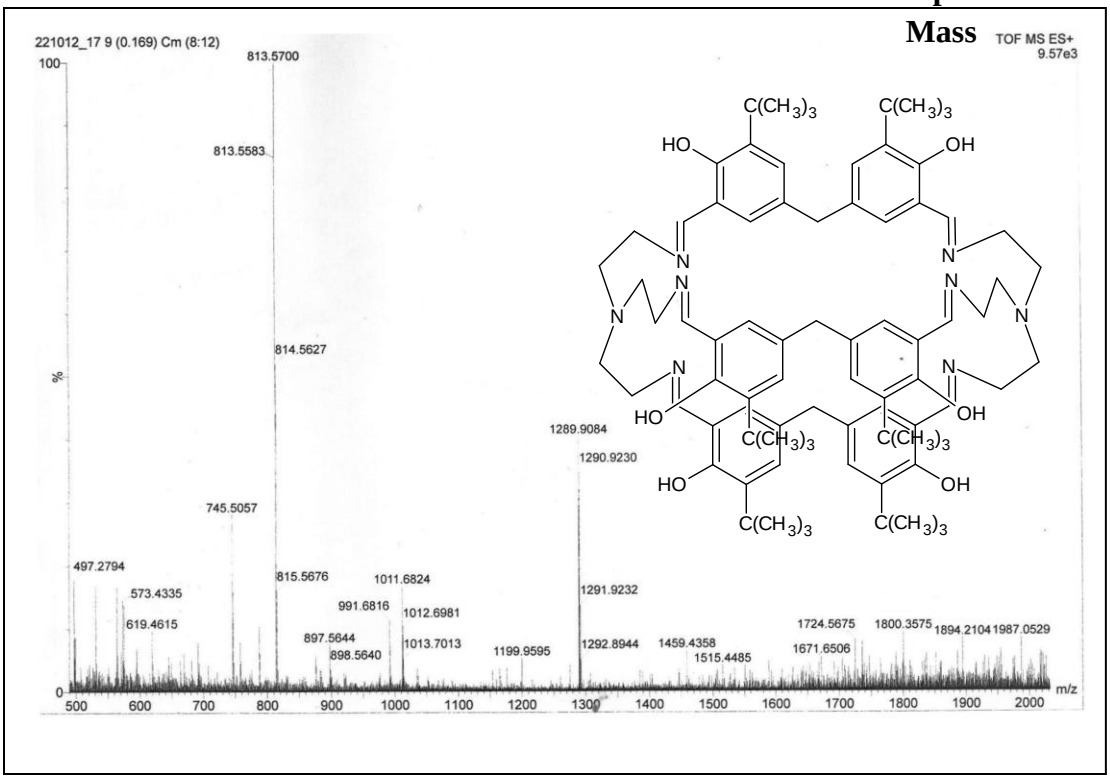

Chromatogram 4.11

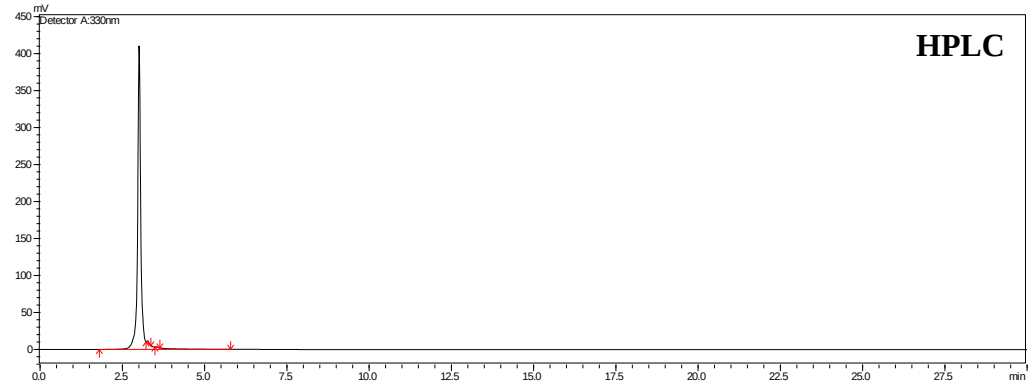

Mobile phase: MDC, Stationary phase : Silica column

Peak	Name	Ret. Time	Area%
1	EXPT C-244(Cryptand from TREN and 5,5'methylene –bis-3-tertbutyl salicylaldehyde)	3.006	99.4670
2	imp 1	3.261	0.4345
3.	imp 2	3.534	0.0985

Spectrum 4.12

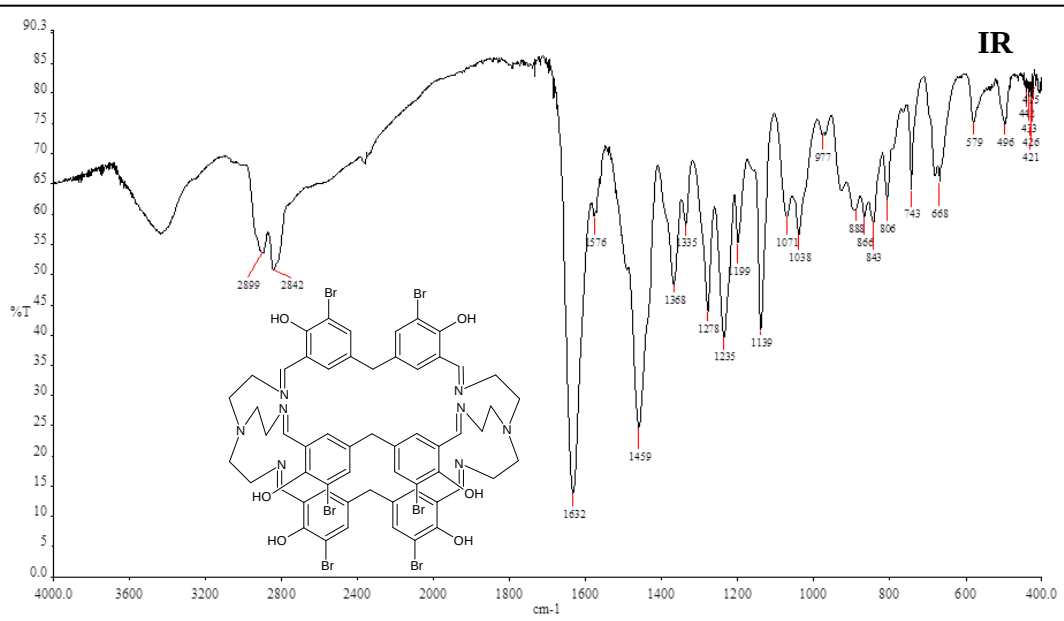

Spectrum 4.13

^{1}H NMR

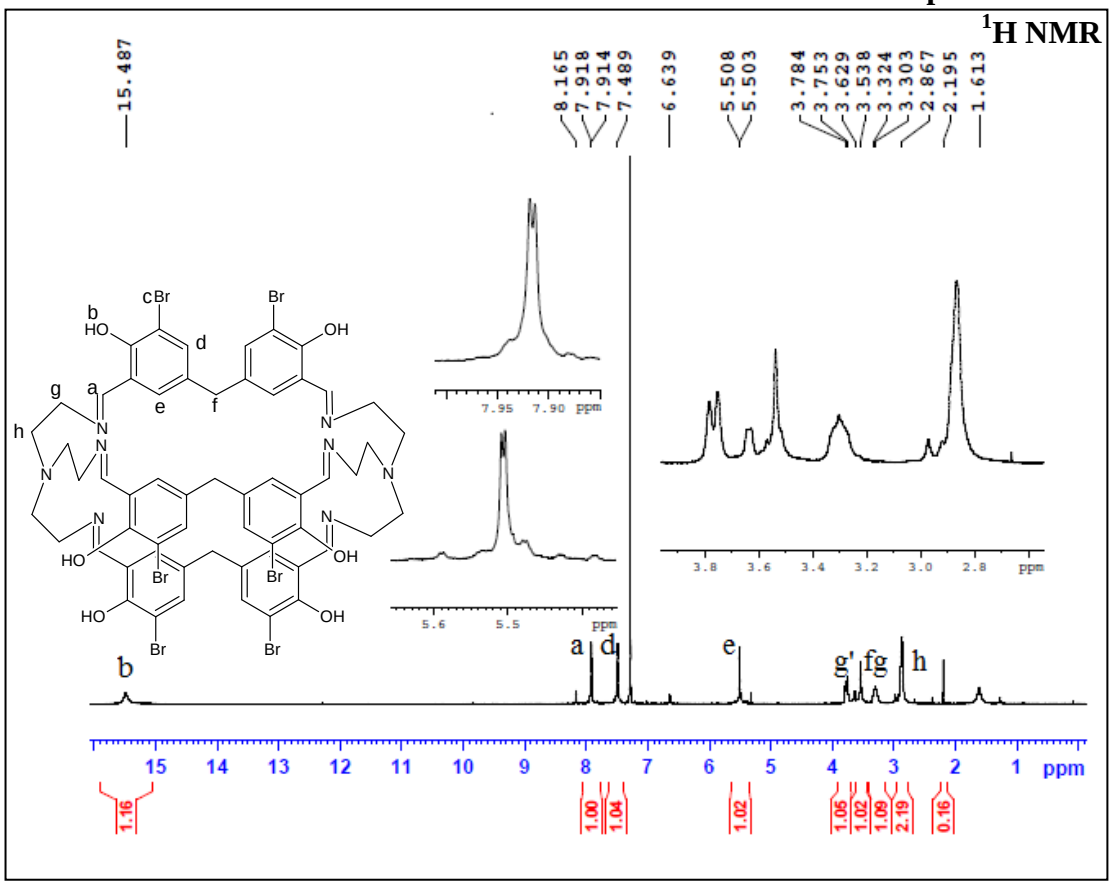

Spectrum 4.14

Mass

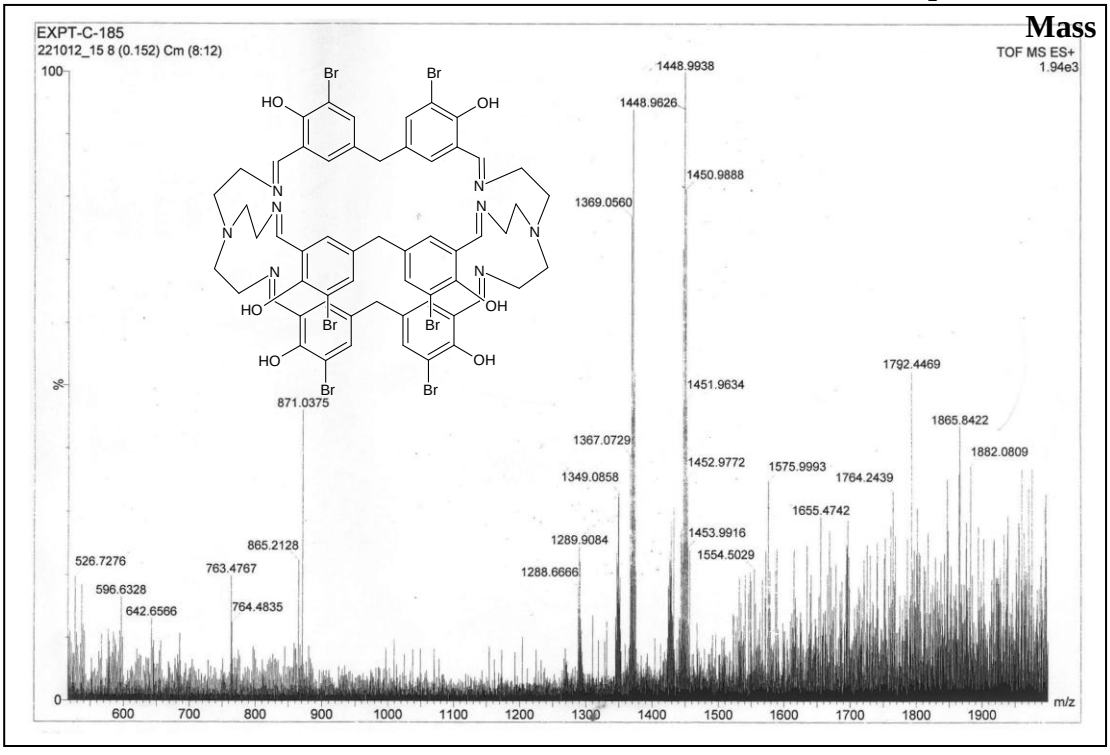

Chromatogram 4.15

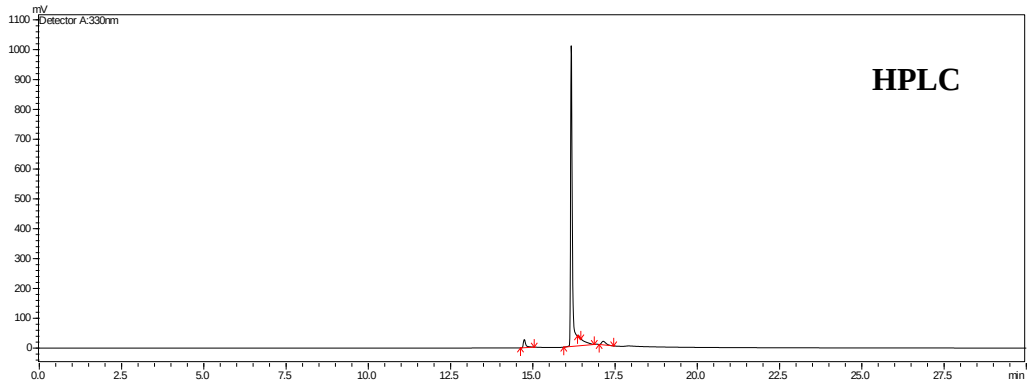

Mobile phase: MDC:MeOH :: 98:2 (v/v), Stationary phase : Silica column

Peak	Name	Ret. Time	Area%
1	imp 1	14.739	3.4113
2	EXPT C-185(Cryptand from TREN and 5,5'methylene –bis-3-bromosalicylaldehyde)	16.165	93.7434
3.	imp 2	16.381	0.2749
4.	imp 3	17.137	2.5704

Spectrum 4.16

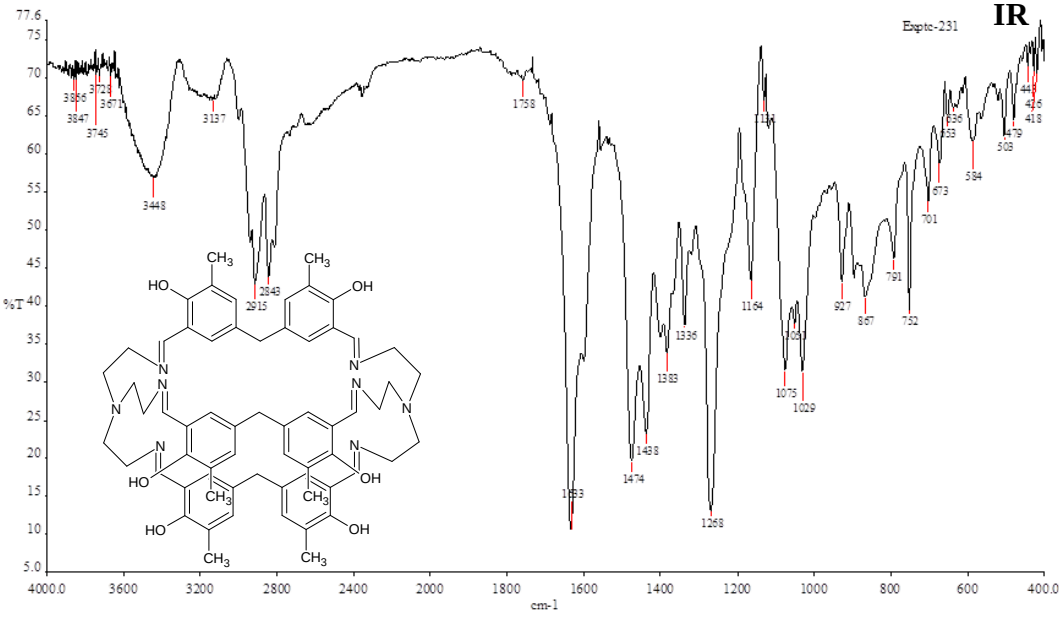

Spectrum 4.17

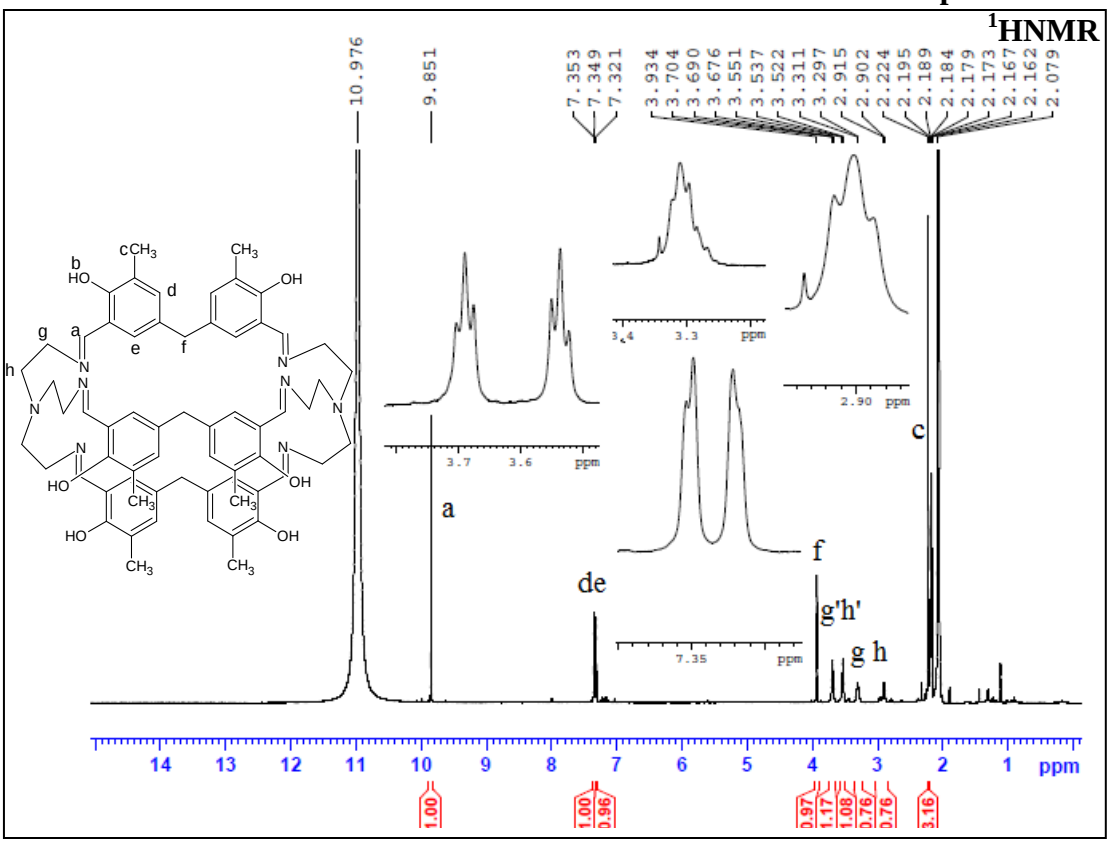

Spectrum 4.18

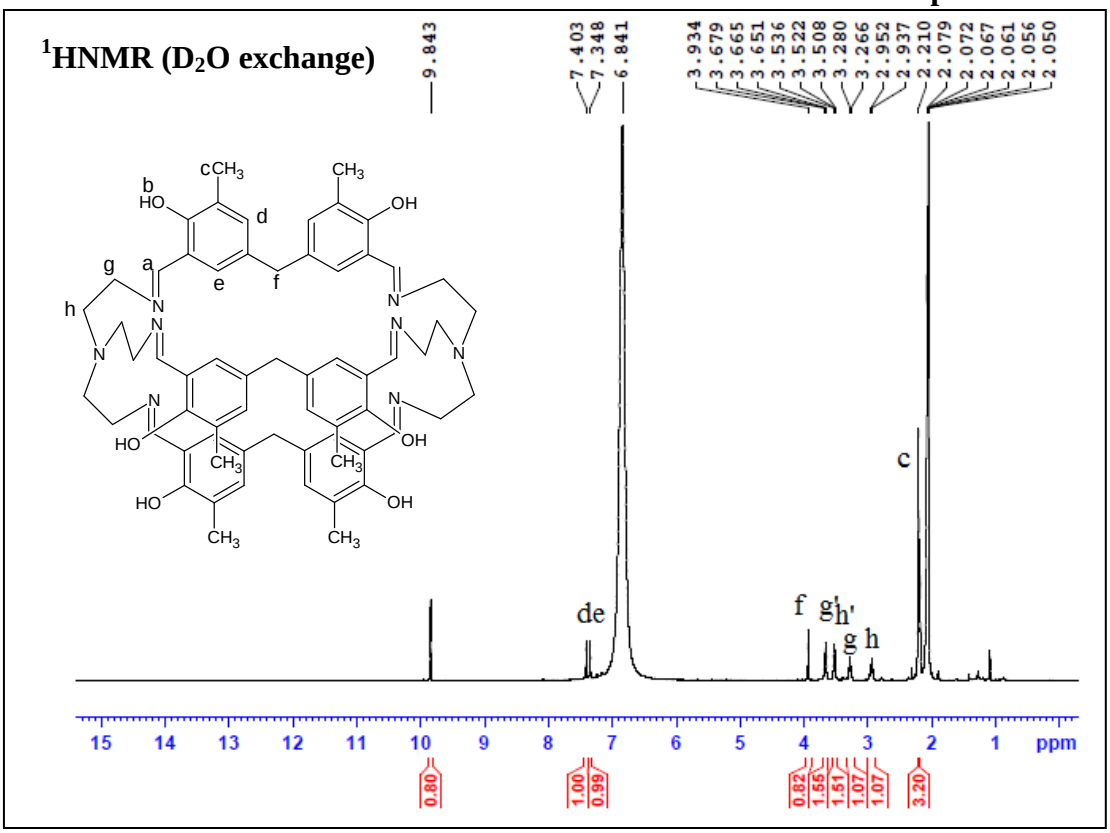

Spectrum 4.19

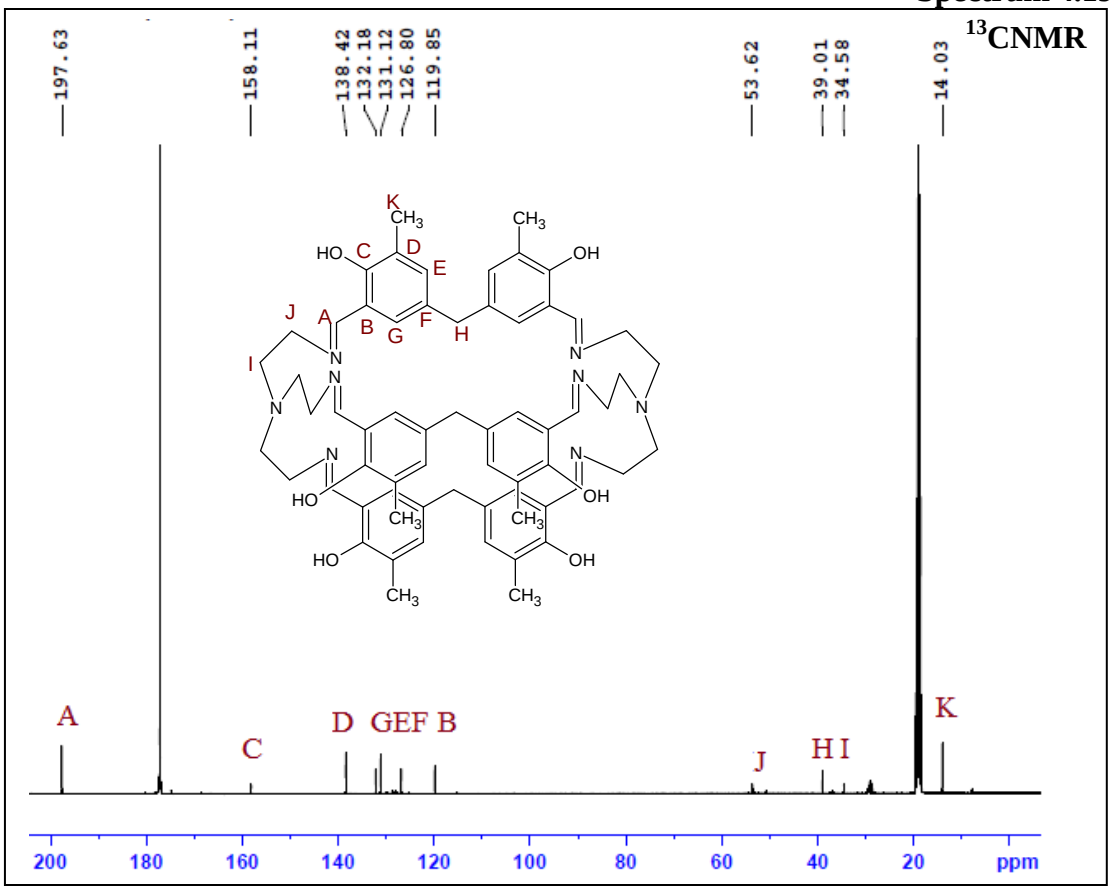

Spectrum 4.20

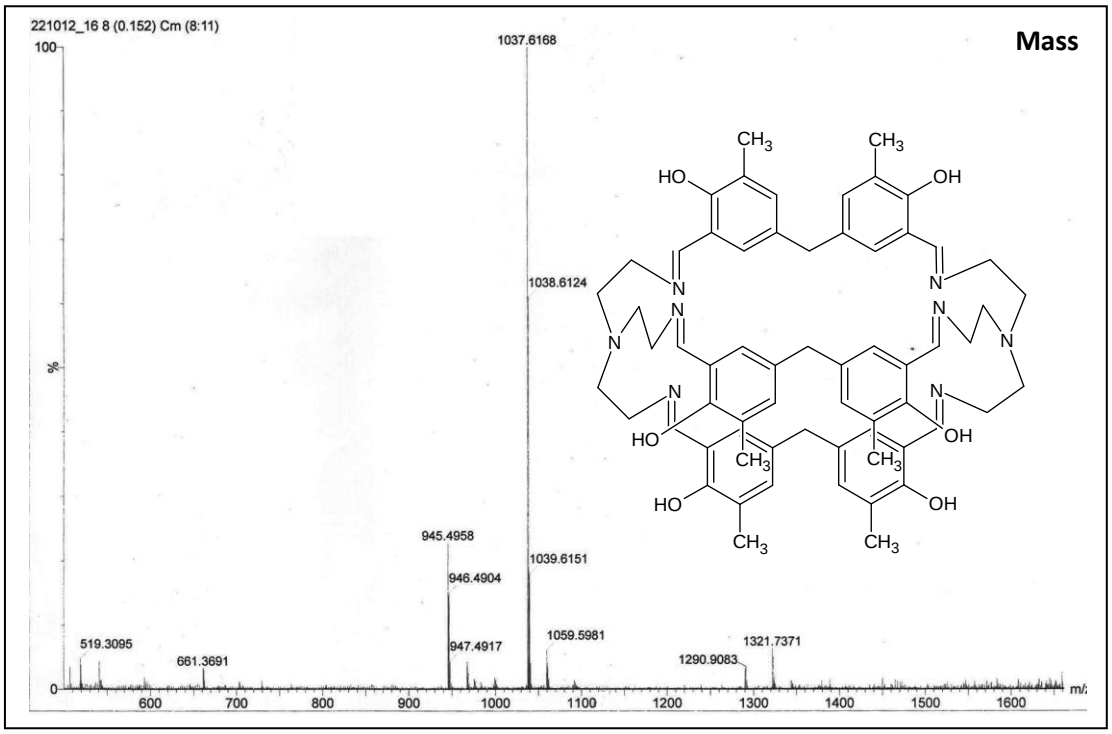

Chromatogram 4.21

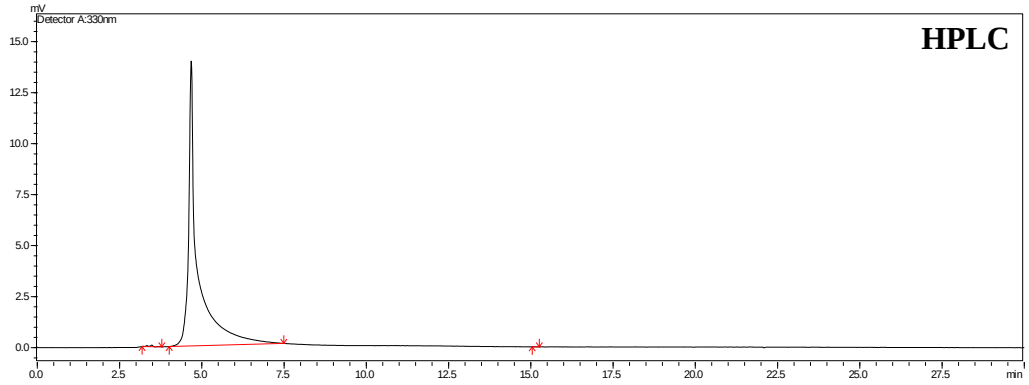

Mobile phase: MDC:MeOH :: 98:2 (v/v), Stationary phase : Silica column

Peak	Name	Ret. Time	Area%
1	EXPT C-231(Cryptand from TREN and 5,5'methylene –bis-3-methylsalicylaldehyde)	3.475	0.2219
2	imp 1	4.675	99.7721
3.	imp 2	15.146	0.0060

4.7 References:

1. McNaught, A. D.; Wilkinson, A. '*IUPAC. Compendium of Chemical Terminology'*, 2nd ed. (the "Gold Book") Blackwell Scientific Publications, Oxford **1997**.

2. Marrs, D. J.; McKee, V.; Nelson, J.; Lu, Q.; Harding, C. J. *Inorg. Chim. Acta*., **1993,** 211, 195.

3. Jazwinski, J.; Lehn,J. M.; Lilienbaum, D.; Ziessel,R.; Guilhem, J.; Pascard C. *J. Chem. Soc., Chem. Commun.*, **1987** 1691.

4. Dera, M. M.; Wichmann K.; Gloeb, K.; Vogtle, F. *Int. J. Mass Spectrom.* **2001**, 210/211, 327.

5. Fenton, D. E.; Najera, B. A. *J. Coord. Chem.*, **20l1**, 54, 239.

6. Kang, S. O.; Llinares, J. M.; Powell, D.; Velde, D. V.; James, K. B. *J. Am. Chem. Soc.* **2003**, 125, 10152.

7. Kang, S.; Lee, S. J.; Yan, S.; Nam, K. C.; Lee, J. Y. *J. Inclusion Phenom. Macrocyclic Chem.*, **2010**, 66, 75.

8. Kang, S. O.; Day, V. W.; James, K. B. *J. Org. Chem.*, **2010**, 75, 277.

9. Wang, Q; Begum, R. A.; Day, V. W.; James, K. B. *Polyhedron,* **2013**, 52, 515.

10.Brooker, S.; Ewing, J. D.; Nelson, J. *Inorg. Chim. Acta.*, **2001**, 317, 53.

11. Brooker, S.; Ewing, J. D.; Nelson, J.; Jeffery J. C. *Inorg. Chim. Acta.,* **2002**, 337 463.

12. Brooker, S.; Ewing, J. D.; Ronson,T. K.; Harding, C. J.; Nelson, J.; Speed D. J. *Inorg. Chem.,* **2003**, 42, 2764.

13. Ronson,T. K.; Nelson, J.; Jameson, G. B.; Jeffery, J. C.; Brooker, S. *Eur. J. Inorg. Chem,*. **2004**, 2570.

14. Kumar, M.; Arin, V. J.; Navarro, P. *Tetrahedron Lett.,* **1995**, 36(12), 2161.

15. Cabezn, B.; Irurzun, M.; Torres T.; Vizquez, P. *Tetrahedron Lett.,* **1998**, 39, 1067.

16. Teulade-Fichou, M.; Vigneron, J.; Lehn, J. *J. Chem. Soc. Perkin Trans.,* 2, **1996** 2169.

17. Martell, A. E.; Motekaitis, R. J.; Lu, Q., Nation, D. A. *Polyhedron*, **1999**, 18, 3203.

18. McKee, V.; Dorrity, M. R. J.; Melone, J. F.; Marrs, D.; Nelson, J. *J. Chem. Soc.,Chem. Commun.*, **1992**, 383.

19. Menif,R.; Reibenspies, J.; Martell, A. E. *Inorg. Chem,*. **1991**, *30*, 3446.

20. Basallote, M. G.; Durán, J.; Fernández-Trujillo, M. J.; Máñez, M. A. *J. Chem. Soc., Dalton Trans*., **1999**, 3817.

21. Basallote, M. G.; Blanco, E.; Blazquez, M.; Ferna´ndez-Trujillo, M. J.; Litran, R.; Manez, M. A. Solar, M. R. *Chem. Mater.*, **2003**, 15, 2025.

22. Basallote, M. G.; Blanco, E.; Blazquez, M.; Ferna´ndez-Trujillo, M. J.; Manez, M. A. Solar, M. R. *Chem. Mater.*, **2002**, *14*, 670.

23. Kang, S. O.; Powell, D.; Velde, D. V.; James, K. B *J. Am. Chem. Soc.*, **2004**, 126, 12272.

24. Alliger, G. E.; Muller,P.; Cummins,C. C.; Nocera, D. G. *Inorg. Chem.,* **2010**. 49, 3697.

25. Lakshminarayanan, P. S.; Suresh, E.; Ghosh, P. *J. Am. Chem. Soc.*, **2005,** 127, 13132.

26. Fabbrizzi, L.; Feravelli, G.; Francese, M.; Licchelli, A.; Perotti, A.; Taglietti, A. *J. Chem. Soc., Chem. Commun.*, **1998**, 971.

27. Li,Y.; Jiang,L.; Feng, X. L.; Lu, T. B. *Cryst. Growth Des.*, **2008,** 8(10), 3689.

28. Brzezik, M.; Jarosz, M.; Jurezak, J. *Polish J. Chem*., **2006**, 80, 1825.

29. Lu, Q.; Latour, J.; Harding, C. J.; Martin, N.; Marrs, D. J.; McKee, V.; Nelson, J. *J. Chem. Soc., Dalton Trans*., **1994**, 1471.

30. Drew, M. G. B.; Marrs, D. J.; Hunter, J.; Nelson, J. *J. Chem. Soc., Dalton Trans*., **1992**, 11.

31. Ravikumar, I.; Suresh, E.; Ghosh, P. *Inorg.Chem*., **2006**, 45(25), 10046.

32. Bandyopadhyay, P.; Bhunia, P. *Colloids Surf. B*, **2007**, 58 14.

33. Avecilla, F.; Blas, A.; Bastida, R.; Fenton, D. E.; Mahía, J.; Macías, A.; Platas, C.; Rodríguez, A.; Rodríguez-Blas T. *J. Chem. Soc*., *Chem. Commun.*, **1999**, 125.

34. Drew, M. G. B.; Howarth, O. W.; Martin, N.; Morgan G.; Nelson, J. *J. Chem. Soc*., *Dalton Trans*., **2000**, 1275.

35. Zhang, J.; Zhanga, W.; Luoa, Q.; Mei Y. *Polyhedron*, **1999**, 18, 3637.

36. Platas, C.; Avecilla, F.; Blas, A.; Rodríguez-Blas T.; Geraldes, C. F. G. C.; Toth, E.; Merbach, A. E.; Bünzli, J. C. G. *J. Chem. Soc*., *Dalton Trans*., **2000**, 611.

37. Chen, Q.; Luo, Q.; Fu, D.; Chen, J. *J. Chem. Soc*., *Dalton Trans*., **2002**, 2873.

38. Lennartsona, A.; McKeeb, V.; Nelsona, J.; Arthurs, M., McKenziea, C. *J. Supramolecular Chemistry*., **2012**, 24(8), 604.

39. Chand, D. K.; Bharadwaj, P. K. *Inorg. Chem.*, **1996**, *35*, 3380.

40. Ghosh, P.; Gupta, S. S.; Bharadwaj, P. K. *J. Chem. Soc*., *Dalton Trans*., **1997**, 935.

41. Mukhopadhyay, P.; Sarkar, B.; Bharadwaj,P. K.; Na1ttinen, K.; Rissanen, K. *Inorg. Chem*., **2003**, 42(16), 4955.

42. Bag, B.; Bharadwaj, P. K. *Inorg. Chem*., **2004**, 43(15), 4626.

43. Sadhu, K. K.; Bharadwaj, P. K. *J. Chem. Soc*., *Chem. Commun*., **2008**, 4180.

44. Chand, D. K.; Bharadwaj, P. K. *Inorg. Chem.*, **1997**, *36*, 5658.

45. Yu, J.; Yang, R. *Synth. Commun*., **2002**, 32(20), 3113.

46. Ziach, K.; Ceborska, M.; Jurczak, J. *Tetrahedron Lett.*, **2011**, 52, 4452.

47. Kanesato, M.; Houjou, H.; Nagawa, Y.; Hiratani, K. *Inorg. Chem. Commun.*, **2002**, 5, 984.

48. Ma, Z.; Yang, R.; Yan, L. *J. Chem. Res. Synop.*, **1999**,712.

49. Panda, A.; Menon, S. C.; Singh, H. B.; Butcher, R. J. *J. Organomet. Chem.,* **2001**, 623, 87.

50. Vyas, T. A., *Ph.D. Thesis,* the M. S. University of Baroda **2004**.

51. Barreiro, E. J.; Kummerle, A. E.; Fraga, C. A. M., *Chem. Rev.*, **2011**, 111(9), 5215.

Chapter 5

Silver ion template synthesis of the cryptates from tris-(2-aminopropyl)amine and their antimicrobial property

5.1 Introduction

Cryptand host on encapsulation of desired guest forms a host-guest complex known as a cryptate. High dilution synthesis of cryptands generally results in lower yields due to greater possibility of oligomerisation or polymerization while template assisted synthesis usually results in fairly good yields of corresponding cryptates.[1]

Several alkali and alkaline earth metals are known to act as templates in various cryptate syntheses. Azacryptands show better affinity for silver ion as compared to the other metal ions. Silver is indeed a suitable guest for azacryptands but also can act as a desirable template for their synthesis. Using nitrate or perchlorate salt of silver as a template, various mononuclear, binuclear or polynuclear silver cryptates have been synthesized and characterized.

Silver(I) is known to form linear two coordinate complexes but in macrocyclic silver cryptates coordination modes vary from near square planner, trigonal pyramidal to distorted octahedral. Occasionally higher coordination modes such as pentagonal pyramidal or trigonal bipyramidal do appear.[2] The silver cryptates of diazabicyclic cryptands (2.2.2), (2.1.1) and (2.2.1) (**Fig. 5.1**) have been reported by J. Gutknecht et. al.[3] Stability constants, kinetics of dissociation and ligand exchange reactions of these cryptates have been studied where Ag(I)-N bonds are found to be quite strong as compared to their alkali metal analogous.[4,5]

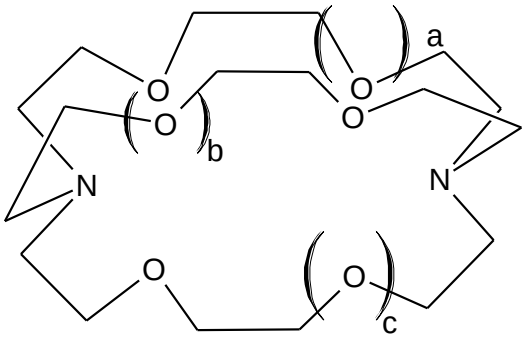

Oxa-diaza cryptand

Fig. 5.1

Bithiazole, bipyridyl linked hybrid cryptand (**Fig. 5.2**) and bithiazole, azacrown linked hybrid cryptand (**Fig. 5.3**) were synthesized and their silver cryptates were formed by Lehn and co-workers.[6]

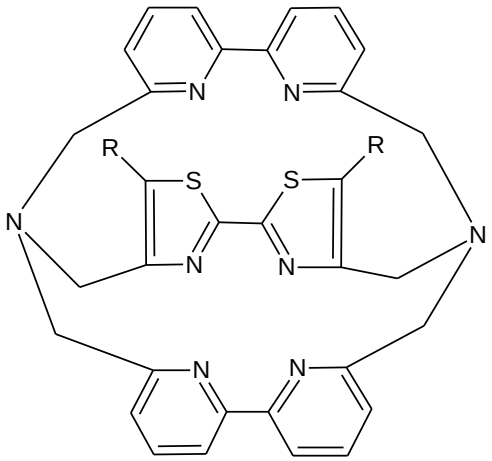

Cryptand with smaller cavity and hybrid heterocyclic linkers

Fig. 5.2

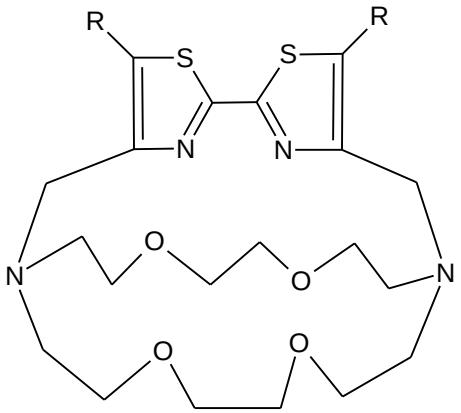

Oxa-aza crown-heterocycle hybrid cryptand

Fig. 5.3

Silver(I) cryptates were prepared by condensation of TRPN (Tris(3-aminopropyl)amine) and 2,5-disubstituted-1,3-phenylenedialdehyde using $AgNO_3$ as template[7,8] (**Fig. 5.4**).

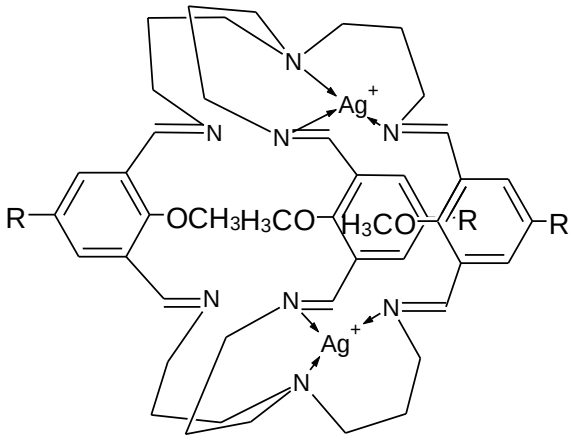

Silver cryptate from TRPN and substituted isothalaldehyde

Fig. 5.4

In template assisted syntheses of these cryptates resulted in differently coordinated cryptates depending on reaction conditions and solvent used. They are named as bridge twisted silver cryptates (**Fig. 5.5**) when having two silver ions diagonally placed, basket shaped silver cryptates (**Fig. 5.6**) when two silver ions were coordinated on one side of the cryptate, while silver ion linked cryptates were termed as polymeric silver cryptate.[7,8]

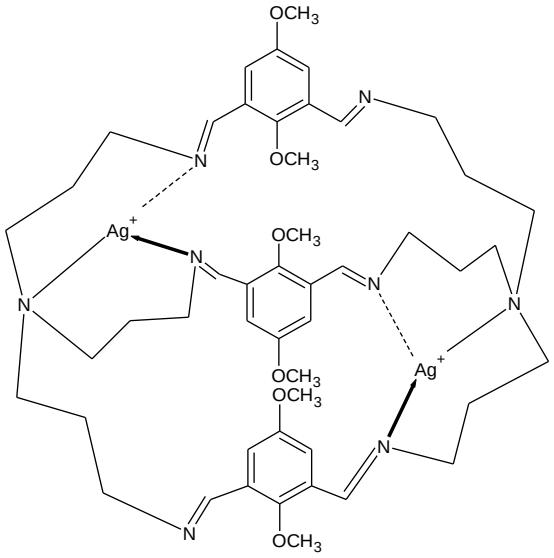

Bridge twisted shaped silver cryptate

Fig. 5.5

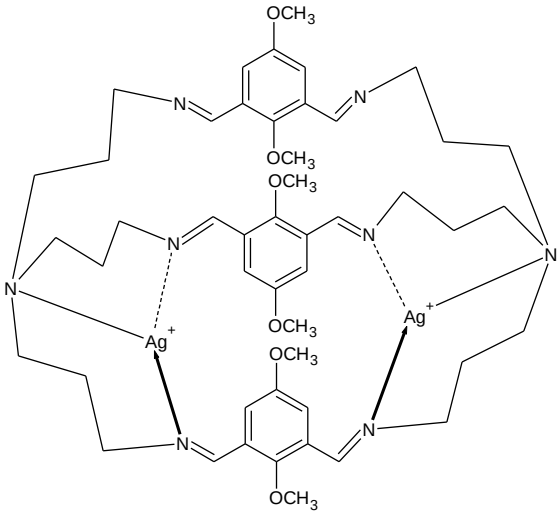

Basket shaped silver cryptate

Fig. 5.6

The binuclear silver cryptate prepared from TRPN and pyridine-2,6-dicarbaldehyde was reported and found to catalyze hydrolysis of acetonitrile included in the cavity.[9] (**Fig. 5.7**)

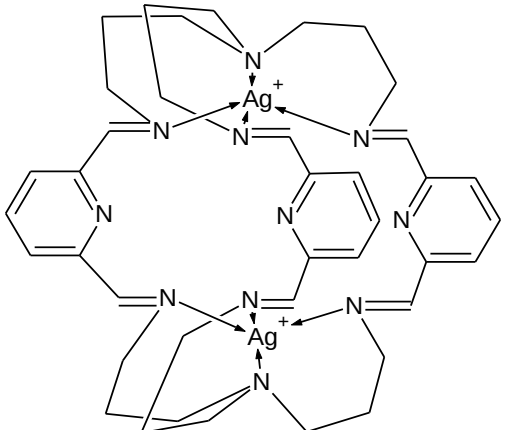

TRPN-pyridine dicarbaldehyde derived silver cryptate

Fig. 5.7

Silver template assisted cryptates by condensation of TRPN with other aromatic or heteroaromatic di-aldehydes have been reported and studied by Nelson and co-workers. It was observed that due to steric factors, silver cation may have different coordination numbers in which all the four nitrogens at one end may not participate in coordination with silver ion. In solution fluxionality may be observed with the help of ^{1}H NMR due to inter conversion of conformers in the solution. Symmetric conformation carries both four coordinated trigonal pyramidal inclusive sites while unsymmetrical conformer possess one four-coordinated trigonal pyramidal site and one three coordinated site [2,10,11] (**Fig. 5.8**).

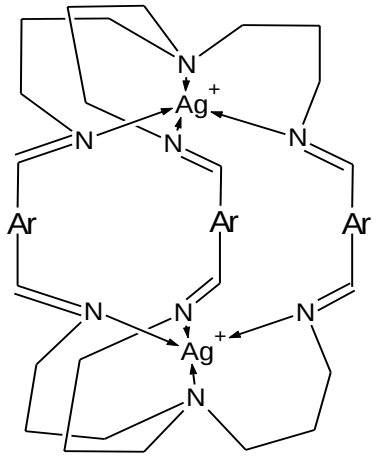

TRPN-aromatic dialdehyde derived silver cryptate

Fig. 5.8

The use of silver ion as a template in the synthesis of cryptand results in the formation of silver cryptates. Compared to other metal ion cryptates, silver cryptates have been widely studied for various applications. Silver cryptate electrode is found to be better reference electrode in non-aqueous solvents as compared to Ag/Ag^{+} electrode due to greater stability of silver ions in form of cryptates.[12] Silver cryptates have also been applied as detectors in gas chromatography for the detection of alkenes and alkynes.[13]

Organosilver compounds have some important application in medical field due to their biological activities. Silver sulphadiazine has been used as an antibacterial agent for the treatment of wounds and ulcers.[14] Nicotinate silver complexes showed antibacterial

activity against antibiotic resistant pathogens.[15] 1,10-Phenanthroline-5,6-dione-silverperchlorate complex has been reported to be most active in aqueous media against human pathogen *Candida albicans.*[16] Bis-imidazole-silver(I) complexes are found to be useful antifungal agents.[17]

5.2 Aim and Objectives:

We aimed to synthesize cryptands with expanded binding pockets by applying tris(3-aminopropyl)amine (TRPN), the higher homologous of TREN by using a variety of linkers prepared by us. The application of Ag^{+} template for achieving the synthesis resulted in isolation of several new silver cryptates which were characterized by various analytical techniques and are included in this chapter. They have also been studied for their antibacterial and antifungal activities.

5.3 Result and Discussion

Following the success in the synthesis of several new cryptands with the help of TREN and methylene-bis-aldehydes, we aimed at the synthesis of the cryptands having larger binding cavity size which could accommodate larger sized guest ions/molecules. For this purpose tris(3-aminopropyl)amine (TRPN), a higher homologue of TREN was thought to be the most suitable selection. Due to increased chain length and greater flexibility in its three arms, it was thought to be a conducive factor for the formation of targeted cryptands under high dilution condition. We also expected improved solubility of the cryptands form TRPN in organic solvents due to increase in the chain length.

The reaction of TRPN with 5,5'-methylene-bis-salicylaldehyde gave product under high dilution conditions was observed on TLC. Isolation of the observed spot after column chromatography of the concentrated reaction mixture was found to be insoluble in organic solvents after removal of solvent from eluted fractions, so it could not be characterized. Attempts to obtain cryptands with the help of the other bis-aldehydes as linkers with TRPN were unsucessful. Higher flexibility of TRPN proved to be a disadvantage rather than an advantage in the synthesis of the desired cryptands. We observed that most of the reports involving a synthesis of macrocyclic structures where TRPN was used involved the use of Ag^+ as template. This prompted us to deviate from high dilution synthesis to template assisted synthesis of the cryptands from TRPN.

We employed silver nitrate dissolved in methanol to offer Ag^+ ion template for macrocyclization. The resulting silver cryptates were isolated in the form of their perchlorates by treating them with sodium perchlorate.

Thus when 5,5'-methylene-bis-salicylaldehyde was reacted with TRPN in excess of methanol in the presence of silver nitrate the resulting cryptate was isolated in form of its perchlorate. The cryptate was found to be soluble in DMSO. (Fig. 5.9) The IR spectrum of the cryptate was indicative of the expected structure of the cryptate. νOH is shifted to 3368 cm^{-1}, νC=N is observed at 1638cm^{-1}, νC-O(phenolic) is observed at 1270cm^{-1}, a typical broad band is observed at 1095cm^{-1} and a sharp medium intensity band is observed at 623 cm^{-1} attributed to ClO_4^- (Spectrum 5.1).

In proton NMR, phenolic OH protons are observed at 13.2δ, CH protons of imine at 8.21δ, aromatic protons are observed at 7.12, 6.85 and 6.74 δ, aliphatic methylene bridge protons (between two aromatic rings) are observed at 3.67 δ and propylene bridge protons at 3.54, 2.45, 1.75 δ (Spectrum 5.2). In ^{13}C NMR more number of signals are observed due to unsymmetrically located silver ions because of which the cryptand is locked in one of the conformations. The nature of the ^{13}C NMR spectrum could also be result of a mixture of different conformer generated due to placement of silver ions in the cryptate[3,7,8,10] (Spectrum 5.3). HPLC analysis of the cryptate in reverse phase silica column shows more than 96% purity. The Q-TOF ESI mass spectrum of the cryptate shows a base peak at 1037.6 corresponding to molecular ion generated from the cryptand alone. This reveals the [2+3] condensation of TRPN and 5,5'-methylene-bis-salicylaldehyde.

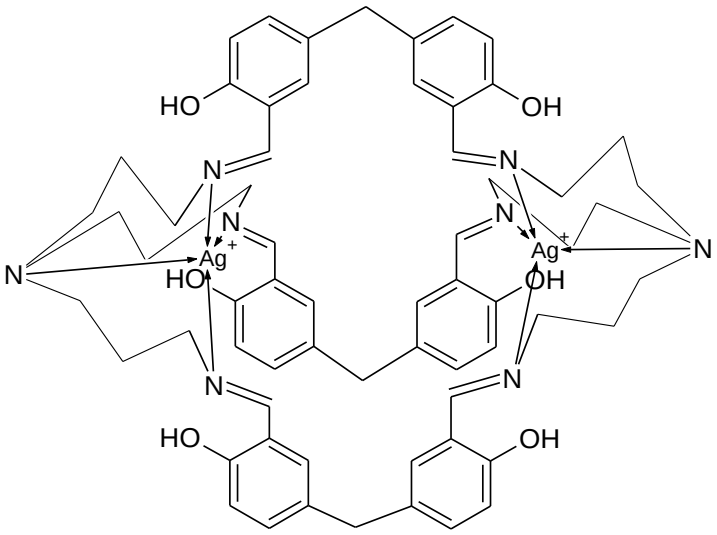

TRPN-(methylene-bis-salicylaldehyde) derived silver cryptate 1

Fig. 5.9

Cyclic voltametric study of the cryptate was carried out. Comparison of cyclic voltamogramme of the cryptate in DMSO with $AgNO_3$ in DMSO and only DMSO proved the presence of Ag^+. The Figures 5.10 a,b,c represent the cyclic voltamogramme of cryptate, silver nitrate and only DMSO respectively.

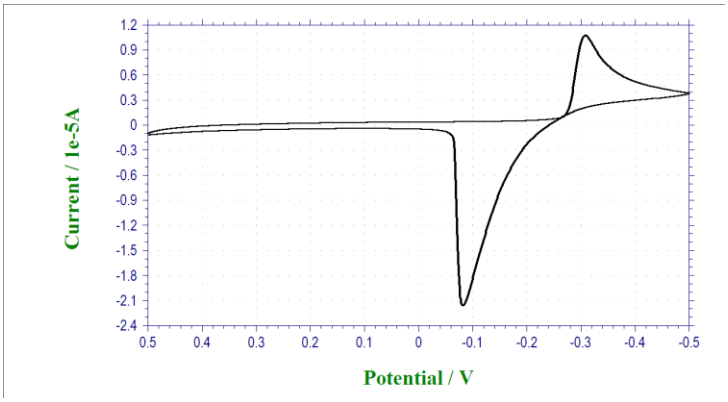

Fig. 5.10-a

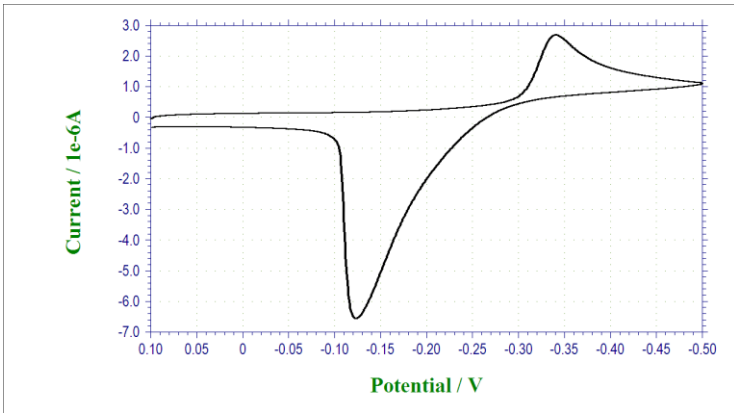

Fig. 5.10-b

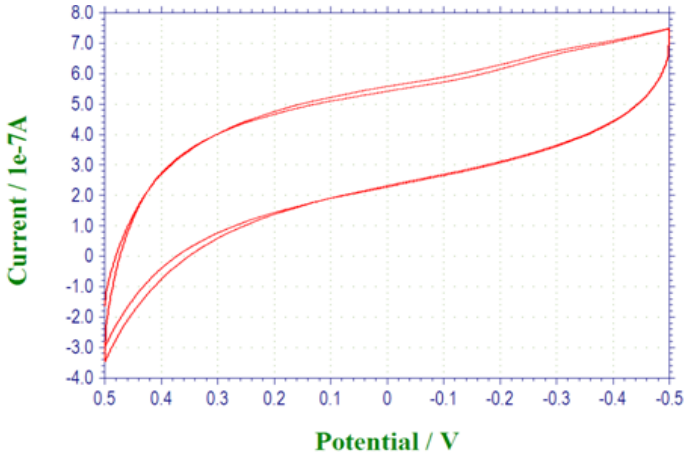

Fig. 5.10-c

CV study of cryptate Fig. 5.10

Following the similar template assisted methodology syntheses of the other silver cryptates were achieved by reacting TRPN with the linkers namely **1.**) 5,5'-methylene-bis-(2-hydroxy-3-methoxy-benzaldehyde) **2**.) 5,5'-methylene-bis-(3-bromo-2-hydroxy-benzaldehyde) **3**.) 5,5'-methylene-bis-(2-hydroxy-3-nitro-benzaldehyde)

4.) 5,5'-methylene-bis-(2-hydroxy-3-methyl-benzaldehyde) and **5**.) 5,5'-methylene-bis-(2-hydroxy-3-*tert*-butyl-benzaldehyde) (Fig. 5.11).

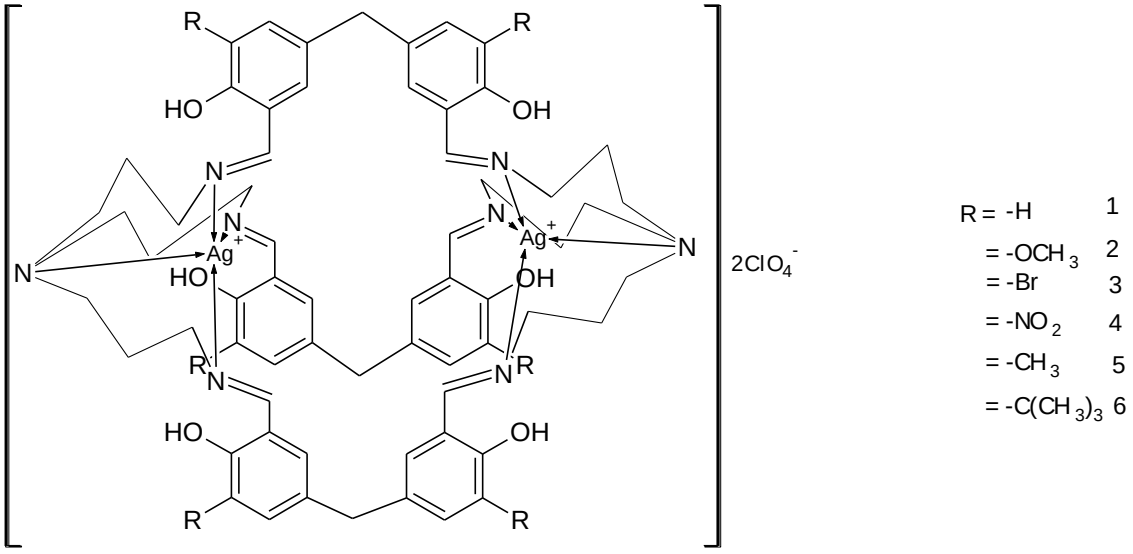

TRPN-(methylene-bis-(3-substitutedsalicylaldehyde)) derived silver cryptates

Fig. 5.11

The cryptates have similar spectral features as discussed above. Some of them show broader signals or signals with more peaks in proton NMR due to non-symmetrical binding in the cryptates. The HPLC analysis of these cryptates show from more than 90% to more than 99% purity. The silver cryptate derived from o-vanillin shows two overlapping peaks in 2:8 ratio in HPLC indicating the presence of isomeric cryptates.

Variable temperature NMR studies were carried out on three of the cryptates (with nitro, methyl and *tert*-butyl substituents) to study conformational changes taking place at higher temperatures. The proton NMR recorded at increasing temperature up to 70 °C at 5 to 10 degree temperature increment. For the nitro derivative multiple peak signals were converted to sharp signals at the temperature of 60 °C and above. The proton signal at 5.58 δ which is due to an aromatic proton, experiencing shielding effect, gradually decreases in intensity with increase in temperature and completely vanishes beyond 60 °C. Thus it can be concluded that due to facile equilibrium process with increase in

temperature NMR gets simplified resulting in a more stable symmetrical structure at high temperatures (Spectrum 5.18). For methyl derivative some noteworthy changes were observed in aliphatic region (Spectrum 5.24), while minor changes were observed for *tert*-butyl derivative because of the presence of six *tert*-butyl groups in the cryptate limiting degree of freedom in the macrocyclic structure up to temperature of 70 °C. (Spectrum 5.30).

Cyclic voltametric study of all the cryptates shows the presence of Ag^{+} having similarity with cyclic voltamogramme of silver nitrate solution in DMSO. The repeated changes in voltage give reproducible cyclic voltamogramme as expected, as was studied for the *tert*-butyl substituted cryptate. Cyclic voltamogramme of silver cryptates **2 to 6** are as below.

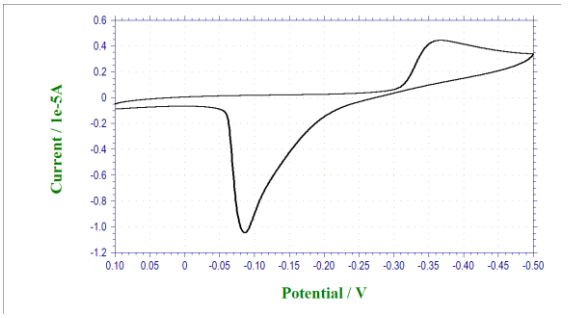

Fig. 5.12 Crptate 2

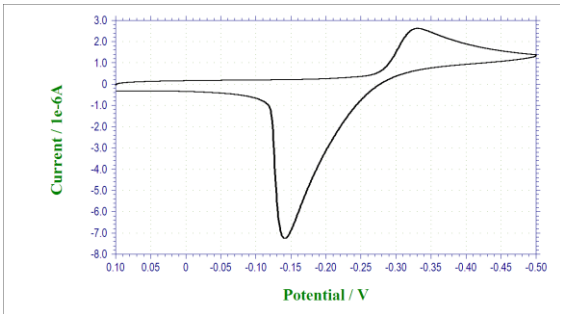

Fig. 5.13 Crptate 3

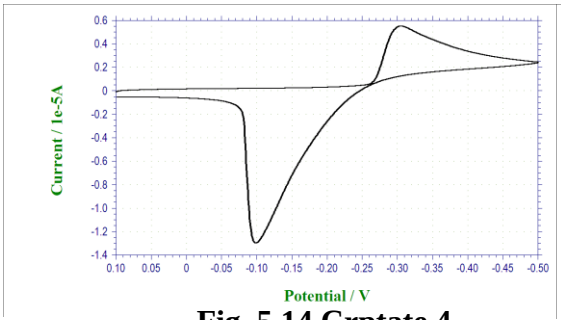

Fig. 5.14 Crptate 4

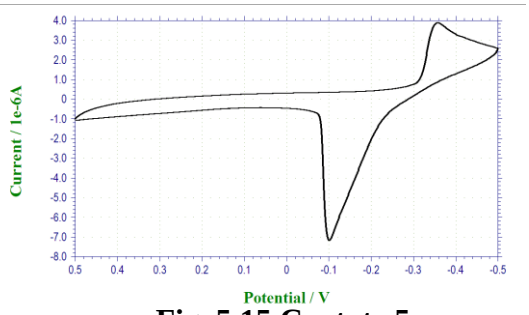

Fig. 5.15 Crptate 5

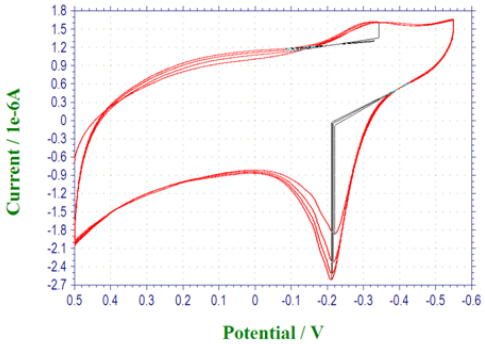

Fig. 5.16 Crptate 6

Q-TOF mass spectrum of the silver cryptate derived from TRPN and 5,5'-methylene-bis-(3-*tert*-butyl-salicylaldehyde) gave a prominent (M+1) peak at 1375 m/z corresponding to the molecular weight of the cryptand and also showed a peak at mass value 1583.75 m/z corresponding to one molecule of $AgClO_4$ indicating inclusion of one silver ion in the cryptate (Spectrum 5.31).

Biological activity studies

As some of the organo-silver compounds form prominent group of antimicrobial agents we decided to study antimicrobial activity of the newly synthesized silver cryptates and to find out structure activity relationship if present. Antibecterial activity of the cryptate was carried out against *S. aureus, S. pyogenus* and *P. vulgaris* as Gram positive bacterial strains and *E. Coli* and *P. aeruginosa* as Gram negative bacterial strains. Ciprofloxacin and silversulphadiazine were used as reference drugs. The minimum inhibitory concentration (MIC) of the cryptates was determined against these bacterial strains for the cryptates using broth dilution method. The MIC values of these silver cryptates are included in Table 5.2. The most prominent activity was observed for the *tert*-butyl-substituted cryptate. It shows MIC of 25 μg/ml against *S. aureus* which is lower than that of ciprofloxacin having MIC of 50 μg/ml and silversulphadiazine having MIC of 100 μg/ml against the same bacterial strain. The MIC of 50 μg/ml agaist *S. pyogenus* is same as the MIC of ciprofloxacin but is lower than that of silversulphadiazine with MIC 125 μg/ml. The cryptates with methyl and methoxy substitutions show prominent activity against *P. aeruginosa* and *S. pyogenus*, both of them have MIC of 100 μg/ml which is comparable to the activity of silversulphadiazine with MIC of 100 -125 μg/ml. Unsubstituted salicylaldehyde cryptate shows the most prominent activity against *S. pyogenus* and *P. vulgaris* with MIC 100 μg/ml comparable to the activity of silver sulphadiazine. The bromo substituted cryptate is having the lowest MIC of 100 μg/ml against *S. aureus.* Further investigation in this direction may lead to a highly potent antibacterial agent in form of *tert*-butyl cryptate.

Table 5.1 MIC of Drugs.

Minimum inhibitory concentration of standard drug					
DRUG	***E.COLI***	***P.AERUGINOSA***	***S.AUREUS***	***S.PYOGENUS***	***P.VULAGARIS***
(µg/ml)	MTCC 443	MTCC 1688	MTCC 96	MTCC 443	MTCC 744
Ciprofloxacin	25	25	50	50	25
Silver-sulphadiazine	50	100	100	125	50

Table 5.2 ANTIBACTERIAL ACTIVITY

MINIMUM INHIBITION CONCENTRATION (µg/ml)						
SR.	**Substituent**	***E.COLI***	***P.AERUGINOSA***	***S.AUREUS***	***S.PYOGENUS***	***P.VULAGARIS***
NO.	**R=**	**MTCC 443**	**MTCC 1688**	**MTCC 96**	**MTCC 443**	**MTCC 744**
1	-H	125	200	200	**100**	100
2	$-OCH_3$	200	**100**	125	**100**	250
3	-Br	250	200	**100**	200	125
4	$-NO_2$	125	500	500	500	250
5	$-CH_3$	150	**100**	200	**100**	200
6	$-C(CH_3)_3$	62.5	125	**25**	**50**	200

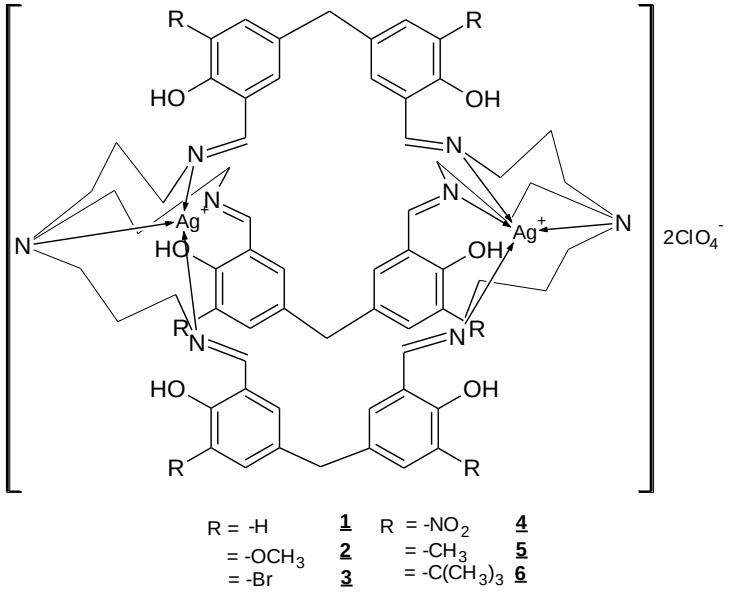

Fig. 5.11

Table 5.3 ANTIFUNGAL ACTIVITY

MINIMAL FUNGICIDAL CONCENTRATION		
SR.	**Substituent**	***C.ALBICANS***
NO.	**R=**	**MTCC 227**
1	-H	1000
2	$-OCH_3$	**500**
3	-Br	>1000
4	$-NO_2$	>1000
5	$-CH_3$	**500**
6	$-C(CH_3)_3$	**250**

The newly synthesized cryptates were also screened for their antifungal activity against *C. albicans.* The reference drugs used were nystatin and greseofulvin. Minimum fungicidal concentration was determined for the silver cryptates and results are shown in table 5.3. The most prominent activity is again shown by the *tert*-butyl derivative having MFC of 250 μg/ml lower than that of greceofulvin with MFC 500 μg/ml. Methyl and methoxy substituted cryptates also have prominent fungicidal activity of 500 μg/ml while cryptates with nitro and bromo functionality were ineffective as antifungal agents with MFC more than 1mg/ml. The study shows that cryptates with electron releasing substituents have effective fungicidal activity while the presence of electron withdrawing groups reduces the antifungal activity of the cryptate. The unsubstituted salicylaldehyde cryptate lies in between the cryptates having electron withdrawing and electron releasing groups. Overall the *tert*-butyl group containing cryptate is found to be most effective antimicrobial agent among the cryptates prepared by us.

5.4 Conclusion

Synthesis of larger cavity cryptands derived from TRPN and bis-aldehydes prepared by us could be achieved in 20 to 30% yields with the help of silver ion template. The need of template assisted synthesis in this case where the high dilution technique failed is attributed to greater flexibility and longer chain length of the tri-arm capping agent TRPN. Solubility of these cryptate in DMSO allowed spectral, voltametric and biological study of the cryptates. Spectral studies indicated the the existence of unsymmetrical nature of the cryptates. Due to amorphous state of cryptates obtained single crystal X-ray structure of the cryptates could not be studied. Attempts to obtain crystalline derivative of the cryptate are in progress. Primary antimicrobial activity study of the cryptates revealed that *tert*-butyl silver cryptate is most active and highly potent antibacterial and antifungal agent among the silver cryptates studied.

5.5 Experimental

General Remarks

All the chemicals and reagents were purchased from Sigma-Aldrich, Merck, and Spectrochem. All solvents were distilled before use. Column chromatography was carried out using silica-gel (60-120 mesh). Thin layer chromatography was performed on pre-coated silicagel $60F_{254}$ (Merck) aluminium sheets.

Infrared spectra were recorded on Perkin-Elmer FT-IR 16PC spectrophotometer as KBr pellets. ^{1}H NMR and ^{13}C NMR were recorded on Bruker 200 or 400 MHz NMR spectrophotometer in $CDCl_3$, DMSO or D_2O. ESI mass were recorded on Shimadzu LC-MS 2010-A and Micromass Quattro micro T. M. API Waters. HPLC was carried out using Shimadzu LC-10AT and UFLC using Shimadzu LC-20AD. Melting points were measured in open capillaries and are uncorrected. Cyclic voltamogrammes were recorded on CH 600 C Potentiostate using Ag/Ag^{+} as reference electrode, Pt disk as working electrode and Pt wire as counter electrode.

Tris(3-aminopropyl)amine(TRPN) derived silver cryptates.

General synthesis.

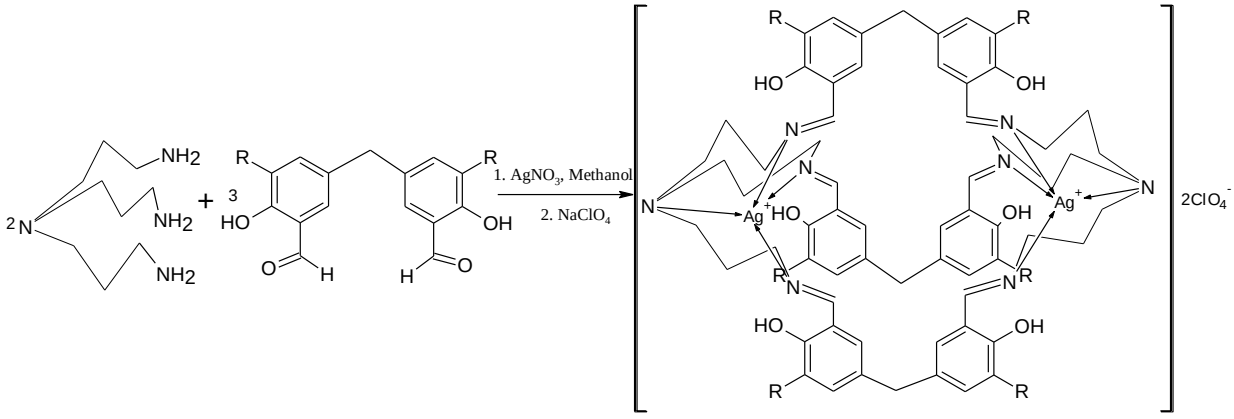

Methanol (120 ml) was placed in 250 ml 2 necked round bottom flask equipped with an addition funnel and a nitrogen balloon. Nitrogen was purged for 30 minutes. 5,5'-Methylene-bis-aldehydes (0.002 mol) and $AgNO_3$(0.002 mol) were added in single charge and stirred for further 30 minutes in dark. TRPN (tris-(3-aminopropyl)amine) (0.001 mol) in methanol (50 ml) was added drop wise from addition funnel over 2 hrs to the magnetically stirred reaction mixture under nitrogen atmosphere. The resulting solution was stirred overnight at 30 ^{o}C. Greenish yellow solution was filtered through cellite under vacuum and yellow clear filtrate was charged to 250 ml round bottom flask. Solution of sodium perchlorate monohydrate (0.004 mol) in methanol (30 ml) was added drop wise to the above solution over 10 minutes and stirred for 4 hrs. Yellow ppts were filtered and dried in vacuum.

Silvercryptate from TRPN and 5,5'-methylene-bis-salicylaldehyde **1**.

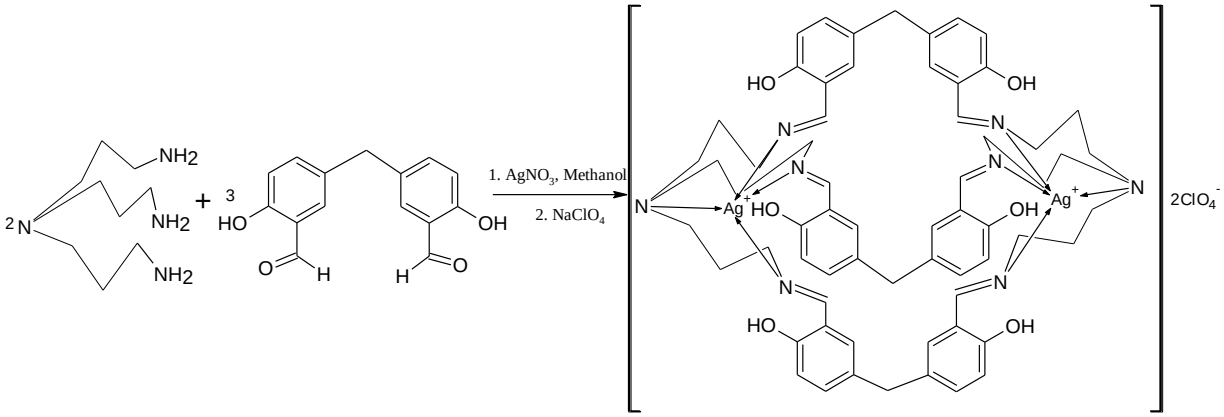

1.

5,5'-Methylene-bis-salicylaldehyde (0.5 g, 0.002mol), TRPN (tris(3-aminopropyl)amine) (0.25 g, 0.001mol), $AgNO_3$ (0.28g, 0.002 mol) and sodium perchlorate monohydrate (0.55g, 0.004mol) were reacted in methanol (200 ml) to yield compound **1**.

Yield: 0.240 g (25%)

M.P .> 300 ^{o}C.

^{1}H NMR (400 MHz, $CDCl_3$): δ 13.19 (1H), 8.21 (1H), 7.12 (1H), 6.85 (1H), 6.74 (1H), 3.67 (1H), 3.54 (2H), 2.45 (2H), 1.75 (2H).

^{13}C NMR (400 MHz, DMSO-d_6): δ 165.9, 164.1, 159.6, 159.2, 156.2, 137.3, 134.3, 133.2, 132.4, 131.9, 131.4, 128.7, 125.4, 118.9, 117.8, 116.9, 116.4, 61.9, 56.9, 53.9, 51.4, 36.4, 31.6, 28.4, 21.8

Mass: 1037.6 [M^+]

HPLC Purity: 96.4%

IR (KBr disc, cm^{-1}) : 3368 (phenol, υ(O-H)), 2923 (methylene, $υ_{as}$(C-H)), 2857 methylene, $υ_s$(C-H)), 2363, 1638 (imine, υ(C=N)), 1542, 1506 (aromatic ring, υ(C=C)), 1438 ($δ_s(CH_2)$), 1270, 1202 (aromatic, υ(C-N)), 1095 (aliphatic, υ(C-N)), 925, 883, 828, 771, 472 (out of plane, δ(C-H)), 623(υClO_4).

Silvercryptate from TRPN and 5,5'-methylene-bis-(3-methoxy-salicylaldehyde) 2.

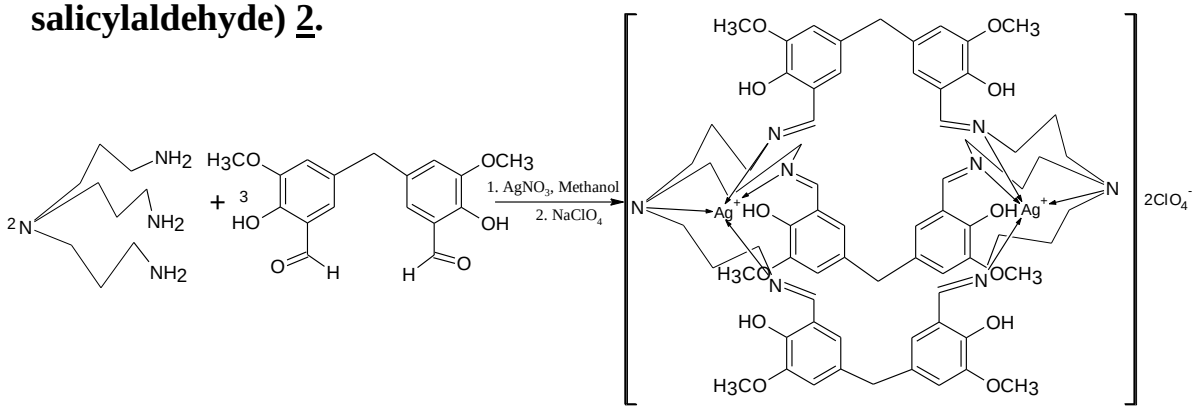

2

5,5'-Methylene-bis-(3-methoxy-salicylaldehyde) (0.5g, 0.002mol), TRPN (tris(3-aminopropyl)amine) (0.20g, 0.001mol), $AgNO_3$ (0.22g, 0.001mol), sodium perchlorate monohydrate (0.44g, 0.003mol) reacted in methanol (200ml) to yield the compound **2**.

Yield: 0.254 g (30%)

M.P. >300 ^{o}C.

^{1}H NMR (400 MHz, DMSO-d_6): δ 13.60 (1H), 8.41 (1H), 6.82 (1H), 3.73 (3H), 3.21 (1H), 2.74 (2H), 2.67 (1H), 1.60 (1H)

^{13}C NMR (400 MHz, DMSO-d_6): δ 166.6, 147.8, 142.9, 131.7, 130.6, 125.2, 122.9, 119.3, 116.0, 112.6, 116.4, 99.7, 56.1, 53.9, 53.8, 28.4

HPLC Purity: 78.6%

IR (KBr disc, cm^{-1}) : 2941 (methylene, υ_{as}(C-H)), 2835 methylene, υ_s(C-H)), 1650,1639 (imine, υ(C=N)), 1541, 1508 (aromatic ring, υ(C=C)), 1457 ($\delta_s(CH_2)$), 1267 (aromatic, υ(C-N)), 1152 (ether, υ_sC-O), 1091 (aliphatic, υ(C-N)), 862, 705,470 (out of plane, δ(C-H)), 621 (υClO_4)

Silvercryptate from TRPN and 5,5'-methylene-bis-(3-bromo-salicylaldehyde) <u>3</u>.

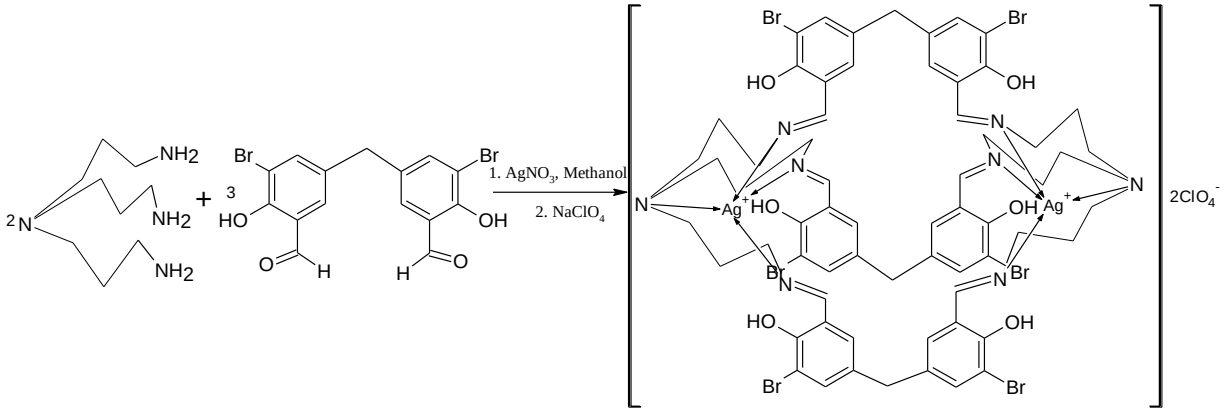

<u>3</u>

5,5'-Methylene-bis-(3-bromo-salicylaldehyde) (1g, 0.002mol), TRPN (tris(3-aminopropyl)amine) (0.30g, 0.002mol), $AgNO_3$ (0.34g, 0.002mol) and sodium perchlorate monohydrate (0.68g, 0.005mol) were reacted in mixture of methanol (200 ml) and MDC (50ml) to yield compound **<u>3</u>**.

Yield: 0.300 g (19%)

M.P.=202 ^{o}C.

^{1}H NMR (400 MHz, DMSO-d_6): δ 14.36 (1H), 8.46 (1H), 7.46 (1H), 7.16 (1H), 3.75 (3H), 3.22 (2H), 1.92 (2H).

^{13}C NMR (400 MHz, DMSO-d_6): δ 166.7, 159.8, 159.3, 137.3, 133.2, 131.6, 131.2, 130.0, 128.7 127.6, 124.7, 122.6, 118.8, 118.4, 117.9, 117.1, 115.9, 111.8, 99.7, 56.1, 53.9, 50.5, 49.1, 25.6

HPLC Purity: 90.0%

IR (KBr disc, cm^{-1}) : 3013 (phenol, υ(O-H)), 2943 (methylene, υ_{as}(C-H)), 2839 (methylene, υ_s(C-H)), 1643 (imine, υ(C=N)), 1493 (aromatic ring, υ(C=C)), 1478 ($\delta_s(CH_2)$), 1381, 1277, 1238 (aromatic, υ(C-N)), 1098 (aliphatic, υ(C-N)), 928, 843 (out of plane, δ(C-H)), 623 (υClO_4)

Silvercryptate from TRPN and 5,5'-methylene-bis-(3-nitro-salicylaldehyde) 4

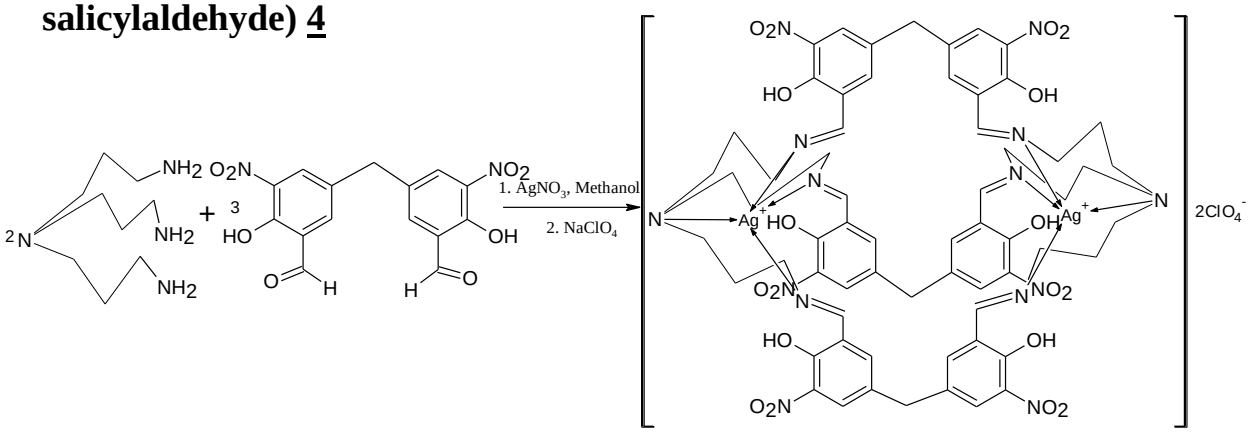

4

5,5'-Methylene-bis-(3-nitro-salicylaldehyde) (0.9g, 0.003mol), TRPN (tris(3-aminopropyl)amine) (0.33g, 0.002mol), $AgNO_3$ (0.37g, 0.002mol) and sodium perchlorate monohydrate (0.73g, 0.005mol) were reacted in a mixture of methanol (200ml) and MDC (50ml) to yield the compound **4**.

Yield : 0.577 g (26%)

M.P.=220 ^{o}C (decomposed).

^{1}H NMR (400 MHz, DMSO-d_6): δ 14.42 (1H), 8.49 (1H), 7.89 (1H), 7.46 (1H), 3.86 (1H), 3.81(2H), 2.44 (2H), 1.83 (2H).

HPLC Purity: 99.7%

IR (KBr disc, cm^{-1}) : 3599, 3065 (phenol, υ(O-H)), 2941 (methylene, $υ_{as}$(C-H)), 2839 methylene, $υ_s$(C-H)), 1649 (imine, υ(C=N)), 1533 (nitro, $υ_{as}$(N--O)), 1468 ($δ_s(CH_2)$), 1350 (nitro, $υ_s$(N--O)),, 1288, 1248 (aromatic, υ(C-N)), 1098 (aliphatic, υ(C-N)), 988, 930, 829, 783, 656, 517 (out of plane, δ(C-H)), 623 ($υClO_4$)

Silvercryptate from TRPN and 5,5'-methylene-bis-(3-methyl-salicylaldehyde) 5

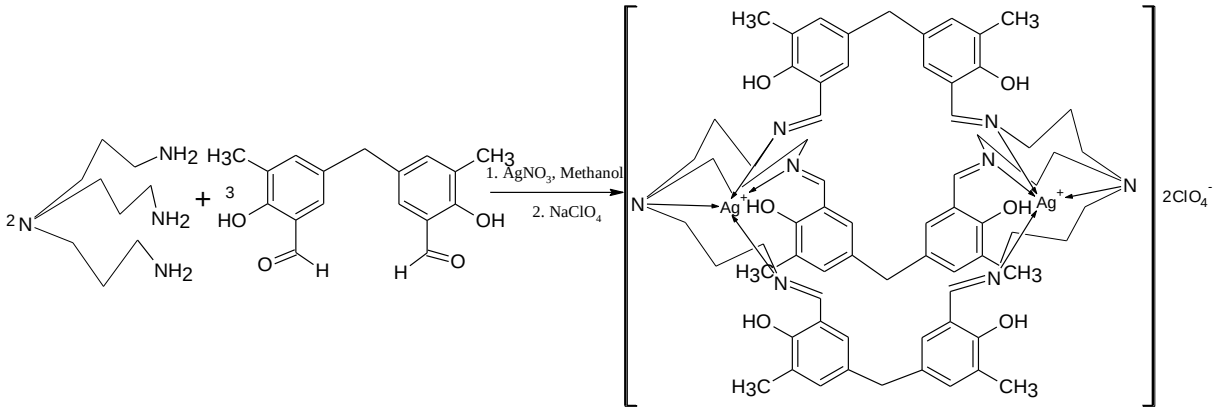

5

5,5'-Methylene-bis-(3-methyl-salicylaldehyde) (0.8g, 0.003 mol), TRPN (tris(3-amino-propyl)amine) (0.35g, 0.002 mol), $AgNO_3$ (0.40g, 0.002 mol), and sodium perchlorate monohydrate (0.79 g, 0.006mol) were reacted in mixture of methanol (200 ml) and MDC (50 ml) to yield the compound **5**.

Yield: 0.425 g (30%)

M.P.=120 ^{o}C (decomposed).

^{1}H NMR (400 MHz, DMSO-d_6): δ 13.58 (1H), 8.32 (1H), 6.98 (2H), 3.76 (1H), 2.68 (2H), 2.03 (2H), 1.66 (2H).

^{13}C NMR (400 MHz, DMSO-d_6): δ 166.4, 157.8, 133.9, 131.5, 129.1 125.2, 117.9, 79.9, 56.6, 49.9, 41.7, 28.5, 15.7

HPLC Purity: 99.2%

IR (KBr disc, cm^{-1}) : 3595, 3329 (phenol, υ(O-H)), 2943 (methylene, $υ_{as}$(C-H)), 2851 (methylene, $υ_s$(C-H)), 1632 (imine, υ(C=N)), 1601, 1545 (aromatic ring, υ(C=C)), 1478 ($δ_s(CH_2)$), 1381, 1335, 1269 (aromatic, υ(C-N)), 1094 (aliphatic, υ(C-N)), 885, 856, 752, 488 (out of plane, δ(C-H)), 623 ($υClO_4$)

Silvercryptate from TRPN and 5,5'-methylene-bis-(3-*tert*-butyl-salicylaldehyde) 6

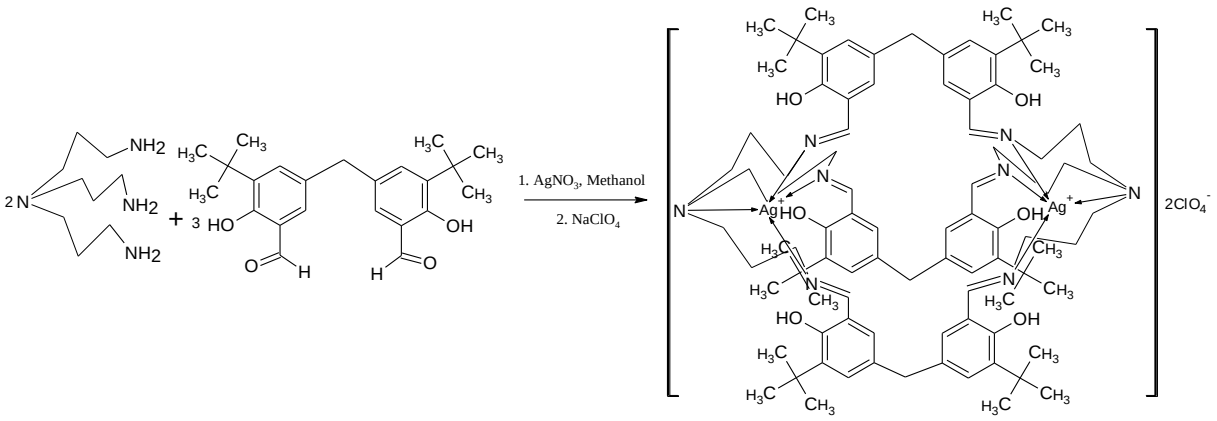

6

5,5'-Methylene-bis-(3-*tert*-butyl-salicylaldehyde) (1g, 0.003mol), TRPN (tris(3-aminopropyl)amine) (0.34g, 0.002mol), $AgNO_3$ (0.38g, 0.002mol), sodium perchlorate monohydrate (0.76g, 0.005mol) were reacted in methanol (200ml) to yield the compound **6**.

Yield: 0.552 g (34%)

M.P. > 300 ^{o}C.

^{1}H NMR (400 MHz, DMSO-d_6): δ 14.21 (1H), 8.31 (1H), 7.08 (1H), 6.86 (1H), 1.64 (4H), 1.26 (9H)

Mass: 1375.0 [M+1]

HPLC Purity:

IR (KBr disc, cm^{-1}) : 3570 (phenol, υ(O-H)), 2955 (methylene, asymmetric υ(C-H)), 2866 (methylene, symmetric υ(C-H)), 2361, 1632, 1633 (imine, υ(C=N)), 1466, 1440 ($\delta_s(CH_2)$), 1389,1266, 1211 (aromatic, υ(C-N)), 1075 (aliphatic, υ(C-N)), 977, 855, 800, 773, 707, 572 (out of plane, δ(C-H)), 623(υClO_4).

Antibacterial and antifungal activity study

Broth dilution method was used to determine minimum inhibitory concentration (MIC) values for gram positive as well as gram negative bacterial strains and to determine minimum fungicidal (MFC) values for *C. albicans*. DMSO was used as diluents / vehicle to get desired concentration of the test compounds to measure their activity against standard bacterial strains. Silversulphadiazine and ciprofloxacin were the standard antibacterial drugs used for the comparison of MIC values while greceofulvin and nystatin were used as standard antifungal dugs for the comparison of MFC values.

Mueller Hinton broth was used as nutrient medium to grow and dilute the drug (or compound) suspension for the test bacteria. Inoculum size for test strain was adjusted to 10^8 CFU [Colony Forming Unit] per milliliter by comparing the turbidity. The strains were procured from Institute of Microbial Technology, Chandigarh.

Procedure:

1. Serial dilutions were prepared in primary and secondary screening.
2. The control tube containing no antibiotic is immediately sub cultured [before inoculation] by spreading a loopful evenly over a quarter of plate of medium suitable for the growth of the test organism and put for incubation at 37 $^{\circ}$C overnight.
3. The MIC of the control organism was read to check the accuracy of the drug concentrations.
4. The lowest concentration inhibiting growth of the organism was recorded as the MIC.
5. The amount of growth from the control tube before incubation [which represents the original inoculum] is compared.
6. Each synthesized drug was diluted obtaining 2000 microgram /ml concentration, as a stock solution.
7. **Primary screen:** In primary screening, 1000 microgram/ml, 500 microgram/ml, and 250 microgram/ml concentrations of the synthesized drugs were taken. The

active drugs found in this primary screening were further tested in a second set of dilution against all microorganisms.

8. **Secondary screen:** The drugs found active in primary screening were similarly diluted to obtain 200 microgram/ml 100 microgram/ml, 50 microgram/ml, 25 micro/ml, 12.5 microgram/ml and 6.25 microgram/ml concentrations.
9. **Reading Result:-** The highest dilution showing at least 99 % inhibition zone is taken as MIC.

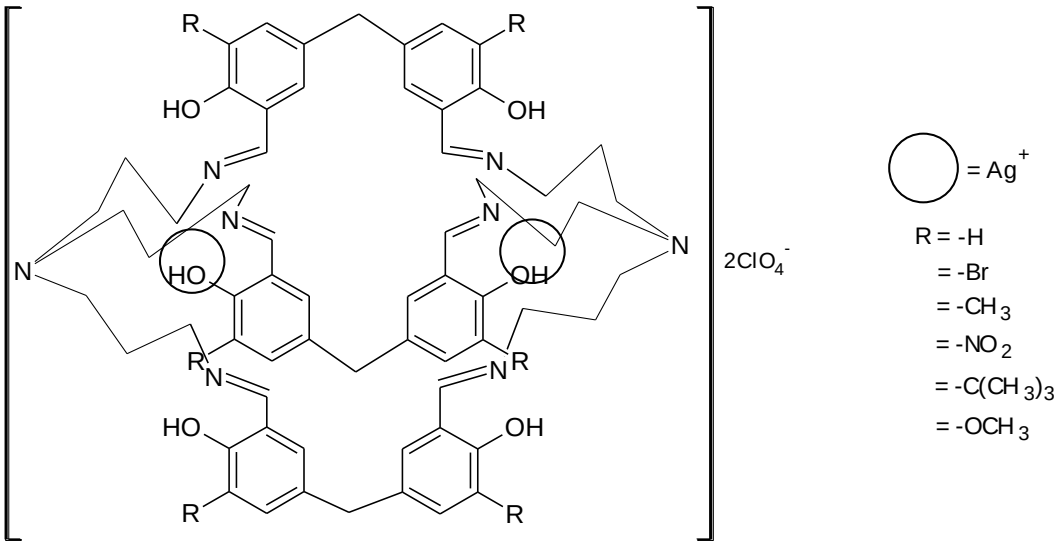

Table: 5.3 Minimum inhibitory concentration values for various bacterial strains

DRUG	*E. COLI*	*P. AERUGINOSA*	*S. AUREUS*	*S. PYOGENUS*	*P. VULAGARIS*
(µg/ml) **R=**	MTCC 443	MTCC 1688	MTCC 96	MTCC 443	MTCC 744
-H	125	200	200	**100**	100
-Br	250	200	**100**	200	125
$-CH_3$	150	**100**	200	**100**	200
$-NO_2$	125	500	500	500	250
$-C(CH_3)_3$	62.5	125	**25**	**50**	200
$-OCH_3$	200	**100**	125	**100**	250
Ciprofloxacin	25	25	50	50	25
Silver-sulphadiazine	50	100	100	125	50

Table: 5.4 Minimum Fungicidal concentration values of various cryptates

DRUG	***C.ALBICANS***
(µg/ml) Sustituent on aromatic ring **R=**	**MTCC 227**
-H	1000
-Br	>1000
$-CH_3$	**500**
$-NO_2$	>1000
$-C(CH_3)_3$	**250**
$-OCH_3$	**500**
NYSTATIN	100
GRESEOFULVIN	500

5.6 Spectra

Spectrum 5.1

IR

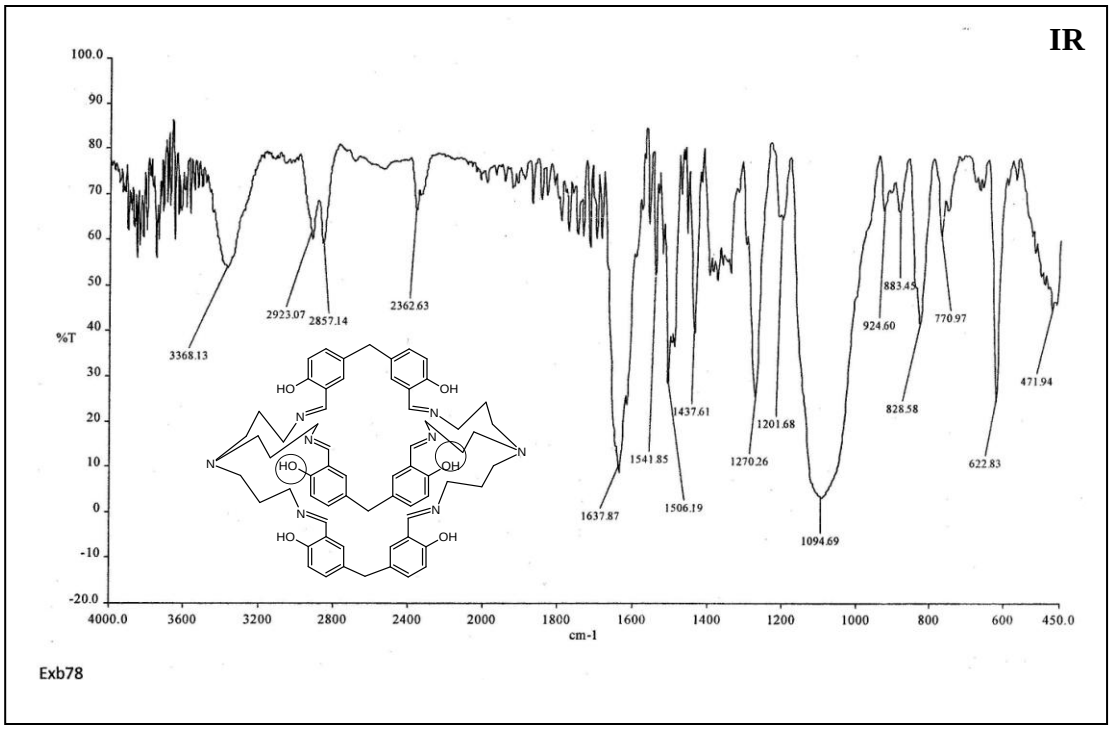

Spectrum 5.2

^{1}HNMR

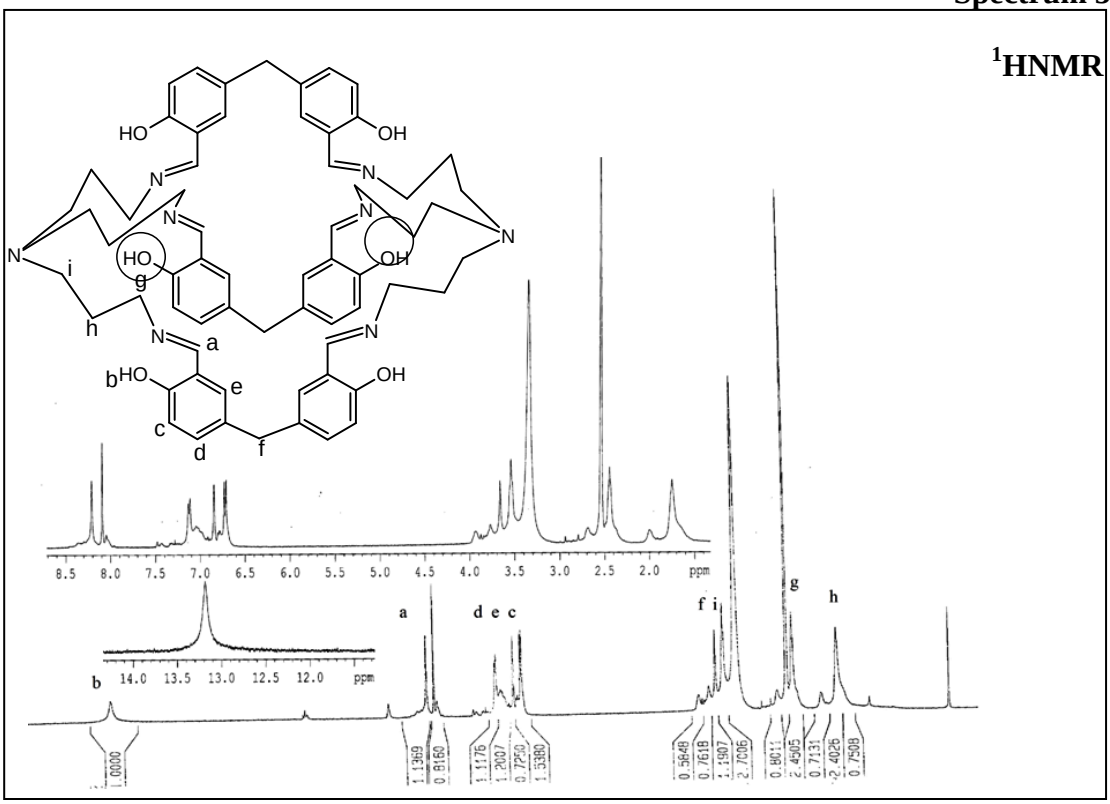

Spectrum 5.3

^{13}CNMR

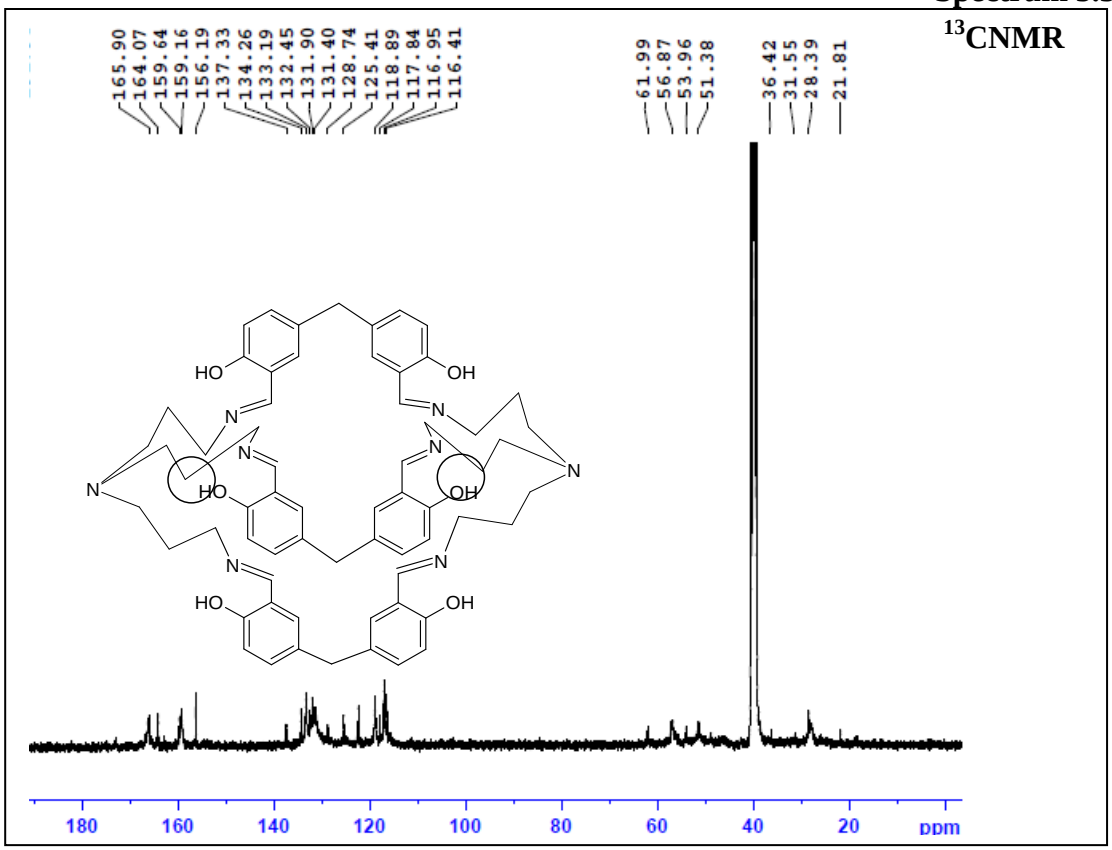

Spectrum 5.4

DEPT 90

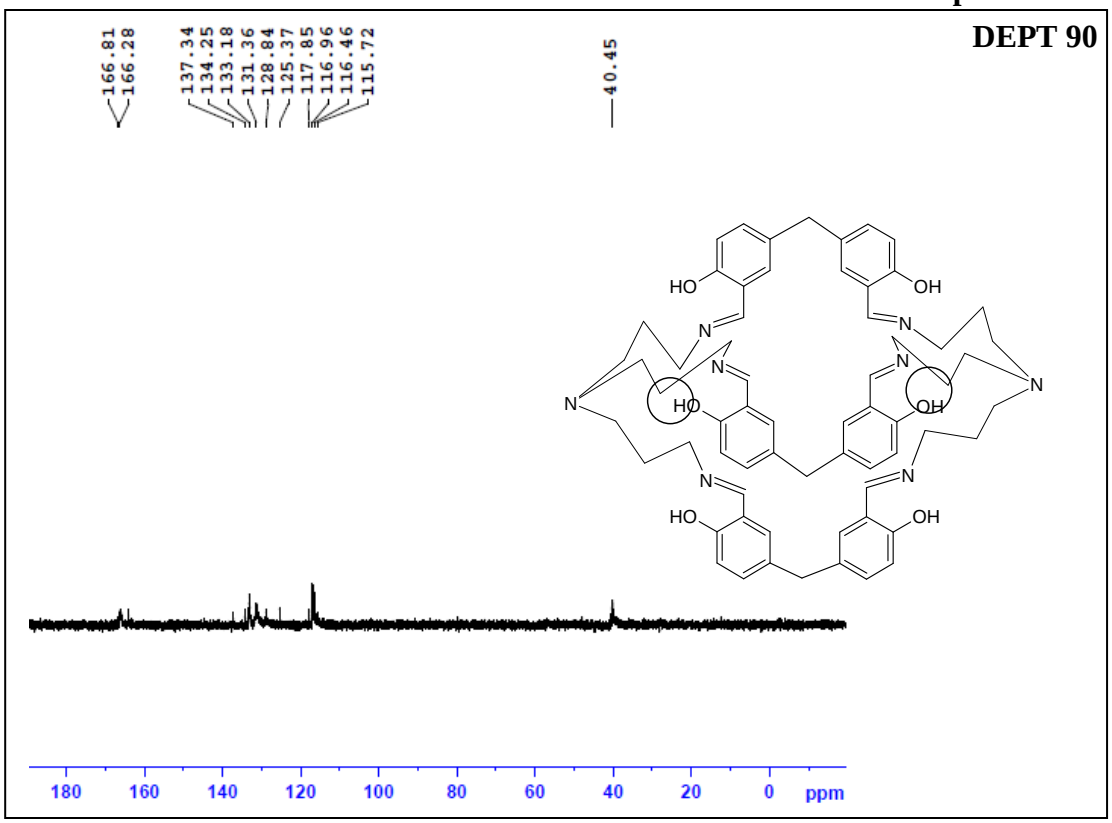

Spectrum 5.5

Mass

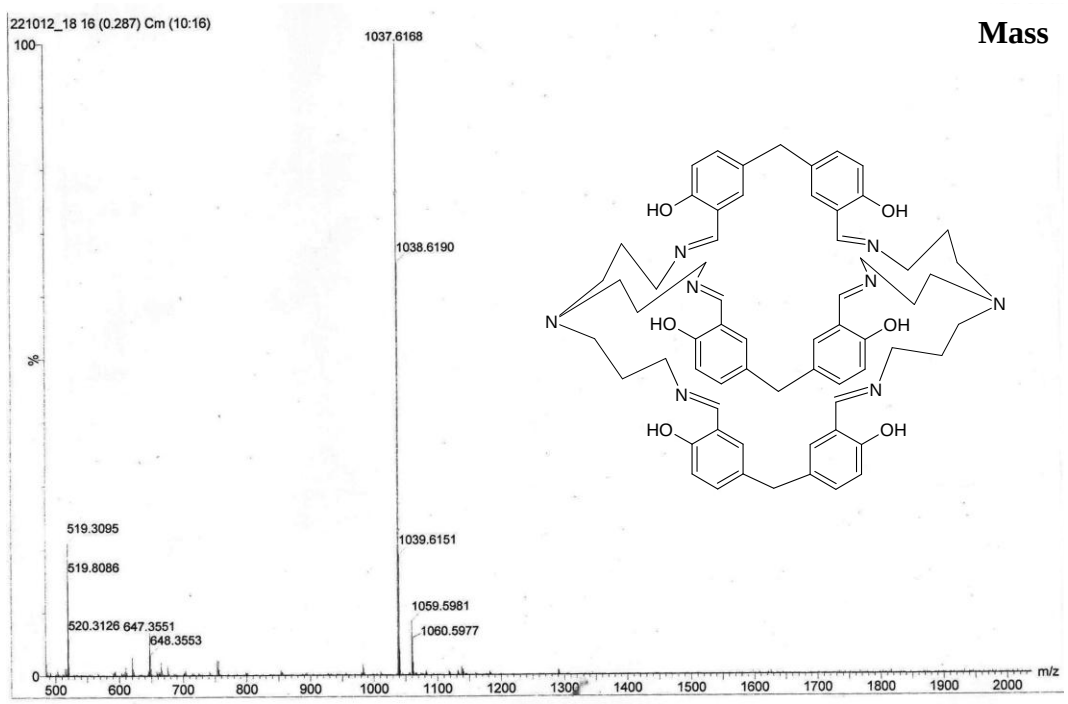

Chromatogram 5.6

HPLC

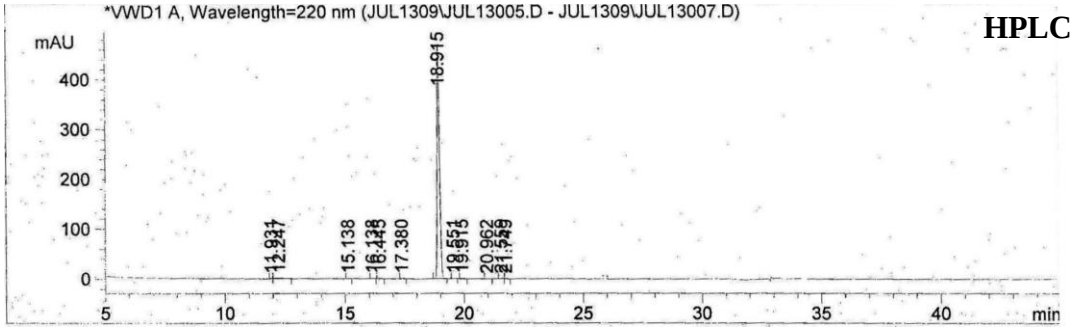

Peak #	RetTime [min]	Type	Width [min]	Area mAU *s	Height [mAU]	Area %
1	1.334	BBA	0.0891	59.66290	10.35569	1.7027
2	11.931	PV	0.0760	2.30479	4.59329e-1	0.0658
3	12.247	VBA	0.3207	28.91982	1.28570	0.8254
4	15.138	BBA	0.1088	2.11224	3.09420e-1	0.0603
5	16.138	BP	0.0987	2.56124	3.96413e-1	0.0731
6	16.445	BBA	0.1309	4.12681	5.01835e-1	0.1178
7	17.380	PB	0.0930	3.62675	5.82768e-1	0.1035
8	18.915	BBA	0.1070	3376.47998	470.81680	96.3627
9	19.551	PBA	0.1053	3.28618	4.76255e-1	0.0938
10	19.915	BP	0.1195	7.93873	1.04118	0.2266
11	20.962	BB	0.1310	2.13795	2.44826e-1	0.0610
12	21.559	PV	0.1045	8.14074	1.16950	0.2323
13	21.749	VBA	0.1130	2.63109	3.42299e-1	0.0751
Totals :				3503.92923	487.98201	

Spectrum 5.7

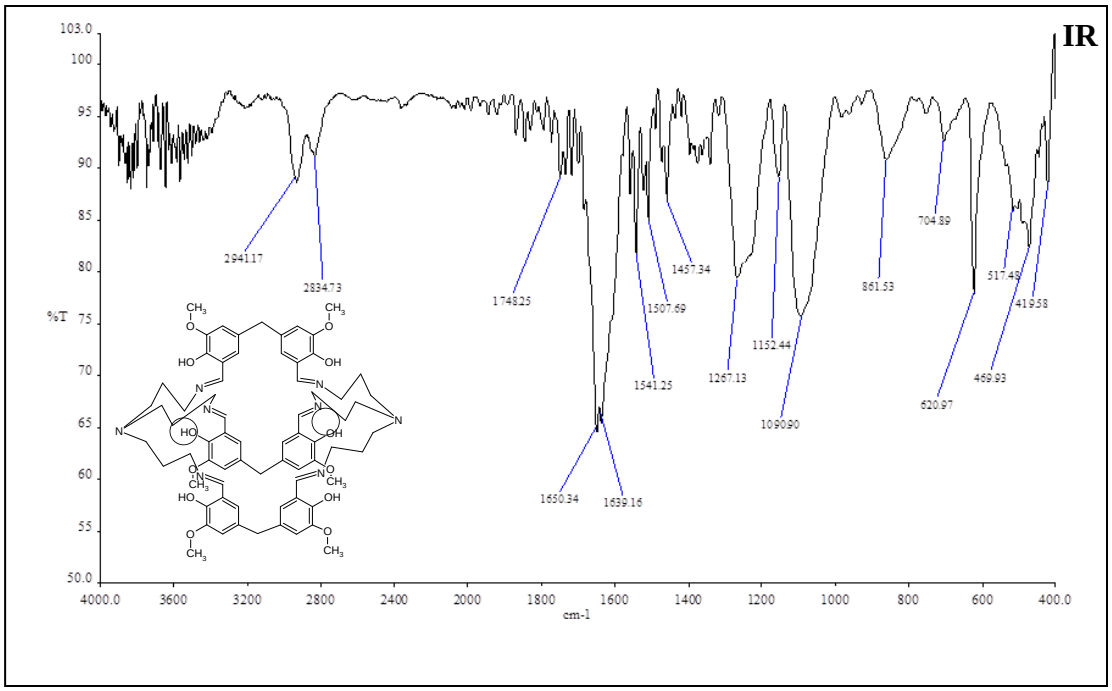

Spectrum 5.8

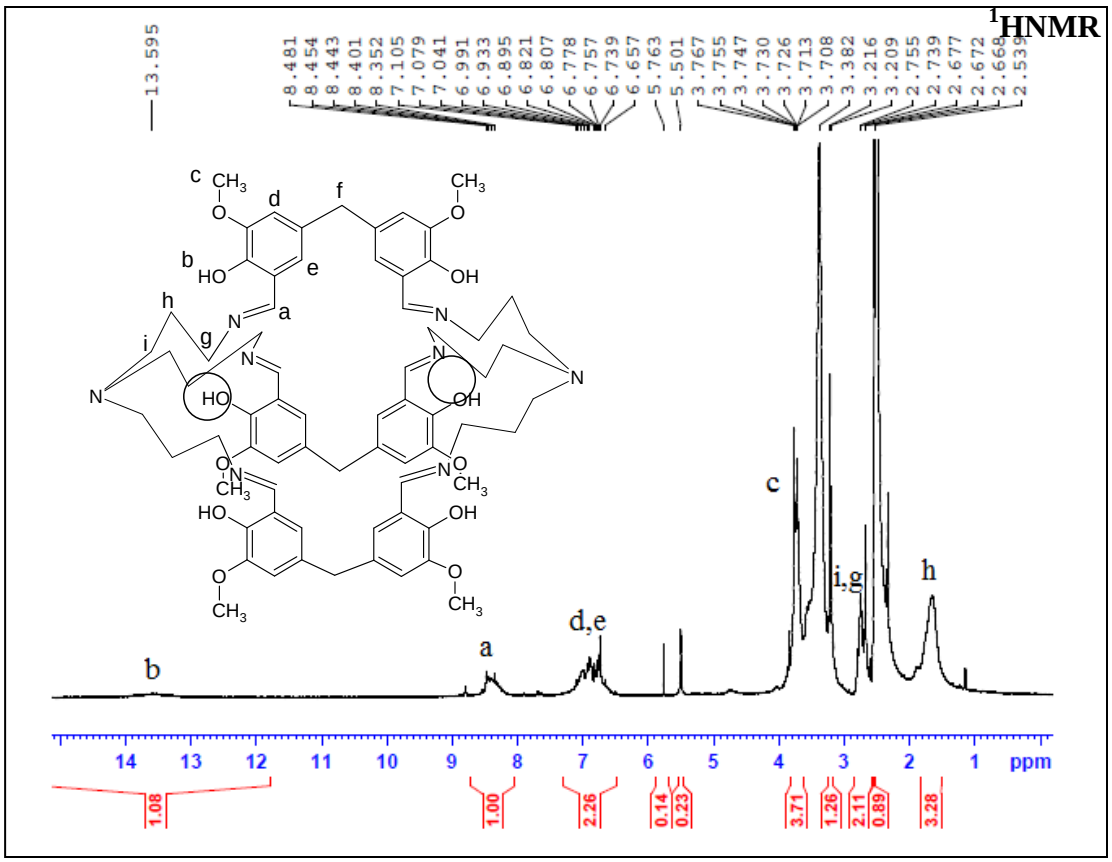

Spectrum 5.9

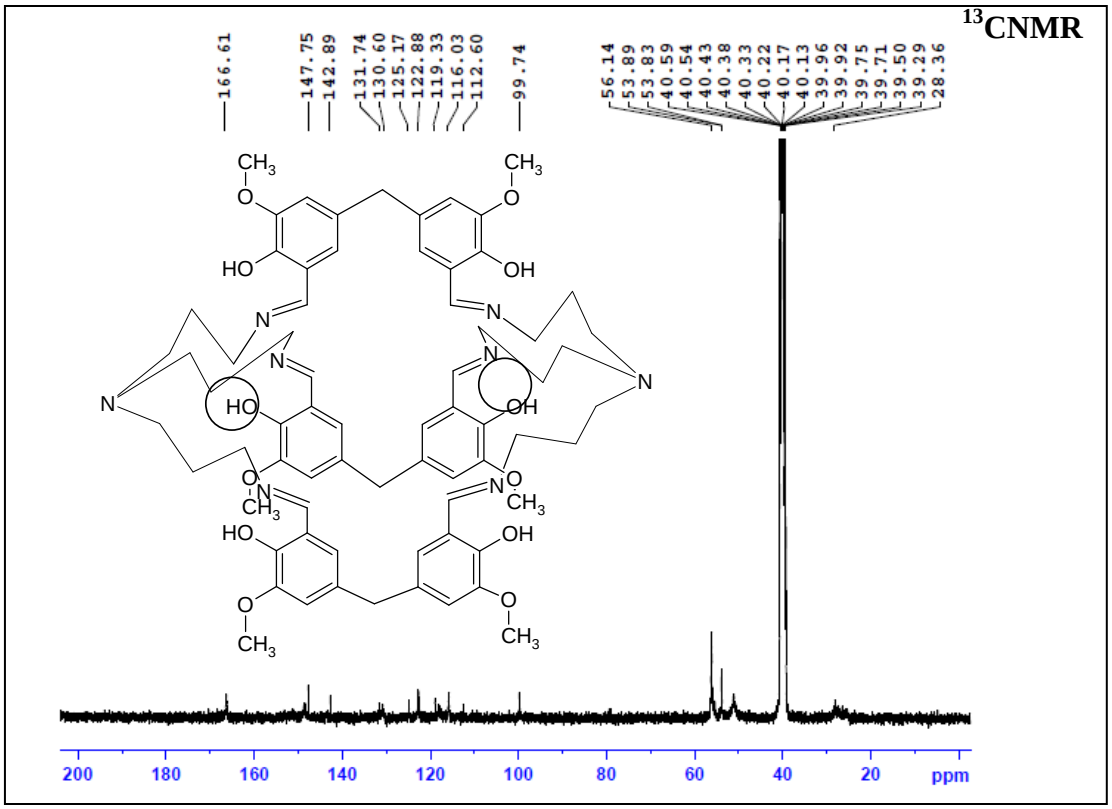

Chromatogram 5.10

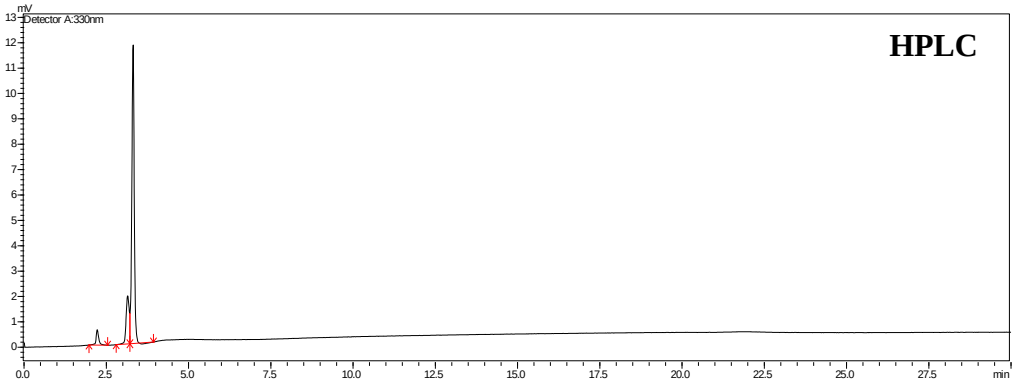

Mobile phase: MDC:MeOH :: 96:4 (v/v), Stationary phase : Silica column

Peak	Name	Ret. Time	Area%
1	imp 1	2.219	4.6120
2	imp 2	3.145	16.7821
3.	EXPT C-226(Silver cryptate from TRPN and 5,5'methylene –bis-3-methoxysalicylaldehyde)	3.310	78.6059

Spectrum 5.11

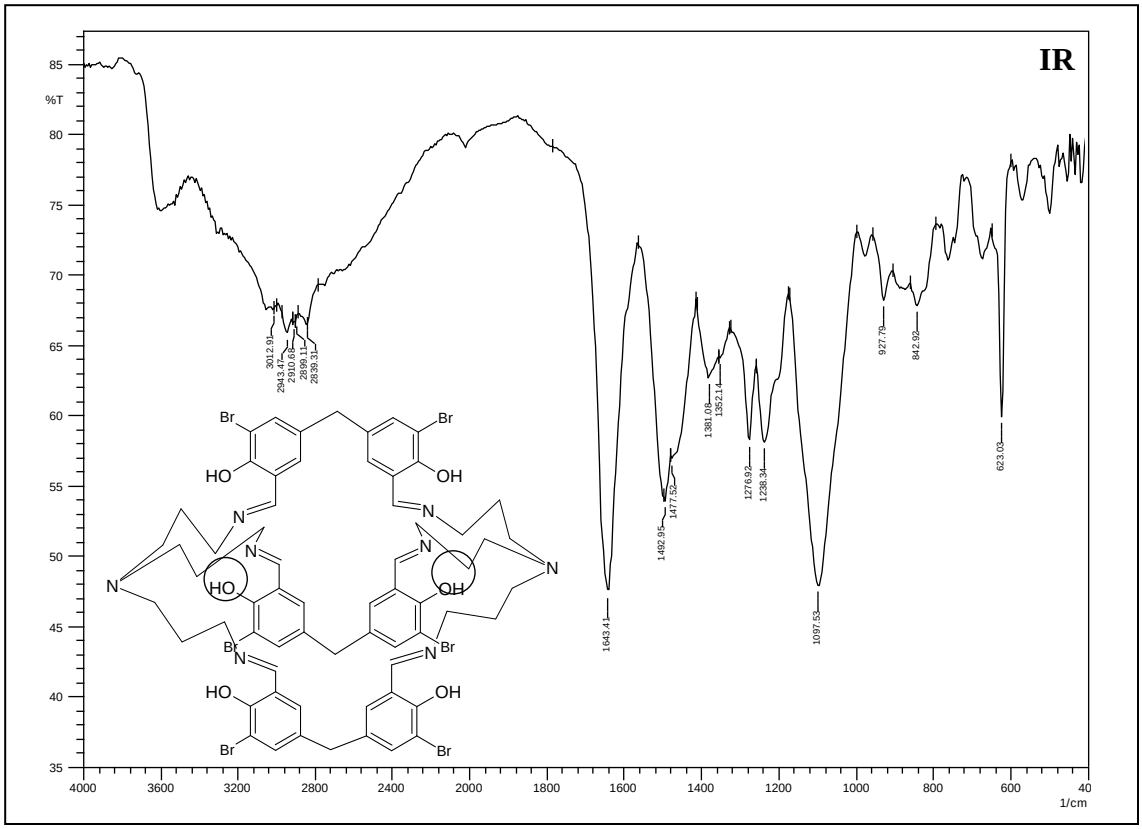

Spectrum 5.12

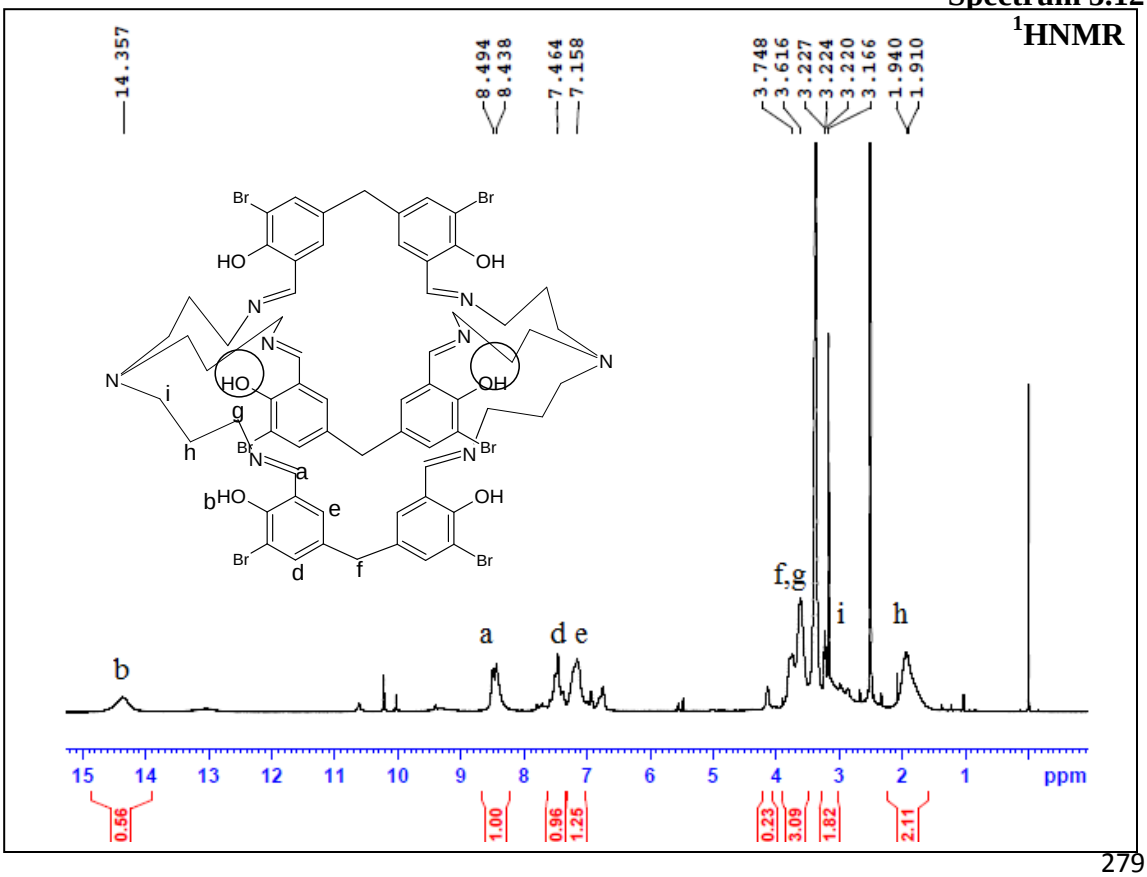

Spectrum 5.13

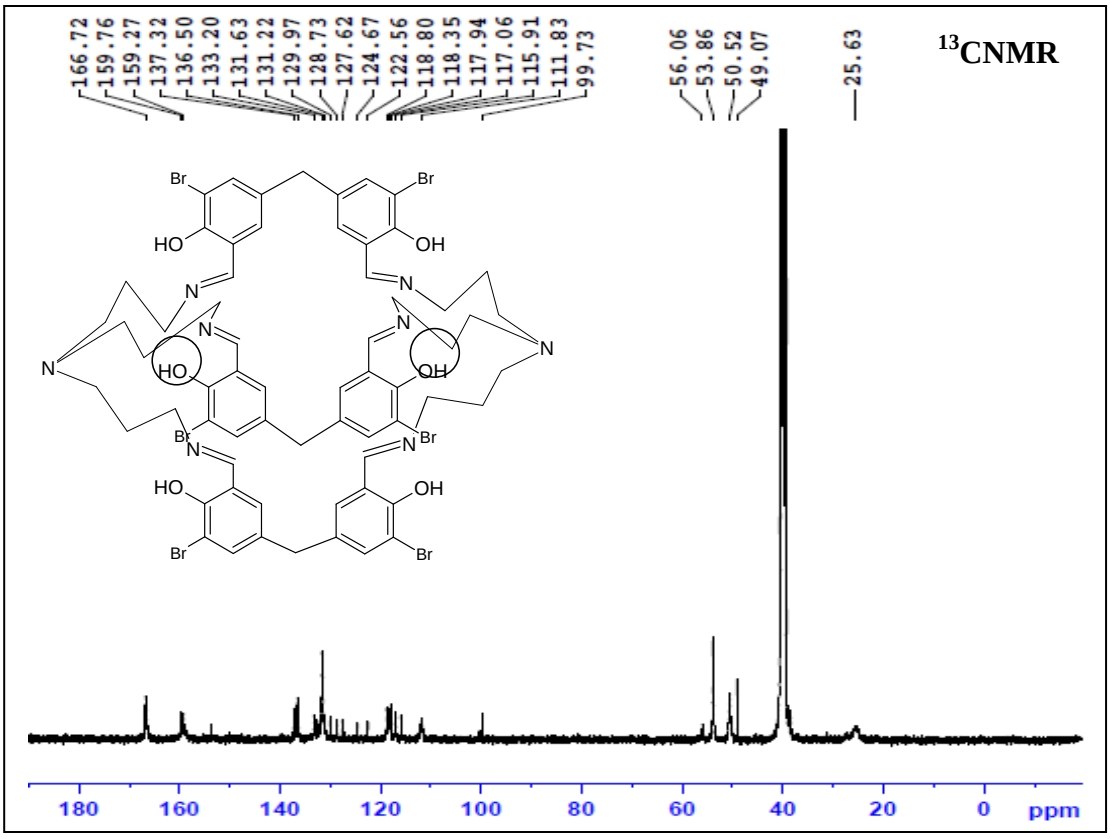

Chromatogram 5.14

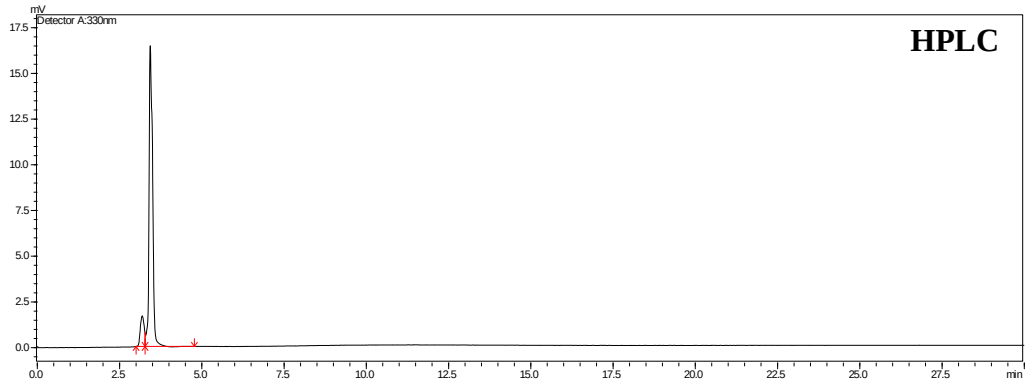

Mobile phase: MDC:MeOH :: 99:1 (v/v), Stationary phase : Silica column

Peak	Name	Ret. Time	Area%
1	EXPT C-222(Silver cryptate from TRPN and 5,5'methylene –bis-3-bromosalicylaldehyde)	3.186	9.9716
2	imp 1	3.428	90.0284

Spectrum 5.15

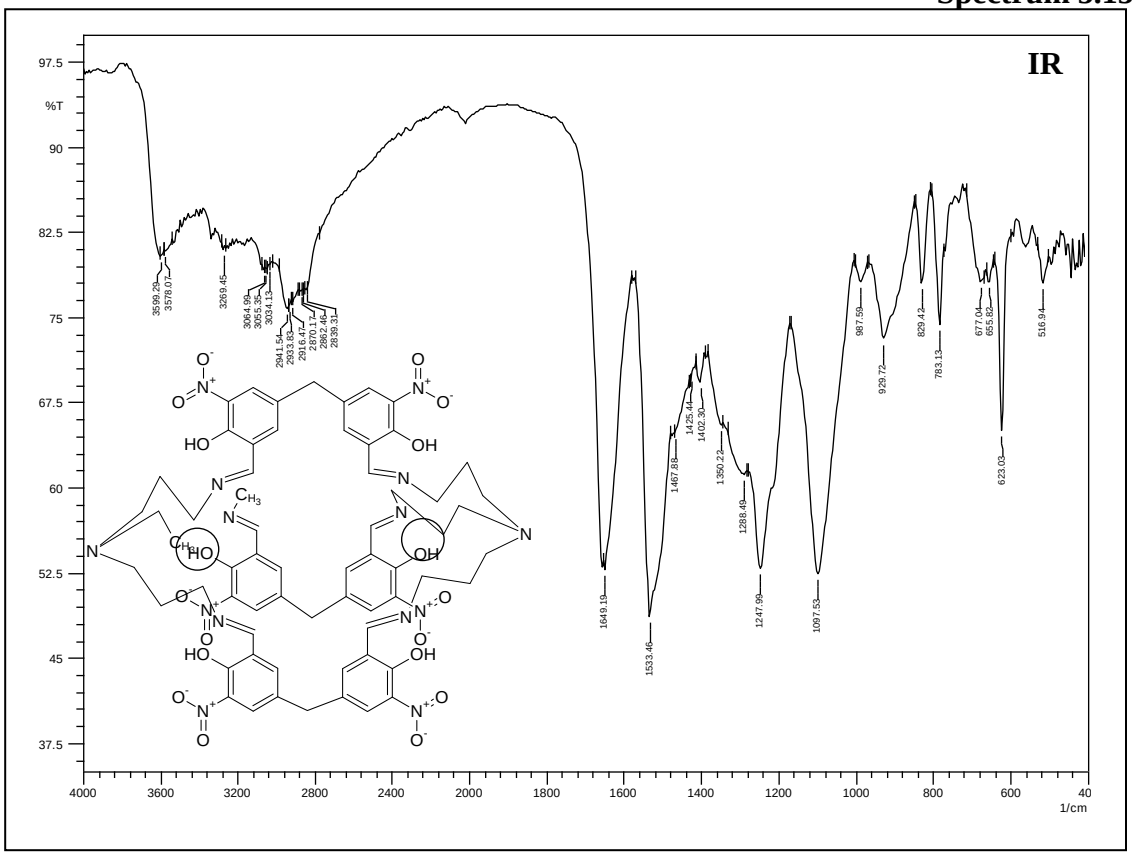

Spectrum 5.16

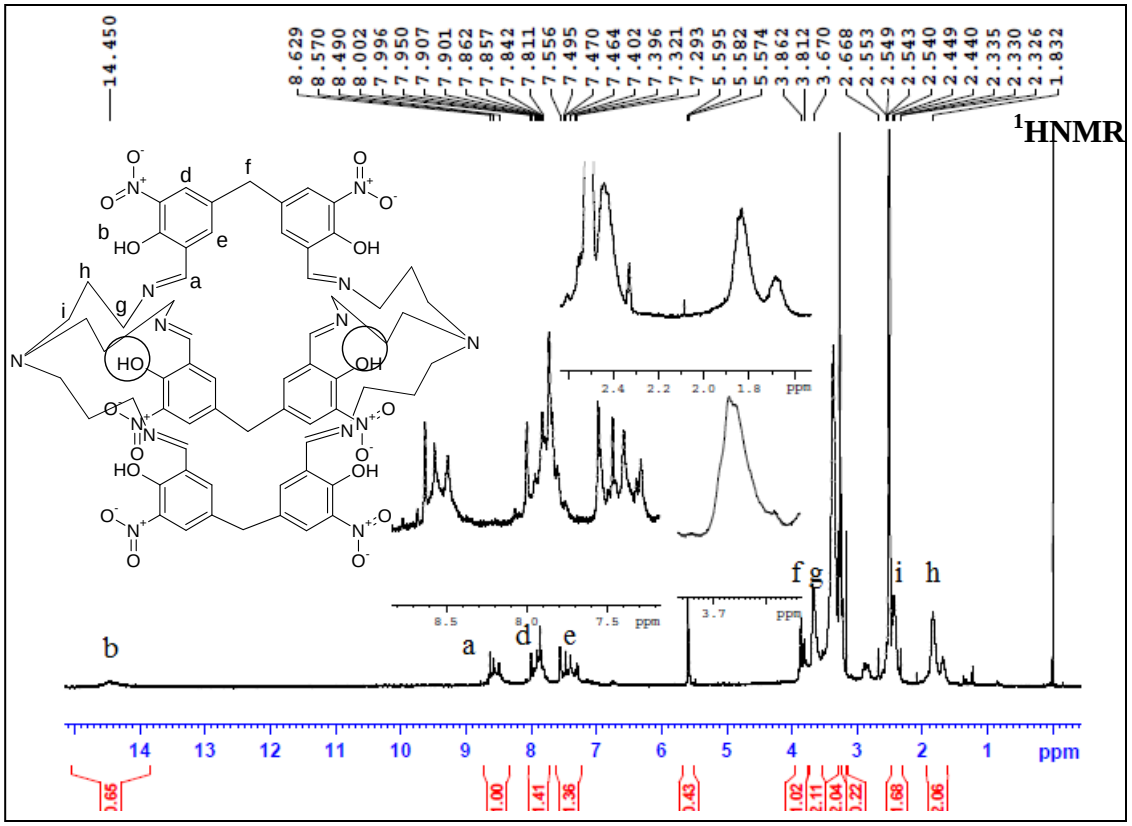

Spectrum 5.17

Variable temperature ^{1}HNMR

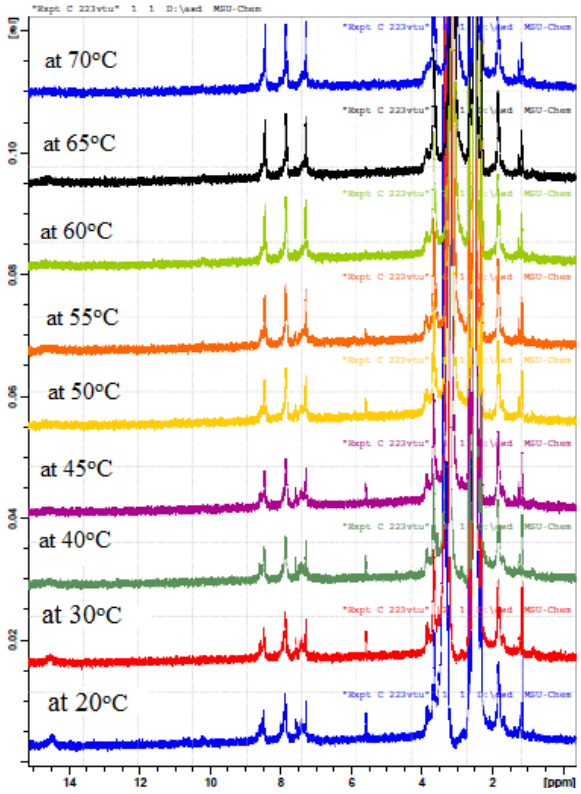

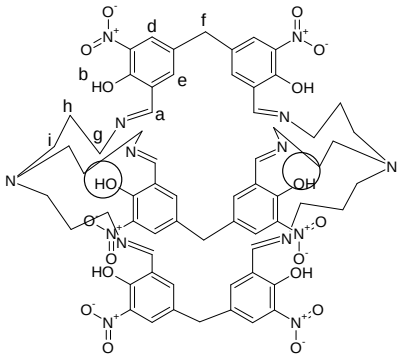

Spectrum 5.18

^{1}HNMR at 70 °C

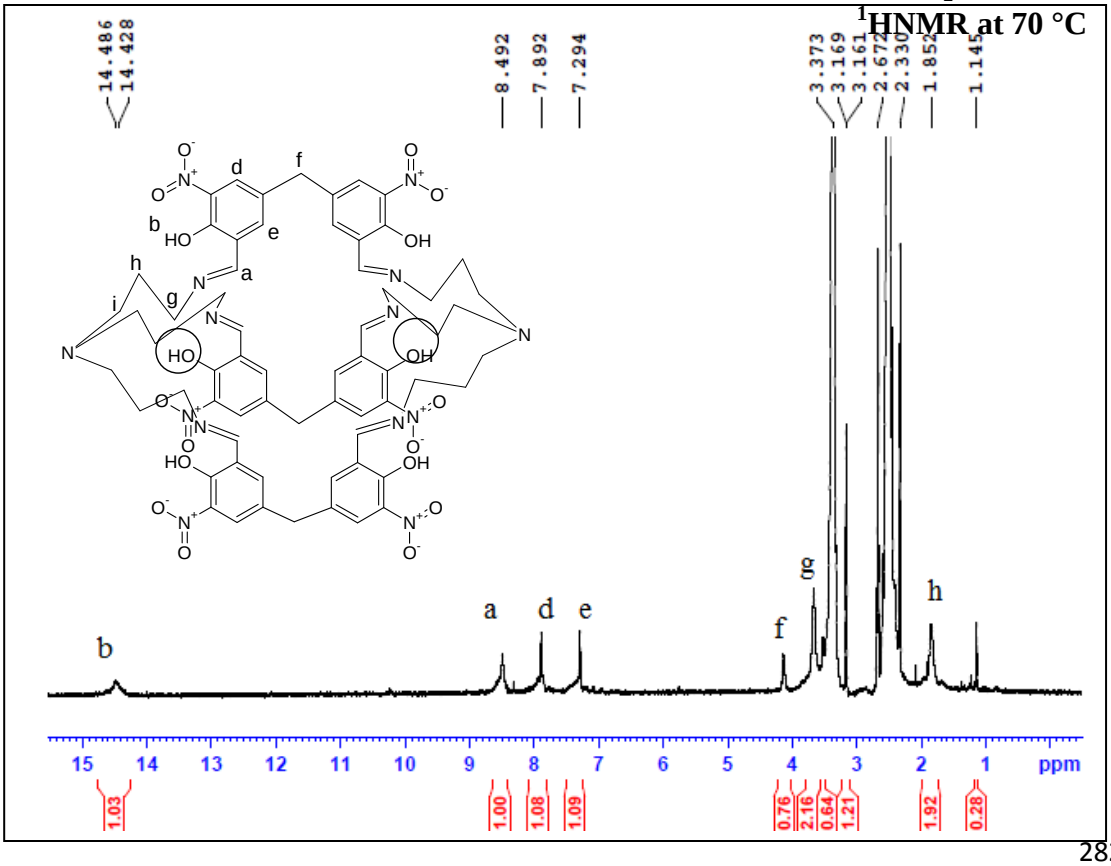

Chromatogram 5.19

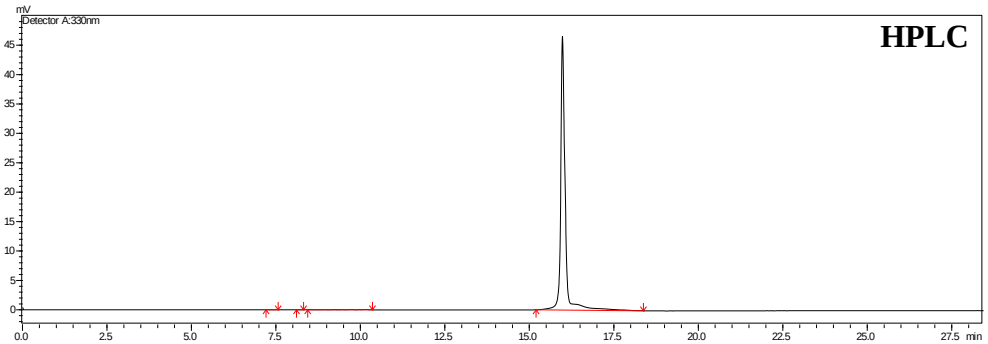

Mobile phase: MDC:MeOH :: 99:1 (v/v), Stationary phase : Silica column

Peak	Name	Ret. Time	Area%
1	imp 1	7.368	0.0020
2	imp 2	8.179	0.0002
3.	imp 3	10.184	0.3107
4.	EXPT C-223(Silver cryptate from TRPN and 5,5'methylene –bis-3-nitrosalicylaldehyde)	15.976	99.6871

Spectrum 5.20

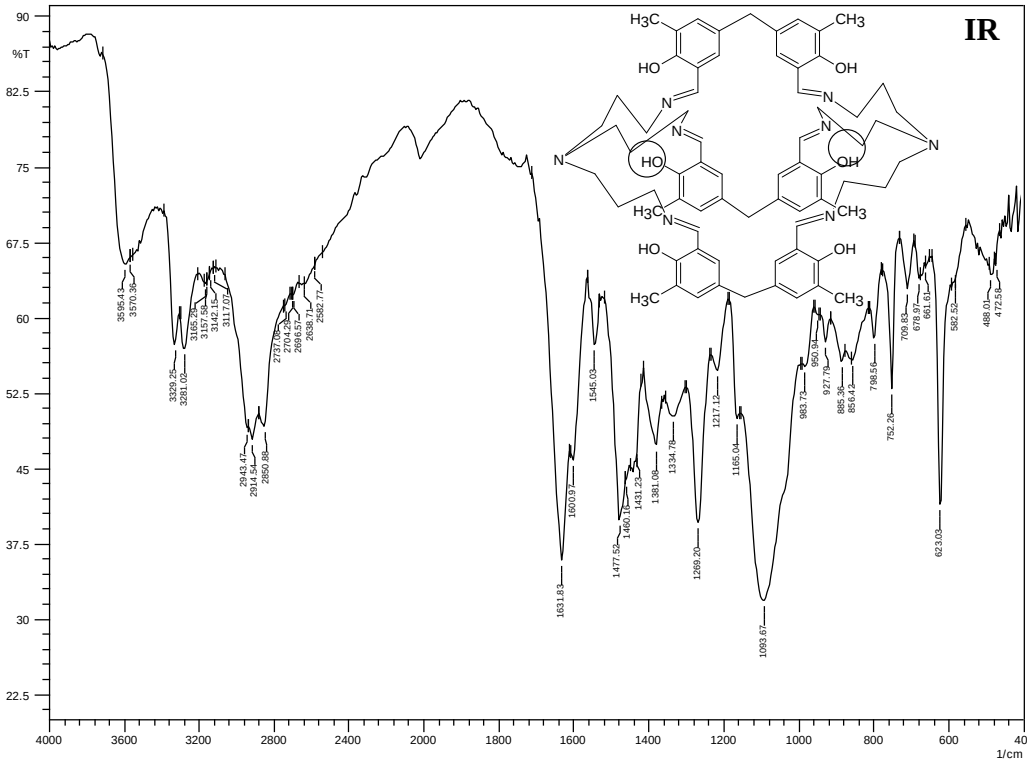

Spectrum 5.21

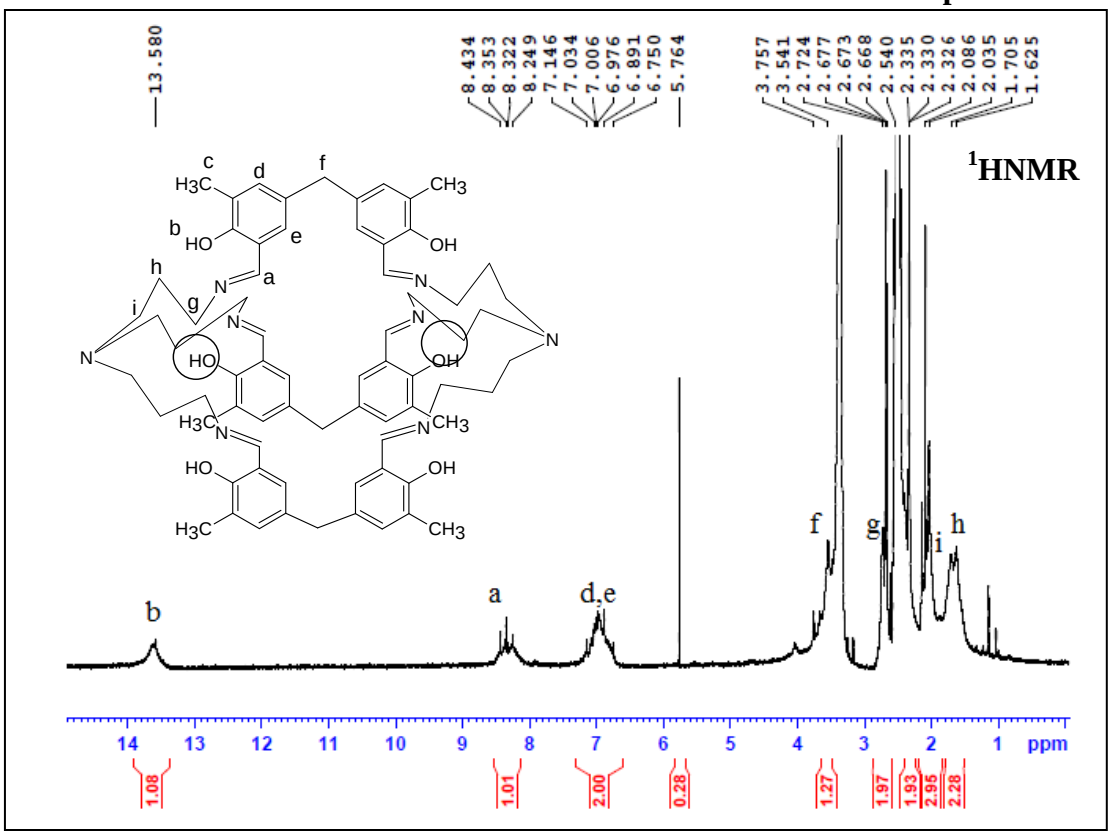

Spectrum 5.22

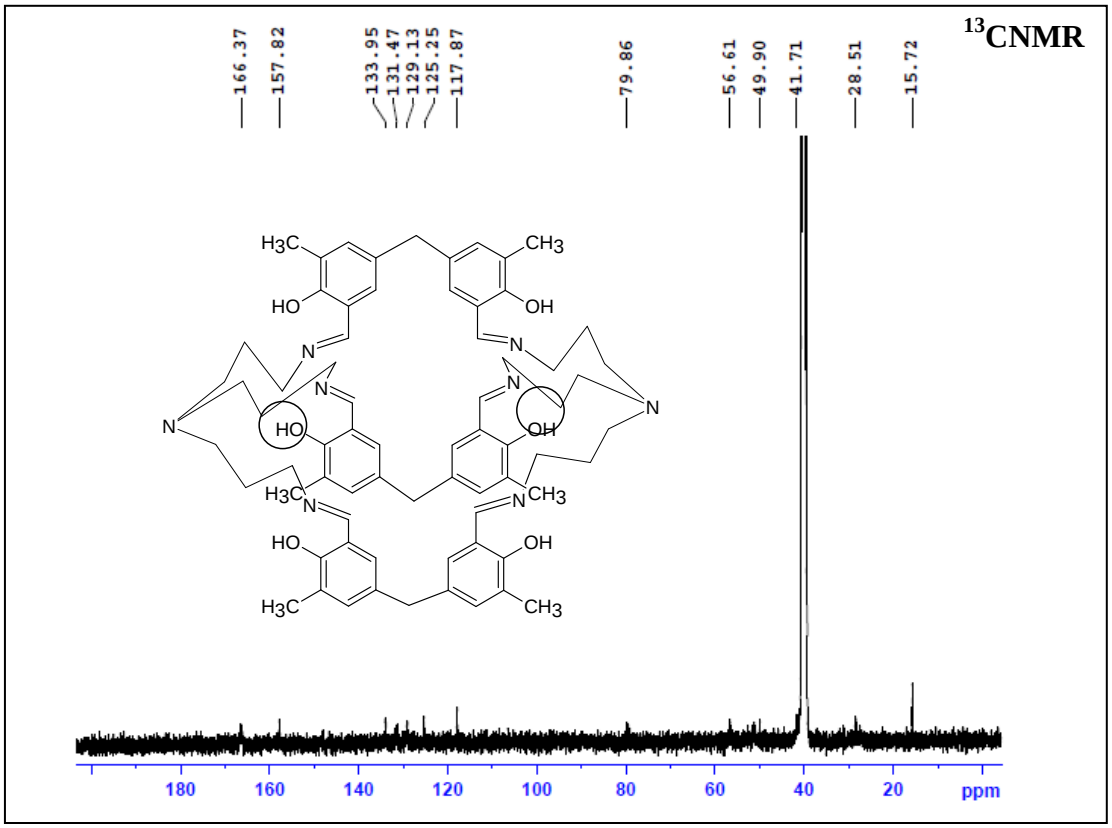

Spectrum 5.23

DEPT 90

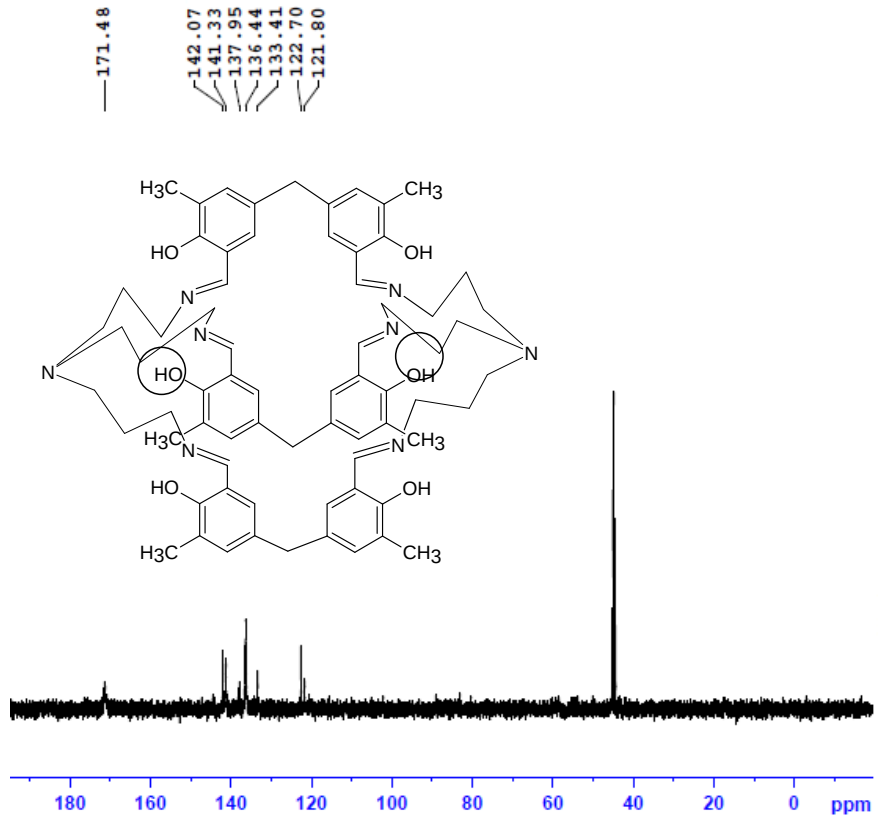

Spectrum 5.24

Variable temperature ^{1}HNMR

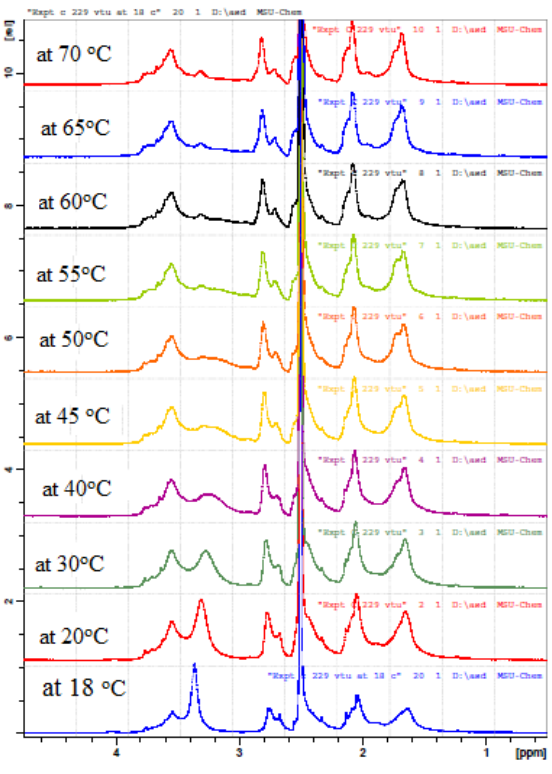

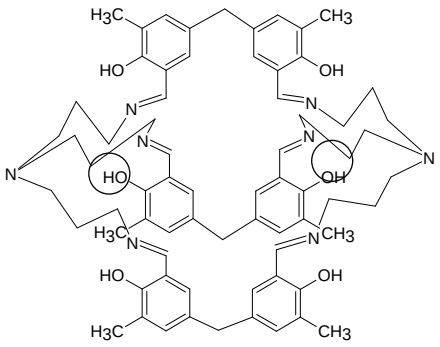

Chromatogram 5.25

HPLC

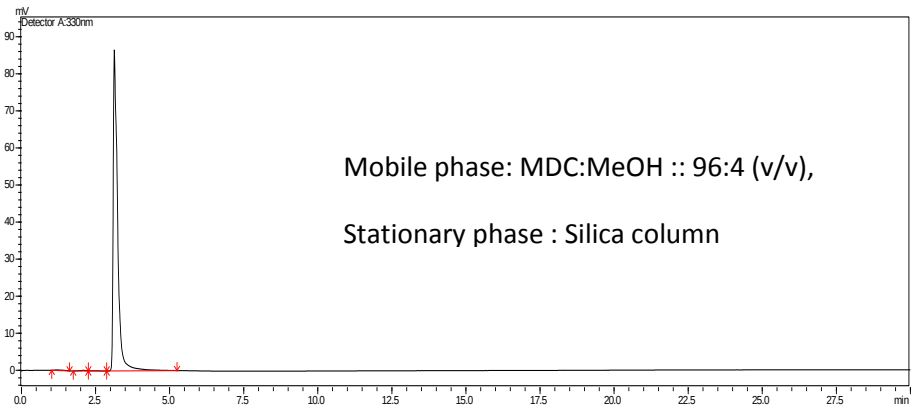

Peak	Name	Ret. Time	Area%
1	imp 1	1.183	0.3633
2	imp 2	2.081	0.2556
3.	imp 3	2.419	0.1561
4.	EXPT C-229 (Silver cryptate from TRPN and 5,5'methylene –bis-3-methylsalicylaldehyde)	3.130	99.2250

Spectrum 5.26

IR

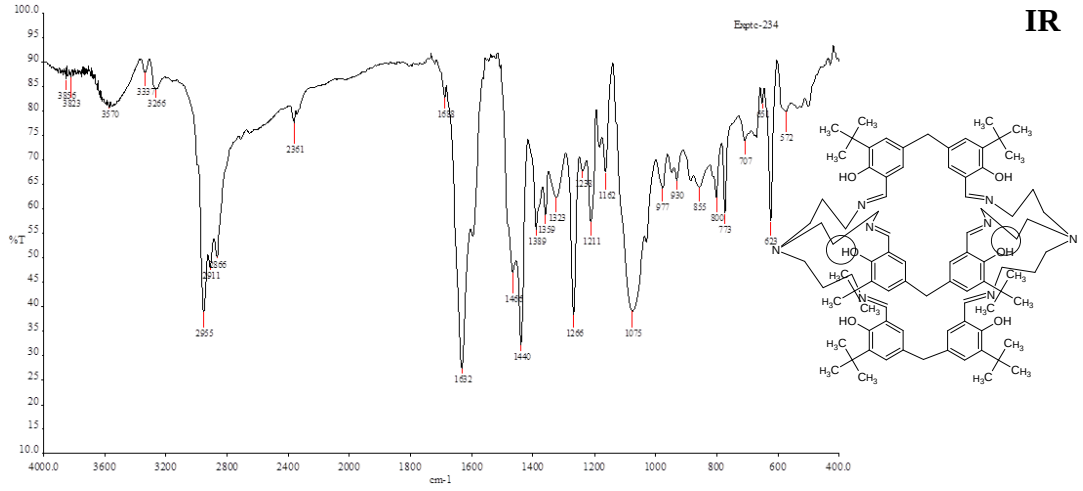

Spectrum 5.27

^{1}HNMR

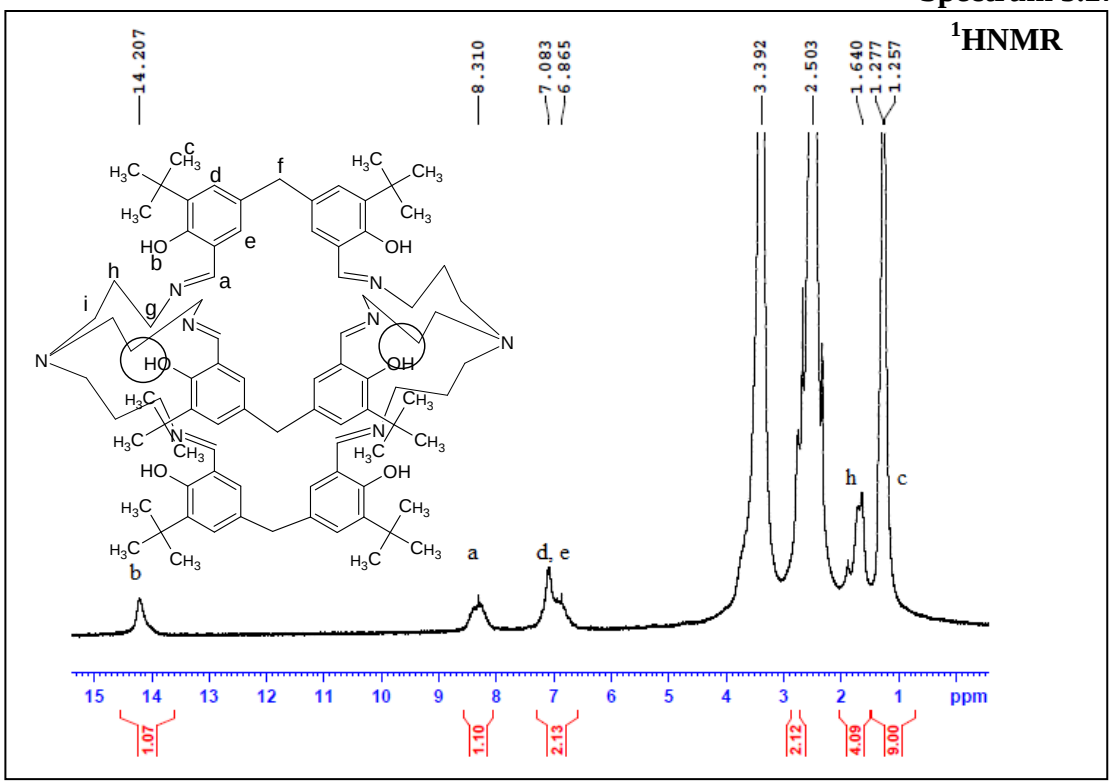

Spectrum 5.28

Variable temperature

^{1}HNMR

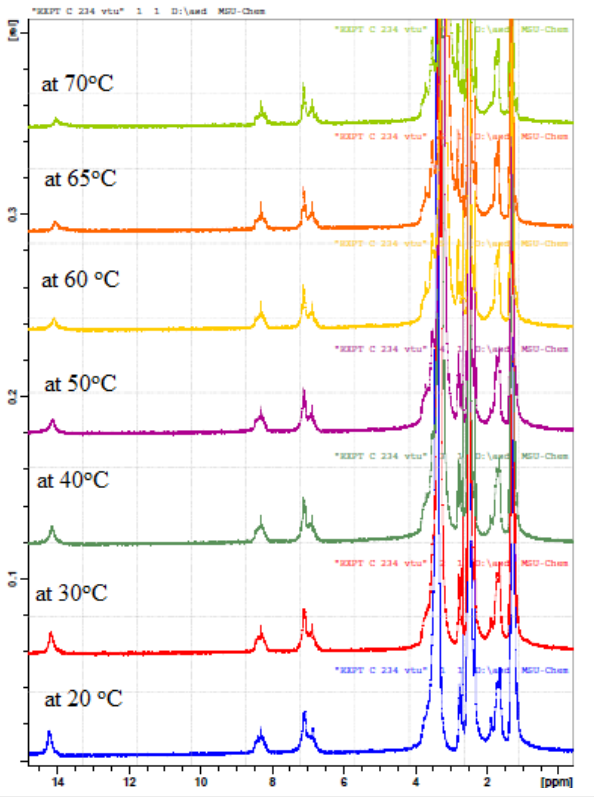

Spectrum 5.29

Mass

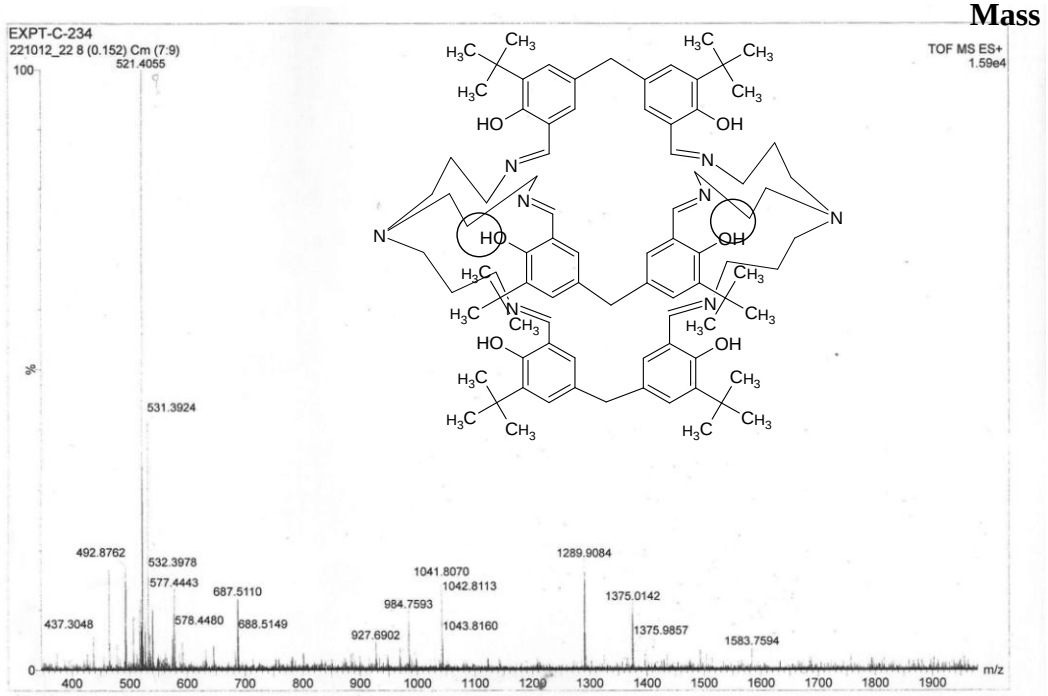

Chromatogram 5.30

HPLC

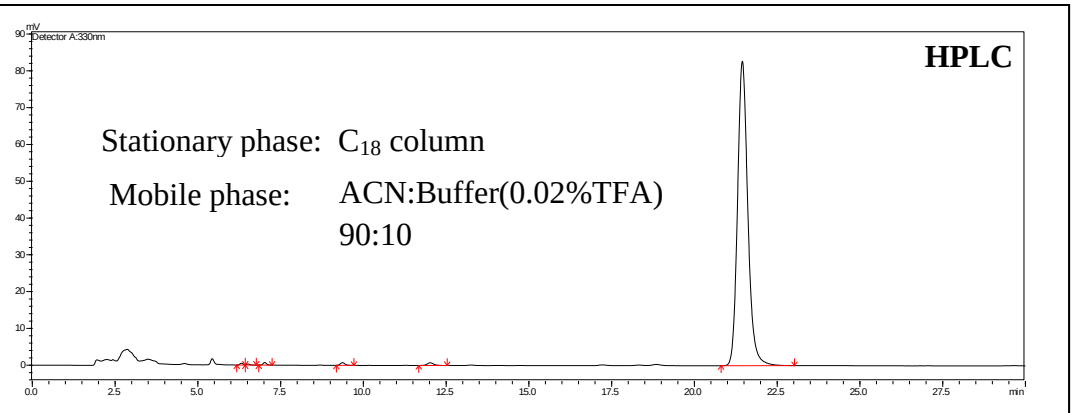

Stationary phase: C_{18} column

Mobile phase: ACN:Buffer(0.02%TFA) 90:10

Peak	Ret. Time	Area%
imp-1	6.314	0.1924
imp-2	6.511	0.1090
imp-3	7.016	0.2944
imp-4	9.365	0.3861
imp-5	12.016	0.5631
cryptand from TRPN and 5,5'-methylene-bis(3-*tert*-butyl-salicylaldehyde)	21.445	98.4550

5.7 References

1. Steed, J. W.; Atwood, J. L. *Supramolecular Chemistry*, John Wiley & Sons, Ltd. **2002**

2. Howarth, O. W.; Morgan, G. G.; McKee, V.; Nelson, J. *J. Chem. Soc., Dalton Trans.*,**1999**, 2097.

3. Gutknecht, J; Schneider, H.; Stroka, J. *Inorg. Chem.*, **1978**, 17(12), 3326.

4. Cox, B. G.; Guminski, C.; Scheider, H. *J. Am. Chem. Soc.*, **1982**, 104, 3789.

5. Cox, B. G.; Truong N. *J. Chem. Soc., Faraday Trans. 1*, **1984**, 80, 3285.

6. Lehn, J.M.; Vains J. R. *Tetrahedron Lett.*, **1989**, 30(17), 2209.

7. Shu-Yan, Y.; Qin-Hui, L.; Meng-Chang, S.; Zheng, Z. *Polyhedron*, **1994**, 13(15/16) 2467.

8. Shu-Yan, Y.; Qin-Hui, L.; Huang, X.; Sheng, T; Wu, T.; Wu, D.; *Polyhedron*, **1997**, 16(3), 453.

9. Luo, R.; Mao, X.; Pan, Z.; Luo, Q. *Spectrochimica Acta Part A*, **2000**, 56, 1675.

10. Drew, M. G. B.; Farrell, D.; Morgan, G. G.; McKee, V.; Nelson, J. *J. Chem. Soc., Dalton Trans.*, **2000**, 1513.

11. Krakowiak, K. E.; Bordunov, A. V.; Bradshaw, J. S. *J. Heterocyclic Chem*., **1998**, 35, 169.

12. Izutsu, K.; Ito, M.; Sarai, E. *Anal. Sci.* **1985**, 1, 341.

13. Hsu, H. P.; Shih, J. S.; *Sens. Actuators B*, **2006**, 114, 720.

14. Aziz, Z; Abu, S. F.; Chong, N. J. *Burns*, **2012**, 38(3), 307.

15. Abu-Youssef, M. A. M.; Dey, R.; Gohar, Y.; Massoud, A. A.; Ohrstrom,L.; Langer, V. *Inorg. Chem*., **2007**, 46(15), 5893.

16. McCann, M.; Coyle, B.; McKay, S.; McCormack, P.; Kavanagh, K.; Devereux, M.; McKee,V.; Kinsella, P.; Oconnor, R.; Clynes,M. *Biometals*, **2004**, 17(6), 635.

17. Abuskhuna, S.; Briody, J.; McCann, M.; Devereux, M.; Kavanagh, K.; Fontecha, J. B.; McKee V. *Polyhedron*, **2004**, 23, 1249.

Chapter 6

Tetrahedral cryptands from tris-(2-aminoethyl)amine and their study

6.1 Introduction

Synthesis of larger sized cryptands from small organic molecules is a challenging task as decrease in entropy is expected. Giant sized molecules are known having metal organic frame work[1-3] but there are only a few reports of only covalently bonded organic cages.

A tetrahedral macro tricyclic cryptand made of four fused triaza[18]crown-6 rings was reported[4] and found to be capable of binding anions such as chloride ion, water or ammonium ion depending on pH of the medium (**Fig. 6.1**).

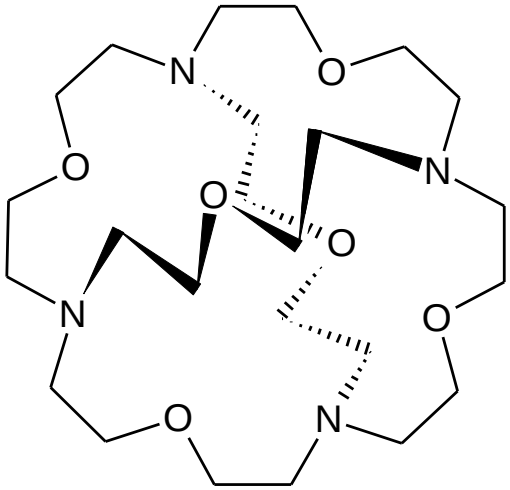

Oxa-aza cryptand , 'Soccer ball' molecule

Fig. 6.1

A chiral tetrahedral iminospherand is synthesized by [6+4] cyclocondensation of 1,2-diaminocyclohexane and 1,3,5-triformyl benzene. It is reported to undergo reversible water uptake.[5-7] Similarly porous covalent organic cages were prepared by cycloimination of 1,3,5-triformylbenzene with (R,R)-1,2-diphenylethylenediamine.[8]

These large cryptands have potential applications in sorption, separation and catalysis due to their large cavity size and can be used for preparation of porous nano particles.[9]

Thus large covalently bonded organic macrocyclic structures have significant importance in material science.

6.2 Aim and Objectives

In the quest of synthesis of macropolycyclic cryptands by applying some of the methylene-bis-aldehydes, we achieved the synthesis of cryptands by condensing these aldehydes with two molecules of TREN as described in Chapter 4. The cryptands formed differed in their physical properties. The reaction of TREN with some of the other bis aldehydes did not result in the synthesis of [2+3] cryptands. The synthesis of cryptands with larger cavity size by replacing TREN with TRPN could be achieved only with the help of template due to greater flexibility in TRPN as discussed in chapter 5. There is a possibility of formation of larger cryptands by reaction of bifunctional linking agents depending on their thermodynamic stability. Some of the larger cryptands could be more stable compared to corands or smaller sized cryptands from the same bifunctional or trifunctional reactants. In this chapter we have included the synthesis and study of cryptands which have resulted in larger macrocyclic structures from the bis-aldehydes and tris-amines. The binding ability study of the resulting cryptands with various transition metal ions forms a part of this chapter.

6.3 Results and Discussion

There are large numbers of cryptands reported by applying reactions of dialdehydes or bis-aldehydes with the tris-amines such as TREN or TRPN.[10-19] These cryptands are formed by the reaction of two molecules of a tris-amine with three molecules of the diformyl linkers. With this background the reaction of 5,5'-methylene-bis-salicylaldehyde was carried out with TREN and the proposed structure of the cryptand was based on [2+3] cyclocondensation of the reactants.[20] In depth investigation of the cryptand lead to the indications that the structure of the cryptand could be different from the proposed [2+3] structure. Detailed 2D NMR and mass studies led to the discovery of a new giant sized cryptand resulting from [4+6] cyclocondensation of TREN and methylene-bis-salicylaldehyde. The ESI-MS spectrum of the cryptand covering extended mass range exhibited mass peak at 1906 and1907 corresponding to M^+ and M+1 which reasserted that it is not among the commonly reported [2+3] cryptands and is a larger cryptand with symmetrical structure involving double the number of reactants than expected (**Fig. 6.2**, Spectrum 6.10).

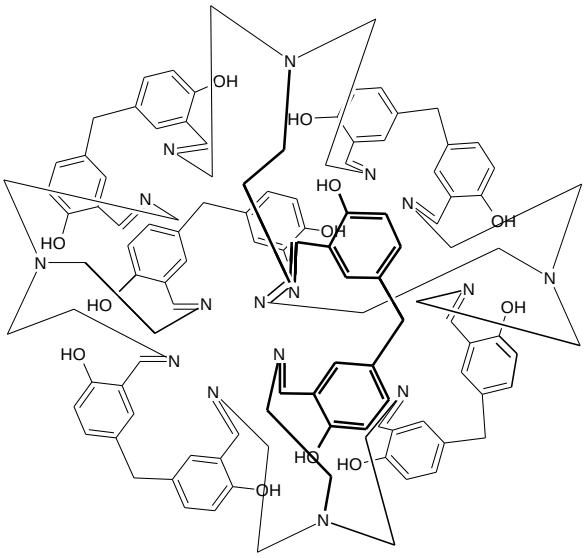

Dodeca-imino, hexadeca-aza tetrahedral cryptand A-10 from 4+6 cyclocondensation

Fig. 6.2

The highly symmetrical nature of the cryptand is reflected in its ^{1}H NMR and ^{13}C NMR characteristics. In proton NMR, phenolic protons are observed as a singlet at 14.04 δ, the CH protons of the imine linkages are observed at 7.52 δ as a doublet with J = 1.2Hz due to allylic coupling with methylene protons. Two of the aromatic protons are observed at 7.42 δ and 7.09 δ with the expected couplings. A signal at 5.47 δ is found to be of the aromatic proton with unusual chemical shift due to shielding effect of aromatic ring of the neighboring bridge. This was also confirmed by 2D NMR experiments. The chemical shift of this aromatic proton placed between the aromatic carbons attached to the methylene bridge and the imine carbon reflects the conformation of the linkers having this carbon pointing inside the cavity of the cryptand while the other edge containing hydroxyl group is shifted on the outer surface of the cryptand. The methylene bridge protons are observed as a singlet at 3.63 δ. Each of the four protons situated on the methylene bridge connecting nitrogens are individually observed at 3.71 δ, 3.14 δ, 2.86 δ and 2.77 δ with expected multiplicity due to rigidity present in macrocyclic structure (Spectrum 6.2).

^{13}C NMR shows signals for 10 carbons between 166 to 40 δ due to the presence of a high element of symmetry present in the cryptand (Spectrum 6.3). Three of the carbons are in the aliphatic region giving negative signals in DEPT 135 while the other are observed at down field due to sp^2 hybridized carbons (Spectra 6.4, 6.5).

The cross peaks in the COSY spectrum of the cryptand confirmed the coupling between various protons. Interestingly only one of the protons of methylene group attached to nitrogen is coupled with the proton on the imine carbon as reflected in COSY spectrum. The coupling between the most up field and most downfield aromatic proton is also observed in COSY spectrum (Spectrum 6.6).

The cross peaks in NOESY spectrum of the cryptand establishes a close proximity in space between the proton attached to imine carbon (proton ‘a’, **Fig. 6.3**) with the down field aromatic proton and with the up field proton of the methylene carbon attached to imine nitrogen (proton ‘g’, **Fig. 6.3**). Similarly proximity is also observed between the methylene bridge protons on the carbon connecting the two aromatic rings with the

aromatic protons (proton ‘e’ and ‘d’, **Fig. 6.3**) situated at the ortho positions to the bridge as reflected in the NOESY spectrum (Spectrum 6.7).

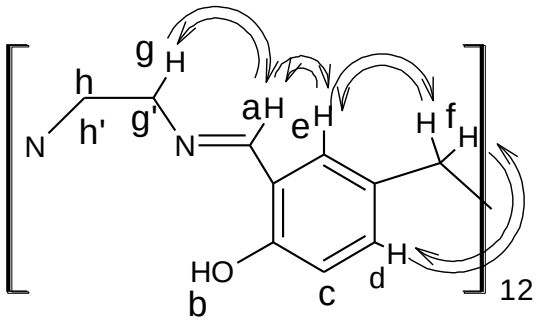

NOESY ^{1}H-^{1}H correlation observed in giant cryptand 1

Fig. 6.3

HSQC and HMBC 2D NMR spectra clearly establish the connectivity between the different protons and carbons showing single bond connectivity and multiple bond connectivity respectively. (Spectra 6.8, 6.9) In IR cryptands exhibit strong bands at 3437 cm^{-1} for νO-H, at 1634 cm^{-} for νC=N, at 1491 cm^{-1} for aromatic ring νC=C and at 1275 cm^{-} for νAr-O. (Spectrum 6.1)

The cryptand could be crystallized in various size crystals in different solvent systems such as dichloromethane-methanol and pyridine–acetone systems. Attempts to collect single crystal X-ray diffraction data were unsuccessful because of highly unstable nature of the solvent supported crystals. Various techniques such as covering the crystals with the help of paraffin or inserting in capillary with the mother liquor were employed for the data collection but crystals were collapsing very fast.

When the cryptand was reduced with sodiumborohydride in methanol-MDC mixture the bright yellow colour disappeared due to reduction of the imine linkages to secondary amine linkages. The isolated reduced cryptand had poor solubility compared to its parent compound (**Fig. 6.4**). Its proton NMR was recorded in CD_3OD-$CDCl_3$ mixture with drastic change in chemical shift of various protons reflecting flexibility introduced in the

reduced cryptand without affecting its symmetry. All the aromatic protons are now observed in normal aromatic region between 6.5 to 7.0 δ. The protons on newly generated benzylic methylene carbon are observed at 3.72 δ as a singlet. Ethylene bridge protons are found as two unresolved triplets near 2.5 δ value and identity of each proton in the parent imine linked cryptand was lost. The NH proton is observed as a singlet at 1.36 δ. (Spectrum 6.12)

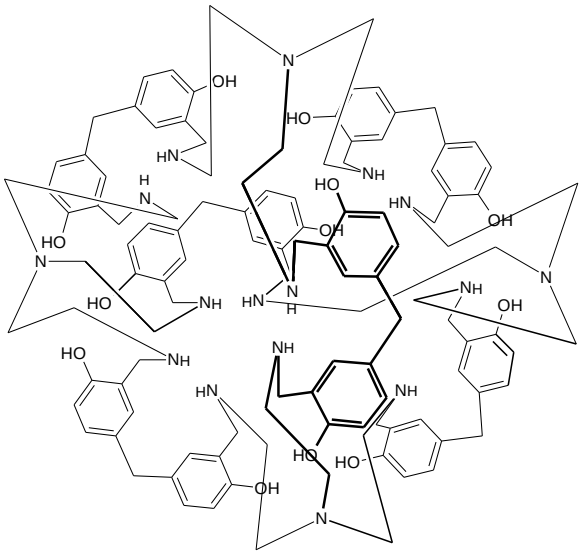

Hexadeca-amino tetrahedral giant cryptand 3 with greater flexibility

Fig. 6.4

Solution studies on this dodeca-imine cryptand (**Fig. 6.2**) revealed that it recognizes Cu^{2+} and forms 1:2 host:guest complex. The copper complex of imine cryptand was prepared by mixing its solution in dichloromethane with solution of copper perchlorate in methanol in 1:4 stoichiometry and removing unbound metal salt by washing with methanol followed by washing with dichloromethane. The resulting copper complex was dirty green in colour (**Fig. 6.5**).

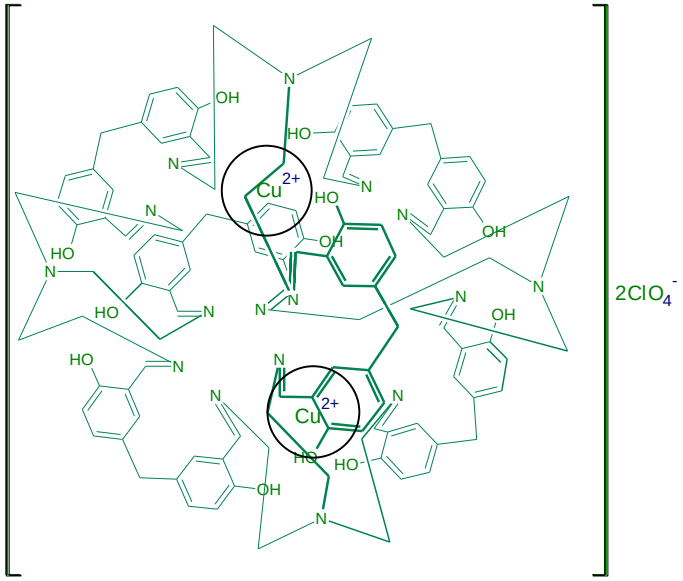

Copper cryptate of dodeca-imino, hexadeca-aza tetrahedral Cryptand 1

Fig. 6.5

IR spectrum of the cryptand shows very broad band at higher wave number region and few new bands due to complexation. A broad band appeared at 1070 cm^{-1} and sharp band at 624 cm^{-1} is also seen due to perchlorate anions (Spectrum 6.13). In proton NMR CH proton of the imine linkage is shifted downfield near 10 δ value while OH protons are shifted up field to 10.5 δ as confirmed by D_2O exchange. Couple of aliphatic protons are seen which are not overlapping with DMSO and DMSO-H_2O signals (Spectra 6.14, 6.15). The copper complex shows a characteristic 4 line ESR spectrum when recorded at low temperature in DMSO. The g_{II} = 2.2332 and A_{II} = 187 x 10^{-4} Cm^{-1}. The perpendicular component was not well resolved and hence not calculated. (Spectrum 6.16). The cyclic voltamogram of copper complex shows two reduction signals, as Cu^{2+} 1^{st} converts to Cu^{1+} and then to $Cu^{(0)}$. The oxidation cycle shows direct conversion of $Cu^{(0)}$ to Cu^{2+}. (**Fig. 6.6**)

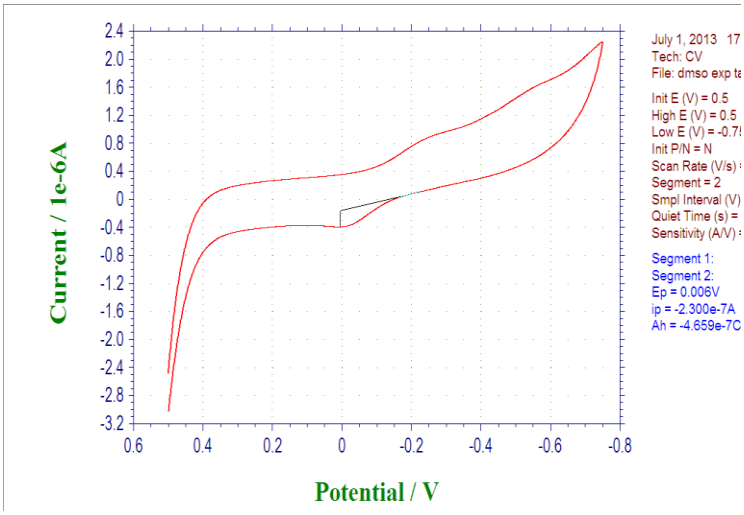

Cyclic voltamogram of copper cryptate

Fig. 6.6

Biological activity of the copper complex was carried out to study its antibacterial and antifungal activities. The antibacterial activity was carried out both on gram positive (*S. aureus, S. pyogenus, P.vulgaris*) and gram negative bacteria (*E. coli and P. aeruginosa*) using broth dilution method. It showed good antibacterial activity and was most effective against *P. aeruginosa* with MIC of 125 µg/ml. Compare to standard antibacterial drugs namely ciprofloxacin and siversulphadiazine which were used as reference, our copper cryptate require 1.2 to 5 times higher concentration for inhibition of bacterial growth. (Table. 6.1)

Table 6.1 Minimum inhibitory concentration

DRUG	***E. coli***	***P. aerugenosa***	***S. aureus***	***S. pyogenus***	***P. vulgaris***
(µg/ml)	MTCC 443	MTCC 1688	MTCC 96	MTCC 443	MTCC 744
Cu^{2+}cryptate	200	**125**	250	250	200
Ciprofloxacin	25	25	50	50	25
Silver-sulphadiazine	50	100	100	125	50

Antifungal activity of the complex was carried out against *C. albicans* and MFC of the complex was found to be equal to the standard drug greseofulvin (500 μg/ml) but was five times higher as compared to nystatin.

Giant Tetrahedral cryptand with methoxy substituents.

The reaction of TREN with 5,5'-methylene-bis-(2-hydroxy-3-methoxybenzaldehyde) under high dilution condition in dichloromethane proceeded with gradual change in the colour of the reaction mixture. Progress of the reaction was also observed on TLC. The resuting cryptand was purified by subjecting the concentrated reaction mixture to column chromatography using MDC-MeOH solvent system in 43% yield with the structure similar to that from bis-salicylaldehyde (**Fig. 6.7**).

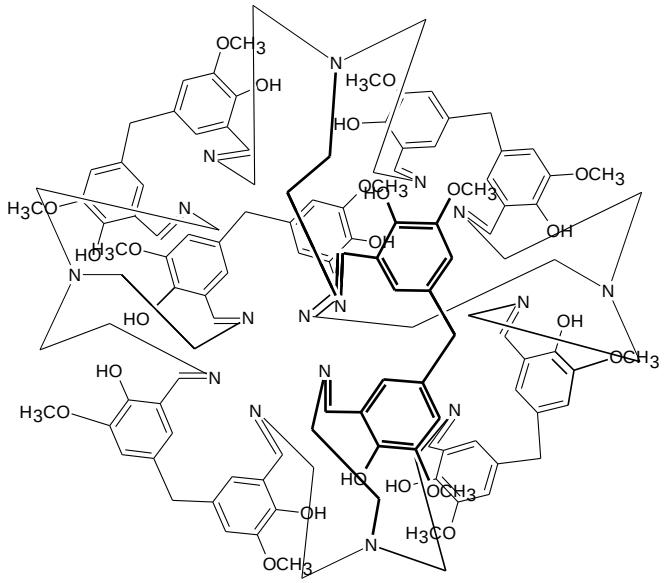

Dodeca-imino, hexadeca-aza tetrahedral cryptand 3 (B-133) from 4+6 cyclocondensation
Fig. 6.7

The cryptand was characterized using various spectroscopic methods. NMR of the cryptand confirms highly symmetrical nature of the cryptand. In proton NMR phenolic protons are observed at 14.66 δ while CH protons of imine linkage are observed at 7.51 δ with allylic coupling (J = 1.6 Hz) as was observed in the earlier case. One of the aromatic protons is observed at 7.17 δ which is coupled with the other aromatic proton observed at

quite up field at 5.23 δ (J = 2 Hz) as discussed earlier. A singlet for methoxy protons is observed at 4.08 δ and methylene bridge protons are observed as a singlet at 3.60 δ while the ethylene bridge protons are observed as three set signals at 3.70 δ for one of the protons near the imine nitrogen at 3.18 δ for the other proton on the same carbon as a multiplet and at 2.83 δ as overlapping signals for the two protons on the carbon towards the tertiary nitrogen (Spectrum 6.18).

^{13}C NMR shows eleven signals between 167 δ to 41 δ. The methoxy carbon is observed at 58.7 δ which is confirmed by DEPT 135 experiment (Spectrum 6.19). COSY spectrum establishes clear coupling between CH proton of the imine linkage with one of the methylene protons on the carbon attached to the nitrogen of the imine linkage and between the aromatic protons' signals situated far apart from each other (Spectrum 6.22).

NOESY spectrum of the cryptand establishes close proximity in space between different protons. One of the protons at the carbon attached to imine nitrogen is falling near to CH proton of imine linkage though not having mutual coupling as in cosy is reflected in NOESY spectrum. The CH proton on imine linkage is also having a NOESY cross peak with the aromatic proton observed at 5.23 δ. The aromatic proton at 7.17 δ has a cross peak with the methoxy protons as well as the methylene protons on the other side. The methylene bridge protons have through space communication with aromatic proton observed at the high field as seen in the NOESY spectrum (Spectrum 6.23).

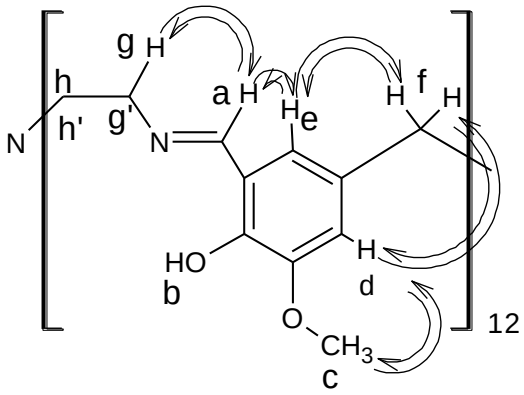

NOESY ^{1}H-^{1}H correlation observed in giant cryptand 3 (B-133)

Fig. 6.8

The HSQC 2D NMR of the cryptand identifies the location of each proton on various carbon atoms (Spectrum 6.24). The Q-TOF mass spectrum of cryptand shows mass peak at 1133.86 corresponding to $M^{+}/2$ which is indicated by the half unit difference with its isotopic peak at 1134.38 (Spectrum 6.25).

In IR spectrum strong bands are observed at 1634cm^{-1} for νC=N, at 1474 cm^{-1} for bending vibrations of methylene and methyl groups and at 1266 cm^{-1} for aryl-O stretching while alkyl-O stretching is observed at 1068 cm^{-1} as a medium intensity band (Spectrum 6.17).

The cryptand from o-vanillin is also crystalline in nature. Crystals developed in (THF: n-Butanol) were found suitable for single crystal X-ray analysis. As these crystals were also solvent supported the single crystal X-ray analysis was carried out by maintaining lower temperature by using nitrogen flow at CSMCRI Bhavnagar using Bruker Smart Apex CCD defractometer. X-ray radiation source was MoK/α with the wavelength of 0.071073 Å. SHELXL-97 was used for structure refinement.

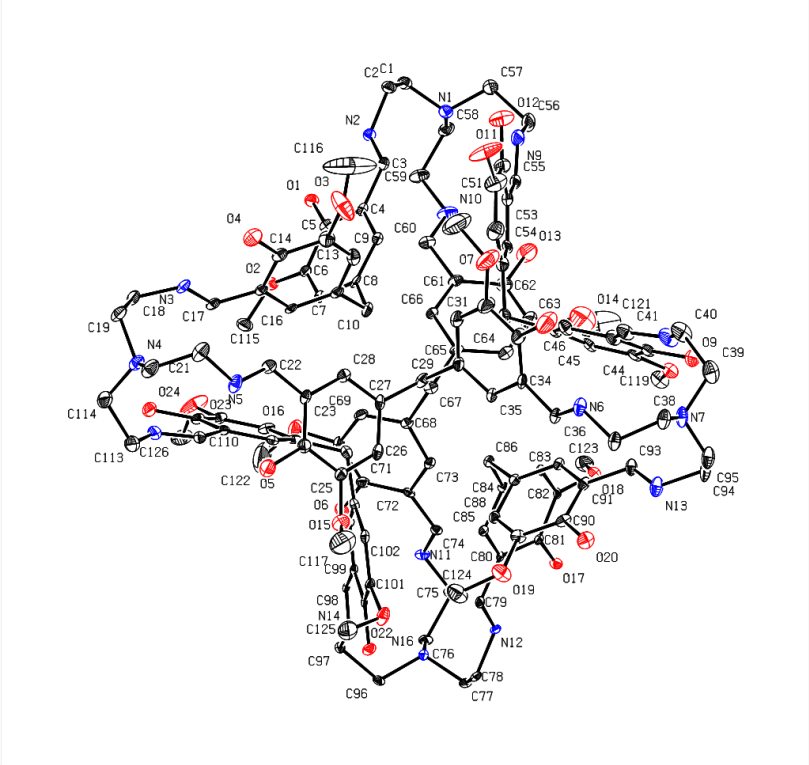

ORTEP diagram of giant tetrahedral cryptand 3 (B-133)
Fig. 6.9

The result confirmed the formation of larger cryptand through [4+6] condensation between TREN and the linker with twelve imine bond formation in single step giving tetrahedral symmetry to the cryptand. The tetrahedral symmetry seems to be thermodynamic driving force for the formation of the giant size macrocyclic compound. The X-ray crystal structure has been presented as ORTEP diagram (**Fig. 6.9**), wire framed projection (**Fig. 6.10**) and as space filling projection (**Fig. 6.11**).

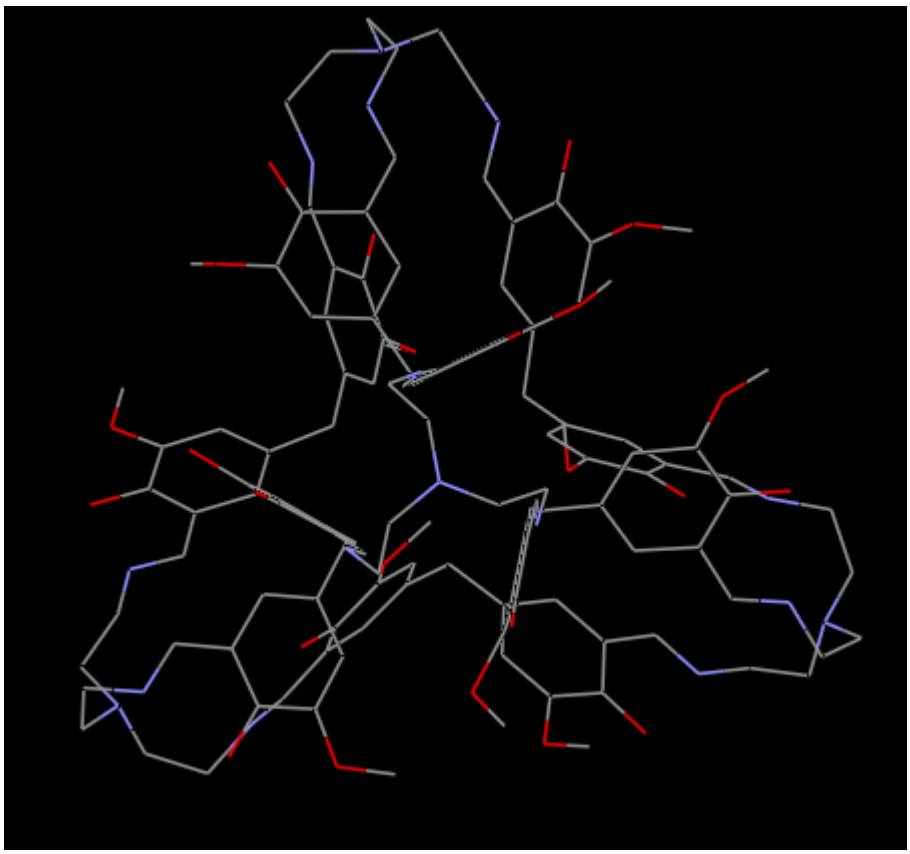

Wire framed structure of tetrahedral cryptand-3 (B-133)
Fig. 6.10

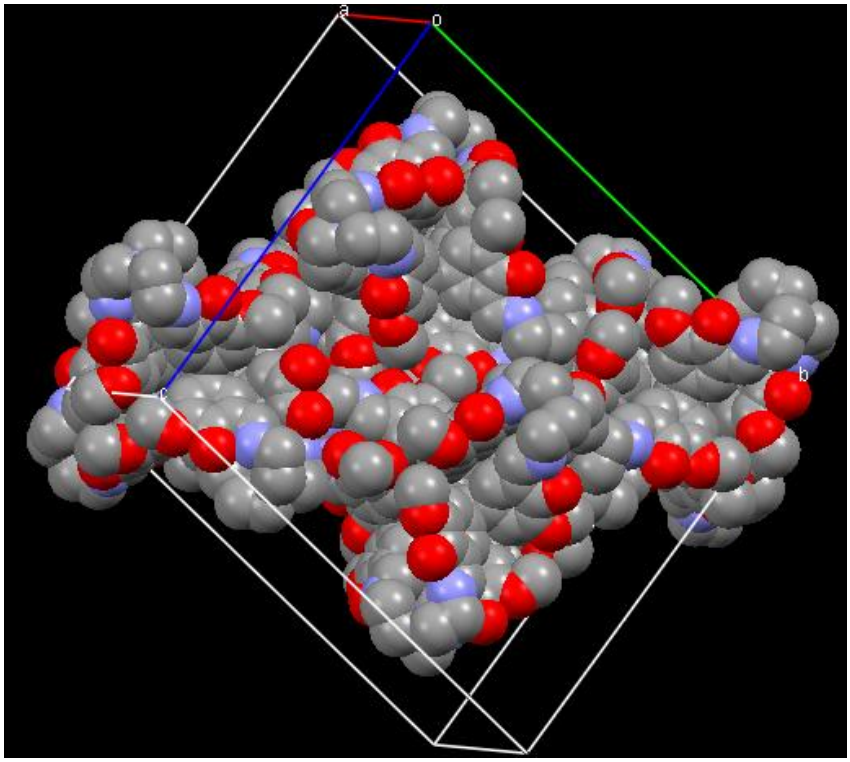

Spacefill model of tetrahedral cryptand 3-(B-133)

Fig. 6.11

Fig. 6.12 shows hydrogen bonding between phenolic -OH group and imine nitrogen.

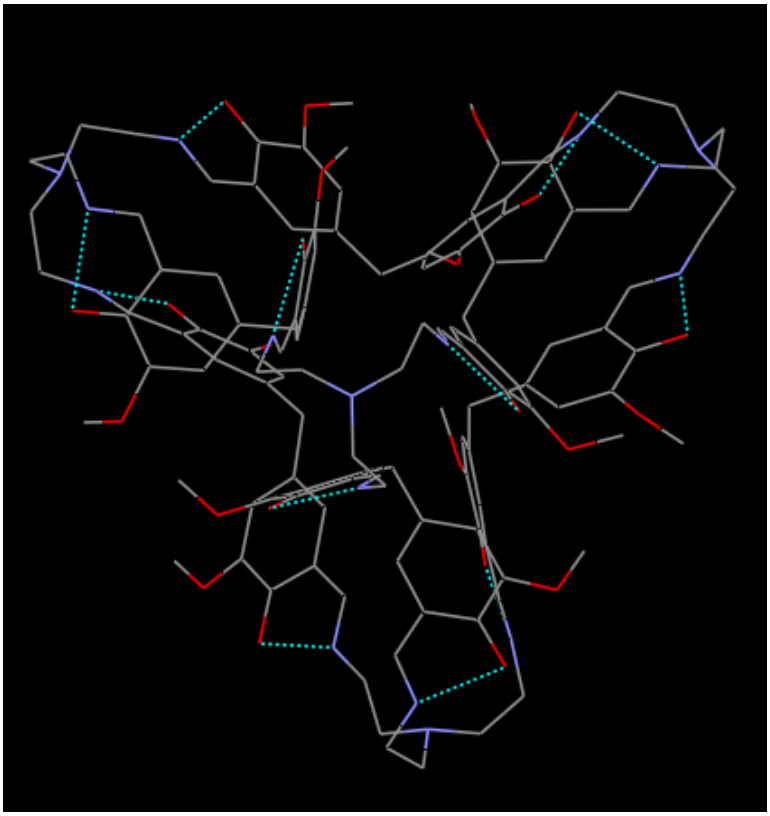

Hydrogen bonding in tetrahedral cryptand 3 (B-133)

Fig. 6.12

Fig. 6.13 shows inter molecular weaker C-H----π interactions and C-H---O soft hydrogen bonding

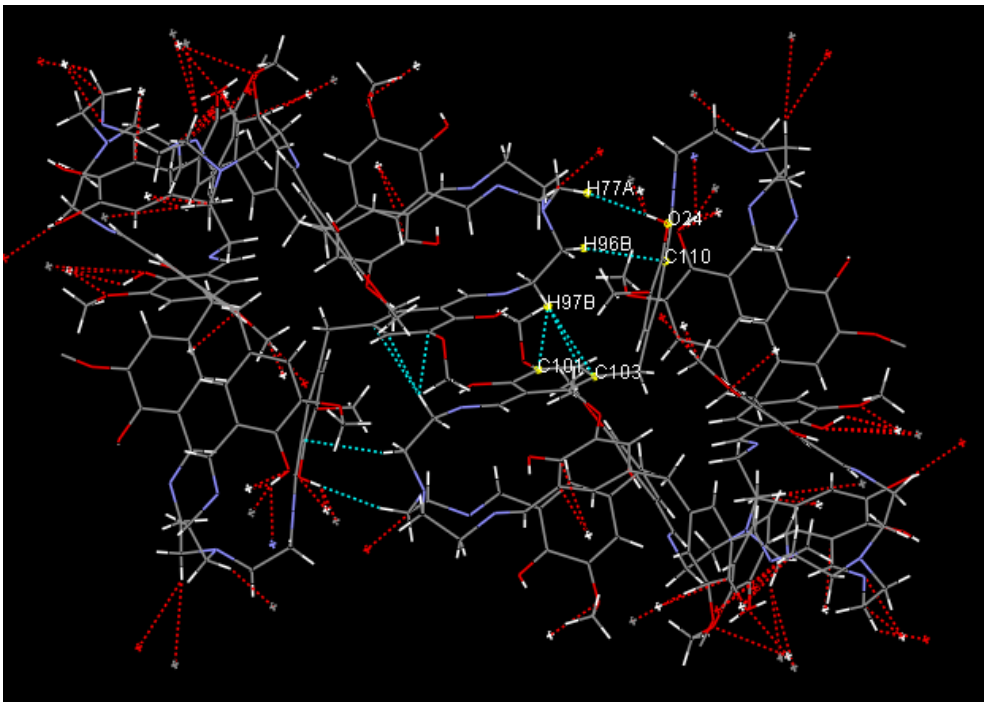

Weaker C-H----π interactions and C-H---O soft hydrogen bonding in tetrahedral cryptand 3 (B-133)

Fig. 6.13

Tabel No. 6.2 Crystal data and structure refinement

1.	Formula	$C_{126}\ H_{136}\ N_{16}\ O_{24}$
2.	Formula Weight	2258.58
3.	Cell Volume (Å)	15091.4
4.	T(K)	100
5.	Crystal system	monoclinic
6.	Space group	P 21/c
7.	Z	4
8.	a Å	15.6010(10)
9.	b Å	32.244(2)
10.	c Å	30.802(2)
11.	α(°)	90.00
12.	β(°)	103.10(10)
13.	γ(°)	90.00
14.	goodness of fit	1.023
15.	Calculated density diffrn ($mg/m^{3)}$	0.989
16.	Absorption coefficient (mm^{-1})	0.069
17.	F(000)	4764
18.	θ ranges for data collection	2.21-19.76
19.	Index ranges	$-17\leq h \leq 18$ $-36\leq k \leq 38$ $-36\leq l \leq 31$
20.	Reflection collected	26559
21.	R indices	11.7

Host-Guest studies between the tetrahedral cryptands and 1st series transition metal ions

Host- Guest stoichiometry

The tetrahedral cryptands contain imine as well as phenolic coordinating sites, which could bind various metal ions. We carried out solution studies using perchlorate salts of 1st transition series metal ions. Job's plot showed 1:2 binding between tetrahedral cryptand and metal ion used to study the stoichiometry. (Fig. 6.14, 6.15)

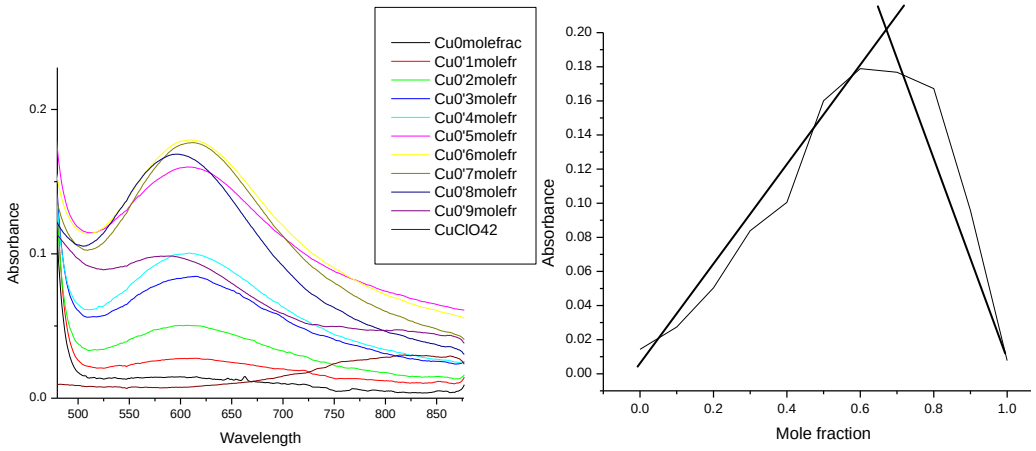

Job's plot for salicylaldehyde derived tetrahedral cryptand (A-10)

Fig. 6.14

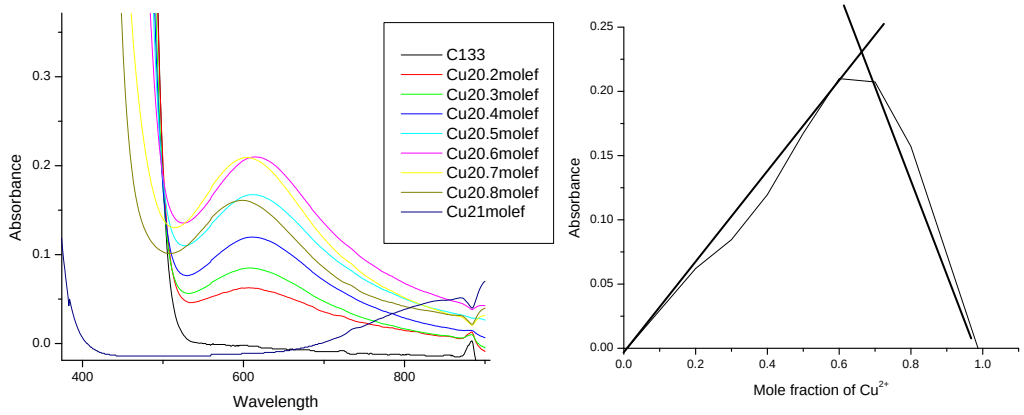

Job's plot for (3-methoxy-salicylaldehyde) derived tetrahedral cryptand (B-133)

Fig. 6.15

Host-guest studies between the two tetrahedral cryptands and 1st transition series metal ions were carried out at $1x10^{-4}$M concentration in DCM of host cryptand and $1x10^{-3}$ M concentration in DMSO of guest ions. Concentration of guest molecules was taken 10 times (in excess) to the host molecule to ensure the complete possible complexation. Study revealed that both the tetrahedral cryptands bind with all transition metal ions and gives specific response for Cu^{2+}, Fe^{3+}, and Fe^{2+}(**Fig.6.16, 6.17**).

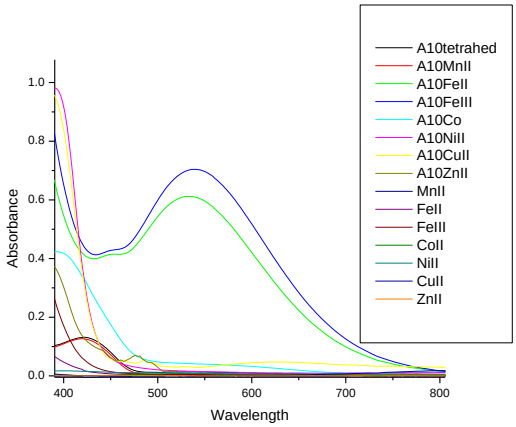

Uv-vis spectra of tetrahedral Cryptand A-10 in presence of 1st transition series metal ions.

Fig. 6.16

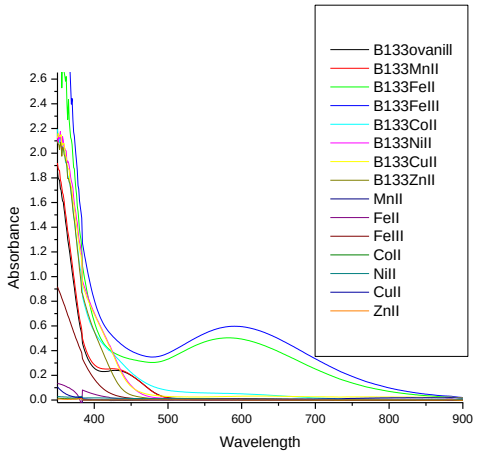

Uv-vis spectra of tetrahedral Cryptand B-133 in presence of 1st transition series metal ions.

Fig. 6.17

Selectivity studies between the mixtures of Fe^{3+} with other transition metal ions were carried out from same stock solutions as mention above by adding 1ml macrocycle solution to the mixture of 1ml Fe^{3+} solution, 1ml other transition metal ion and 1ml DMSO. The result shows that all 1st series transition metal ions except Cu^{2+} shows same response as that of Fe^{3+} but Cu^{2+} retained its characteristic when mixed with Fe^{3+} which prompted us to carry out copper(II) selectivity studies.(**Fig.6.18,6.19**)

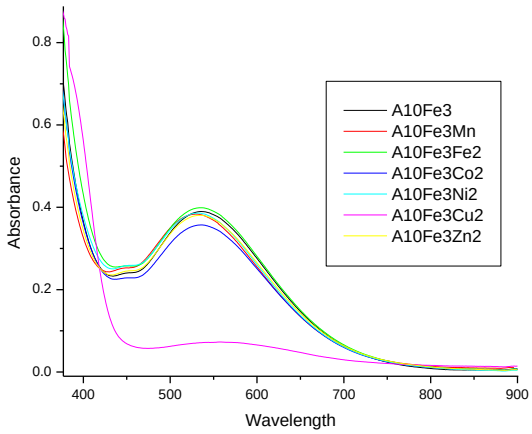

Fe^{3+} selectivity study with tetrahedral cryptand A-10

Fig. 6.18

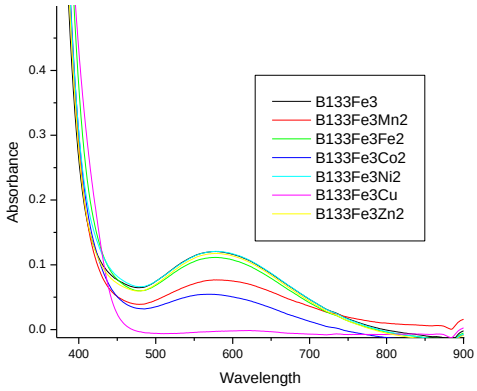

Fe^{3+} selectivity study with tetrahedral cryptand B-133

Fig. 6.19

Selectivity studies between mixture of Cu^{2+} with other transition metal ions were carried out by adding solution of host macrocycle having concentration of $1x10^{-3}$ M to the solution mixture of two metal ions at a time having concentration of $1x10^{-2}$ M each. Results show that cryptands show similar response when added to mixture of different metal ions with Cu^{2+} as that of Cu^{2+} alone which proveS that macrocycles has greater affinity for Cu^{2+} with very small interference of iron. The green colored complex was immediately formed due to Cu^{2+} complexation even in the mixtures of different metal ions with Cu^{2+} (Fig. 6.20, 6.21). Interference of iron is more for o-vanillin based cryptands than for salicylaldehyde based cryptands. (Fig. 6.20, 6.21) Thus bis-salicylaldehyde based cryptand (A-10) can serve as a better colorimetric sensor for detection of Cu^{2+} than the o-vanillin derived cryptand (B-133).

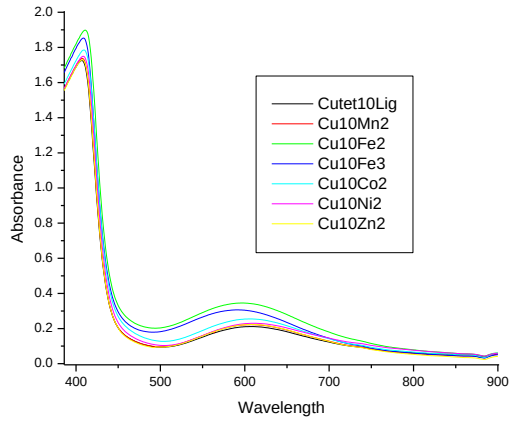

Cu^{2+} selectivity study with tetrahedral cryptand A-10

Fig. 6.20

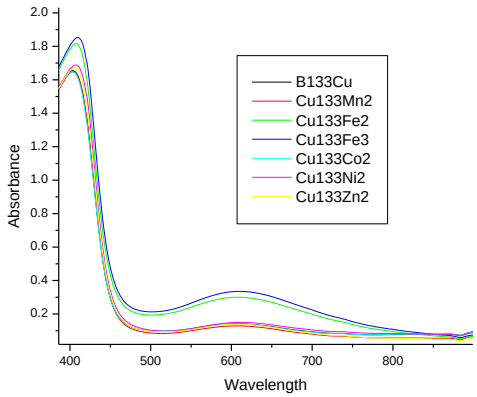

Cu^{2+} selectivity study with tetrahedral cryptand B-133

Fig. 6.21

Photoluminescence study was also carried out with the tetrahedral cryptands (1x 10^{-4} M in DCM) and 1st transition series metal ions (1x 10^{-3} M in DMSO) to evaluate them as fluorescence sensors. Zn^{2+} showed an excellent enhancement in fluorescence intensity of the tetrahedral cryptands while the other metal ions did not show any enhancement, this revealed specific recognition of Zn^{2+} compared to the other metal ions. (Fig. 6.22, 6.23) Interference of Cu^{2+} and Fe^{3+} was observed during selectivity studies of cryptands with mixture of metal ions.

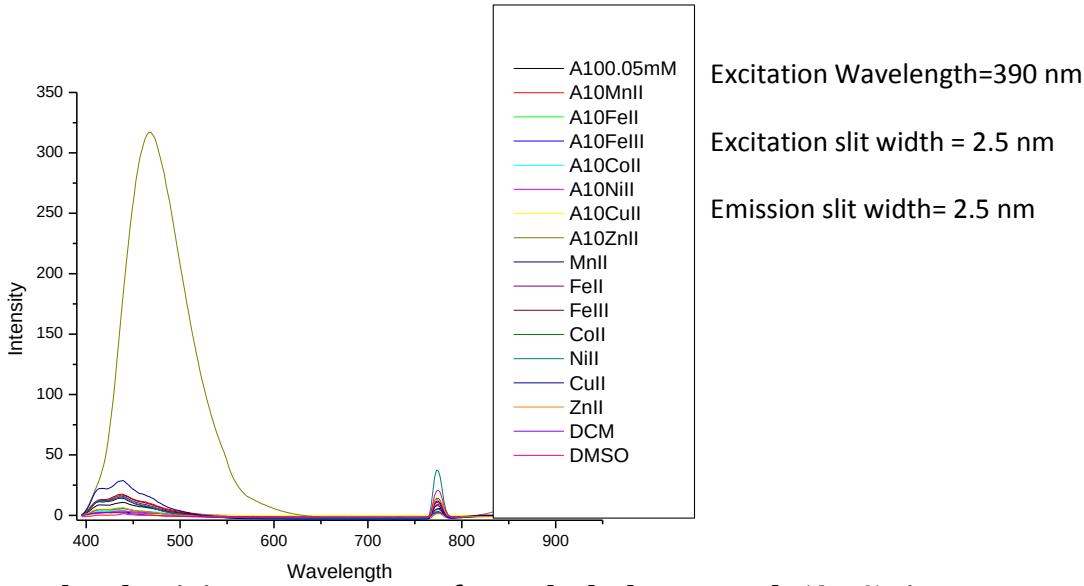

Photoluminiscence spectra of tetrahedral cryptand (A-10) in presence of 1st transition series metal ions.

Fig. 6.22

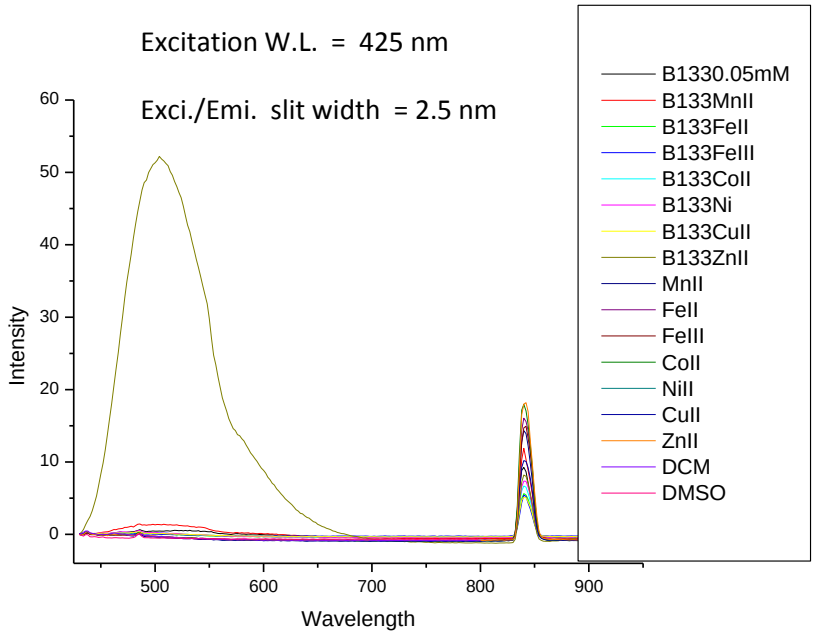

Photoluminiscence spectra of tetrahedral cryptand (B-133) in presence of 1st transition series metal ions.

Fig. 6.23

6.4 Conclusion

The synthesis of the giant sized macropolycyclic supramolecular cryptands with unique tetrahedral symmetry has been achieved by the reaction of TREN with methylene-bis-salicylaldehdye and methylene-bis-o-vanillin. Highly symmetrical tetrahedral cryptands are characterized by detailed NMR studies, mass spectral analysis and single crystal X-ray diffraction results. The newly synthesized cryptands have been studied for their binding capabilities with the transition metal ions. They show significant difference in recognition of Fe^{3+}, Cu^{2+} and Zn^{2+}. The Cu^{2+} cryptate obtained from bis-salicylaldehyde cryptand was studied for its antibacterial and antifungal activities. Various in depth studies of these novel cryptands have been undertaken and are in progress.

6.5 Experimental

General Remarks

All the chemicals and reagents were purchased from Sigma-Aldrich, Merck, and Spectrochem. All solvents were distilled before use. Column chromatography was carried out using silic-gel (60-120 mesh). Thin layer chromatography was performed on pre-coated silicagel $60F_{254}$ (Merck) aluminium sheets.

Infrared spectra were recorded on Perkin-Elmer FT-IR 16PC spectrometer as KBr pellets. ^{1}H NMR and ^{13}C NMR were recorded on Bruker 200, 300 or 400 MHz NMR spectrometer in $CDCl_{3,}$ DMSO or D_2O. Elemental analysis was carried out on Perkin-Elmer C, H, N analyser. ESI mass were recorded on Shimadzu LC-MS 2010-A and Waters micromass Quattro micro T. M. API. EI and CI mass was recorded on Thermofisher DSQ II mass spectrometer. Uv analysis was carried out on Perkin-Elmer Lambda 35 Uv-Vis spectrometer. HPLC was carried out using Shimadzu LC-10AT and UFLC using Shimadzu LC-20AD. Photoluminescence was measured using Jasco FP6300 Spectrofluorometer. Melting points were recorded in open capillaries and are uncorrected.

Tris(3-aminoethyl)amine (TREN) derived tetrahedral cryptands.

General Procedure.

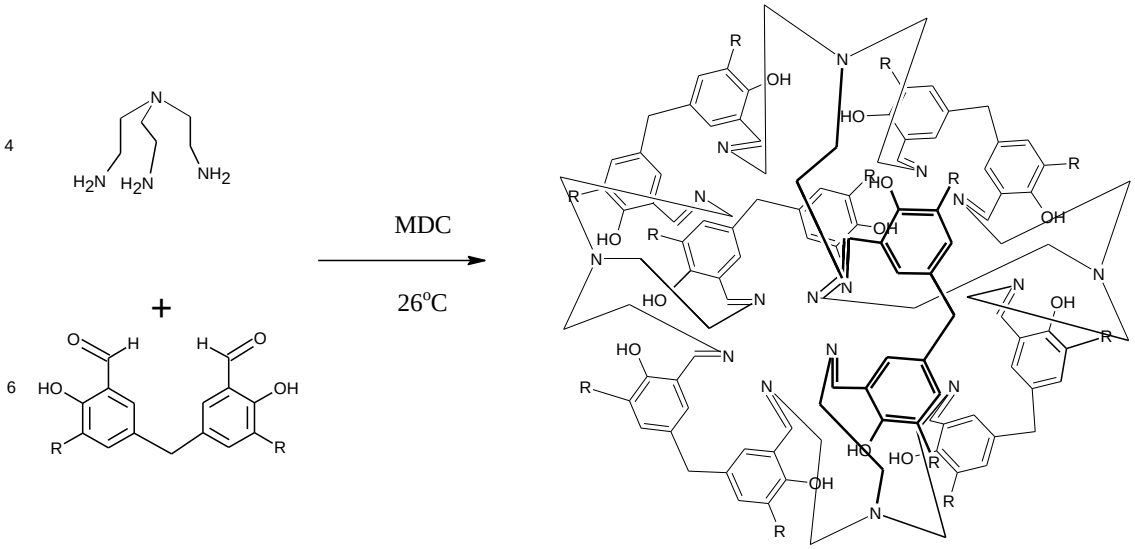

Dichloromethane (500ml) was placed in a 2L three necked round bottom flask equipped with two addition funnels and N_2 balloon. N_2 was purged for 30 minutes. Solution of 5,5' methylene-bis-aldehydes (0.003 mol) in 600ml dichloromethane and TREN (tris(3-aminoethyl)amine) (0.002 mol) in 400ml dichloromethane was added drop wise from addition funnels over 12 hrs to the magnetically stirred dichloromethane under nitrogen atmosphere. Yellow colour was developed on progress of the reaction. After stirring for further twelve hours time the solvent was removed on rotary evaporator to small volume of 50 ml solution, which was adsorbed on silica-gel for column chromatography. TLC showed very small amount of starting material, nonpolar product spot and many polar impurities. Starting material was separated by elution with MDC followed by single spot yellow product on further elution with MDC: Methanol system (gradient).

Tetrahedral Cryptand from TREN and 5,5'-Methylene-bis-salicylaldehyde (A-10).

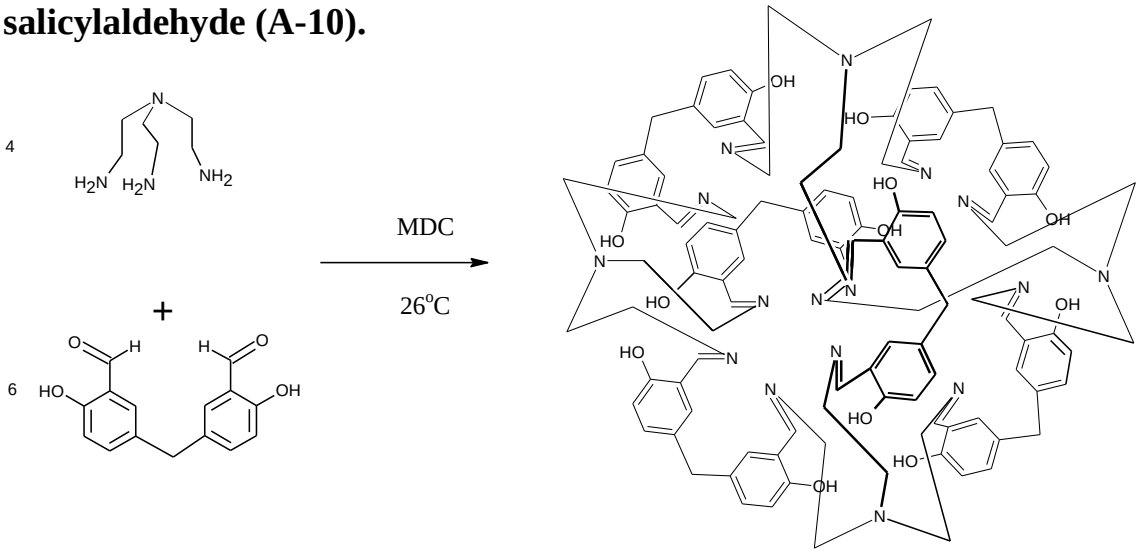

5,5'-Methylene-bis-salicylaldehyde (1g, 0.004mol) and tris(3-aminoethyl)amine (TREN) (0.38g, 0.002mol) were reacted in 1800ml MDC to yield the cryptand (A-10).

Yield: 0.186 g (15%), M.P.= 225 °C (decomposed).

^{1}H NMR (400 MHz, $CDCl_3$): δ 14.04 (s, 1H), 7.52 (d, *J* = 1.2 Hz, 1H), 7.42 (dd, J_1 = 1.6 Hz, J_2 = 6.8 Hz, 1H), 7.09 (d, *J* = 6.8 Hz, 1H), 5.47 (d, *J* = 1.6 Hz, 1H), 3.71 (d, *J* = 9.4 Hz, 1H), 3.63 (s ,1H), 3.14 (t, *J* = 9.4 Hz, 1H), 2.86 (t, *J* = 9.1 Hz, 1H), 2.77 (d, *J* = 9.4 Hz, 1H).

^{13}C NMR (400 MHz, $CDCl_3$): δ 165.9, 160.1, 132.4, 131.2, 130.8, 119.2, 117.4, 58.4, 56.2, 40.4

ESI Mass: 1907 m/z

HPLC Purity: 99.2%

IR (KBr disc, cm^{-1}) : 3437 (phenol, υ(O-H)), 2919 (methylene, υ_{as}(C-H)), 2846 methylene, υ_s(C-H)), 1634 (imine, υ(C=N)), 1588, 1491 (aromatic ring, υ(C=C)), 1441 ($\delta_s(CH_2)$), 1367, 1275, 1223 (aromatic, υ(C-N)), 1155, 1039 (aliphatic, υ(C-N)), 923, 822, 780, 665, 630, 578, 460 (out of plane, δ(C-H))

Tetrahedral Cryptand from TREN and 5,5'-Methylene-bis-(3-methoxy-salicylaldehyde) B-133

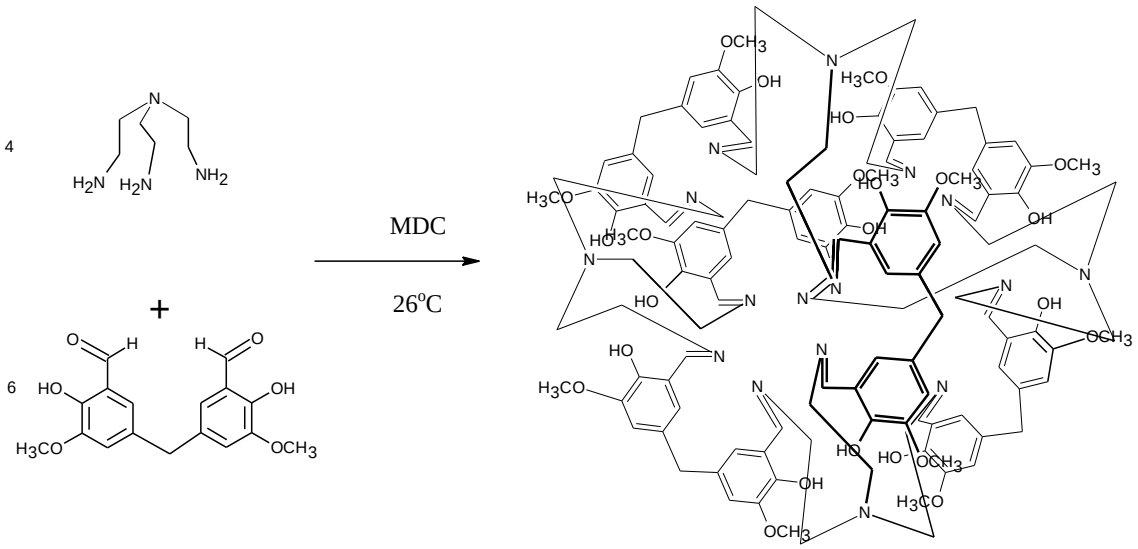

5,5'-Methylene-bis-(3-methoxy-salicylaldehyde) (1g, 0.003mol) and tris(3-aminoethyl)amine (TREN) (0.31g, 0.002mol) were reacted in MDC (1500ml) to yield the cryptand (B-133).

Yield: 0.509 g (43%), M.P.= 250 °C (decomposed).

^{1}H NMR (400 MHz, $CDCl_3$): δ 14.66 (s, 1H), 7.51 (s, 1H), 7.17 (s, 1H), 5.23 (s, 1H), 4.08 (s, 3H), 3.70 (d , *J* = 12.0 Hz, 1H), 3.60 (s,1H), 3.18 (t, *J* = 9.4 Hz, 1H), 2.83 (d, *J* = 7.6 Hz, 2H).

^{13}C NMR (400 MHz, $CDCl_3$): δ 166.1, 153.2, 149.2, 131.7, 123.4, 118.9, 118.1, 58.7, 57.6, 56.1, 41.3

QTOF mass m/z: 1133.4 (M^+/2)

HPLC Purity: 96.8%

IR (KBr disc, cm^{-1}) : 2937 (methylene, υ_{as}(C-H)), 2838 (methylene, υ_s(C-H)), 2361, 1634 (imine, υ(C=N)), 1591, 1474 (aromatic ring, υ(C=C)), 1403 ($\delta_s(CH_2)$), 1338, 1266 (aromatic, υ(C-N)), 1154 (ether, υ_sC-O), 1068 (aliphatic, υ(C-N)), 1040 (ether, υ_{as}C-O), 986,932, 802, 758, 700, 674, 590 (out of plane, δ(C-H))

Copper cryptate from tetrahedral cryptand (A10 Cu)

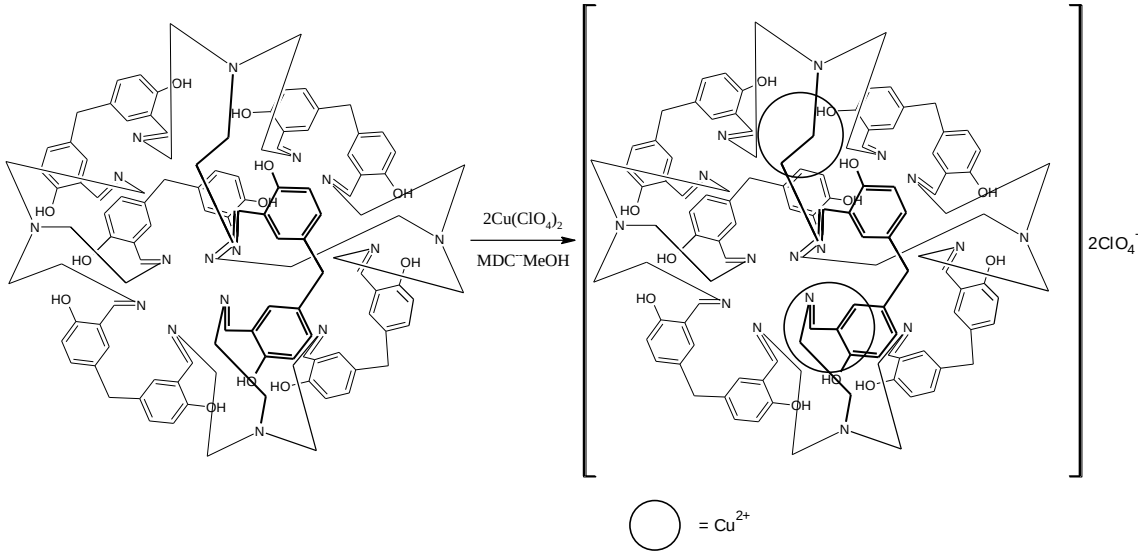

Tetrahedral cryptand (A-10) (0.2g, 0.0001 mol) in MDC (50ml) and $Cu(ClO_4)_2x6H_2O$ (0.155g, 0.0004 mol) in methanol (20ml) were reacted at 40 °C to give dirty green precipitates which were filtered and washed with methanol (5x 20ml) and MDC (3x 50ml) to yield the cryptate (A-10-Cu).

Yield: 0.24g (94%)

M.P. > 300 °C (decomposed)

^{1}H NMR (400 MHz, DMSO-d_6): δ 10.56 (d,1H), 10.22 (s, 1H), 7.85 (s, 1H), 7.46 (s, 1H), 6.93 (s, 1H), 3.84 (s, 1H), 2.94 (s, 1H).

IR (KBr disc, cm^{-1}) : 3345 (phenol, υ(O-H)), 2913 (methylene, $υ_{as}$(C-H)), 1636 (imine, υ(C=N)), 1534, (aromatic ring, υ(C=C)), 1472 ($δ_s(CH_2)$), 1388, 1274, (aromatic, υ(C-N)), 1070 (aliphatic, υ(C-N)), 828, 624 (out of plane, δ(C-H))

Tetrahedral Amino Cryptand

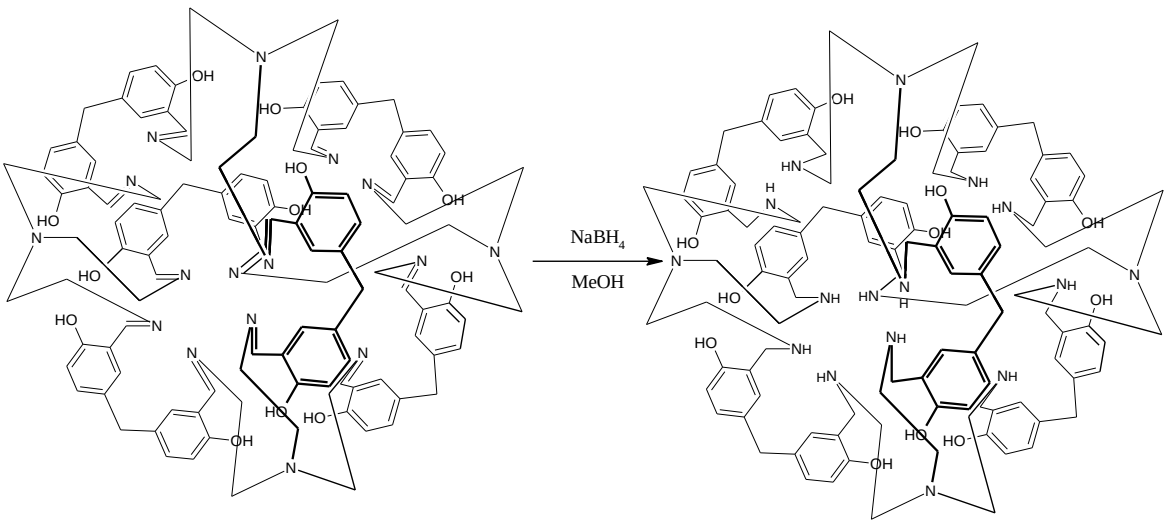

Tetrahedral cryptand (A-10) (0.2 g, 0.0001mol) was suspended in methanol (40 ml) in 50 ml round bottom flask. Sodiumborohydride 1g (excess) added gradually in portions. Yellow coloured cryptand solution was changed to colourless product which was filtered and washed with excess of methanol to yield reduced tetrahedral cryptand.

Yield : 0.168 g (83%)

M.P. > 300 °C

^{1}H NMR (400 MHz, $CDCl_3$+CD_3OD): δ 6.85 (d, *J* = 7.8 Hz, 1H), 6.68 (s, 1H), 6.54 (d, *J* = 8.1 Hz, 1H), 3.72 (s, 2H), 3.65 (s, 1H), 2.53 (d, 4H), 1.26 (s, 1H).

Antibacterial and antifungal activities

Broth dilution method was used to determine minimum inhibitory concentration (MIC) values for the gram positive as well as gram negative bacterial strains and to determine minimum fungicidal concentration (MFC) values for *C. albicans*. DMSO was used as diluents/vehicle to get desired concentration of drugs (test compounds) to test upon standard bacterial strains. Silversulphadiazine and ciprofloxacin were used as standard antibacterial drugs for comparison of MIC values while greceofulvin and nystatin were used as standard antifungal dugs for comparison of MFC values.

Mueller Hinton broth was used as nutrient medium to grow and dilute the drug suspension for the test bacteria. Inoculum size for test strain was adjusted to 10^8 CFU [Colony Forming Unit] per milliliter by comparing the turbidity. The strains were procured from Institute of Microbial Technology, Chandigarh.

Procedure:

1. Serial dilutions were prepared in primary and secondary screening.
2. The control tube containing no antibiotic is immediately sub cultured [before inoculation] by spreading a loopful micro organism evenly over a quarter of plate of medium suitable for the growth of the test organism and put for incubation at 37 $^{\circ}$C overnight.
3. The MIC of the control organism is read to check the accuracy of the compound concentrations.
4. The lowest concentration inhibiting growth of the organism is recorded as the MIC.
5. The amount of growth from the control tube before incubation [which represents the original inoculum] is compared.
6. Each test compound was diluted obtaining 2000 microgram /ml concentration, as a stock solution.
7. **Primary screen:** In primary screening 1000 microgram/ml, 500 microgram/ml, and 250 microgram/ml concentrations of the synthesized drugs

were taken. The active synthesized drugs found in this primary screening were further tested in a second set of dilution against all microorganisms.

8. **Secondary screen:** The drugs found active in primary screening were similarly diluted to obtain 200 microgram/ml 100 microgram/ml, 50 microgram/ml, 25 micro/ml, 12.5 microgram/ml and 6.25 microgram/ml concentrations.

Reading Result:- The highest dilution showing at least 99 % inhibition zone is taken as MIC. The result of this is much affected by the size of the inoculum. The test mixture should contain 10^8 organism/ml.

Table 6.1 Minimum inhibitory concentration.

DRUG	***E. coli***	***P. aeruginosa***	***S. aureus***	***S. pyogenus***	***P. vulgaris***
(μg/ml)	MTCC 443	MTCC 1688	MTCC 96	MTCC 443	MTCC 744
Cu^{2+}cryptate	200	**125**	250	250	200
Ciprofloxacin	25	25	50	50	25
Silver-sulphadiazine	50	100	100	125	50

Table 6.2 Minumium Fungicidal Concentration.

DRUG	***C. albicans***
	MTCC 227 (μg/ml)
Cu^{2+}cryptate	500
NYSTATIN	100
GRESEOFULVIN	500

Solution Studies for Host-Guest Stoichiometry Determination:

Job's method was used for determination of Host : Guest stoichiometry. Stock solution of 1mM bis-salicylaldehyde derived tetrahedral cryptand was prepared in DCM while 1mM $Cu(ClO_4)_2$ solution was prepared in DMSO. Solutions were mixed in proportion shown in the following table and their electronic spectra were recorded at 26 °C. Similar procedure using same concentrations was used for bis-3-methoxy-salicylldehyde derived cryptand for determination of the its binding staichiometry with Cu^{2+}.

Table : 6.3

Tetrahedral cryptand	5ml	4.5ml	4ml	3.5ml	3ml	2.5ml	2ml	1.5ml	1ml	0.5ml	0ml
$Cu(ClO_4)_2$	0ml	0.5ml	1ml	1.5ml	2ml	2.5ml	3ml	3.5ml	4ml	4.5ml	5ml

Host-Guest Recognition Studies Using UV Spectral Characteristics:

Host-guest studies between the tetrahedral cryptands (A10: bis-salicylaldehyde based cryptand and B133: o-vanillin based cryptand) with 1st transition series metal ions were carried using $1x10^{-4}$M concentration in DCM of host cryptand and $1x10^{-3}$ M concentration in DMSO of guest ions. Both solutions of host and guest molecules were mixed in equal volumes.

Selectivity studies between the mixtures of Fe^{3+} with other transition metal ions were carried out from same stock solutions as mentioned above by adding 1ml cryptand solution to the mixture of 1ml Fe^{3+} solution, 1ml another transition metal ion and 1ml DMSO. The response of all test solutions were compared with the reference solution prepared by addition of 1ml cryptand solution to the mixture of 1ml $Fe(ClO_4)_3$ solution and 2ml DMSO. Selectivity studies between mixture of Cu^{2+} with the other transition metal ions were carried out by adding 1ml solution of host macrocycle having

concentration of $1x10^{-3}$ M in DCM to the solution mixture of two metal ions at a time having concentration of $1x10^{-2}$ M in DMSO (1ml each) and 1ml DMSO. Their responses were compared with the reference solution prepared by adding 1 ml cryptand solution to the mixture of 1ml $Cu(ClO_4)_2$ solution and 2 ml DMSO.

Fluorescence studies were carried out using 0.1mM stock solutions of tetrahedral cryptands (A10 and B133) in DCM and $1x10^{-3}$ M solutions of 1^{st} transition series metal ions in DMSO. Spectroscopy grade DCM and DMSO were used for the study. The host-guest complexes were excited at 390 nm with 2.5 mm excitation and emission slit width using Jasco FP6300 spectrophotometer. Photoluminescence spectra for blank solvents were also recorded with no response in the 390 to 400 nm range. Please see result and discussion for the graphs obtained.

6.6 Spectra

Spectrum 6.1

IR

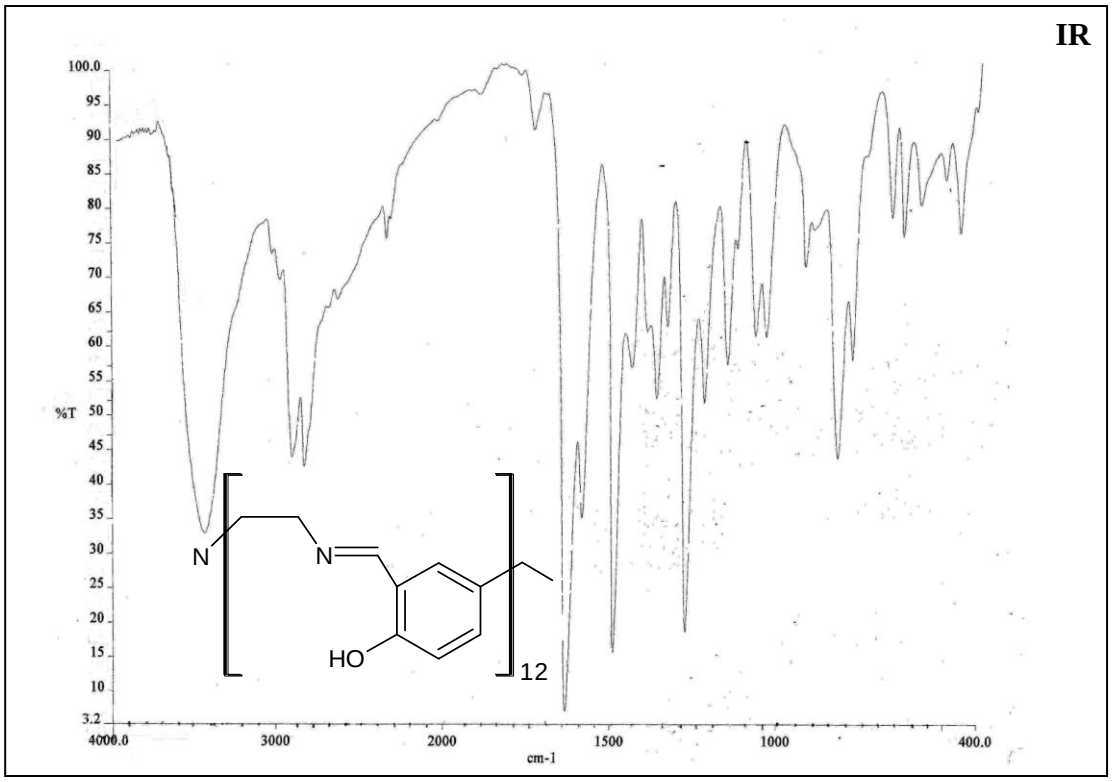

Spectrum 6.2

^{1}HNMR

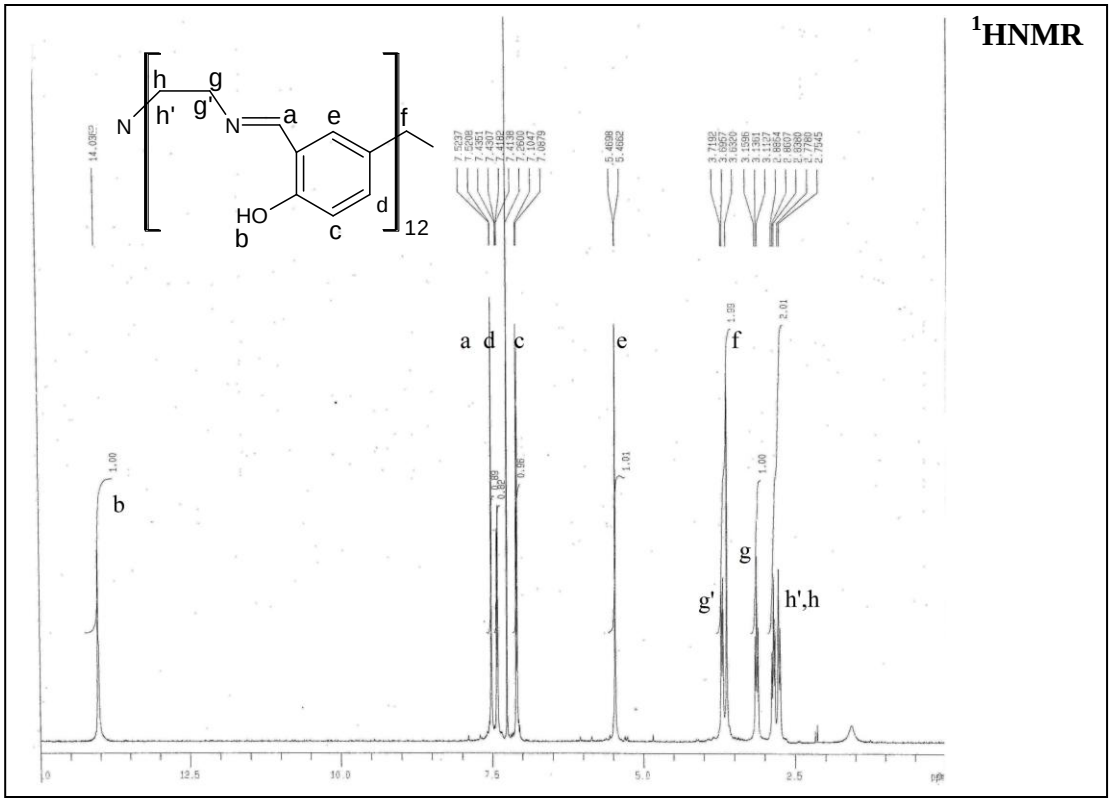

Spectrum 6.3

^{13}CNMR

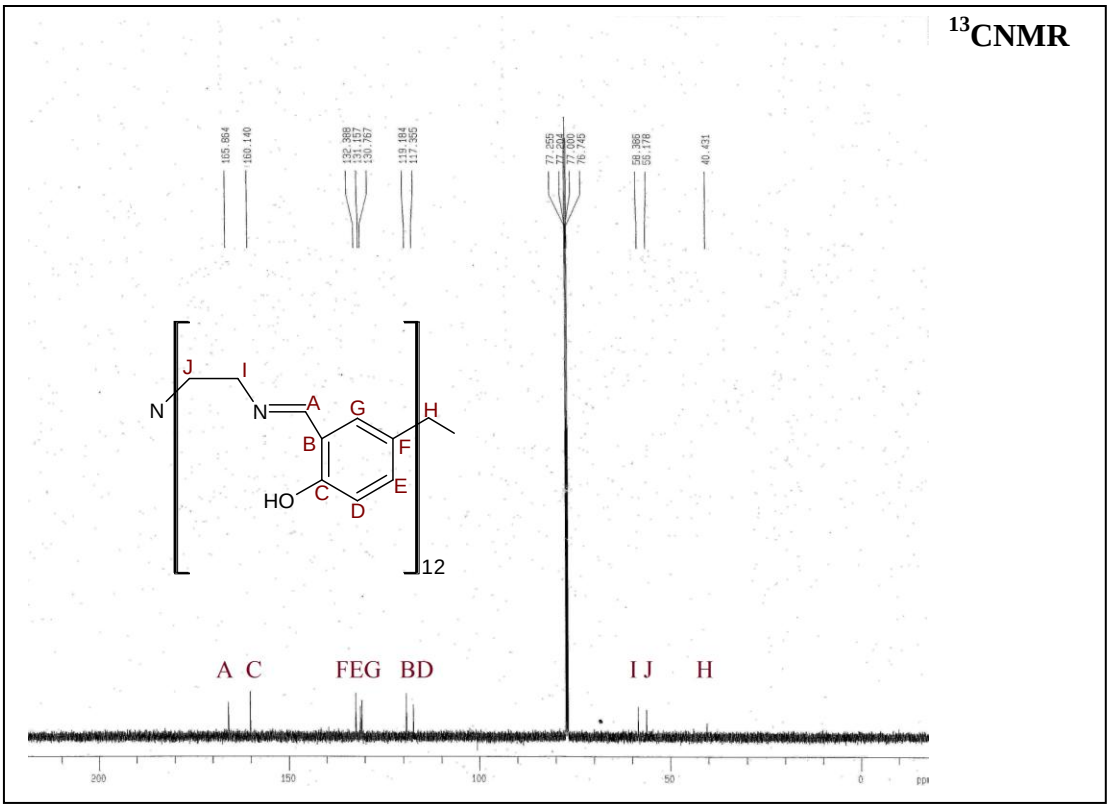

Spectrum 6.4

DEPT 90

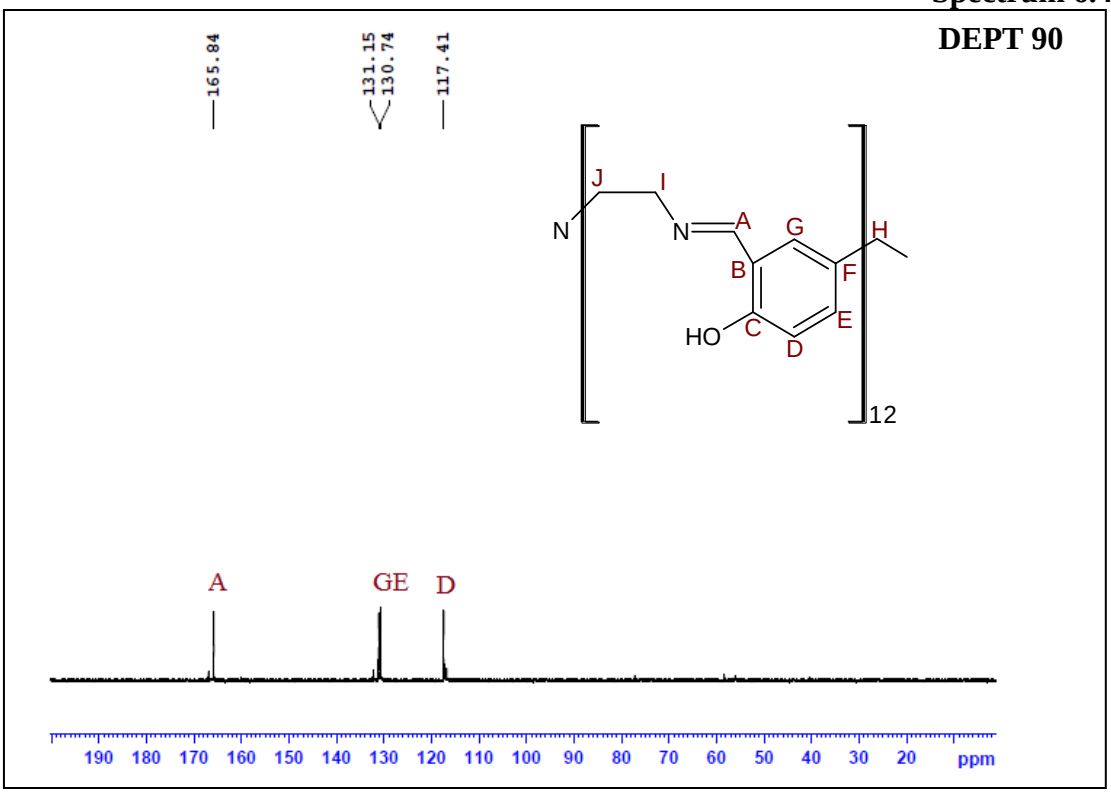

Spectrum 6.5

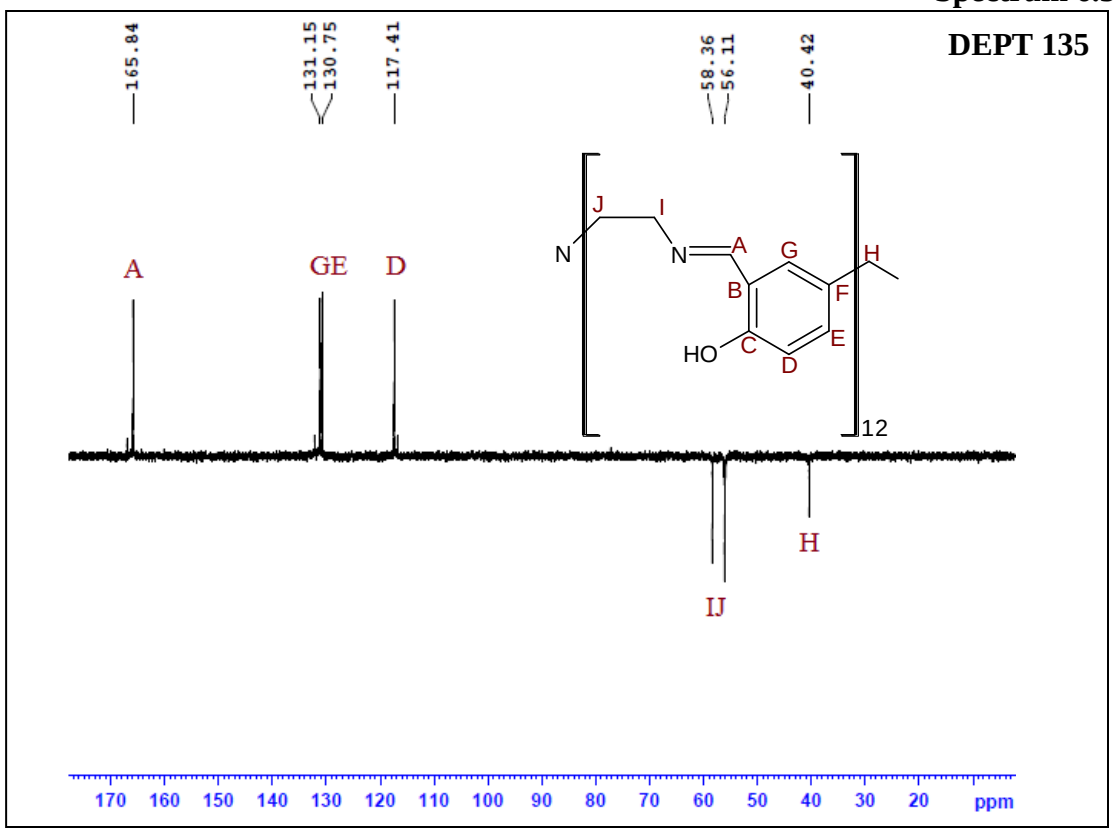

Spectrum 6.6

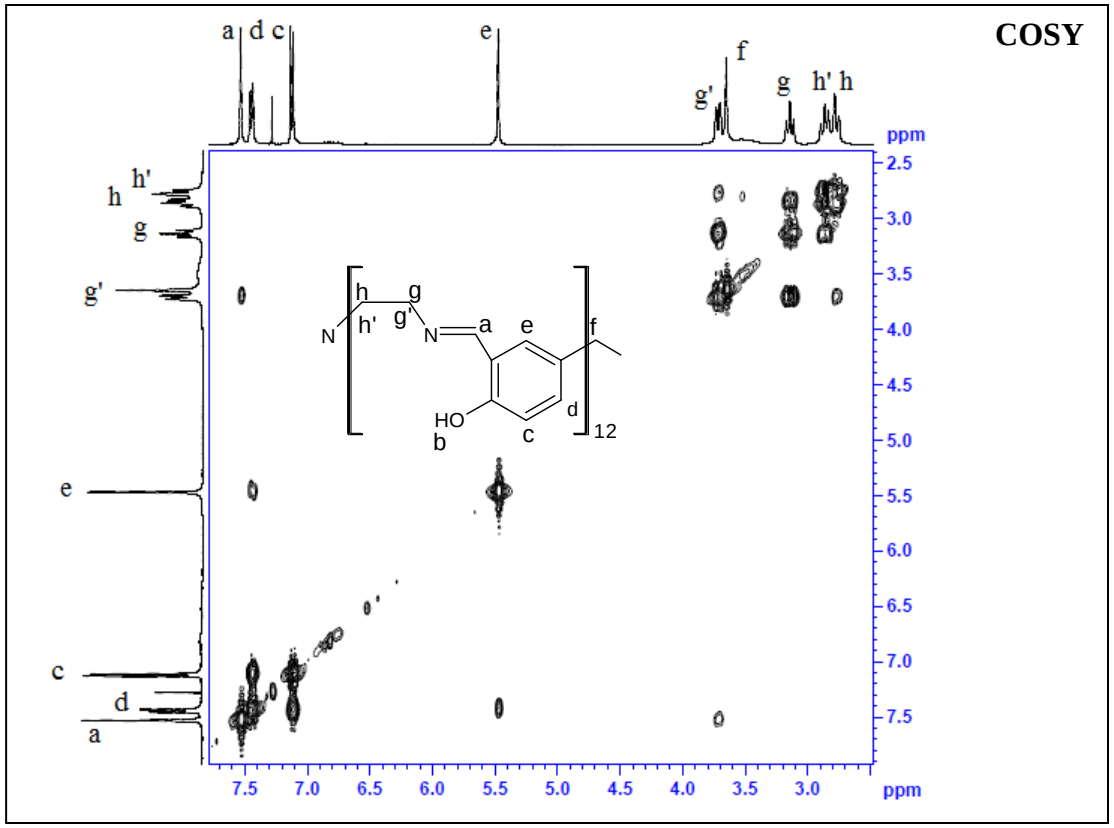

Spectrum 6.7

NOESY

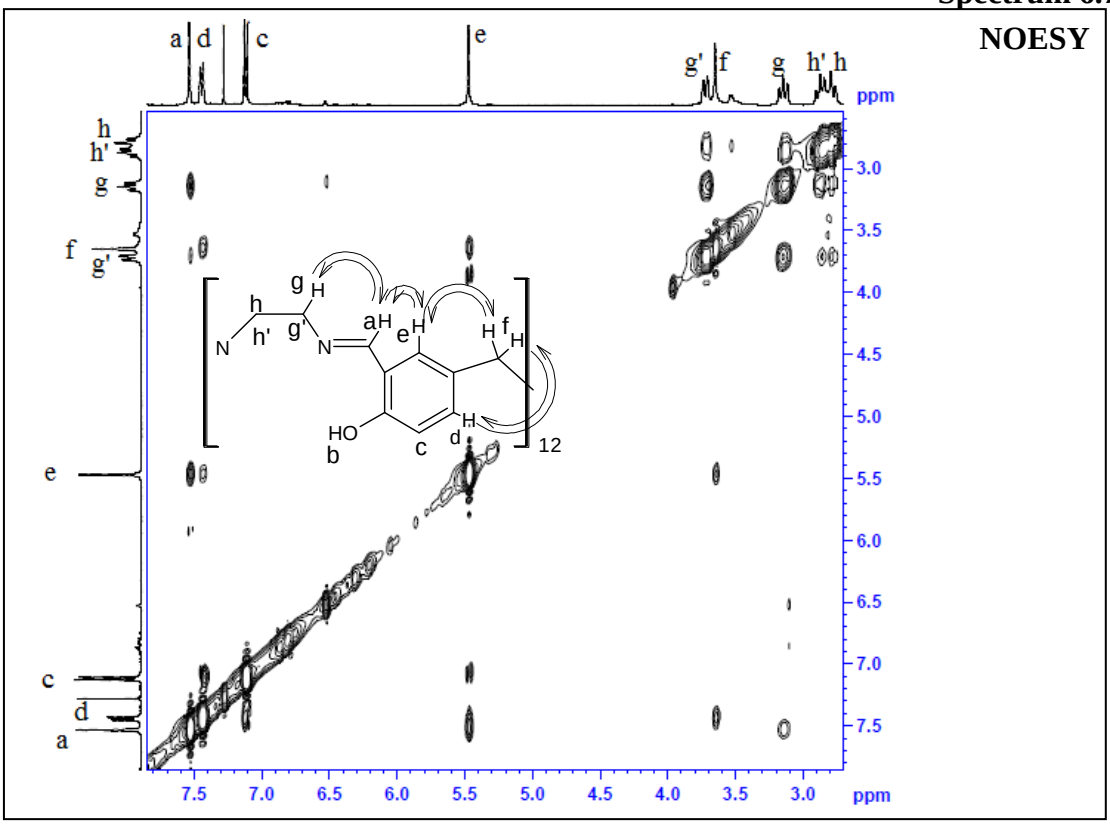

Spectrum 6.8

HMQC

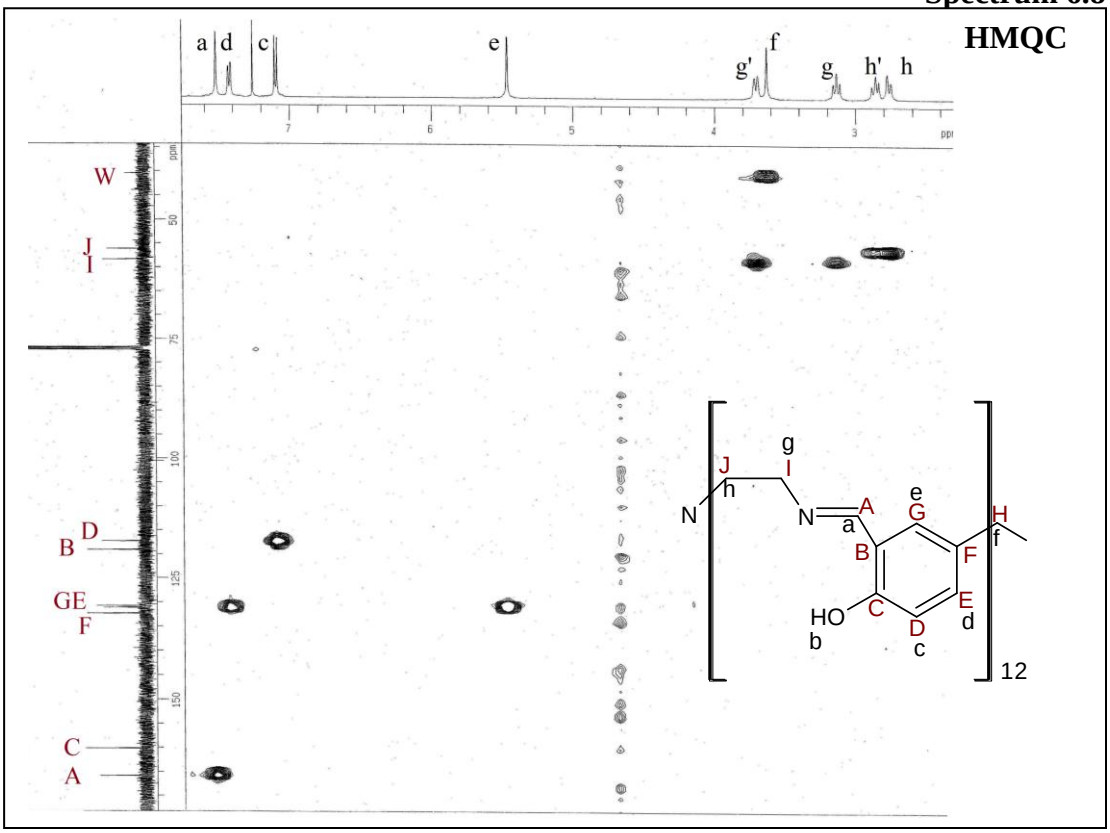

Spectrum 6.9

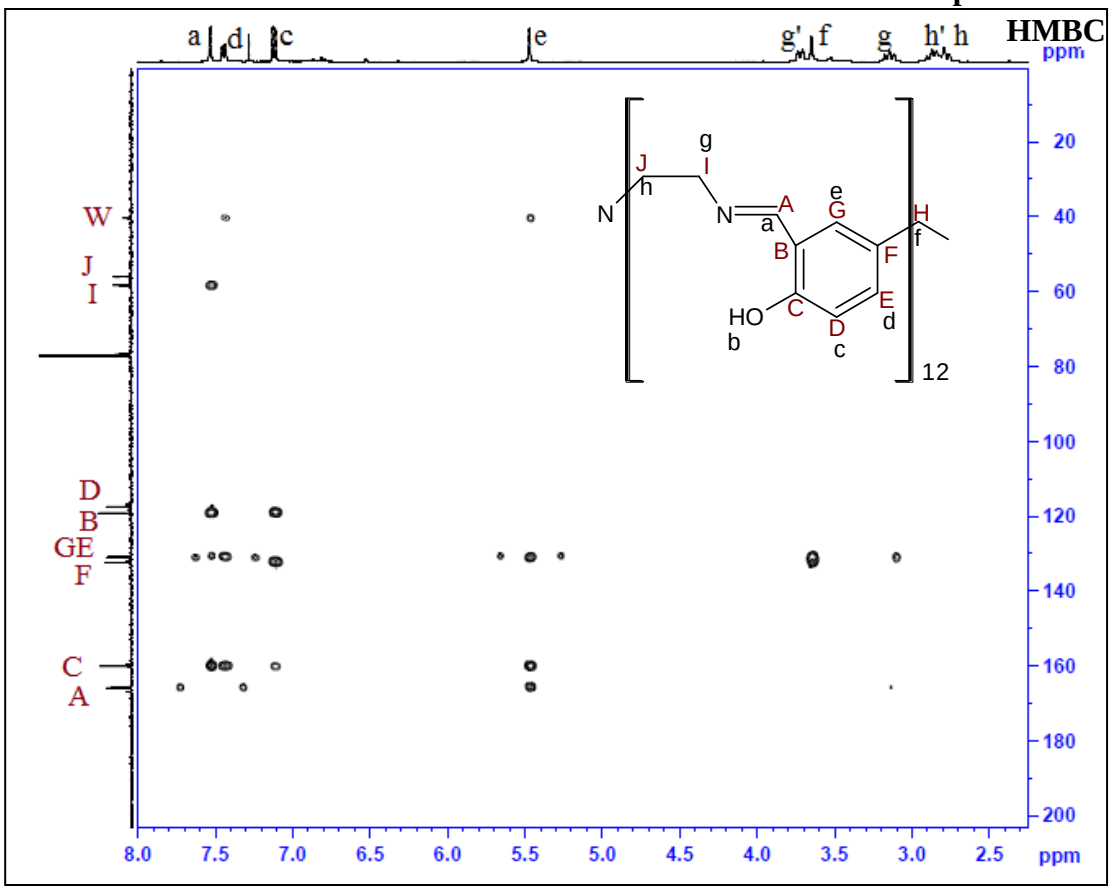

Spectrum 6.10

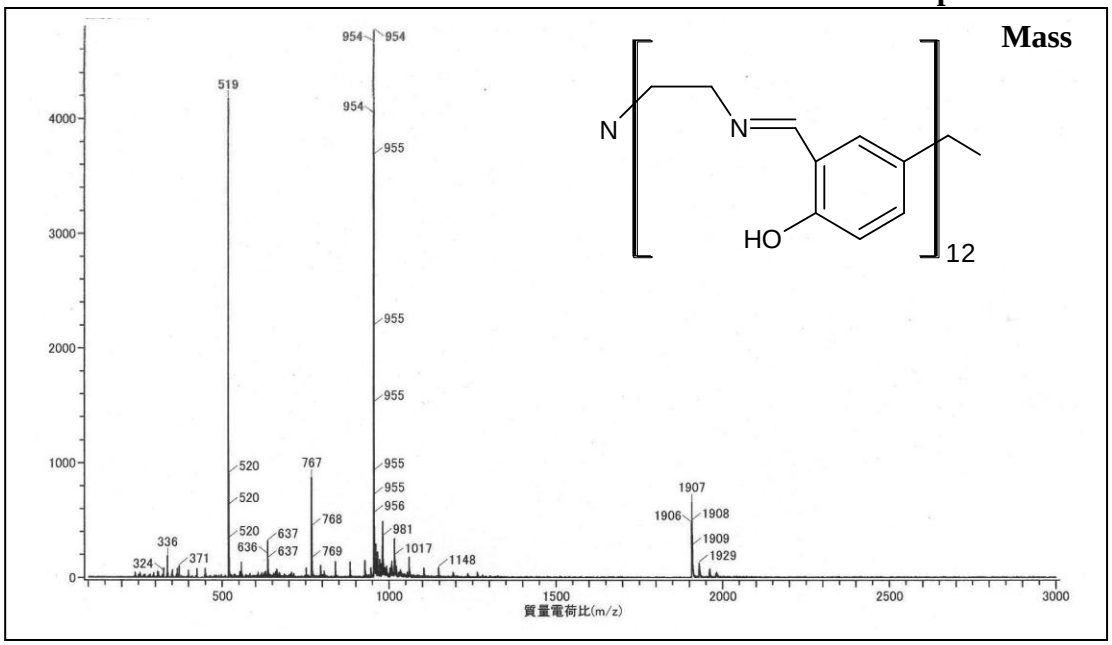

Chromatogram 6.11

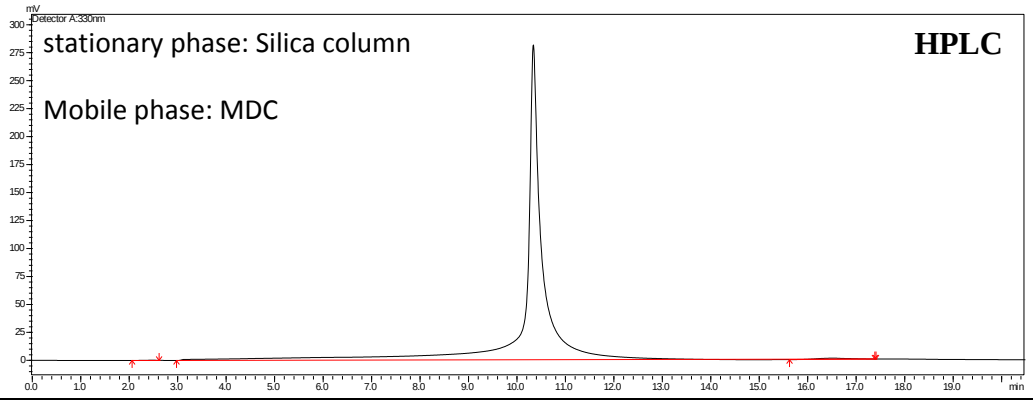

Peak	Name	Ret. Time	Area%
1	imp-1	2.503	0.0711
2	EXPT A-10(Tetrahedron from TREN and 5,5'methylene –bis-salicylaldehyde	10.334	99.2090
3.	imp 2	16.521	0.7199

Spectrum 6.12

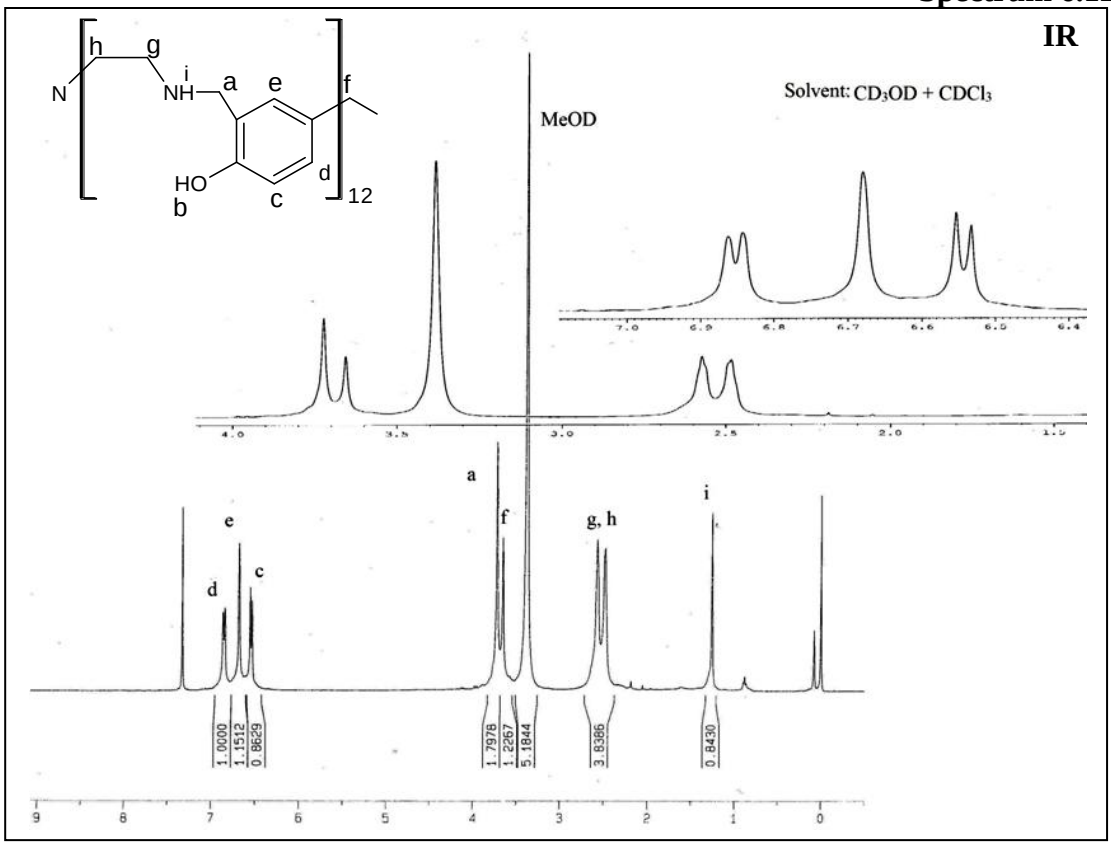

Spectrum 6.13

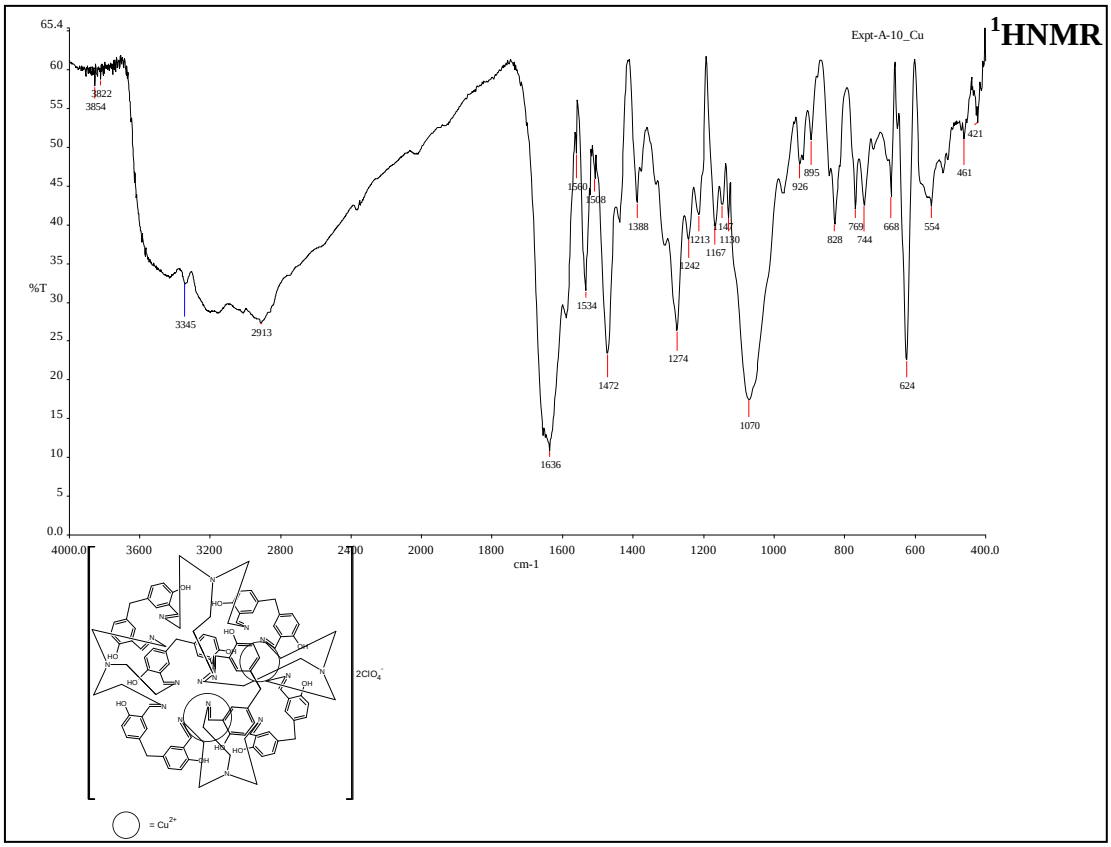

Spectrum 6.14

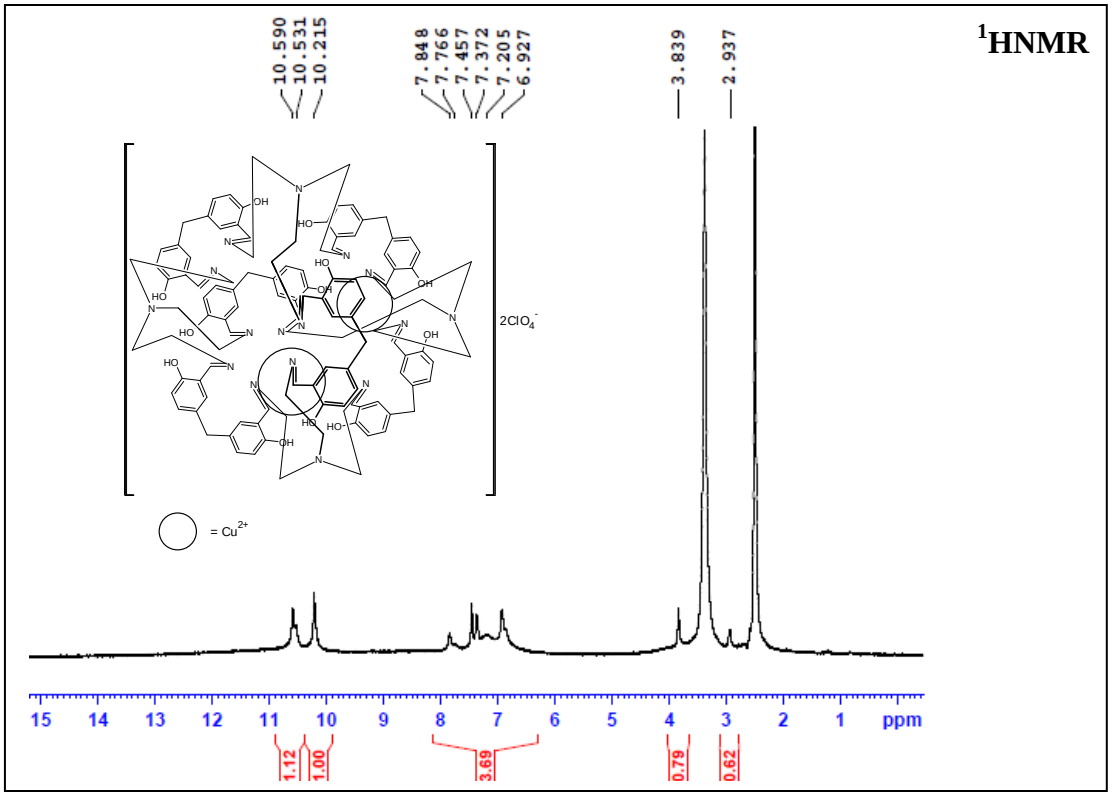

Spectrum 6.15

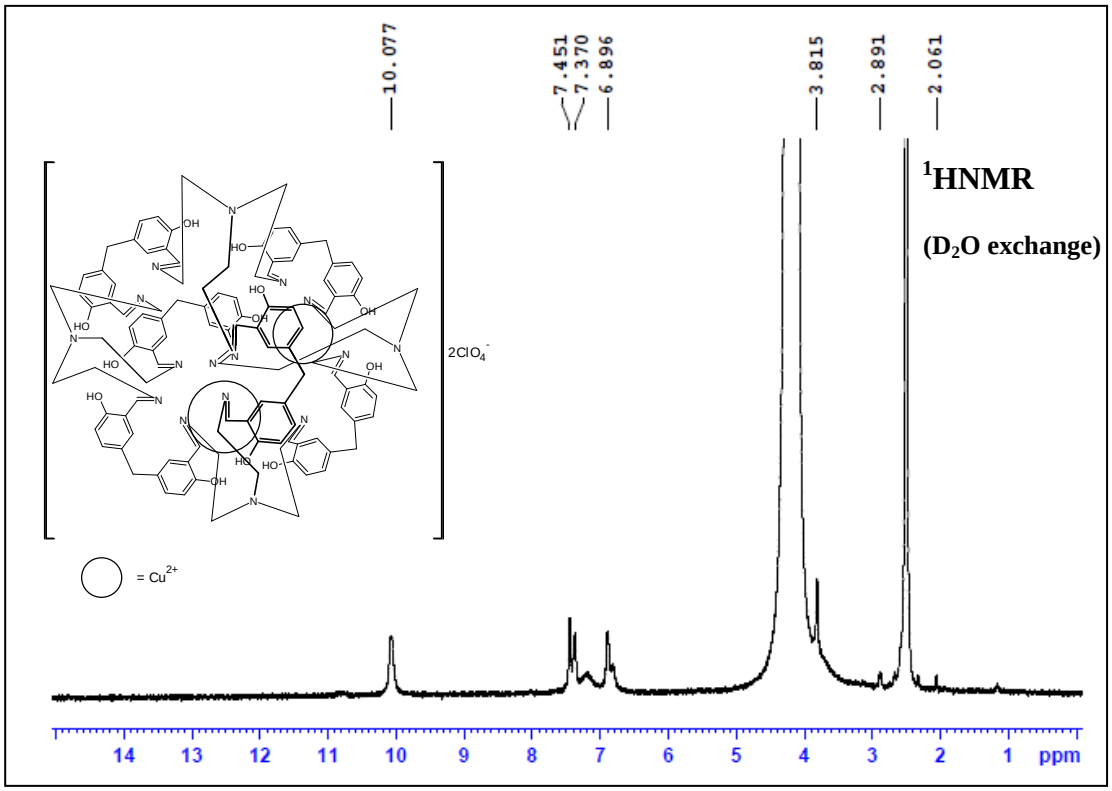

Spectrum 6.16

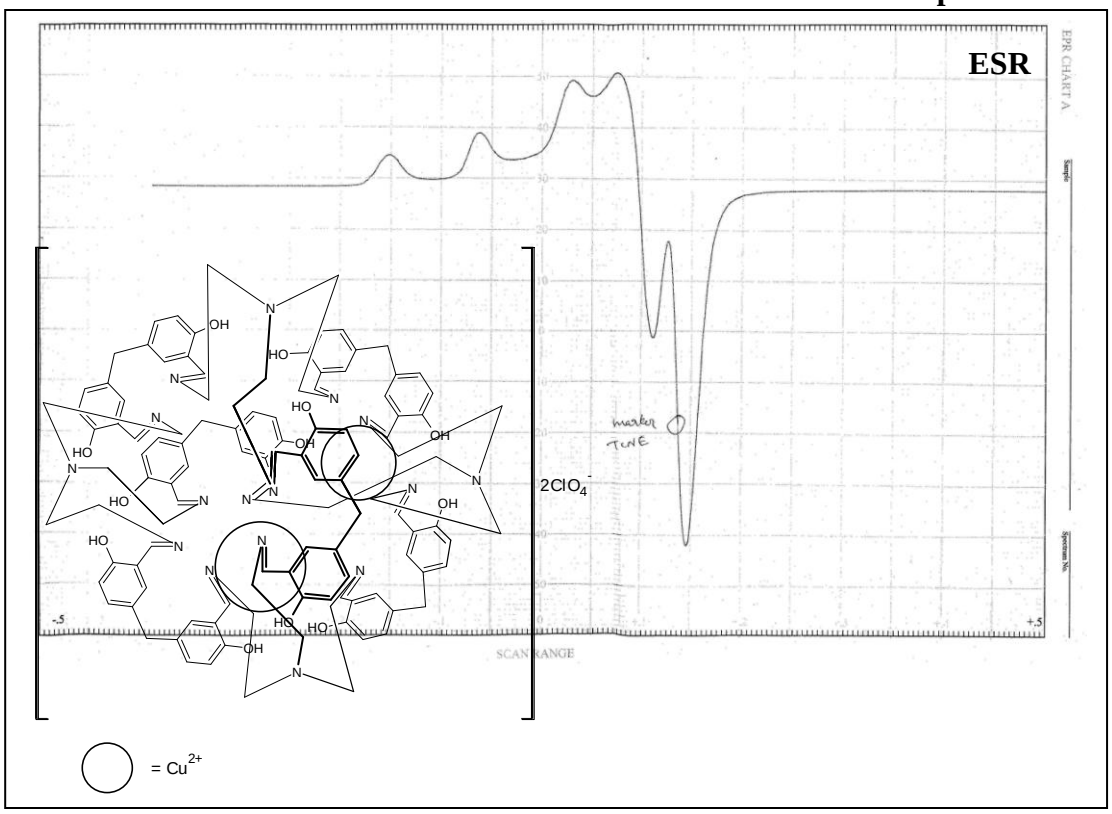

Spectrum 6.17

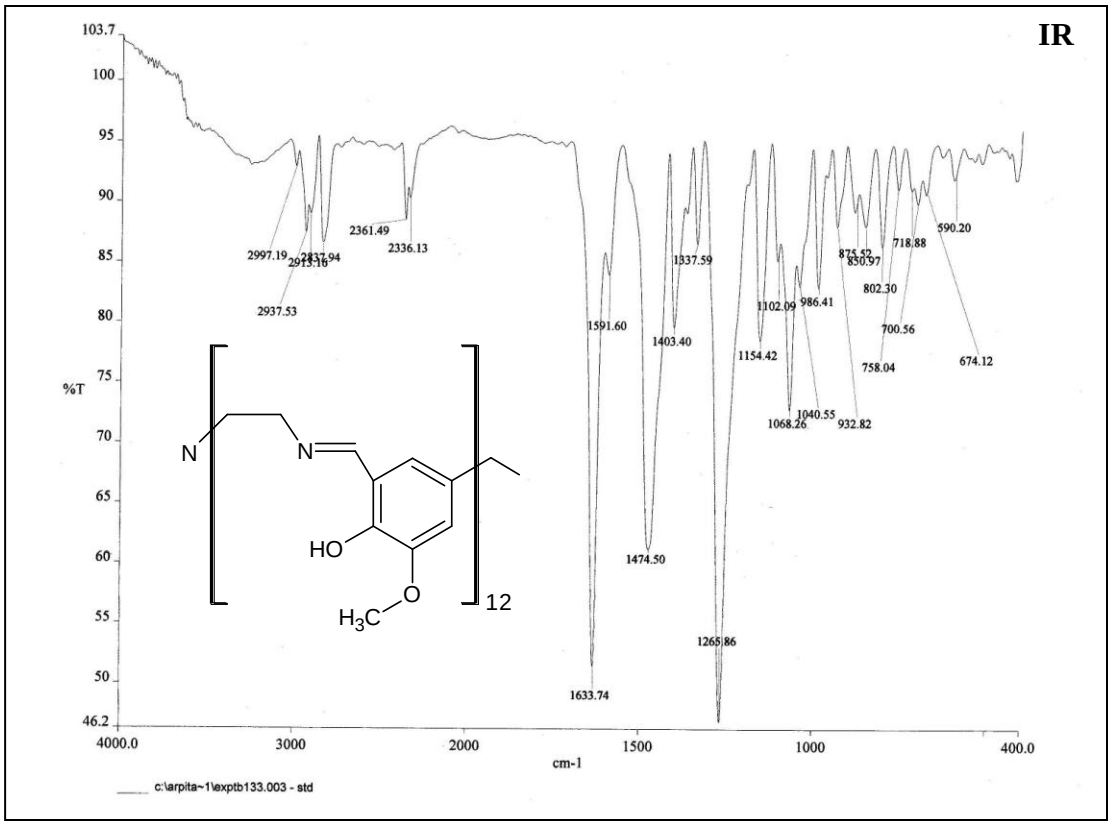

Spectrum 6.18

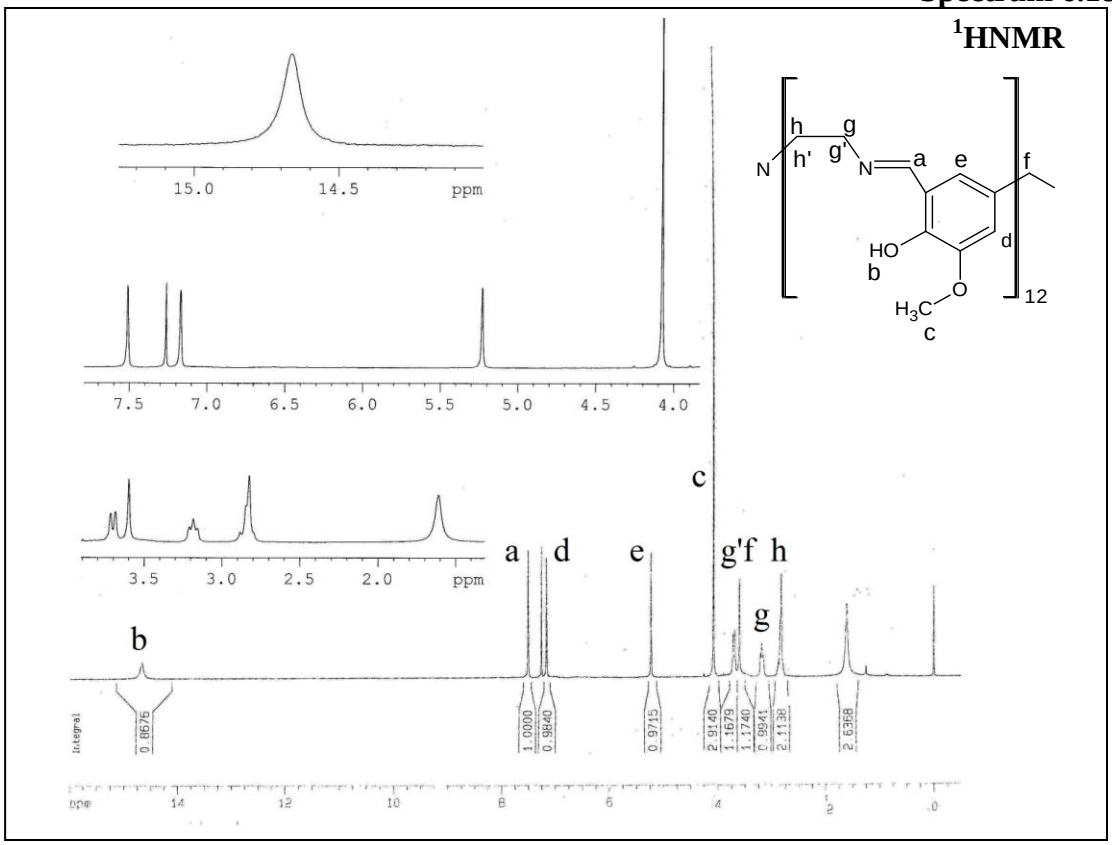

Spectrum 6.19

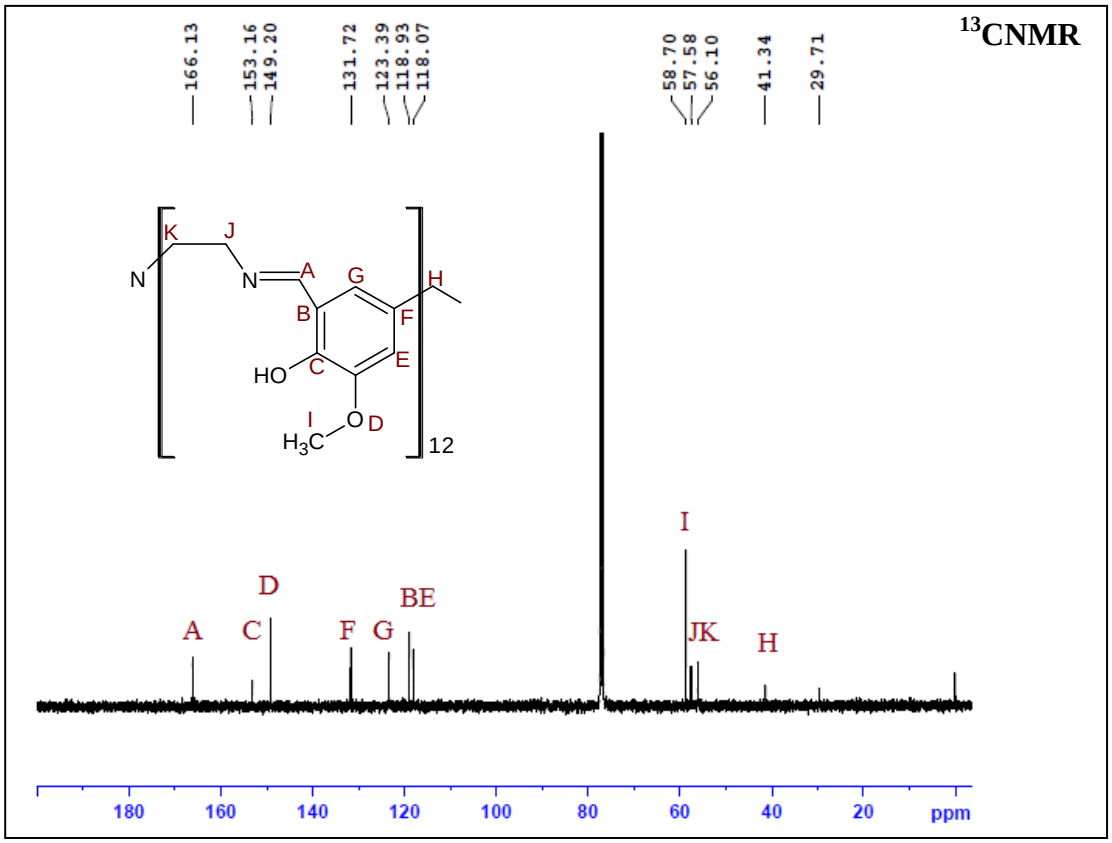

Spectrum 6.20

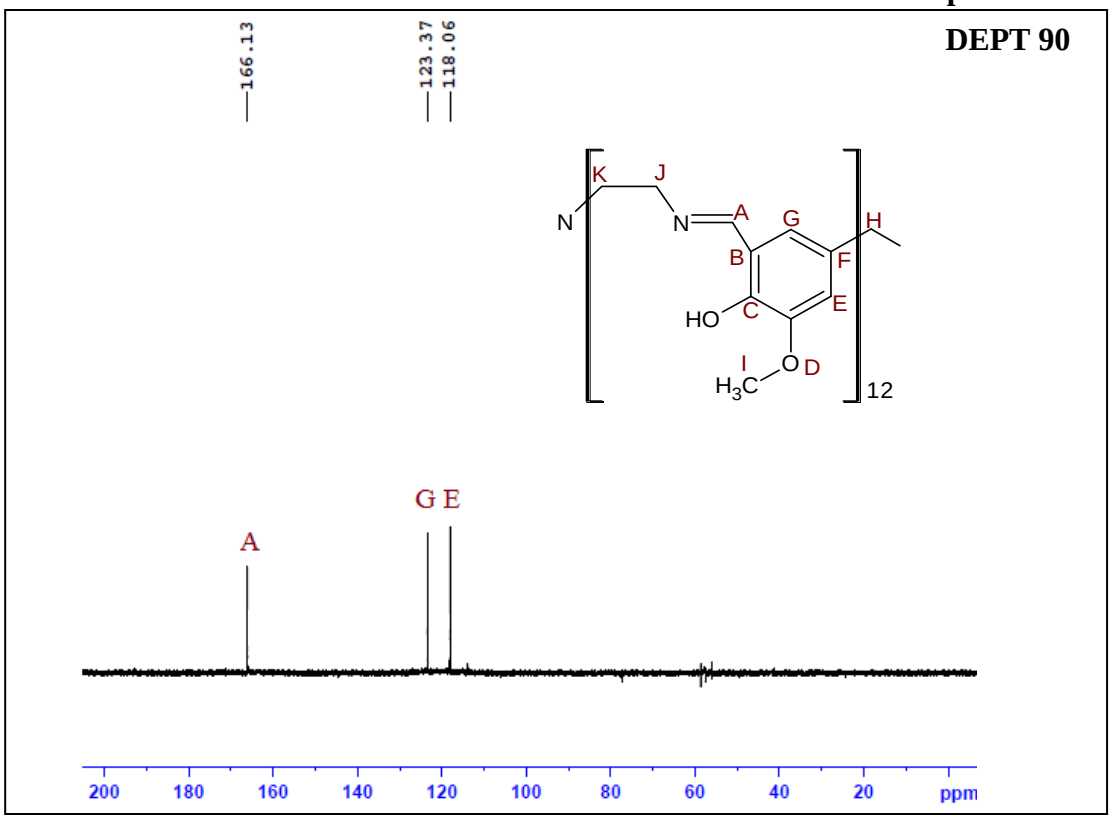

Spectrum 6.21

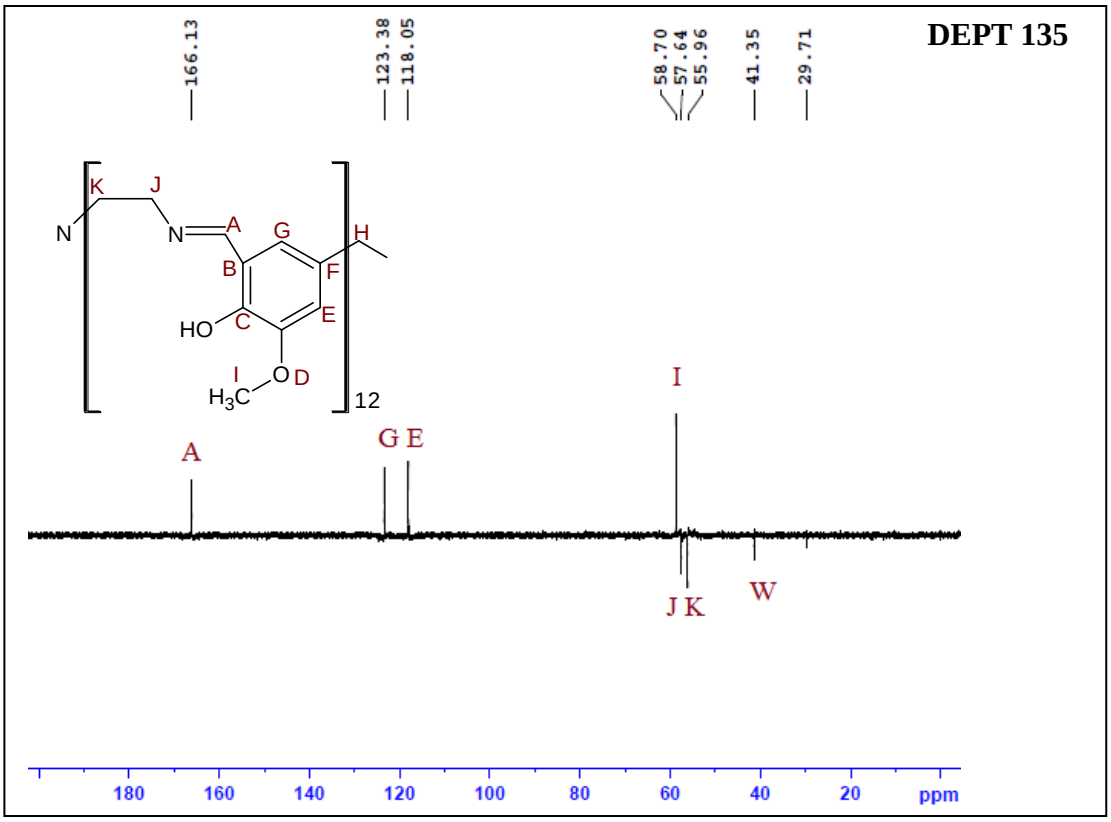

Spectrum 6.22

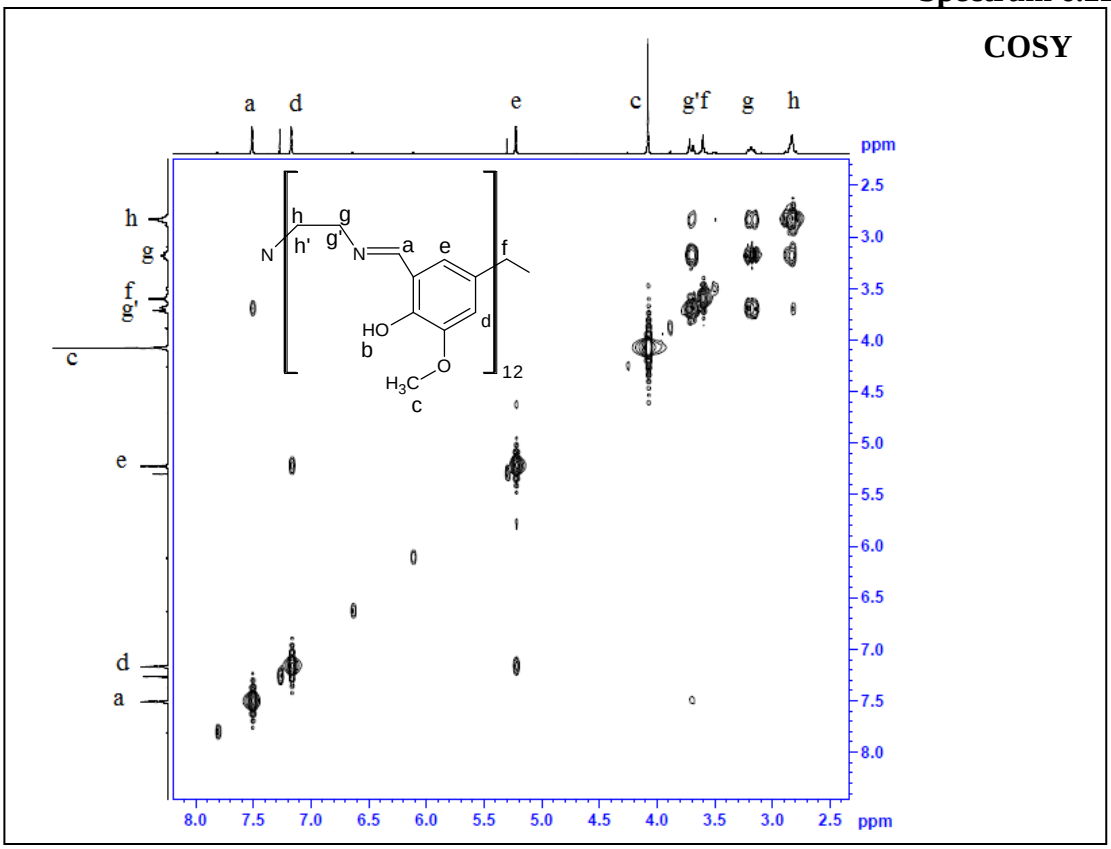

Spectrum 6.23

NOESY

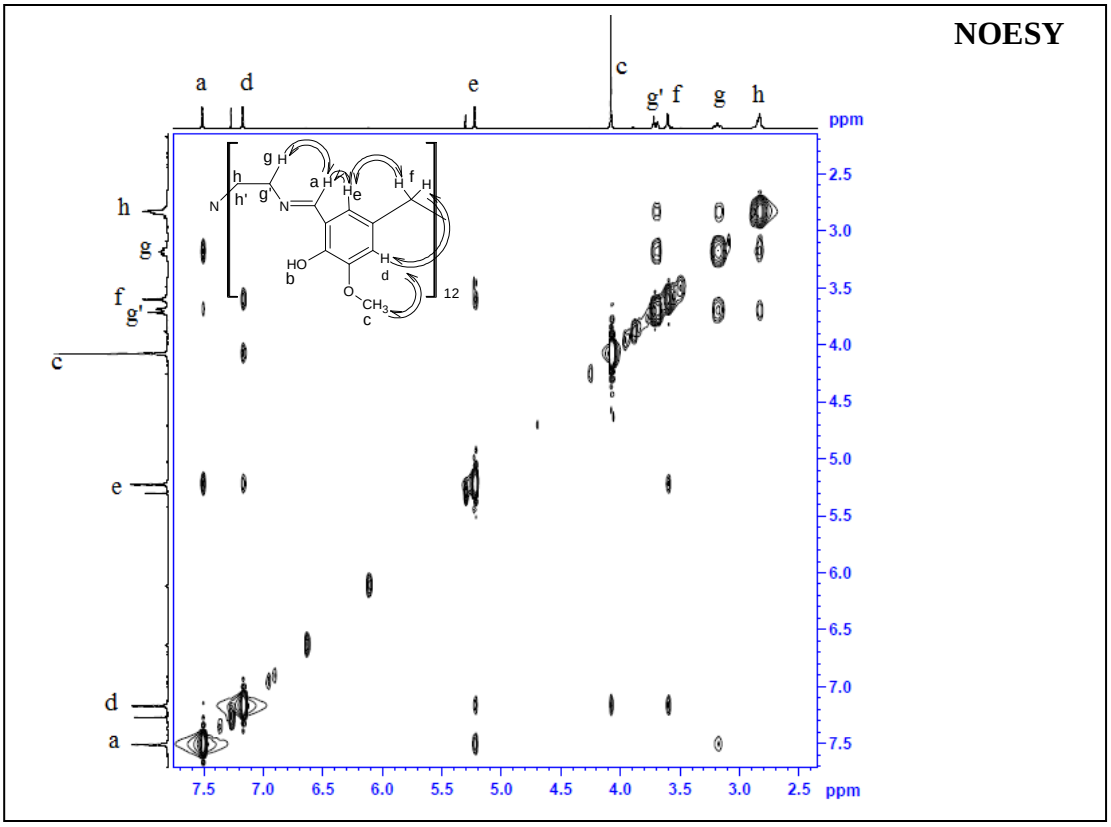

Spectrum 6.24

HSQC

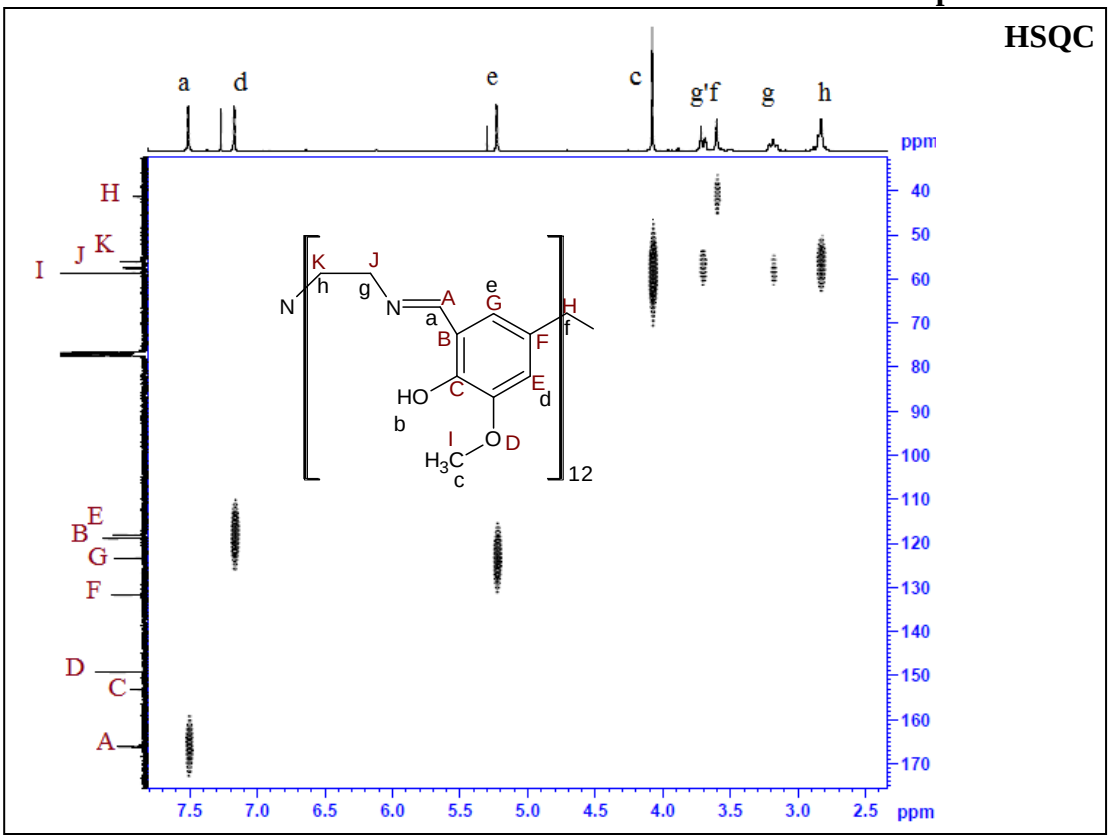

Spectrum 6.25

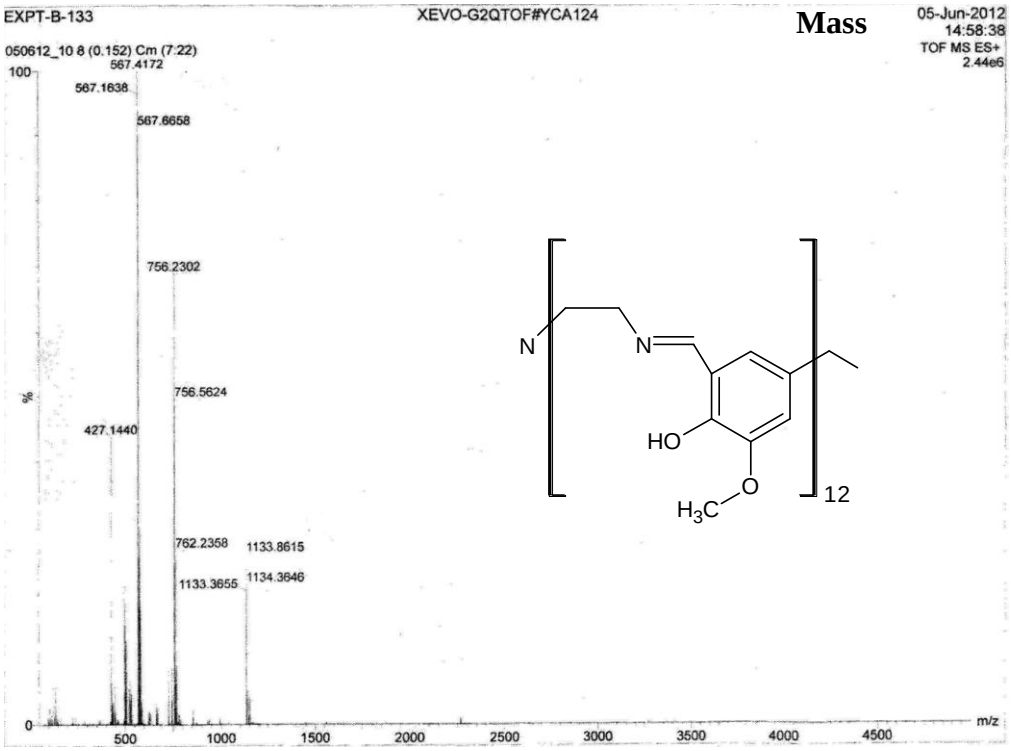

Chromatogram 6.26

HPLC

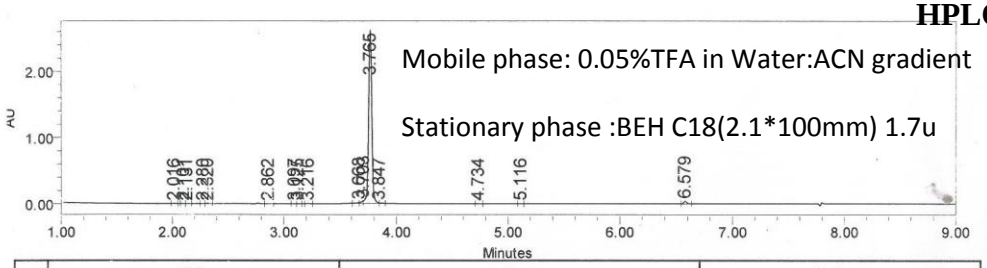

	RT	Area	% Area
1	2.016	2940	0.06
2	2.101	2057	0.04
3	2.131	1947	0.04
4	2.280	1838	0.03
5	2.320	4832	0.09
6	2.862	3036	0.06
7	3.097	2026	0.04
8	3.125	1587	0.03
9	3.216	4722	0.09
10	3.668	18571	0.35
11	3.703	46729	0.88
12	3.765	5144850	96.85
13	3.847	8272	0.16
14	4.734	874	0.02
15	5.116	1144	0.02
16	6.579	66863	1.26

6.7 References:

1. Cui, Y; Yue, Y.; Qian, G.; Chen, B.; *Chem. Rev*., **2012**, 112, 1126.

2. Kreno, L. E.; Leong, K.; Farha, O. K.; Allendorf, M.; Van Duyne, R. P.; Hupp, J. T.; *Chem. Rev*., **2012**, 112, 1105.

3. Horcajada, P.; Gref, R.; Baati, T.; Allan, P. K.; Maurin, G.; Couvreur, P.; Ferey, G.; Morris, R. E.; Serre, C. *Chem. Rev*., **2012**, 12, 1232.

4. Dietrich, B. *Pure Appl. Chem*., **1993,** 65, 1457.

5. Skowronek, P.; Gawronski, J. *Org. Lett.*, **2008**, 10 (21), 4755.

6. Hasell, T.; Schmidtmann, M.; Stone, C. A.; Smith, M. W.; Cooper, A. I. *J. Chem. Soc*., *Chem. Commun*., **2012**, 48, 4689.

7. Hasell, T.; Chong, S. Y.; Jelfs, K. E.; Adams, D. J.; Cooper, A. I. *J. Am. Chem. Soc*., **2012**, 134, 588.

8. Bojdys,M. J.; Briggs, M. E.; Jones,J. T. A.; Adams, D. J.; Chong, S. Y. Schmidtmann, M.; Cooper, A. I. *J. Am. Chem. Soc*., **2011**, 133, 16566.

9. Jones,J. T. A.; Hasell, T.; Xiaofengwu, J. B.; Jelfs, K. E.; Schmidtmann, M.; Chong, S. Y.; Adams, D. J.; Trewin, A.; Schiffman, F.; Cora, F.; Slater, B.; Steiner, A.; Day, G. M.; Cooper, A. I. *Nature*, **2011**, 474, 367.

10. Jazwinski, J.; Lehn,J. M.; Lilienbaum, D.; Ziessel,R.; Guilhem, J.; Pascard C. *J. Chem. Soc., Chem. Commun.*, **1987** 1691.

11. Kang, S. O.; Llinares, J. M.; Powell, D.; Velde, D. V.;James, K. B. *J. Am. Chem. Soc.* **2003**, 125, 10152.

12.Wang, Q; Begum, R. A.; Day, V. W.; James, K. B. *Polyhedron* **2013**, 52, 515.

13. Menif,R.; Reibenspies, J.; Martell, A. E. *Inorg. Chem.* 1991, *30*, 3446

14. Basallote, M. G.; Blanco, E.; Blazquez, M.; Ferna´ndez-Trujillo, M. J.; Litran, R.; Manez, M. A. Solar, M. R. *Chem. Mater*. **2003**, 15, 2025.

15. Avecilla, F.; Blas, A.; Bastida, R.; Fenton, D. E.; Mahía, J.; Macías, A.; Platas, C.; Rodríguez, A.; Rodríguez-Blas T. . *J. Chem. Soc., Chem. Commun.*, **1999**, 125.

16. Shu-Yan, Y.; Qin-Hui, L.; Meng-Chang, S.; Zheng, Z. *Polyhedron*, **1994**, 13(15/16) 2467.

17. Shu-Yan, Y.; Qin-Hui, L.; Huang, X.; Sheng, T; Wu, T.; Wu, D.; *Polyhedron*, **1997**, 16(3), 453.

18. Drew, M. G. B.; Farrell, D.; Morgan, G. G.; McKee, V.; Nelson, J. *J. Chem. Soc., Dalton Trans.*, **2000**, 1513.

19. Howarth, O. W.; Morgan, G. G.; McKee, V.; Nelson, J. *J. Chem. Soc., Dalton Trans.*,**1999**, 2097.

20. Vyas, T. A., *PhD Thesis*, The M. S. University of Baroda **2004**.

List of papers presented in conferences

Sr. No.	Title of the paper presented	Title of conference or seminar	Dates of the event and place
1.	Design of container molecules: synthesis of new azacryptates	International conference on Supramolecular and Nanomaterials Research and Applicaitons	6-8 February 2012 Ahmedabad
2.	Synthesis and characterization of chiral corands	Regional Science Congress on Science for shaping the future of India.	15-16 September 2012 Baroda
3.	Synthesis and study of chiral calix-salen corands	Mordern Trends in Chemistry-MTC-2013	21-23 March 2013 Baroda